NASA Technical Memorandum 102230

IN-02
116463
P.430

Transonic Wind Tunnel Test of a 14% Thick Oblique Wing

Robert A. Kennelly, Jr., Ilan M. Kroo,
James M. Strong, and Ralph L. Carmichael

August 1990

(NASA-TM-102230) TRANSONIC WIND TUNNEL TEST OF A 14 PERCENT THICK OBLIQUE WING (NASA) 430 p

N92-32213

Unclas

G3/02 0116463

National Aeronautics and
Space Administration

NASA Technical Memorandum 102230

Transonic Wind Tunnel Test of a 14% Thick Oblique Wing

Robert A. Kennelly, Jr., James M. Strong, and Ralph L. Carmichael
Ames Research Center, Moffett Field, California

Ilan M. Kroo
Department of Aeronautics and Astronautics
Stanford University, Stanford, California

August 1990

NASA
National Aeronautics and
Space Administration

Ames Research Center
Moffett Field, California 94035-1000

TABLE OF CONTENTS

TRANSONIC WIND TUNNEL TEST OF A 14% THICK OBLIQUE WING

Robert A. Kennelly, Jr., Ilan M. Kroo,* James M. Strong, and Ralph L. Carmichael

Ames Research Center

SUMMARY

An experimental investigation was conducted in the NASA Ames 11- by 11-Foot Transonic Wind Tunnel as part of the Oblique Wing Research Aircraft program to study the aerodynamic performance and stability characteristics of a 0.087-scale model of an F-8 airplane fitted with an oblique wing designed by Rockwell International. The aspect ratio 10.3, straight-tapered wing of 0.14 thickness/chord ratio was tested at two different mounting heights above the fuselage. Additional tests were conducted to assess low-speed behavior with and without flaps, aileron effectiveness at representative flight conditions, and transonic drag divergence with 0° wing sweep.

Longitudinal stability data were obtained at sweep angles of 0°, 30°, 45°, 60°, and 65°, at Mach numbers ranging from 0.25 to 1.40. Test Reynolds number varied from 3.2 to 6.6 ¥ 10^6/ft. Angle of attack ranged from -5° to +18°. Most data were taken at zero sideslip, but a few runs were made at sideslip angles of ±5°.

The raised wing position proved detrimental overall, although side force and yawing moment were reduced at some conditions. Maximum lift coefficient with the flaps deflected was found to fall short of the value predicted in the preliminary design document. The performance and trim characteristics of the present wing are generally inferior to those obtained for a previously tested wing designed at Ames.

INTRODUCTION

An F-8 fighter aircraft model fitted with an oblique wing was tested in the NASA Ames 11- by 11-Foot Transonic Wind Tunnel during July 1988. The wing was designed by Rockwell International under the Oblique Wing Research Aircraft (OWRA) program (Contract NAS2-12229, Report NA-87-1033 (draft)). Simplicity of manufacture was among the design objectives in order to limit the cost of the proposed flight vehicle. Test conditions included Mach numbers from 0.25 to 1.40 and wing sweep angles from 0° to 65°. Unit Reynolds number varied from 3.2 to 6.6 ¥ 10^6/ft for most of the runs.

One of the primary test objectives was to determine whether an elevated pivot design would reduce side force and yawing moment, as had been observed by Rockwell in low-speed tests.

---

*Dept. of Aeronautics and Astronautics, Stanford University, Stanford, Calif.

Therefore, two wing pivot heights were tested. Although the primary emphasis of the test was upon the transonic and low supersonic characteristics of these two configurations in pitch, several other studies were done. Low-speed behavior was investigated both for the clean wing and with landing flaps deflected, and aileron effectiveness was measured for a range of Mach numbers and sweep angles. A few runs were devoted to varying sideslip angle and dynamic pressure. Complete results for the Rockwell-designed wing are presented in this report, with essentially no analysis. An index to the data figures is included.

A second wing of comparable size but differing in leading-edge sweep, pivot location, and airfoil section was designed at NASA Ames and has also been tested. A brief comparison of the two designs is presented in the appendix. Detailed results and analysis for the Ames wing are the subject of a report to be published.

NOMENCLATURE

The reference axis systems and sign conventions used are illustrated in figure 1 (of the quantities illustrated, only those actually used in the test are defined in the list that follows). Lift and drag are presented in the stability-axis system, and the other forces and moments are presented in the body-axis coordinate system. The reference values of parameters b, c, and S used for the force and moment coefficients are given in table 1; they are identical to those used in several previous tests and thus differ slightly from the dimensions of the present model.

Symbols

b	wing span
c	wing chord
c_{root}	wing root chord (unswept)
C_D	drag coefficient, drag/qS
C_L	lift coefficient, lift/qS
C_L (max)	maximum lift coefficient as angle of attack is increased past stall
C_l	rolling moment coefficient, rolling moment/qSb
C_m	pitching moment coefficient, pitching moment/qSc
C_n	yawing moment coefficient, yawing moment/qSb
C_Y	side force coefficient, side force/qS

L/D	lift/drag ratio
q	free-stream dynamic pressure
Re	Reynolds number
S	wing area
x	Cartesian coordinate along axis parallel to model centerline; positive downstream
y	Cartesian coordinate along wing span perpendicular to centerline; positive to the right
z	Cartesian coordinate vertical from model centerline; positive upward

Greek symbols

α	angle of attack referenced to fuselage centerline (deg)
β	sideslip angle (deg)
Λ	sweep angle of the wing in the horizontal plane, measured between the (straight) leading edge of the wing and a perpendicular to the body axis; positive indicates right tip forward (deg)

Configuration and control surface codes

LP	low pivot (denoted L in data plots)
HPF	high pivot with fairing (denoted F in data plots)
LA	left aileron
LO	left outboard flap
RO	right outboard flap
RA	right aileron

MODEL DESCRIPTION

The wing was mounted on a 0.087-scale model of an F-8 fighter-type aircraft as shown in figure 2. The fuselage, empennage, and ventral fins were similar to those of the Ames-Dryden F-8C Digital-Fly-by-Wire testbed vehicle, except that the model's engine inlet was faired over. In addition, the wing was mounted above the fuselage. The wing was tapered, with a straight leading edge and forward-swept trailing edge. The wing aspect ratio was approximately 10.3 in the unswept position. Lofting of the wing surface was linear from root to tip. The airfoil section was SC (2)-0714, designed at NASA Langley for a lift coefficient of 0.70 at Mach 0.735 (ref. 1). A sketch of the airfoil and its normalized coordinates are given in figure 3. There was no twist between wing root and tip. The horizontal and vertical tail surfaces had NACA 65A006 airfoil sections and a 45° swept quarter-chord line. The horizontal tail was mounted at 0° incidence relative to the fuselage centerline. Pertinent dimensions of the wing, fuselage, and tail are given in table 1.

The wing bank angle, 0° with the wing unswept, was 10° (right tip down) with 65° sweep, viewed along the long axis of the fuselage. The pivot axis inclination was 7.894° forward and 5.0° to the right. This choice of axis tilt yields the desired wing bank angle at 65° sweep and results in a section angle of attack of zero at both 0° and 65° sweep.

Both high and low mounting positions were used, and the wing could be swept 0°, 30°, 45°, 60°, or 65°. The high pivot had a fairing around the mounting post, as shown in figure 4, whereas a short section of the post was left exposed with the wing in the low position. The flaps, plain deflectable segments extending from 34.3% to 65.1% semispan and hinged at x/c = 70%, could be deflected 30° (positive downward). A second pair of flaps located closer to the fuselage was not available for low-speed use. The aileron surfaces were of similar design and were located outboard of the flaps, from 65.1% to 92.1% semispan. Installation photographs of the model in the wind tunnel, with the wing mounted on the low pivot, are presented in figure 5.

To ensure consistent boundary layer transition, a row of (nominal) 0.0054-in.-raised dots was placed at 10% x/c from the leading edge on the upper and lower wing surfaces. The dots were of approximately 0.045-in. diameter and were spaced 0.100 in. center to center. Strips of 0.0058-in.-diameter grit, 0.10 in. wide, were glued onto the tail and in a ring 1.0 in. from the nose of the fuselage. The sizes of the dots and of the grit were calculated to induce transition on the unswept wing at a tunnel Reynolds number of 3.3×10^6/ft.

TEST FACILITY

The tests were conducted in the Ames Research Center 11- by 11-Foot Transonic Wind Tunnel, part of the Unitary Plan Wind Tunnel system. The tunnel is a closed-circuit, continuous-flow facility capable of operation at stagnation pressures of 0.5 to 2.25 atm, corresponding to unit Reynolds numbers of 1.5×10^6/ft to 9.4×10^6/ft. The Mach number is variable from 0.25 to 1.40. The test section has ventilated walls, floor, and ceiling, permitting testing through the transonic range.

TEST PROCEDURE AND DATA REDUCTION

The model was supported by a sting through the base of the fuselage, and forces and moments were measured by an internally mounted six-component electrical strain gauge balance selected for its high rolling moment capacity. The 2.5-in. Mark XXA balance capacities are 4000 in.-lb in roll, and 600 lb of axial force. Using measured values of sting cavity pressure, the balance data were adjusted to a condition corresponding to free-stream static pressure on the base of the model.

The reference area for the aerodynamic coefficients was 326.97 in.^{2}, corresponding to a nominal full-scale planform area of 300 ft^2. The chord and span reference values used for pitching and rolling/yawing moments were also the same as in the test of the Ames-designed wing (see table 1). The moment center was located on the model centerline, aligned longitudinally beneath the wing pivot at $0.26c_{root}$.

Most runs were conducted at a constant q of 700 psf, corresponding to chord Reynolds numbers between 2.5 and 3.9 ¥ 10^6. Tunnel Mach number ranged from 0.25 to 1.40 for this test, and was held to within ±0.002 of the nominal value for each series of runs. Angle of attack varied from −5° to +18°. The sweep and Mach number combinations tested for the pivot height comparison are shown in table 2. Once the pivot height was chosen, additional studies were made of stall behavior, transonic drag divergence, aileron effectiveness for ±10° deflections, and low-speed C_L (max) for 30° flaps.

Angles f attack and sideslip were measured by the angular "knuckle-sleeve" drive system of the model support, located downstream of the sting, with corrections for balance and sting deflection based on pretest calibrations. Flow angularity was measured by comparison of lift data taken with the model upright and inverted, over a range of Mach numbers for sweep angles of 0° and 65°. The estimated angle-of-attack corrections applied to the data were all less than 0.07°.

RESULTS AND DISCUSSION

Selection of Baseline Pivot Height

After low-speed tests at 65° wing sweep, Rockwell had proposed that the wing height above the fuselage be increased in order to reduce wing/fuselage interference. Results for the high and low pivot configurations are presented in figure 6. The high wing position offers few advantages. The side force is reduced at a few conditions, but overall the force and moment breaks are more irregular with the high pivot, and the drag is higher, especially at high speeds. In addition, a small transonic pitch instability at intermediate sweep angles is exacerbated by raising the wing (see, for example, the C_m plot for Mach 0.90, sweep 45°). For these reasons, the low pivot was chosen as the baseline configuration for the balance of the test.

Aerodynamic Characteristics in Pitch

The low-wing data are replotted in figure 7 to show the effect of sweep angle on the forces and moments at each Mach number. A similar overview of the effect of Mach number is presented in figure 8 for the various sweep angles tested. Finally, a summary of the derived aerodynamic characteristics is presented in figure 9. All sweep angles are grouped together, and the various quantities are plotted against Mach number.

Additional data were taken at zero sweep with the base configuration (low pivot, LP) at a number of subsonic Mach numbers to study stall characteristics and transonic drag divergence. The low-speed data, Mach 0.25 to 0.50, are presented in figure 10, and a similar set of plots, figure 11, covers the range 0.50 to 0.80.

Effect of Sideslip

The base configuration was tested at sideslip angles of ±5° for Mach 0.80 at sweep angle 45°. These force and moment data are presented in figure 12. Here, as elsewhere, the drag data labeled C_D is actually C_{D_S}.

Landing-Flap Effectiveness

The flaps were deflected by 30° to study high-lift performance at low speeds with the wing unswept. The (untrimmed) results are presented in figure 13. The value of C_L (max) at Mach 0.25 is 1.73 with full flap deflection (vs. 1.60 for the clean wing), which is significantly lower than the trimmed value of greater than 2.0 which was quoted in the preliminary design document. This apparent discrepancy requires further analysis to account for Mach and Reynolds number effects, and for the additional download on the model's tail which would be required for trim in pitch.

Effect of Aileron Deflection

Aileron effectiveness was measured for an asymmetric deflection of 10° in both roll directions (except for the symmetric zero sweep case, where only left-positive deflections were evaluated). Force and moment results for these configurations are presented in figure 14, grouped by sweep angle.

Effect of Dynamic Pressure

A single run was made at reduced q to study Reynolds number sensitivity. As shown in figure 15, the difference between the Mach 0.80, sweep 45° baseline run (q = 700, Re ≈ 4.5×10^6/ft) and the special run with q = 300 psf (Re ≈ 2.1×10^6/ft) is not large, although there is a systematic shift in drag revealed by the L/D results. This is apparently the result of the change in Reynolds number, rather than an aeroelastic effect, since the pitching and rolling moments, which are sensitive to wing twist, were unchanged.

ERROR ANALYSIS

Although no formal analysis of the accuracy or precision of these results has been performed, data from some of the repeat runs are presented in figure 16. The data agree fairly well; there was apparently little run-to-run variation, except at very high angles of attack. The data for Mach 0.30 were the least reproducible. The reason for the shifts in the C_L–α and C_L–C_D curves is unknown.

CONCLUDING REMARKS

An examination of the aerodynamic characteristics of an oblique wing of relatively simple design proposed for the F-8 OWRA has resolved one major design question and raised several other issues which may merit further investigation. The high pivot configuration proposed on the basis of low-speed tests caused high drag with little reduction in wing/fuselage interference, and was less stable in pitch at certain transonic conditions than the low pivot configuration was. Further testing, with the wing in the lower position, suggests that the maximum lift coefficient anticipated by its designers would not be obtained in flight. The exact magnitude of this discrepancy is uncertain, since a complete study of the trimmed low-speed characteristics at flight Reynolds number was beyond the scope of the test.

As discussed in the appendix, comparison with a slightly more complex wing shows that better performance and handling properties can be obtained if desired. The Ames-designed wing tested previously offers higher L/D ratios at most conditions, higher C_L (max), and more moderate force and moment breaks than the present design does. Both wings, however, exhibit the usual oblique wing nonl. 1earities, exaggerated by the rigidity of the wind tunnel models.

APPENDIX

Additional data (to be published), on the Ames 300 ft^2 wing, were obtained along with the results reported here for the Rockwell-designed wing. Since the two wings are fairly similar (they differ in airfoil, pivot location, and leading-edge sweep), were mounted on the same body, and were tested under the same conditions, it is possible to compare the basic results. These comparisons are presented in figure A.1, in which the forces and moments are plotted for conditions ranging from Mach 0.30, 0° sweep to Mach 1.40, 65° sweep. The Ames wing, 14% thick at the root and 12% at the tip, is somewhat thinner than the Rockwell design and has more camber because the airfoils were designed for higher lift coefficients. The Ames wing's spanwise variation in airfoil section, which would require somewhat higher manufacturing costs, is common in production aircraft but was felt by Rockwell to be too expensive for a one-of-a-kind demonstrator. This simplicity comes at a high price, however. The 0° sweep performance of the Rockwell wing is superior only for Mach 0.76 and 0.78, and then only for $C_L \leq 0.50$. (And, since the OWRA wing would normally be swept with increasing Mach number, even this comparison is not significant.) The higher lift capacity of the sections used in the Ames wing is reflected in wider regimes of linear behavior for the swept wing cases as well, and there are milder force and moment breaks when stall does occur. The difference between the two wings diminishes as the wing sweep increases: at Mach 1.40 with sweep 65°, for example, maximum L/D for the Ames wing is only about 7% higher than for the Rockwell design.

REFERENCE

1. Harris, Charles D.: Aerodynamic Characteristics of a 14-Percent-Thick NASA Supercritical Airfoil Designed for a Normal-Force Coefficient of 0.7. NASA TM X–72,712, July 1975.

TABLE 1.— MODEL DIMENSIONS.

Fuselage			
Length			55.677 in.
Maximum depth (at station 11.850)			6.589 in.
Maximum width (at station 32.828)			5.278 in.
Base diameter			3.750 in.
Wing			
Span	Model		57.752 in.
	Reference		58.524 in.
Area	Model, straight TE		324.00 sq in.
	Reference		326.98 sq in.
Chord	Root, straight TE		8.217 in.
	Tip		1.808 in.
	Reference		5.587 in.
Aspect ratio	Model	Sweep 0°	10.29
		Sweep 30°	8.91
		Sweep 45°	7.28
		Sweep 60°	5.15
		Sweep 65°	4.35
Section (see figure 3)			SC(2)-0714
Incidence	Root		0°
	Tip		0°
Leading edge sweep			0°
Dihedral			1.0°
Horizontal tail			
Span			18.868 in.
Area			101.74 sq in.
Chord	Root (on fuselage centerline)		9.396 in.
	Tip		1.388 in.
Aspect ratio			3.50
Section			NACA 65A006
Incidence			0°
0.25 chord sweep			45°
Dihedral			6°
Vertical tail			
Span			12.608 in.
Area			107.85 sq in.
Chord	Root (on fuselage centerline)		13.570 in.
	Tip		3.539 in.
Aspect ratio			1.45
Section			NACA 65A006
Incidence			0°
0.25 chord sweep			45°

TABLE 2. — TEST CONDITIONS FOR PIVOT HEIGHT COMPARISON.

Sweep	Alpha	Beta	Q	Mach .30	.40	.60	.70	.80	.90	.95	1.10	1.20	1.40
0°	vary	0°	250	•									
0°	vary	0°	440		•								
0°	vary	0°	700			•	•	•					
30°	vary	0°	700			•	•	•	•				
45°	vary	0°	700			•		•	•	•	•	•	
60°	vary	0°	700					•		•	•	•	•
65°	vary	0°	700			•		•			•	•	•

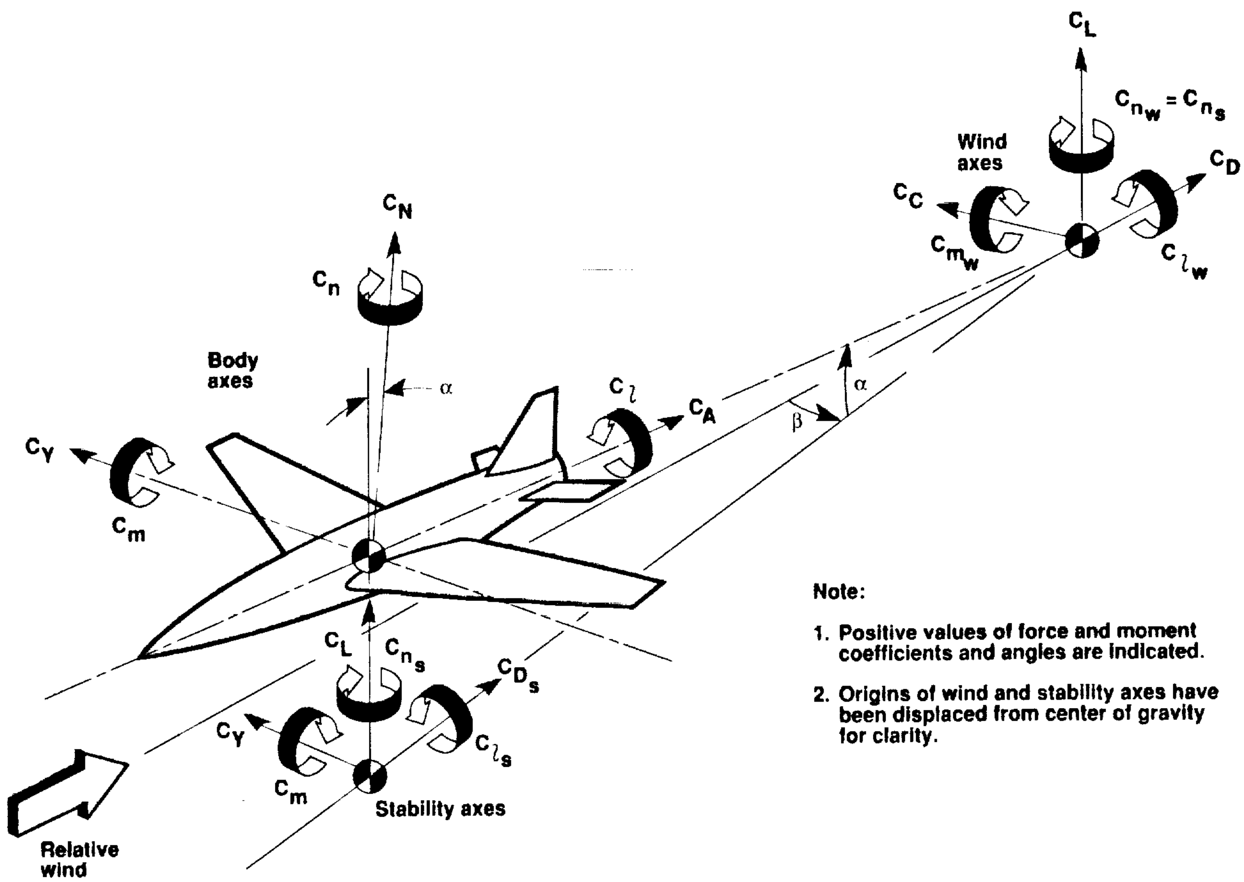

Figure 1. Reference axis systems.

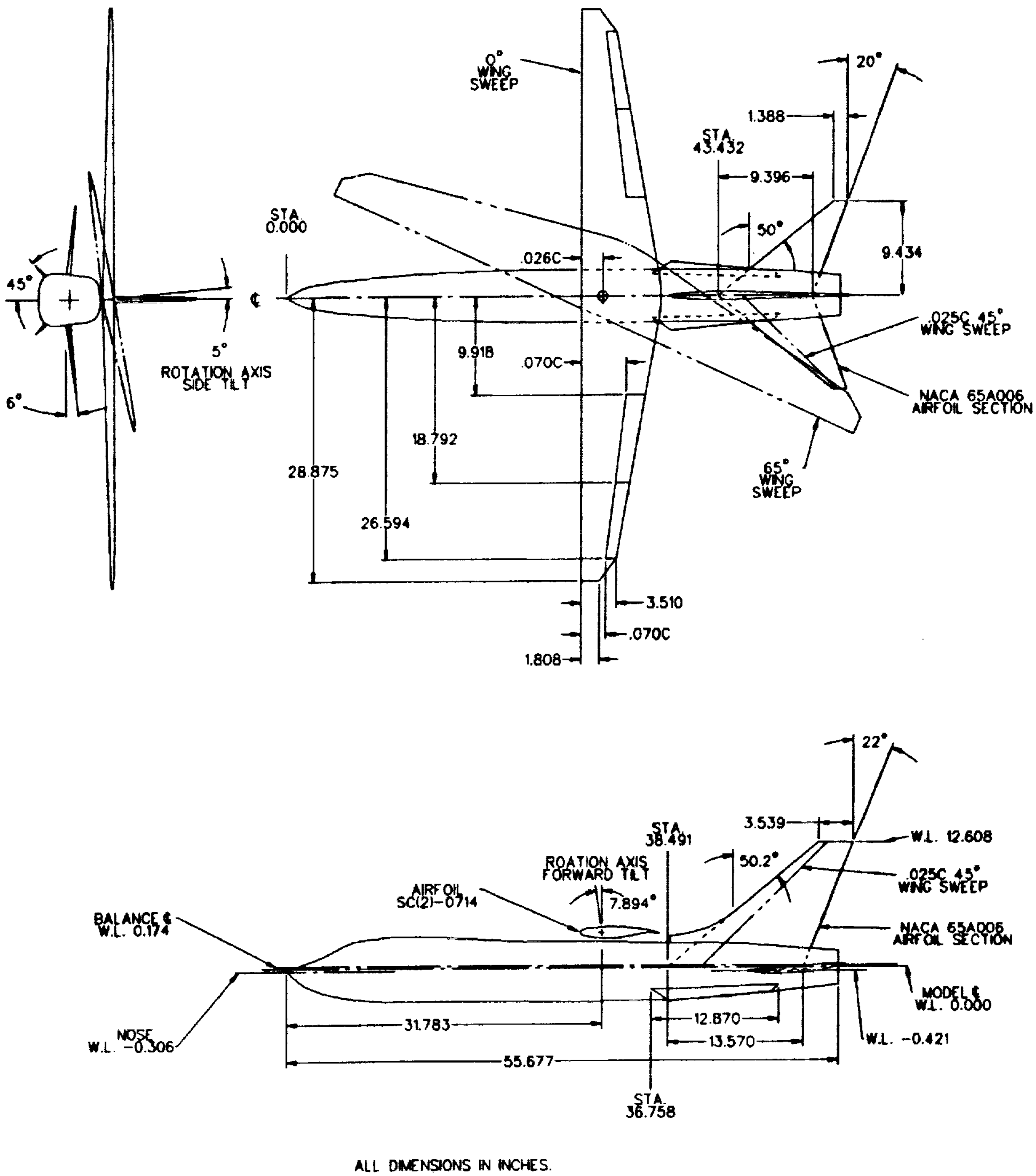

Figure 2. F-8 model with Rockwell oblique wing.

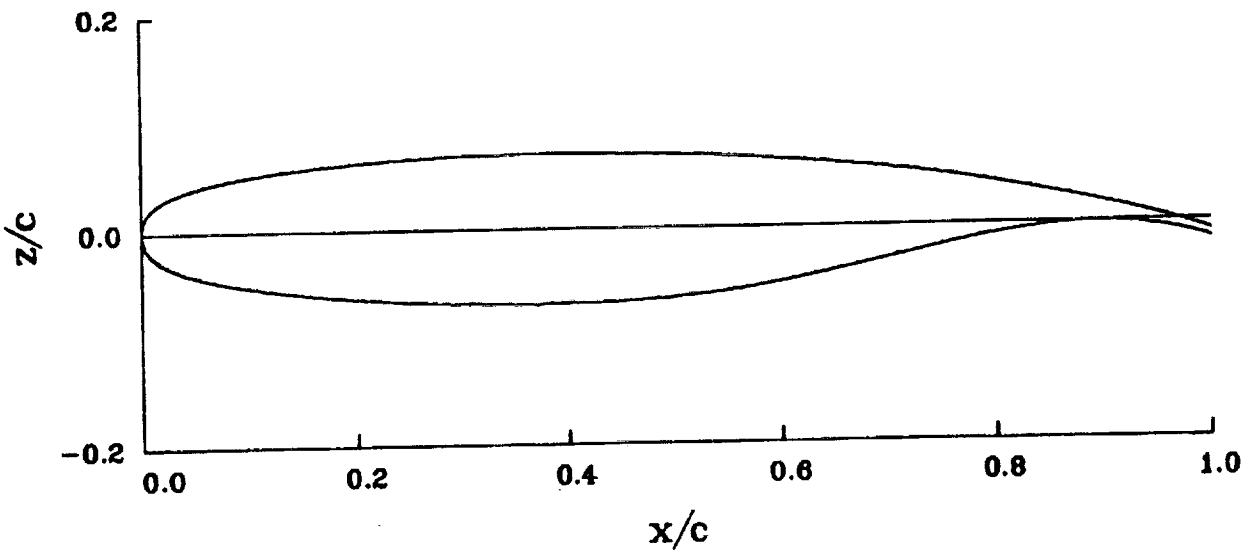

x/c	z/c upper	z/c lower	camber	thickness
0.000000	0.000000	0.000000	0.000000	0.000000
0.002000	0.010800	-0.010800	0.000000	0.021600
0.005000	0.016700	-0.016500	0.000100	0.033200
0.010000	0.022500	-0.022300	0.000100	0.044800
0.020000	0.029700	-0.029500	0.000100	0.059200
0.030000	0.034600	-0.034300	0.000150	0.068900
0.040000	0.038300	-0.038100	0.000100	0.076400
0.050000	0.041400	-0.041100	0.000150	0.082500
0.060000	0.044000	-0.043800	0.000100	0.087800
0.070000	0.046300	-0.046100	0.000100	0.092400
0.080000	0.048400	-0.048100	0.000150	0.096500
0.090000	0.050200	-0.050000	0.000100	0.100200
0.100000	0.051900	-0.051700	0.000100	0.103600
0.110000	0.053500	-0.053300	0.000100	0.106800
0.120000	0.054900	-0.054700	0.000100	0.109600
0.130000	0.056200	-0.056100	0.000050	0.112300
0.140000	0.057400	-0.057400	0.000000	0.114800
0.150000	0.058500	-0.058500	0.000000	0.117000
0.160000	0.059600	-0.059600	0.000000	0.119200
0.170000	0.060600	-0.060600	0.000000	0.121200
0.180000	0.061500	-0.061600	-0.000050	0.123100
0.190000	0.062400	-0.062500	-0.000050	0.124900
0.200000	0.063200	-0.063300	-0.000050	0.126500
0.210000	0.064000	-0.064100	-0.000050	0.128100
0.220000	0.064700	-0.064800	-0.000050	0.129500

Figure 3. Airfoil SC (2)-0714 sketch and coordinates.

x/c	z/c upper	z/c lower	camber	thickness
0.230000	0.065300	-0.065500	-0.000100	0.130800
0.240000	0.065900	-0.066100	-0.000100	0.132000
0.250000	0.066500	-0.066700	-0.000100	0.133200
0.260000	0.067000	-0.067200	-0.000100	0.134200
0.270000	0.067500	-0.067700	-0.000100	0.135200
0.280000	0.067900	-0.068100	-0.000100	0.136000
0.290000	0.068300	-0.068500	-0.000100	0.136800
0.300000	0.068600	-0.068800	-0.000100	0.137400
0.310000	0.068900	-0.069100	-0.000100	0.138000
0.320000	0.069200	-0.069300	-0.000050	0.138500
0.330000	0.069400	-0.069500	-0.000050	0.138900
0.340000	0.069600	-0.069600	0.000000	0.139200
0.350000	0.069800	-0.069700	0.000050	0.139500
0.360000	0.069900	-0.069700	0.000100	0.139600
0.370000	0.070000	-0.069700	0.000150	0.139700
0.380000	0.070000	-0.069600	0.000200	0.139600
0.390000	0.070000	-0.069500	0.000250	0.139500
0.400000	0.070000	-0.069300	0.000350	0.139300
0.410000	0.069900	-0.069100	0.000400	0.139000
0.420000	0.069800	-0.068900	0.000450	0.138700
0.430000	0.069700	-0.068600	0.000550	0.138300
0.440000	0.069600	-0.068200	0.000700	0.137800
0.450000	0.069400	-0.067800	0.000800	0.137200
0.460000	0.069200	-0.067300	0.000950	0.136500
0.470000	0.068900	-0.066700	0.001100	0.135600
0.480000	0.068600	-0.066100	0.001250	0.134700
0.490000	0.068300	-0.065400	0.001450	0.133700
0.500000	0.068000	-0.064600	0.001700	0.132600
0.510000	0.067600	-0.063700	0.001950	0.131300
0.520000	0.067200	-0.062700	0.002250	0.129900
0.530000	0.066800	-0.061600	0.002600	0.128400
0.540000	0.066300	-0.060400	0.002950	0.126700
0.550000	0.065800	-0.059100	0.003350	0.124900
0.560000	0.065200	-0.057700	0.003750	0.122900
0.570000	0.064600	-0.056200	0.004200	0.120800
0.580000	0.064000	-0.054600	0.004700	0.118600
0.590000	0.063400	-0.052900	0.005250	0.116300
0.600000	0.062700	-0.051100	0.005800	0.113800
0.610000	0.062000	-0.049300	0.006350	0.111300

Figure 3. Continued.

x/c	z/c upper	z/c lower	camber	thickness
0.620000	0.061300	-0.047400	0.006950	0.108700
0.630000	0.060500	-0.045400	0.007550	0.105900
0.640000	0.059600	-0.043400	0.008100	0.103000
0.650000	0.058700	-0.041300	0.008700	0.100000
0.660000	0.057800	-0.039200	0.009300	0.097000
0.670000	0.056800	-0.037100	0.009850	0.093900
0.680000	0.055800	-0.034900	0.010450	0.090700
0.690000	0.054700	-0.032700	0.011000	0.087400
0.700000	0.053600	-0.030500	0.011550	0.084100
0.710000	0.052400	-0.028300	0.012050	0.080700
0.720000	0.051200	-0.026100	0.012550	0.077300
0.730000	0.049900	-0.023900	0.013000	0.073800
0.740000	0.048600	-0.021700	0.013450	0.070300
0.750000	0.047200	-0.019500	0.013850	0.066700
0.760000	0.045700	-0.017300	0.014200	0.063000
0.770000	0.044200	-0.015200	0.014500	0.059400
0.780000	0.042600	-0.013200	0.014700	0.055800
0.790000	0.040900	-0.011300	0.014800	0.052200
0.800000	0.039200	-0.009500	0.014850	0.048700
0.810000	0.037400	-0.007900	0.014750	0.045300
0.820000	0.035600	-0.006400	0.014600	0.042000
0.830000	0.033700	-0.005000	0.014350	0.038700
0.840000	0.031700	-0.003800	0.013950	0.035500
0.850000	0.029700	-0.002800	0.013450	0.032500
0.860000	0.027600	-0.002000	0.012800	0.029600
0.870000	0.025500	-0.001400	0.012050	0.026900
0.880000	0.023300	-0.001000	0.011150	0.024300
0.890000	0.021000	-0.000800	0.010100	0.021800
0.900000	0.018600	-0.000800	0.008900	0.019400
0.910000	0.016200	-0.001100	0.007550	0.017300
0.920000	0.013700	-0.001600	0.006050	0.015300
0.930000	0.011100	-0.002400	0.004350	0.013500
0.940000	0.008400	-0.003500	0.002450	0.011900
0.950000	0.005700	-0.004900	0.000400	0.010600
0.960000	0.002900	-0.006600	-0.001850	0.009500
0.970000	0.000000	-0.008600	-0.004300	0.008600
0.980000	-0.003000	-0.010900	-0.006950	0.007900
0.990000	-0.006200	-0.013600	-0.009900	0.007400
1.000000	-0.009500	-0.016500	-0.013000	0.007000

Figure 3. Concluded.

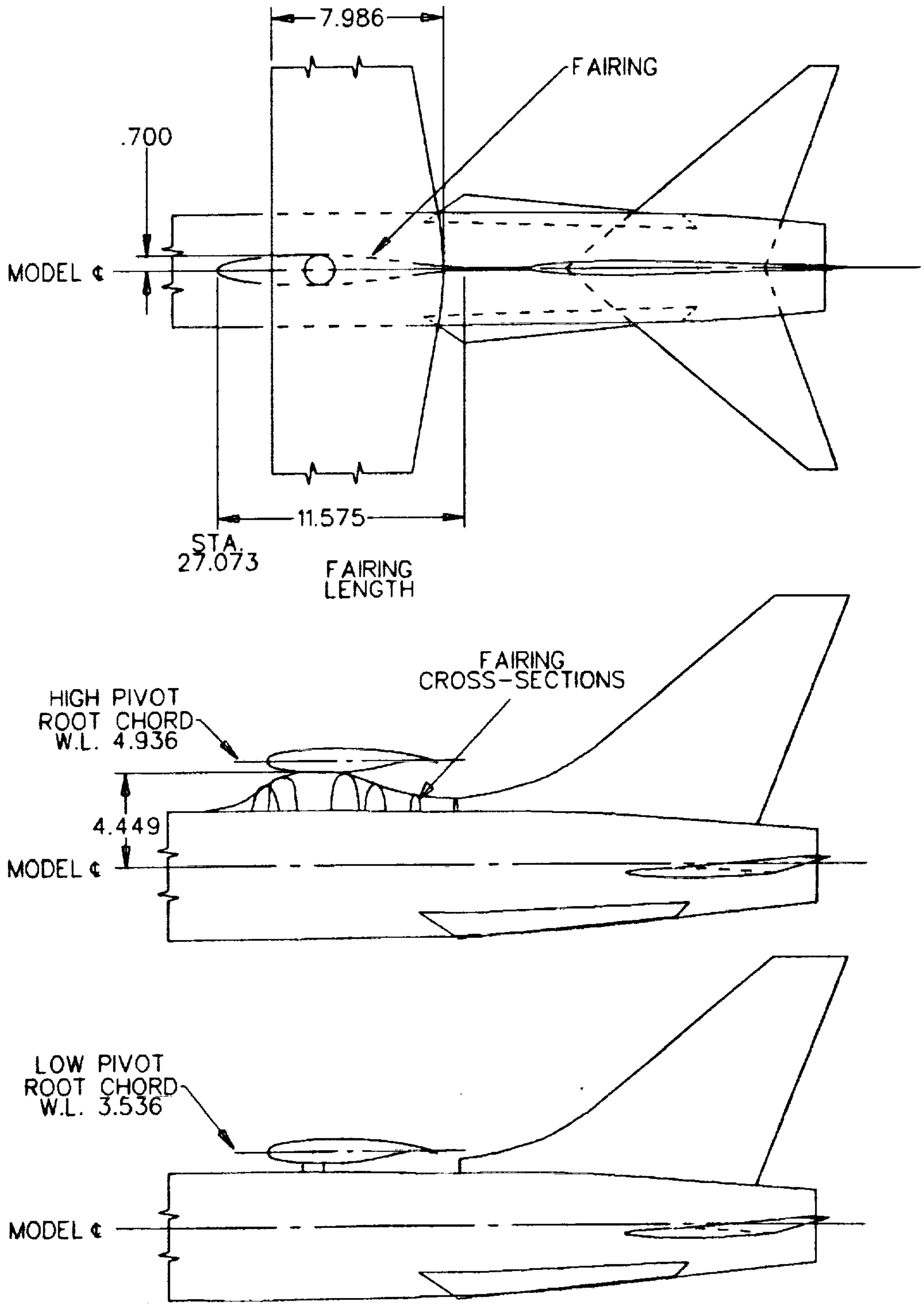

ALL DIMENSIONS IN INCHES.

Figure 4. High pivot and fairing detail.

ORIGINAL PAGE
BLACK AND WHITE PHOTOGRAPH

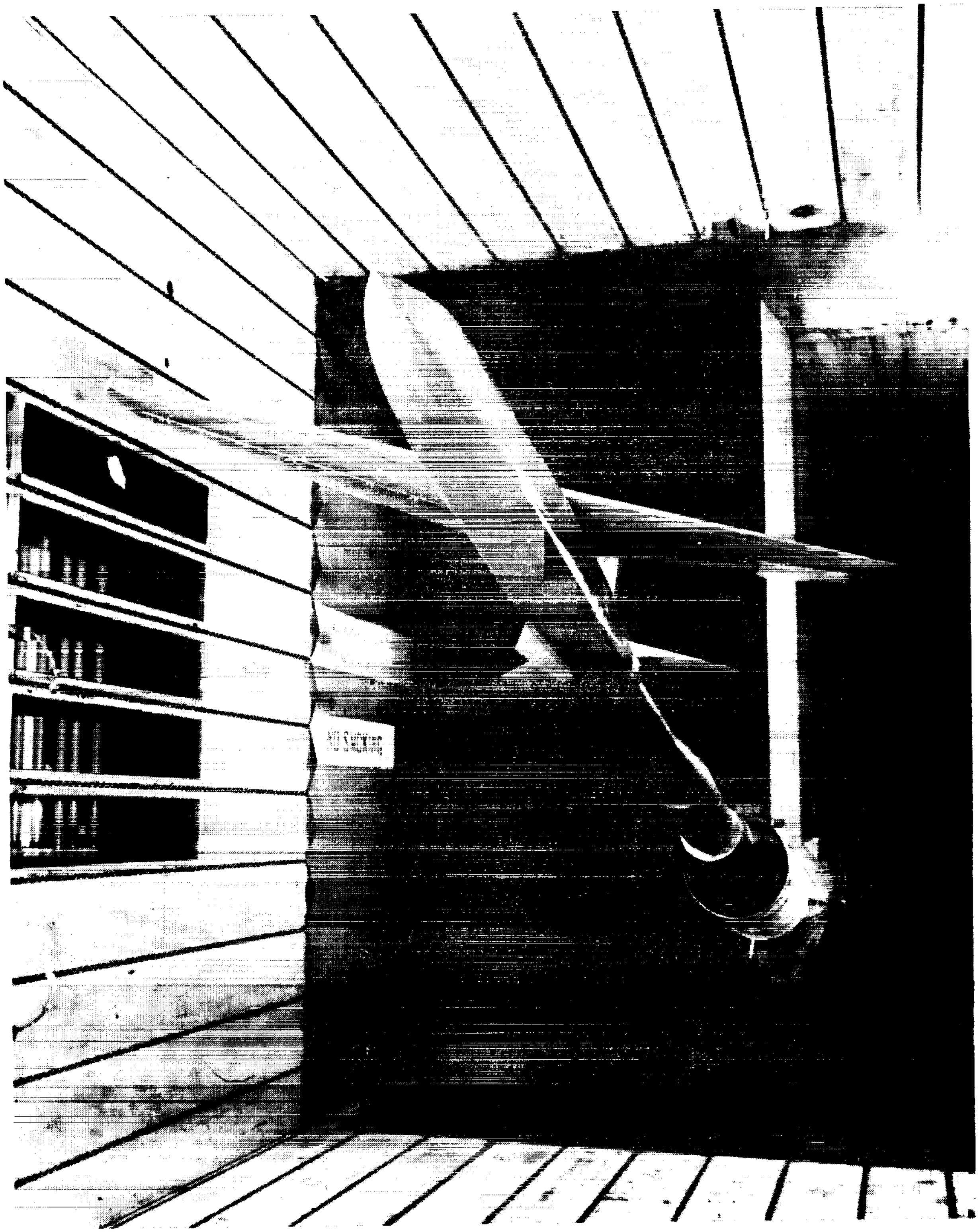

Figure 5. Installation photographs of F-8/OWRA model in the Ames 11- by 11-Foot Transonic Wind Tunnel.

ORIGINAL PAGE
BLACK AND WHITE PHOTOGRAPH

Figure 5. Continued.

ORIGINAL PAGE
BLACK AND WHITE PHOTOGRAPH

Figure 5. Concluded.

INDEX TO DATA FIGURES

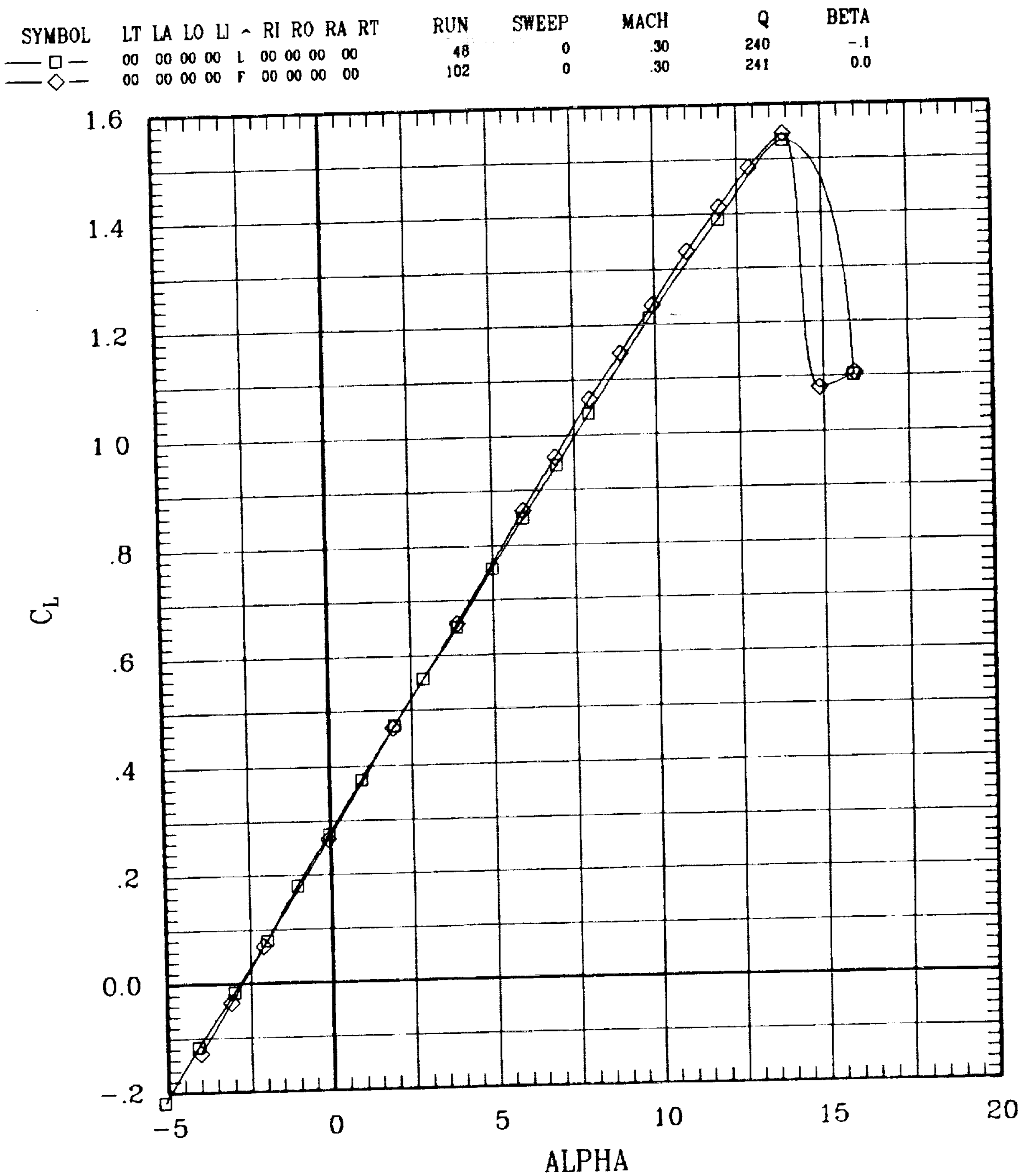

Figure 6(a). Effect of pivot height for sweep = 0 deg.

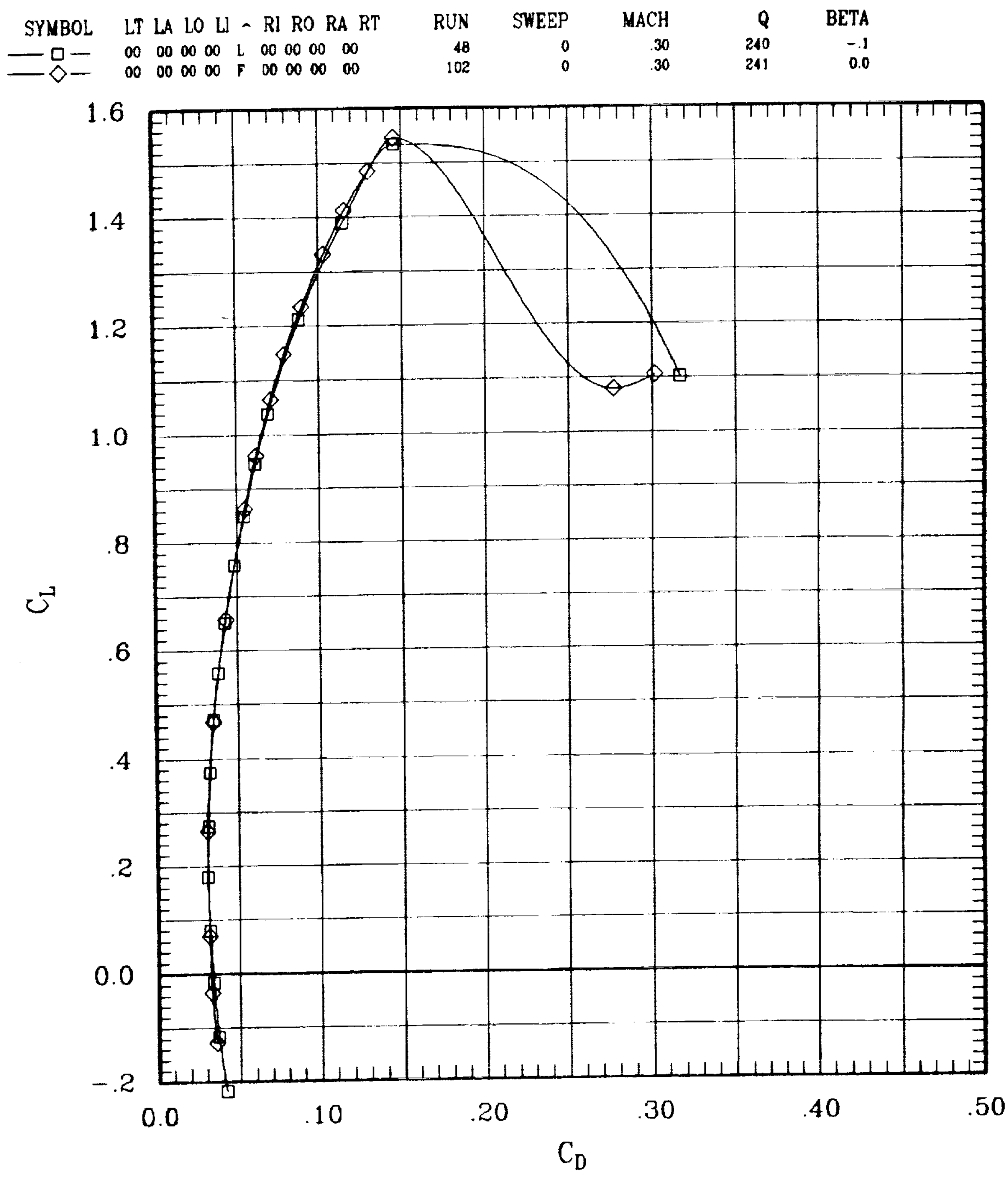

Figure 6(a). Effect of pivot height for sweep = 0 deg.

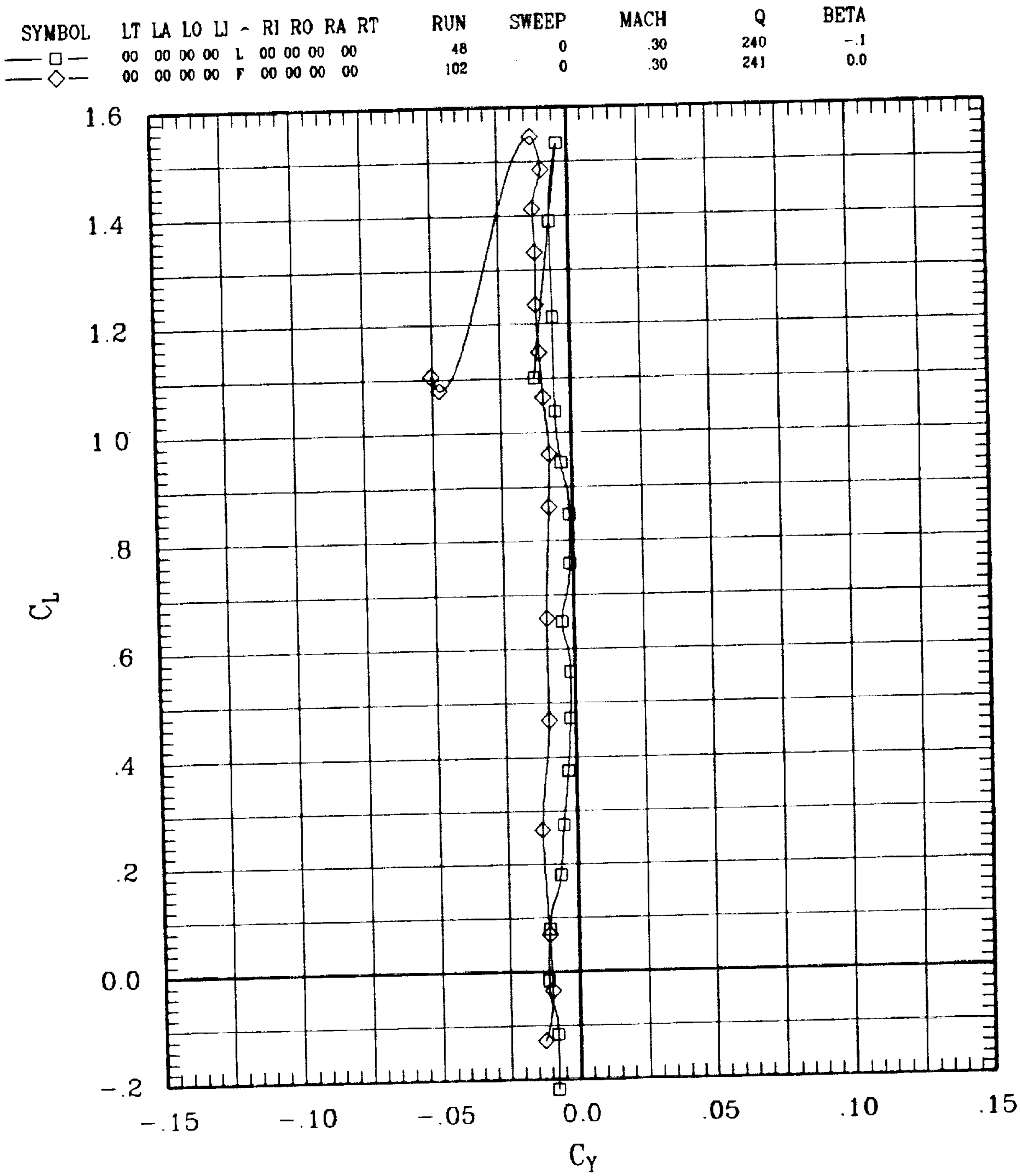

Figure 6(a). Effect of pivot height for sweep = 0 deg.

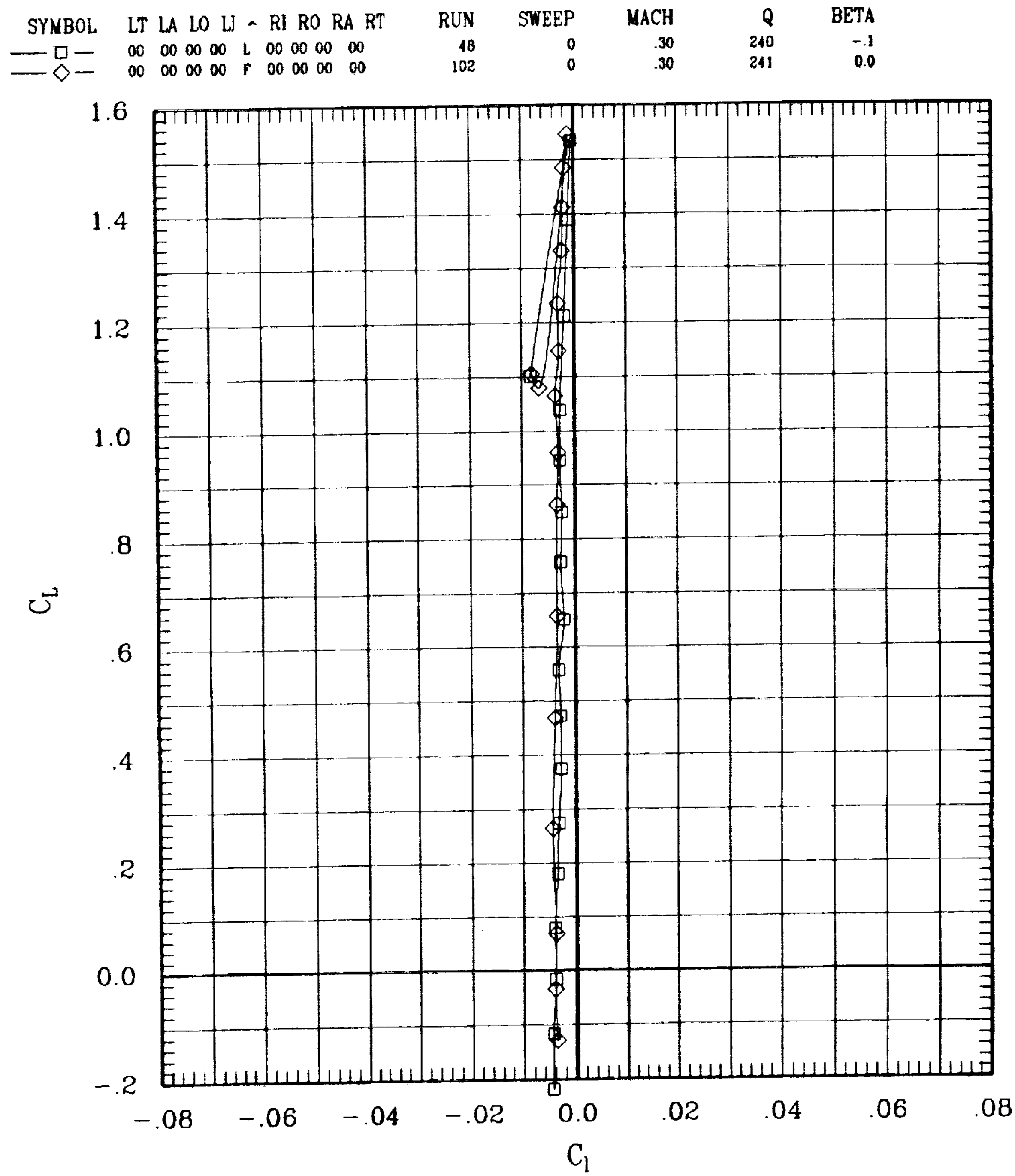

Figure 6(a). Effect of pivot height for sweep = 0 deg.

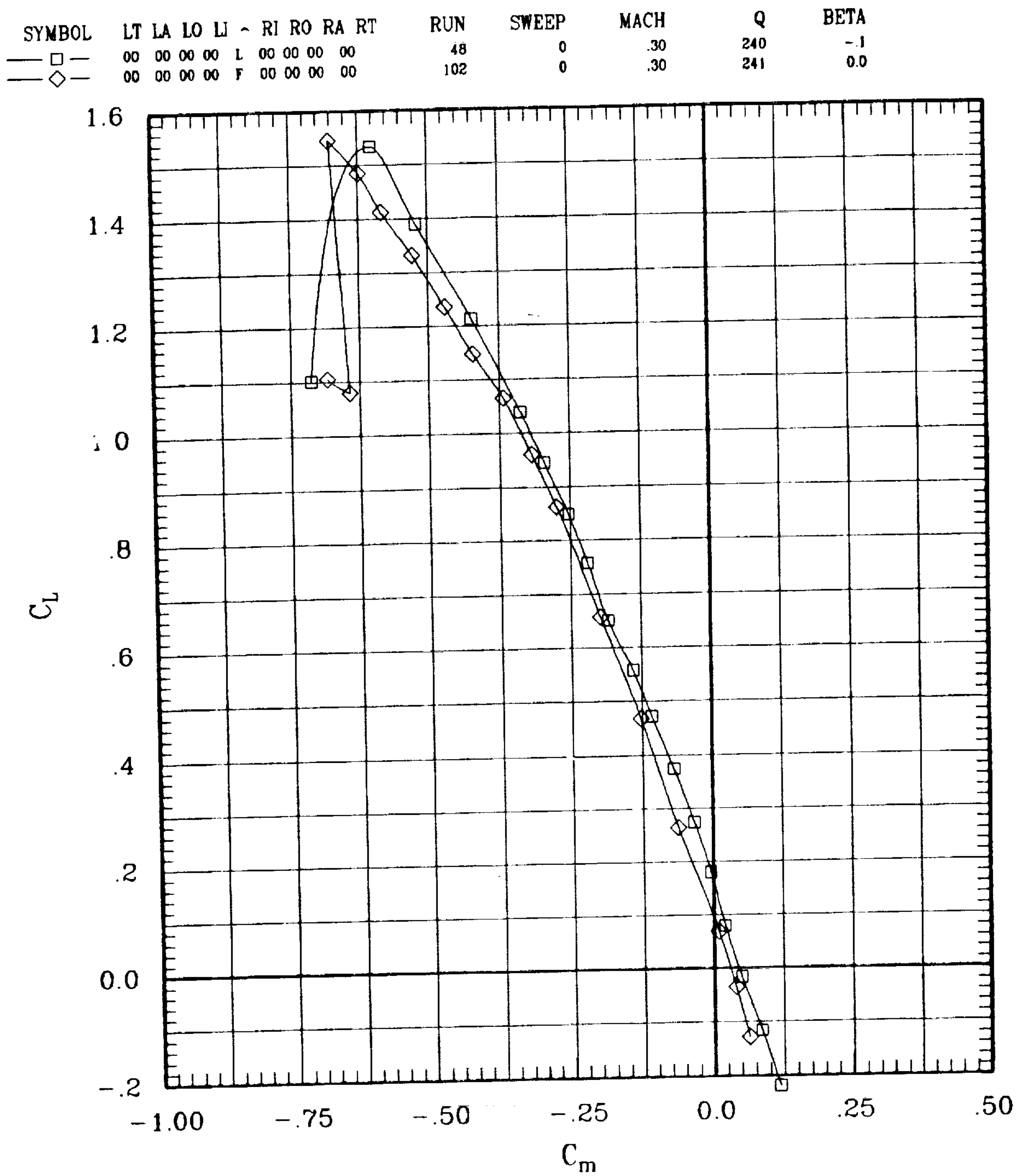

Figure 6(a). Effect of pivot height for sweep = 0 deg.

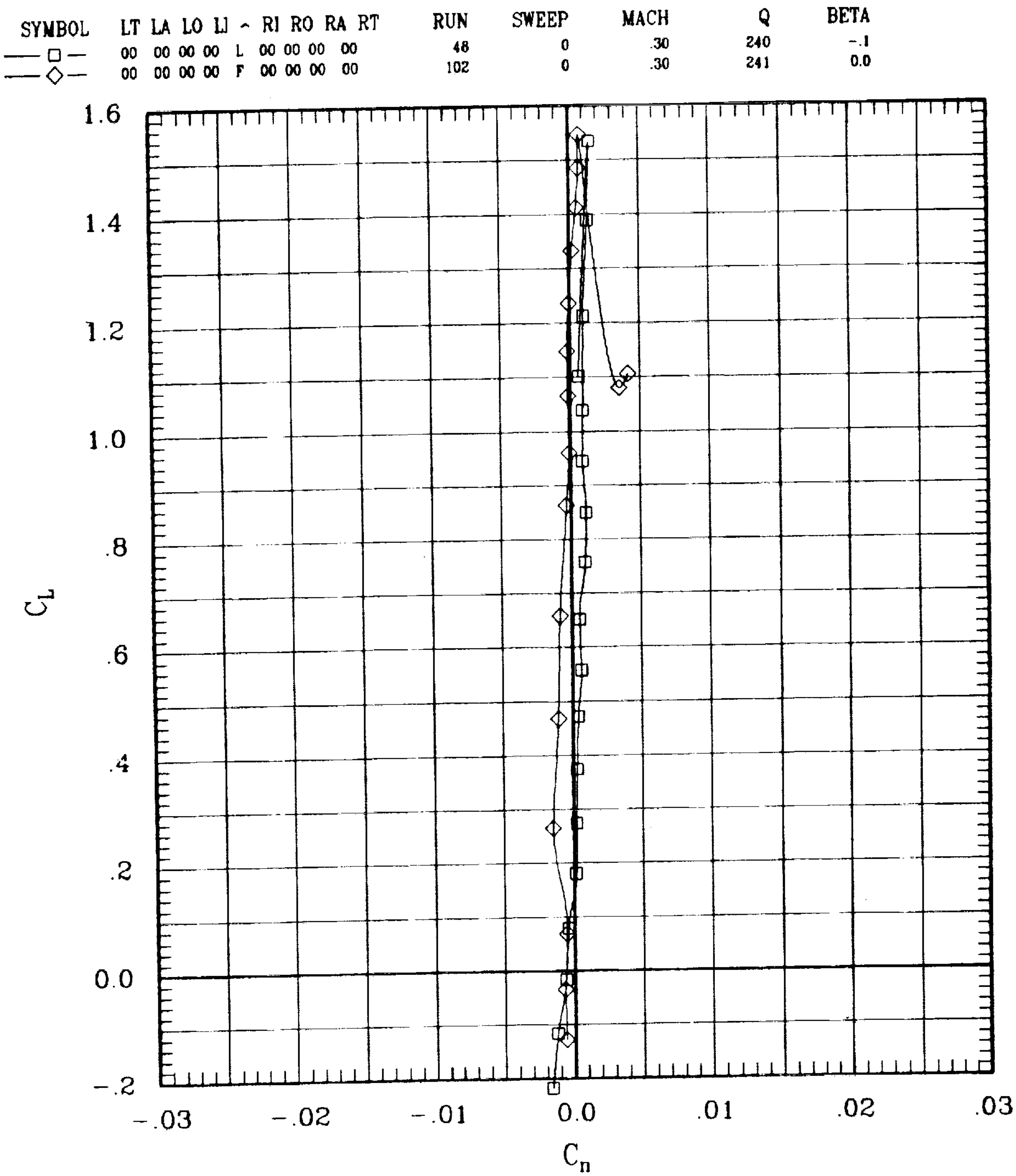

Figure 6(a). Effect of pivot height for sweep = 0 deg.

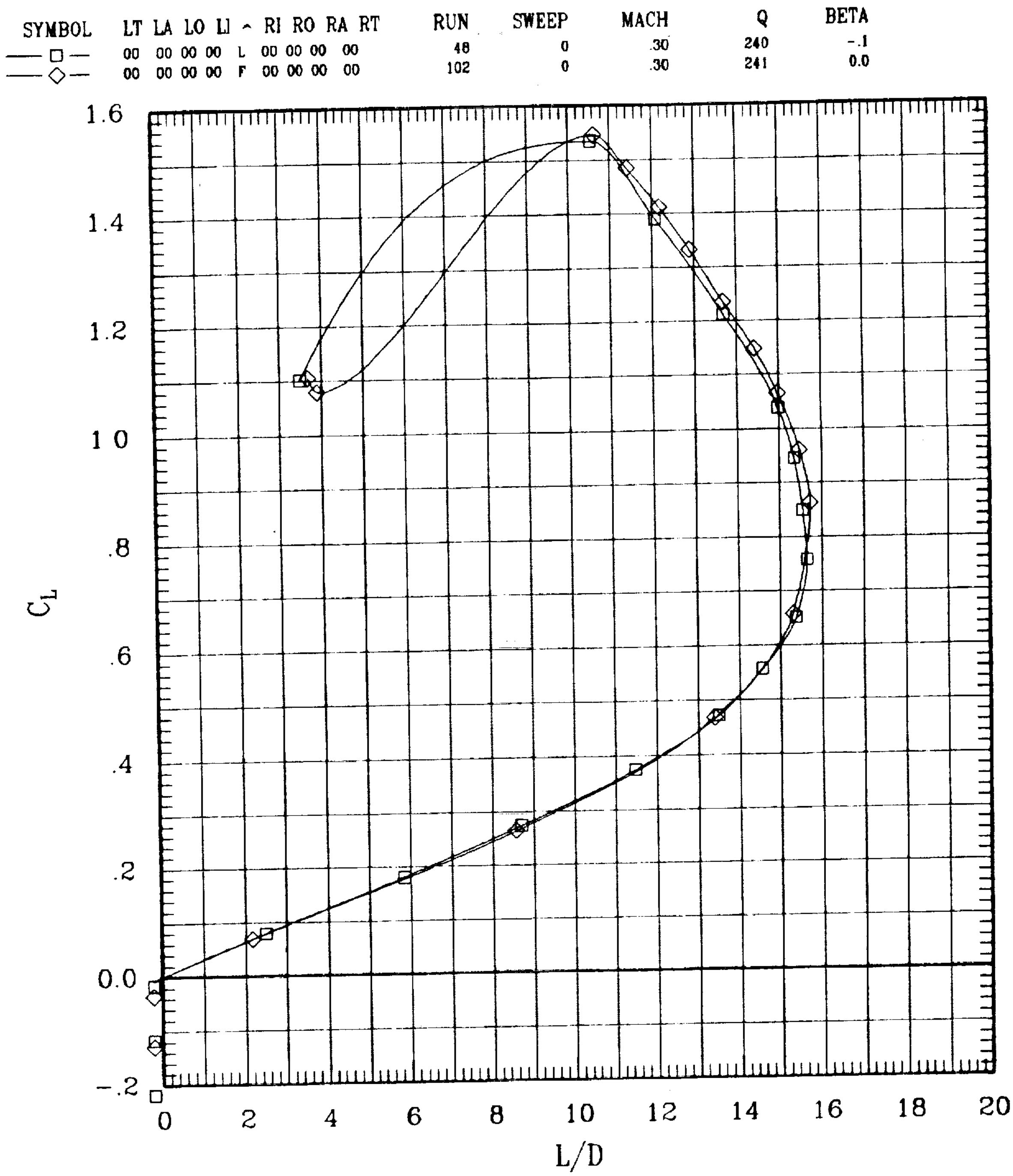

Figure 6(a). Effect of pivot height for sweep = 0 deg.

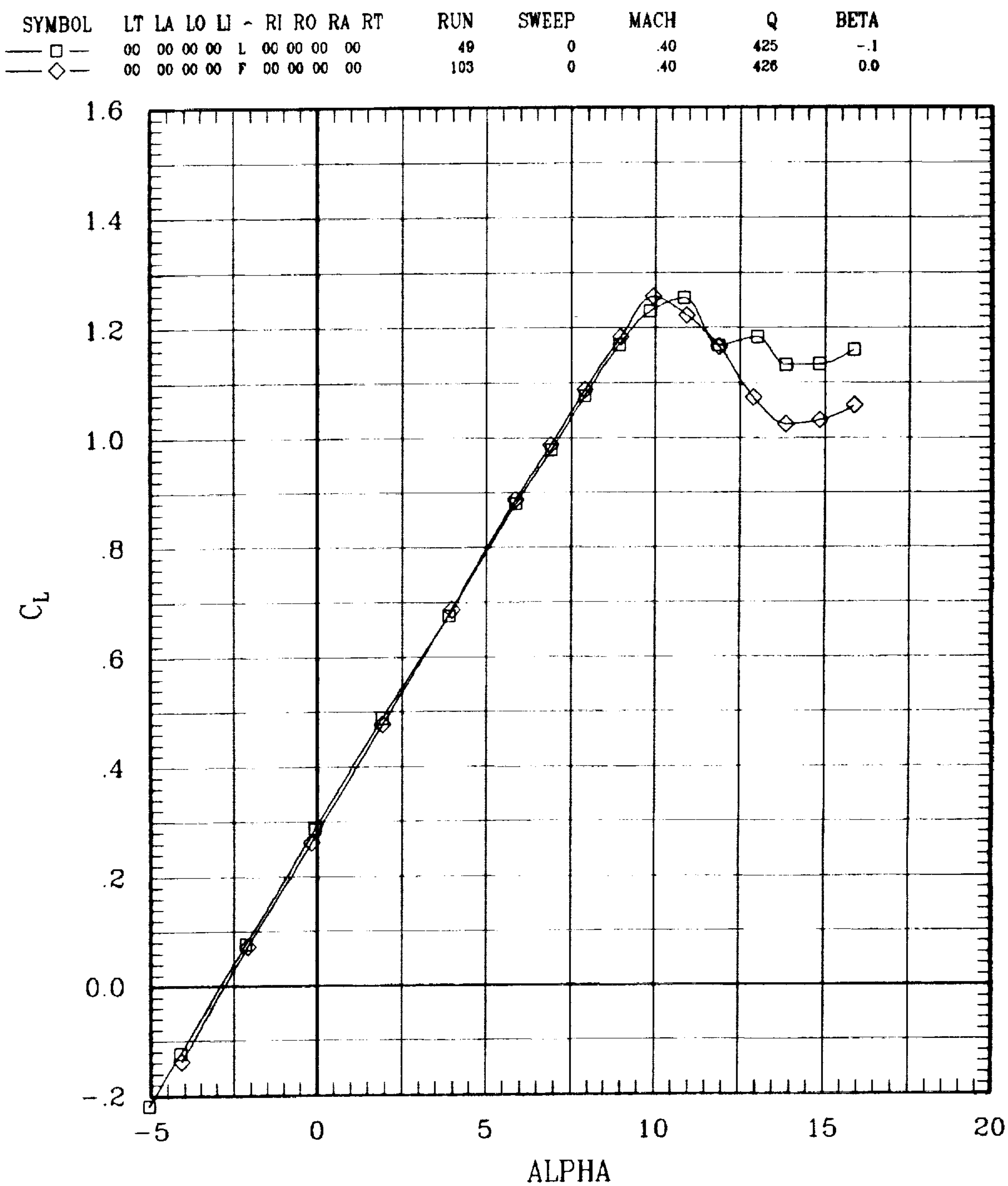

Figure 6(a). Effect of pivot height for sweep = 0 deg.

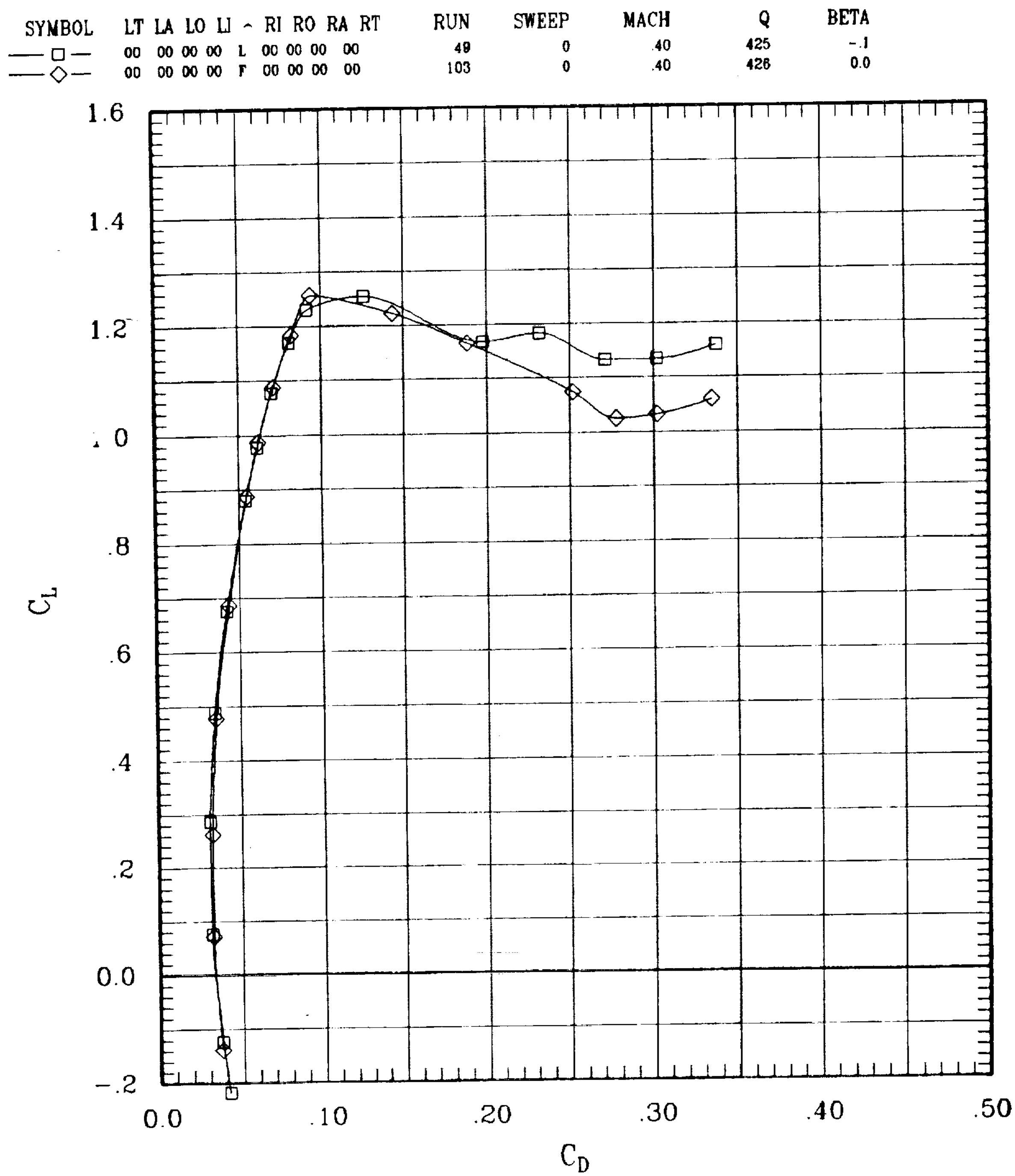

Figure 6(a). Effect of pivot height for sweep = 0 deg.

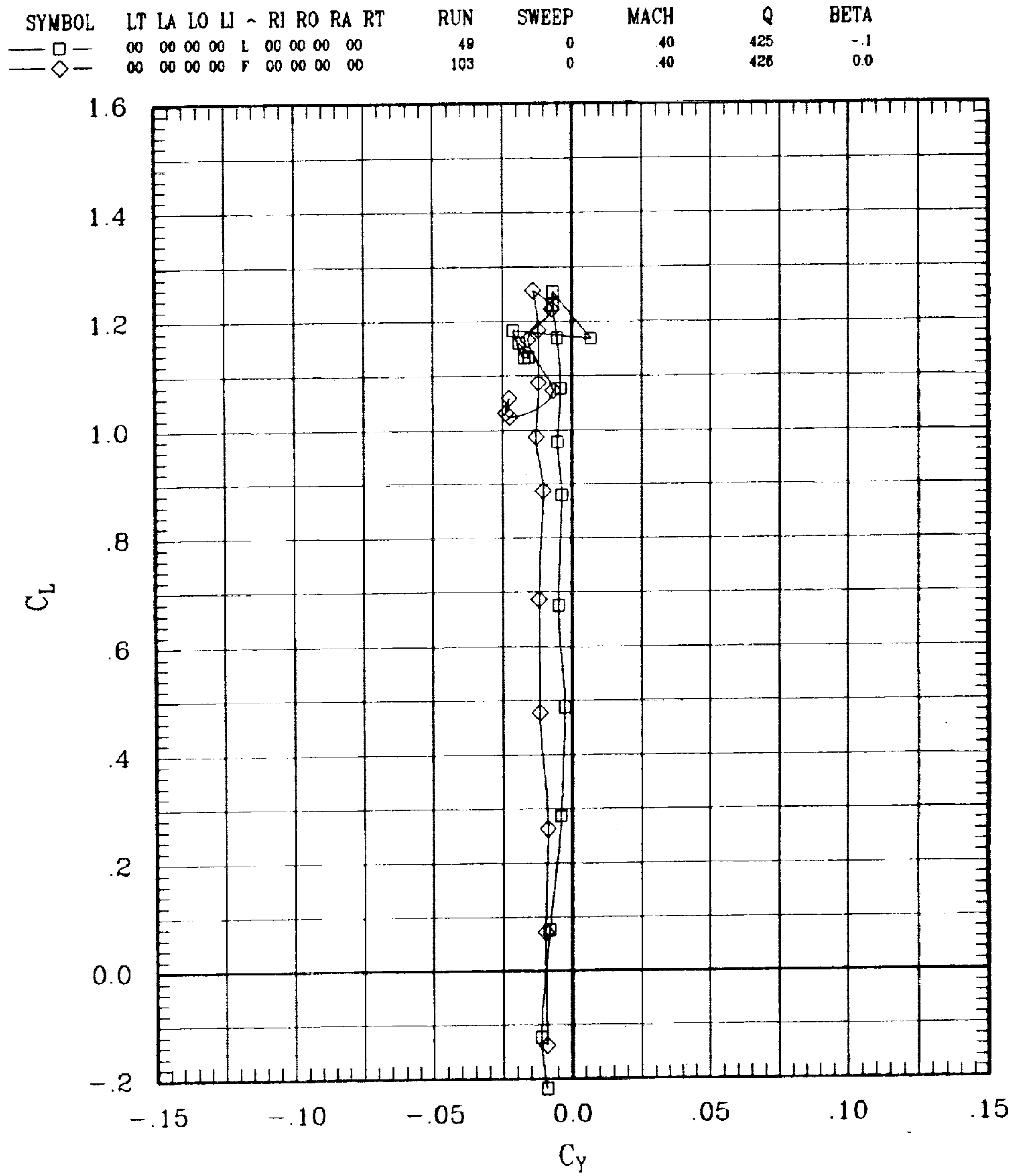

Figure 6(a). Effect of pivot height for sweep = 0 deg.

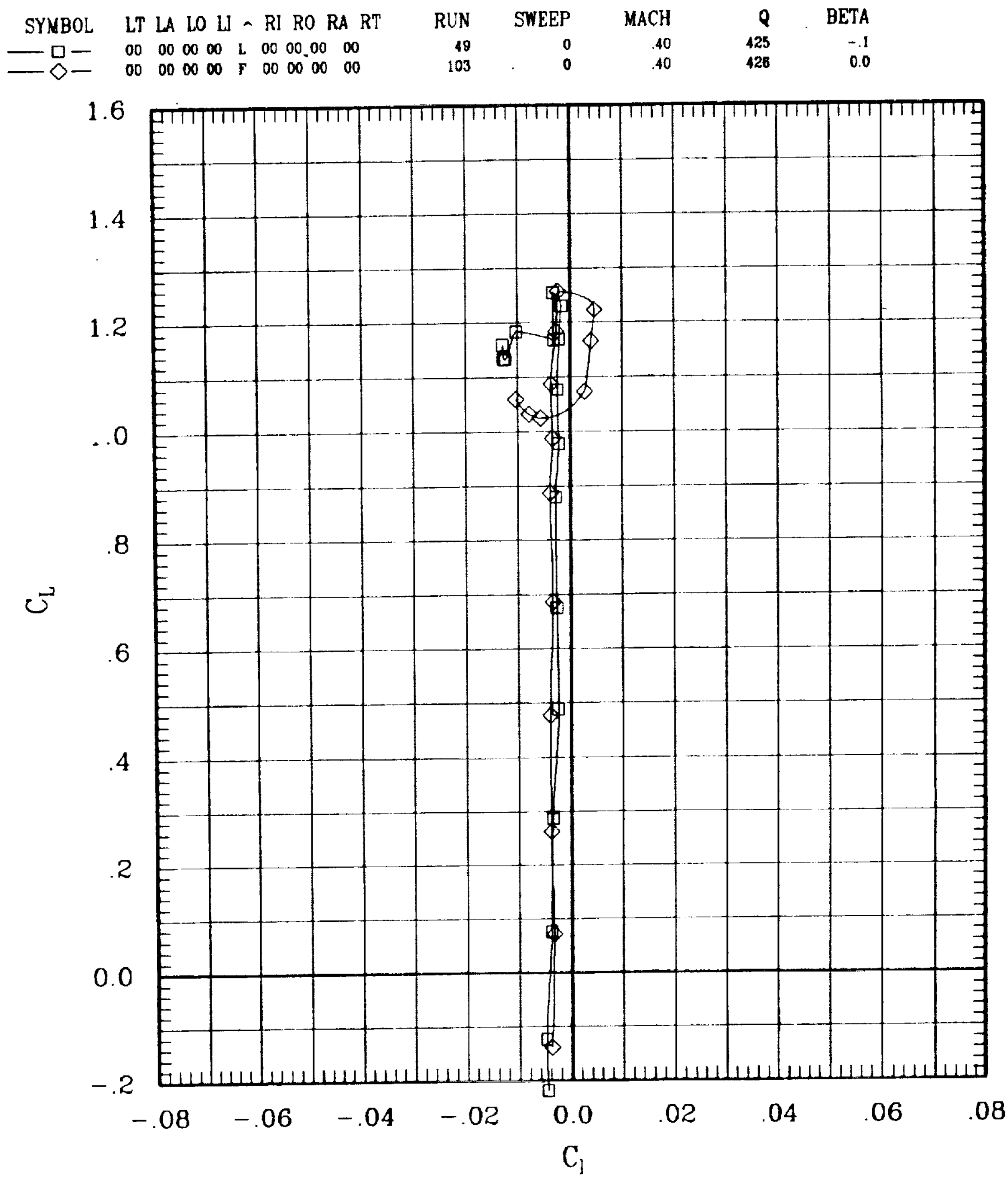

Figure 6(a). Effect of pivot height for sweep = 0 deg.

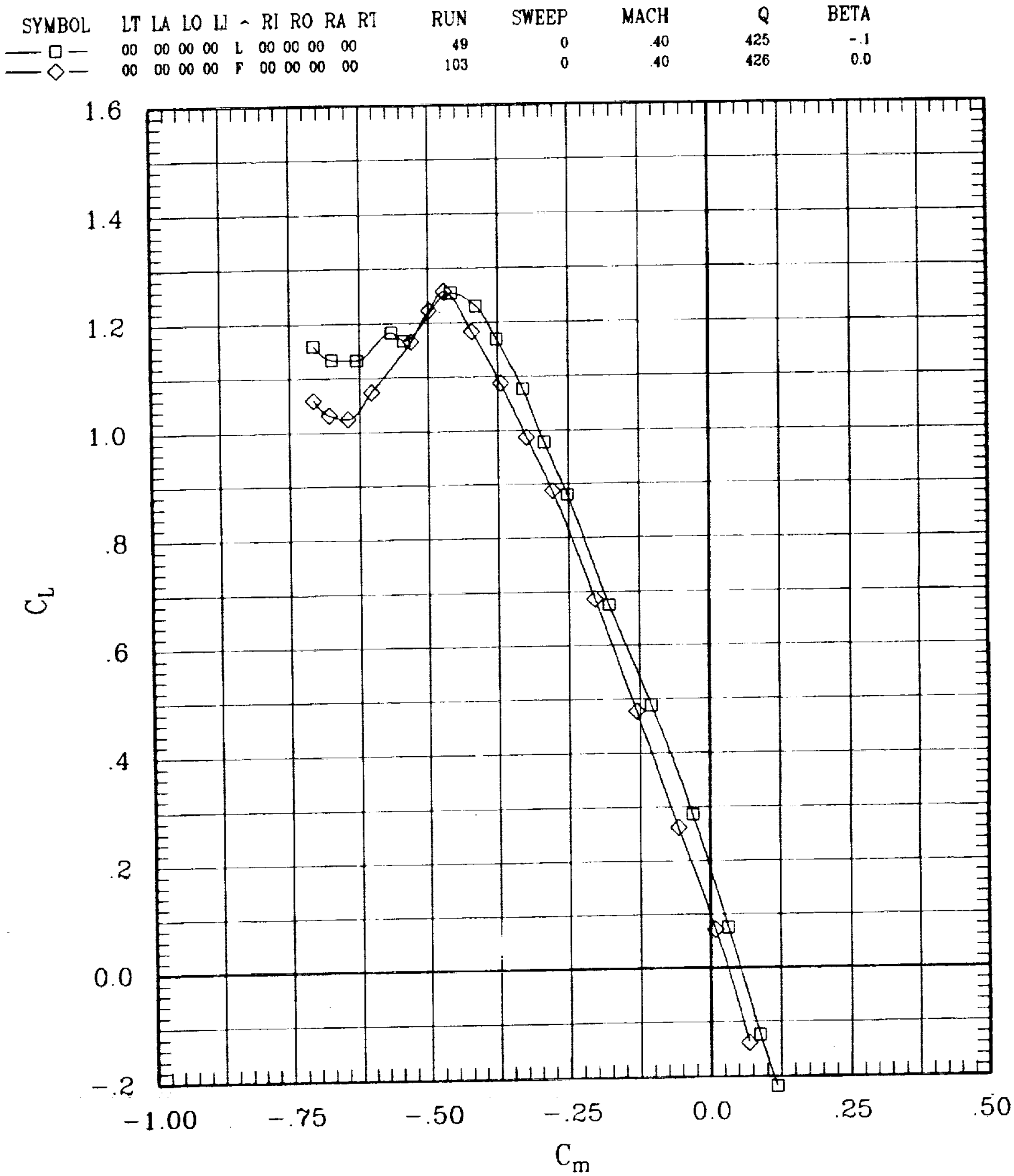

Figure 6(a). Effect of pivot height for sweep = 0 deg.

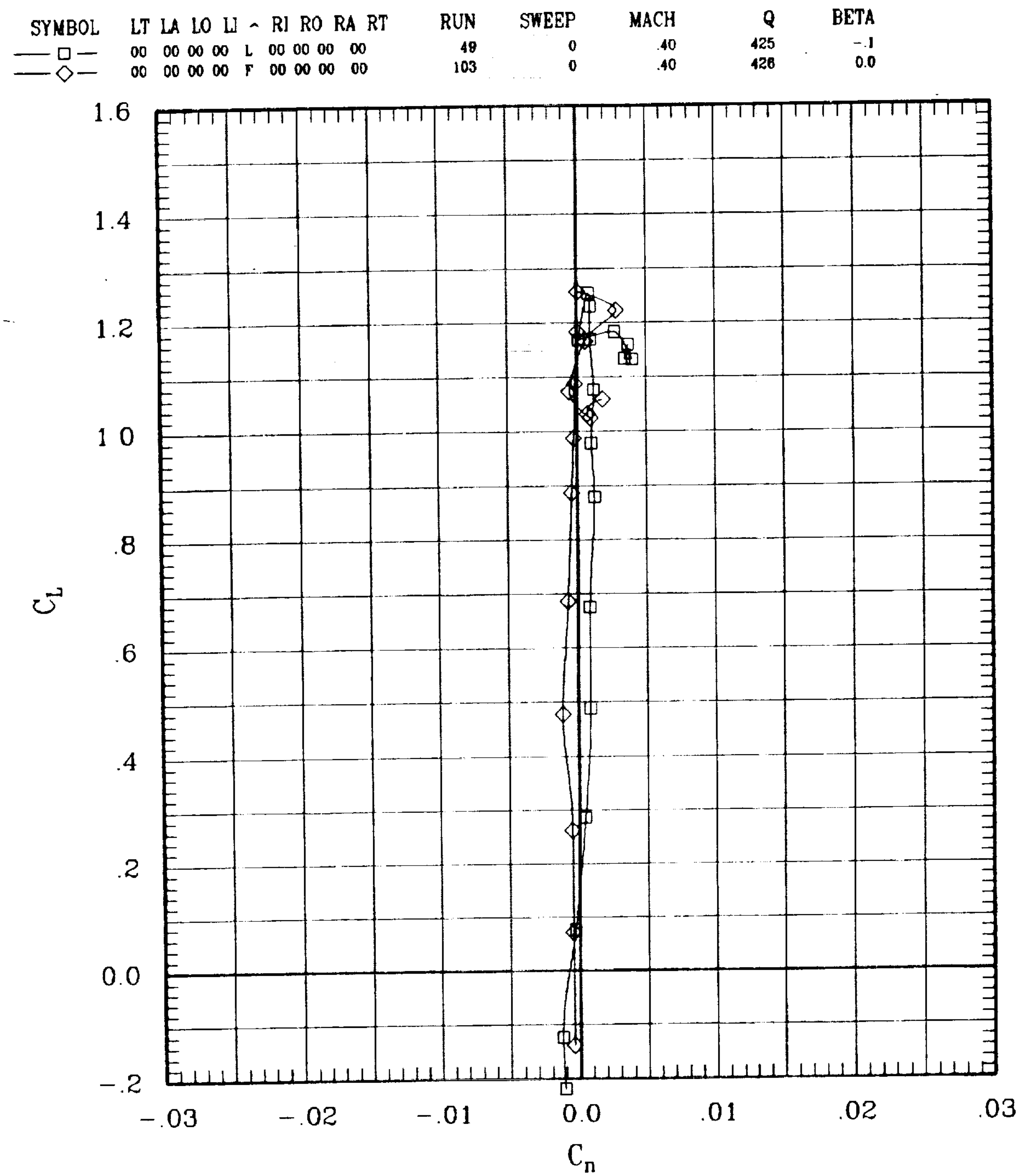

Figure 6(a). Effect of pivot height for sweep = 0 deg.

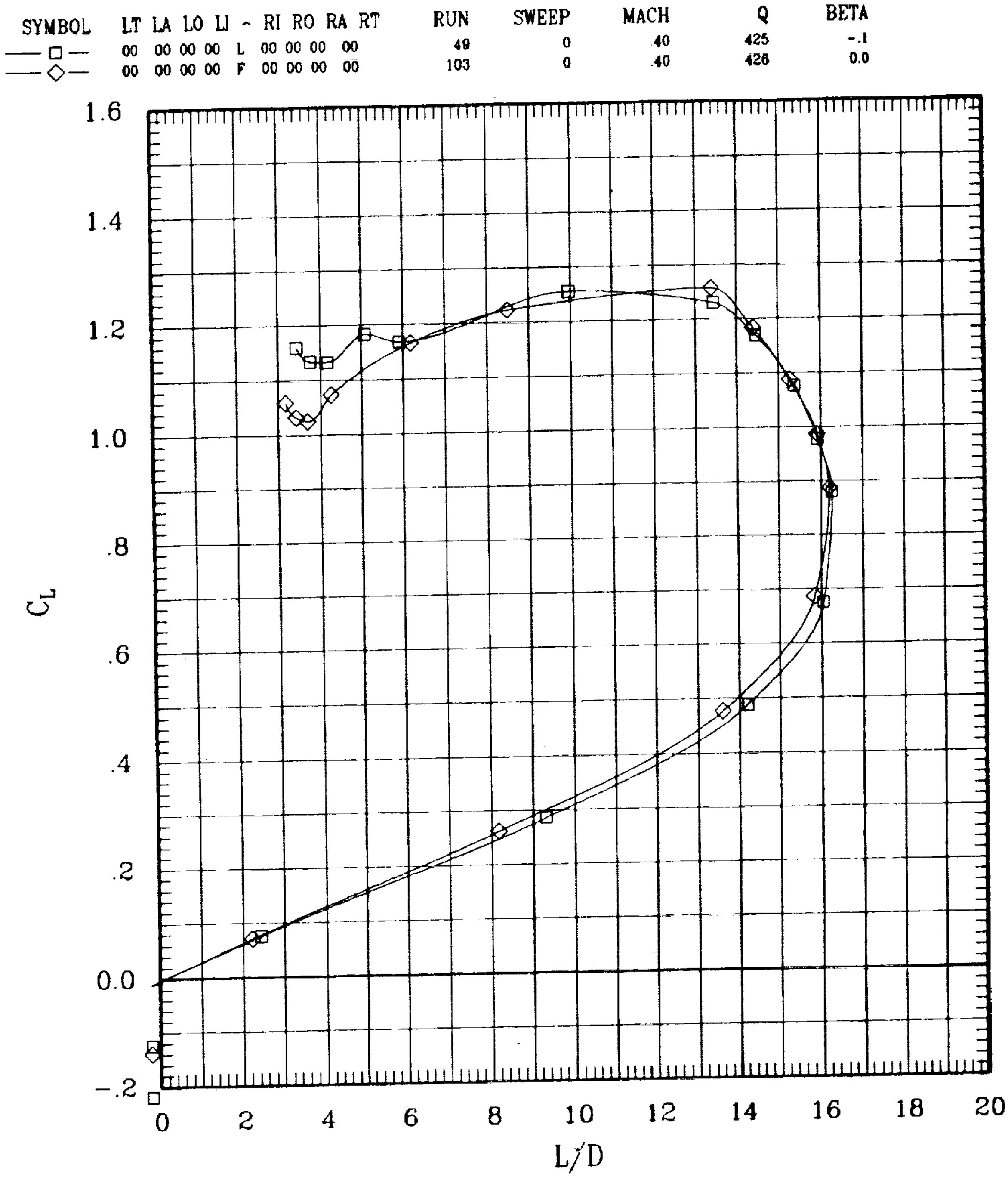

Figure 6(a). Effect of pivot height for sweep = 0 deg.

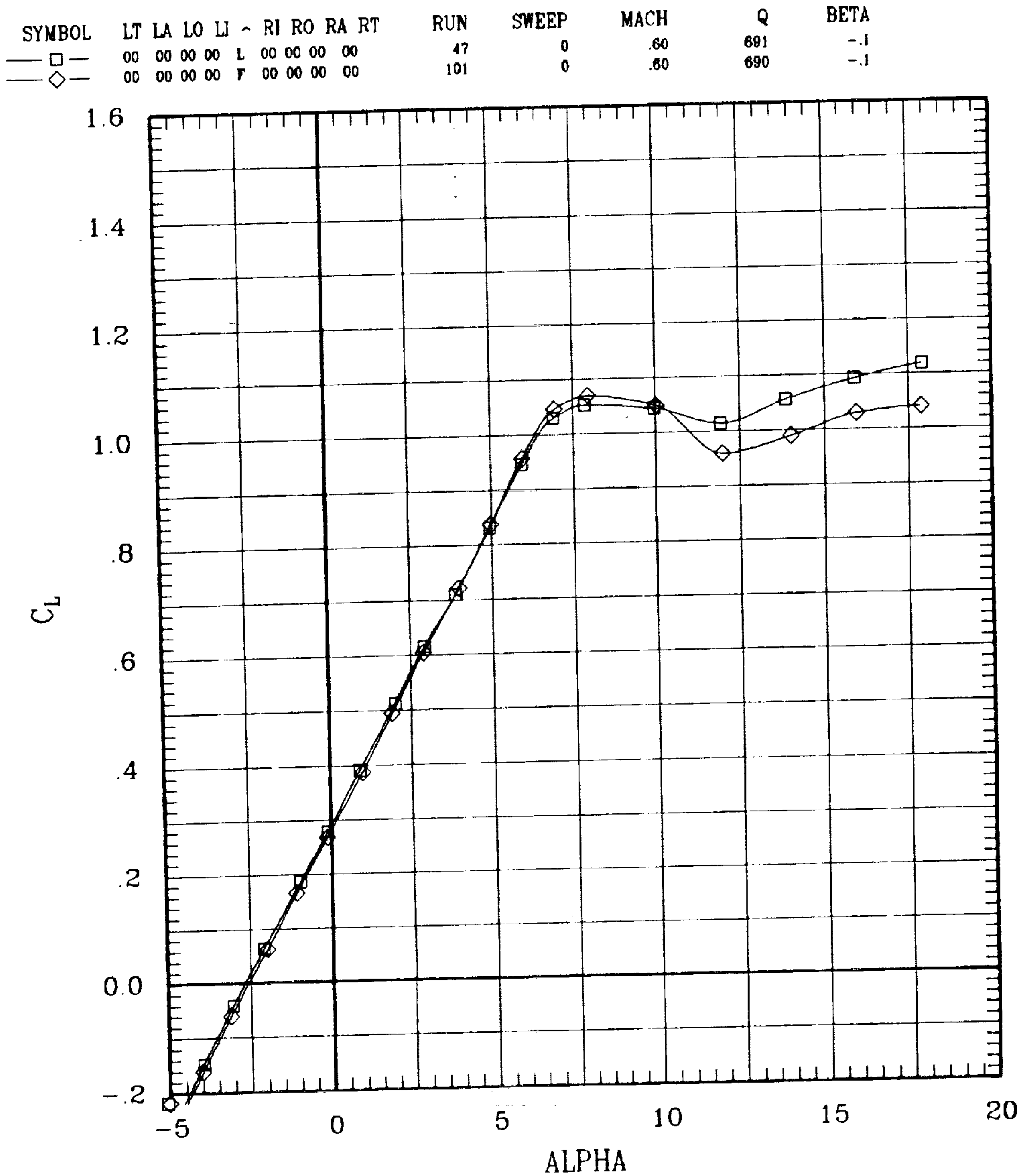

Figure 6(a). Effect of pivot height for sweep = 0 deg.

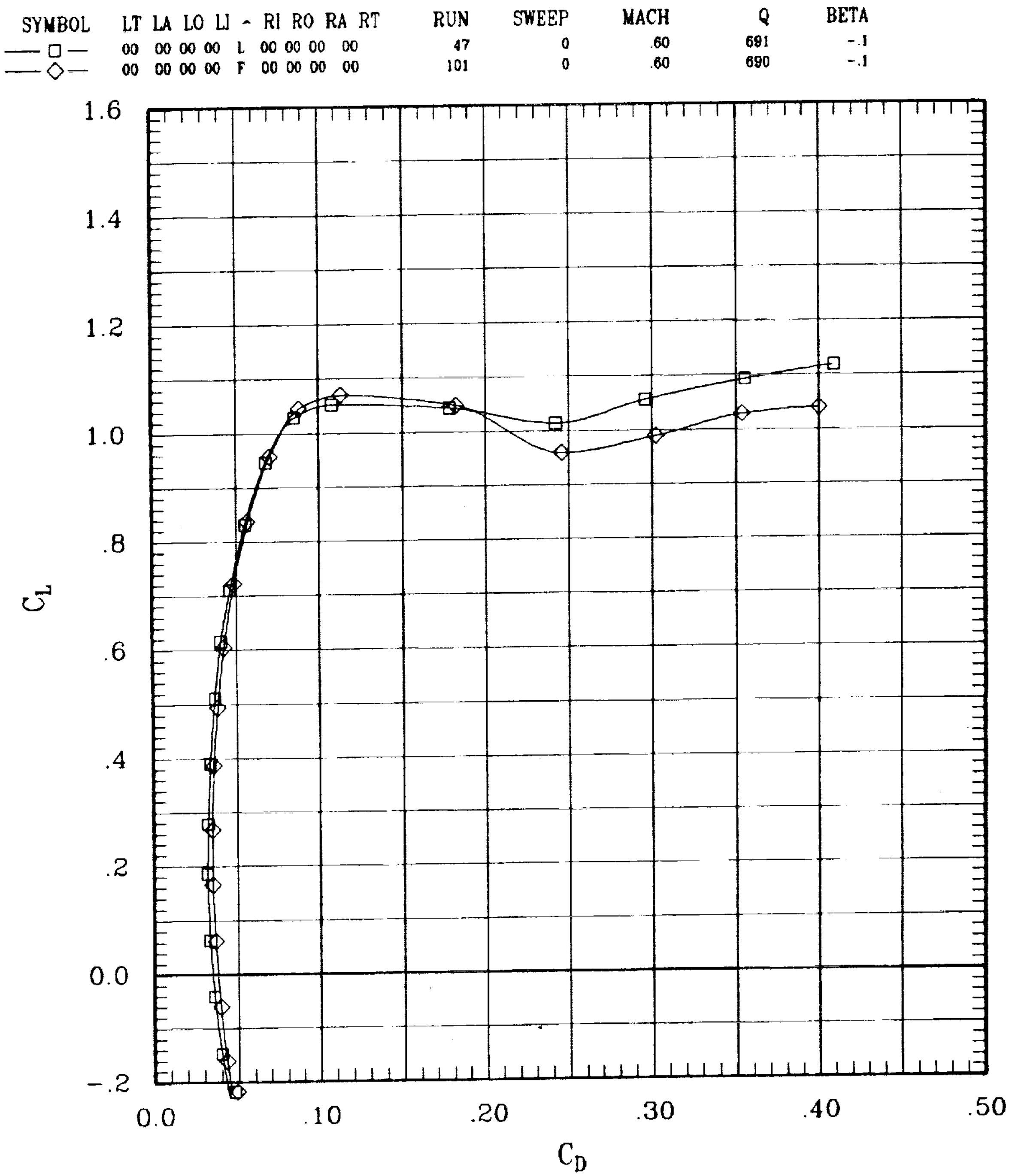

Figure 6(a). Effect of pivot height for sweep = 0 deg.

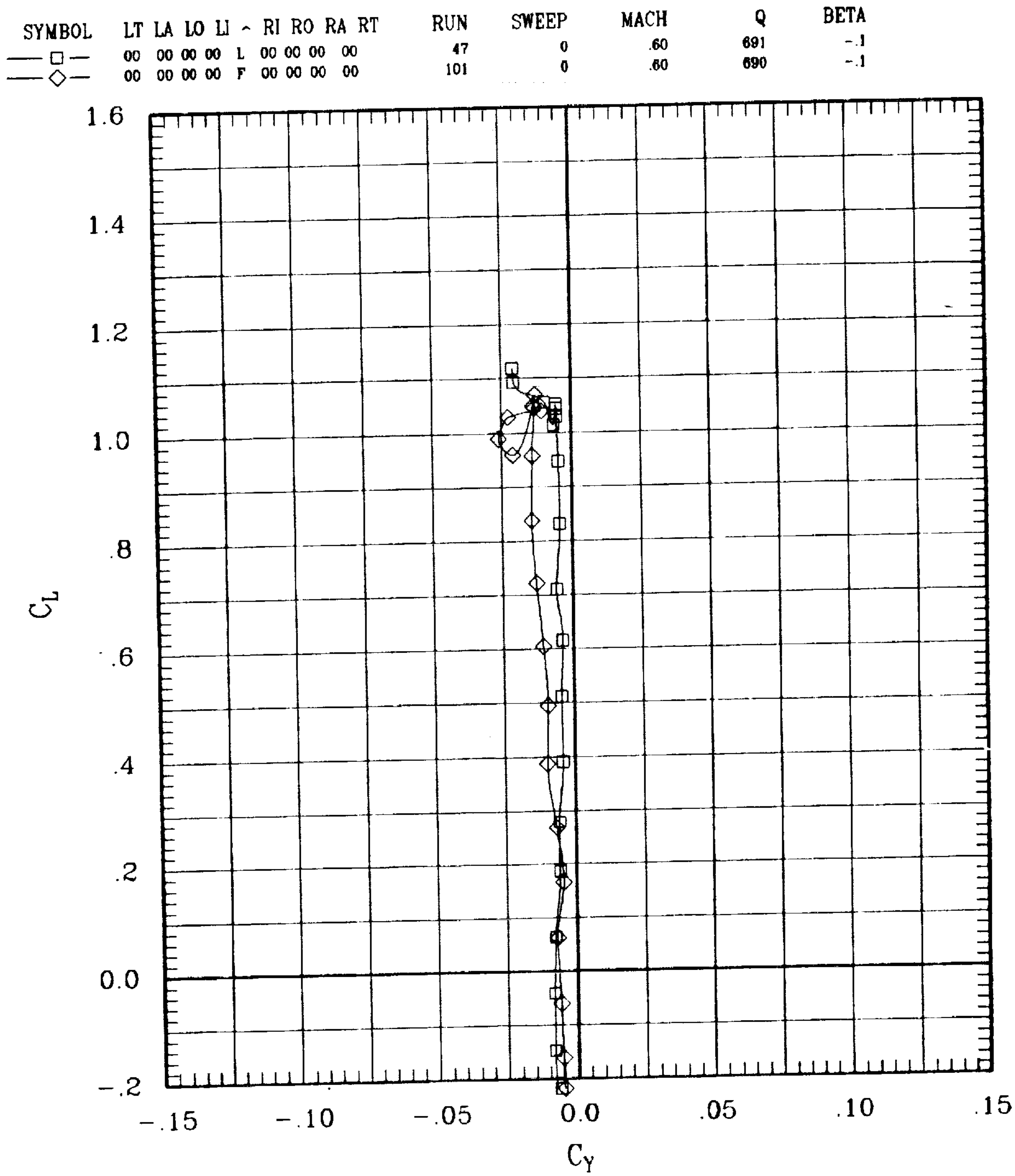

Figure 6(a). Effect of pivot height for sweep = 0 deg.

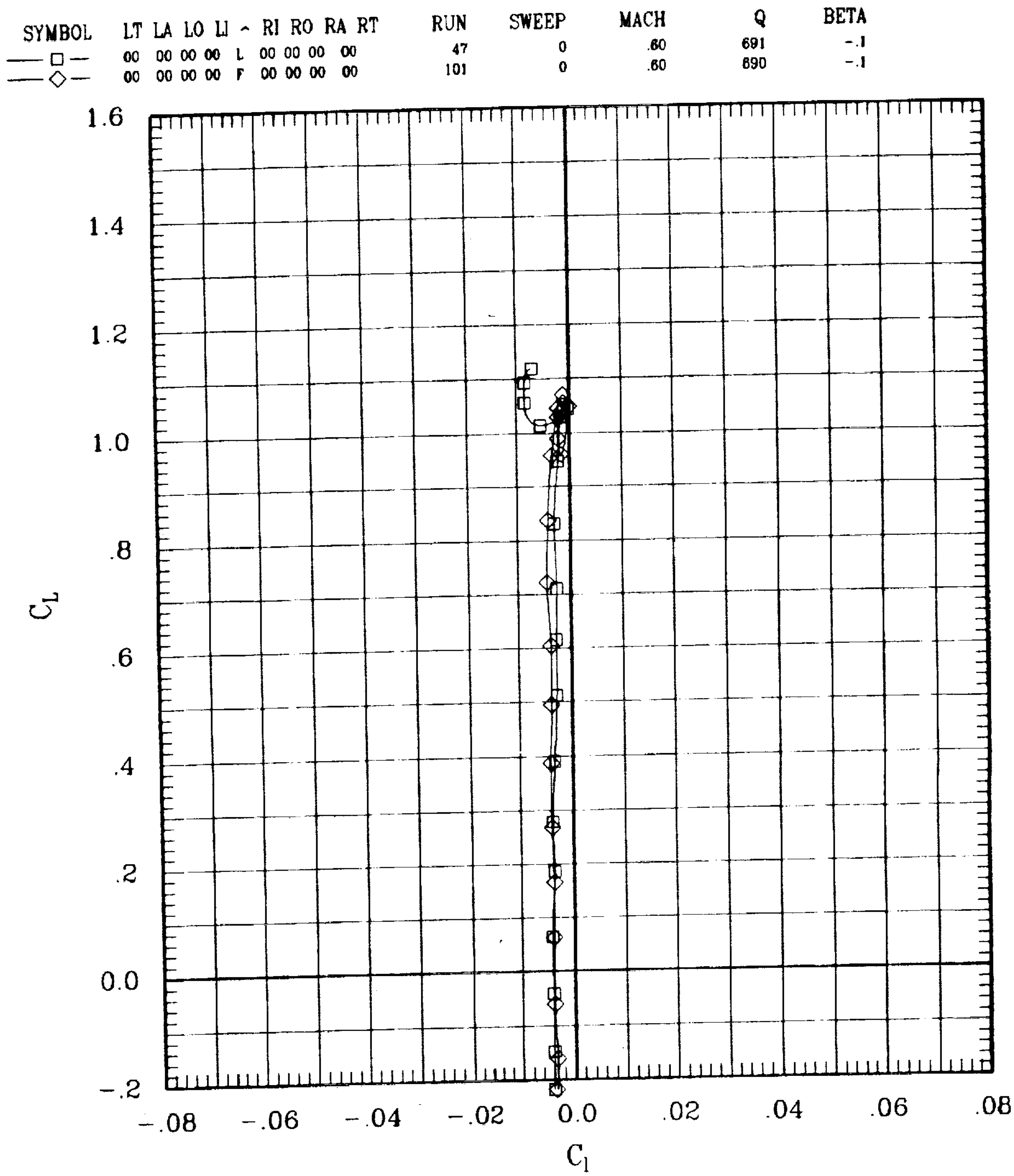

Figure 6(a). Effect of pivot height for sweep = 0 deg.

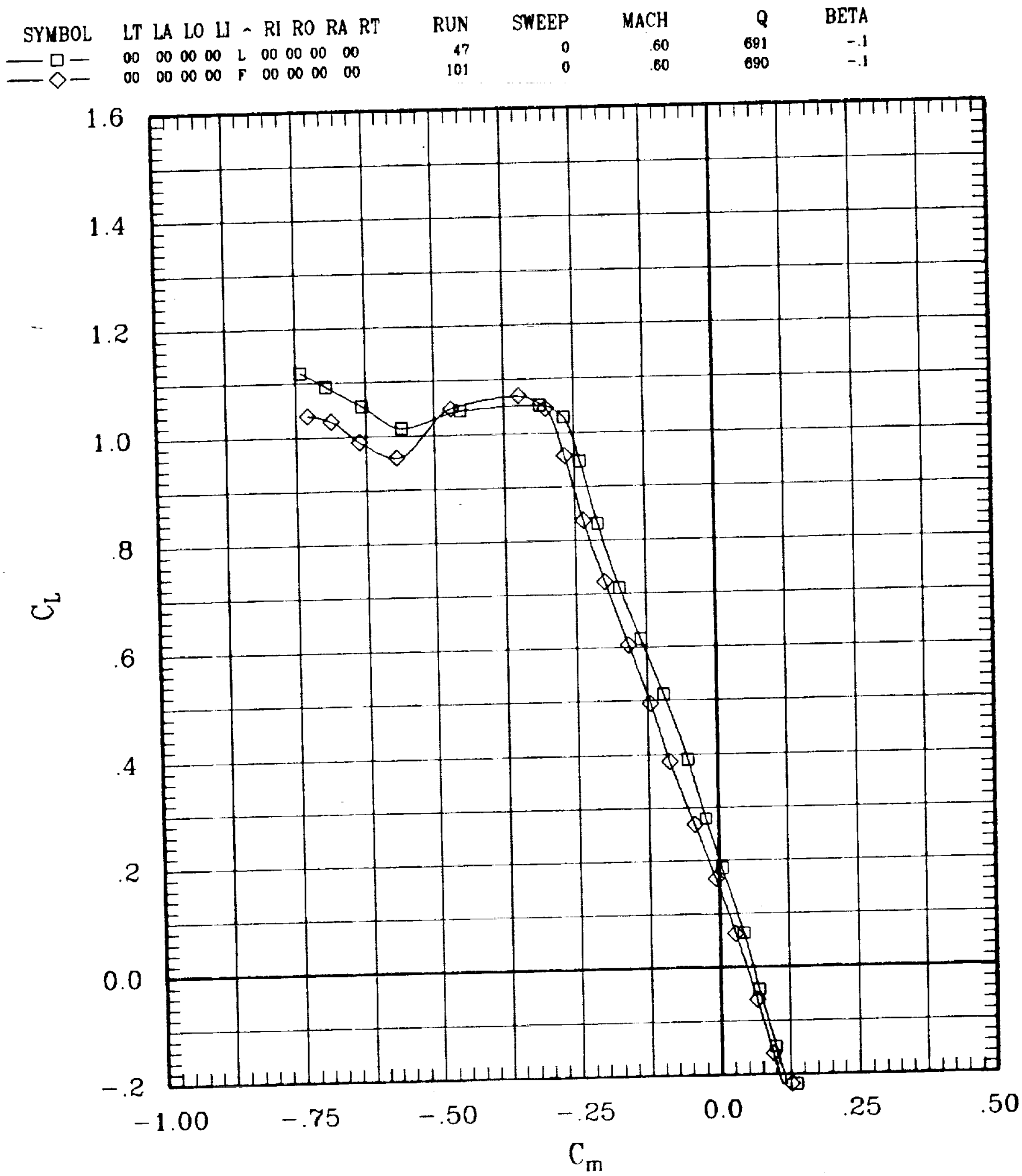

Figure 6(a). Effect of pivot height for sweep = 0 deg.

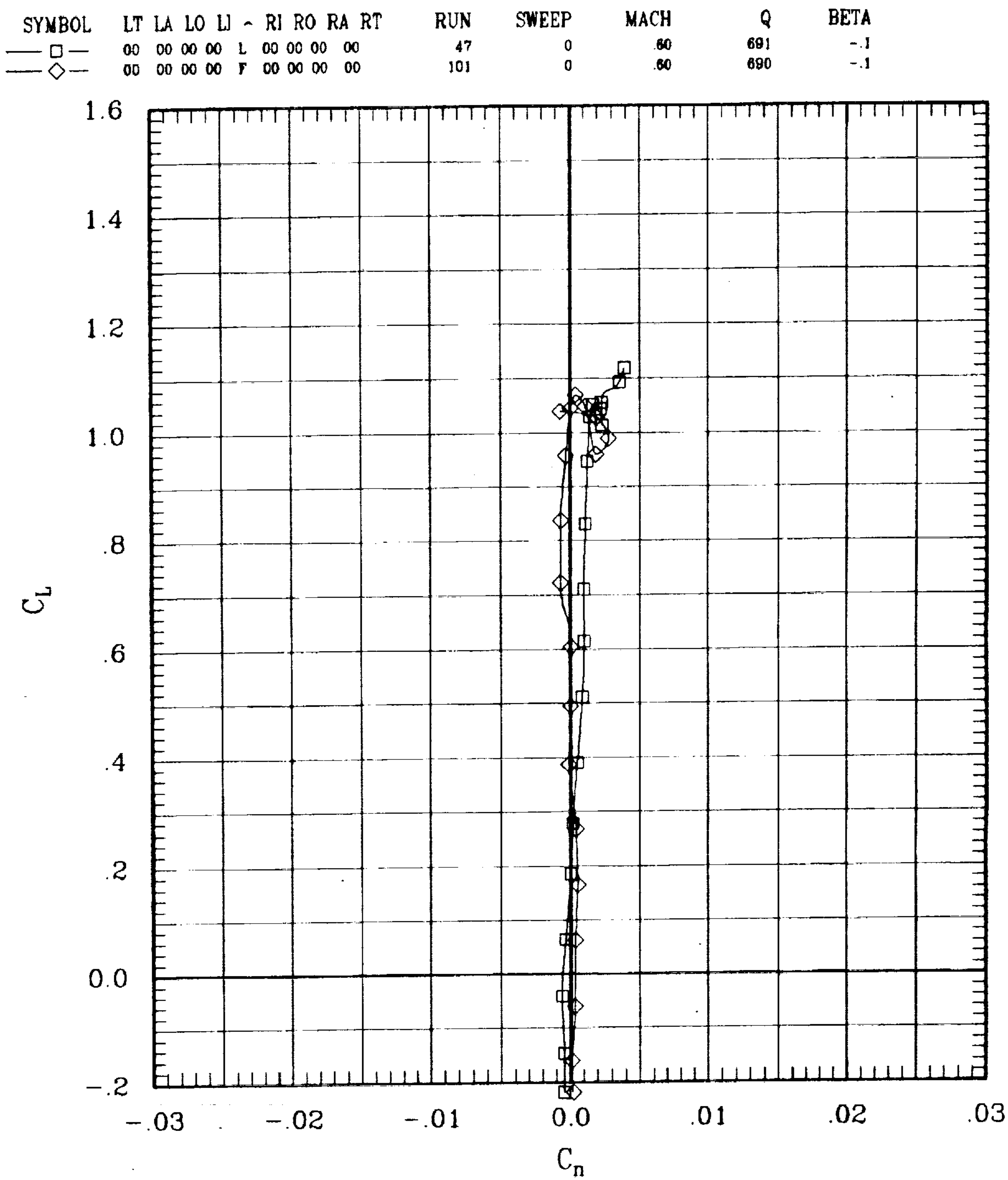

Figure 6(a). Effect of pivot height for sweep = 0 deg.

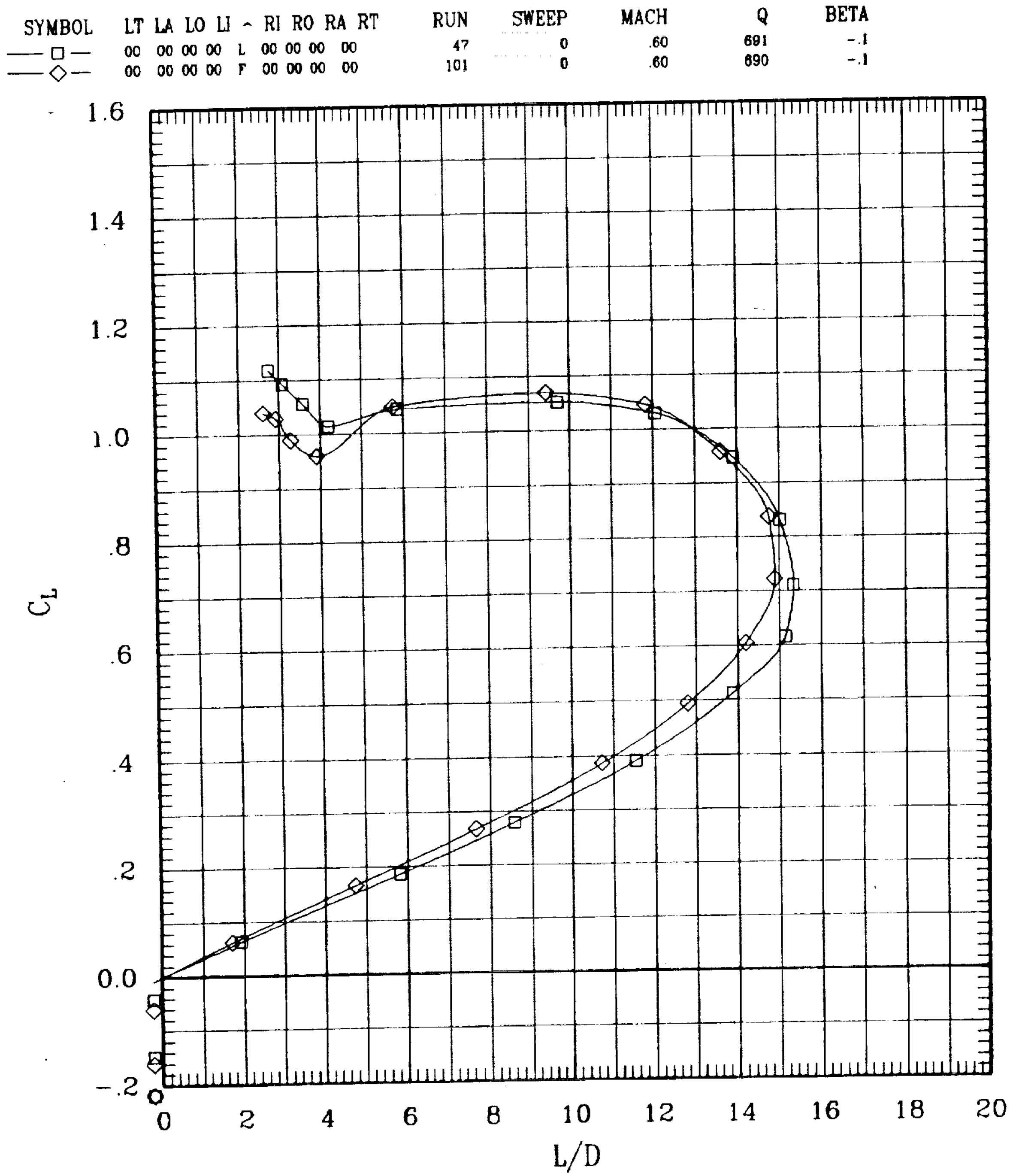

Figure 6(a). Effect of pivot height for sweep = 0 deg.

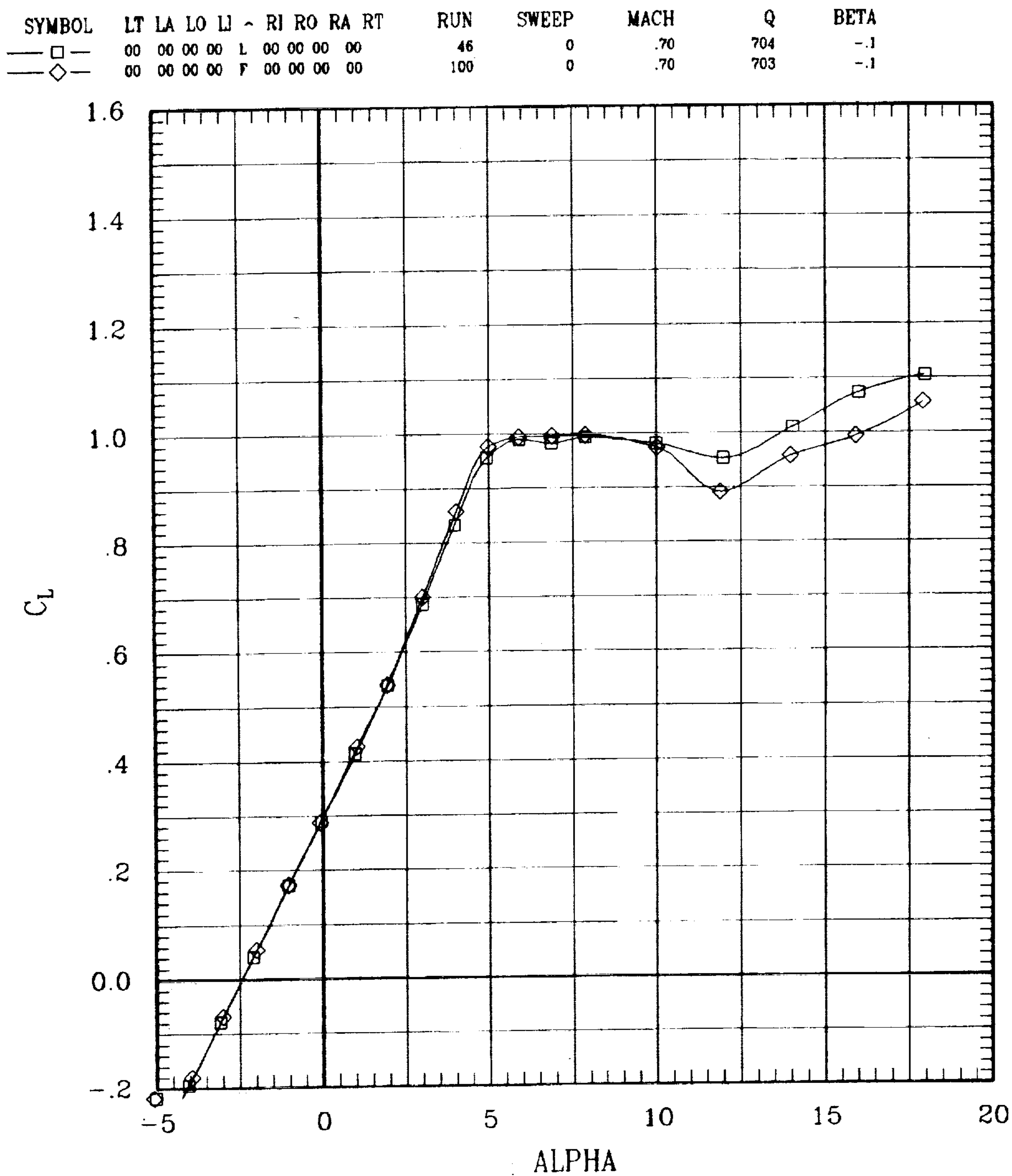

Figure 6(a). Effect of pivot height for sweep = 0 deg.

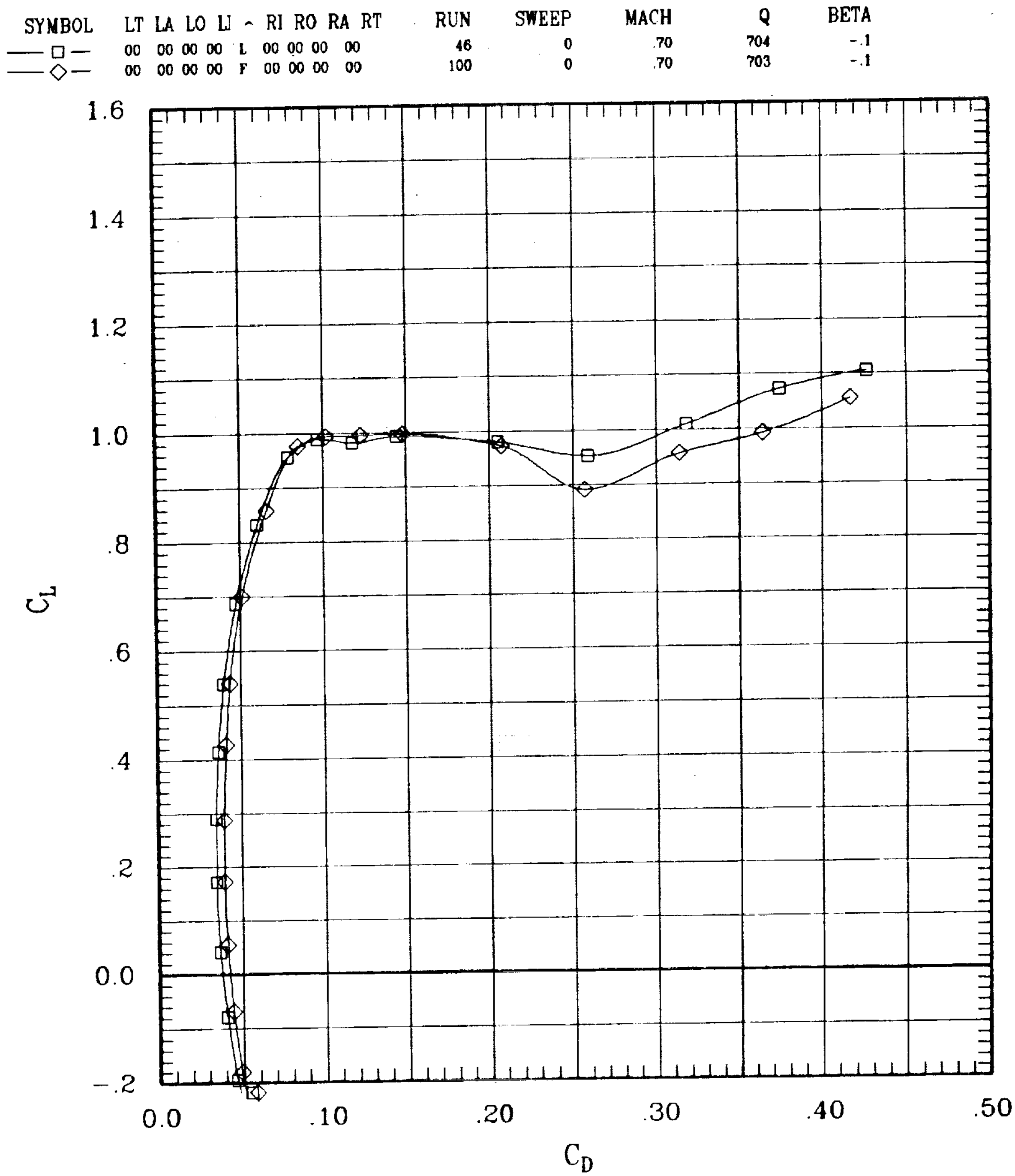

Figure 6(a). Effect of pivot height for sweep = 0 deg.

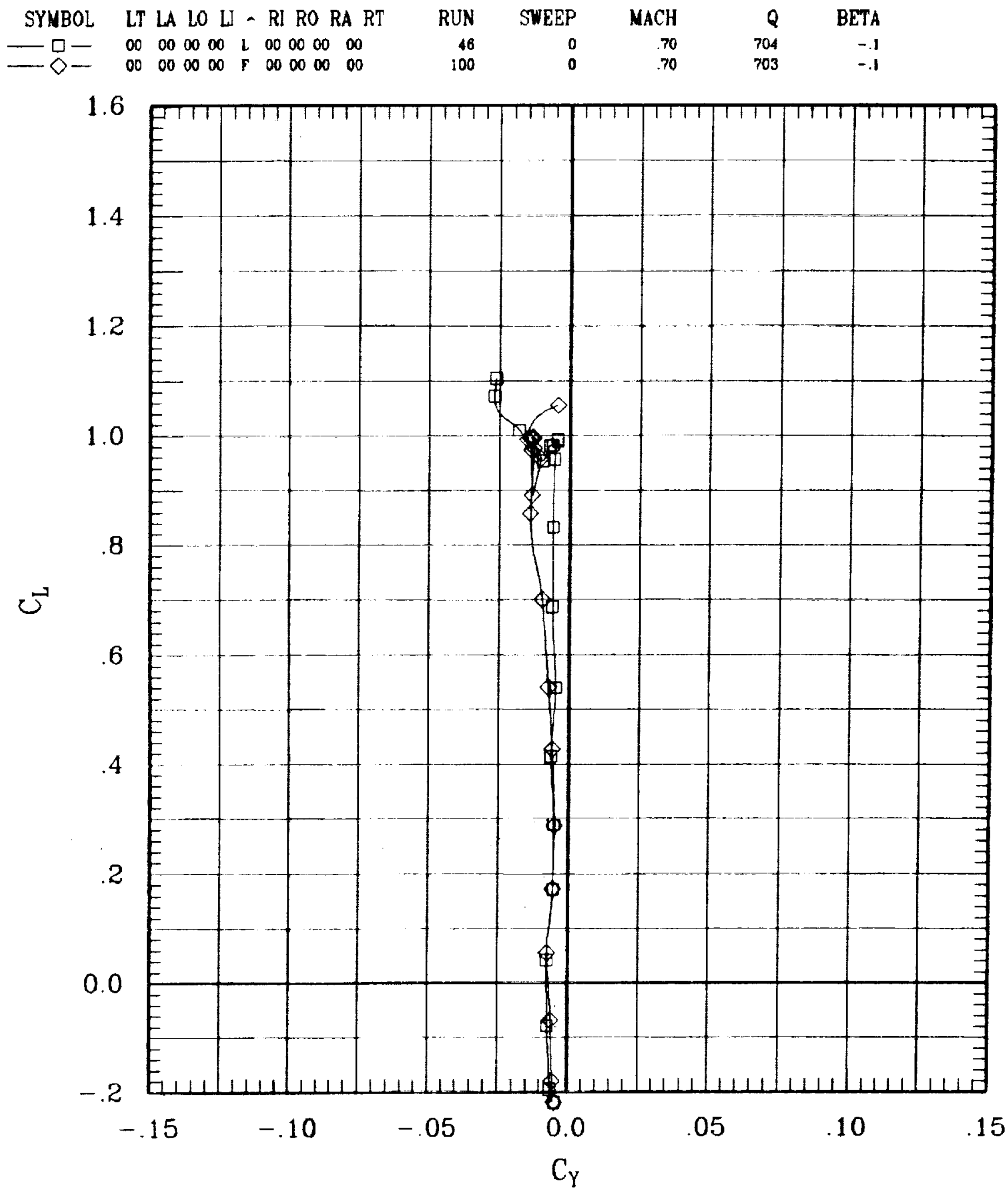

Figure 6(a). Effect of pivot height for sweep = 0 deg.

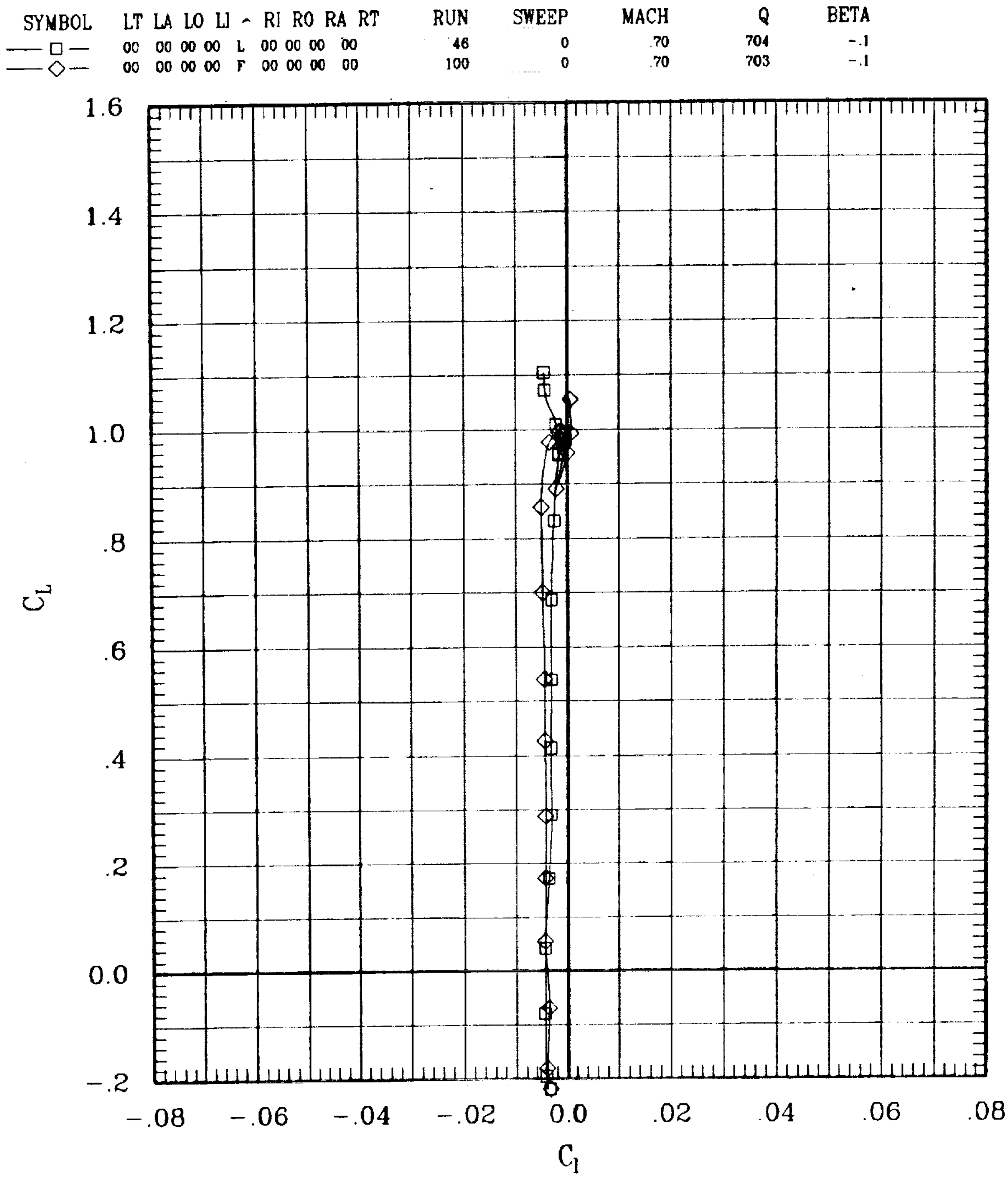

Figure 6(a). Effect of pivot height for sweep = 0 deg.

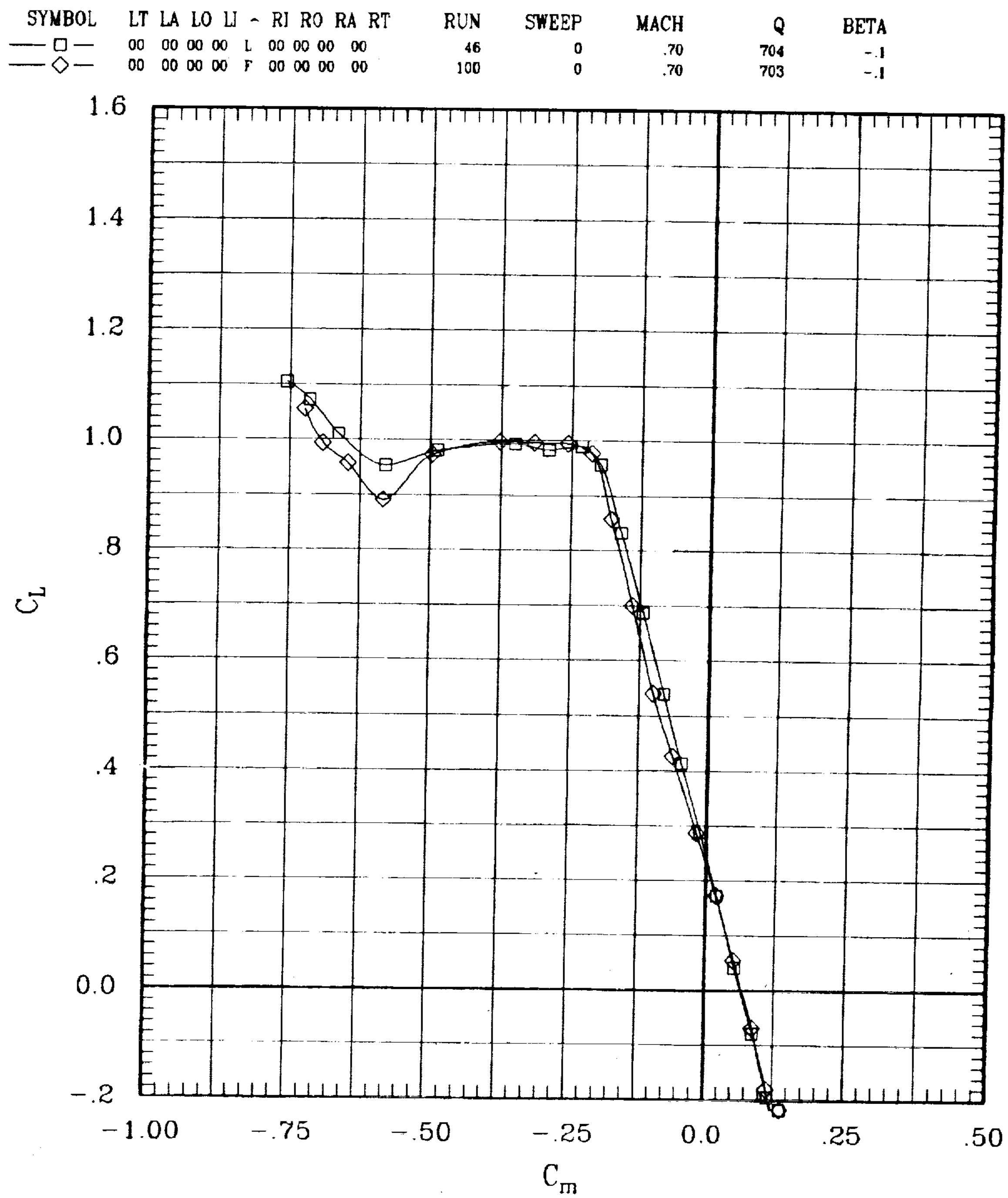

Figure 6(a). Effect of pivot height for sweep = 0 deg.

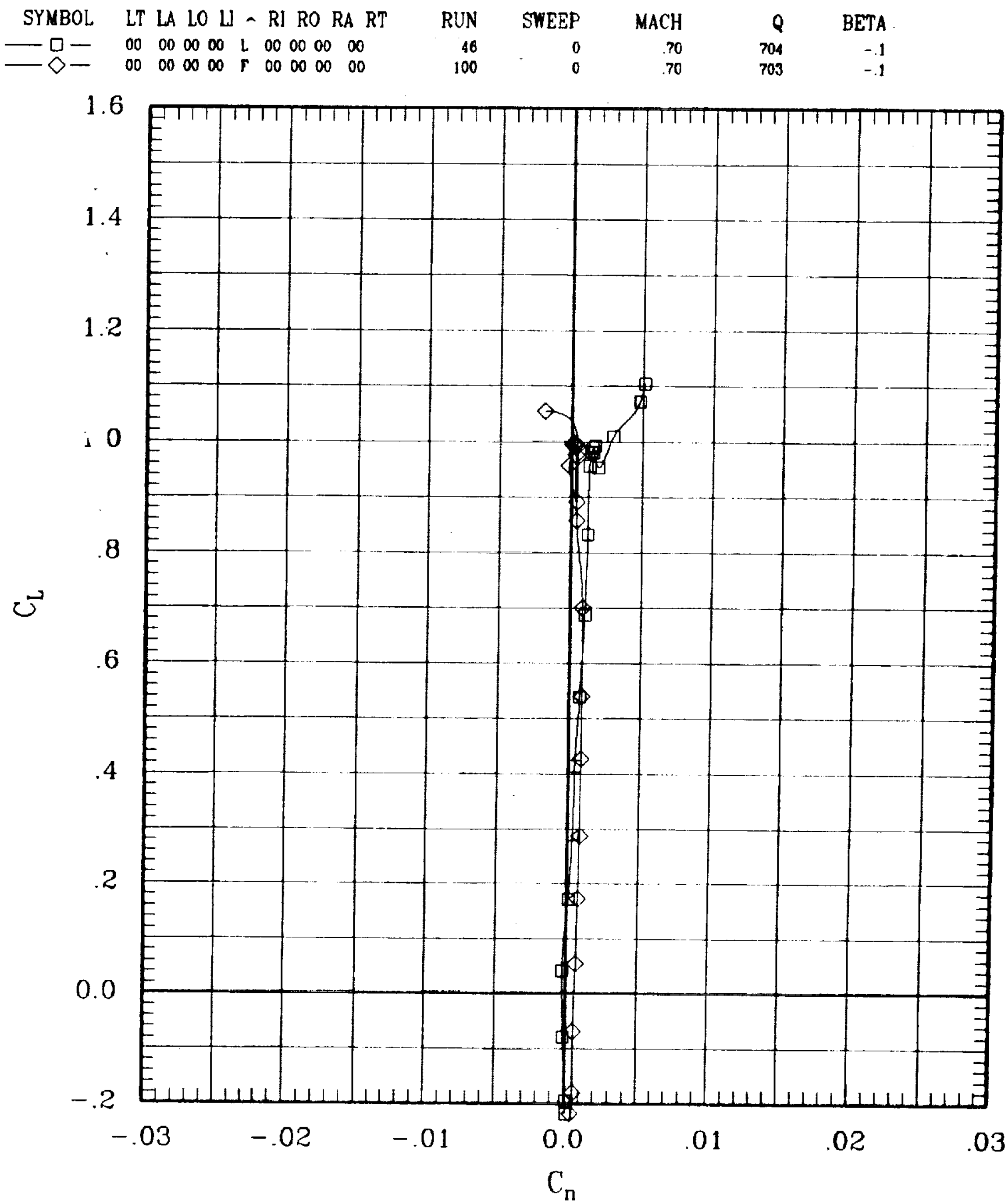

Figure 6(a). Effect of pivot height for sweep = 0 deg.

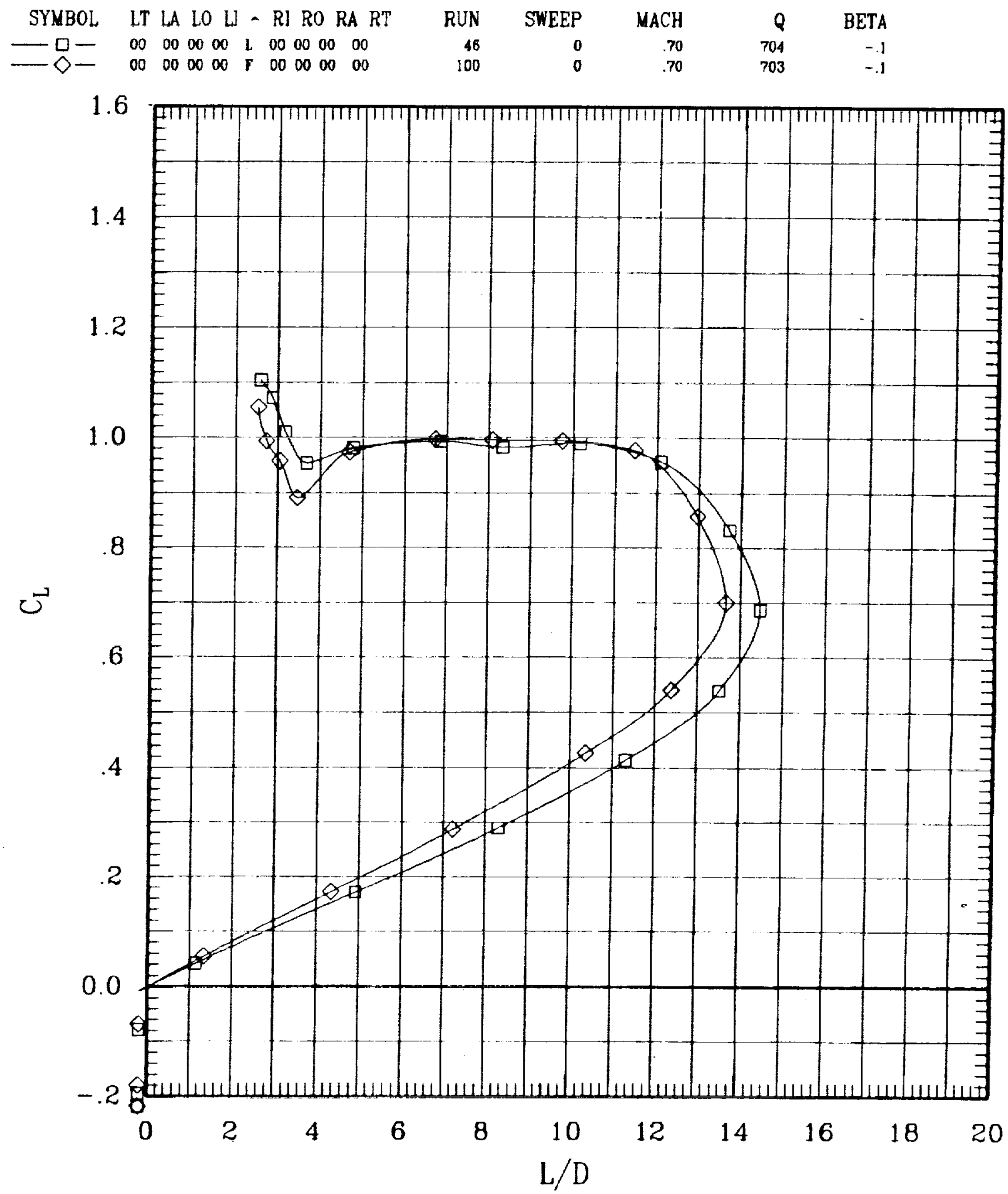

Figure 6(a). Effect of pivot height for sweep = 0 deg.

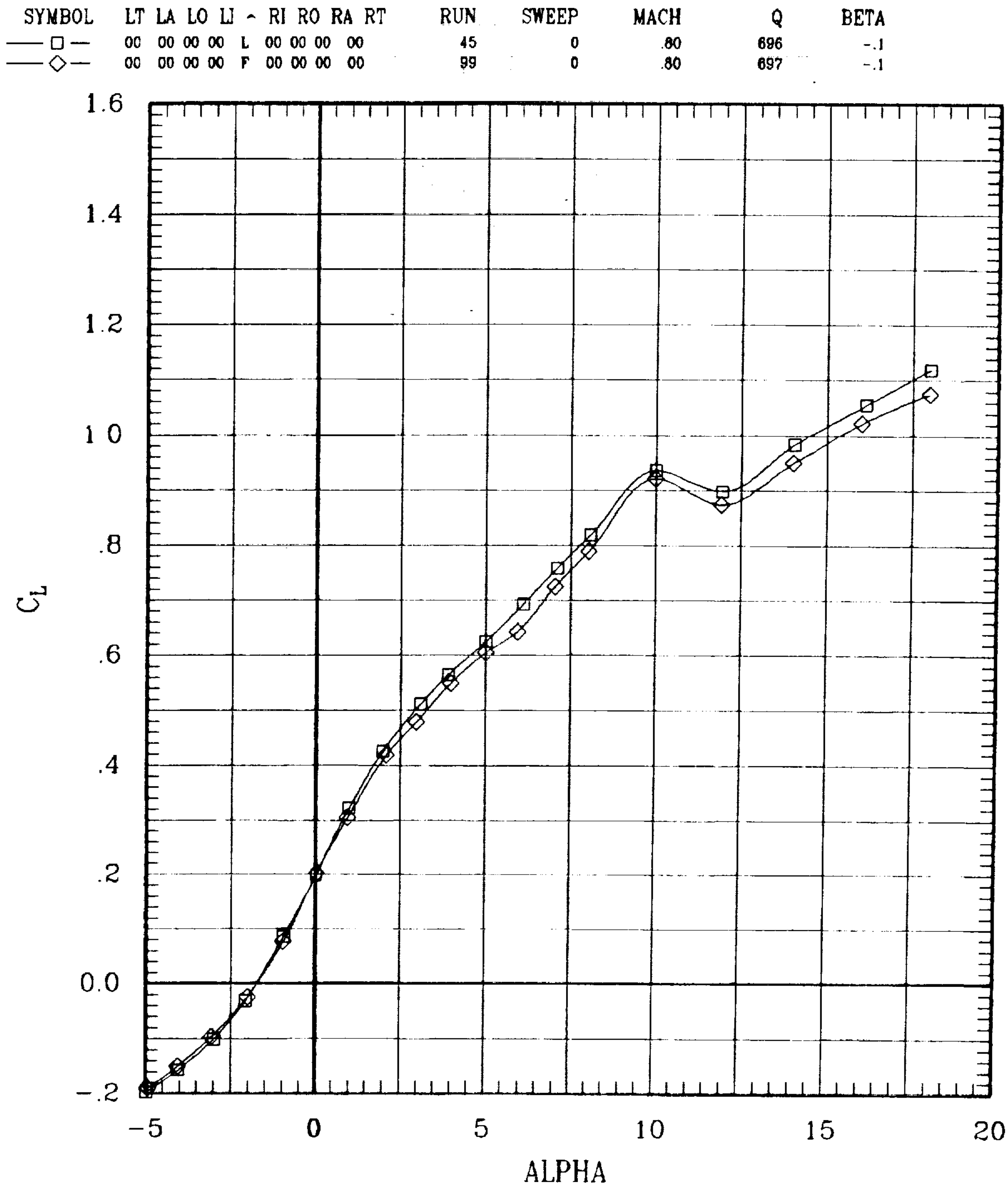

Figure 6(a). Effect of pivot height for sweep = 0 deg.

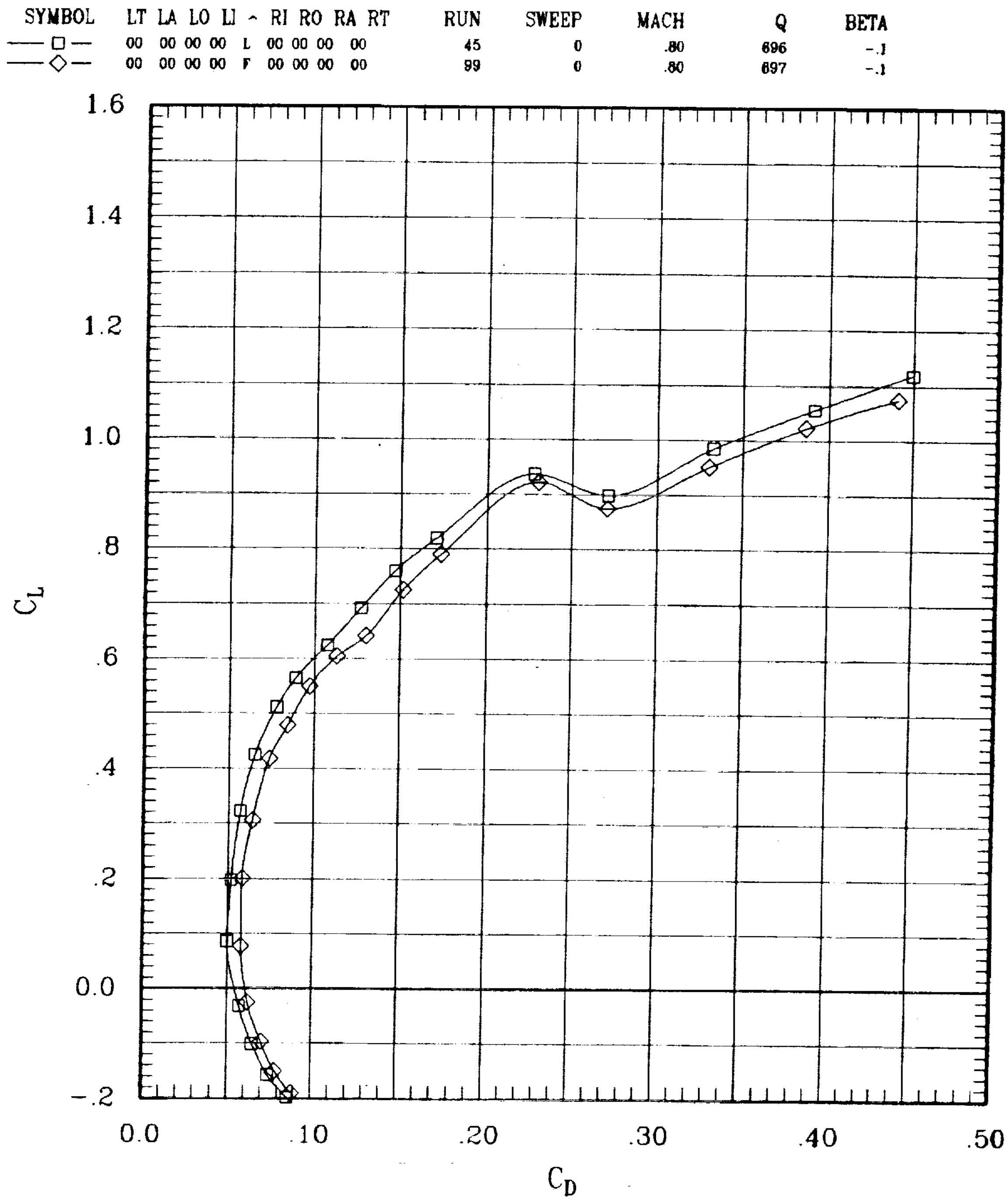

Figure 6(a). Effect of pivot height for sweep = 0 deg.

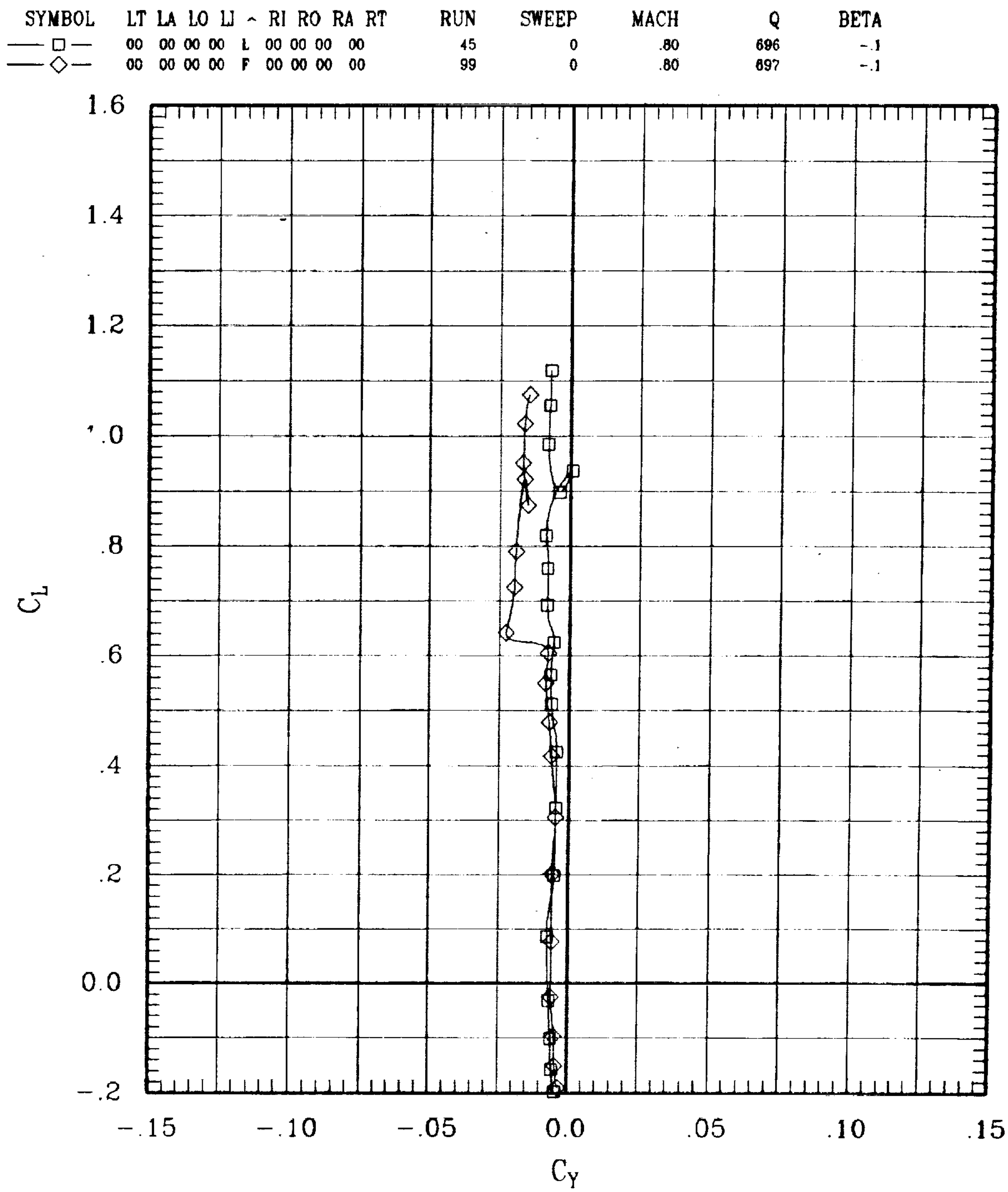

Figure 6(a). Effect of pivot height for sweep = 0 deg.

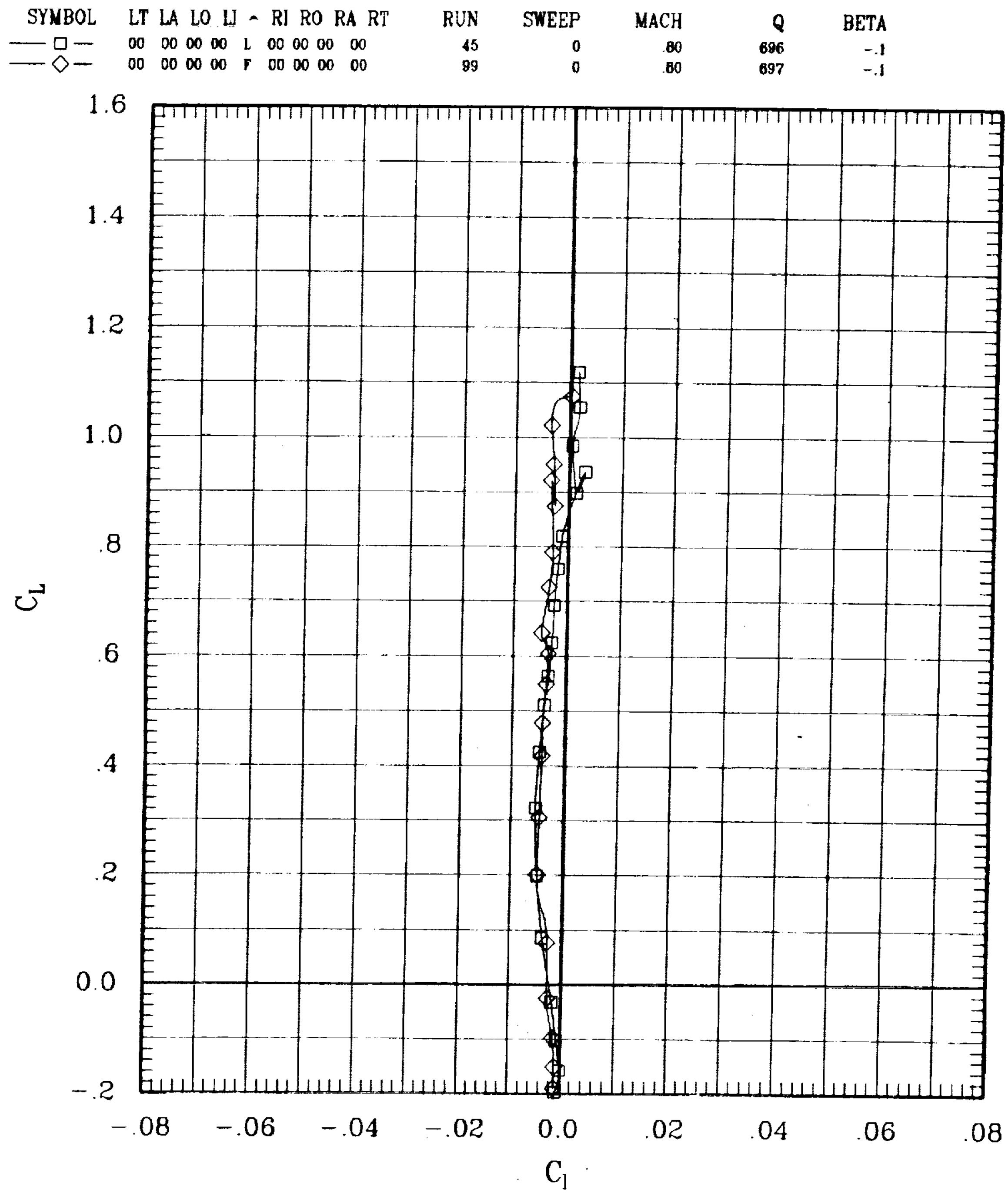

Figure 6(a). Effect of pivot height for sweep = 0 deg.

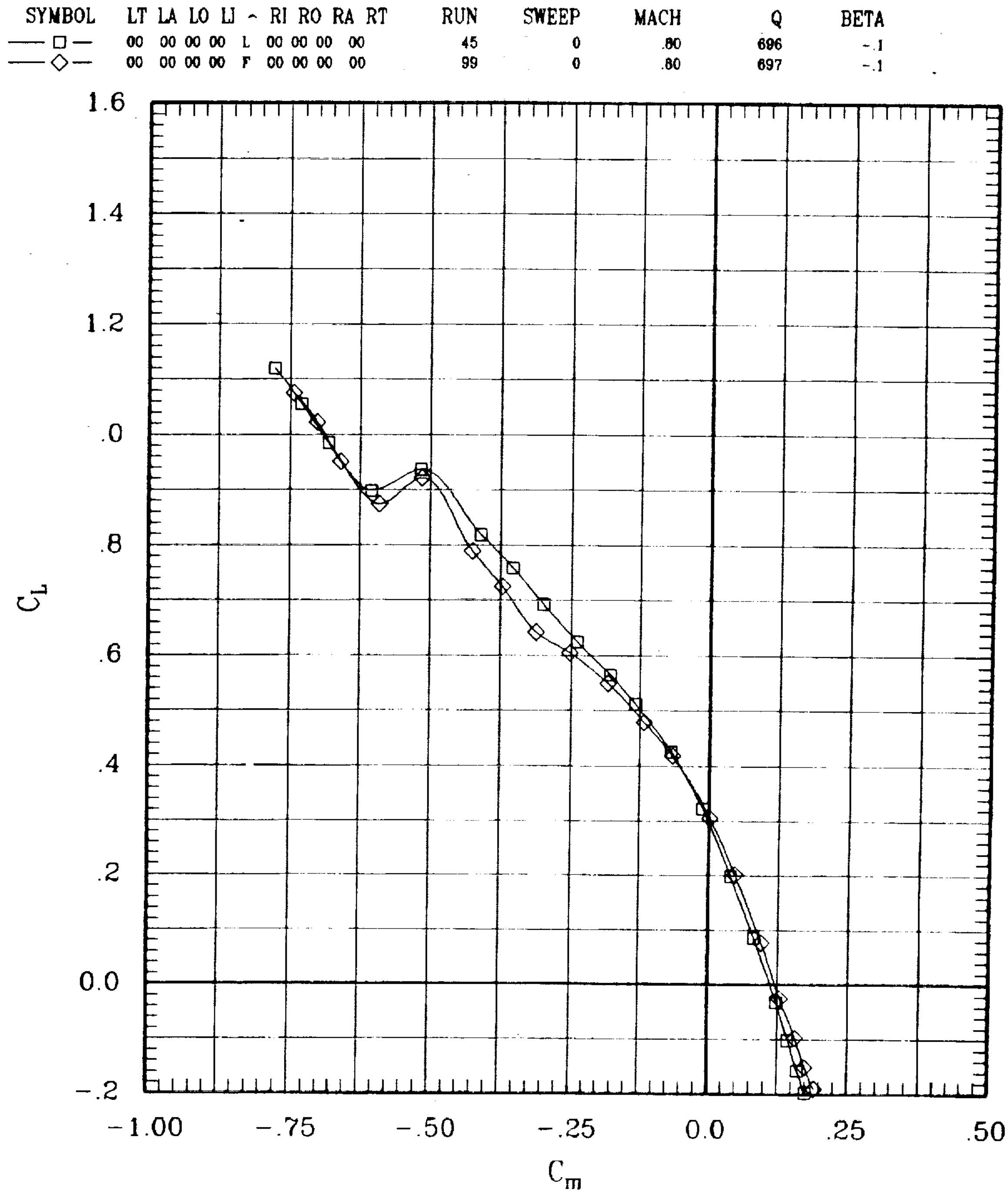

Figure 6(a). Effect of pivot height for sweep = 0 deg.

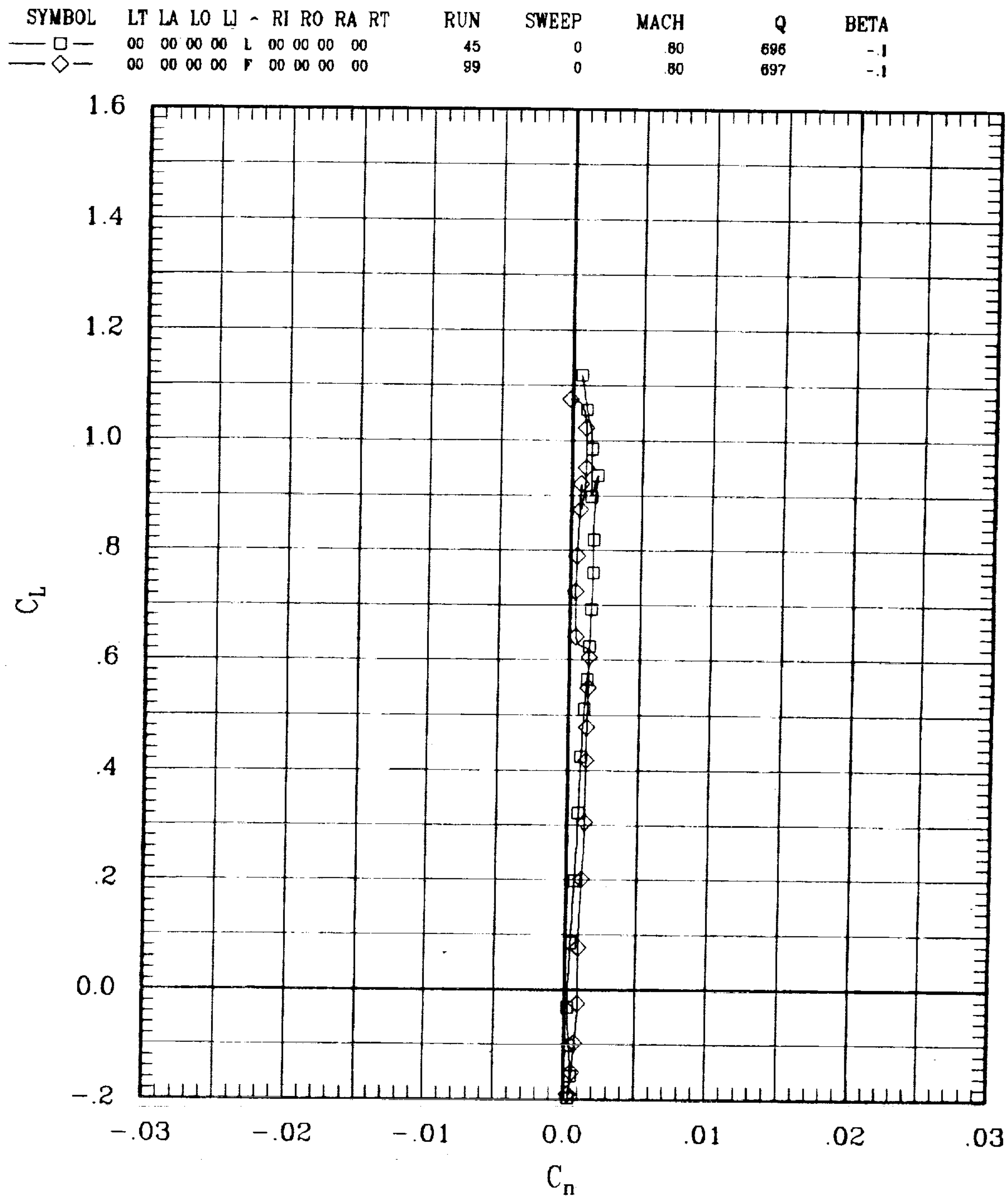

Figure 6(a). Effect of pivot height for sweep = 0 deg.

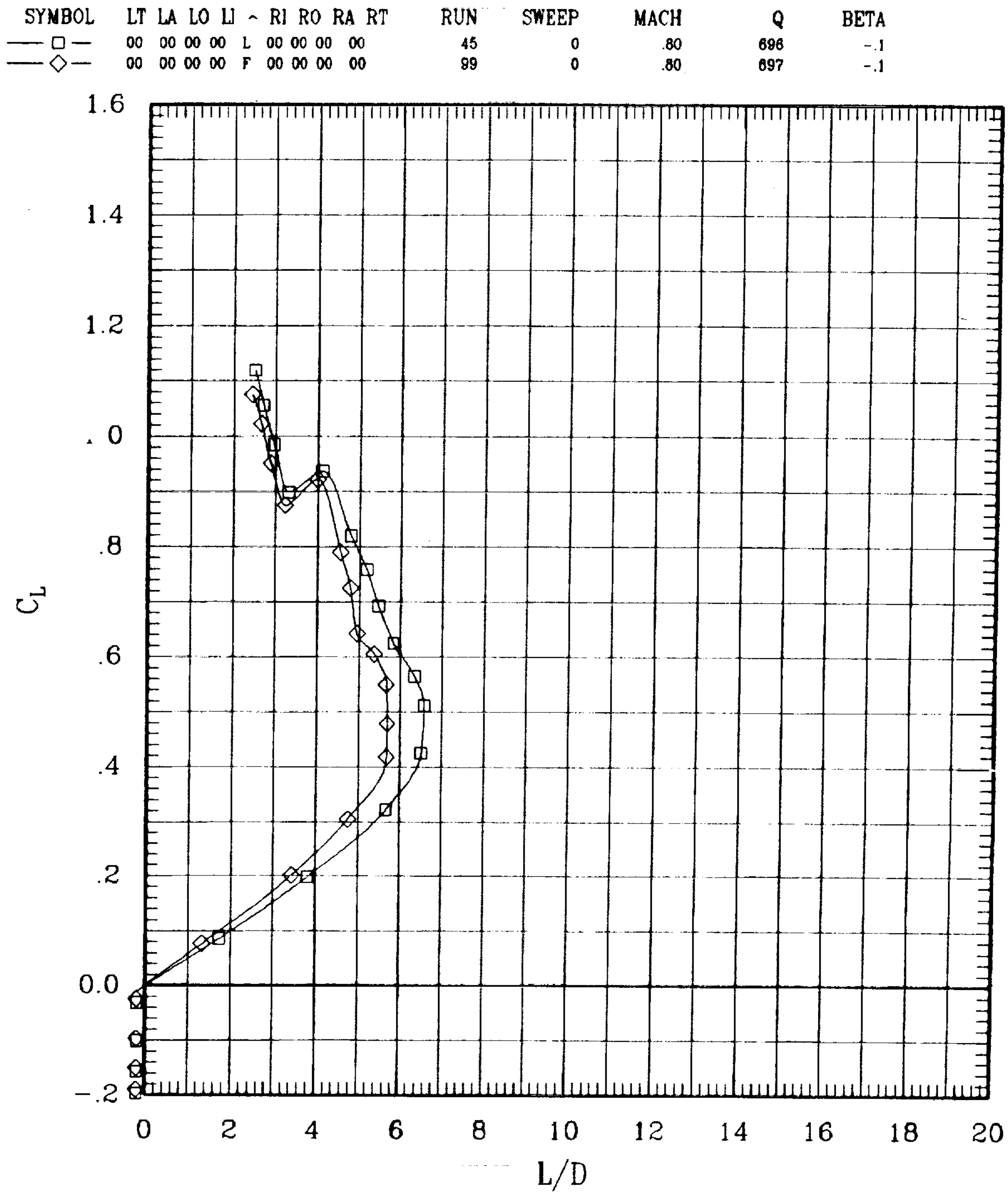

Figure 6(a). Effect of pivot height for sweep = 0 deg.

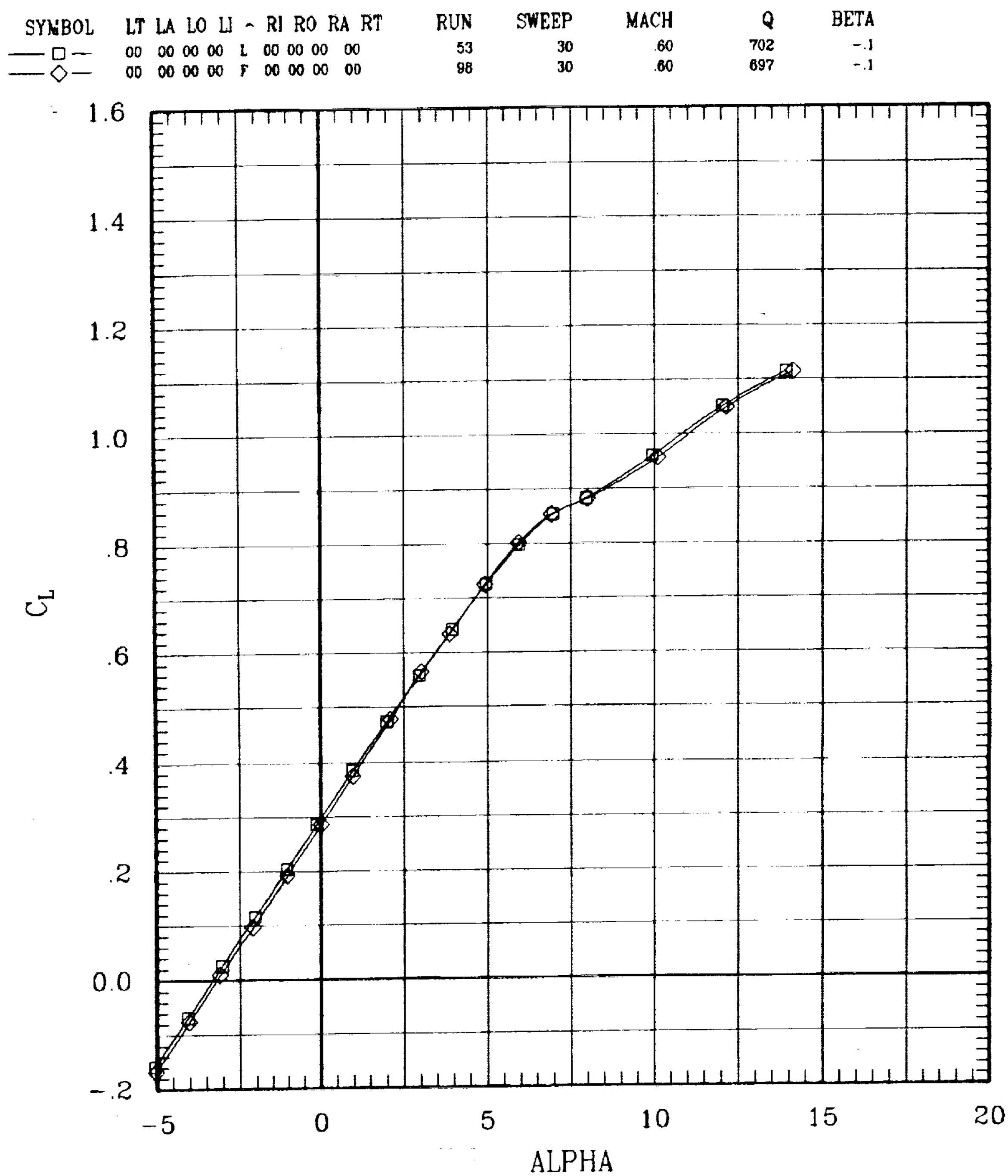

Figure 6(b). Effect of pivot height for sweep = 30 deg.

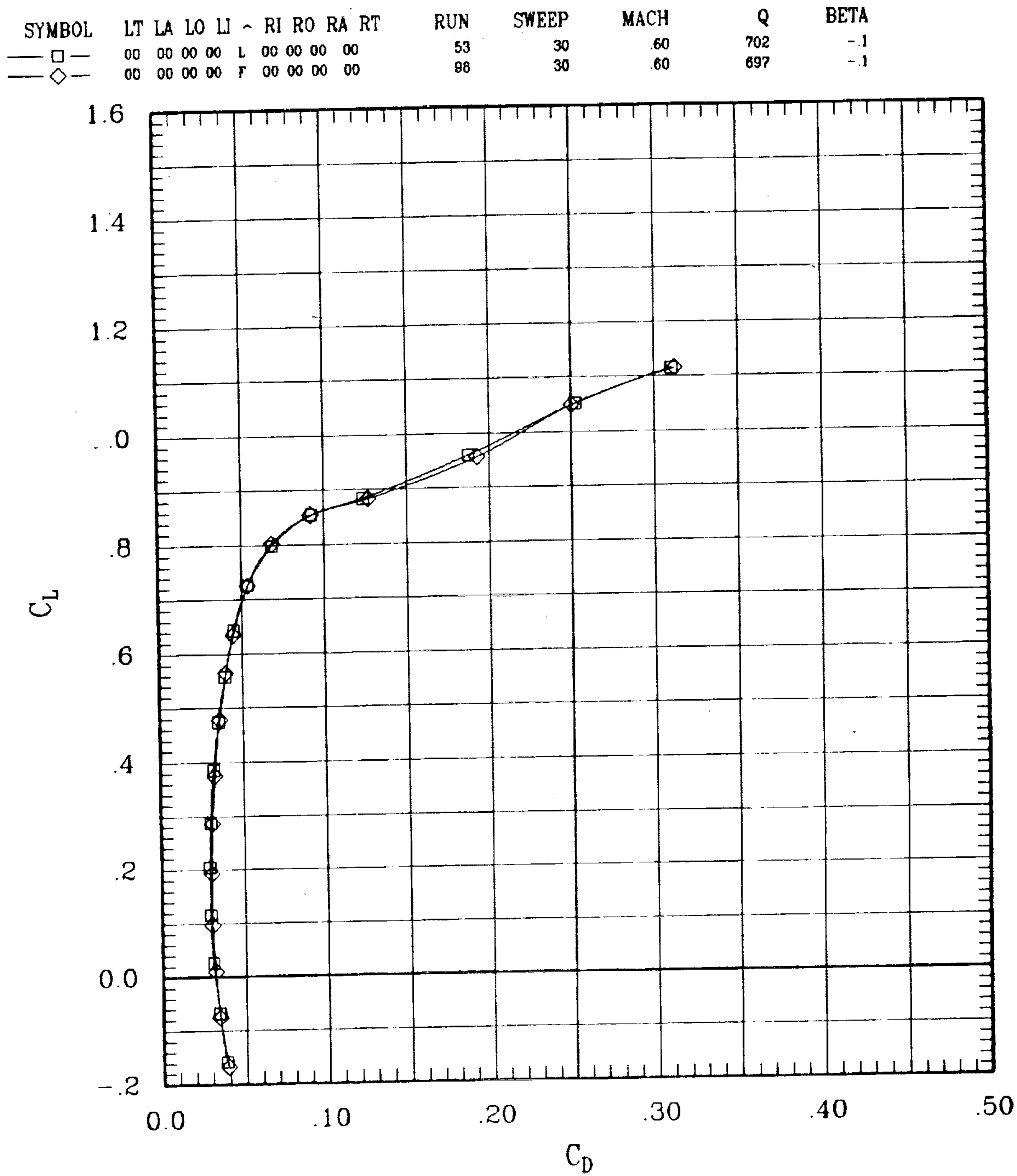

Figure 6(b). Effect of pivot height for sweep = 30 deg.

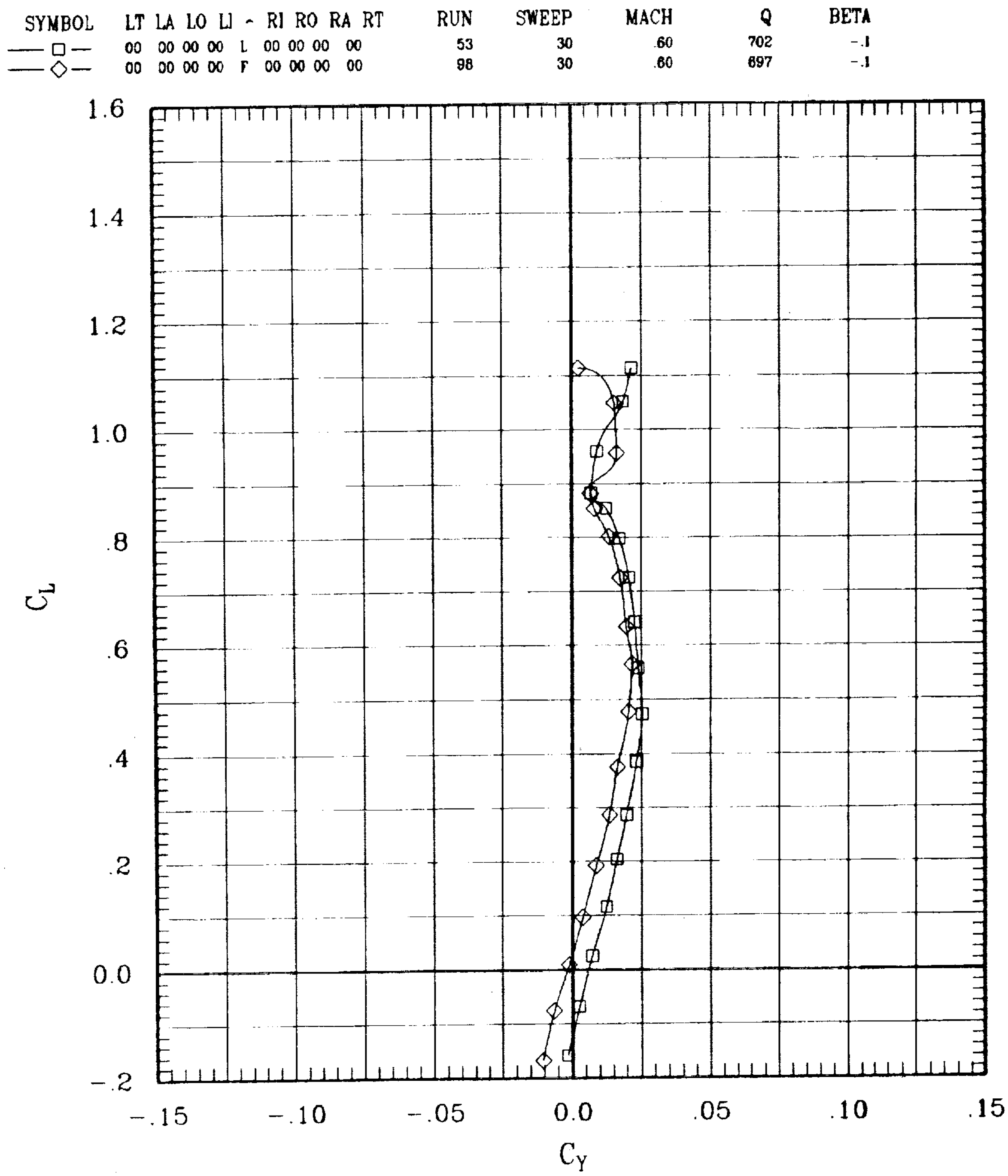

Figure 6(b). Effect of pivot height for sweep = 30 deg.

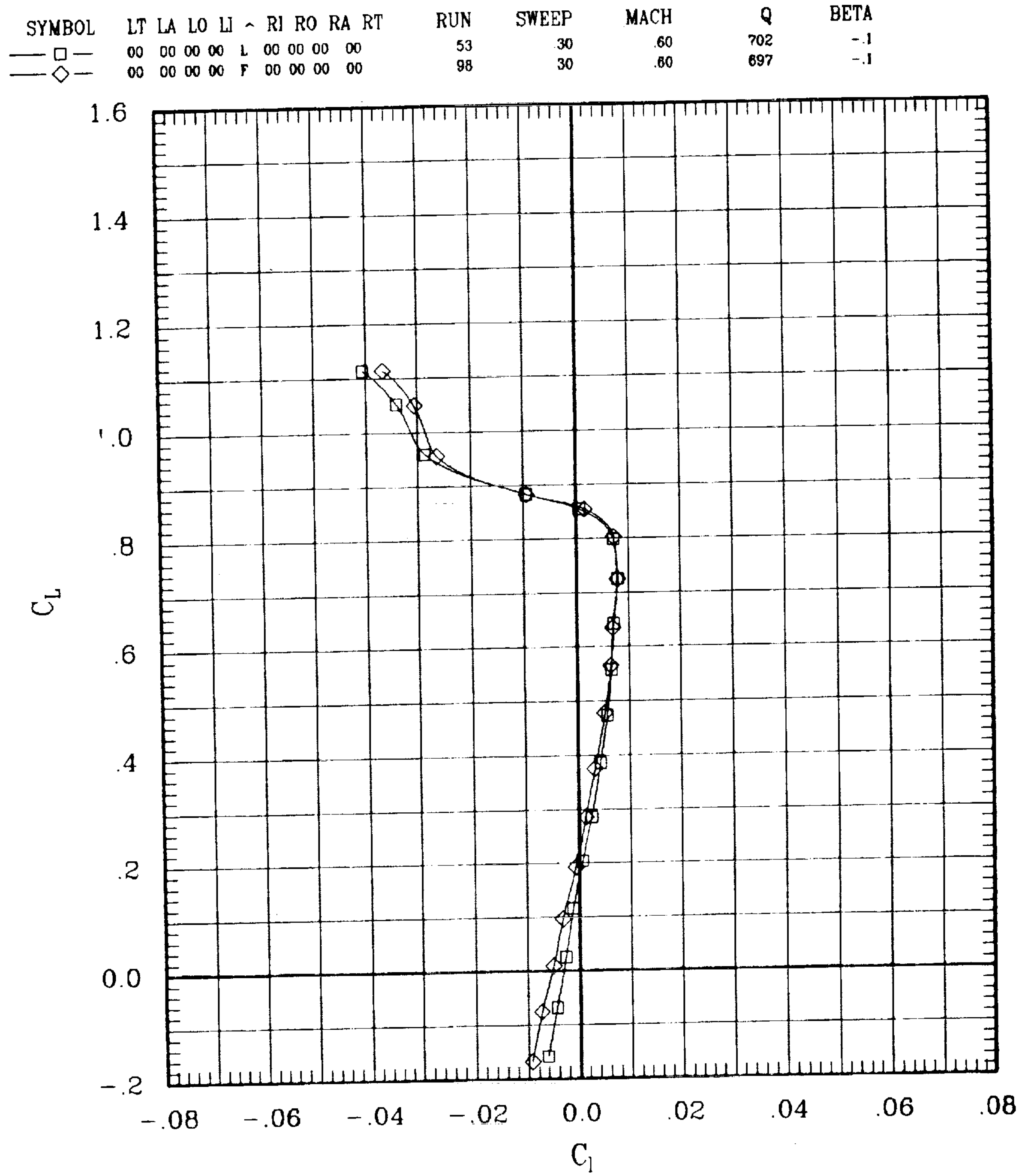

Figure 6(b). Effect of pivot height for sweep = 30 deg.

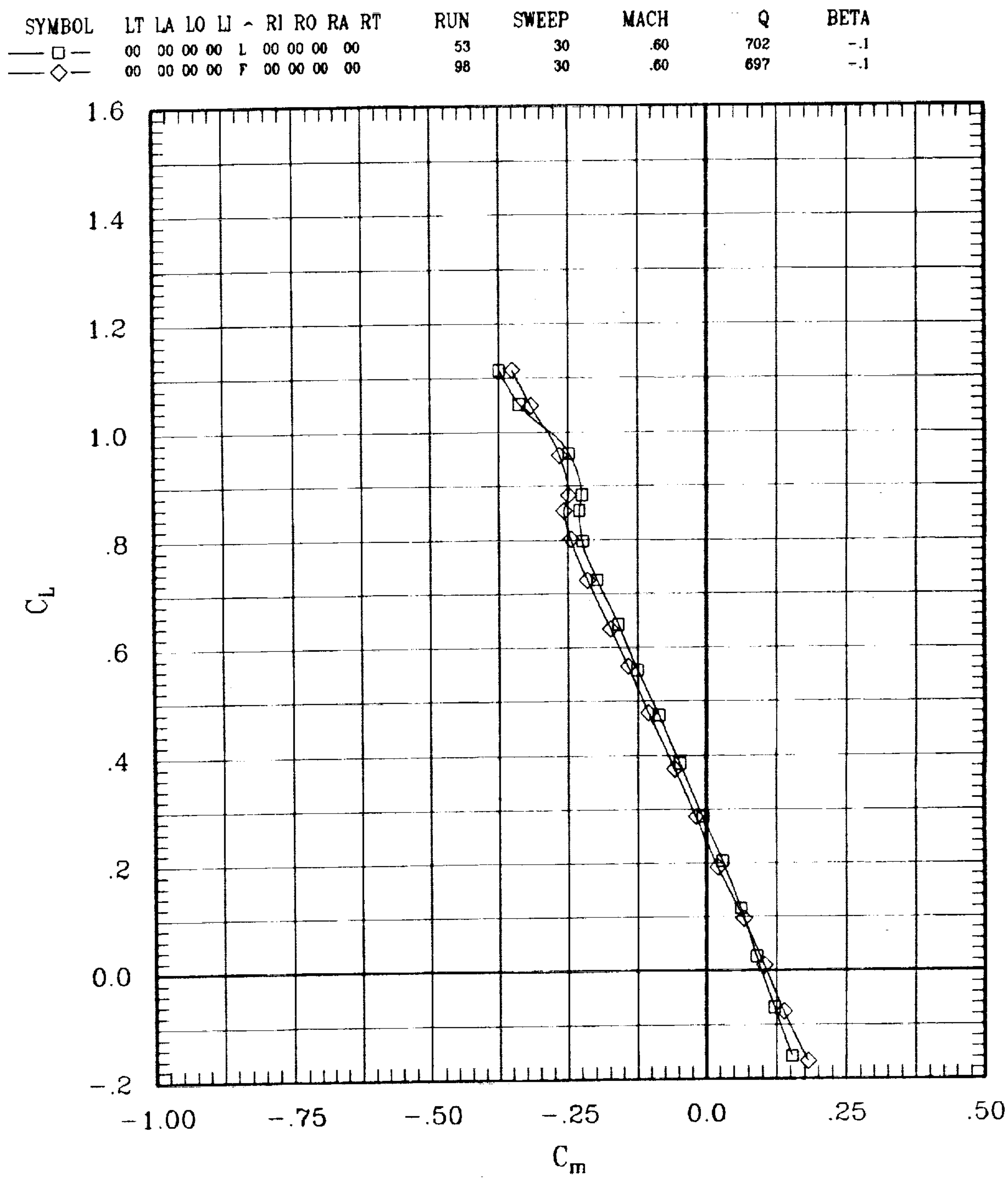

Figure 6(b). Effect of pivot height for sweep = 30 deg.

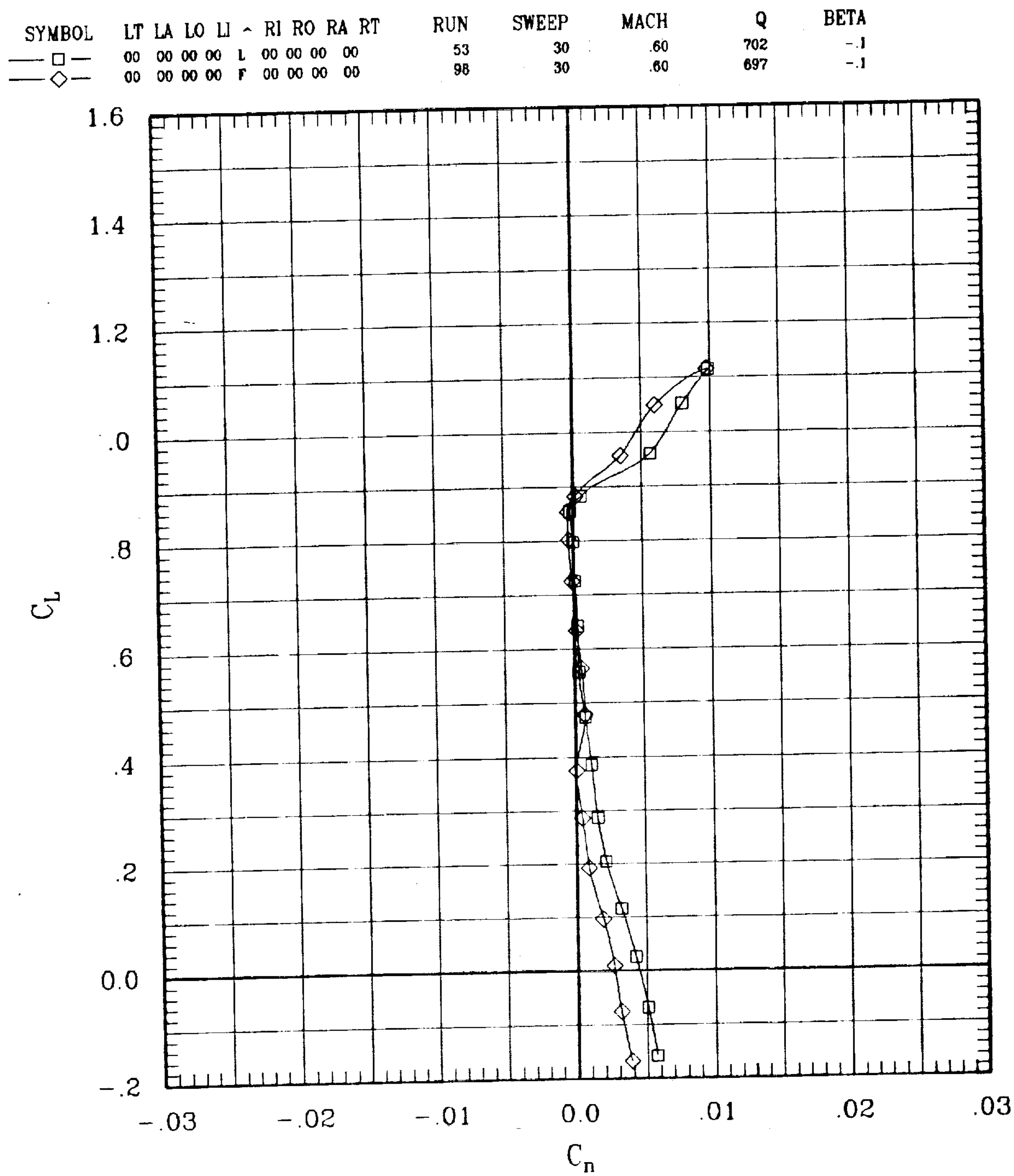

Figure 6(b). Effect of pivot height for sweep = 30 deg.

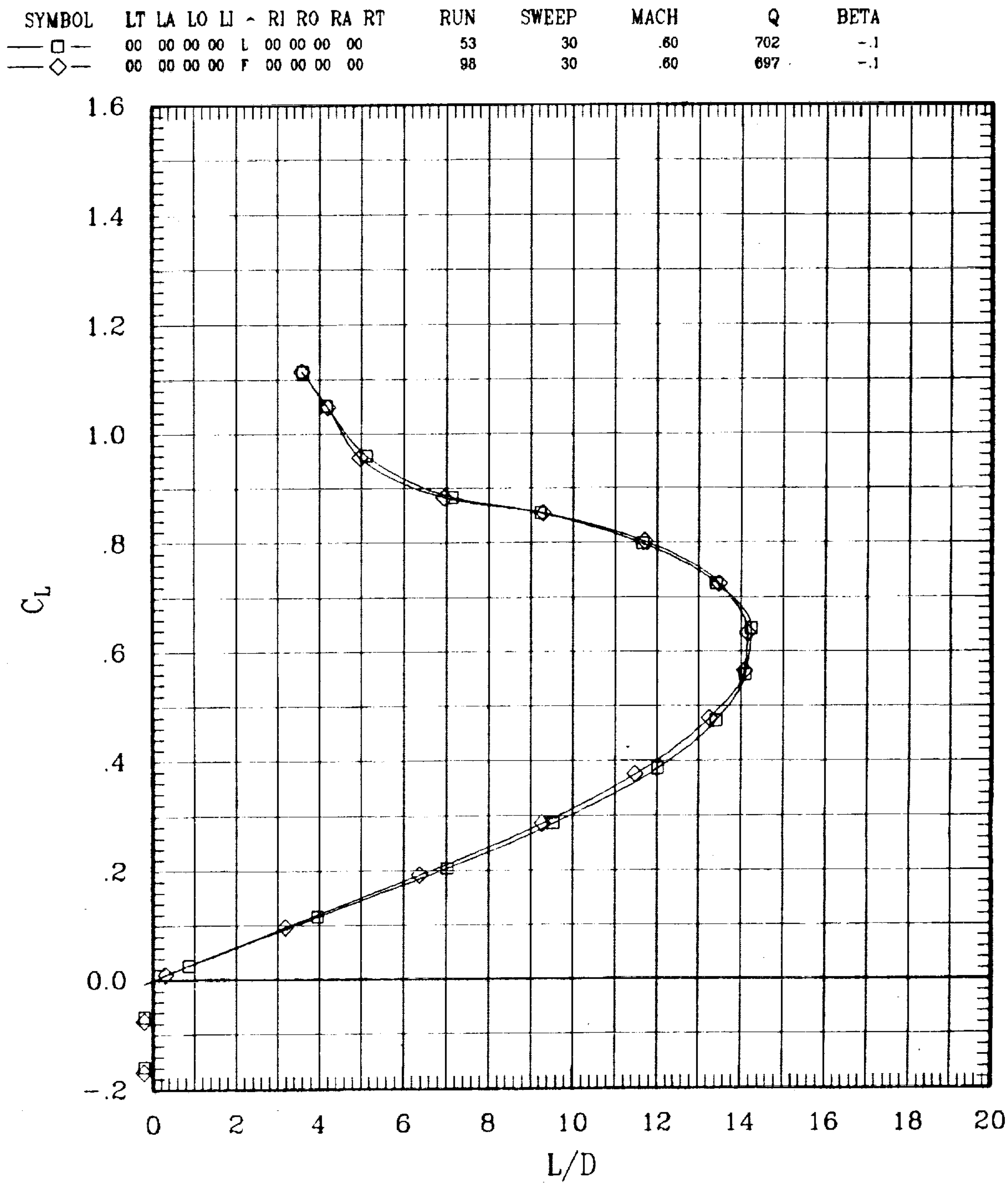

Figure 6(b). Effect of pivot height for sweep = 30 deg.

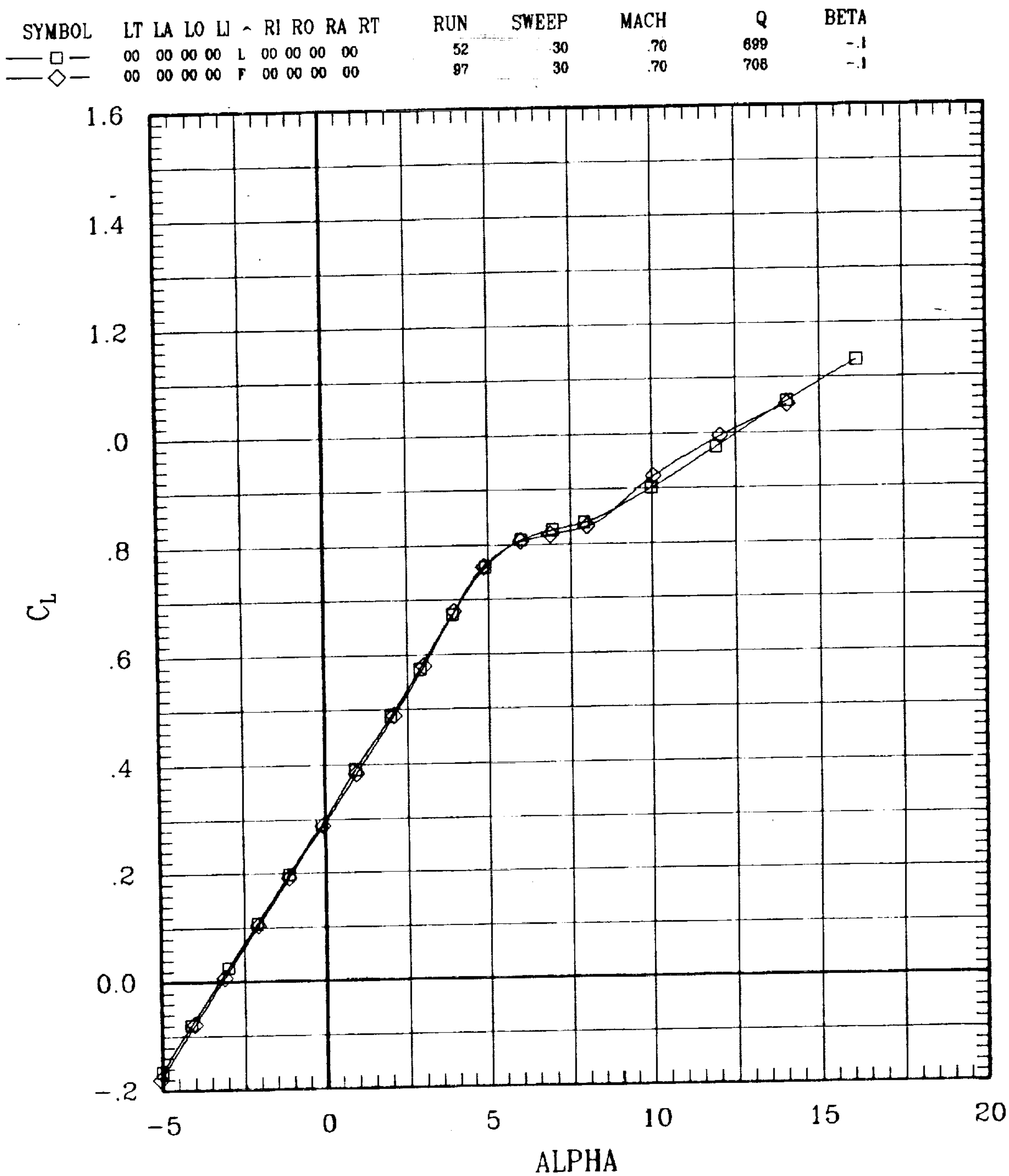

Figure 6(b). Effect of pivot height for sweep = 30 deg.

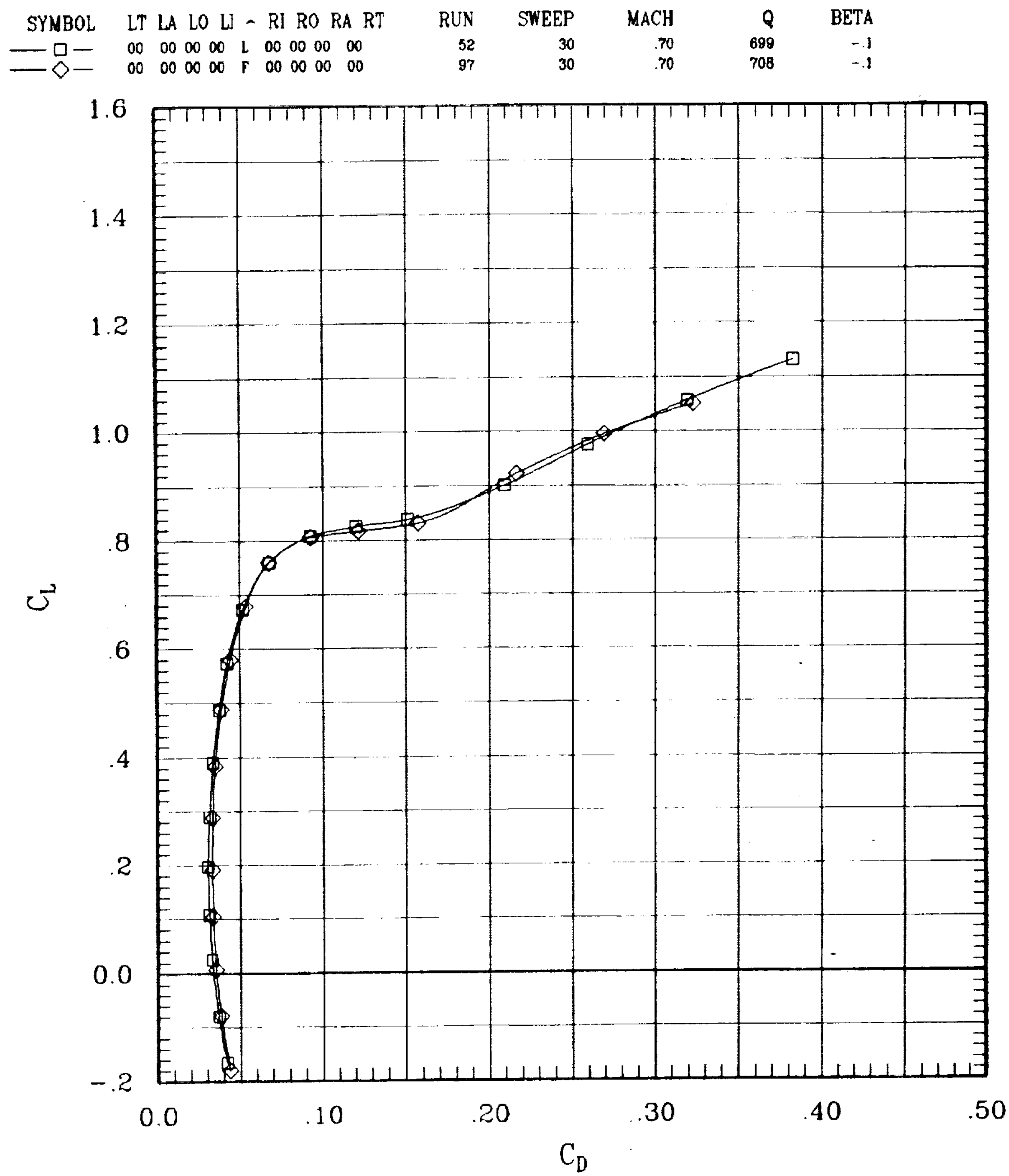

Figure 6(b). Effect of pivot height for sweep = 30 deg.

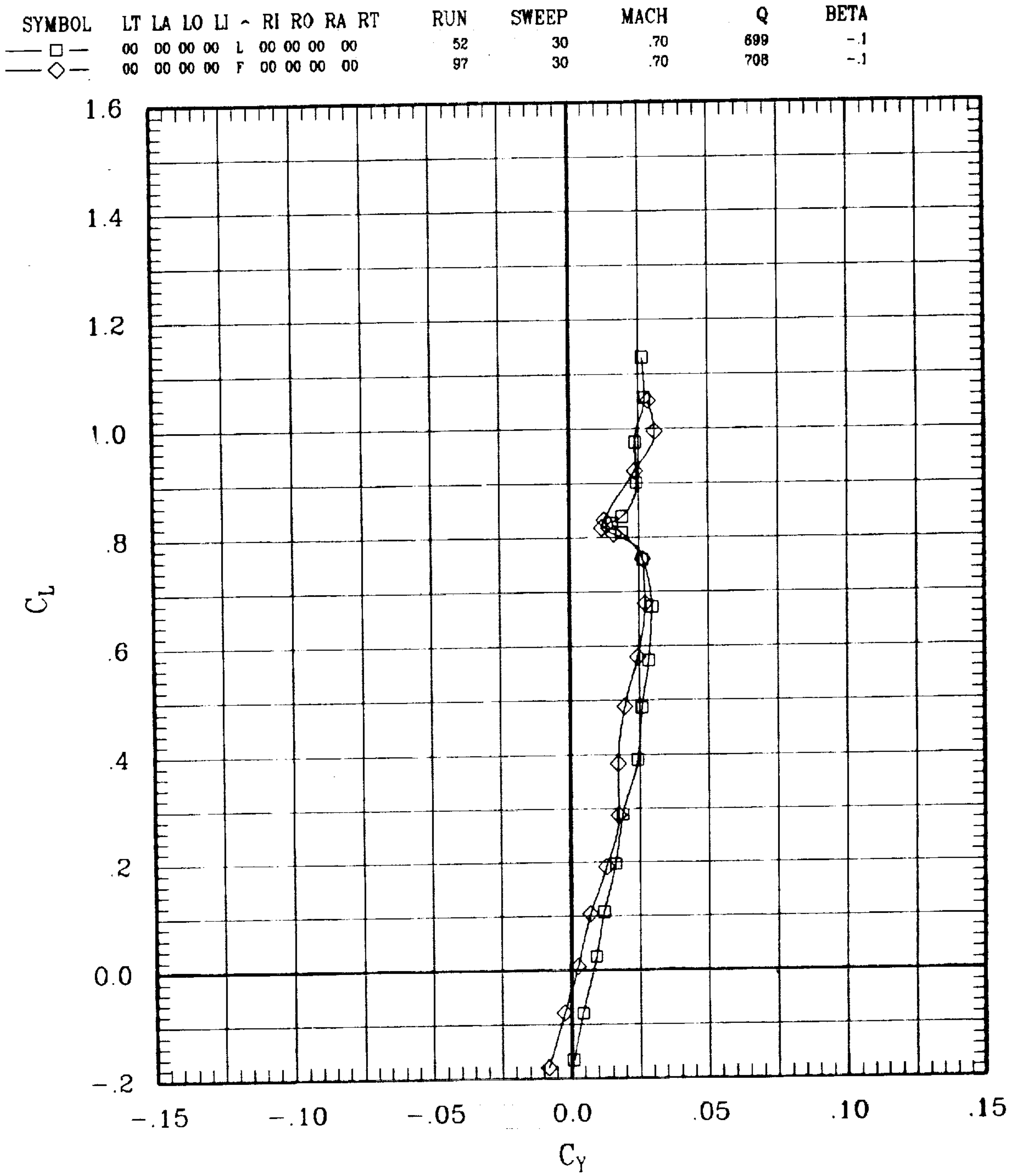

Figure 6(b). Effect of pivot height for sweep = 30 deg.

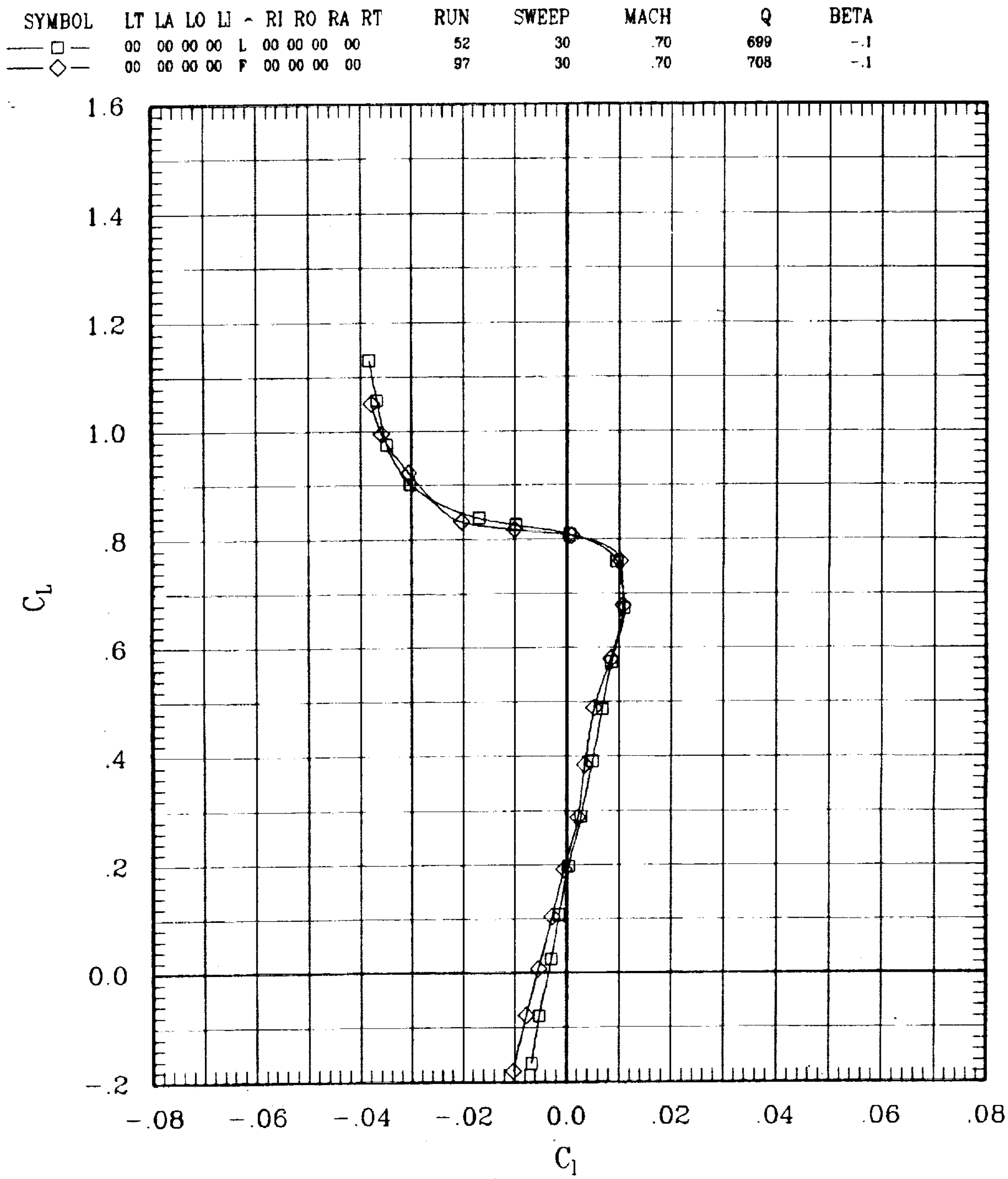

Figure 6(b). Effect of pivot height for sweep = 30 deg.

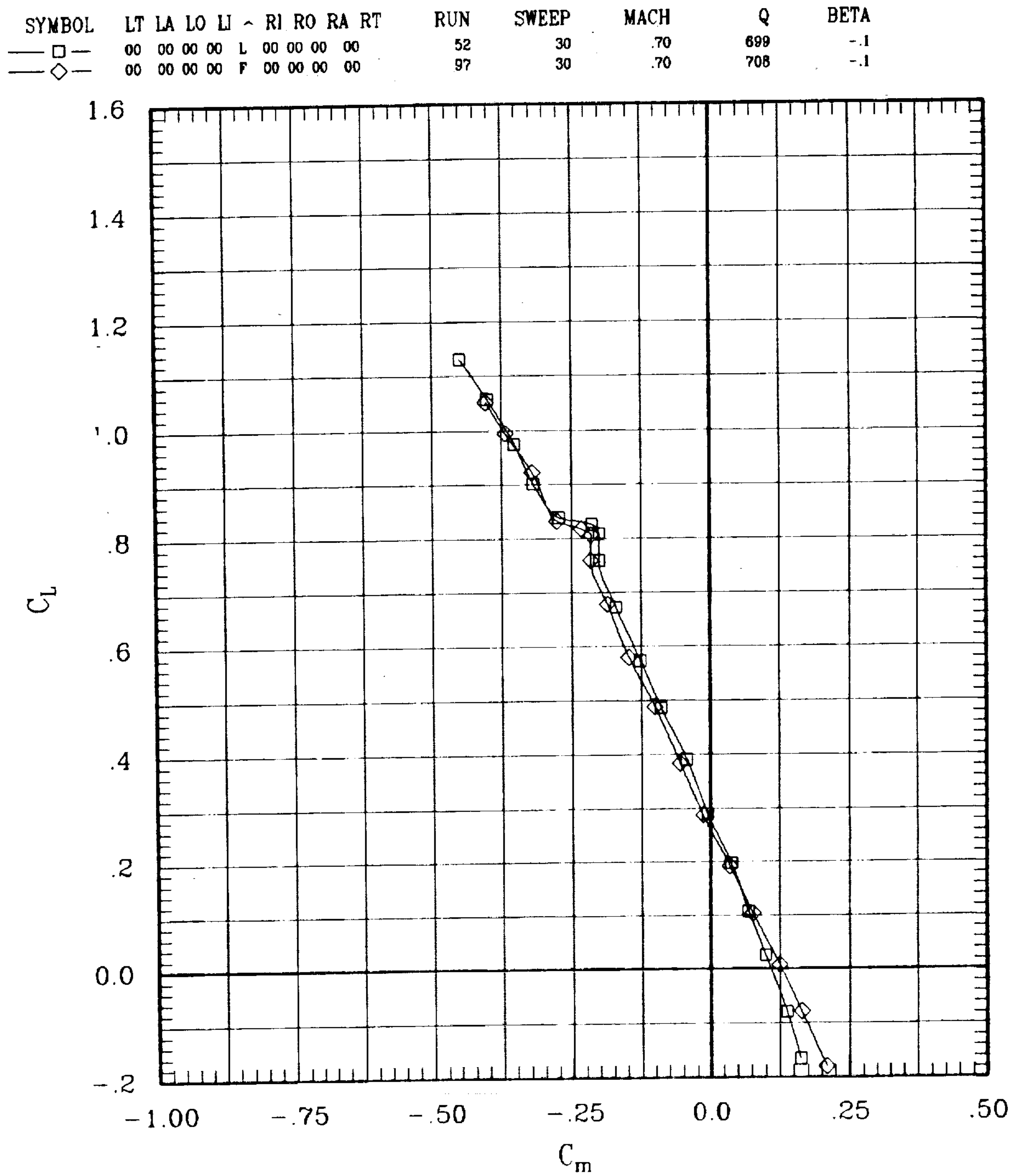

Figure 6(b). Effect of pivot height for sweep = 30 deg.

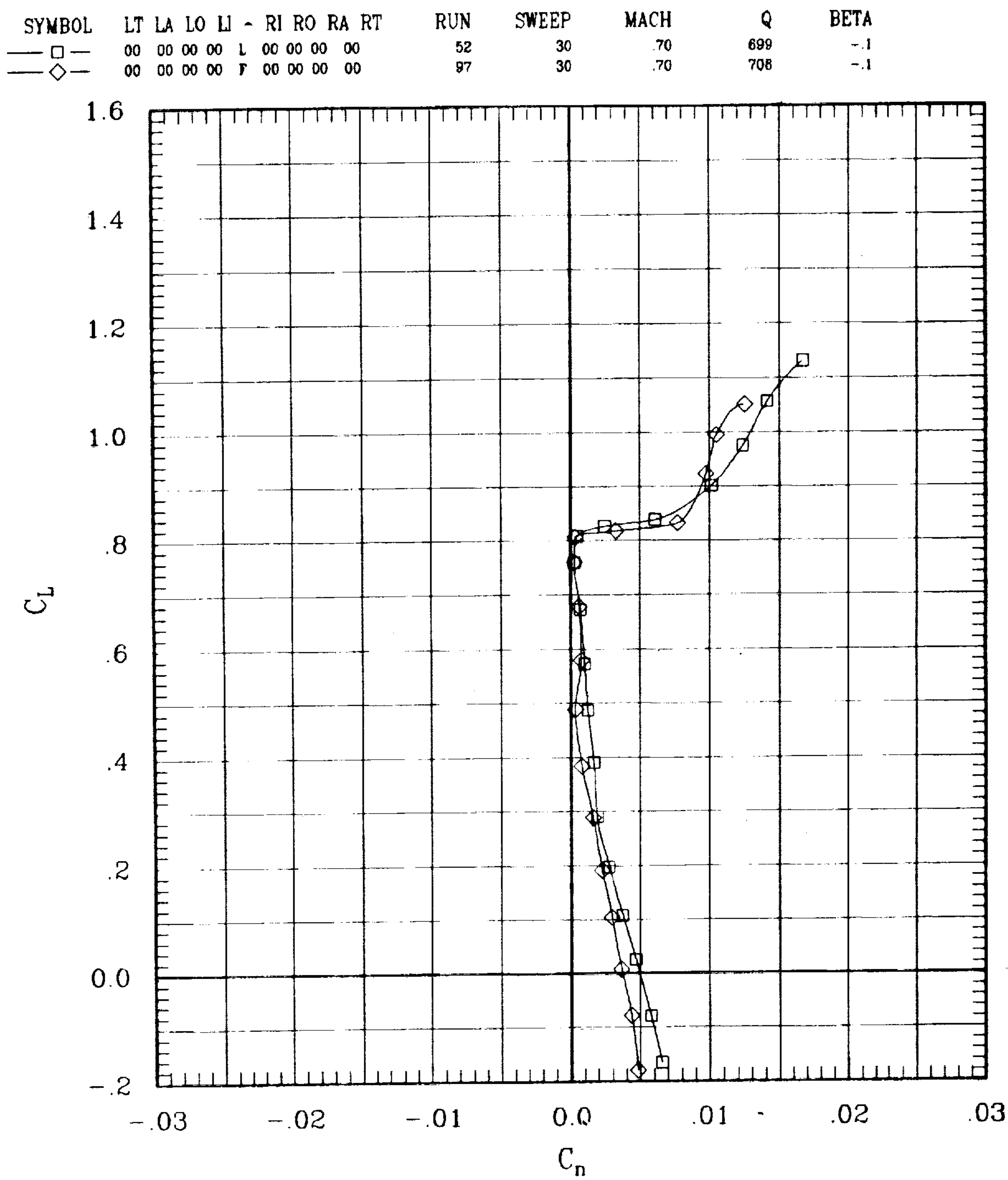

Figure 6(b). Effect of pivot height for sweep = 30 deg.

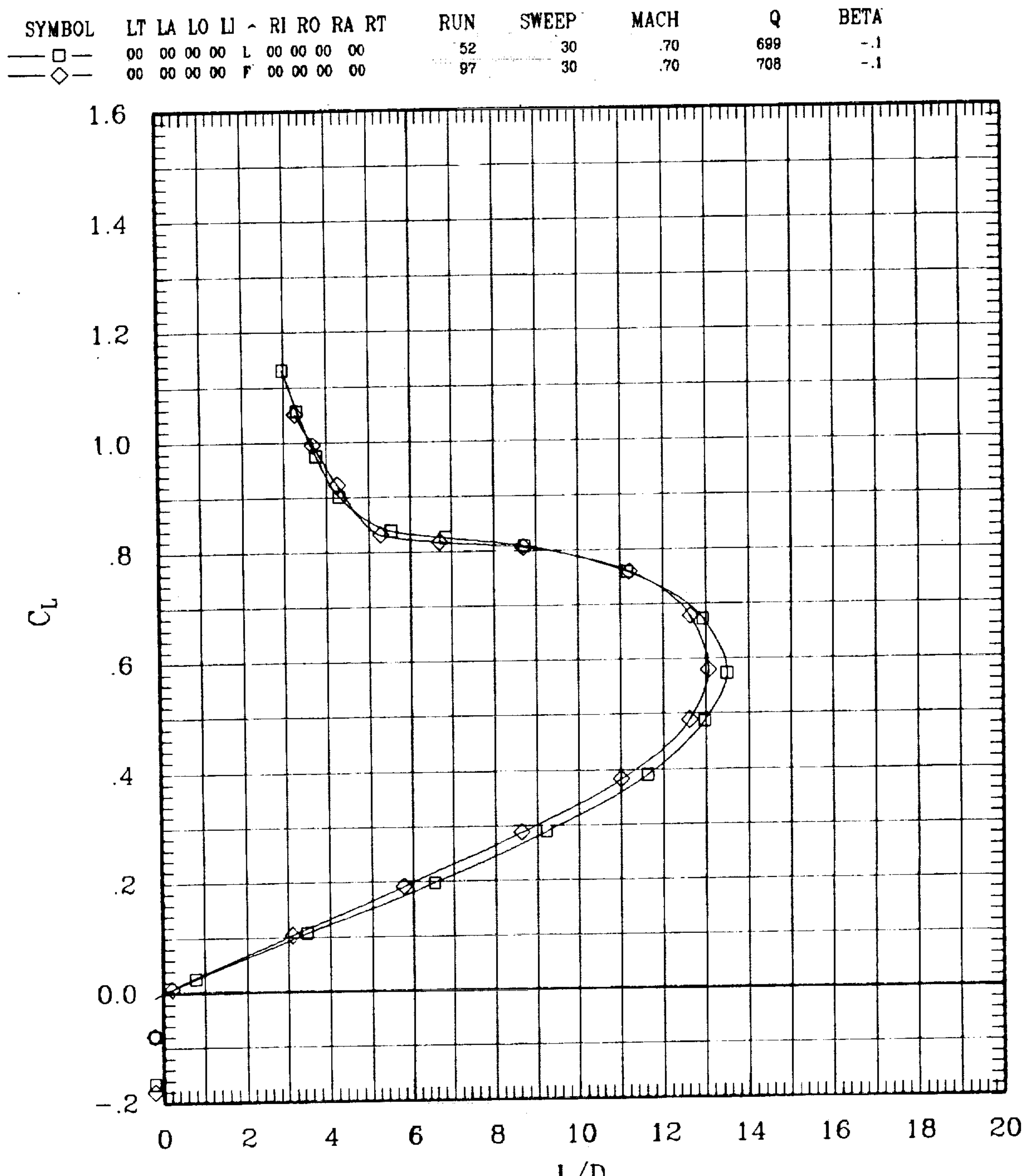

Figure 6(b). Effect of pivot height for sweep = 30 deg.

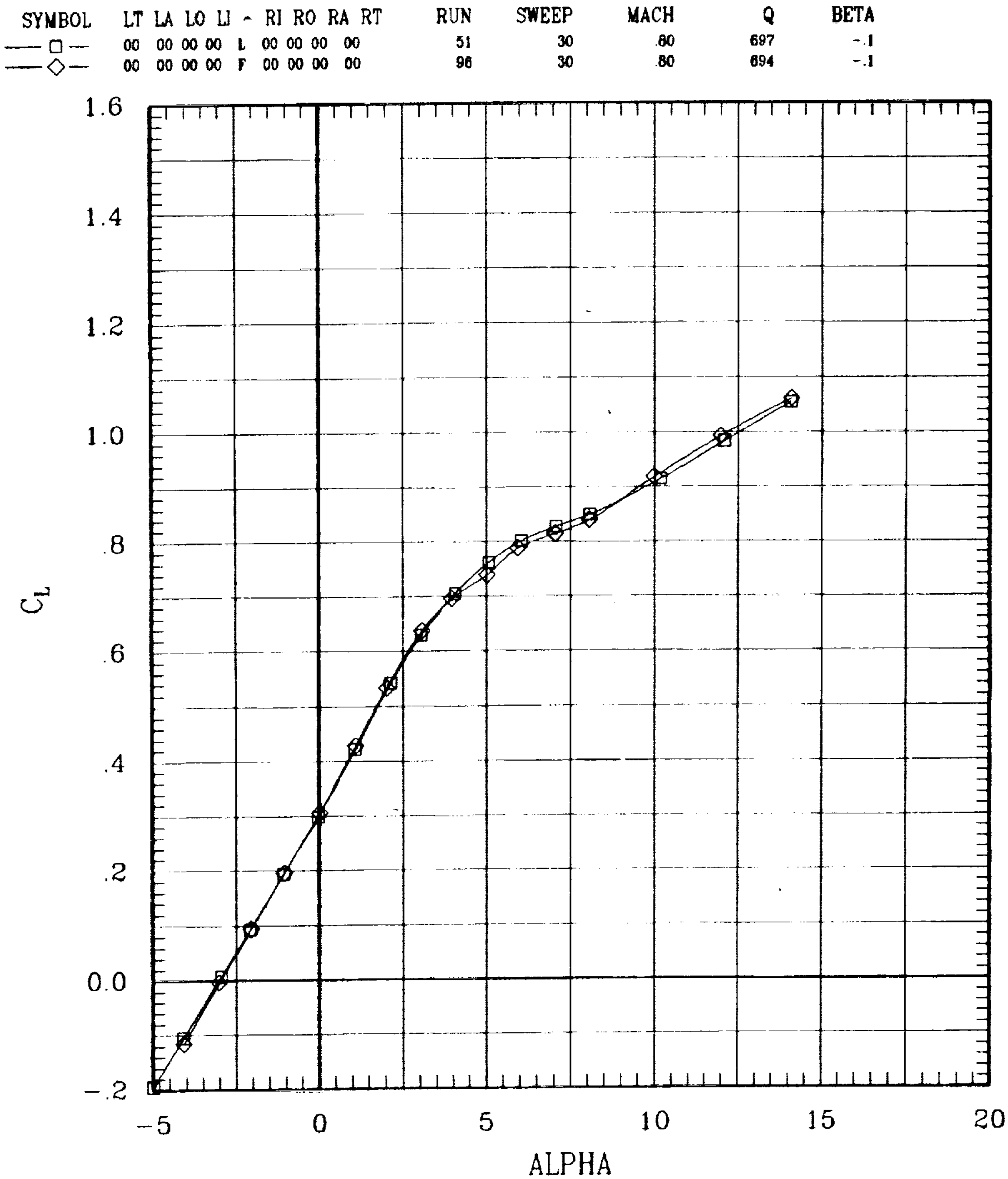

Figure 6(b). Effect of pivot height for sweep = 30 deg.

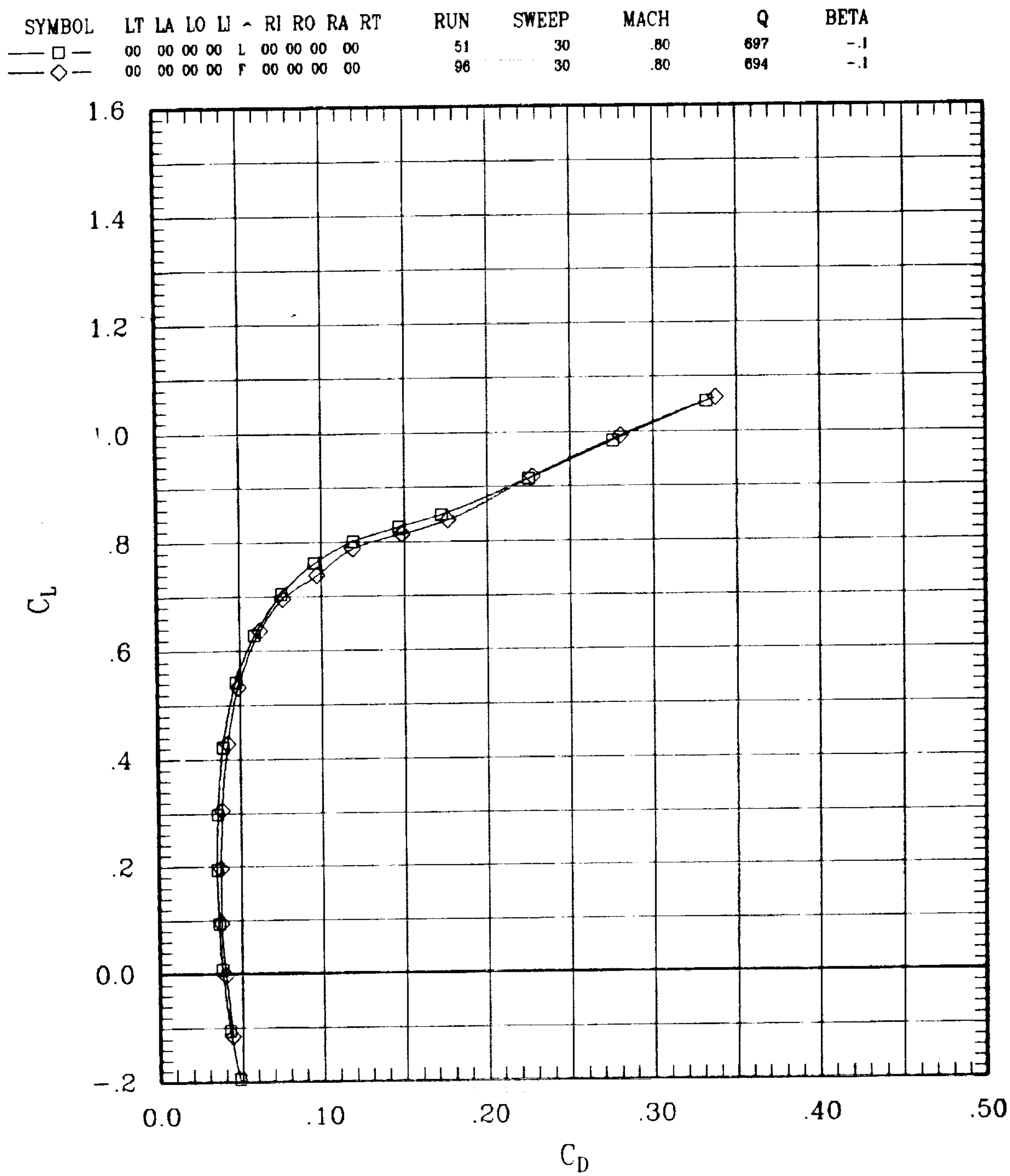

Figure 6(b). Effect of pivot height for sweep = 30 deg.

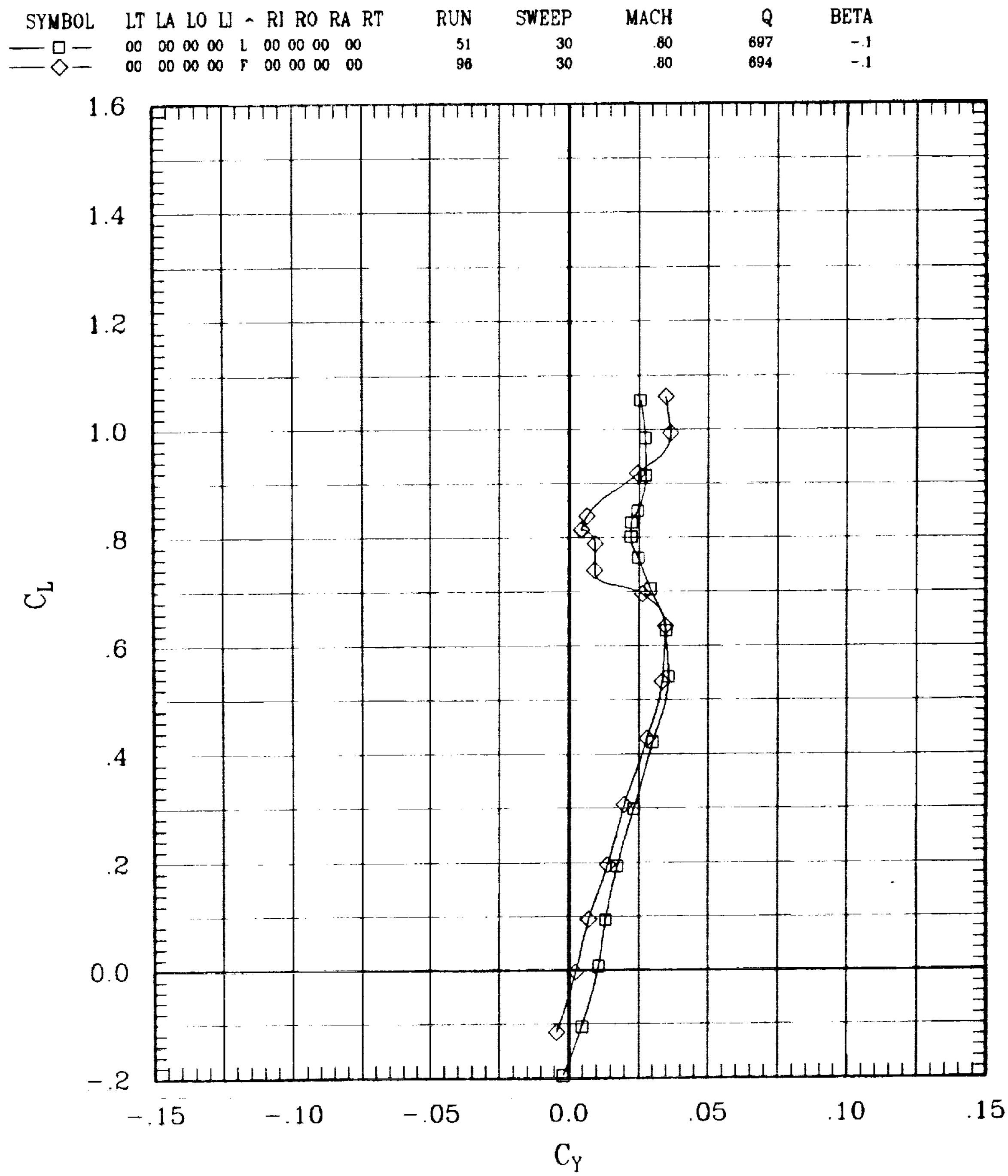

Figure 6(b). Effect of pivot height for sweep = 30 deg.

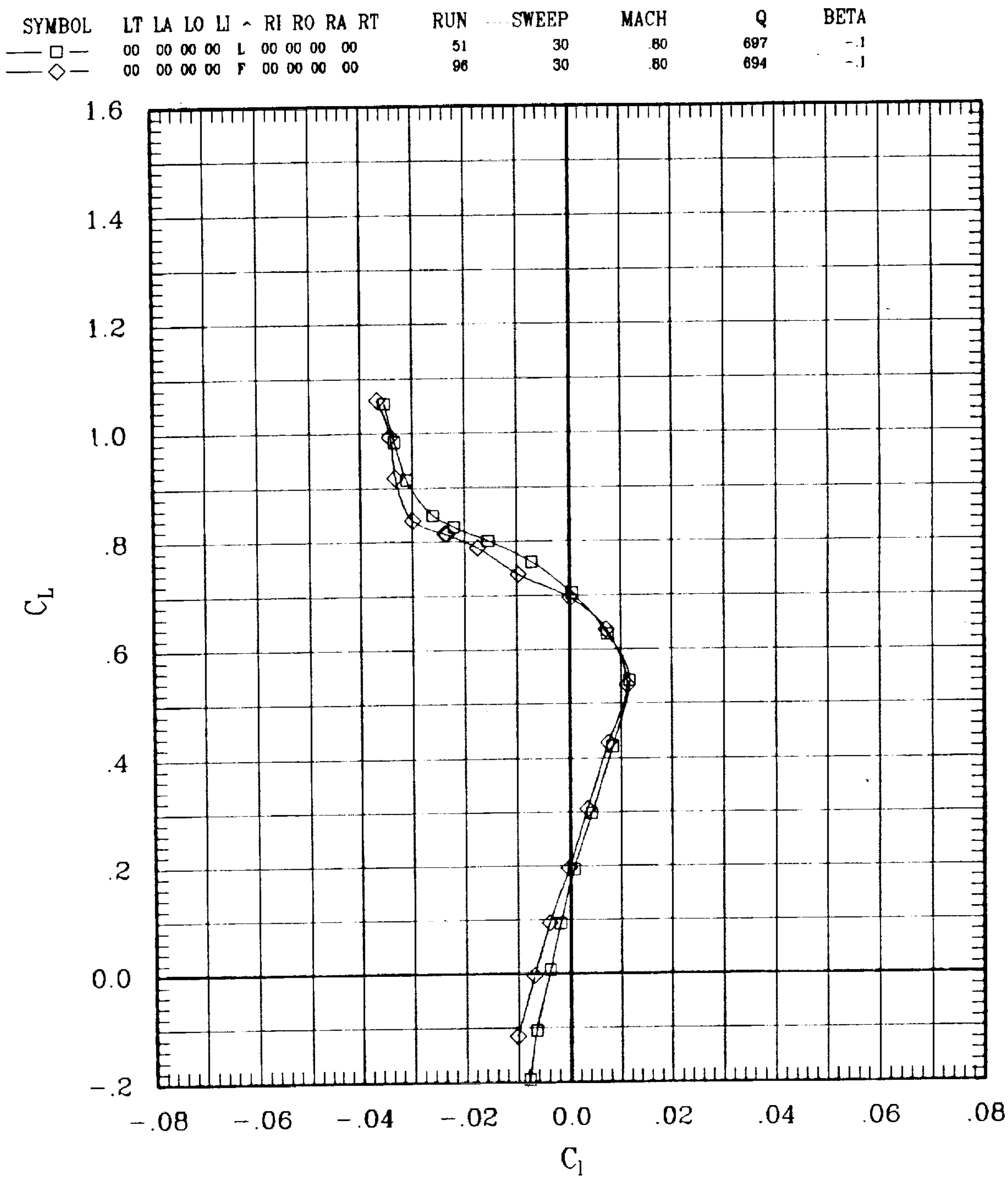

Figure 6(b). Effect of pivot height for sweep = 30 deg.

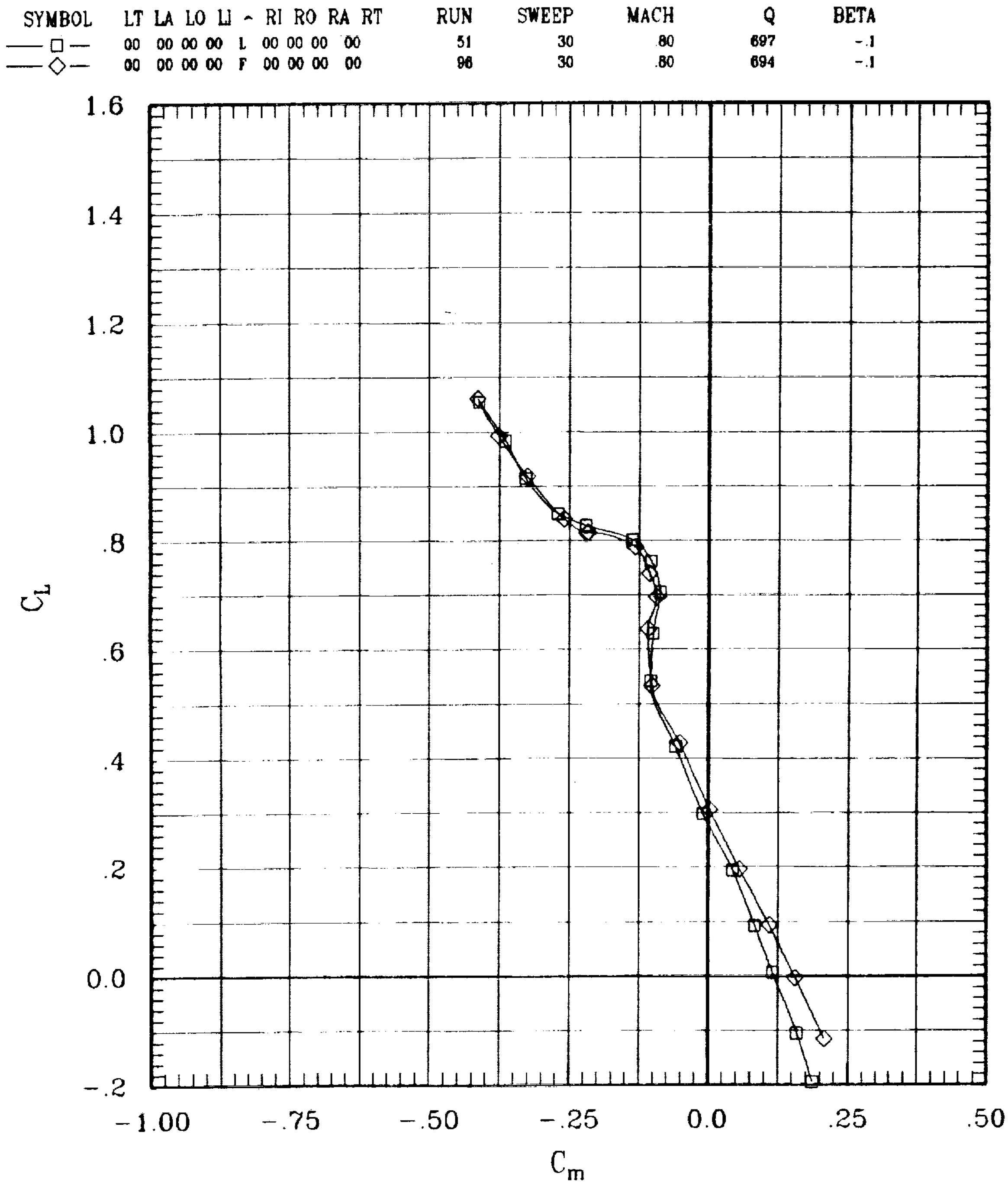

Figure 6(b). Effect of pivot height for sweep = 30 deg.

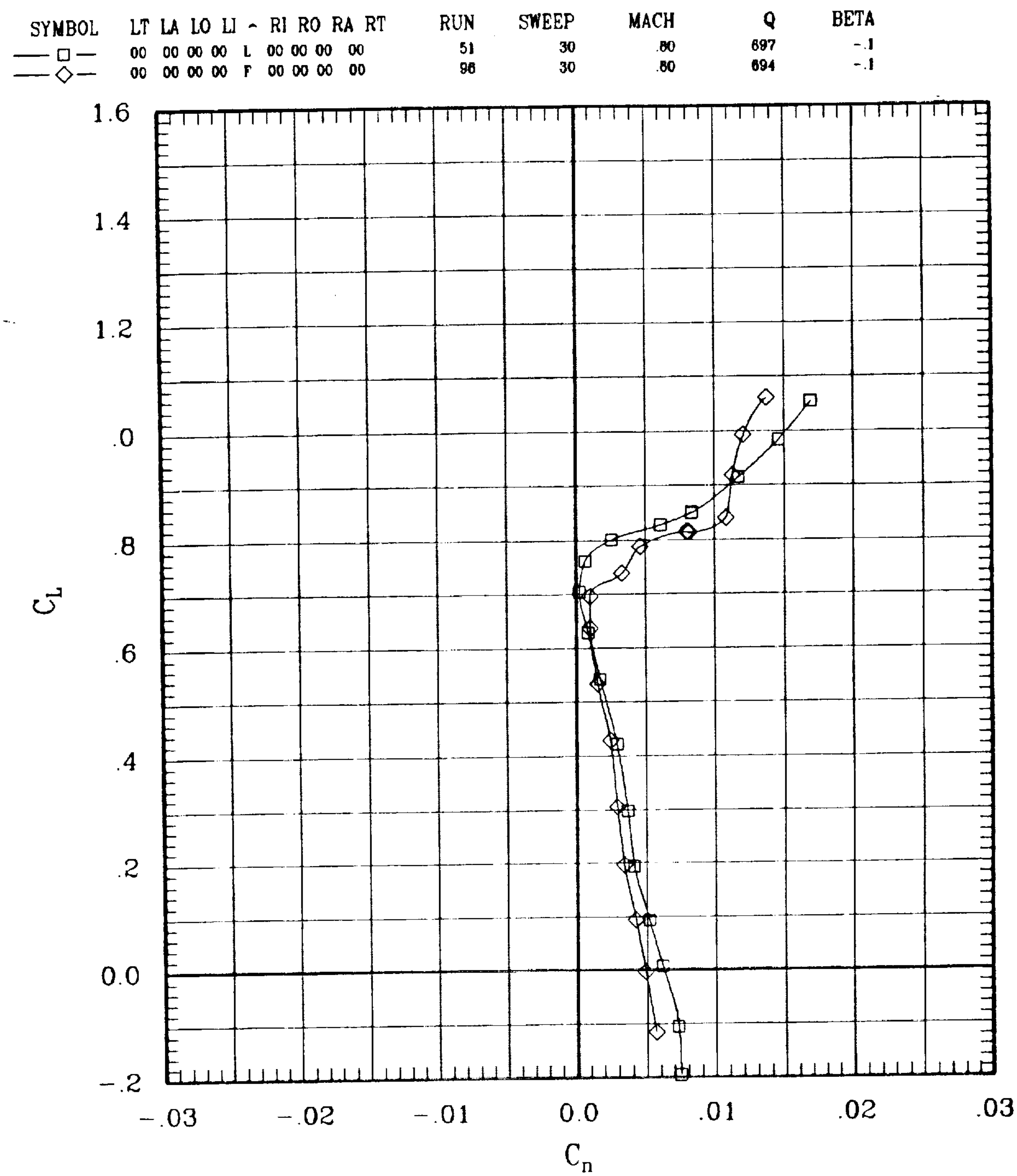

Figure 6(b). Effect of pivot height for sweep = 30 deg.

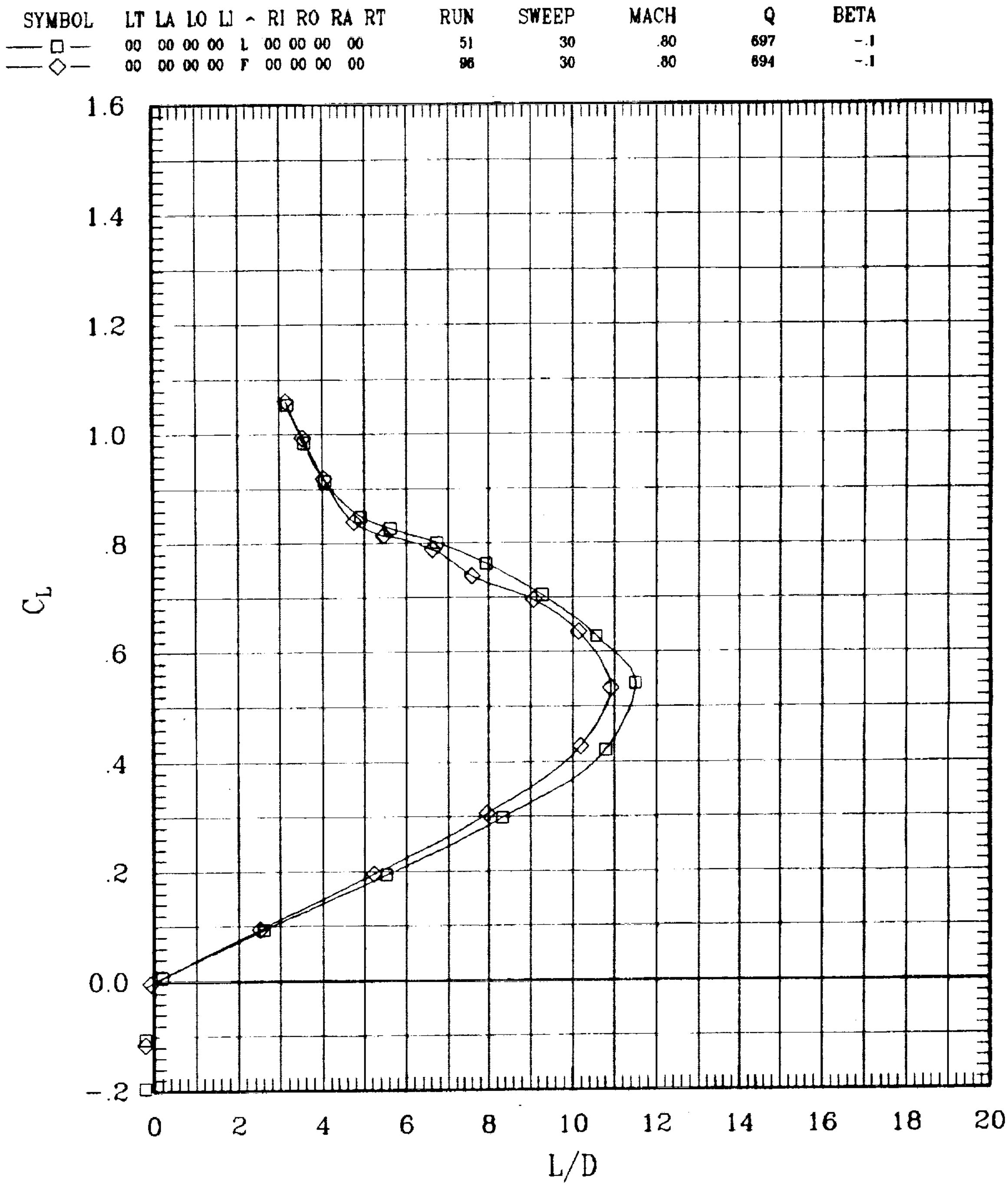

Figure 6(b). Effect of pivot height for sweep = 30 deg.

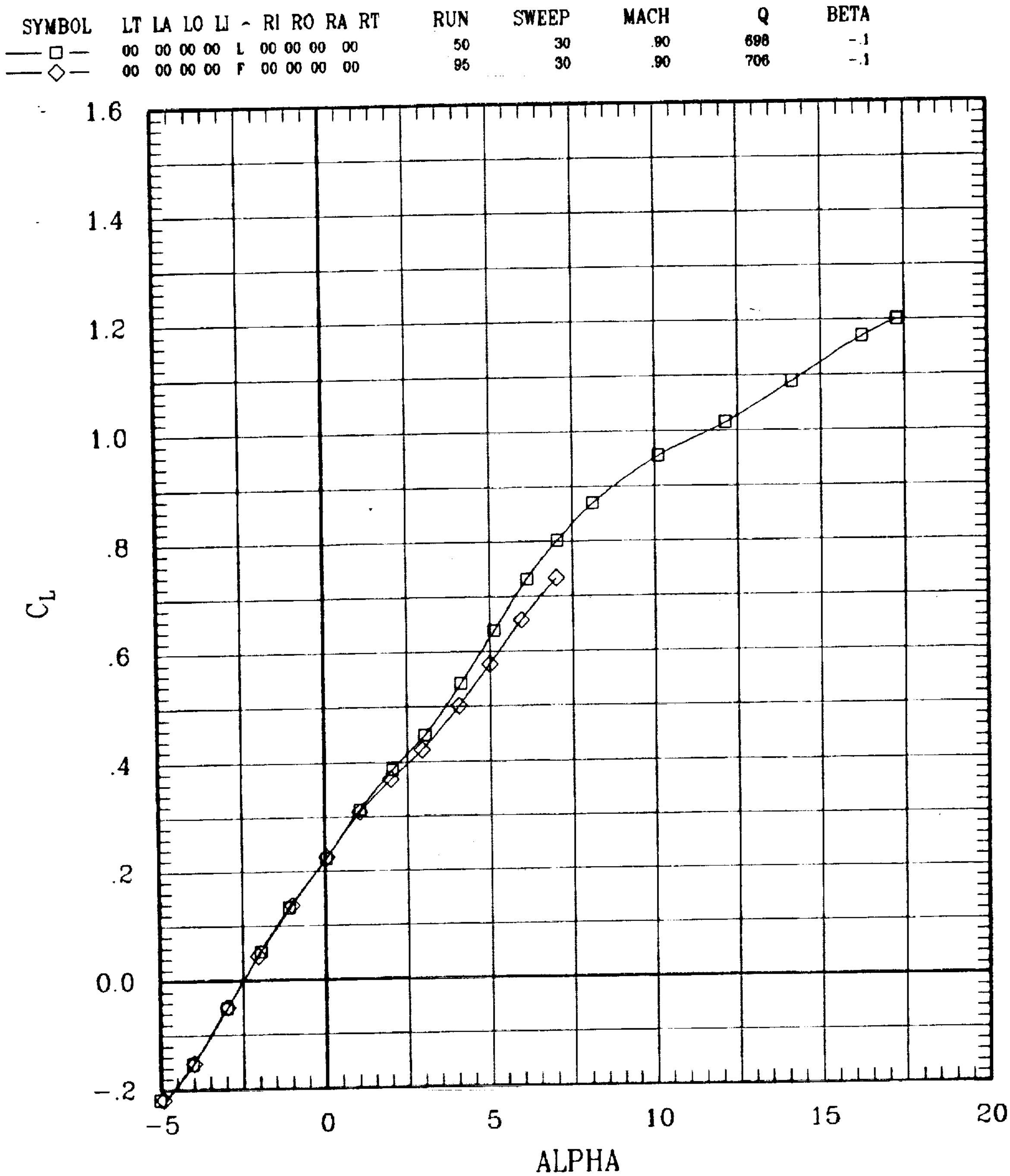

Figure 6(b). Effect of pivot height for sweep = 30 deg.

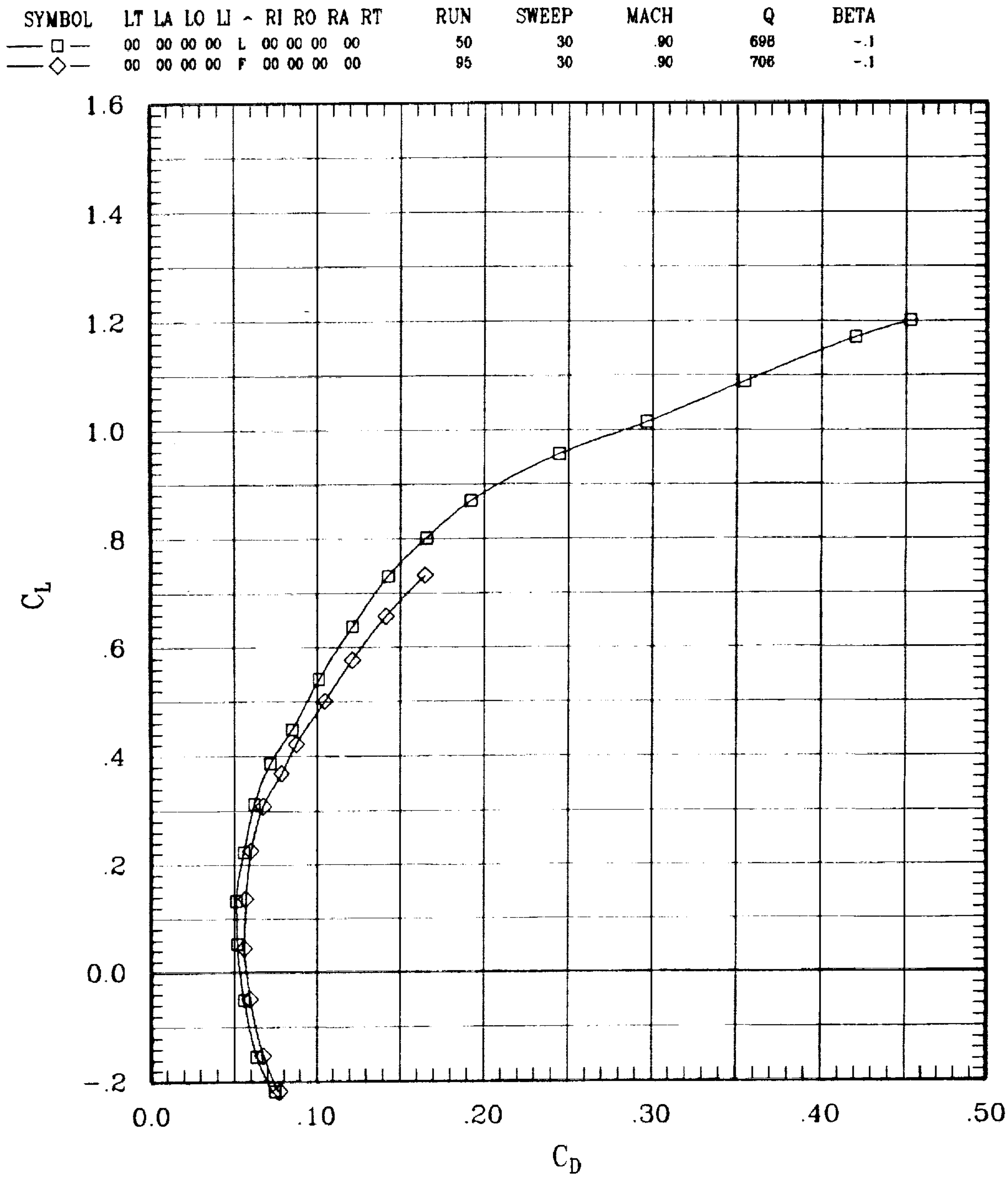

Figure 6(b). Effect of pivot height for sweep = 30 deg.

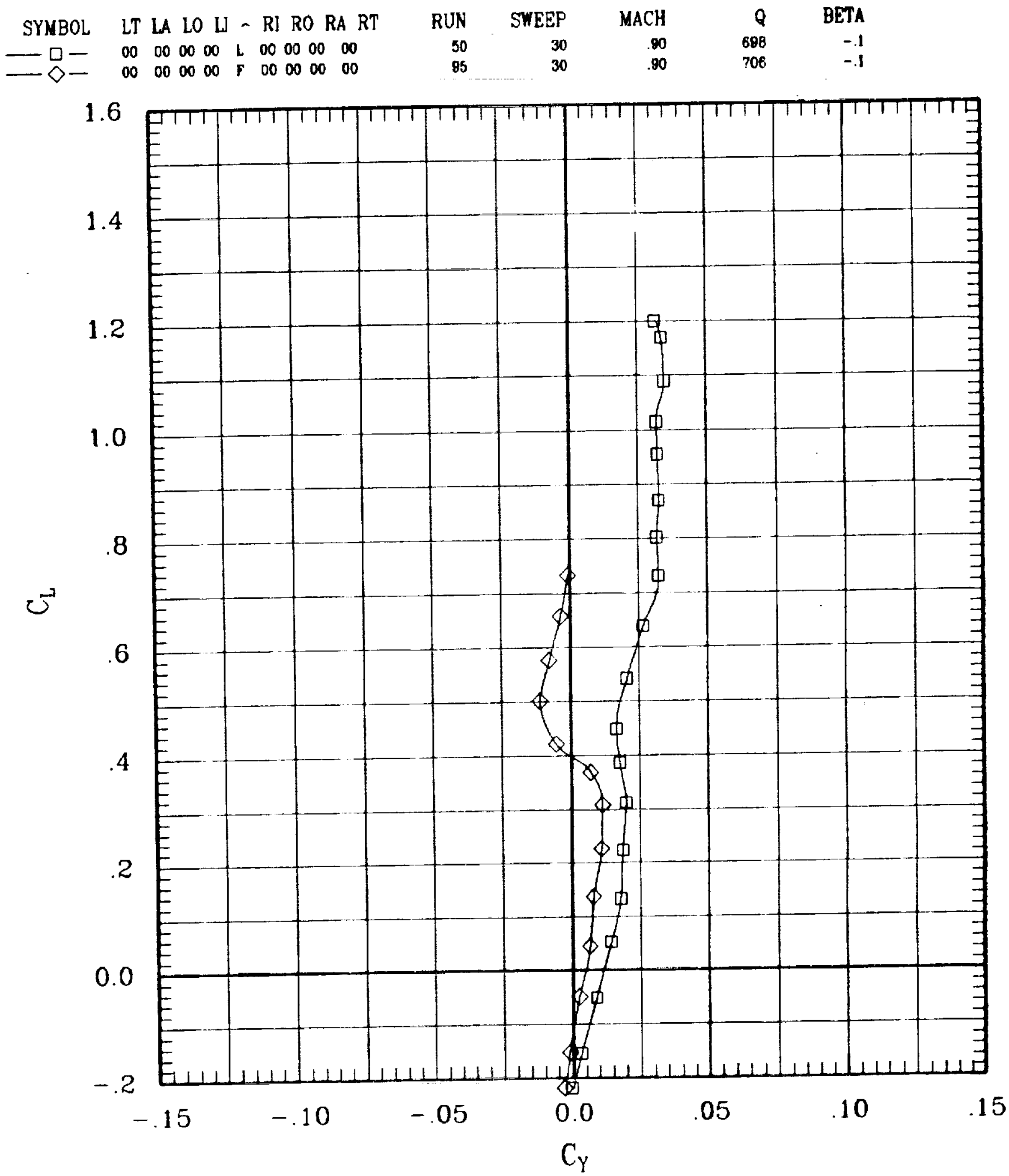

Figure 6(b). Effect of pivot height for sweep = 30 deg.

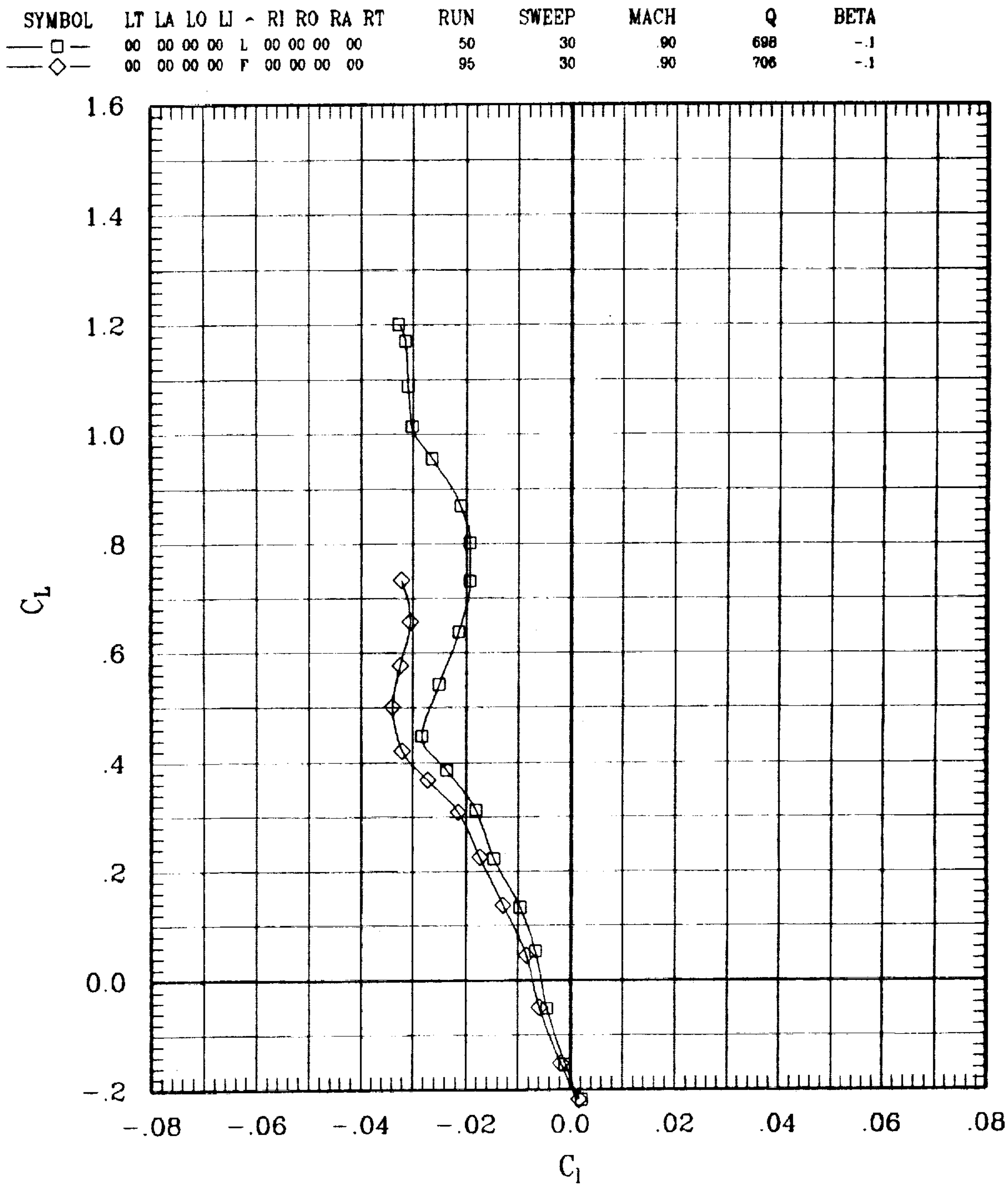

Figure 6(b). Effect of pivot height for sweep = 30 deg.

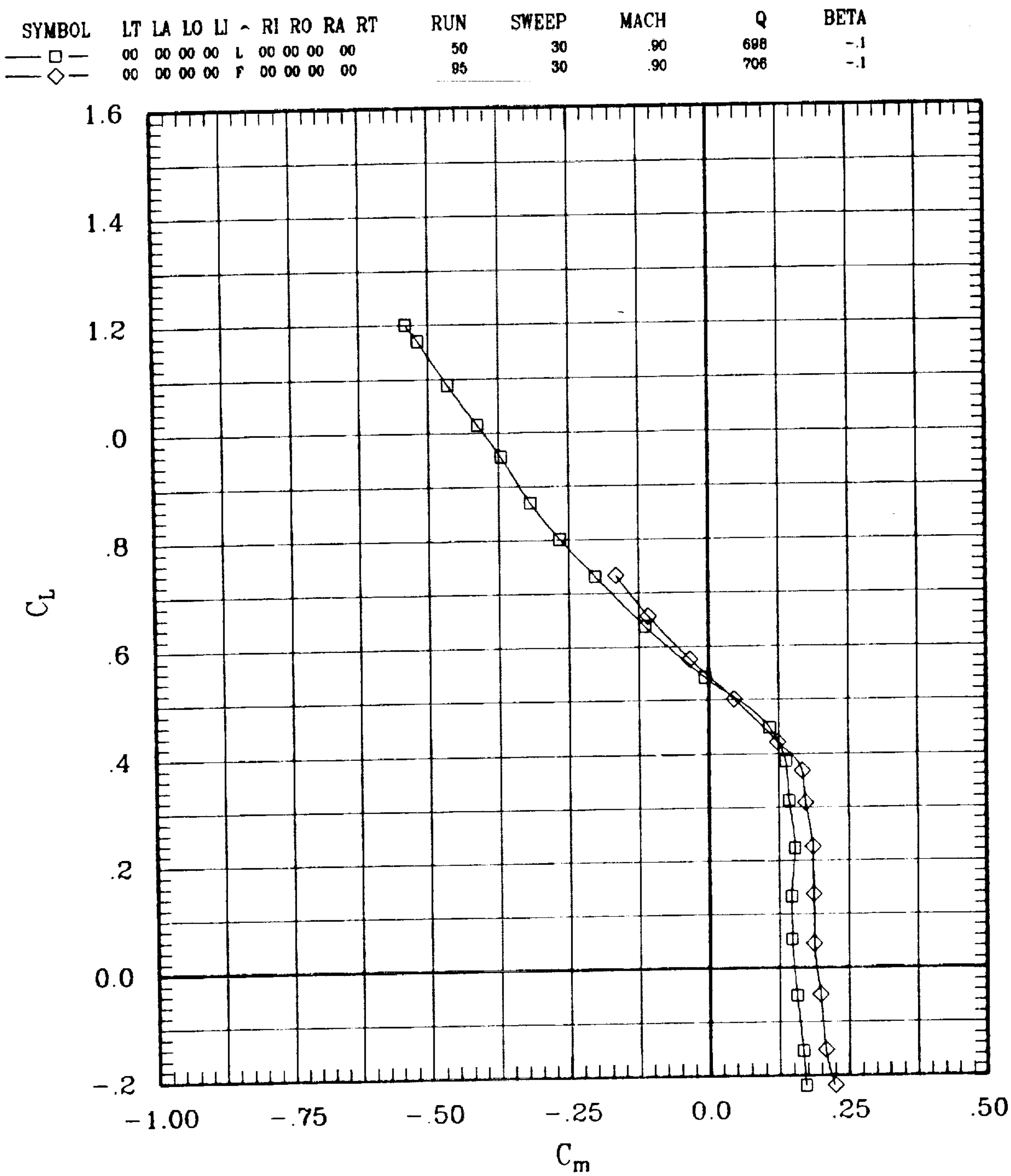

Figure 6(b). Effect of pivot height for sweep = 30 deg.

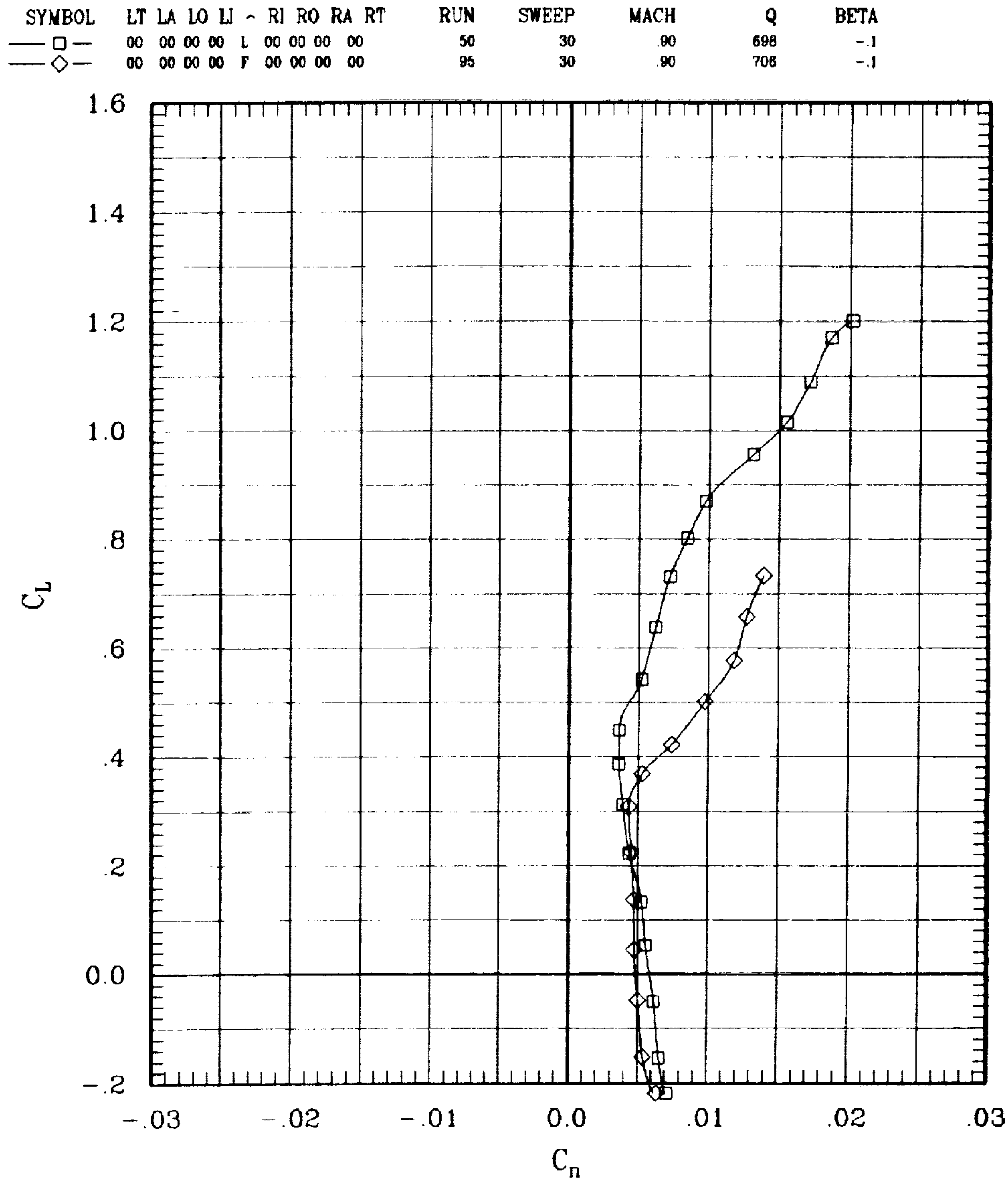

Figure 6(b). Effect of pivot height for sweep = 30 deg.

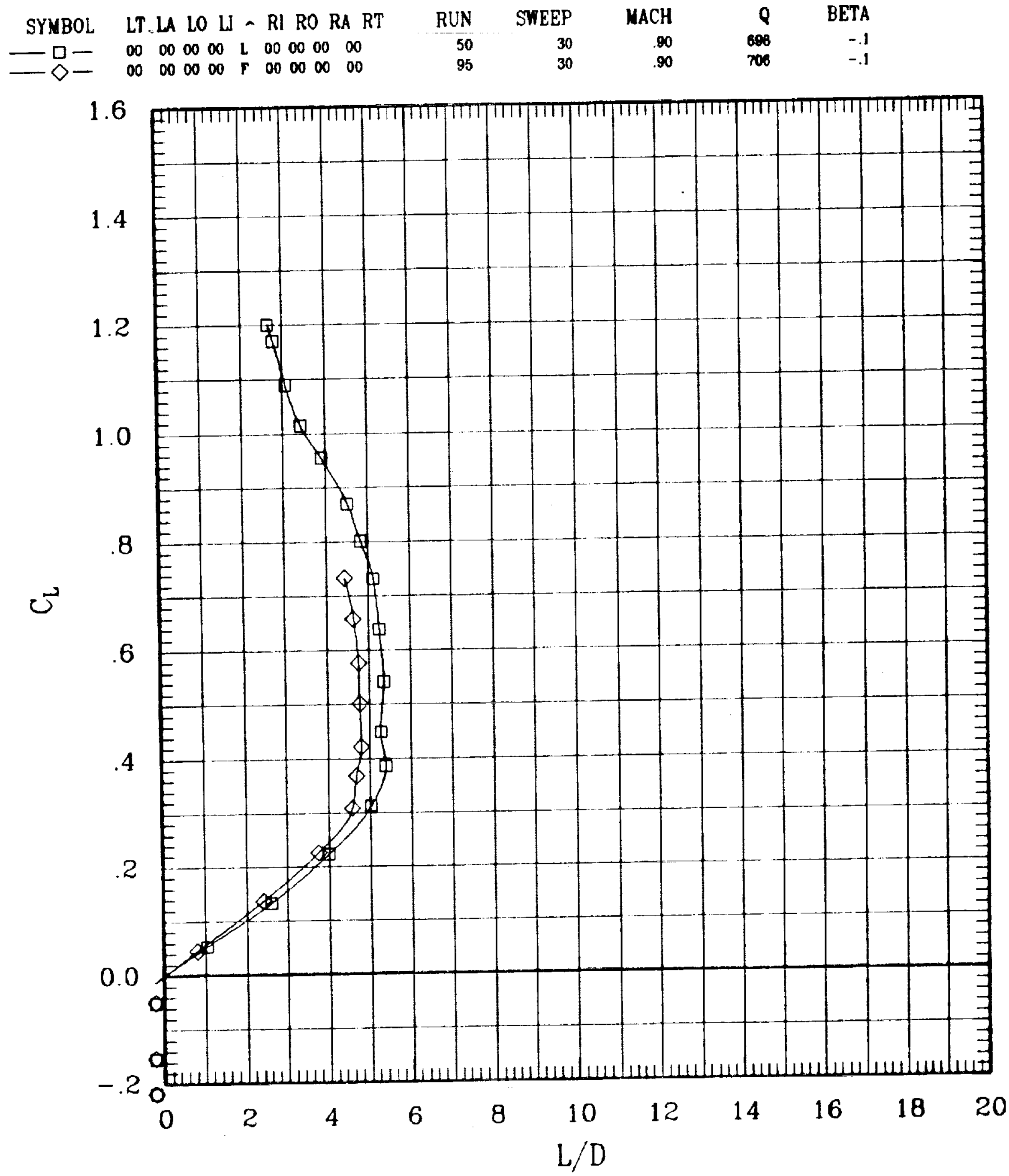

Figure 6(b). Effect of pivot height for sweep = 30 deg.

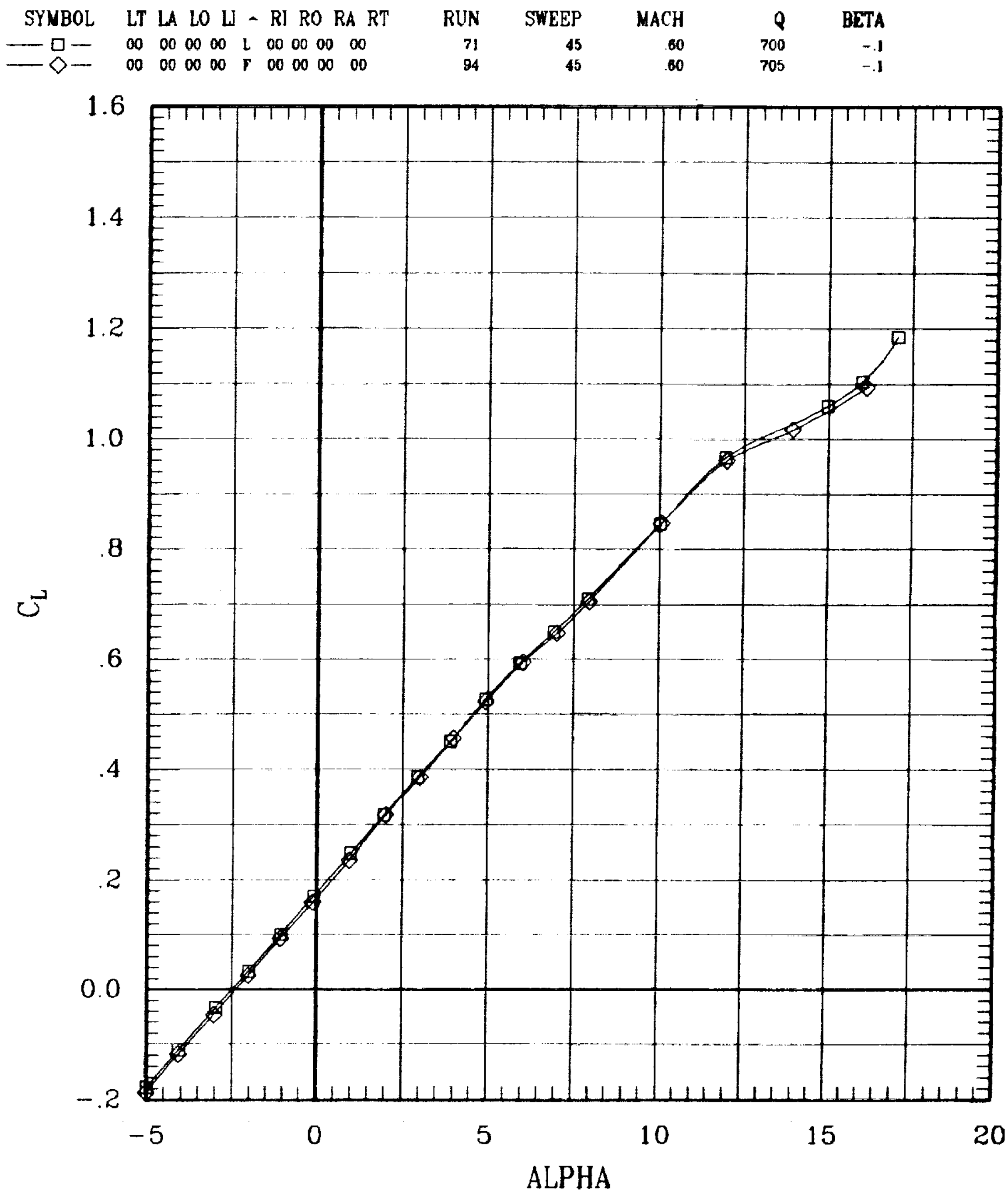

Figure 6(c). Effect of pivot height for sweep = 45 deg.

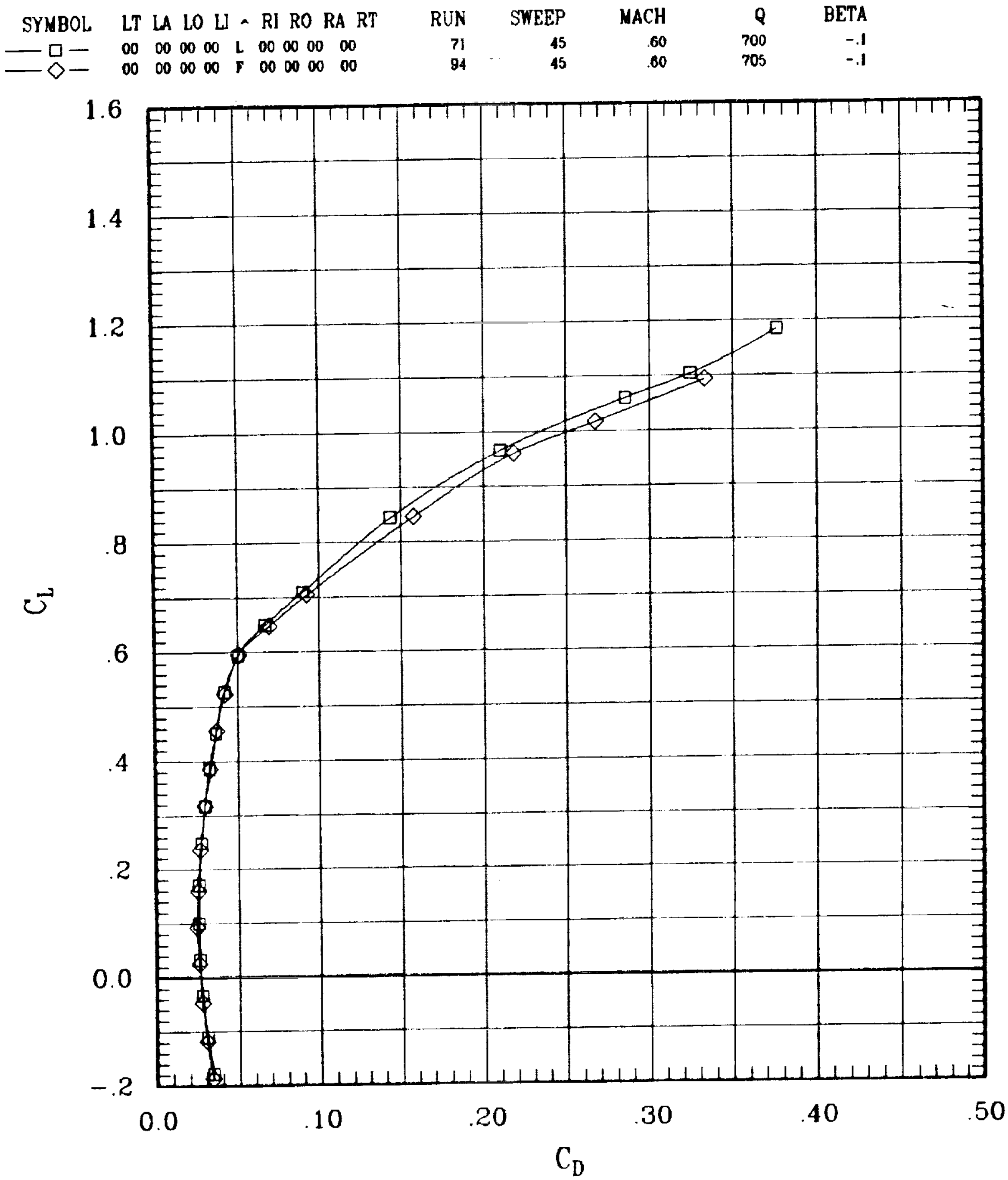

Figure 6(c). Effect of pivot height for sweep = 45 deg.

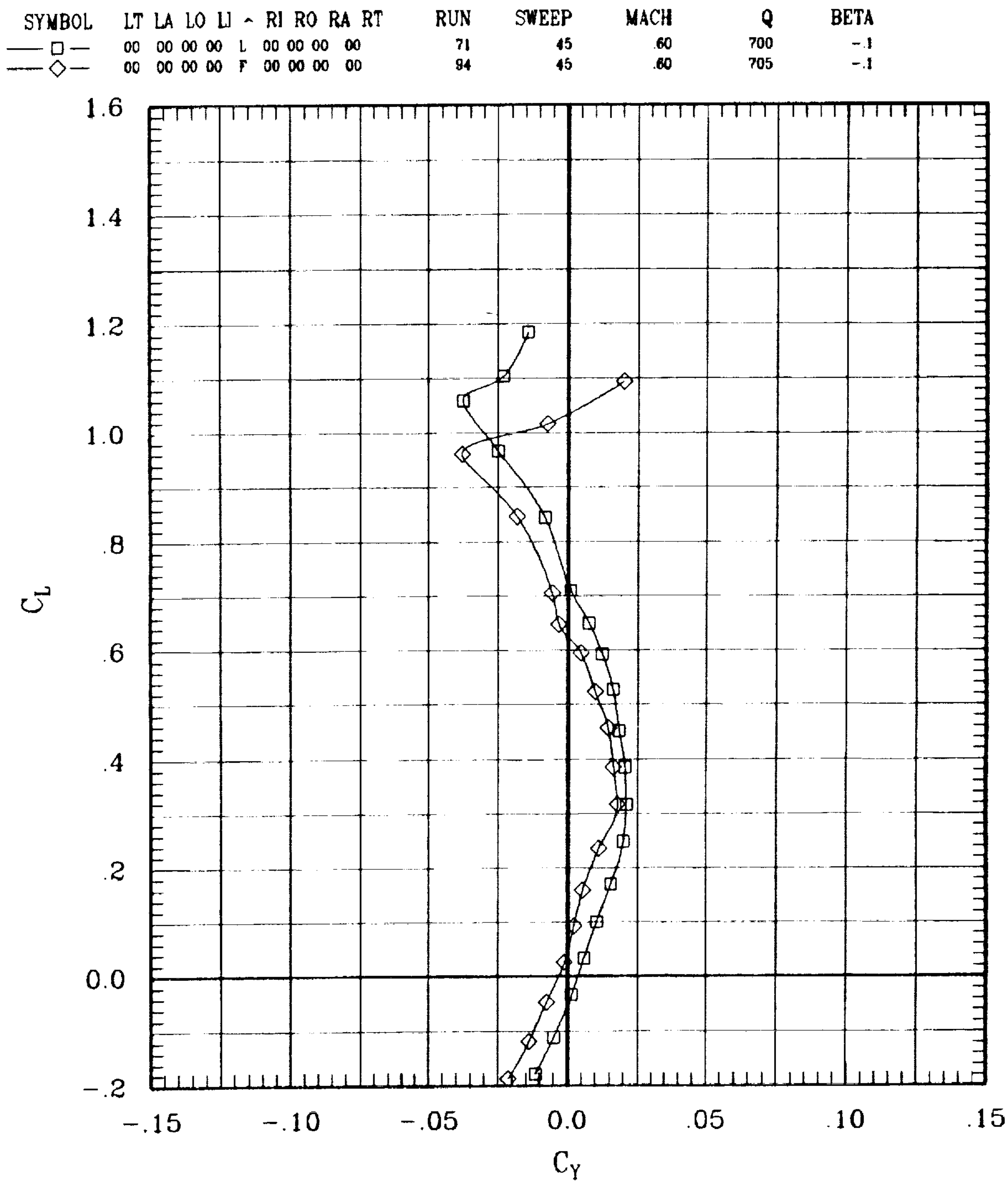

Figure 6(c). Effect of pivot height for sweep = 45 deg.

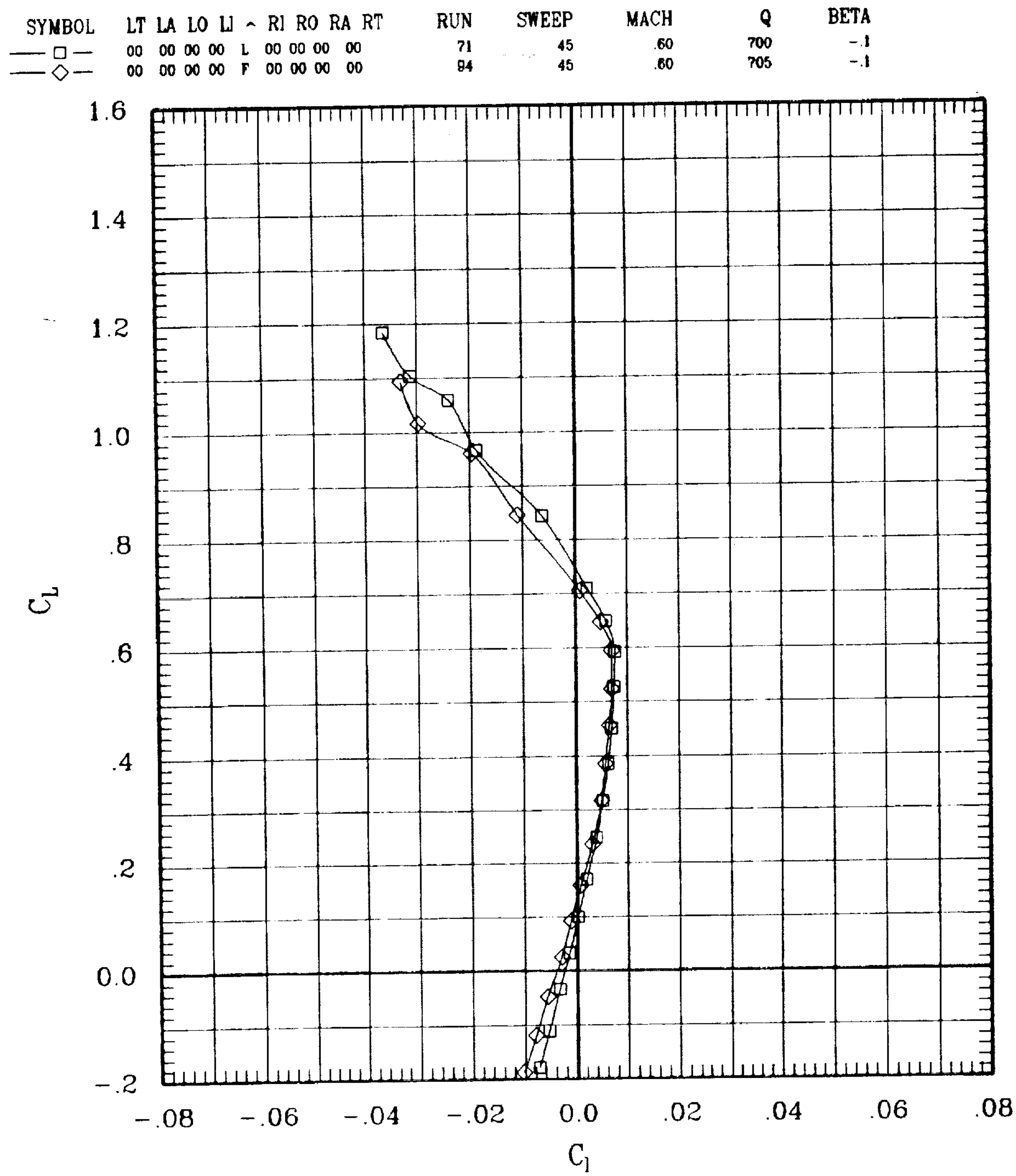

Figure 6(c). Effect of pivot height for sweep = 45 deg.

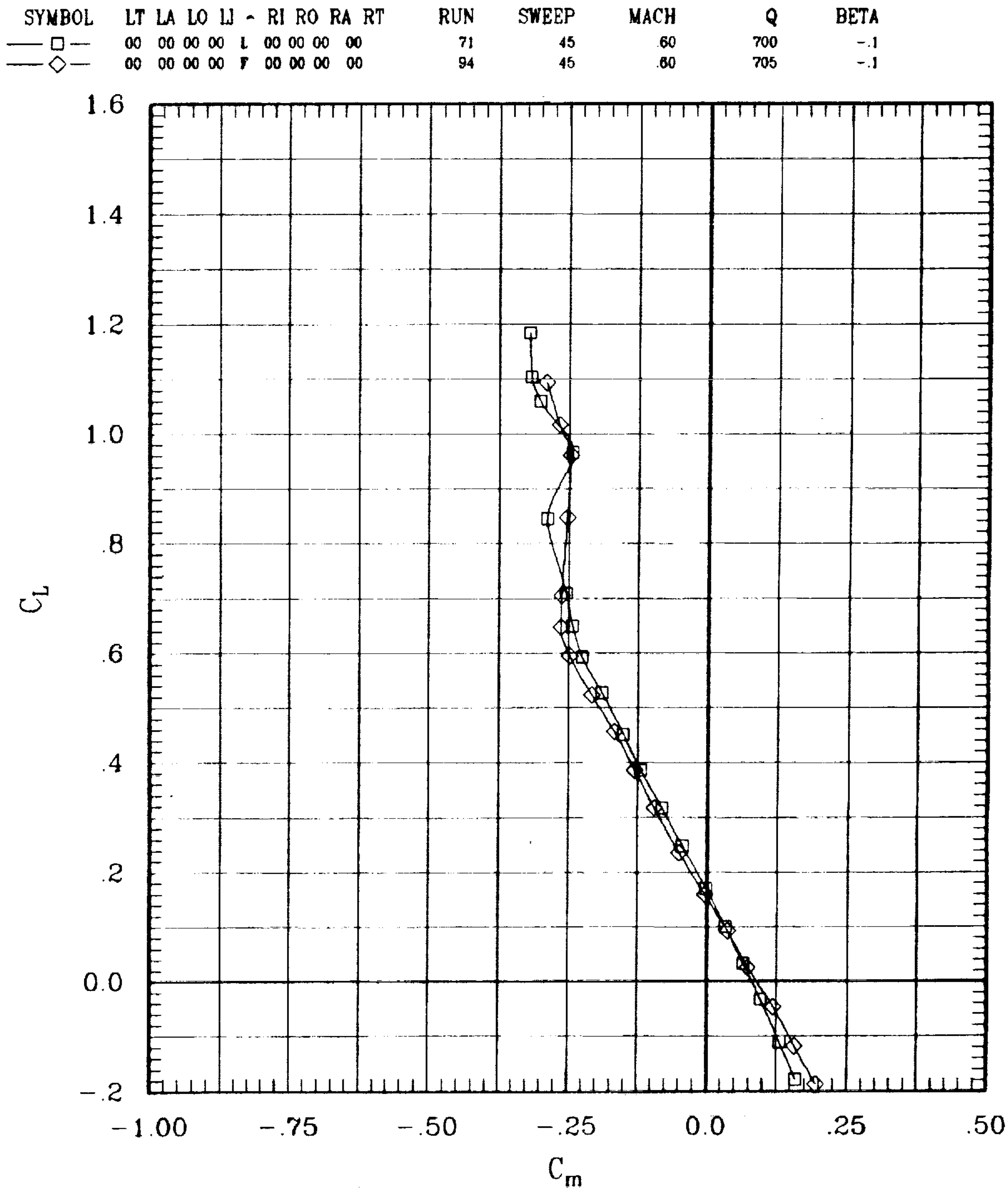

Figure 6(c). Effect of pivot height for sweep = 45 deg.

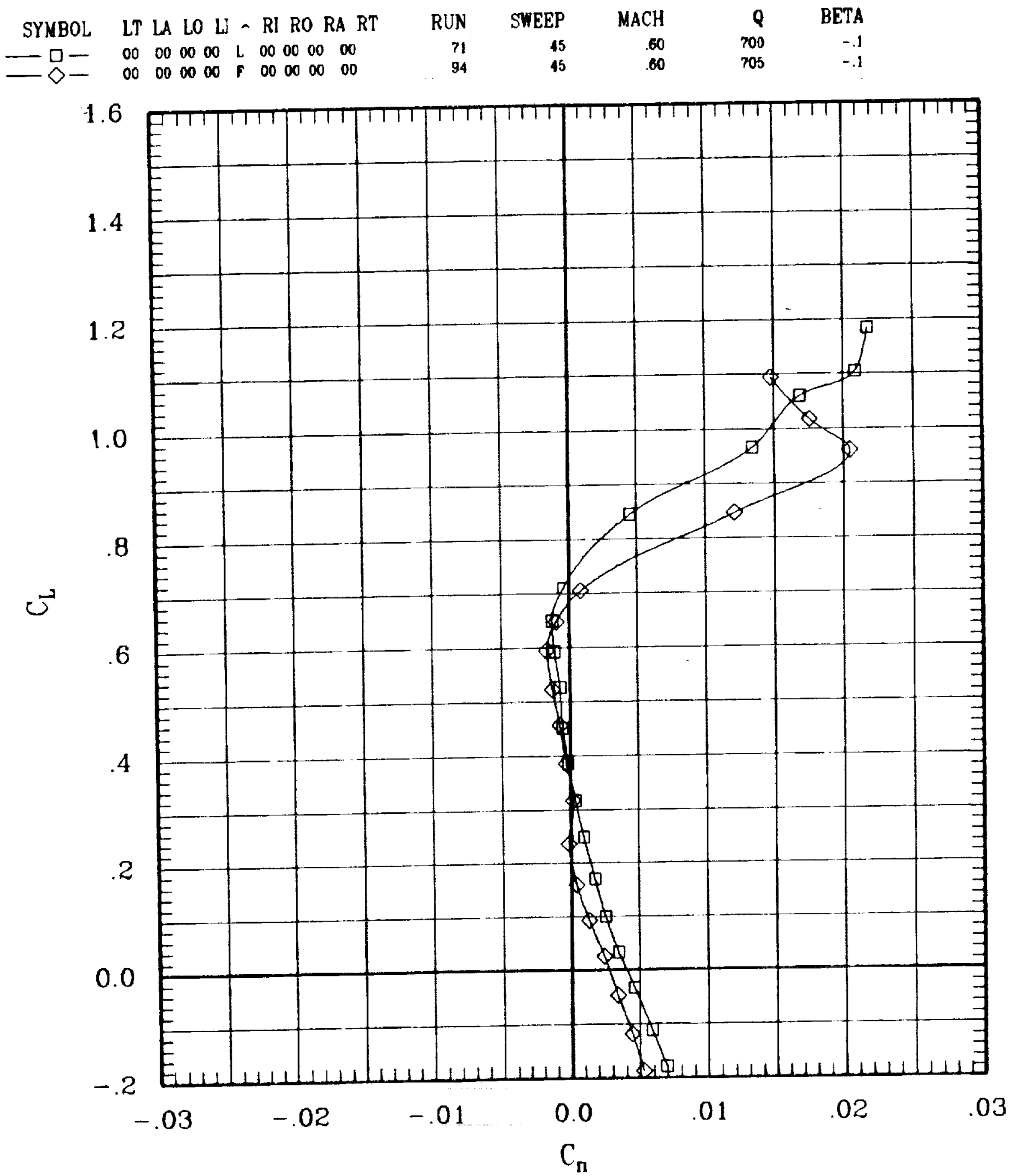

Figure 6(c). Effect of pivot height for sweep = 45 deg.

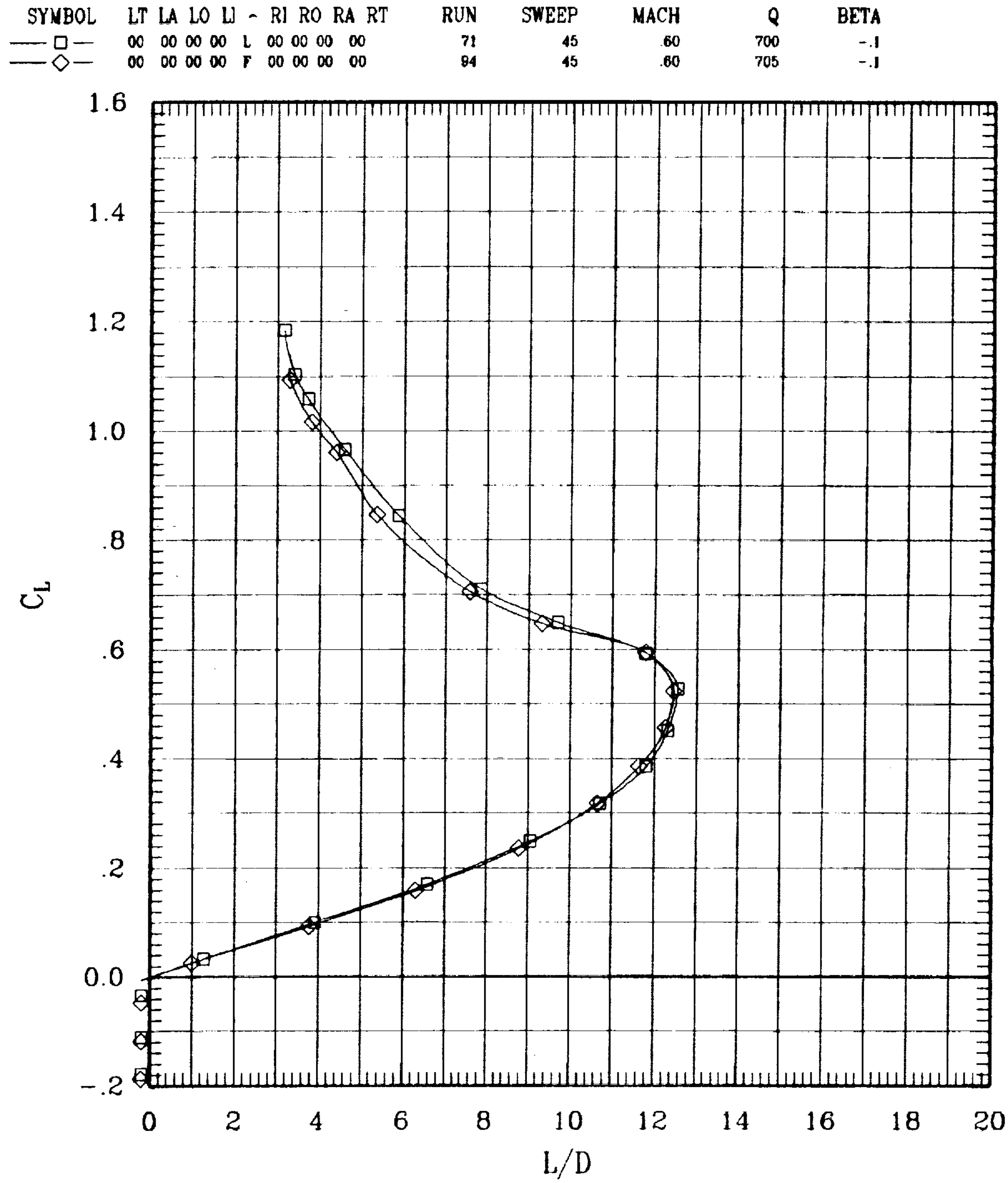

Figure 6(c). Effect of pivot height for sweep = 45 deg.

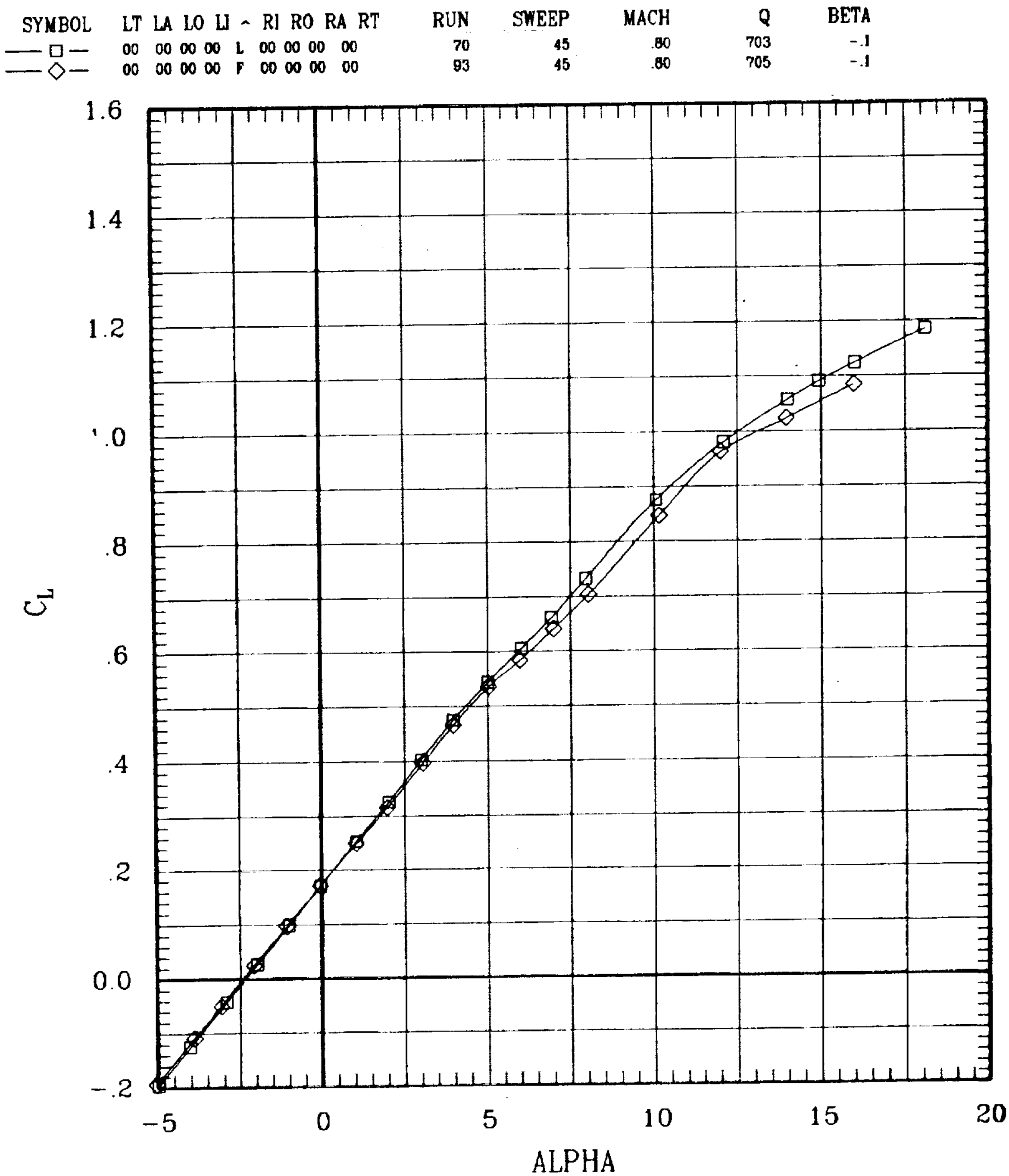

Figure 6(c). Effect of pivot height for sweep = 45 deg.

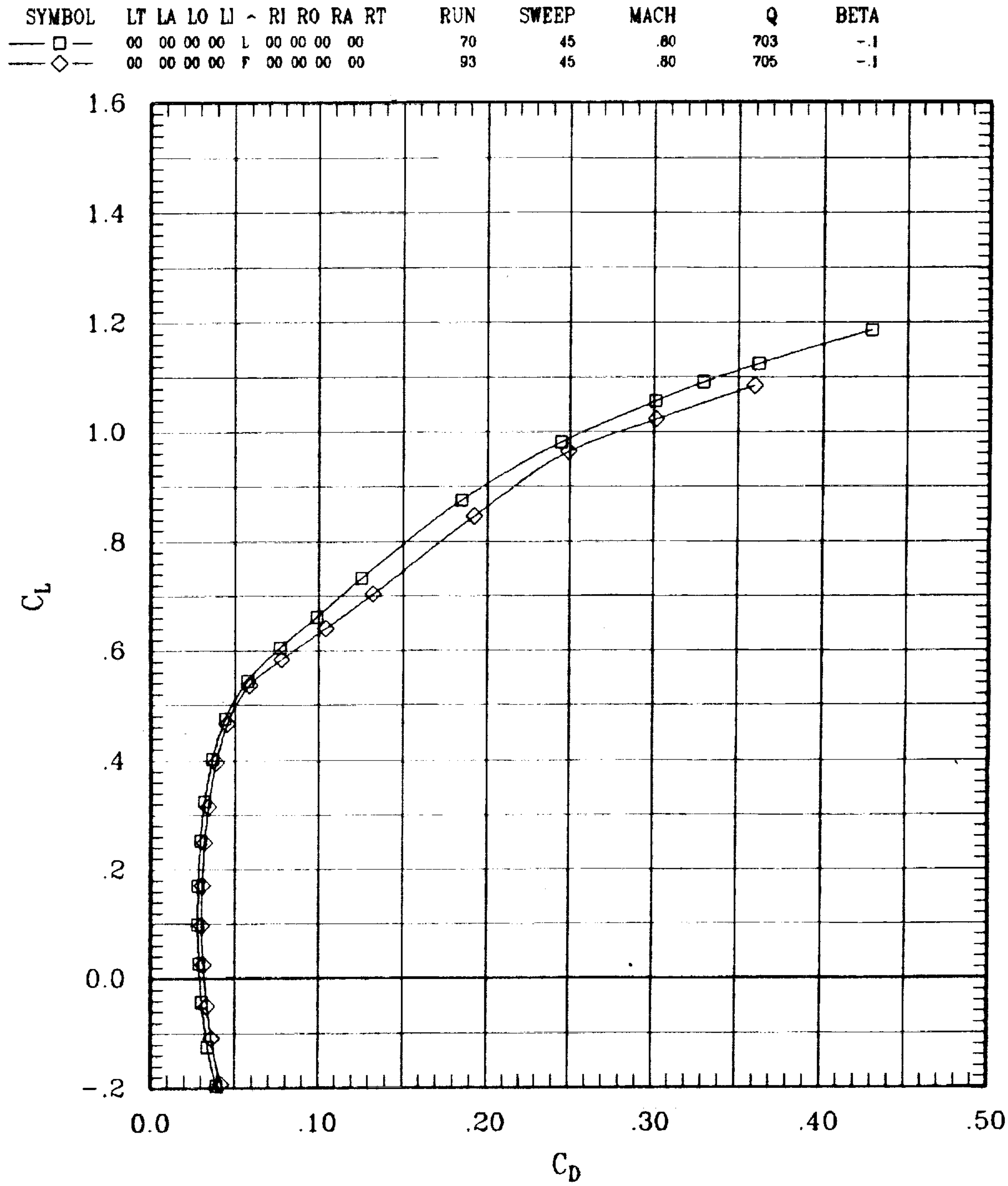

Figure 6(c). Effect of pivot height for sweep = 45 deg.

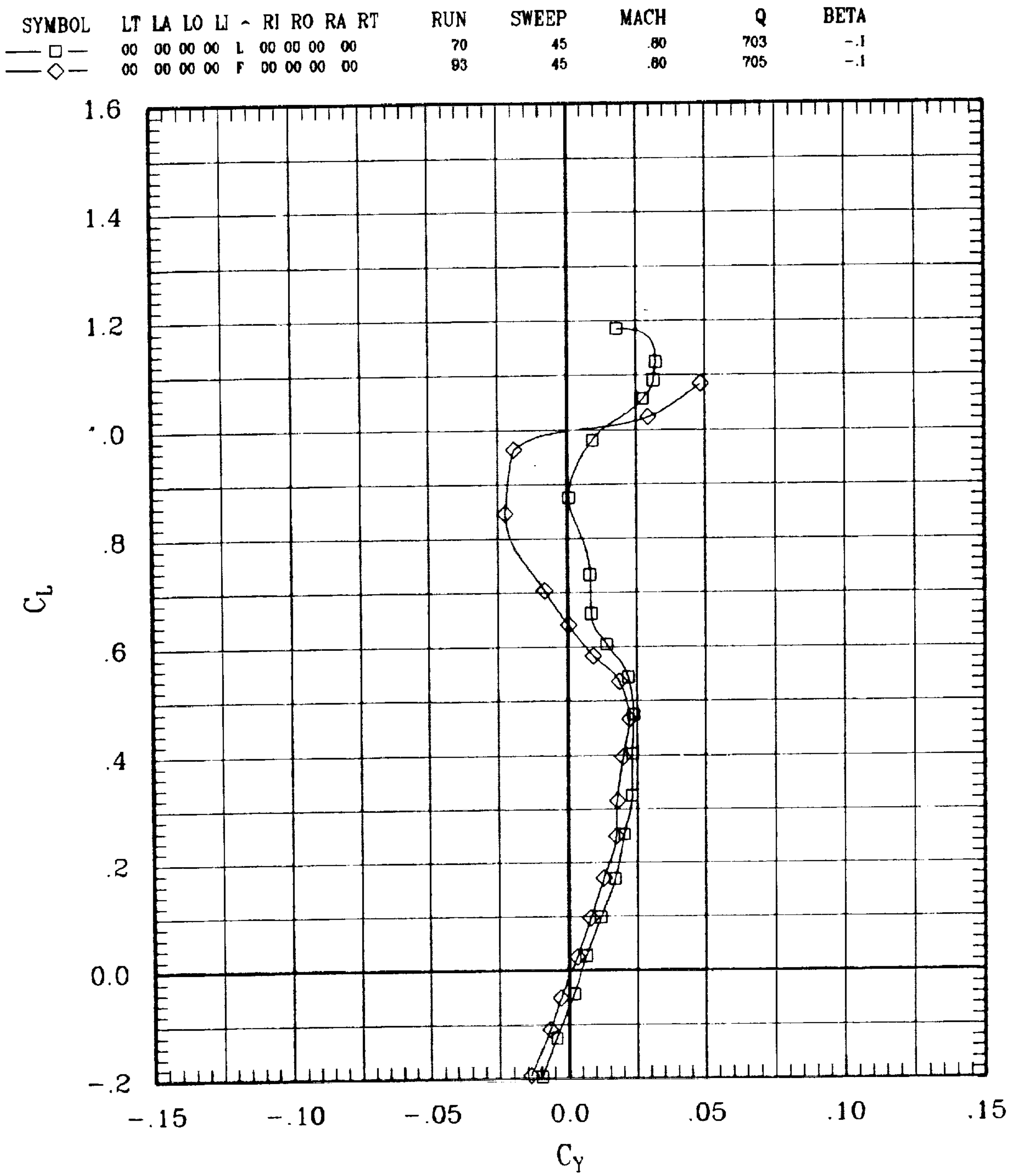

Figure 6(c). Effect of pivot height for sweep = 45 deg.

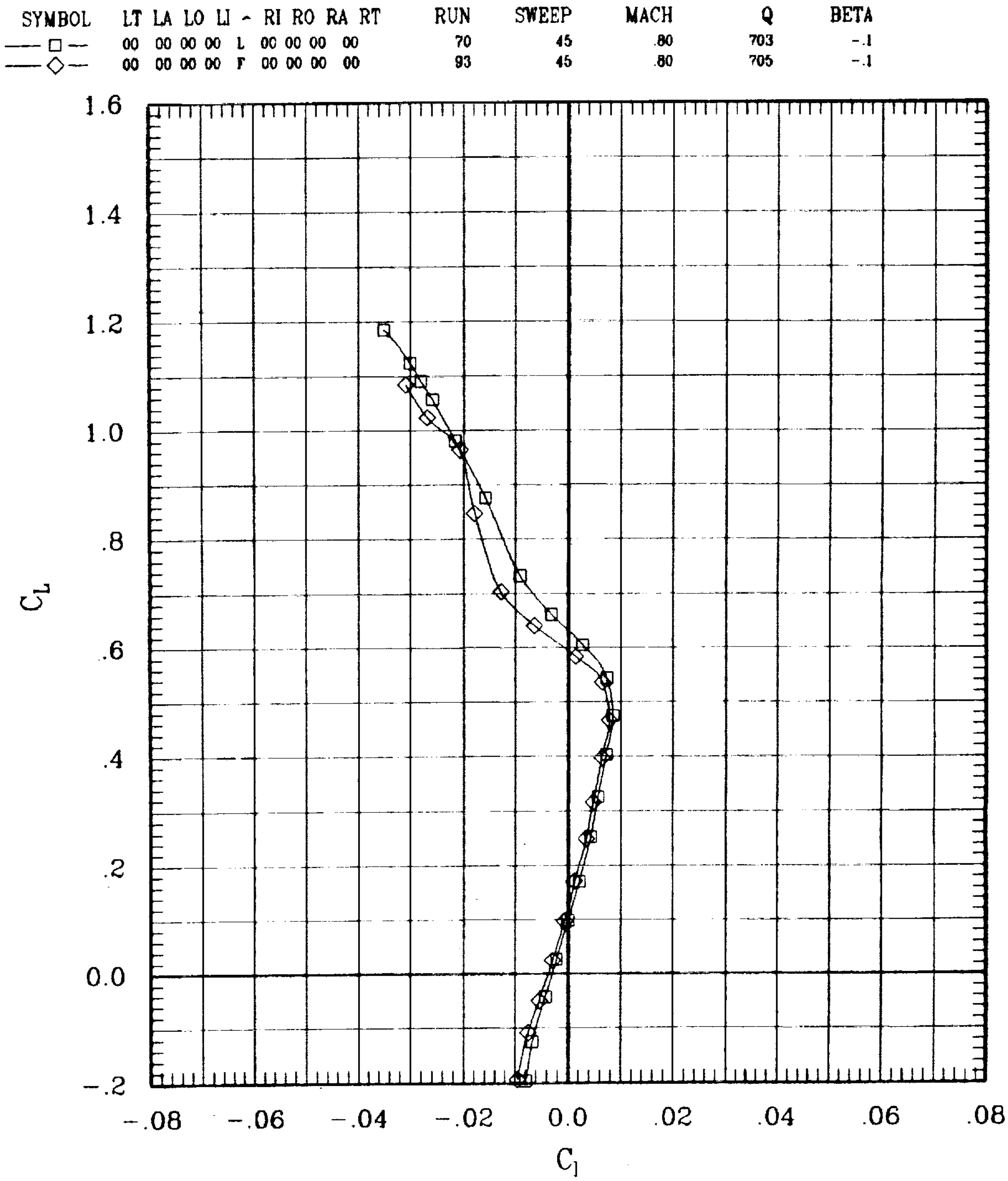

Figure 6(c). Effect of pivot height for sweep = 45 deg.

C-2

SYMBOL	LT LA LO LI - RI RO RA RT	RUN	SWEEP	MACH	Q	BETA
—□—	00 00 00 00 L 00 00 00 00	70	45	.80	703	-.1
—◇—	00 00 00 00 F 00 00 00 00	93	45	.80	705	-.1

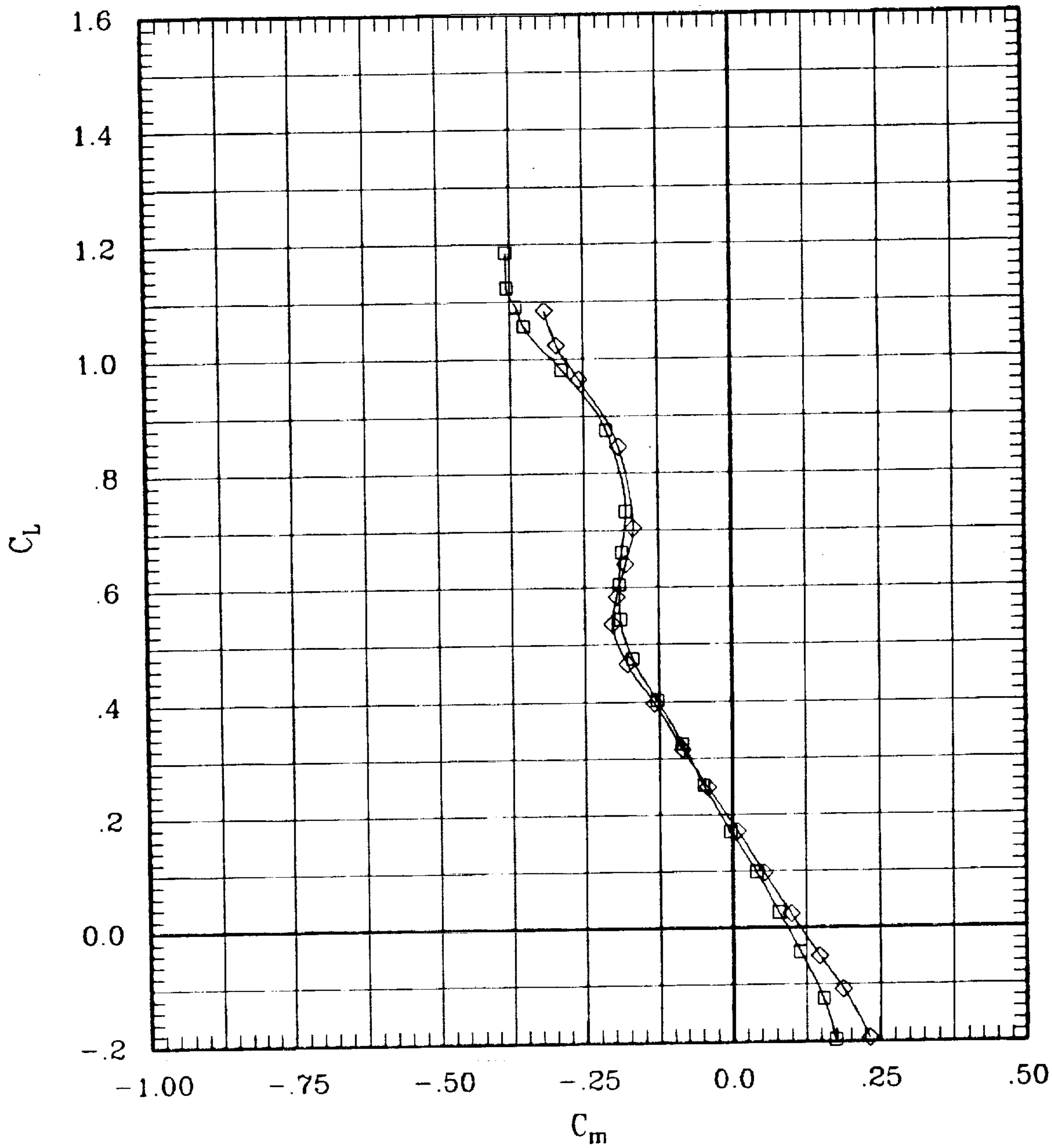

Figure 6(c). Effect of pivot height for sweep = 45 deg.

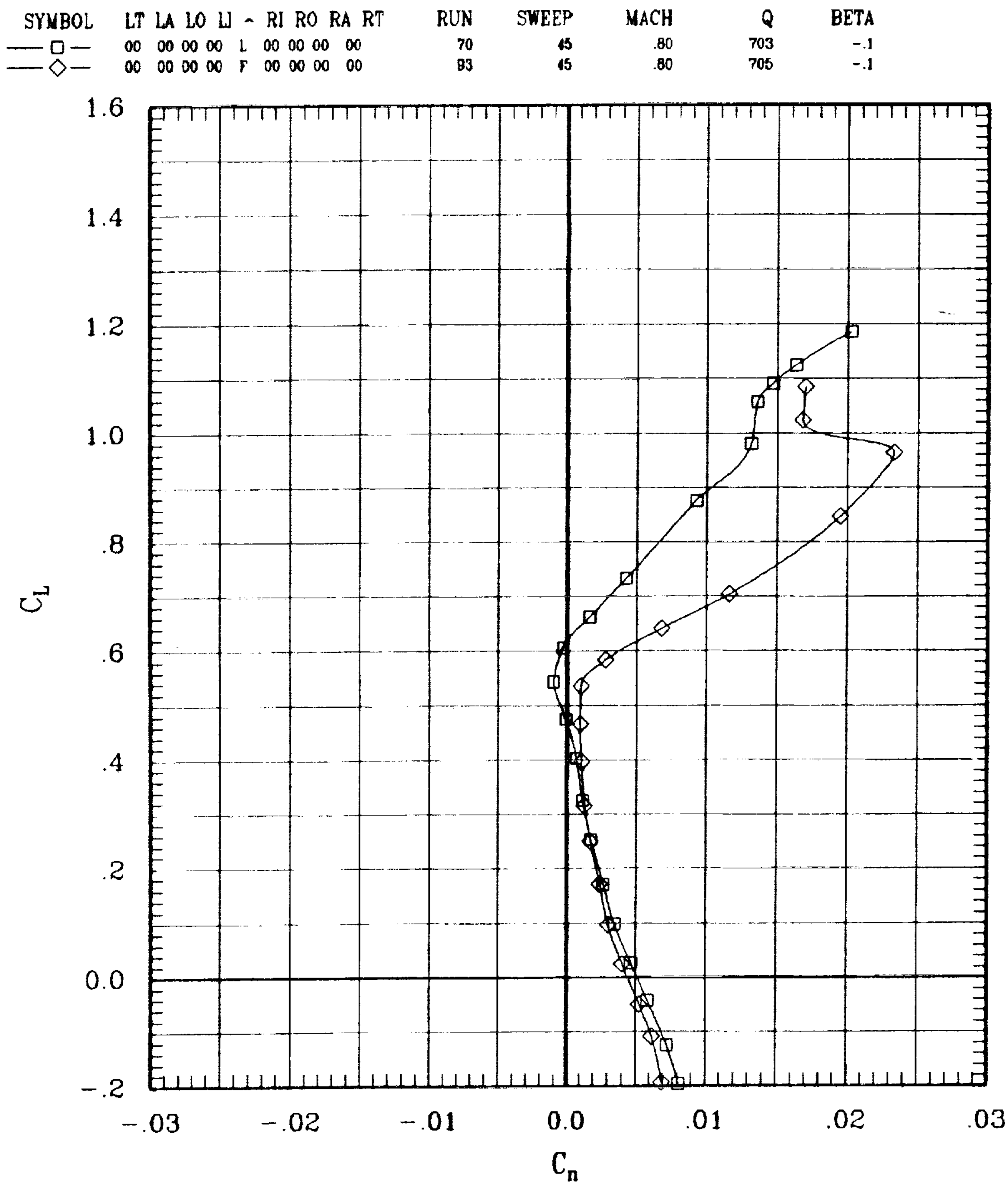

Figure 6(c). Effect of pivot height for sweep = 45 deg.

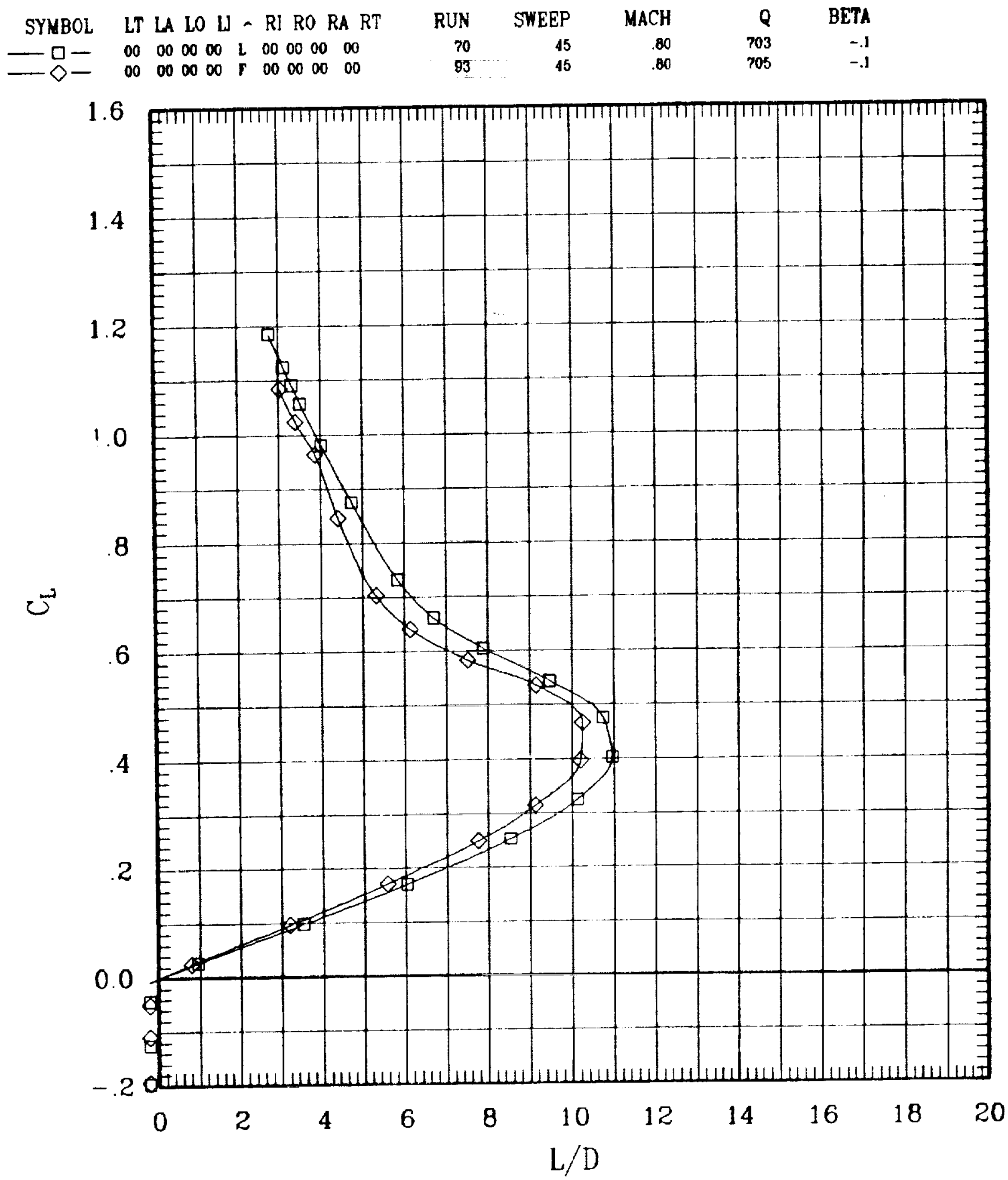

Figure 6(c). Effect of pivot height for sweep = 45 deg.

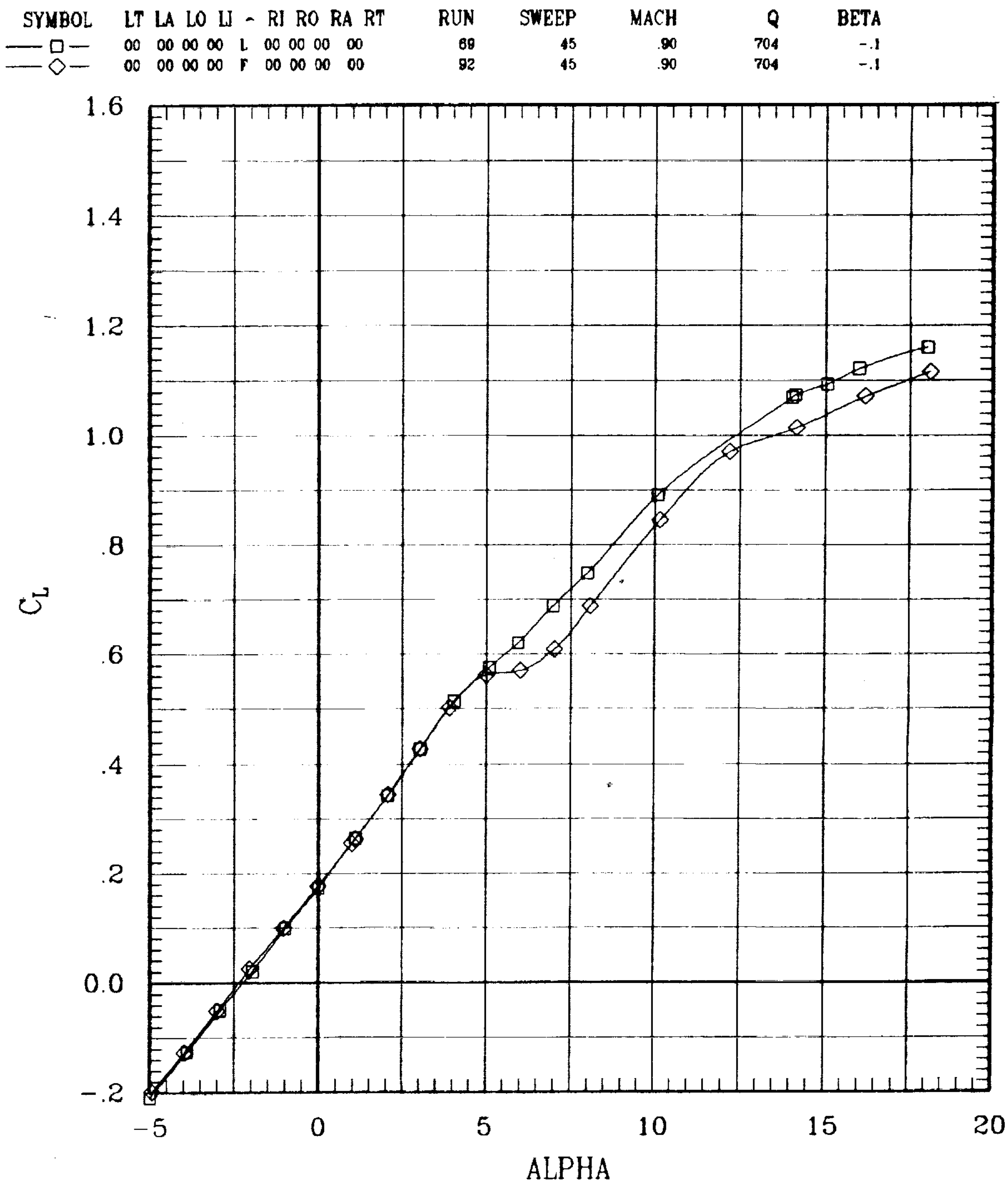

Figure 6(c). Effect of pivot height for sweep = 45 deg.

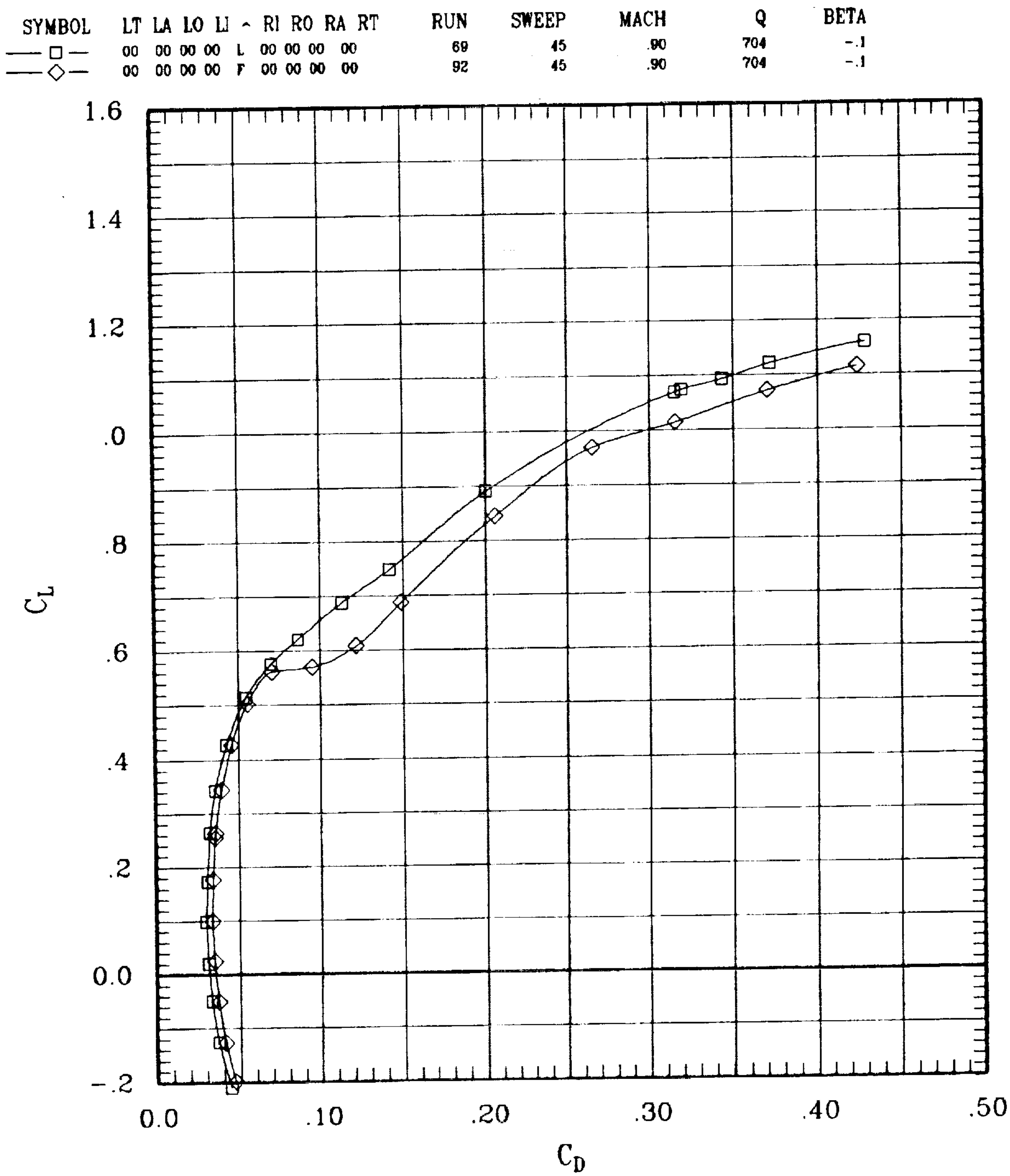

Figure 6(c). Effect of pivot height for sweep = 45 deg.

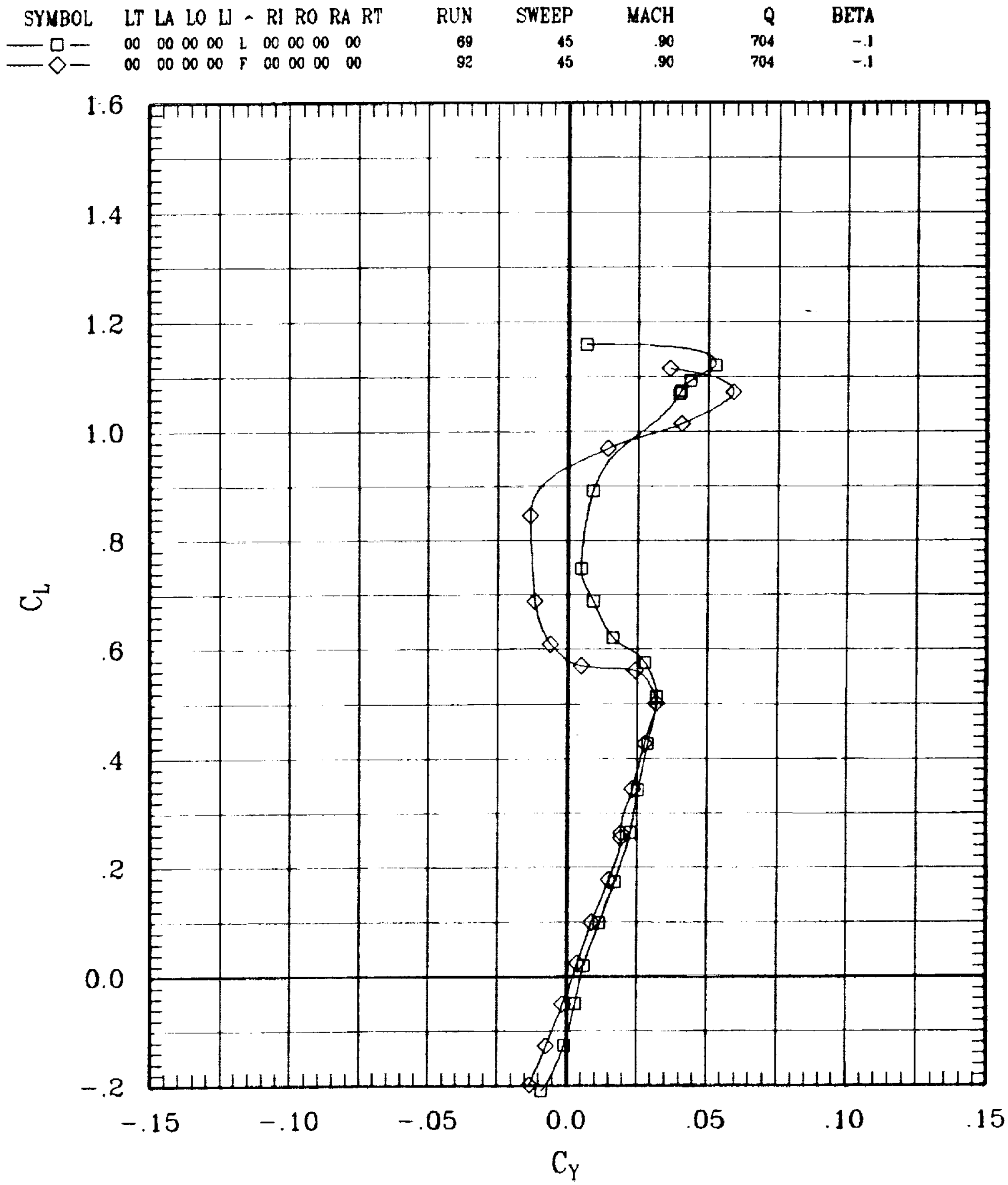

Figure 6(c). Effect of pivot height for sweep = 45 deg.

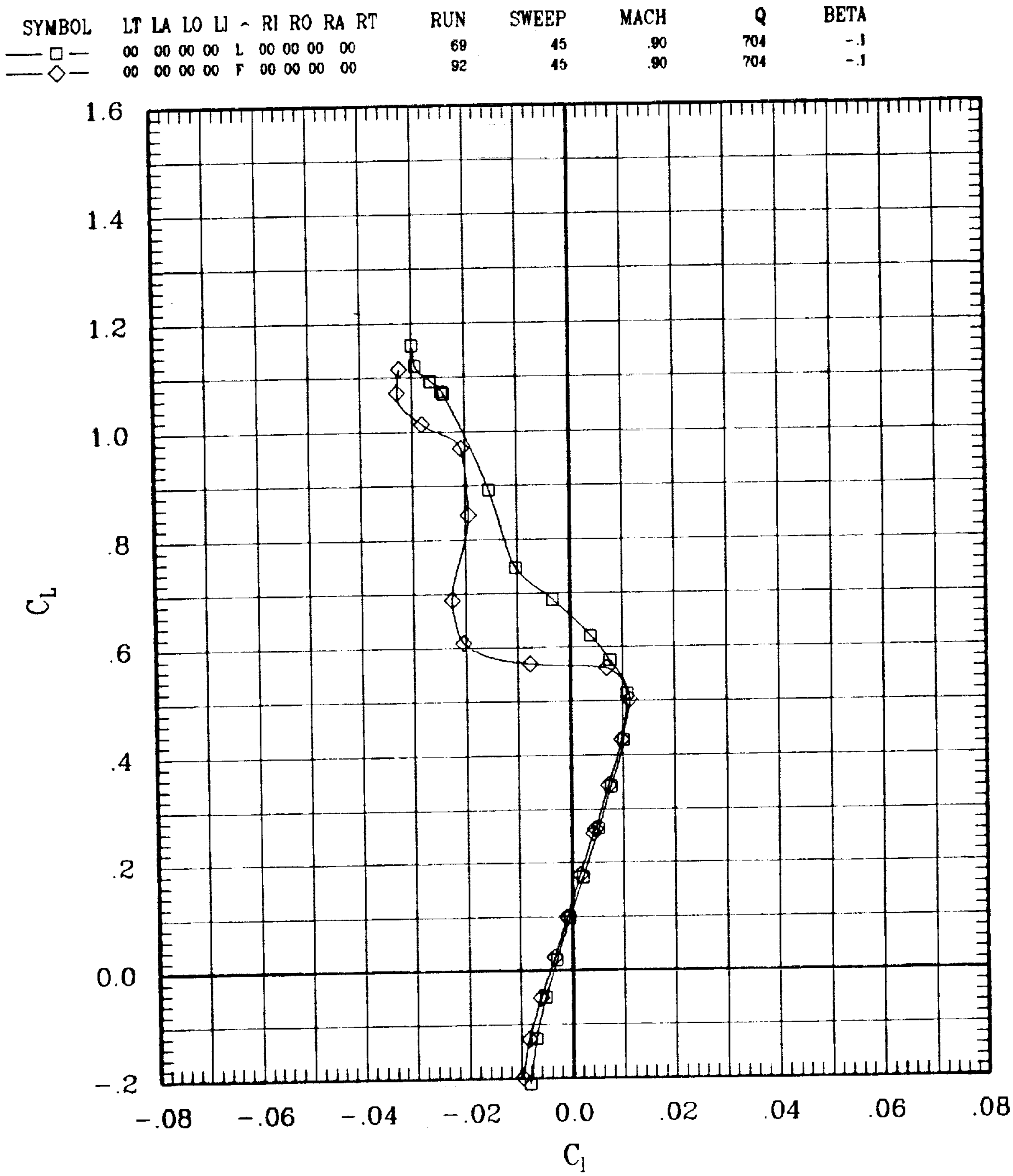

Figure 6(c). Effect of pivot height for sweep = 45 deg.

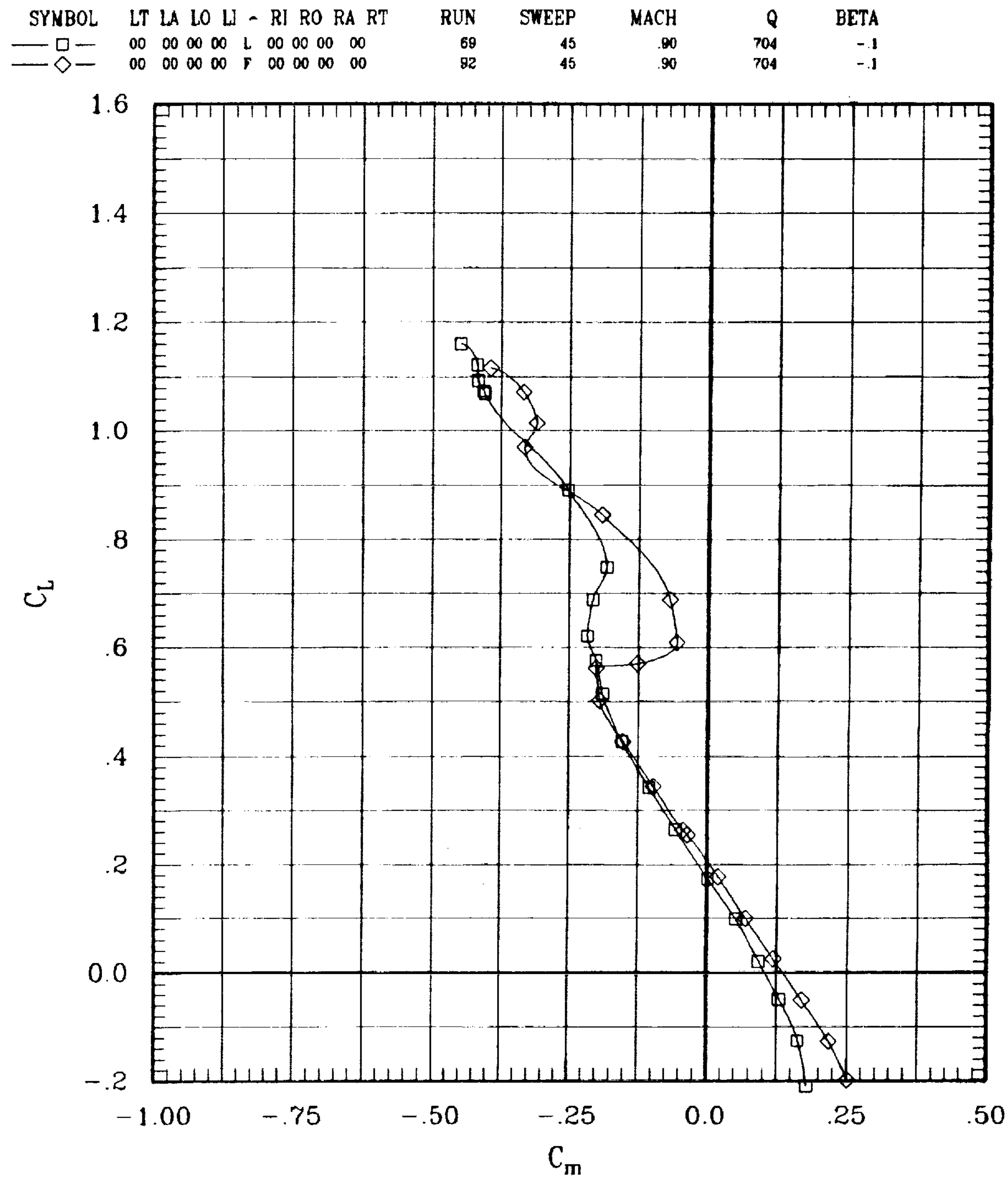

Figure 6(c). Effect of pivot height for sweep = 45 deg.

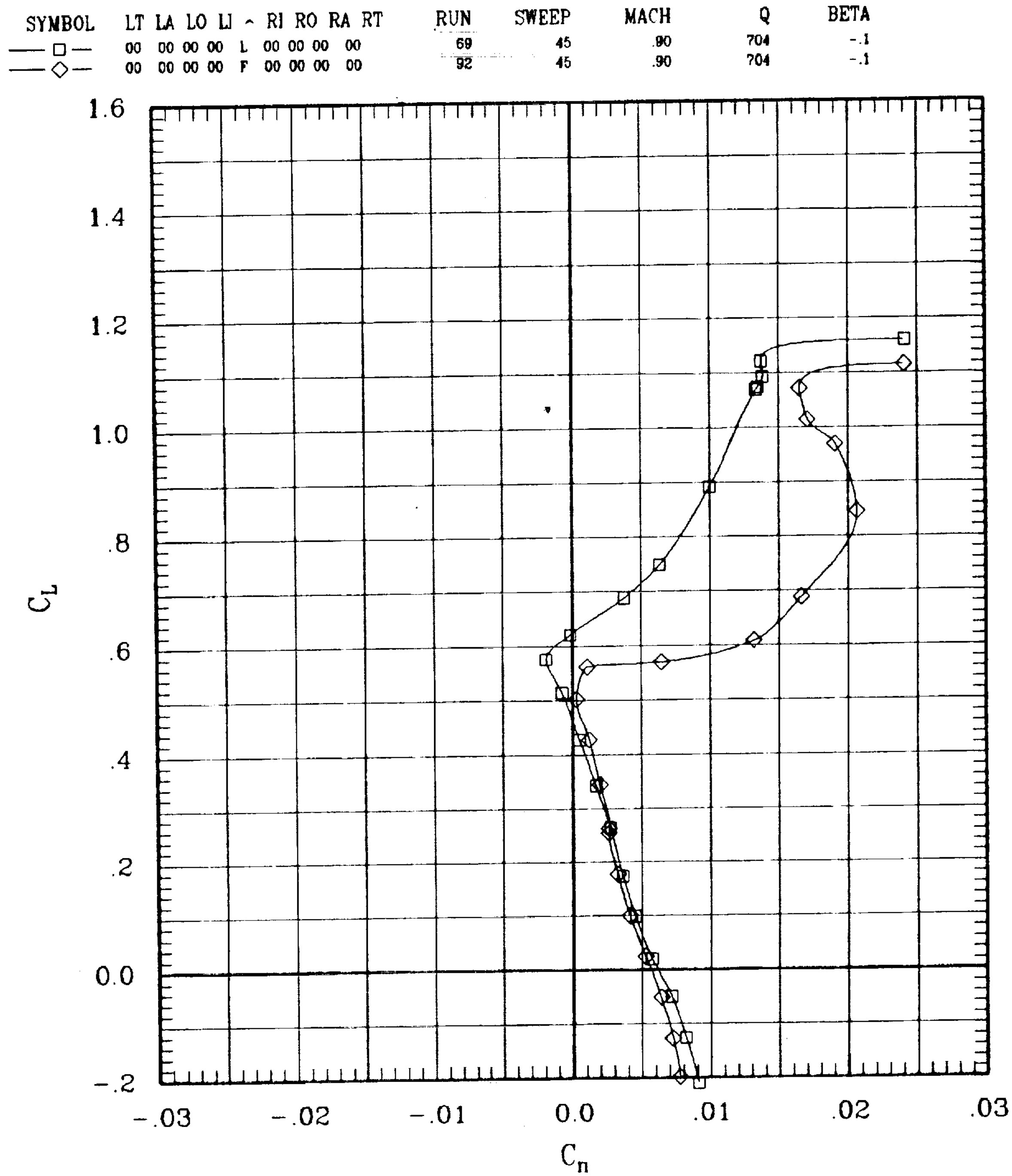

Figure 6(c). Effect of pivot height for sweep = 45 deg.

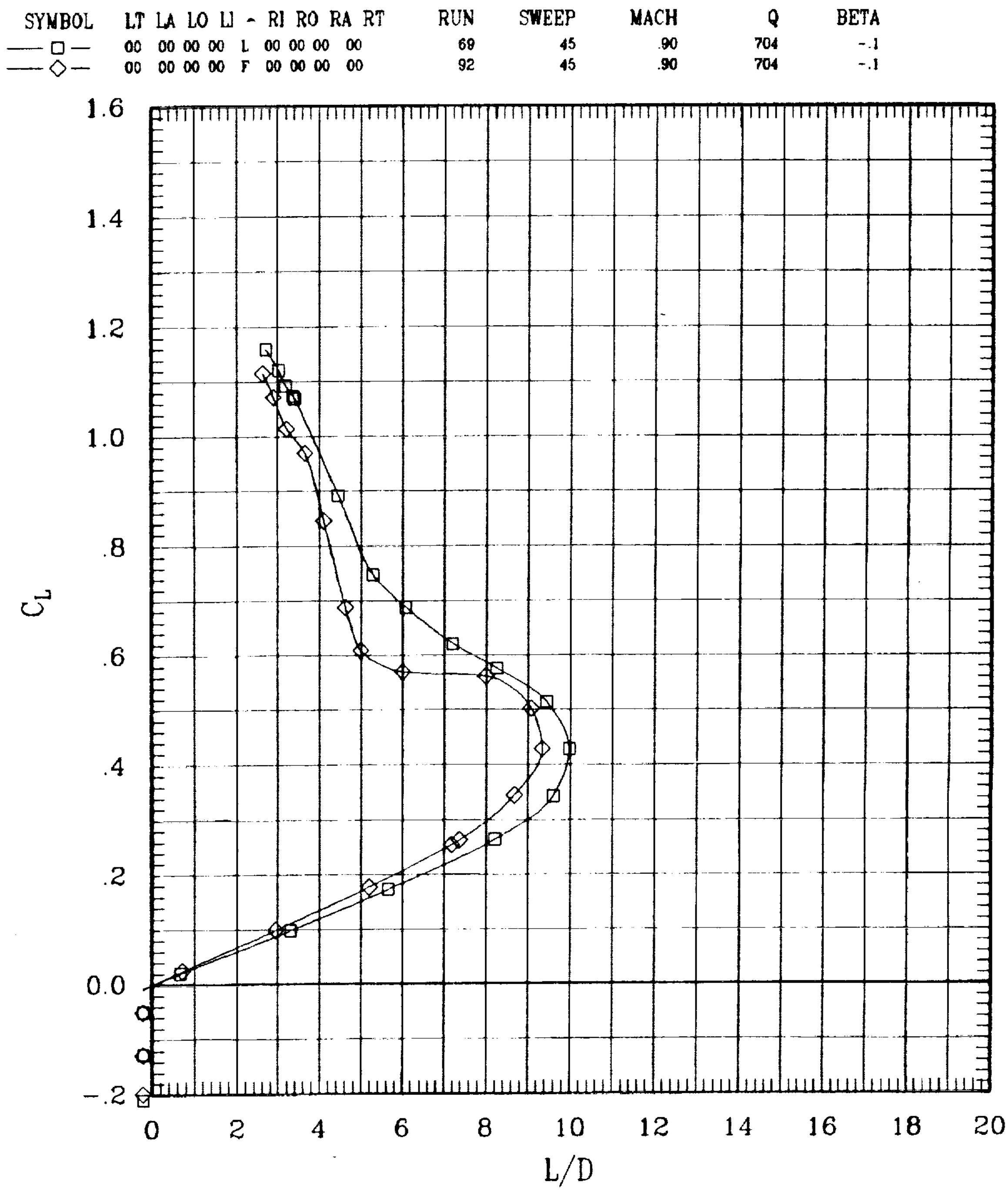

Figure 6(c). Effect of pivot height for sweep = 45 deg.

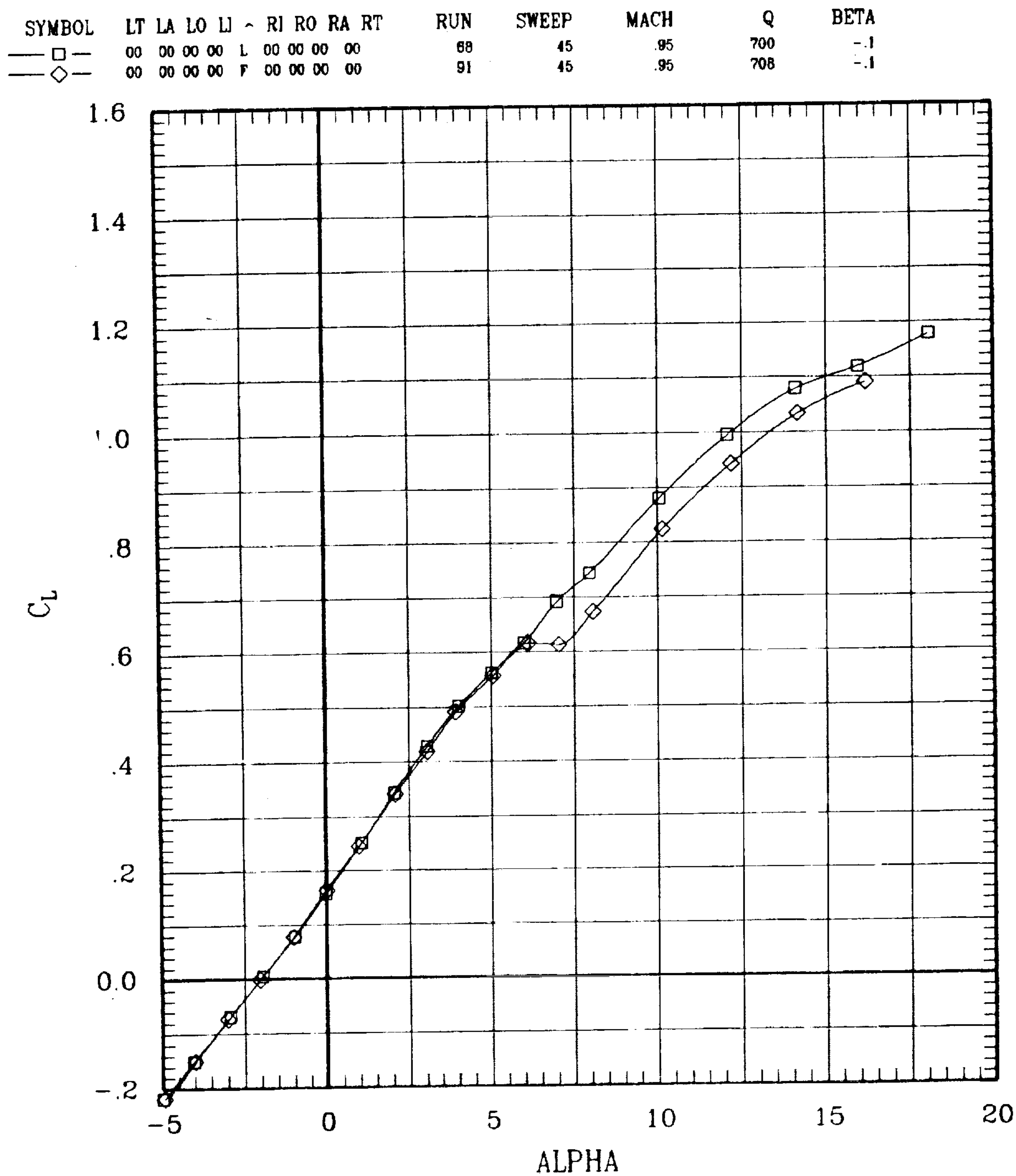

Figure 6(c). Effect of pivot height for sweep = 45 deg.

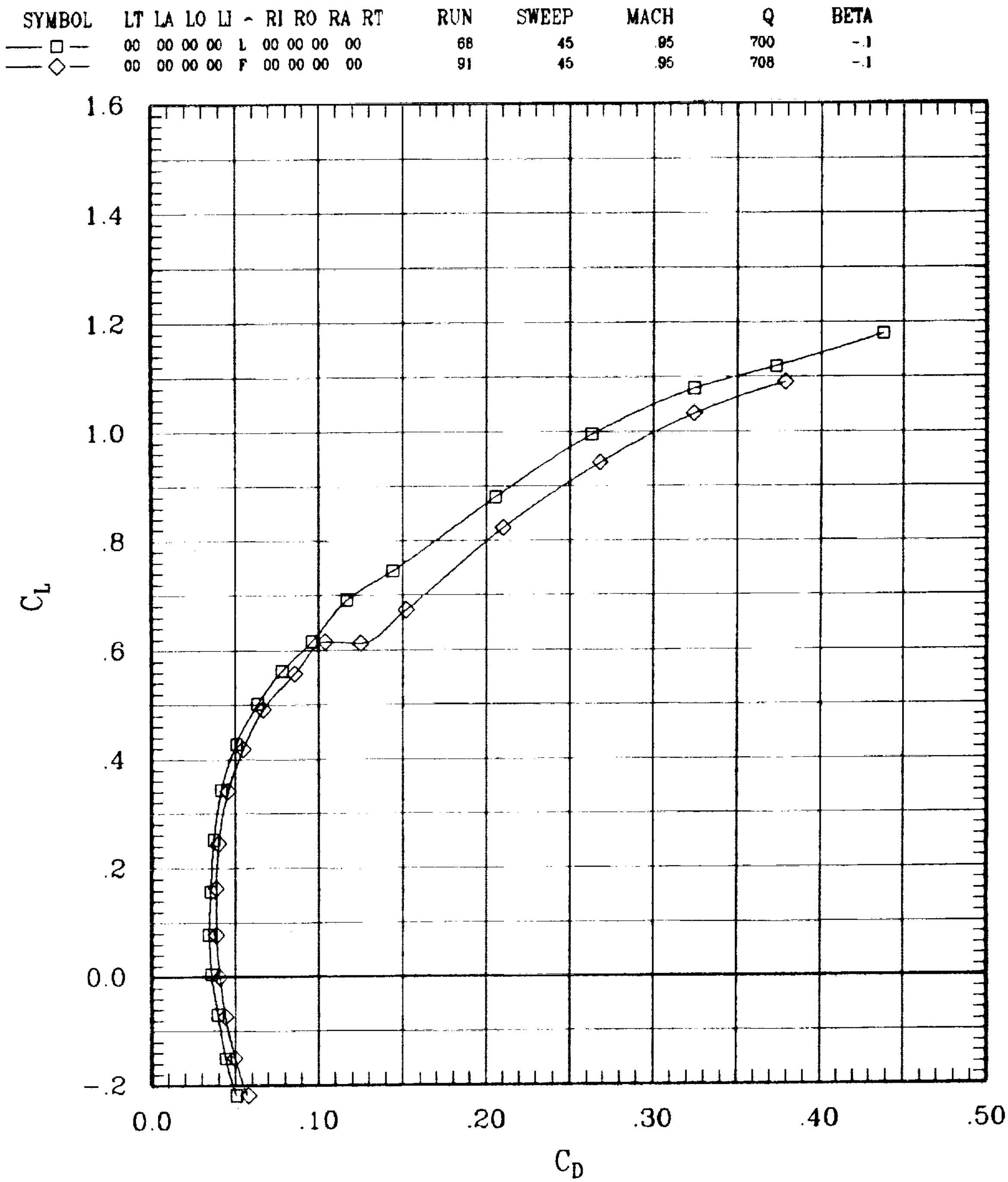

Figure 6(c). Effect of pivot height for sweep = 45 deg.

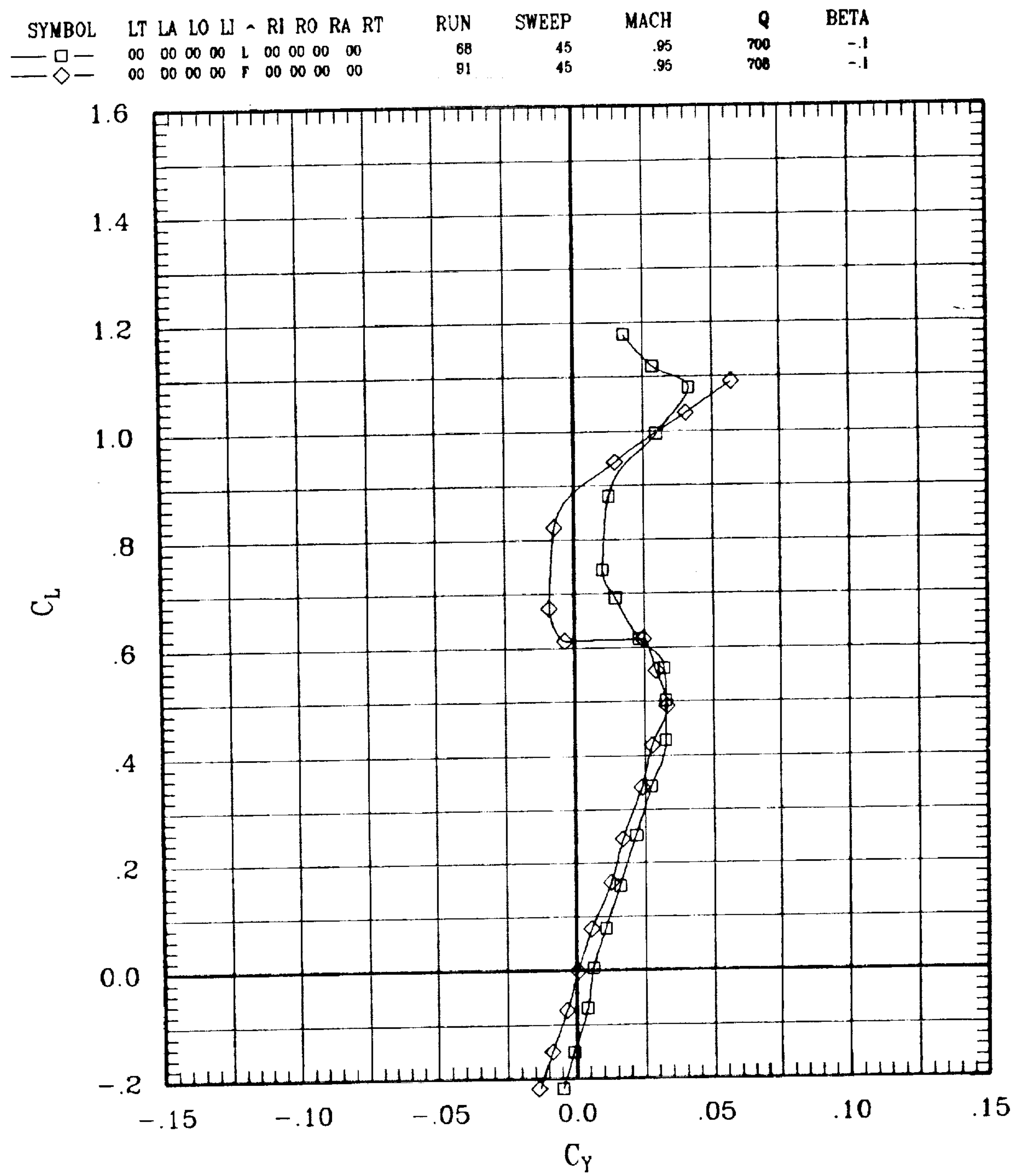

Figure 6(c). Effect of pivot height for sweep = 45 deg.

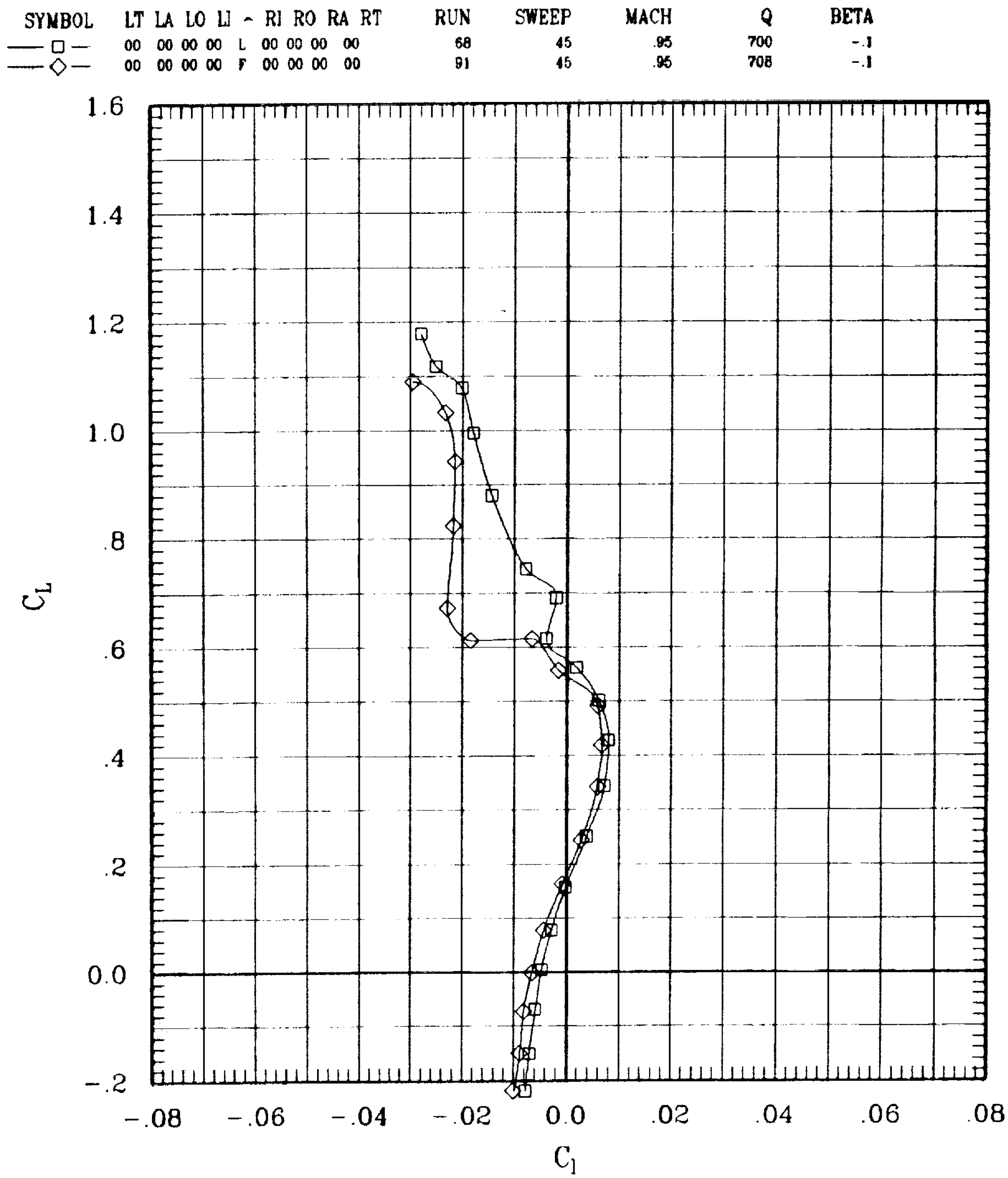

Figure 6(c). Effect of pivot height for sweep = 45 deg.

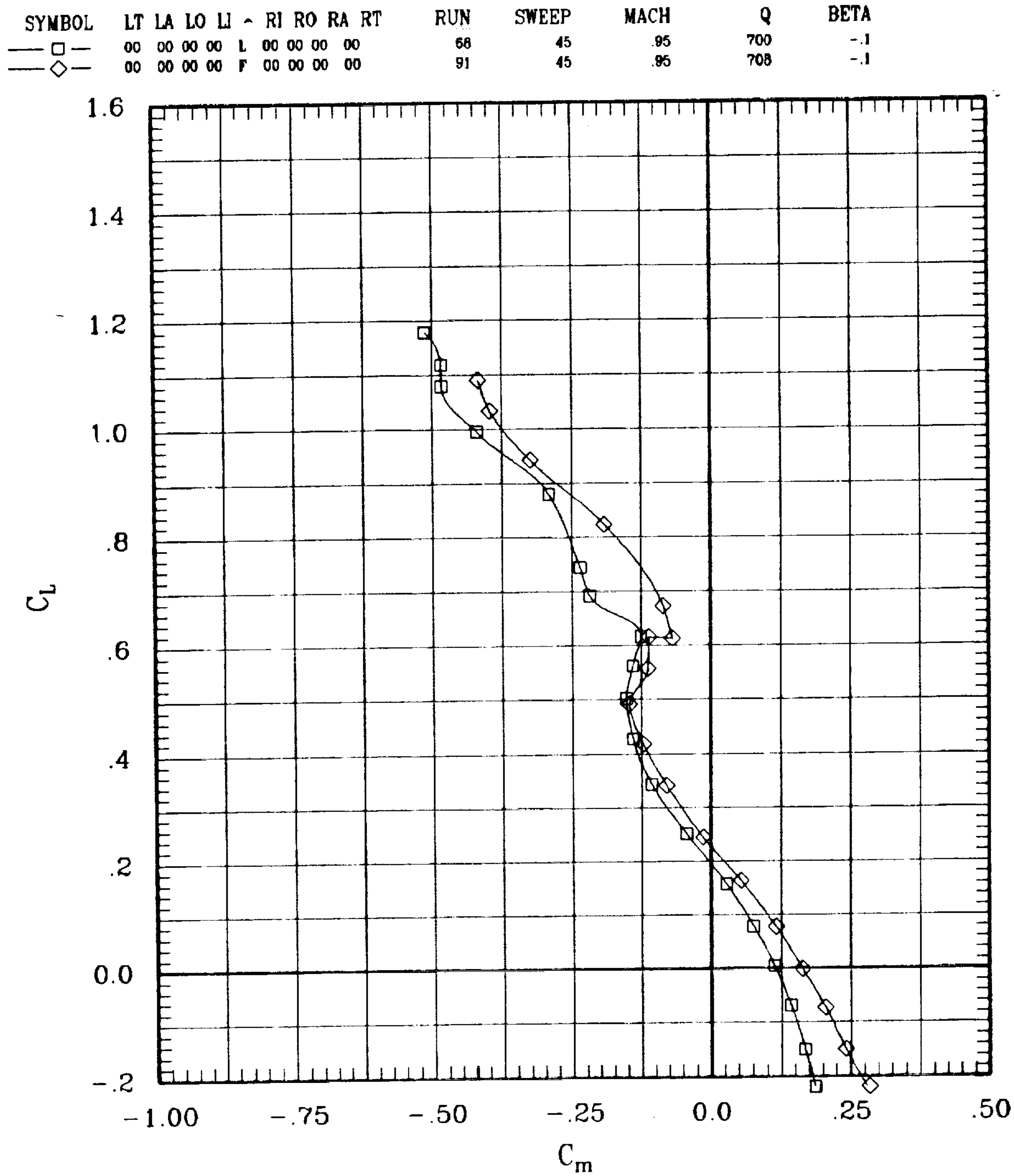

Figure 6(c). Effect of pivot height for sweep = 45 deg.

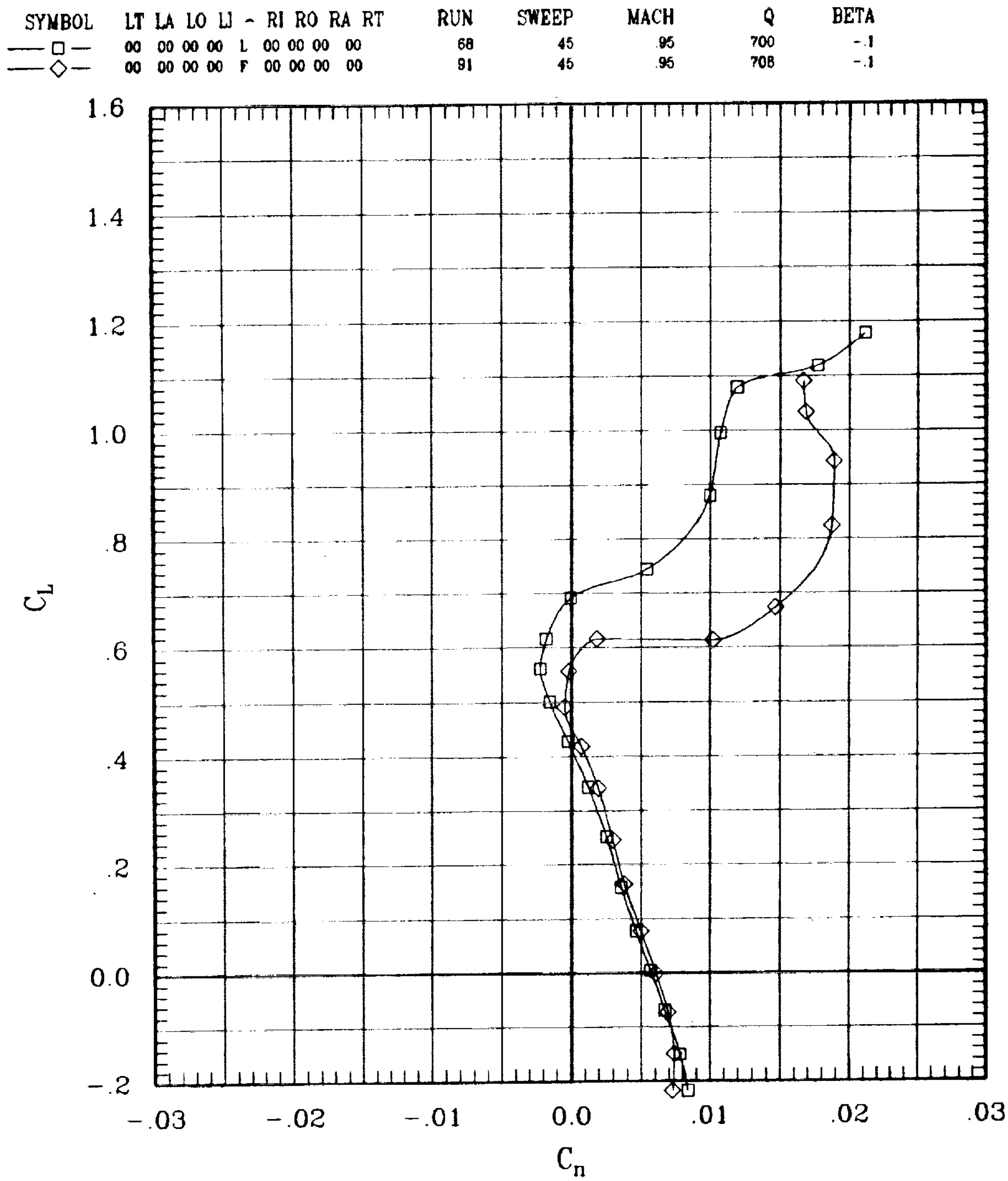

Figure 6(c). Effect of pivot height for sweep = 45 deg.

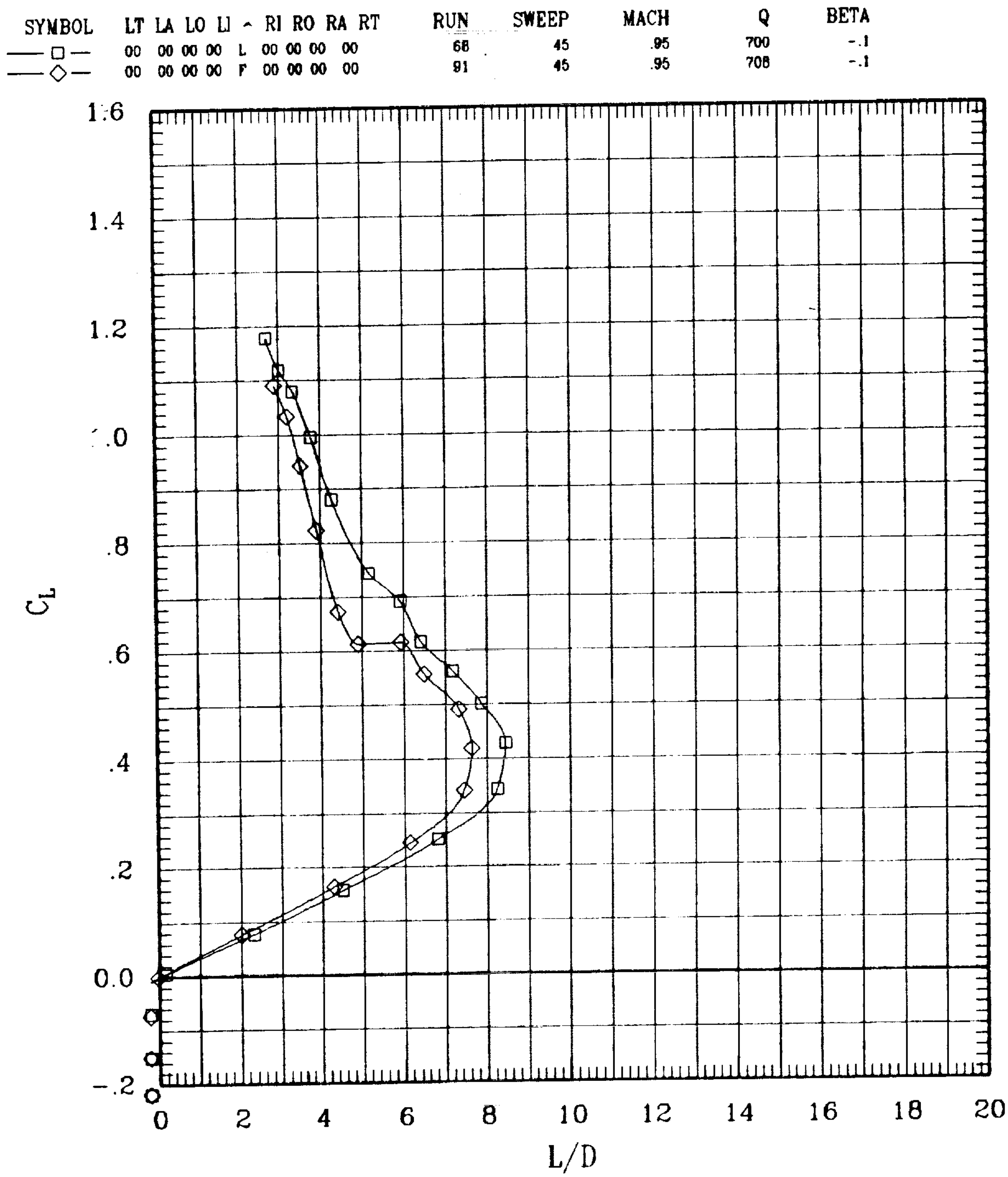

Figure 6(c). Effect of pivot height for sweep = 45 deg.

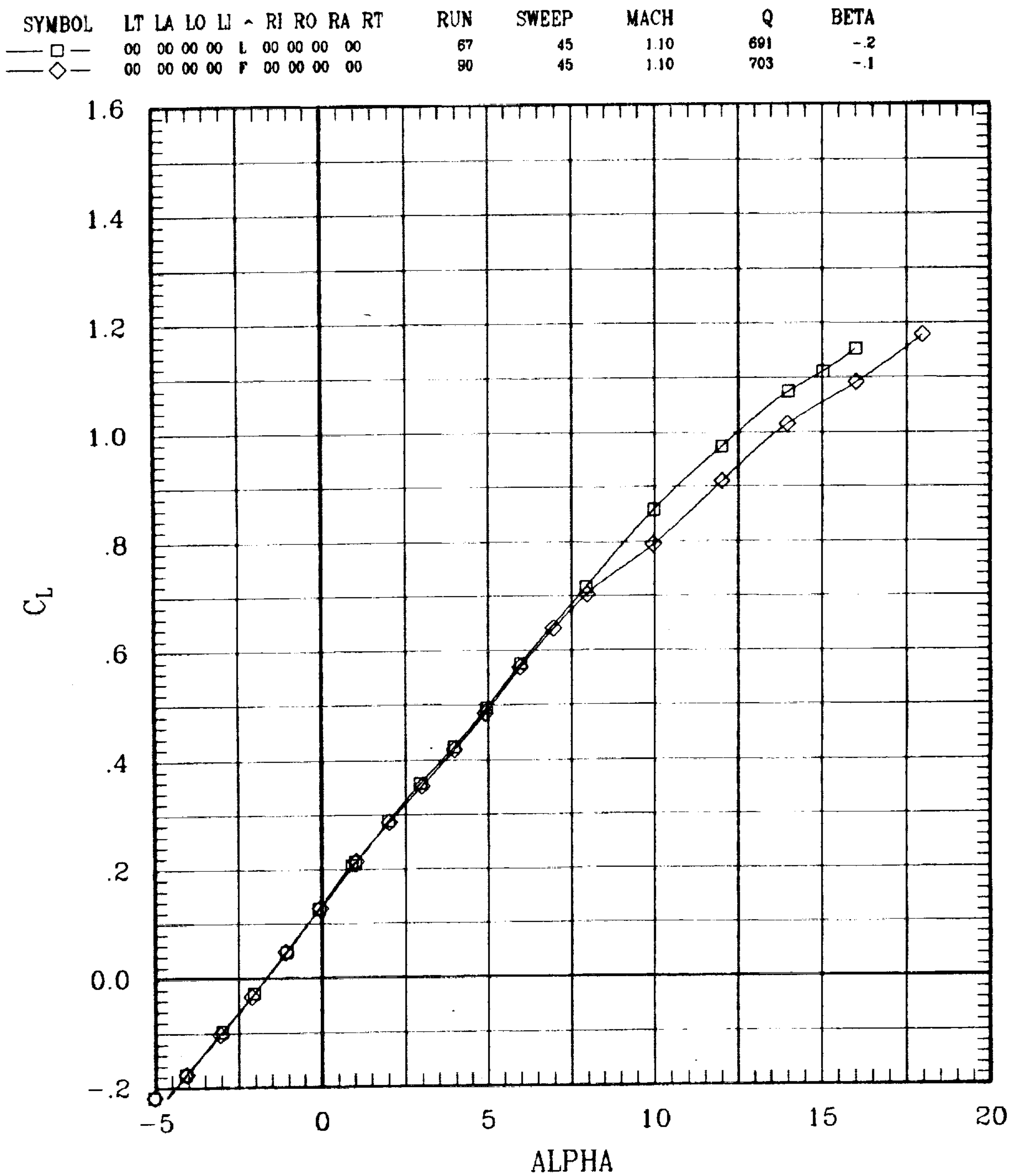

Figure 6(c). Effect of pivot height for sweep = 45 deg.

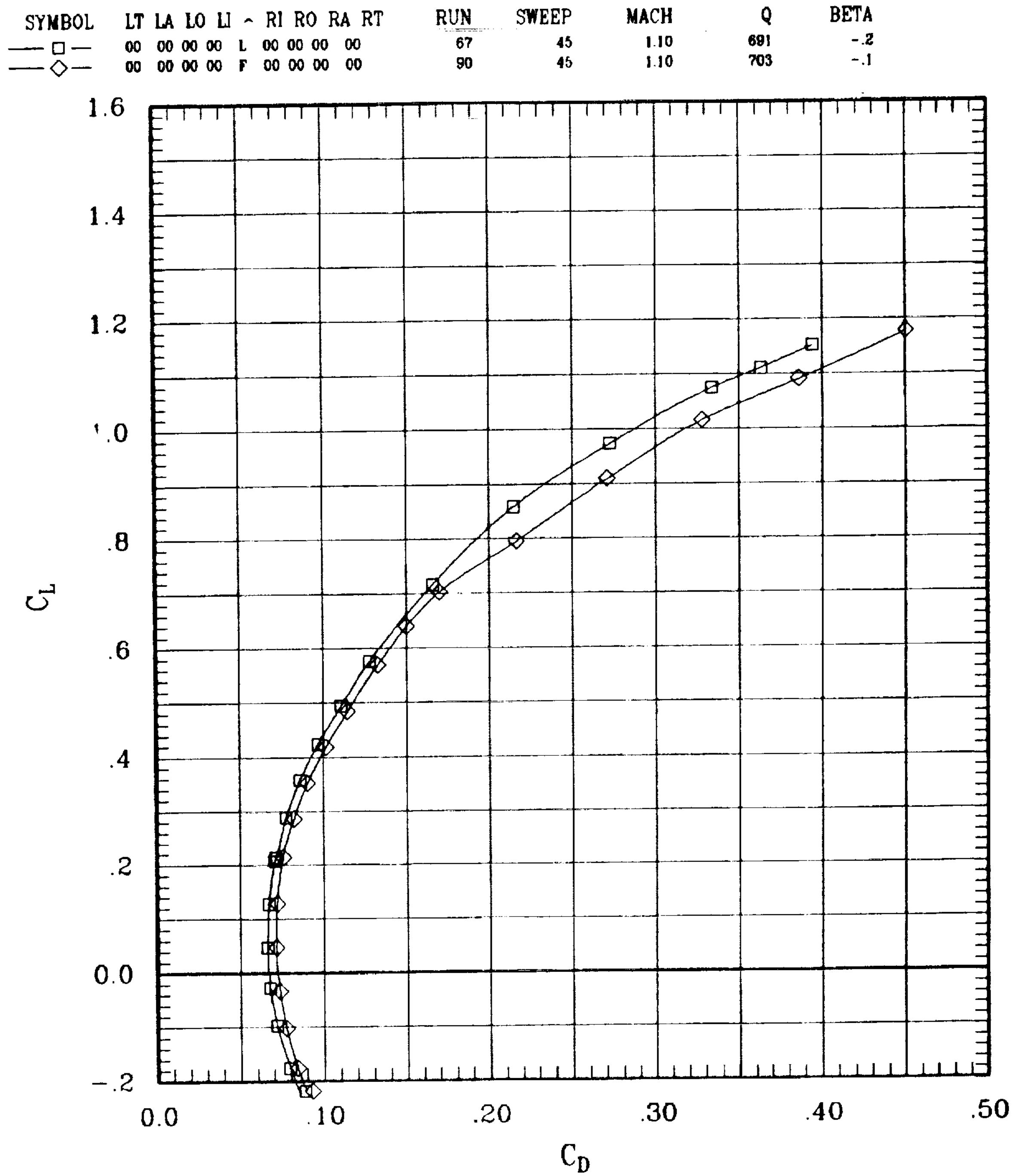

Figure 6(c). Effect of pivot height for sweep = 45 deg.

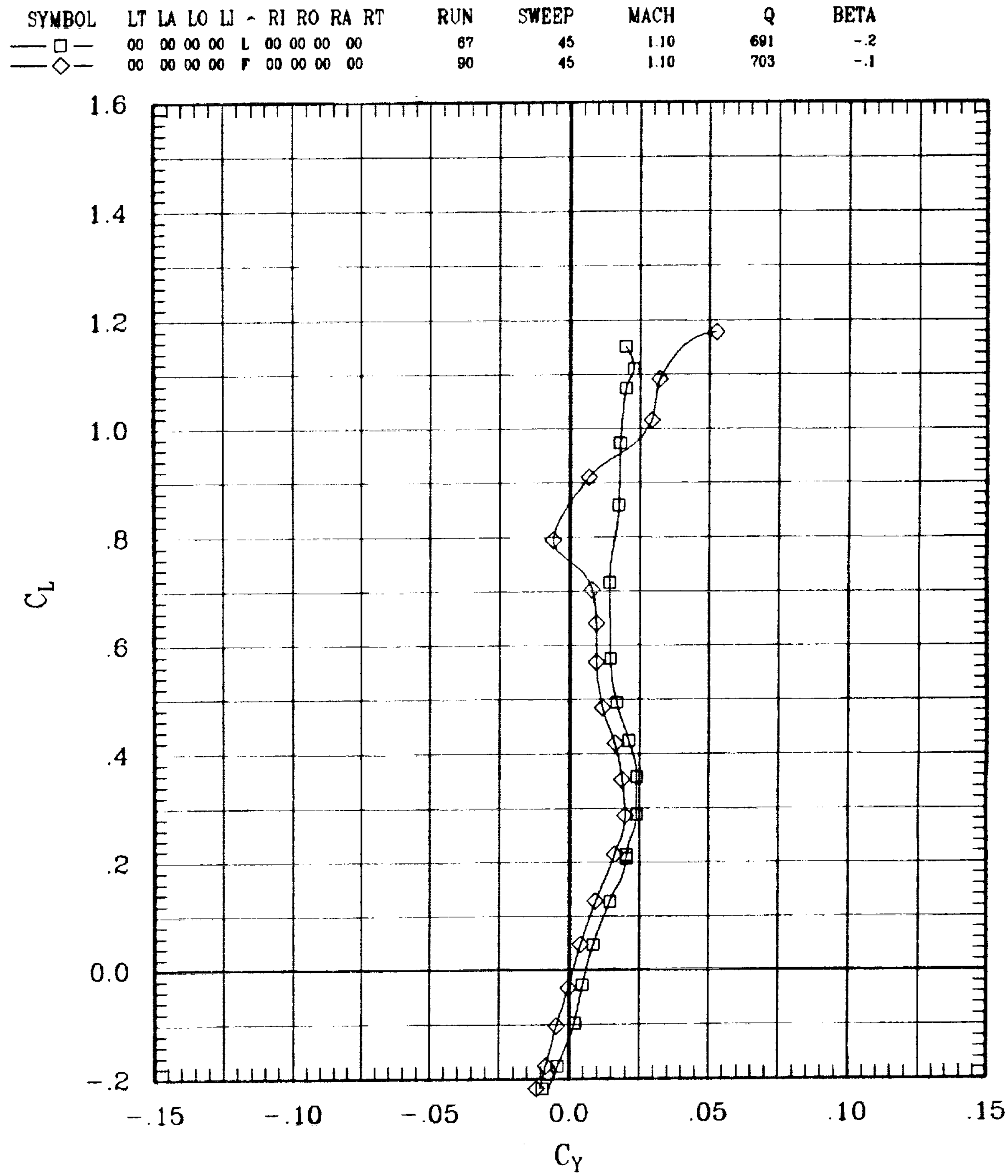

Figure 6(c). Effect of pivot height for sweep = 45 deg.

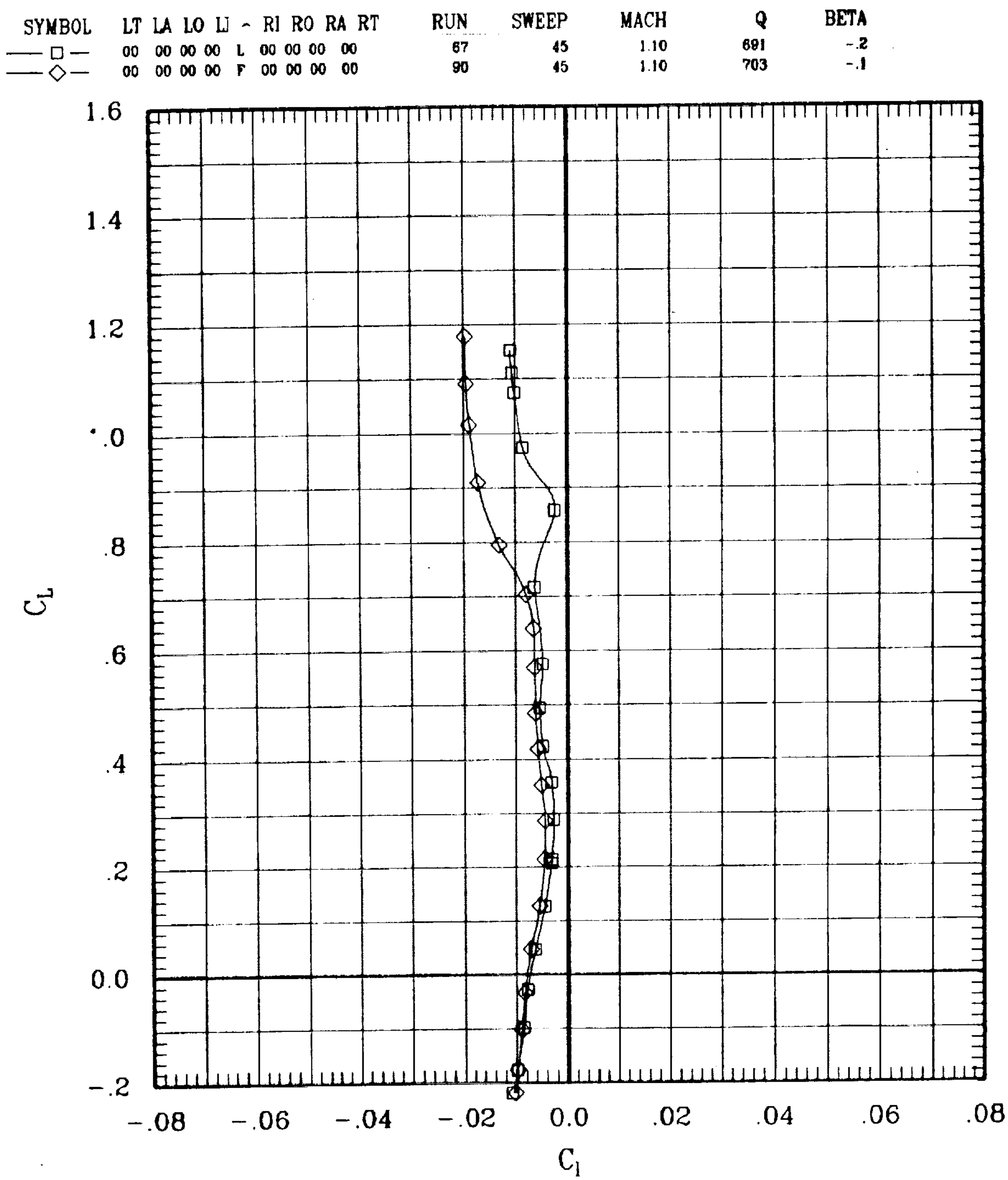

Figure 6(c). Effect of pivot height for sweep = 45 deg.

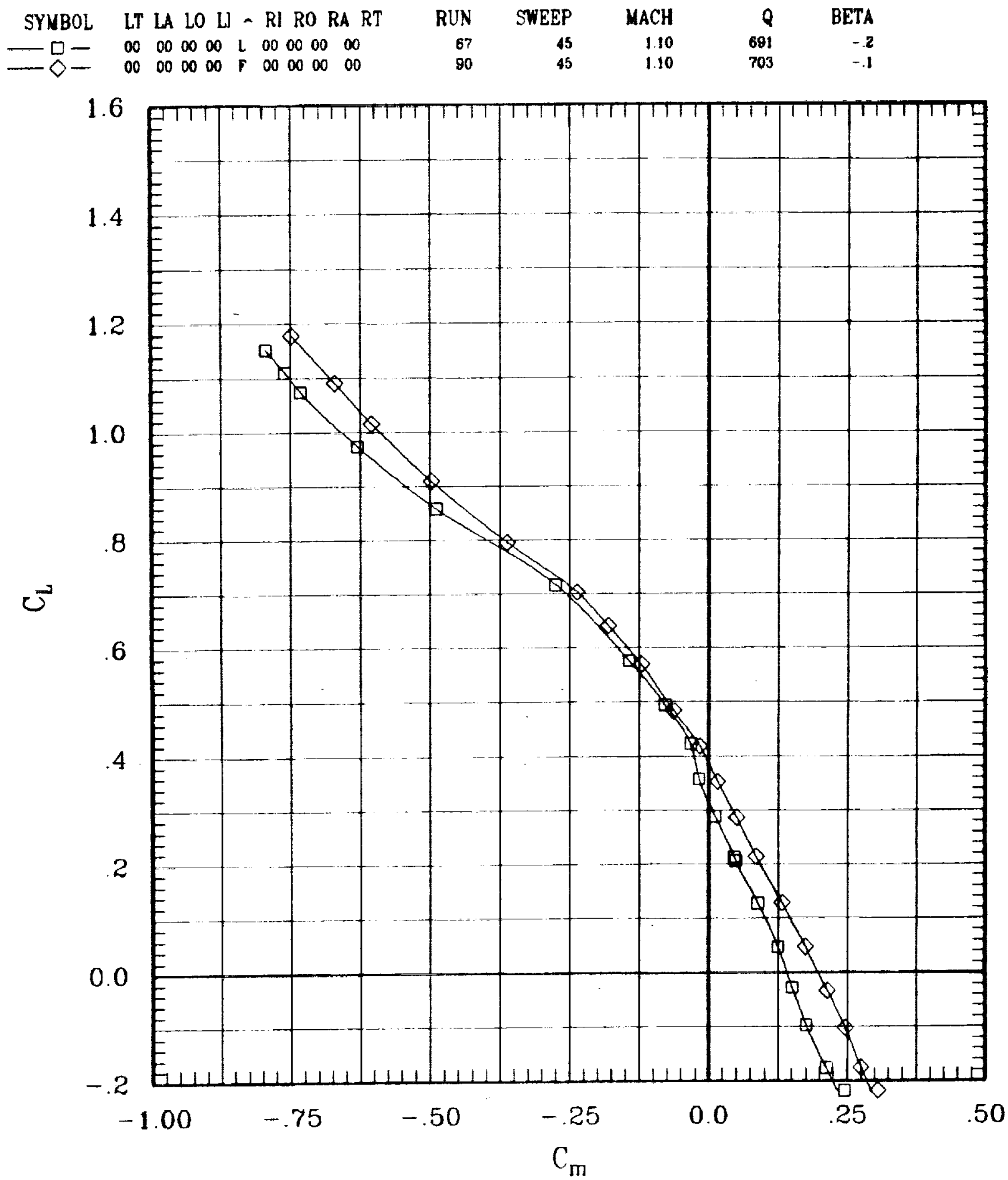

Figure 6(c). Effect of pivot height for sweep = 45 deg.

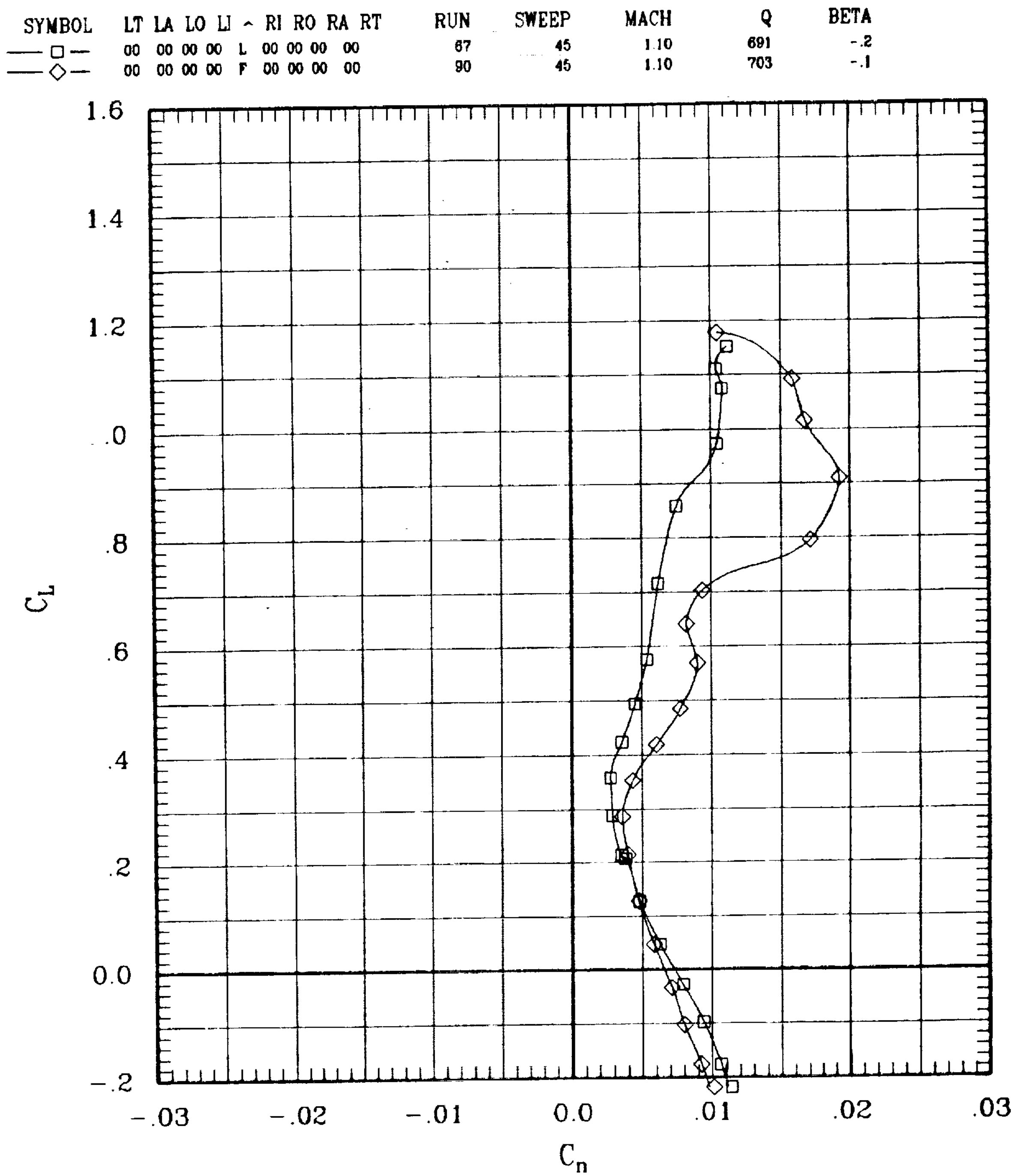

Figure 6(c). Effect of pivot height for sweep = 45 deg.

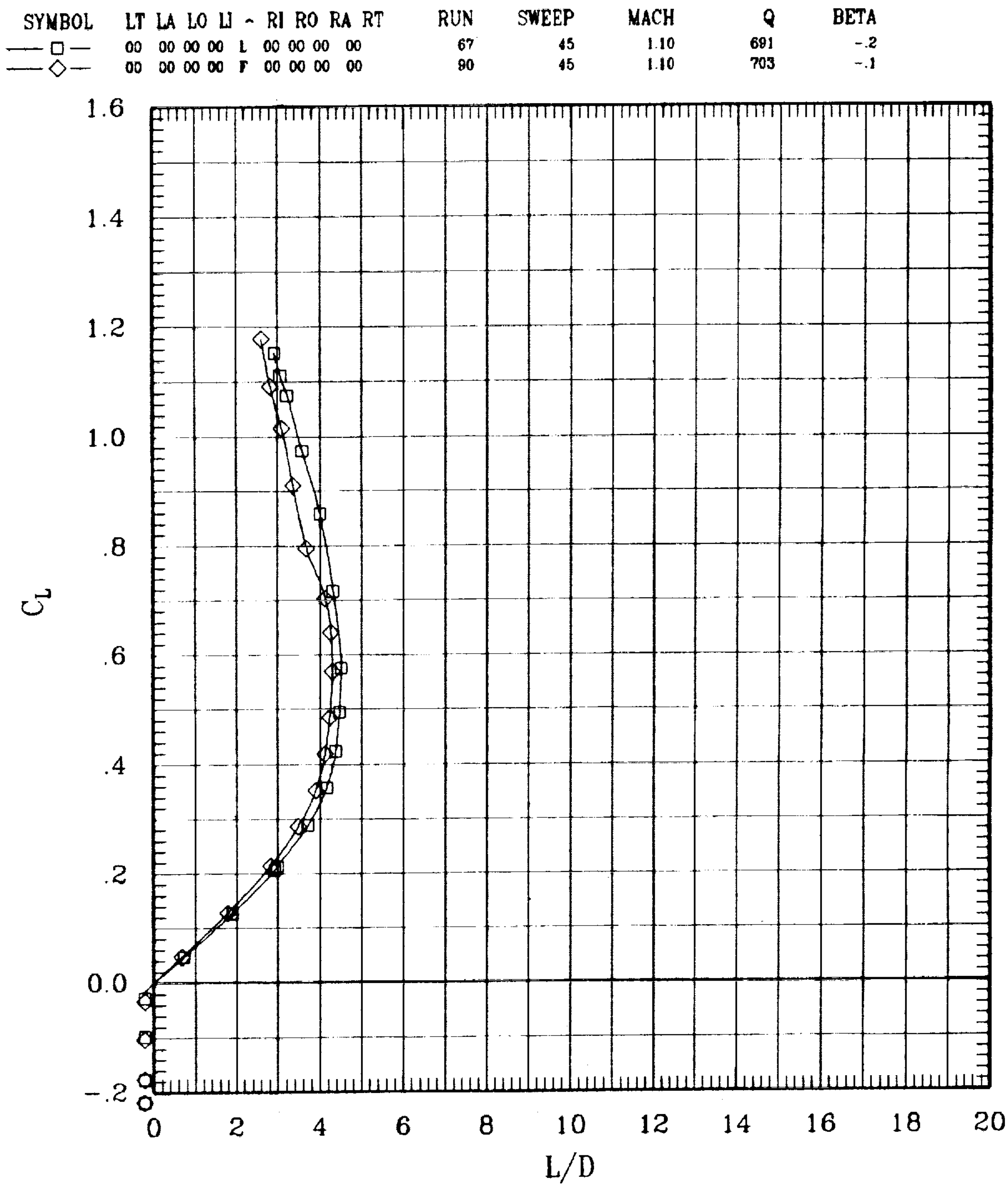

Figure 6(c). Effect of pivot height for sweep = 45 deg.

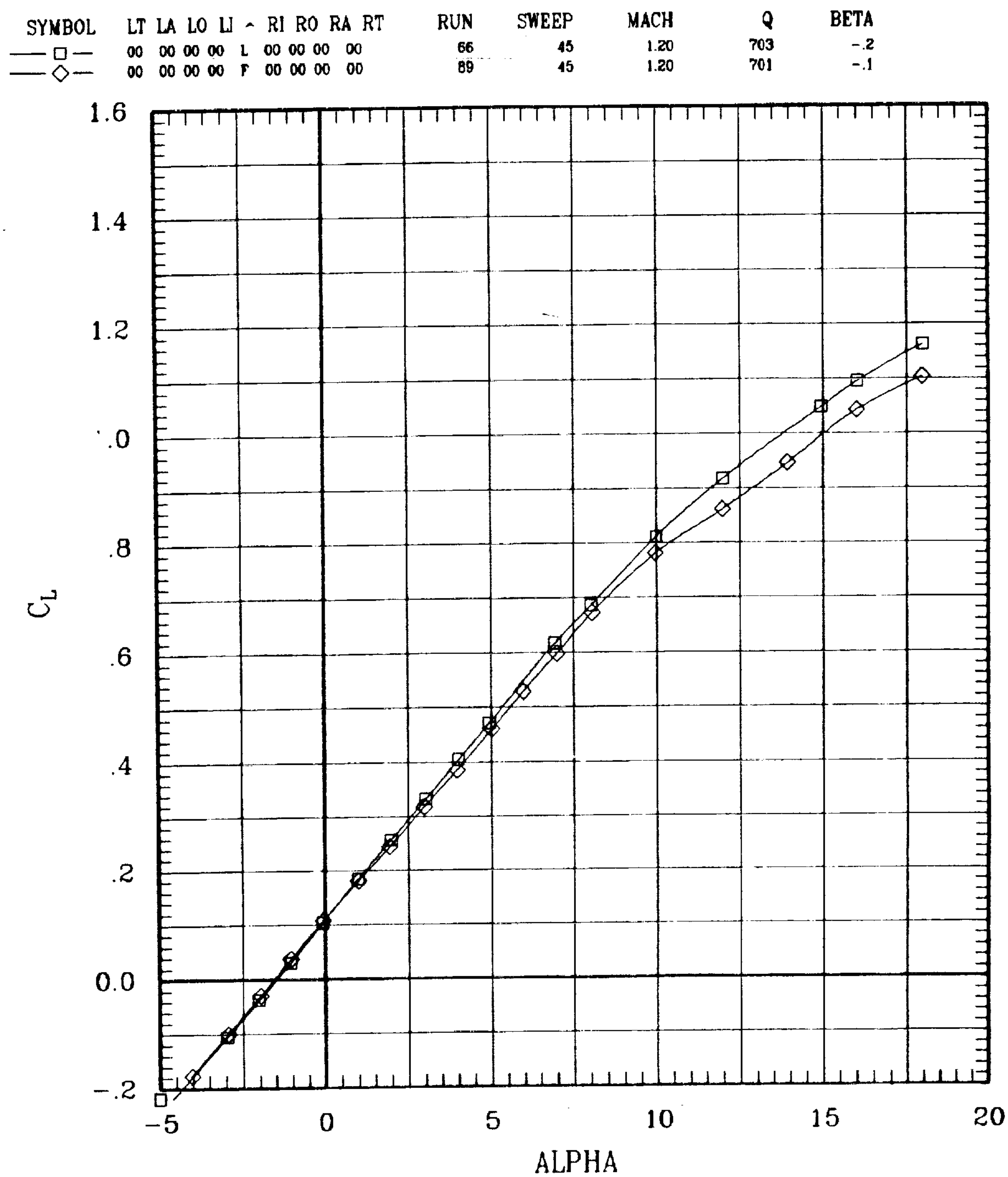

Figure 6(c). Effect of pivot height for sweep = 45 deg.

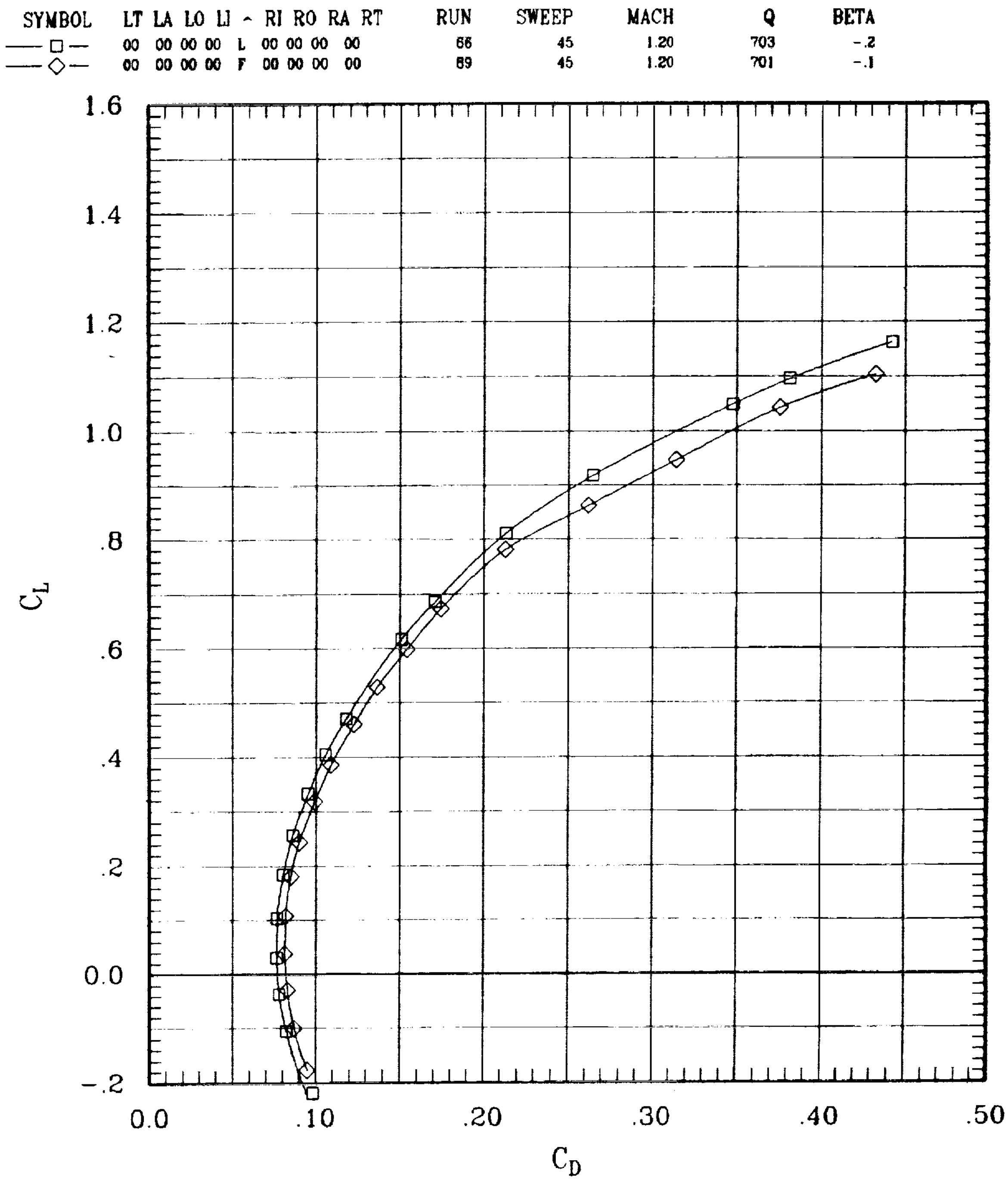

Figure 6(c). Effect of pivot height for sweep = 45 deg.

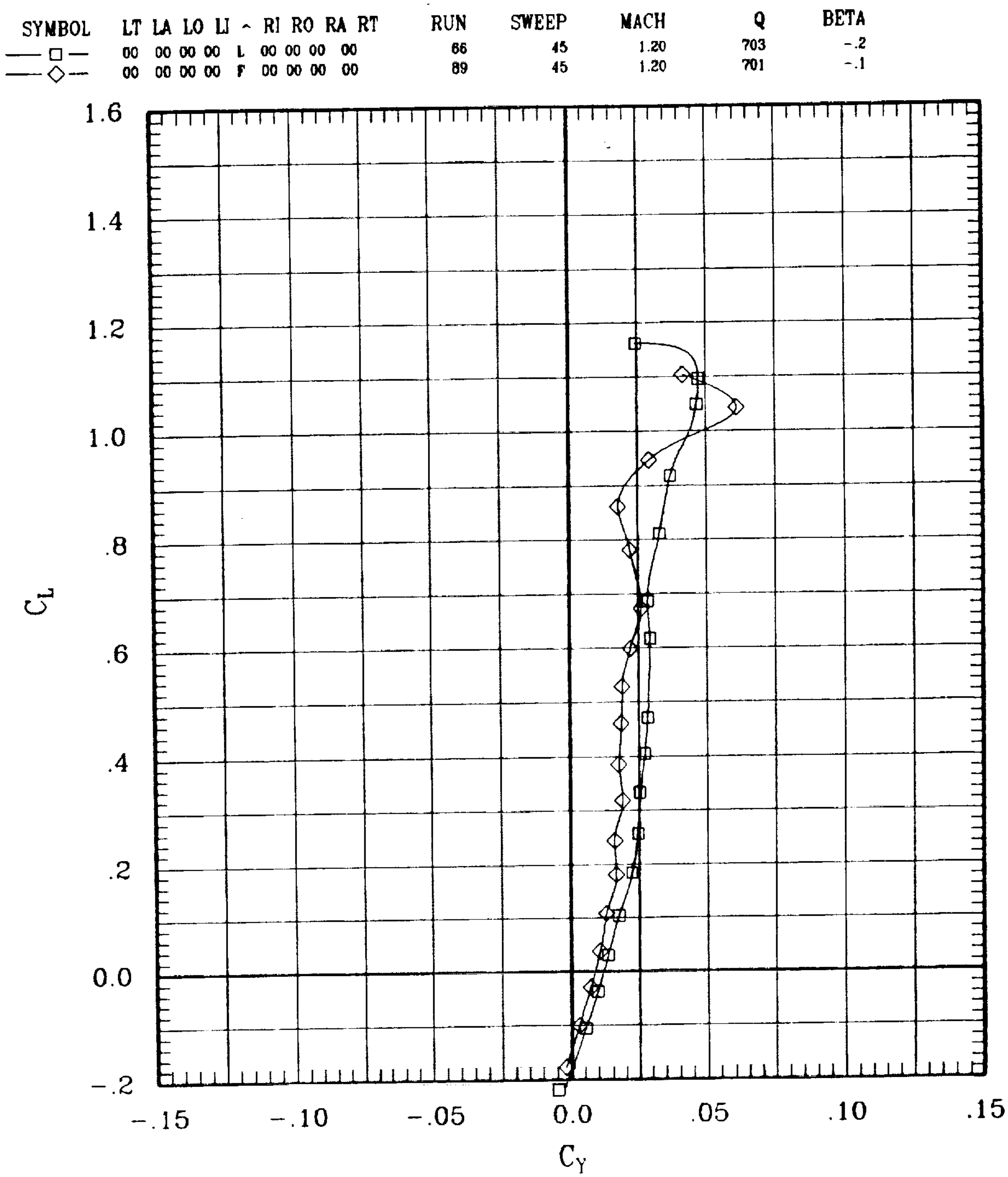

Figure 6(c). Effect of pivot height for sweep = 45 deg.

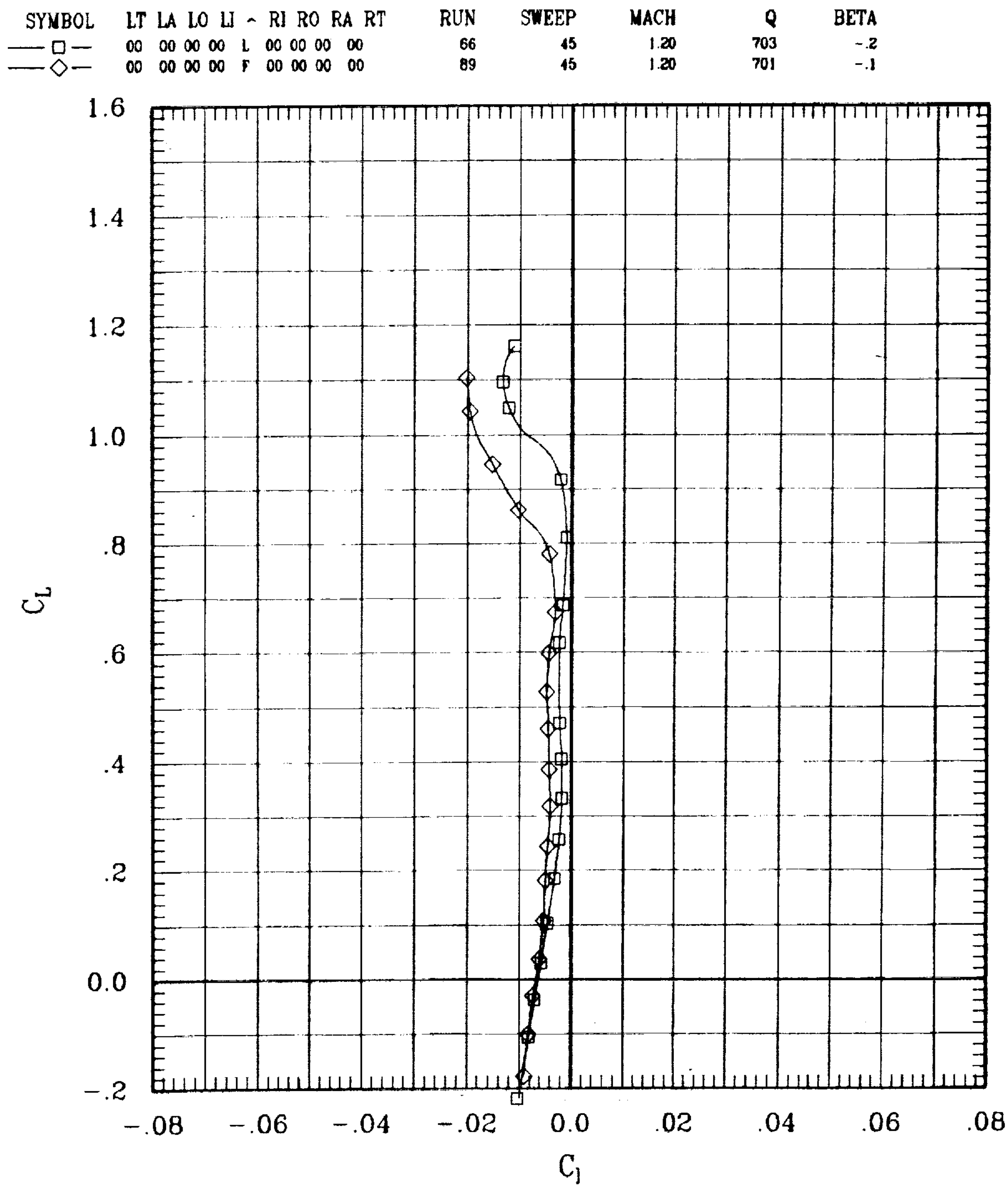

Figure 6(c). Effect of pivot height for sweep = 45 deg.

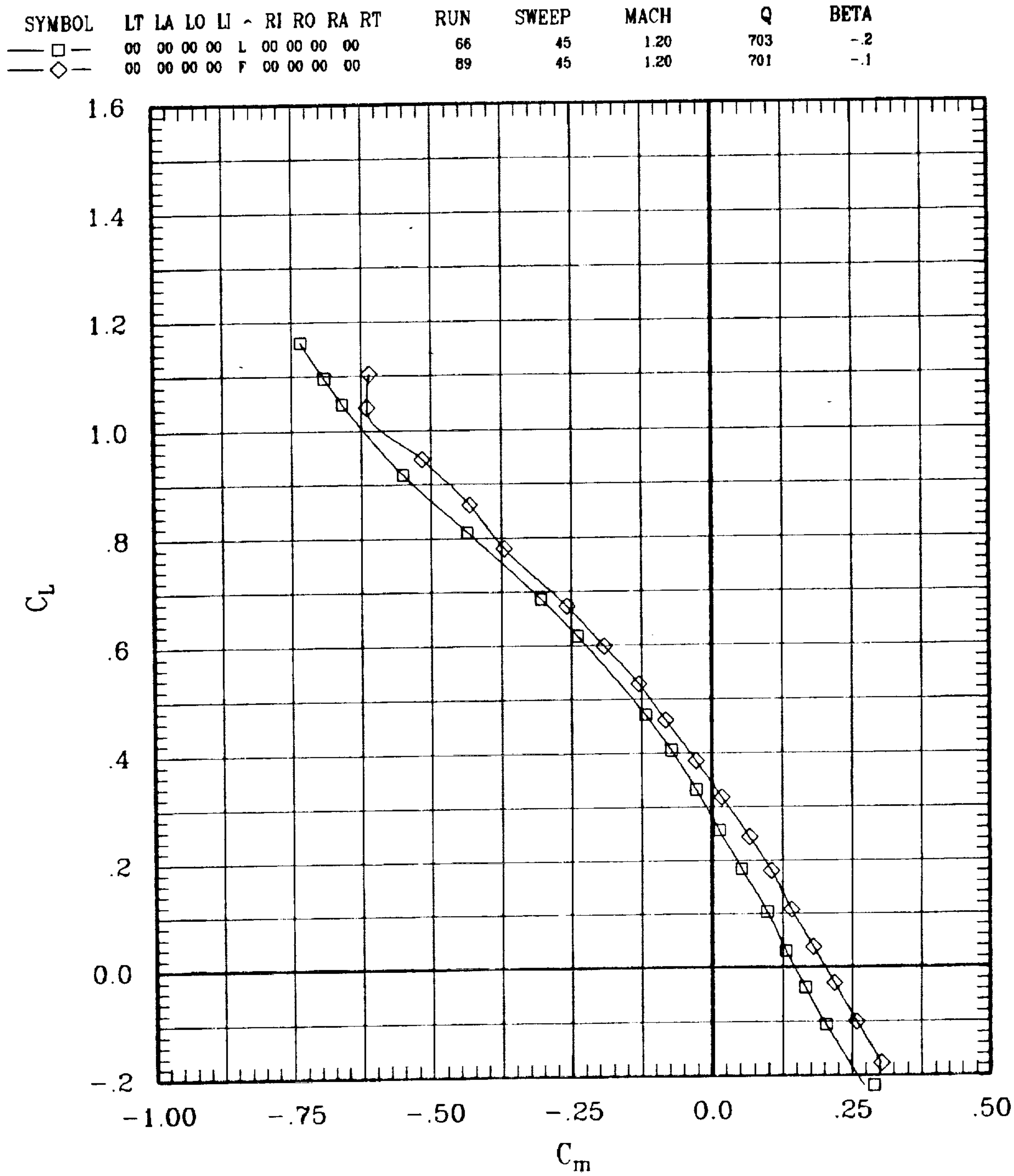

Figure 6(c). Effect of pivot height for sweep = 45 deg.

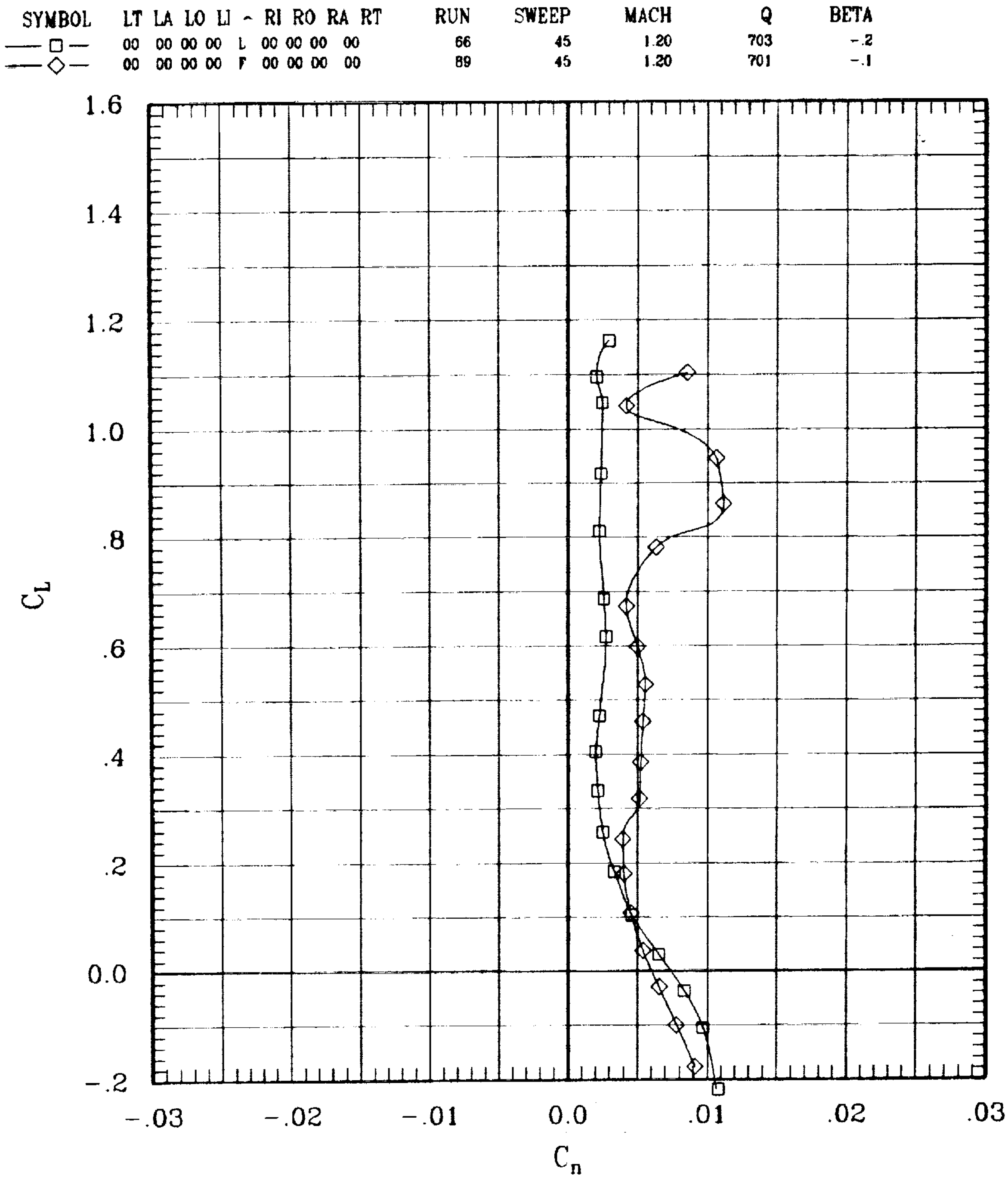

Figure 6(c). Effect of pivot height for sweep = 45 deg.

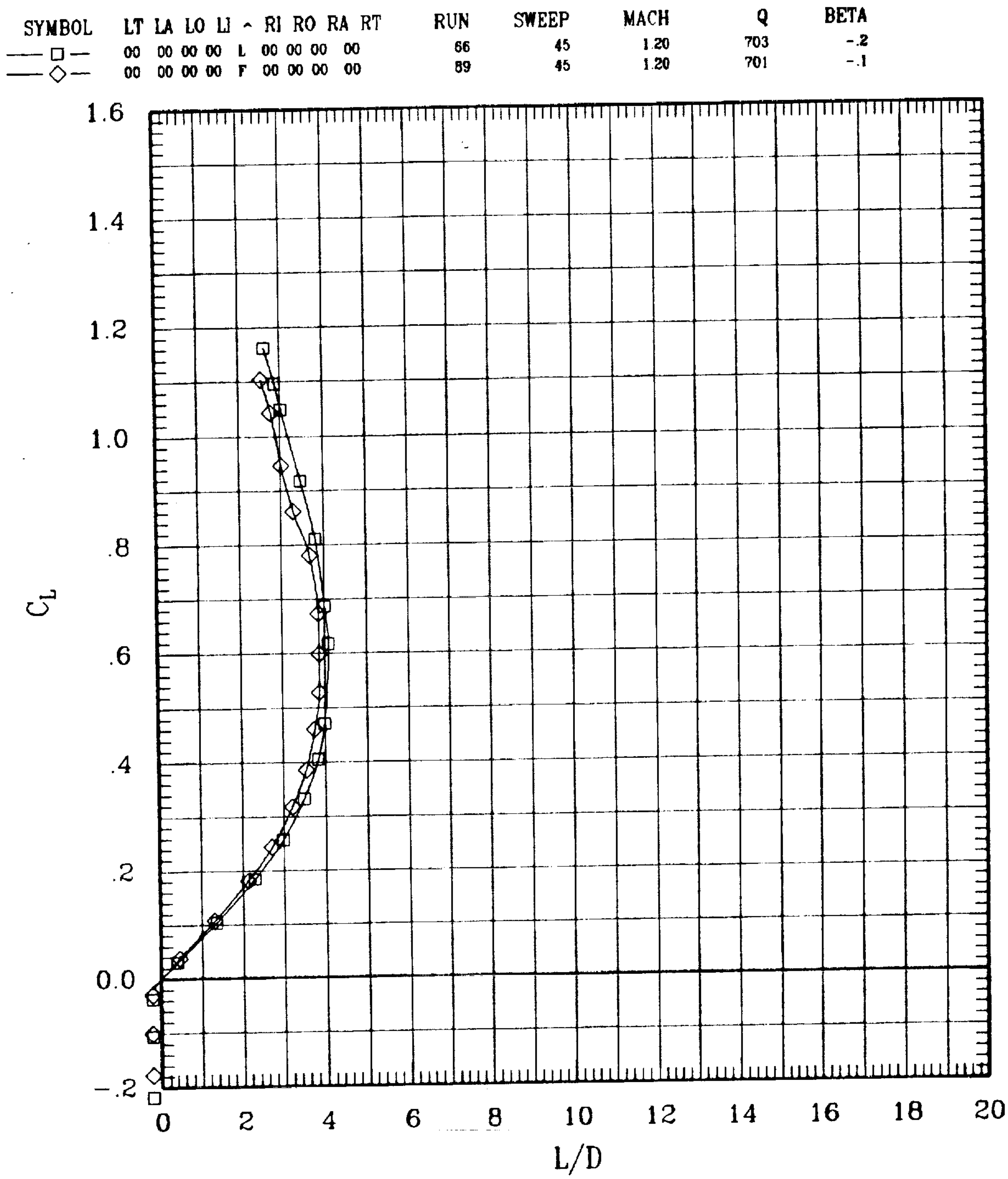

Figure 6(c). Effect of pivot height for sweep = 45 deg.

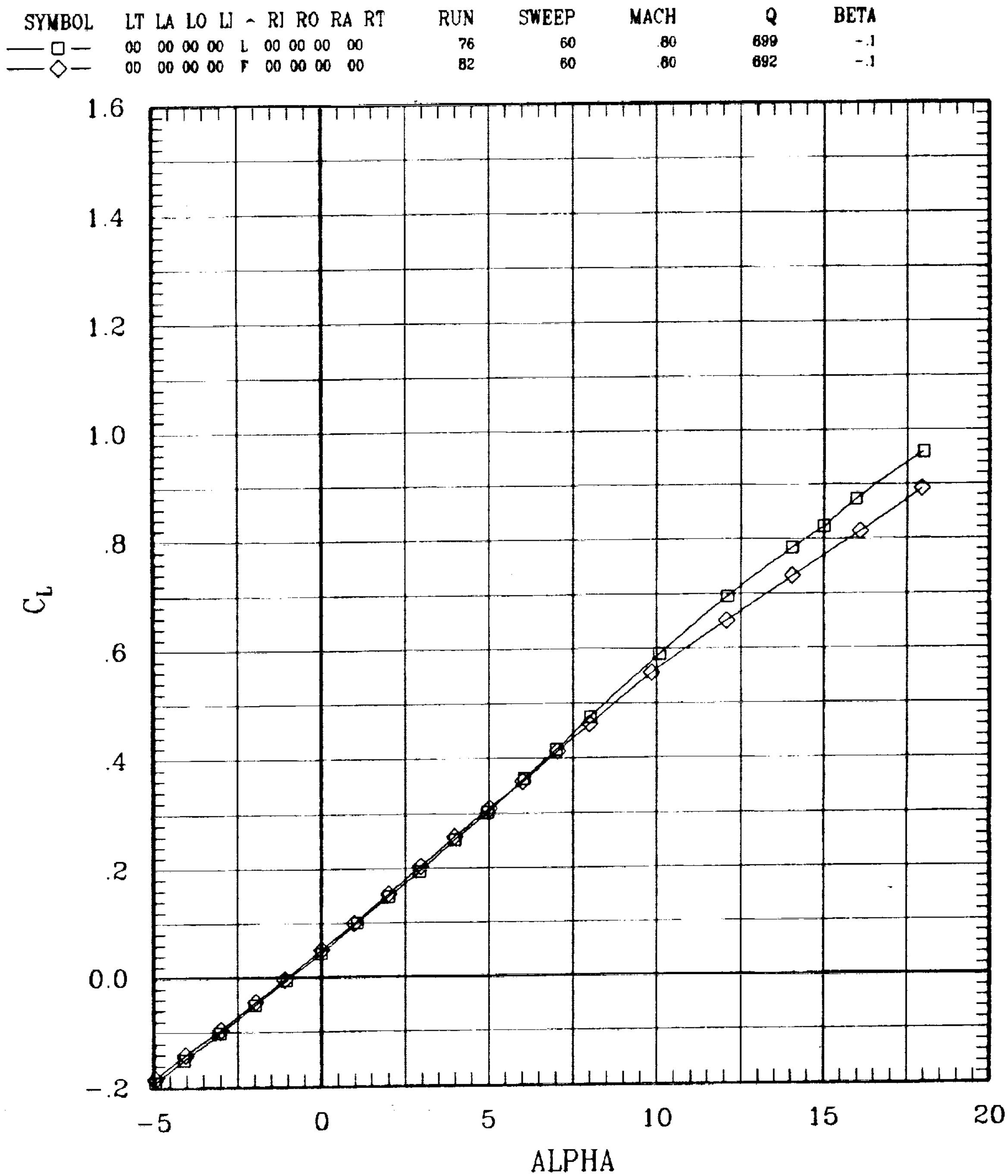

Figure 6(d). Effect of pivot height for sweep = 60 deg.

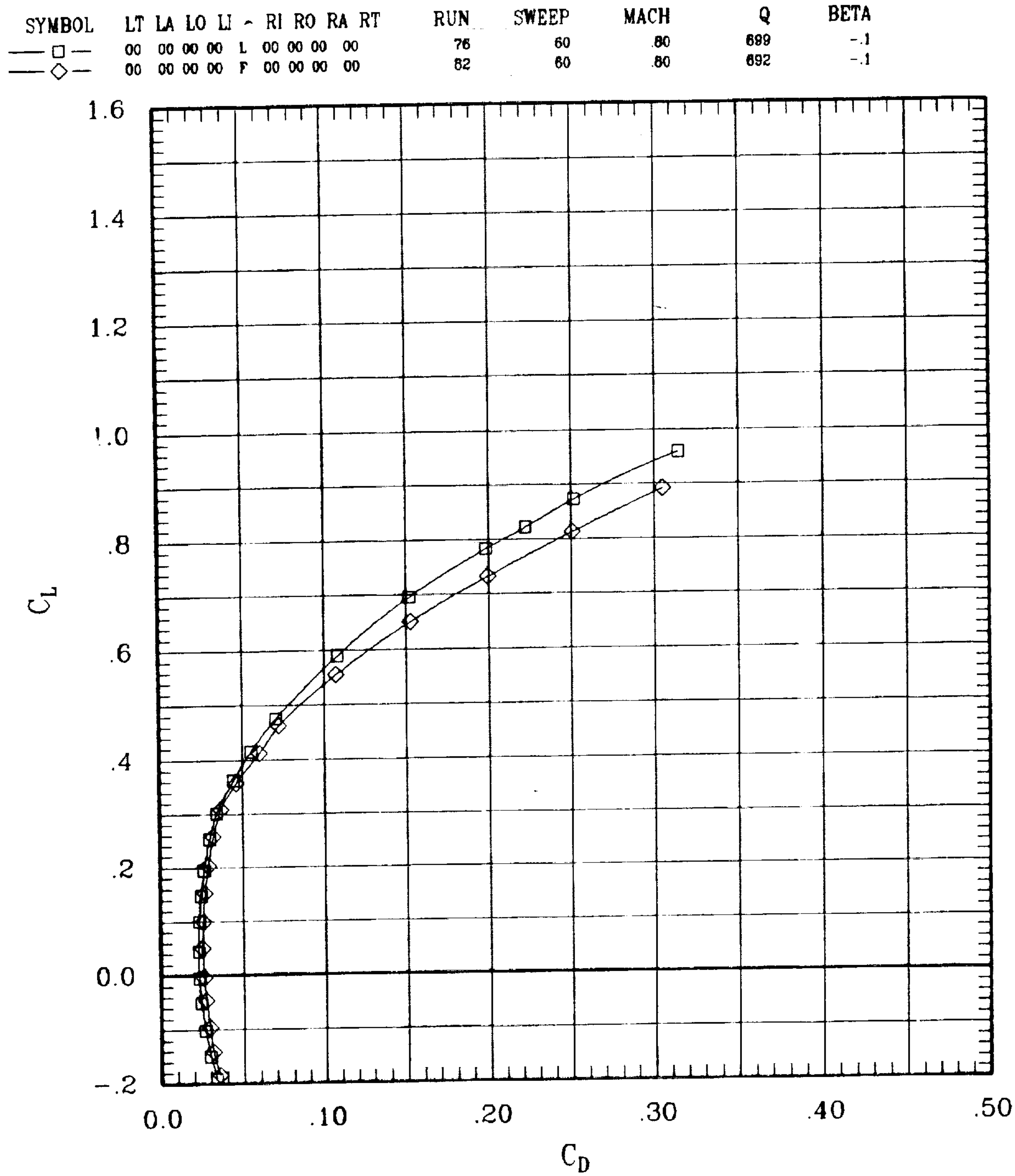

Figure 6(d). Effect of pivot height for sweep = 60 deg.

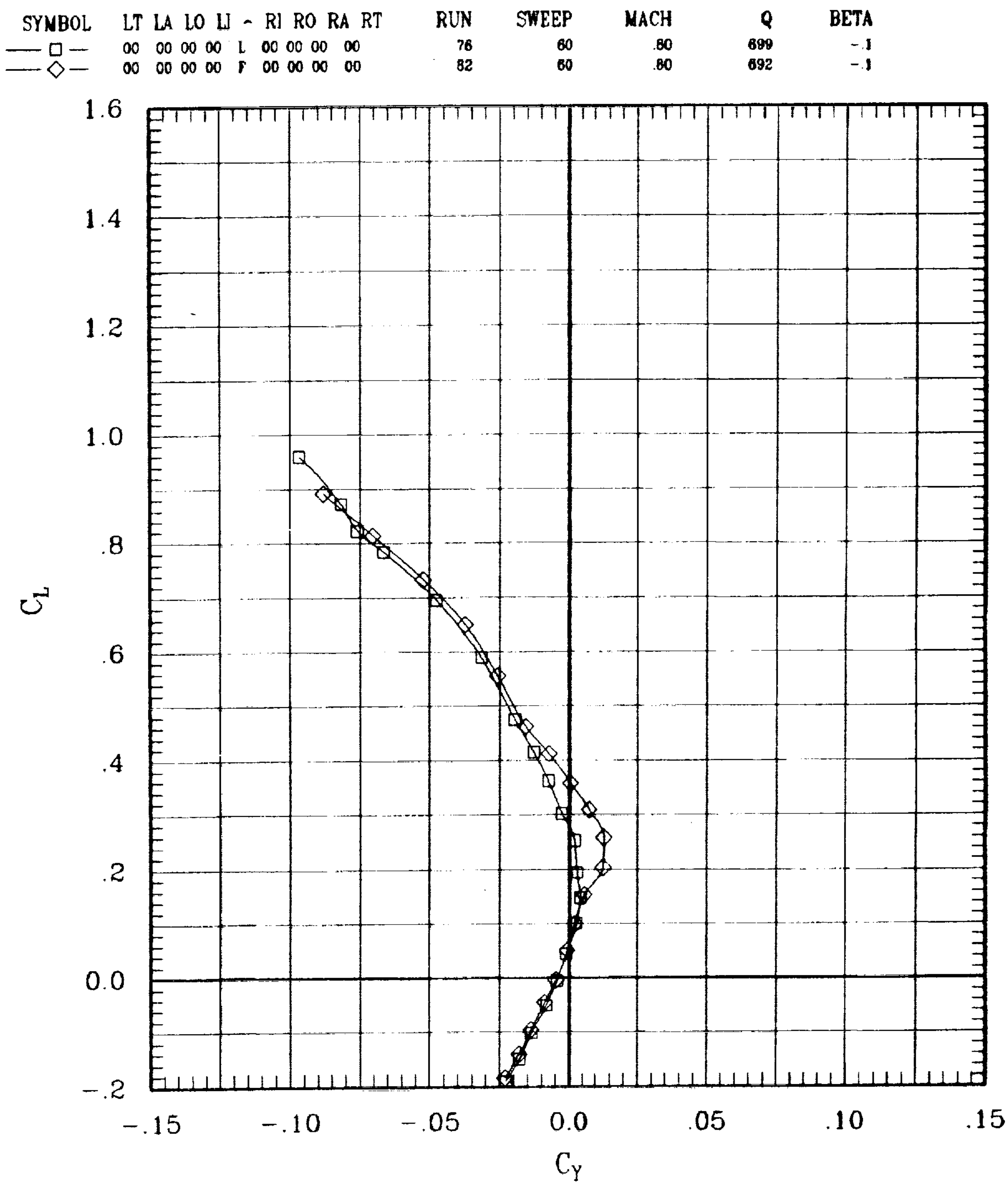

Figure 6(d). Effect of pivot height for sweep = 60 deg.

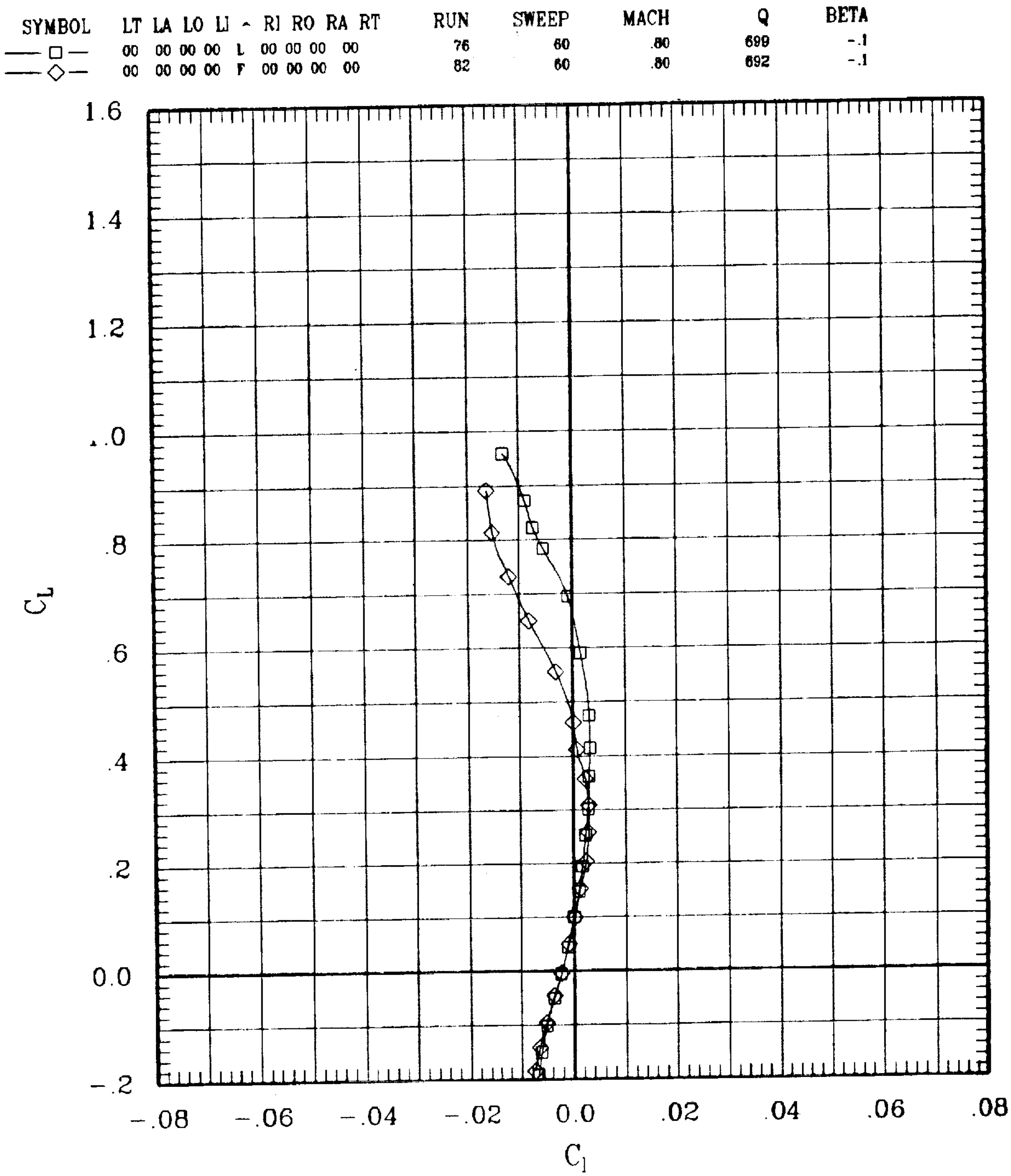

Figure 6(d). Effect of pivot height for sweep = 60 deg.

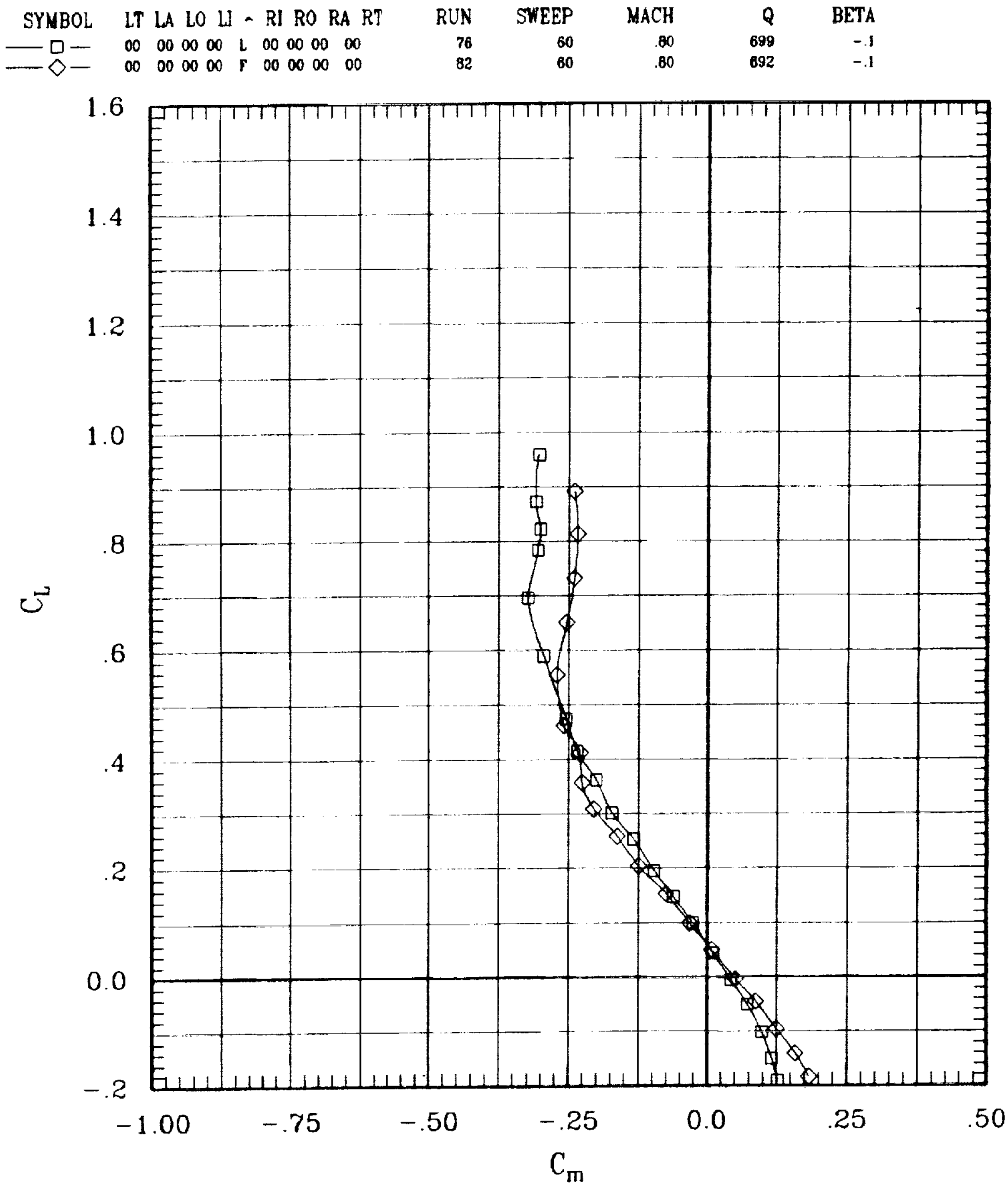

Figure 6(d). Effect of pivot height for sweep = 60 deg.

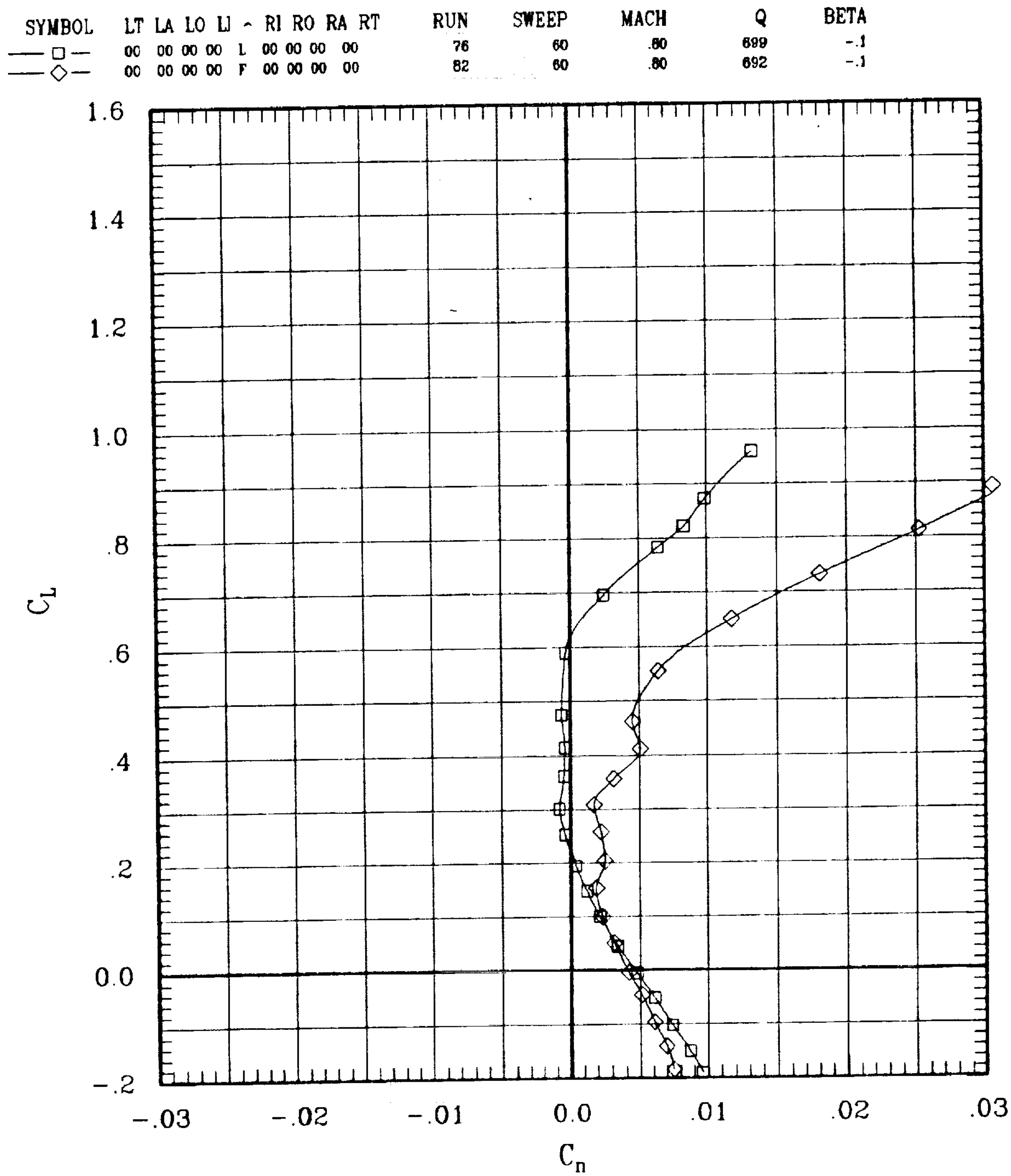

Figure 6(d). Effect of pivot height for sweep = 60 deg.

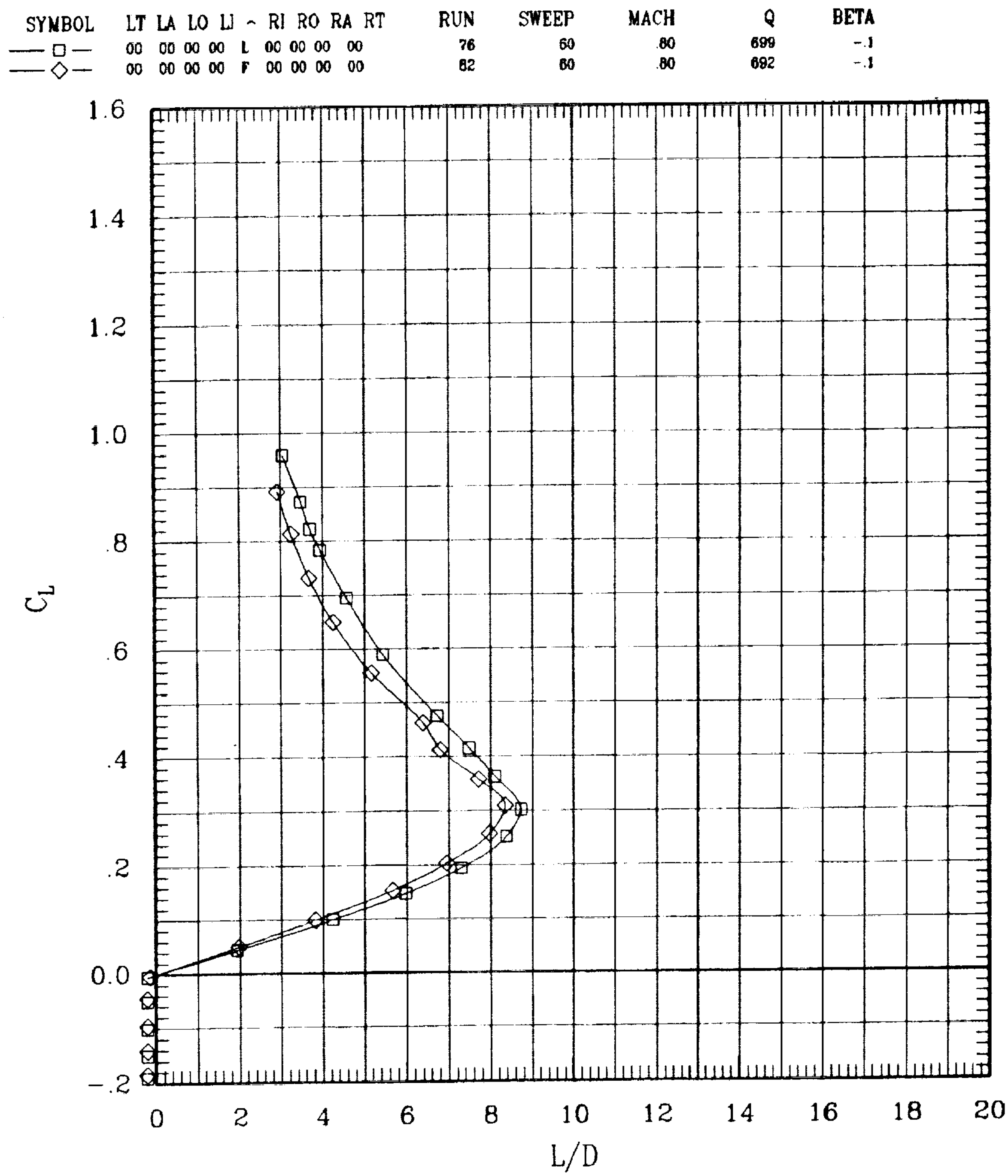

Figure 6(d). Effect of pivot height for sweep = 60 deg.

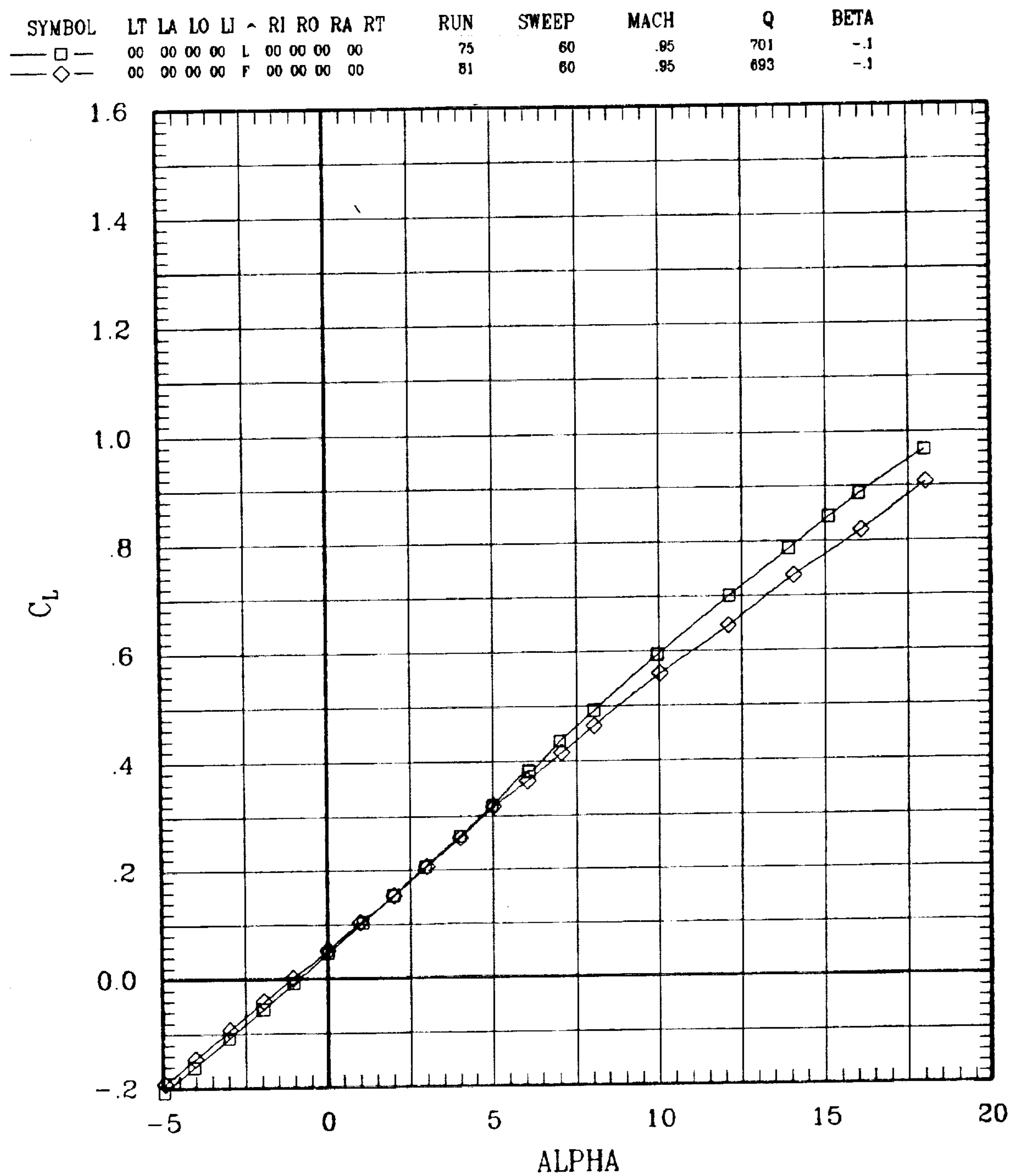

Figure 6(d). Effect of pivot height for sweep = 60 deg.

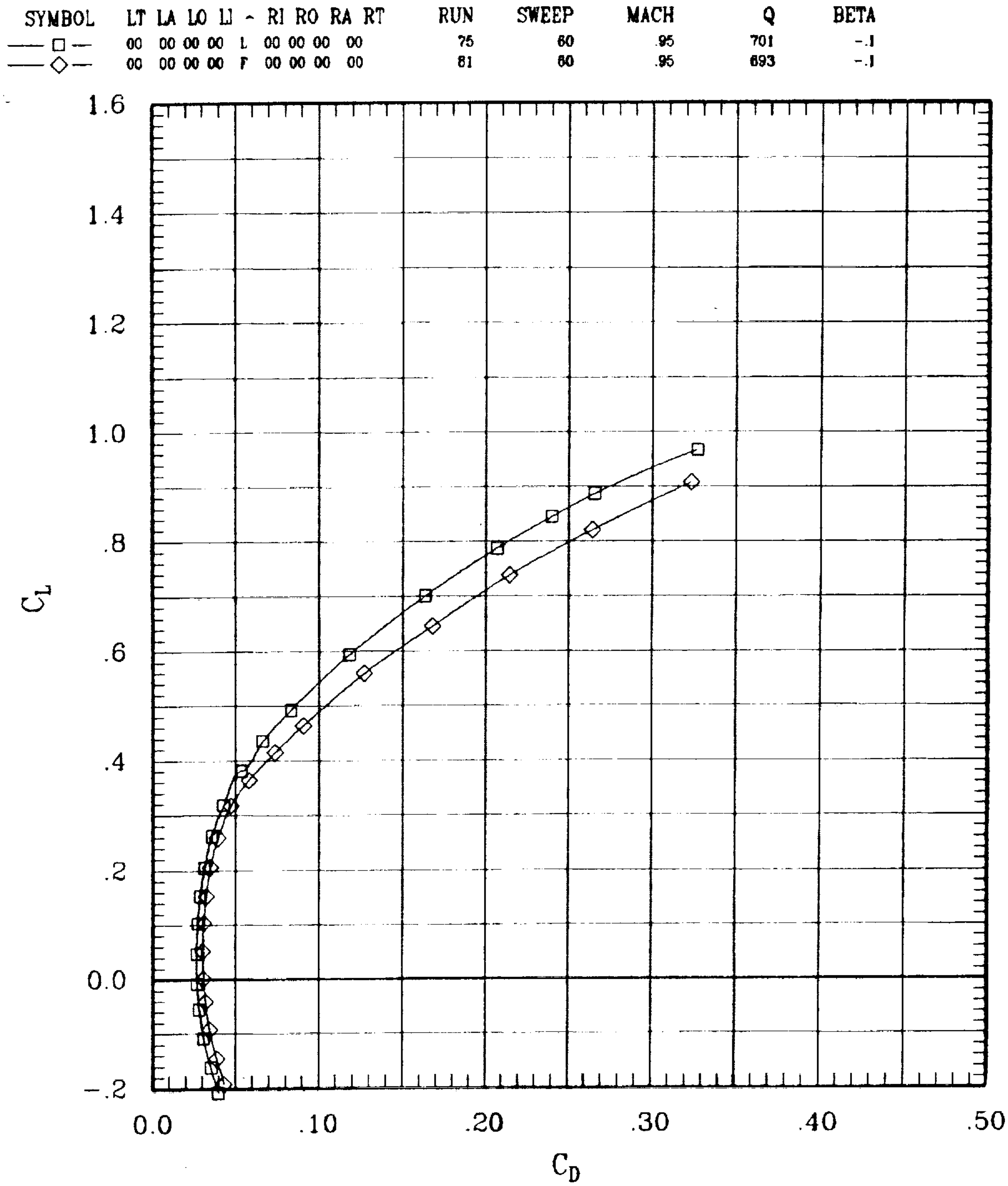

Figure 6(d). Effect of pivot height for sweep = 60 deg.

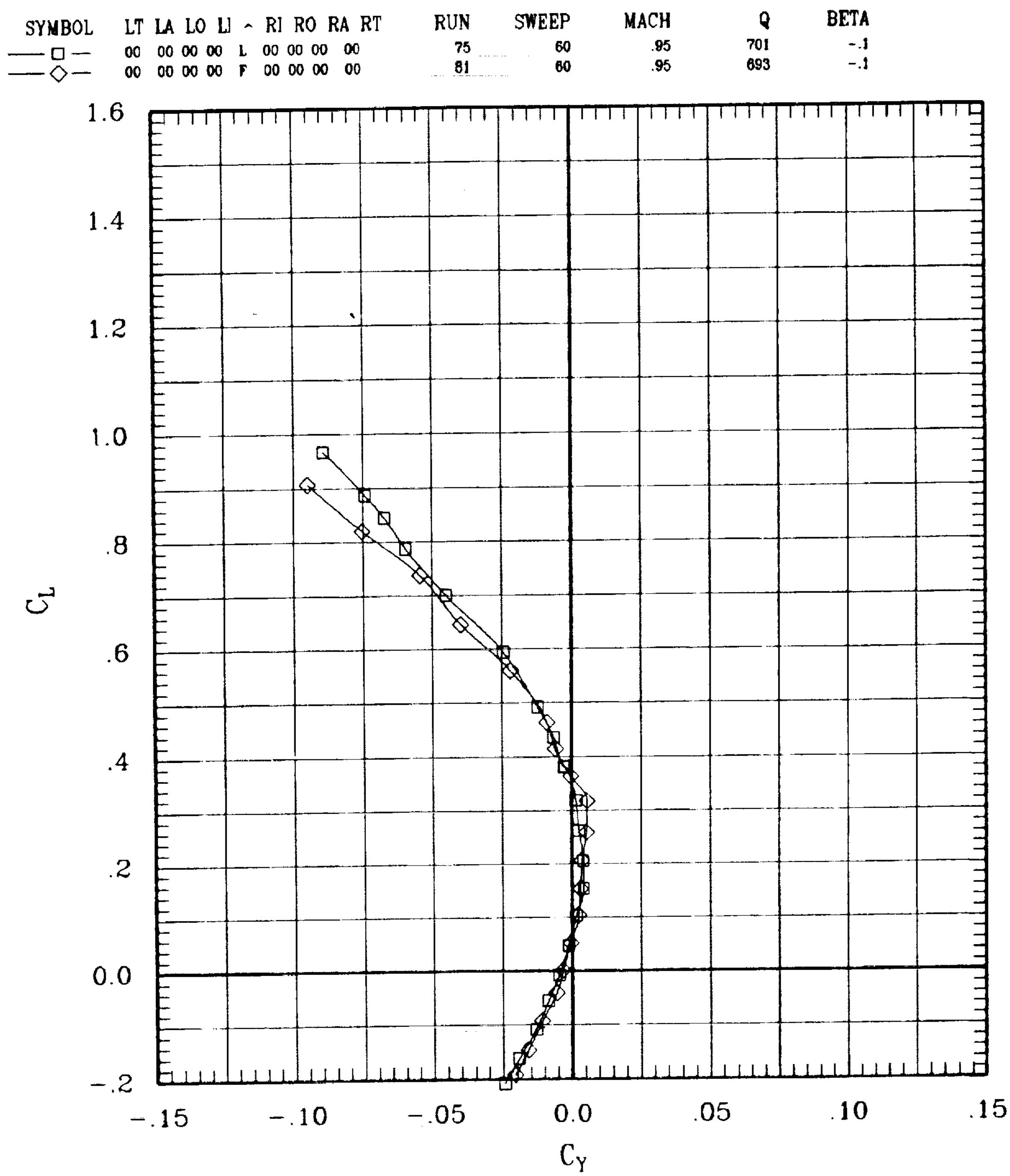

Figure 6(d). Effect of pivot height for sweep = 60 deg.

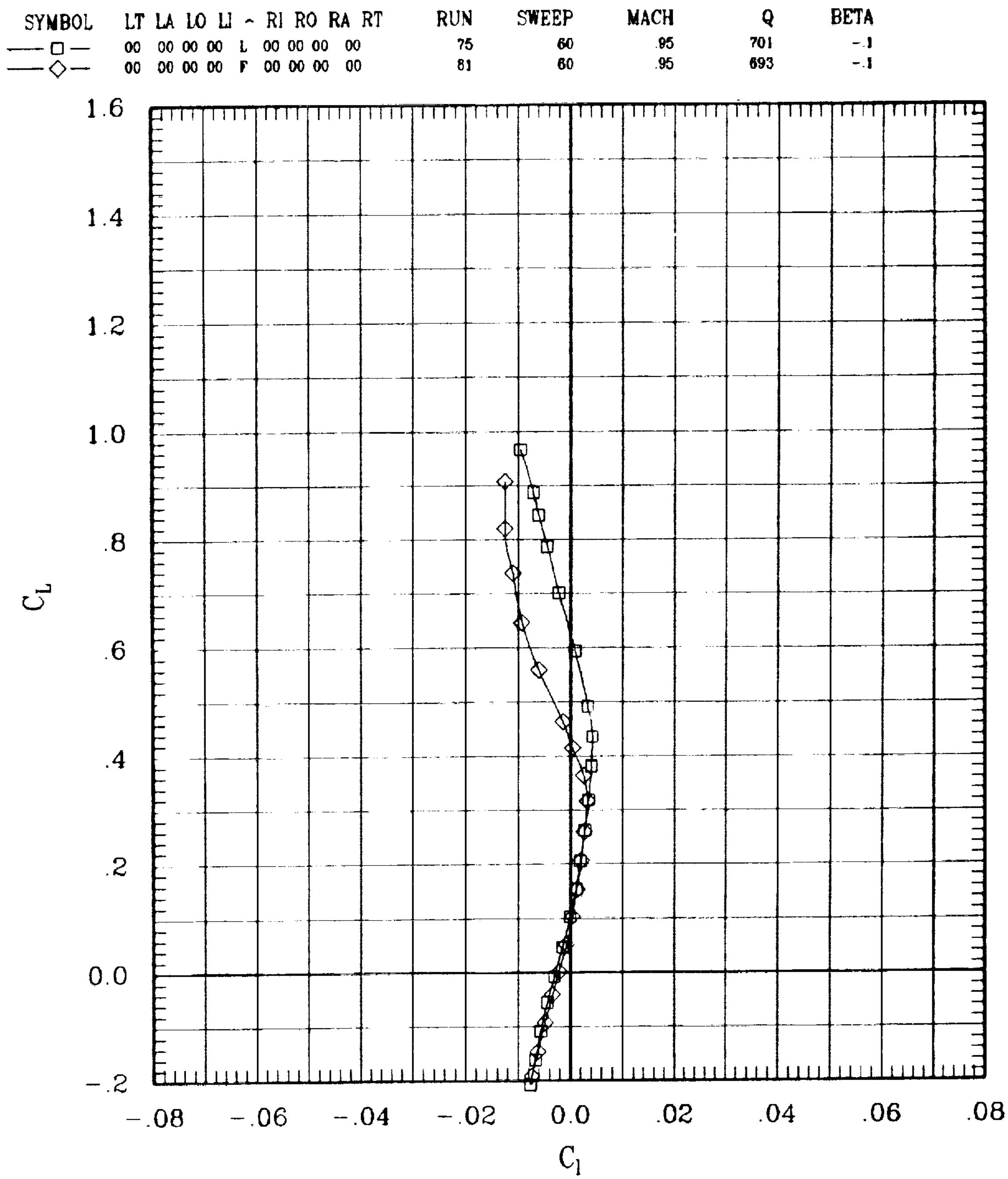

Figure 6(d). Effect of pivot height for sweep = 60 deg.

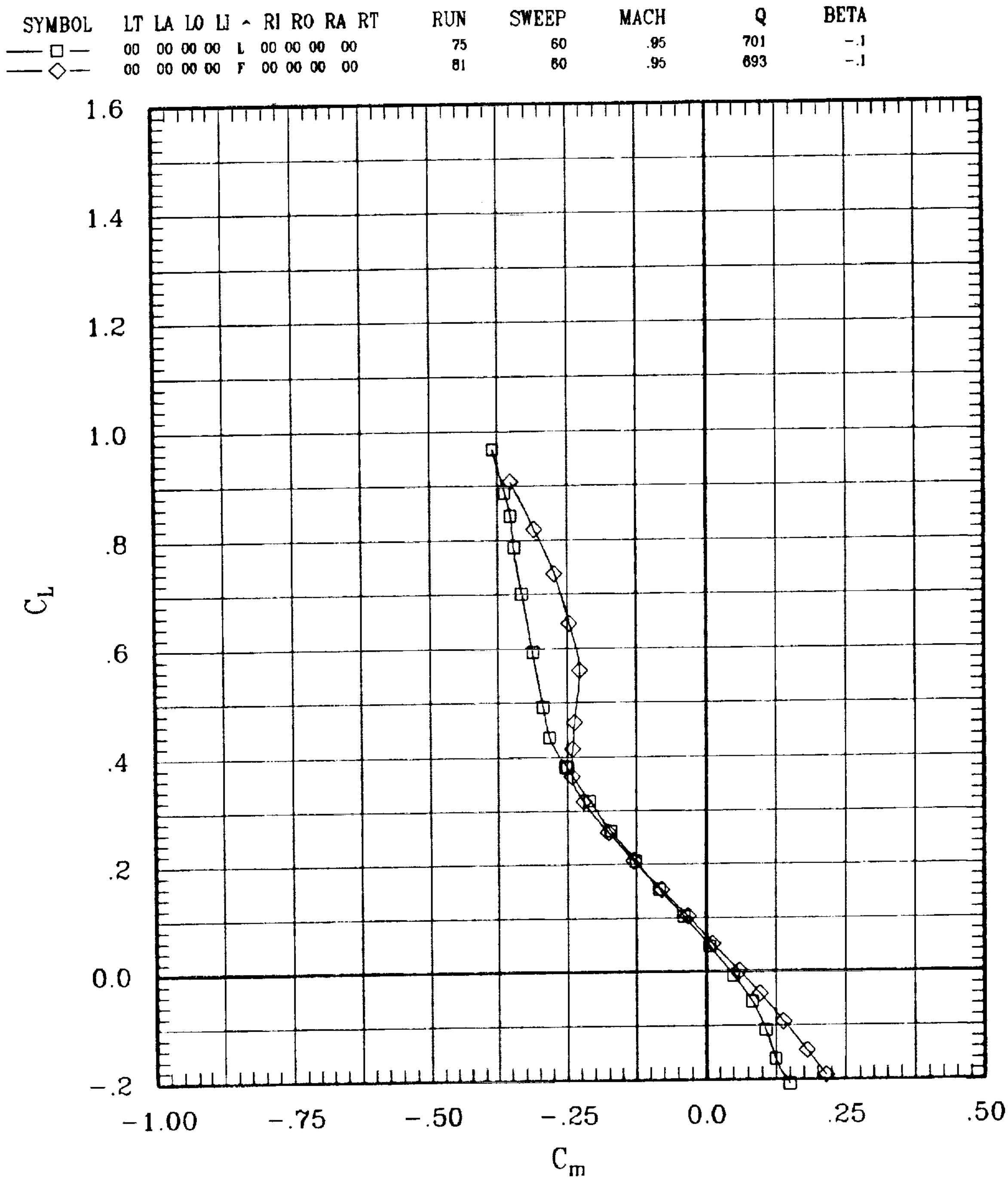

Figure 6(d). Effect of pivot height for sweep = 60 deg.

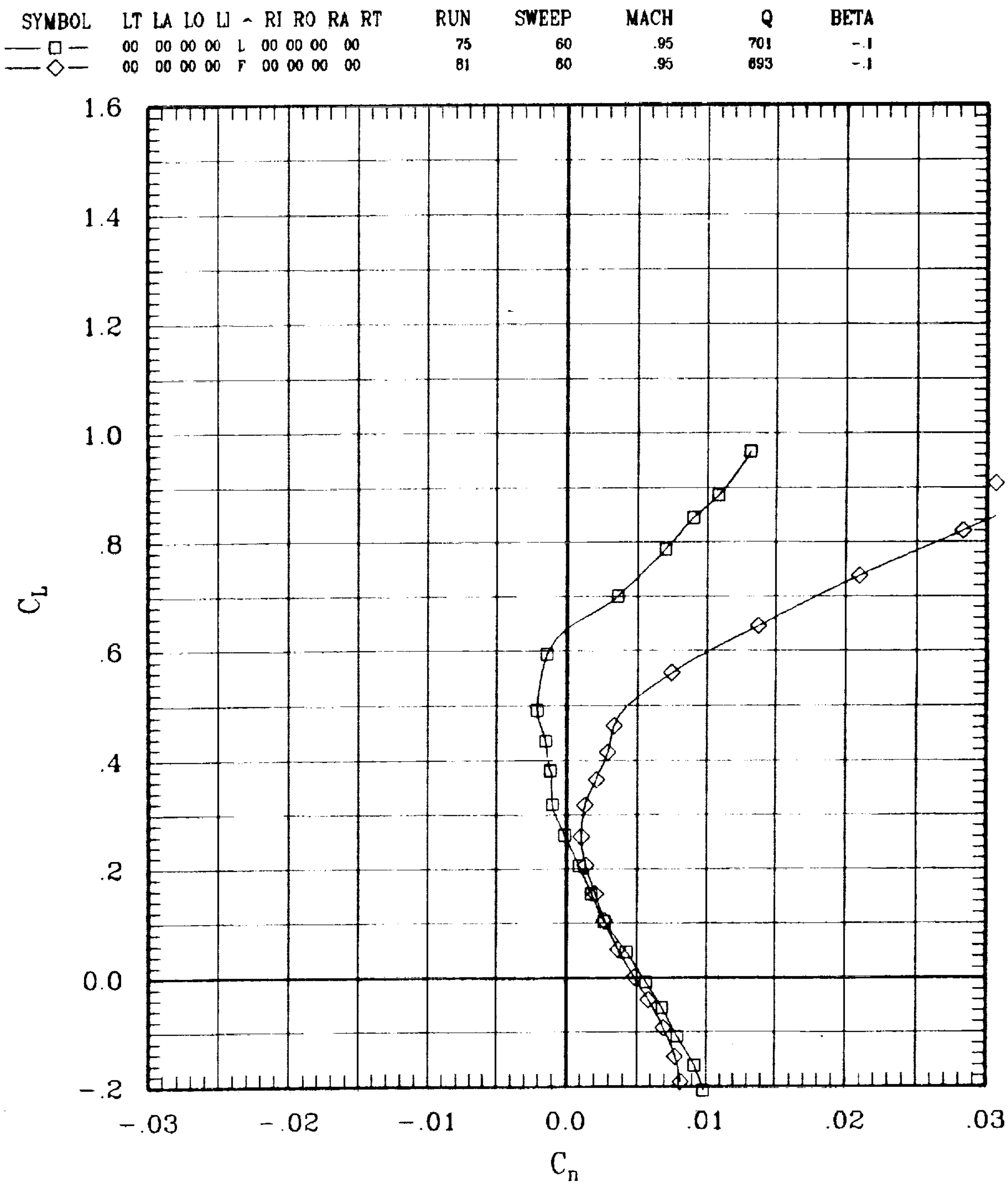

Figure 6(d). Effect of pivot height for sweep = 60 deg.

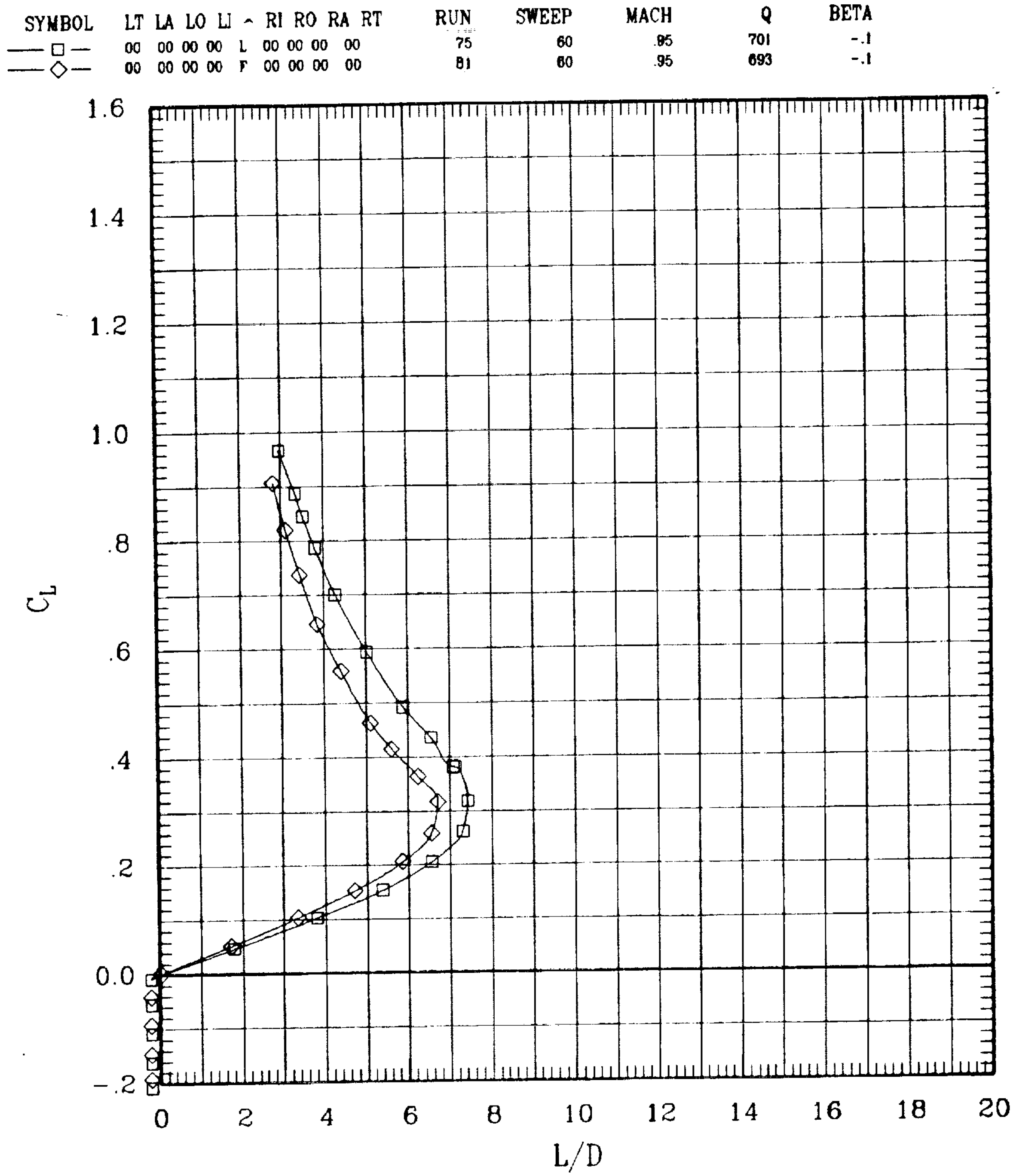

Figure 6(d). Effect of pivot height for sweep = 60 deg.

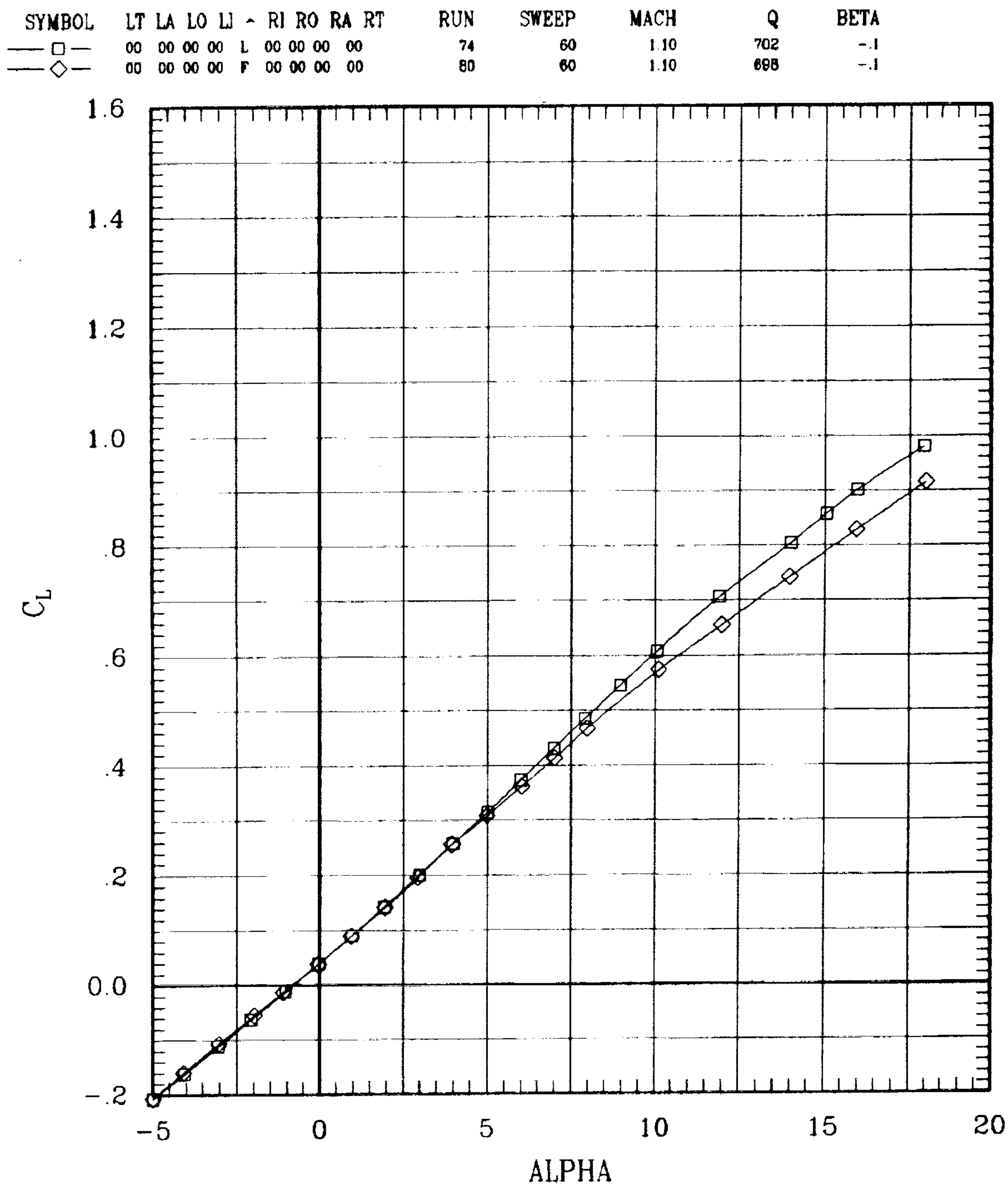

Figure 6(d). Effect of pivot height for sweep = 60 deg.

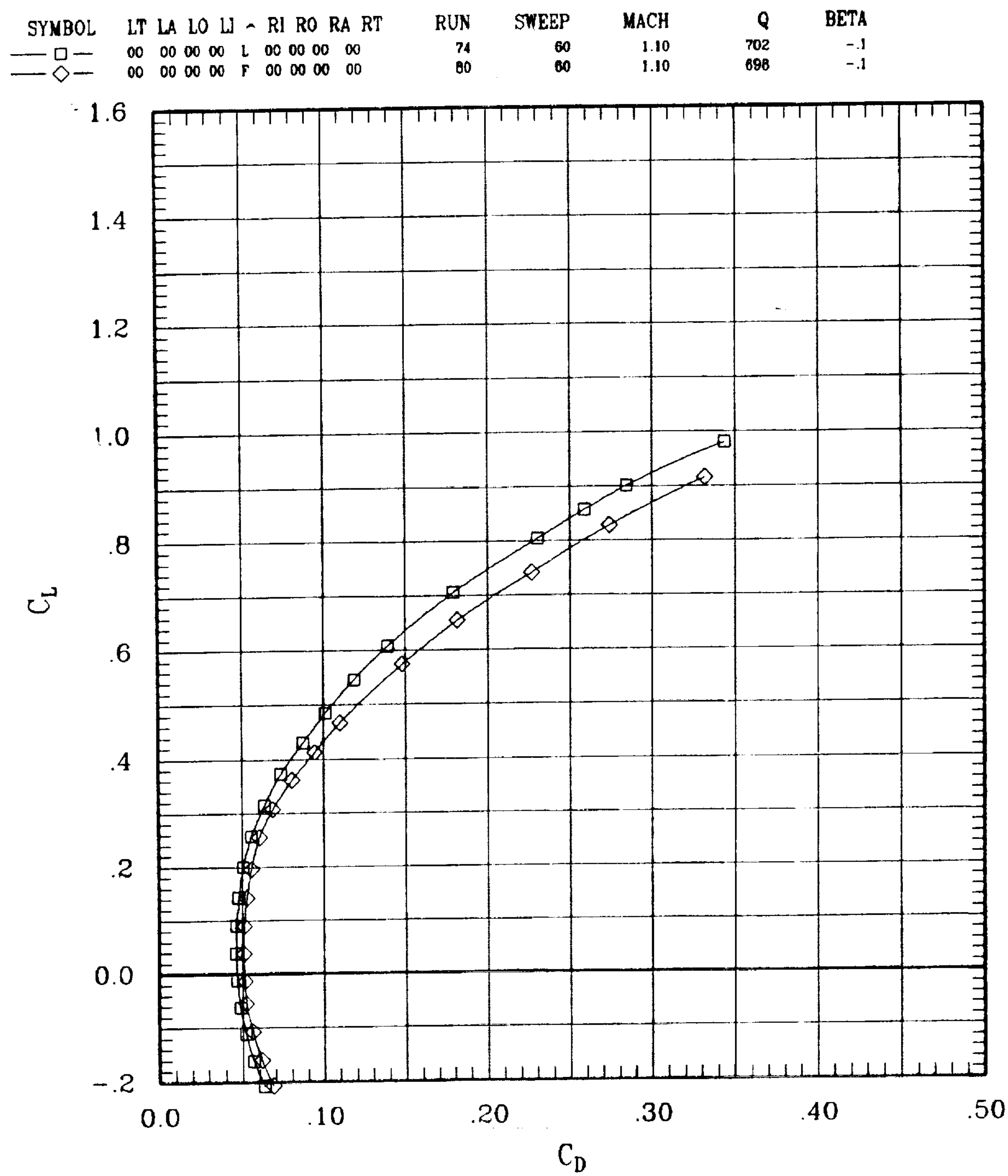

Figure 6(d). Effect of pivot height for sweep = 60 deg.

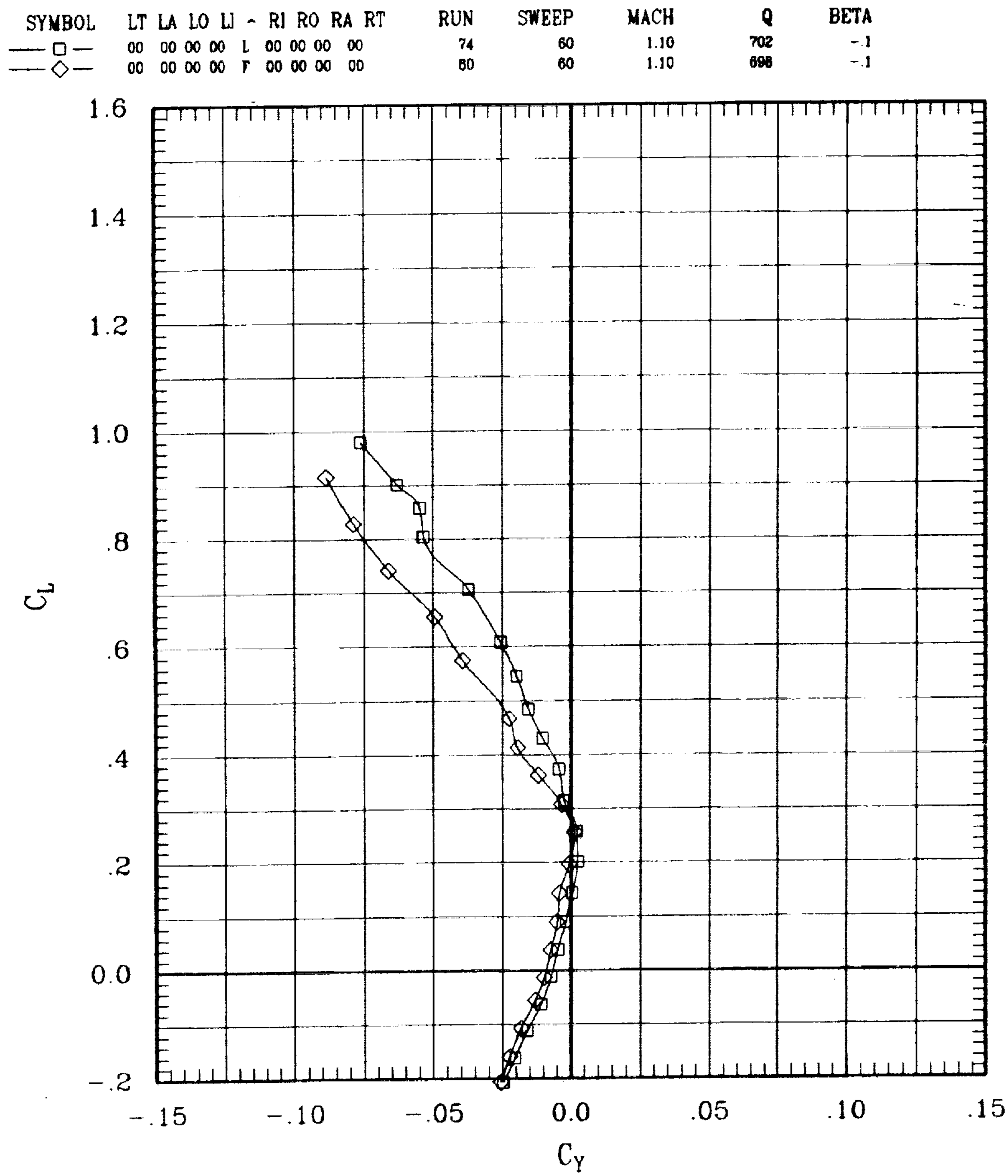

Figure 6(d). Effect of pivot height for sweep = 60 deg.

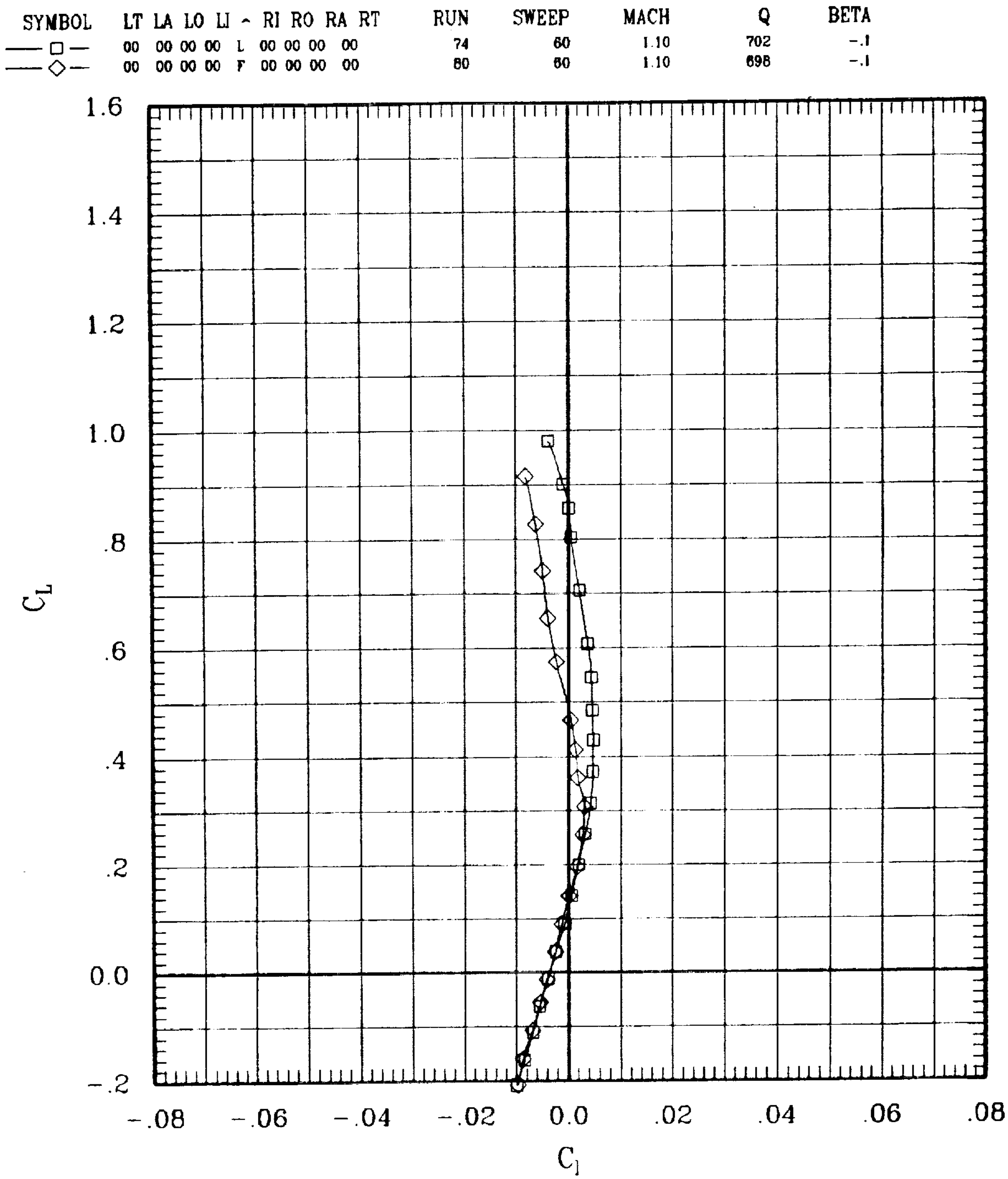

Figure 6(d). Effect of pivot height for sweep = 60 deg.

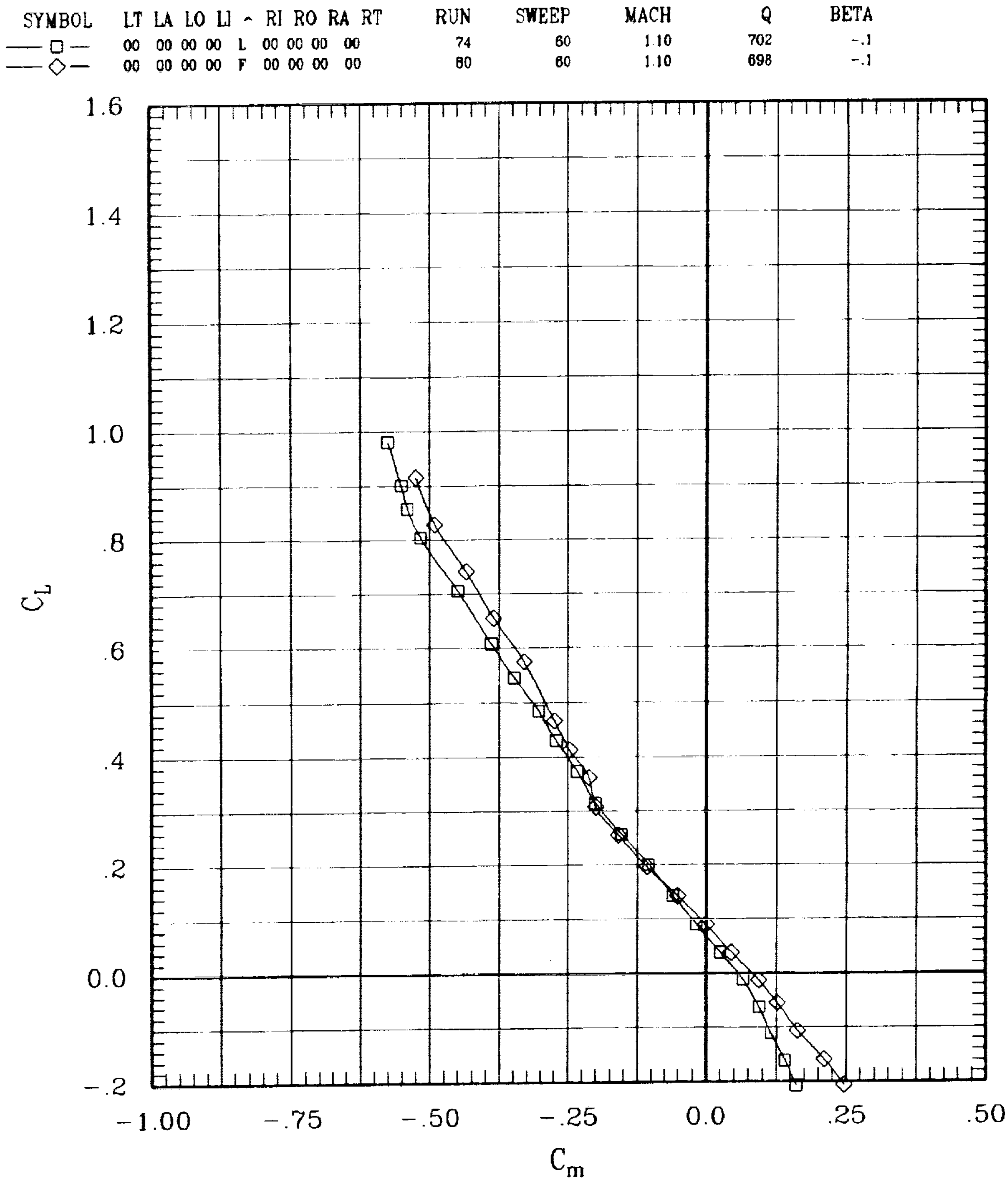

Figure 6(d). Effect of pivot height for sweep = 60 deg.

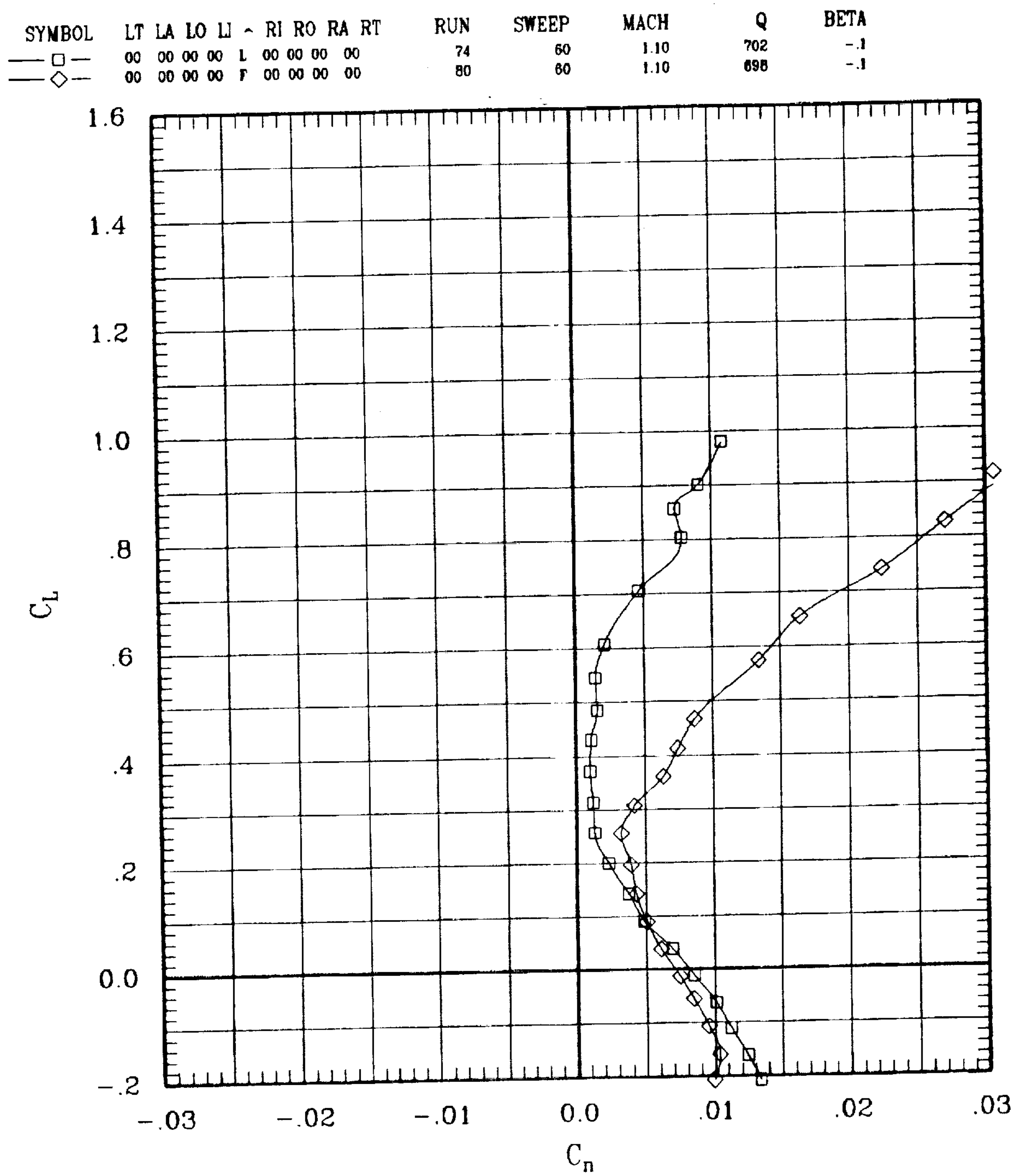

Figure 6(d). Effect of pivot height for sweep = 60 deg.

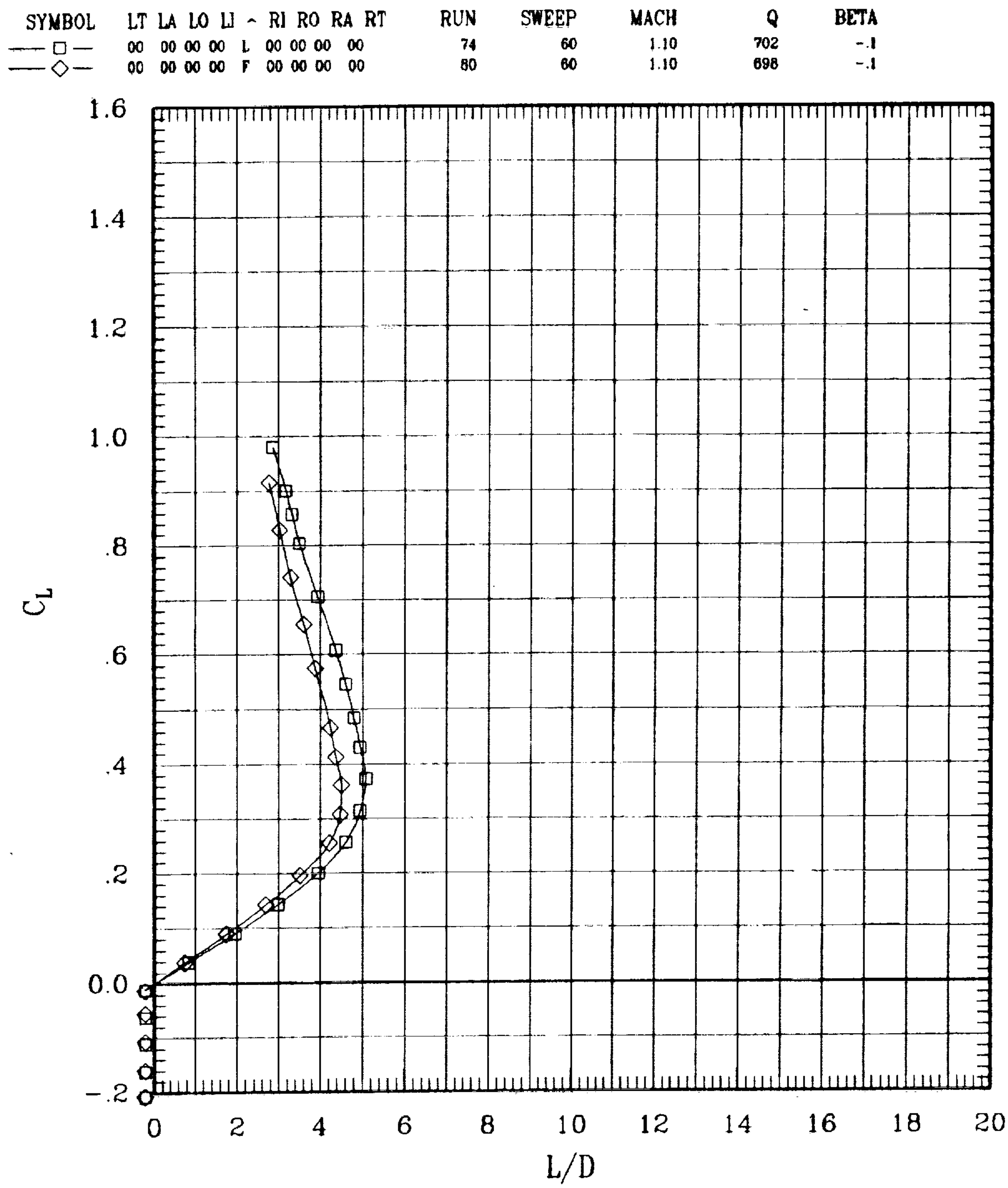

Figure 6(d). Effect of pivot height for sweep = 60 deg.

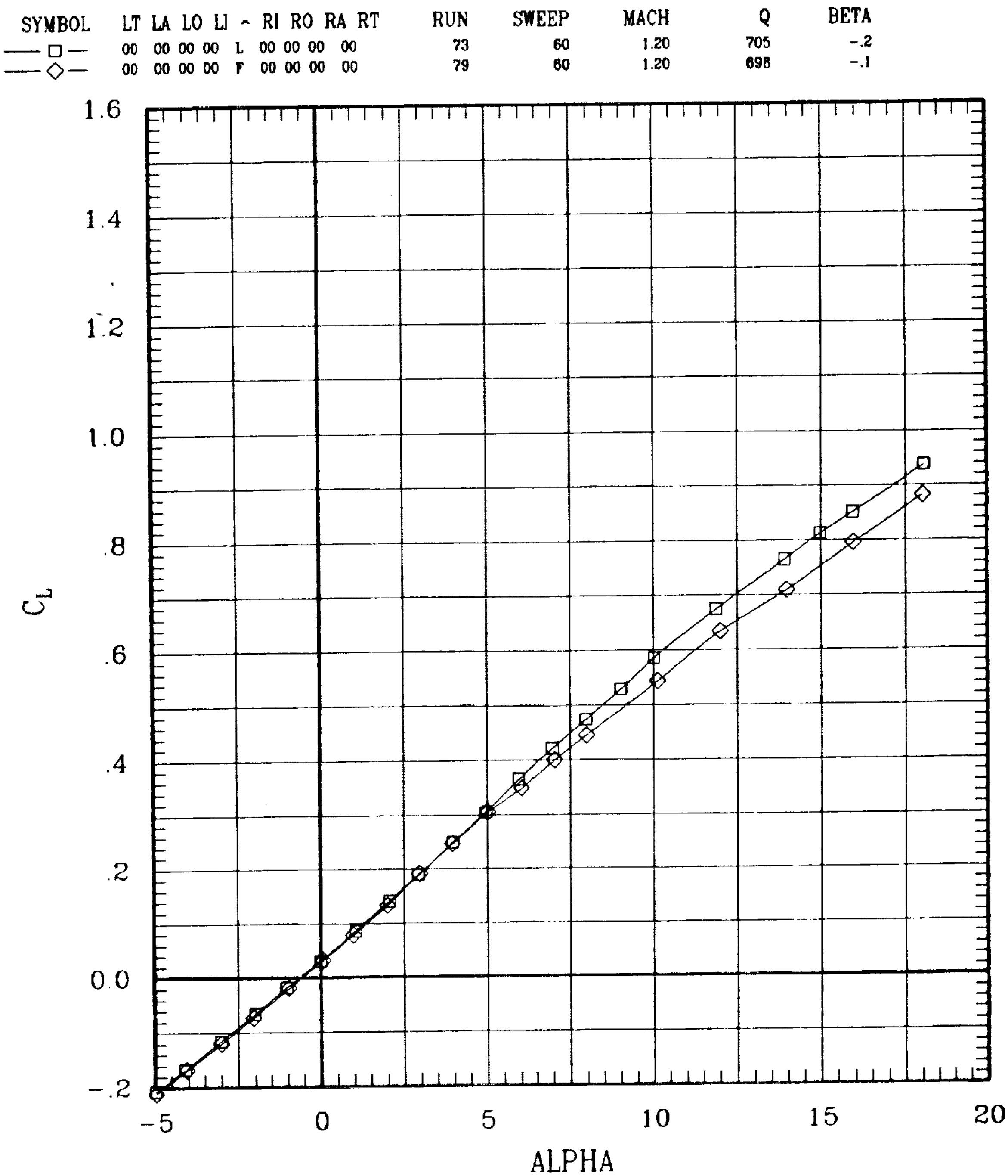

Figure 6(d). Effect of pivot height for sweep = 60 deg.

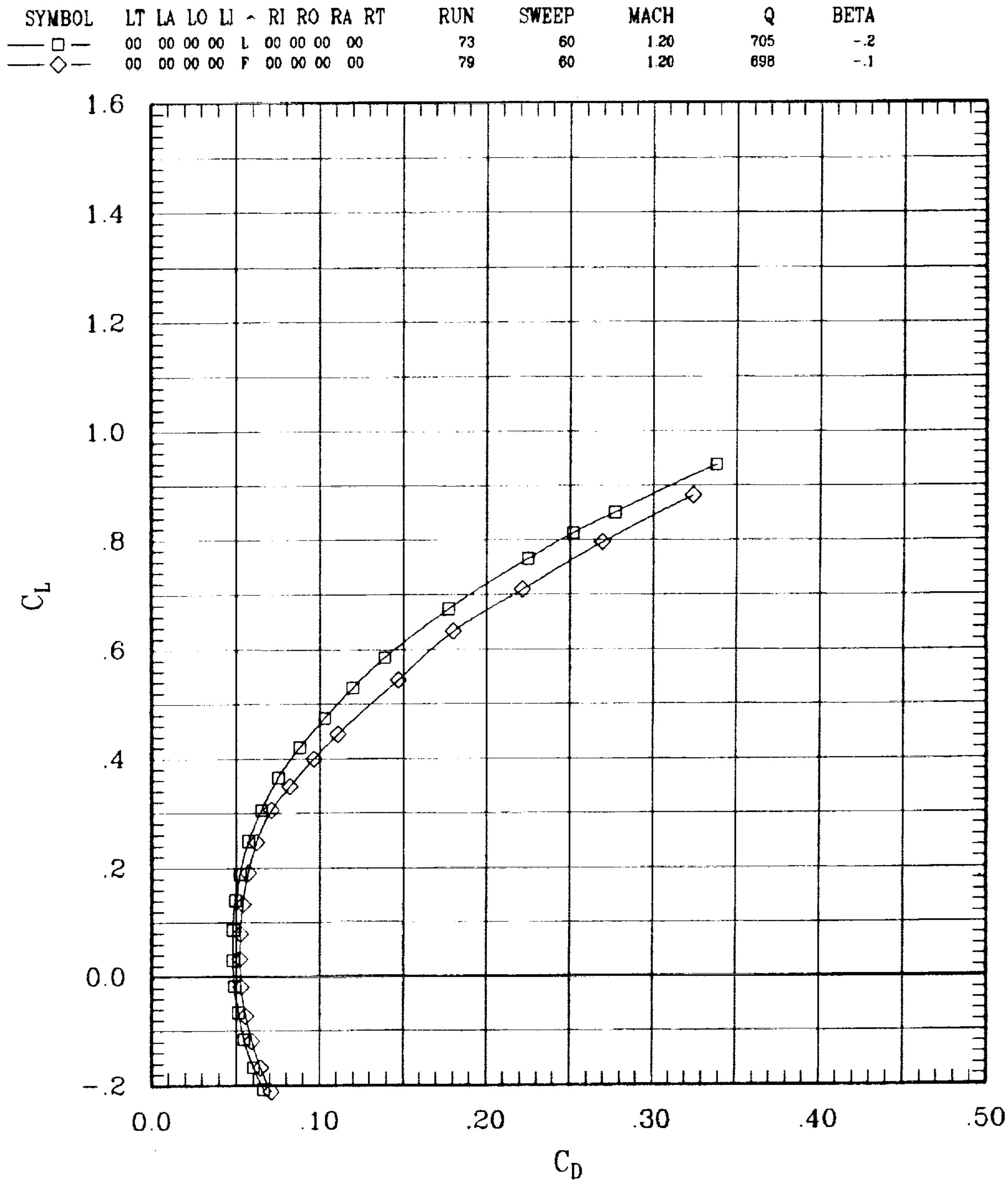

Figure 6(d). Effect of pivot height for sweep = 60 deg.

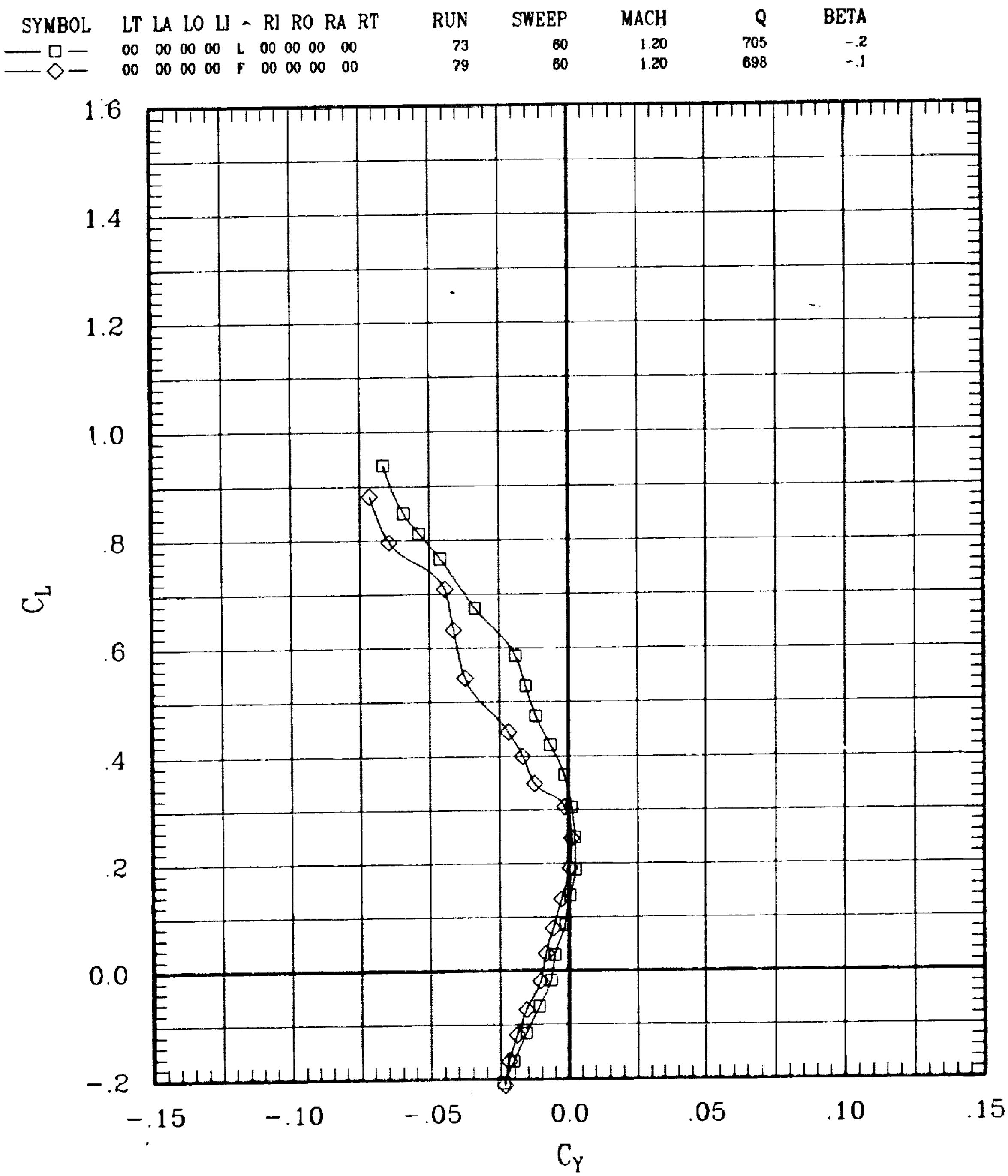

Figure 6(d). Effect of pivot height for sweep = 60 deg.

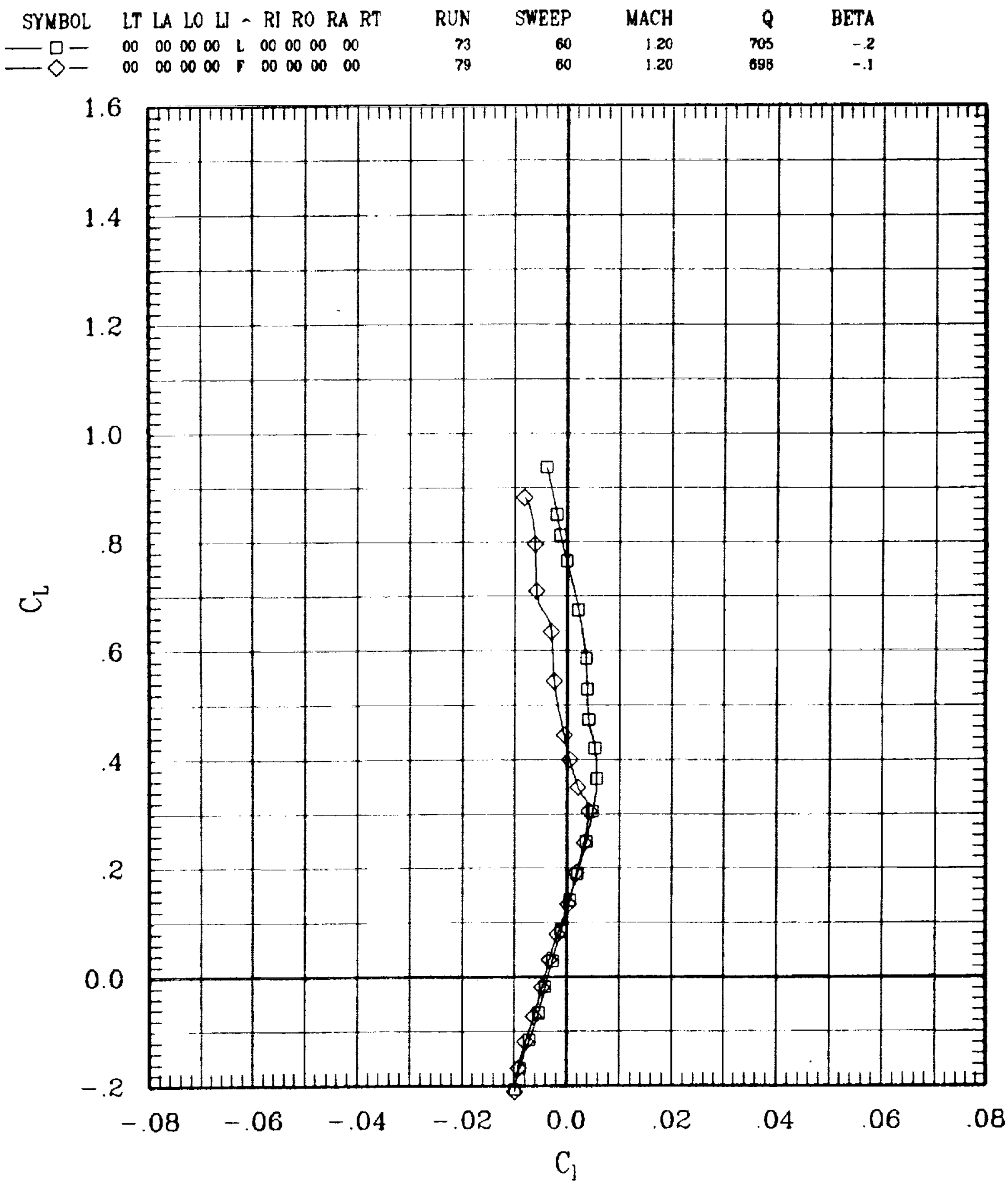

Figure 6(d). Effect of pivot height for sweep = 60 deg.

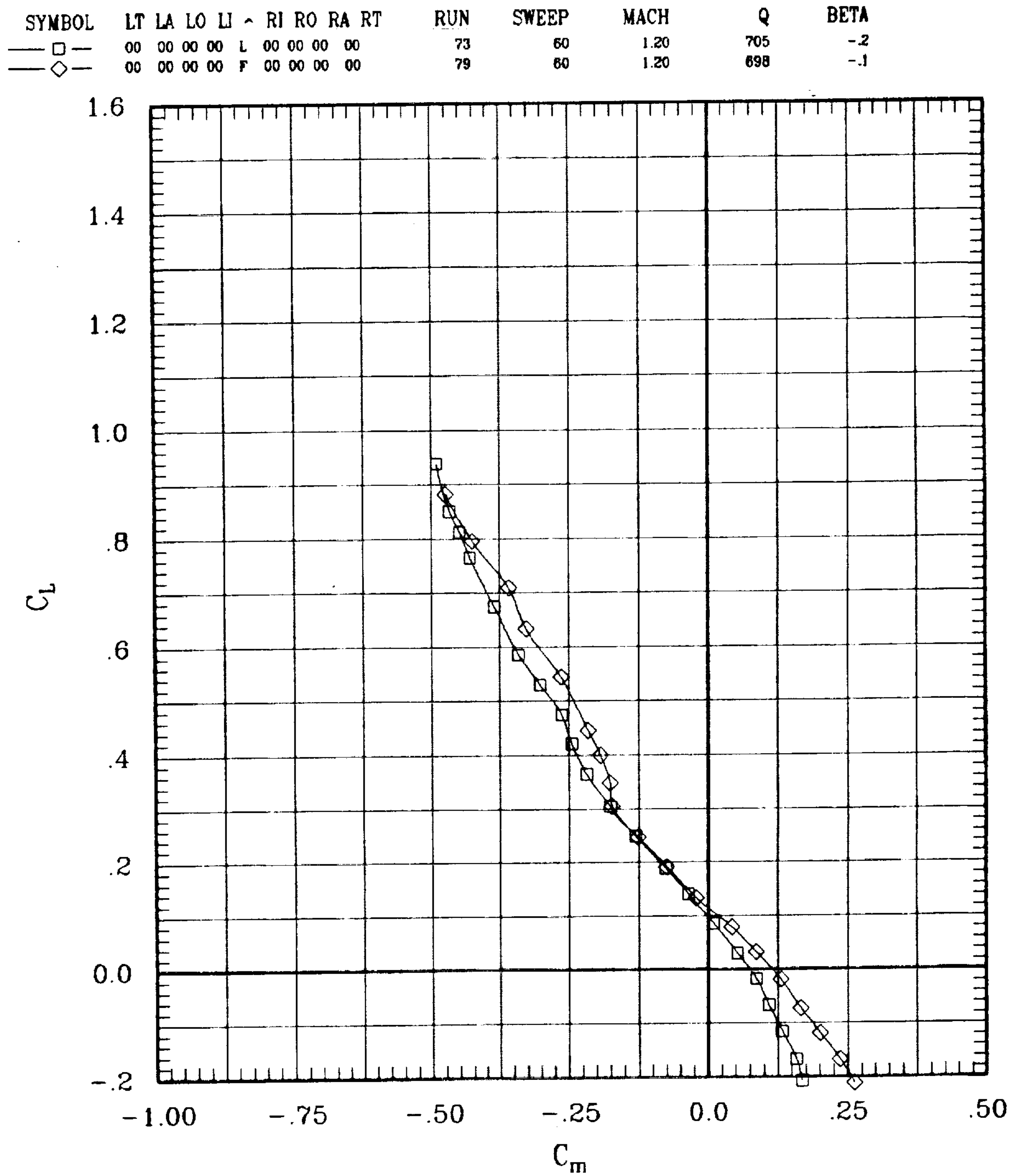

Figure 6(d). Effect of pivot height for sweep = 60 deg.

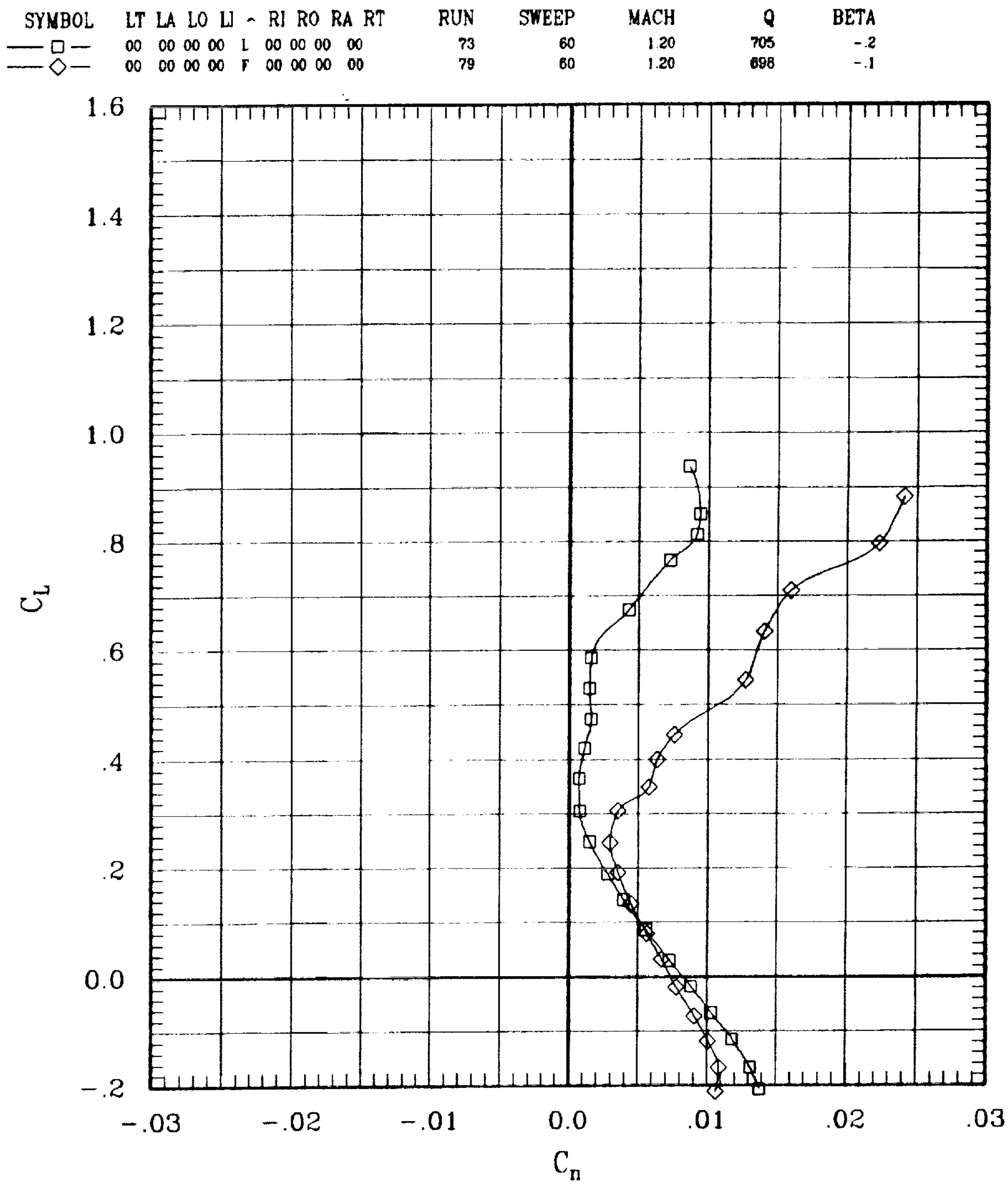

Figure 6(d). Effect of pivot height for sweep = 60 deg.

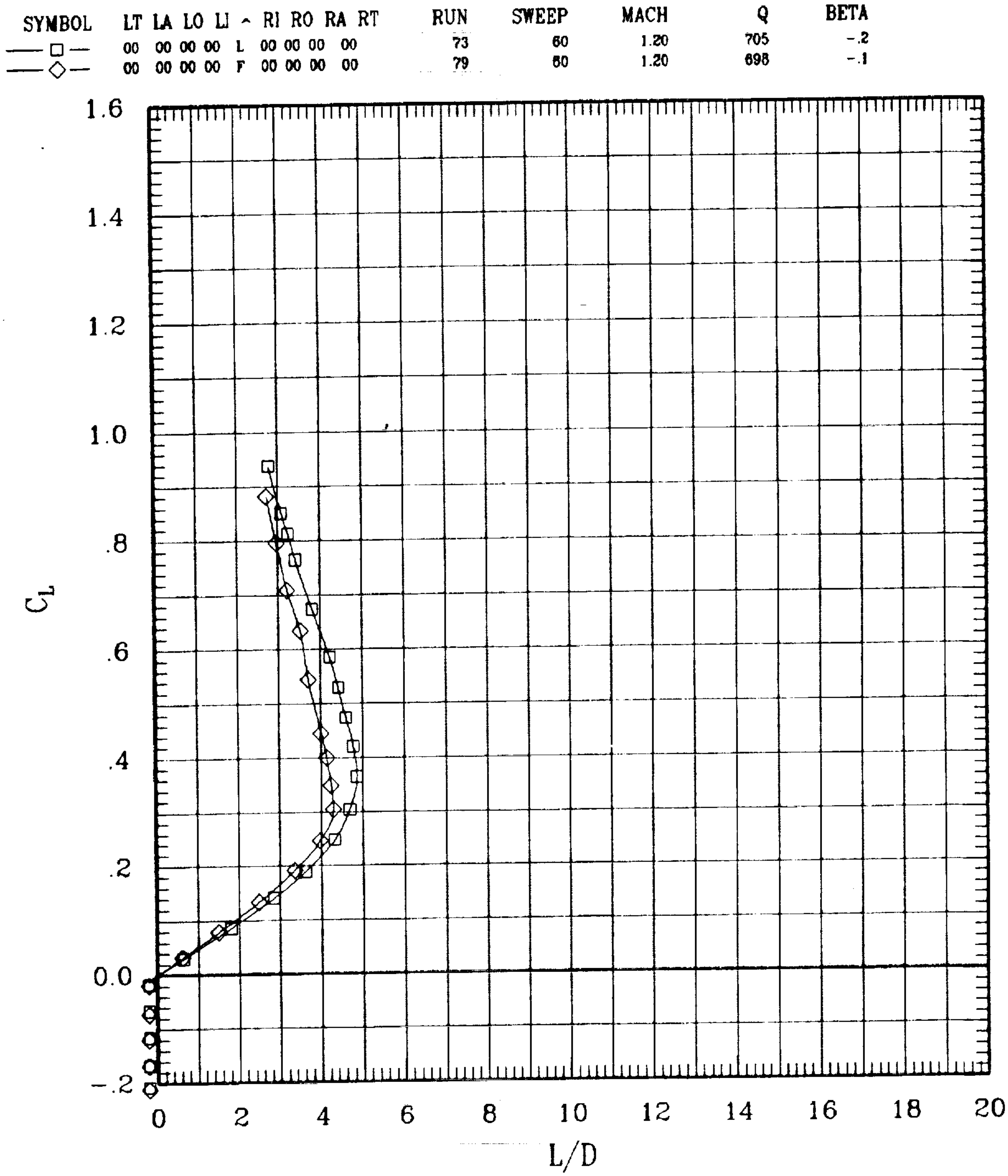

Figure 6(d). Effect of pivot height for sweep = 60 deg.

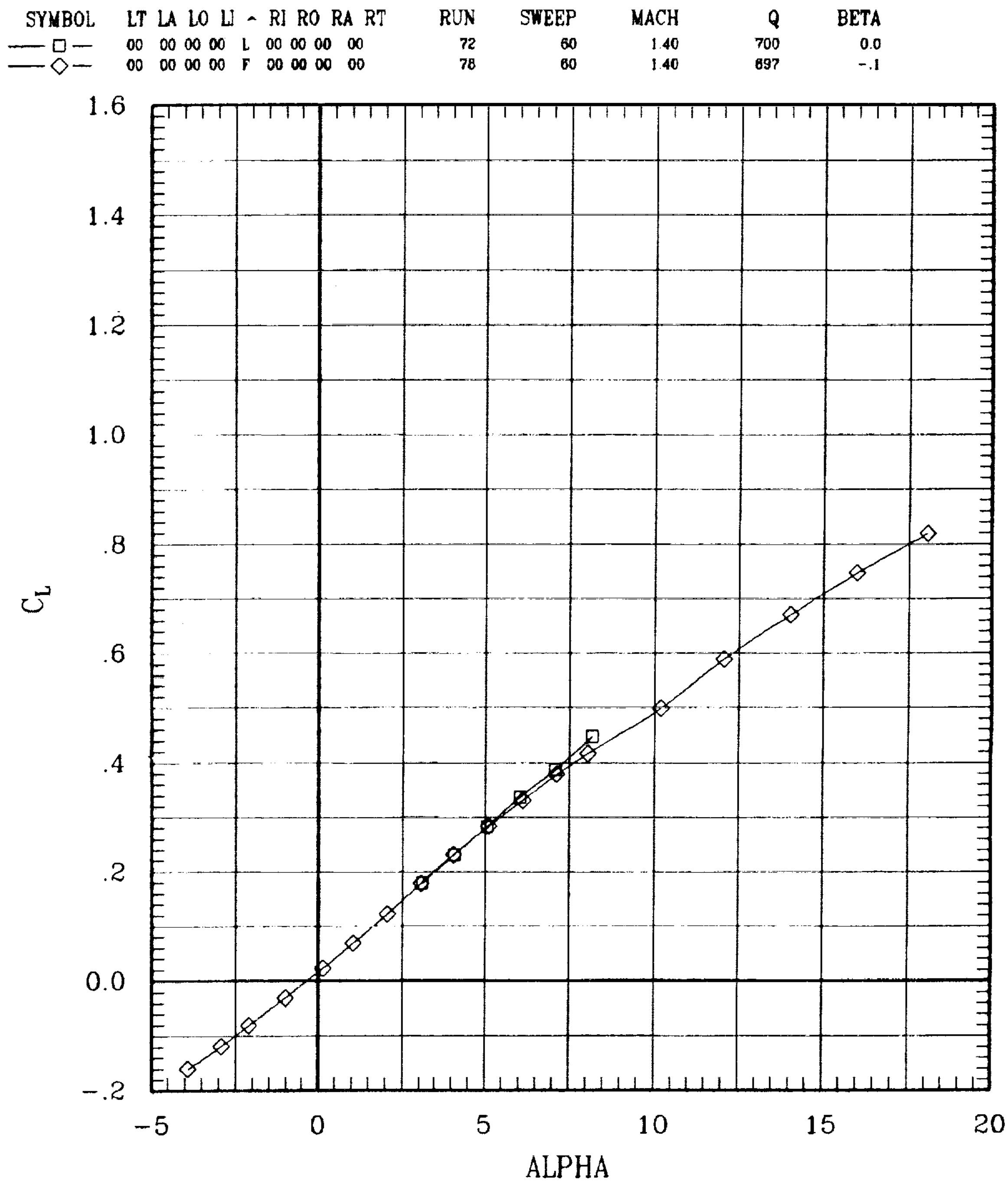

Figure 6(d). Effect of pivot height for sweep = 60 deg.

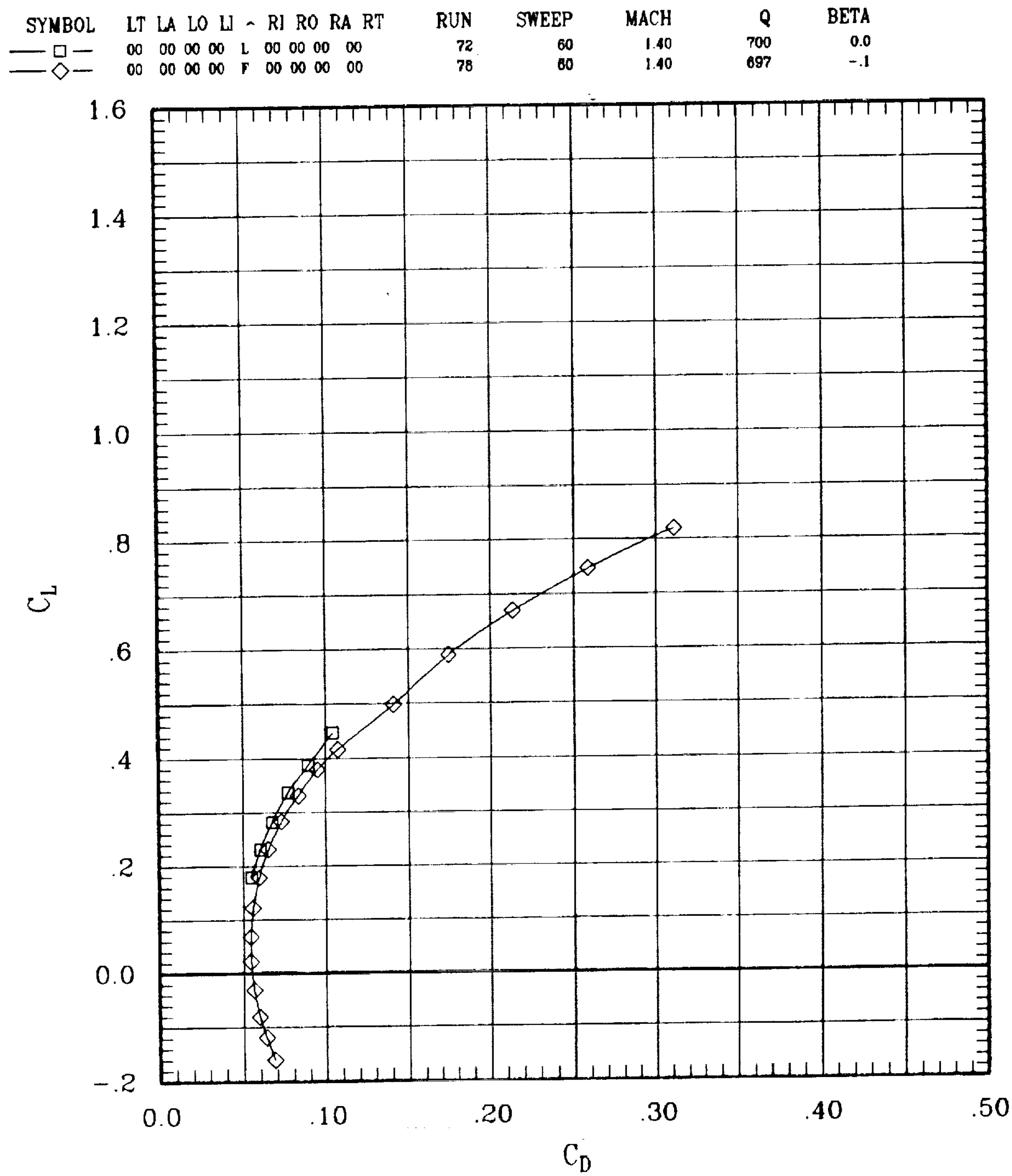

Figure 6(d). Effect of pivot height for sweep = 60 deg.

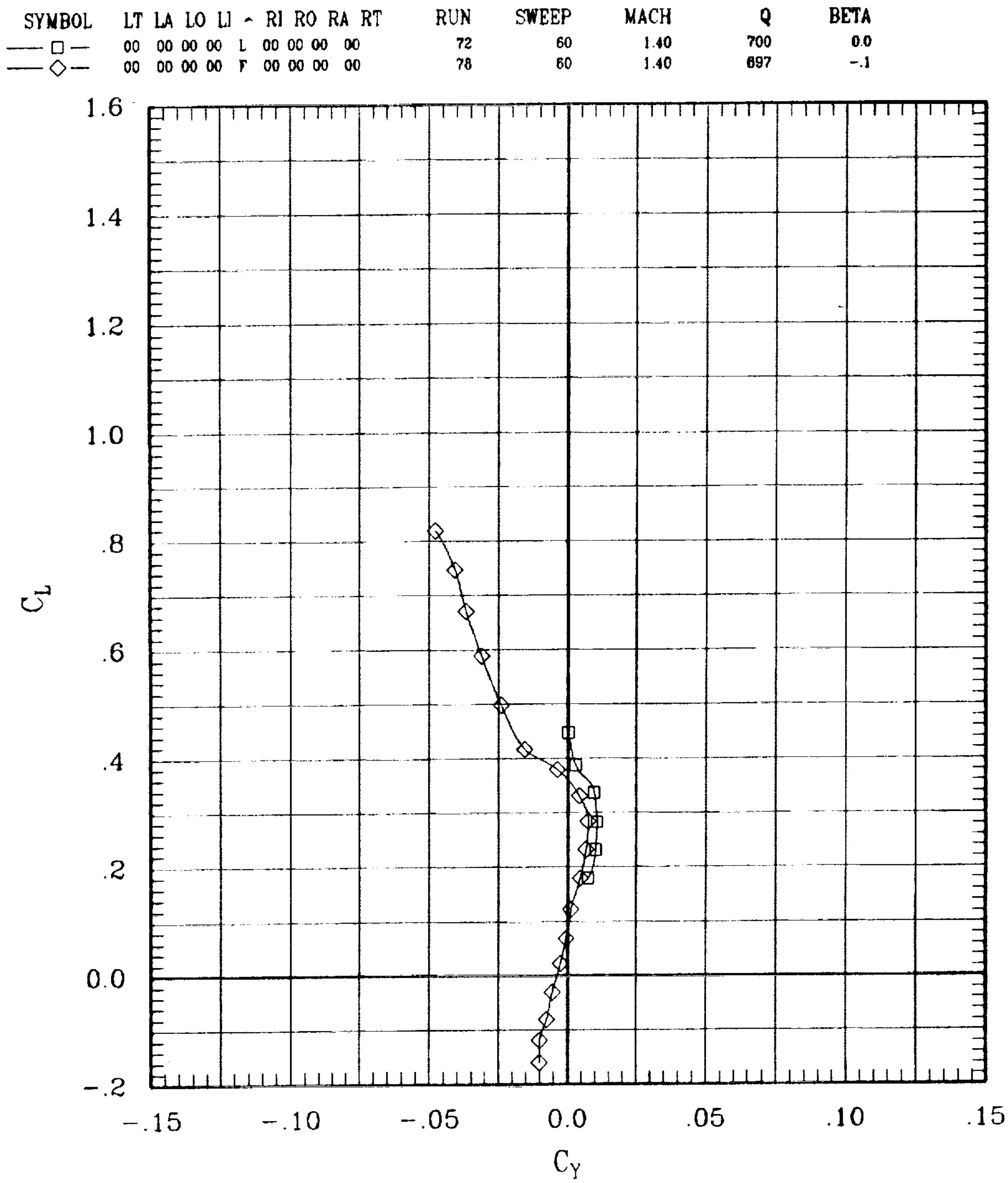

Figure 6(d). Effect of pivot height for sweep = 60 deg.

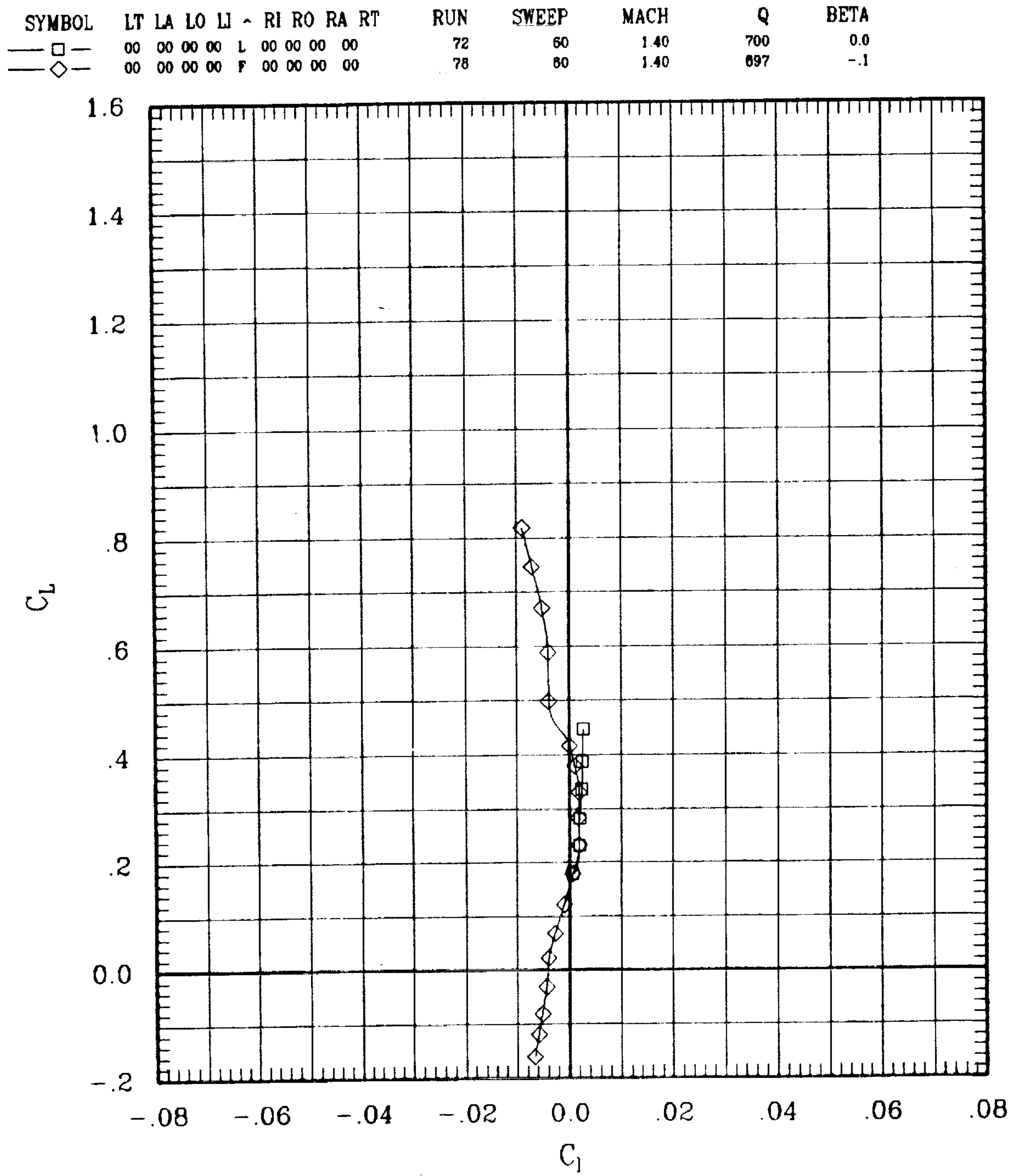

Figure 6(d). Effect of pivot height for sweep = 60 deg.

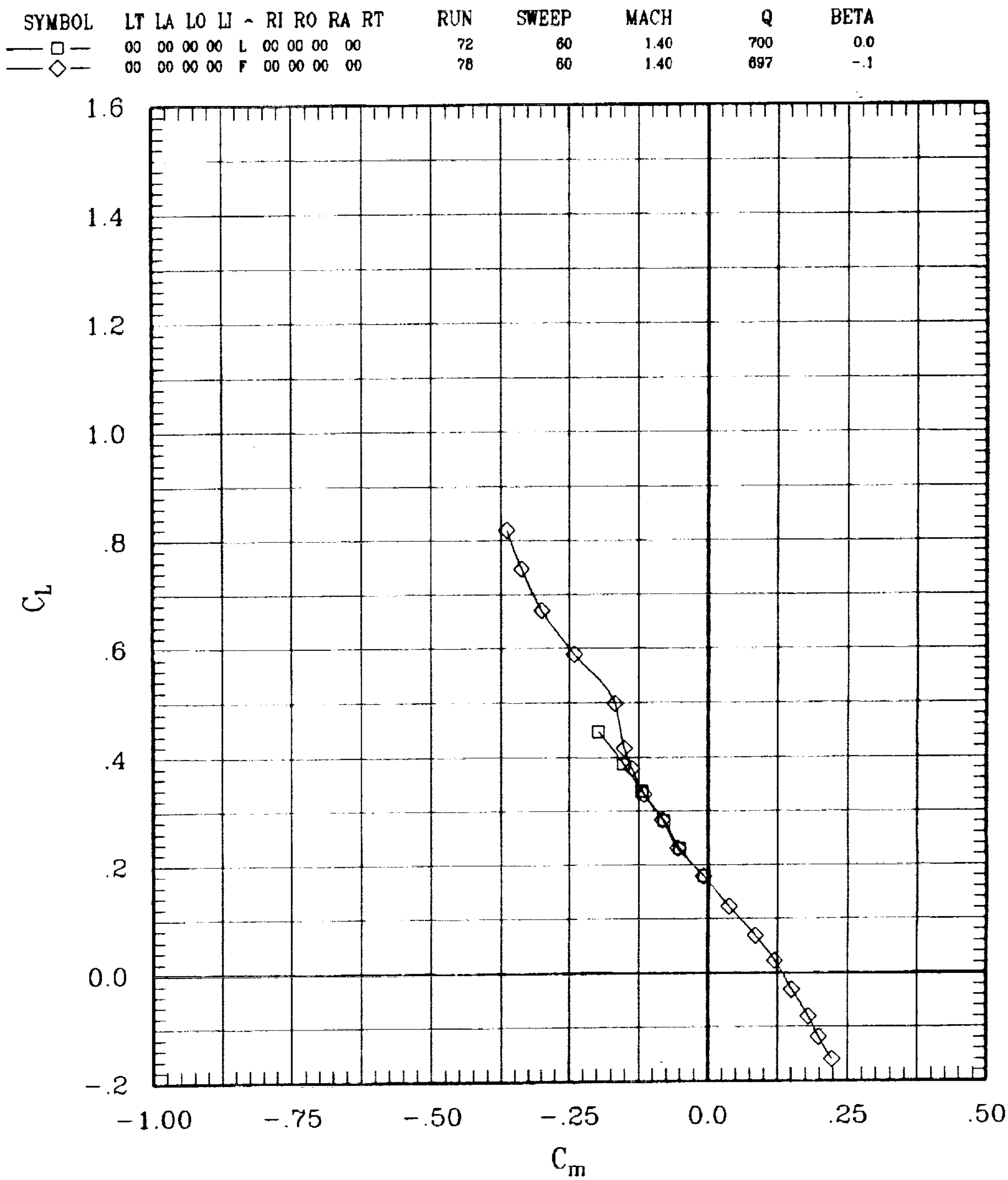

Figure 6(d). Effect of pivot height for sweep = 60 deg.

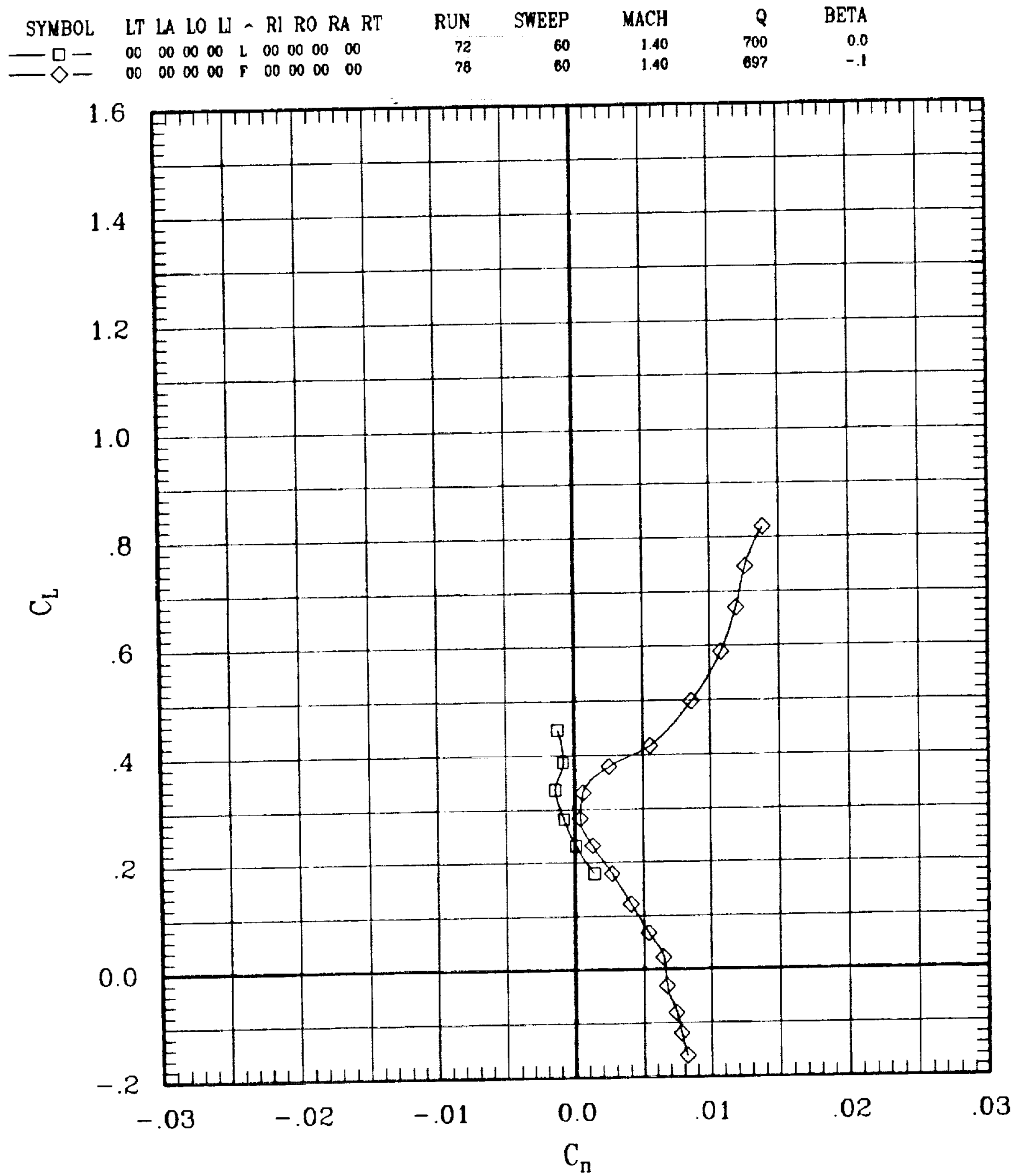

Figure 6(d). Effect of pivot height for sweep = 60 deg.

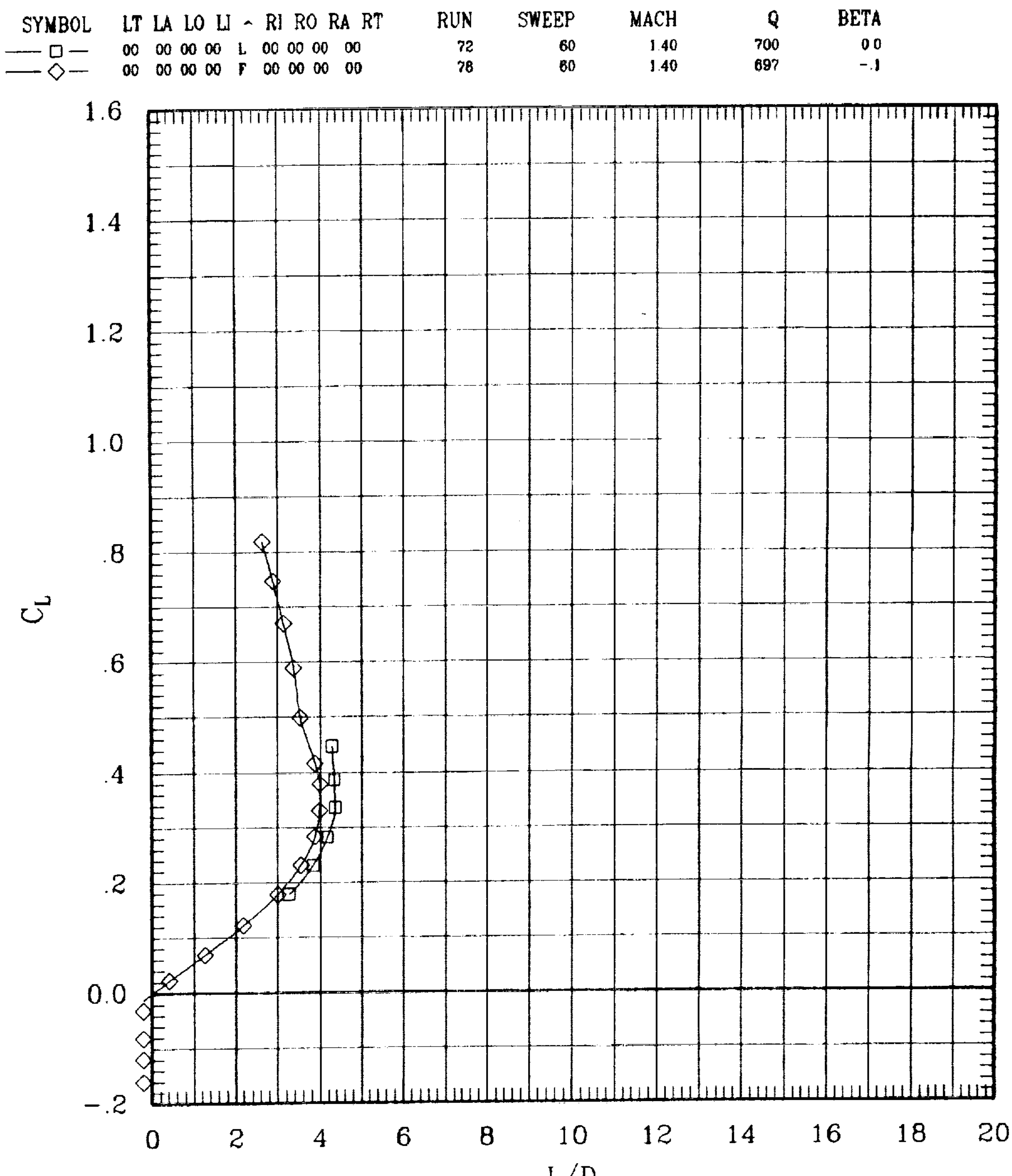

Figure 6(d). Effect of pivot height for sweep = 60 deg.

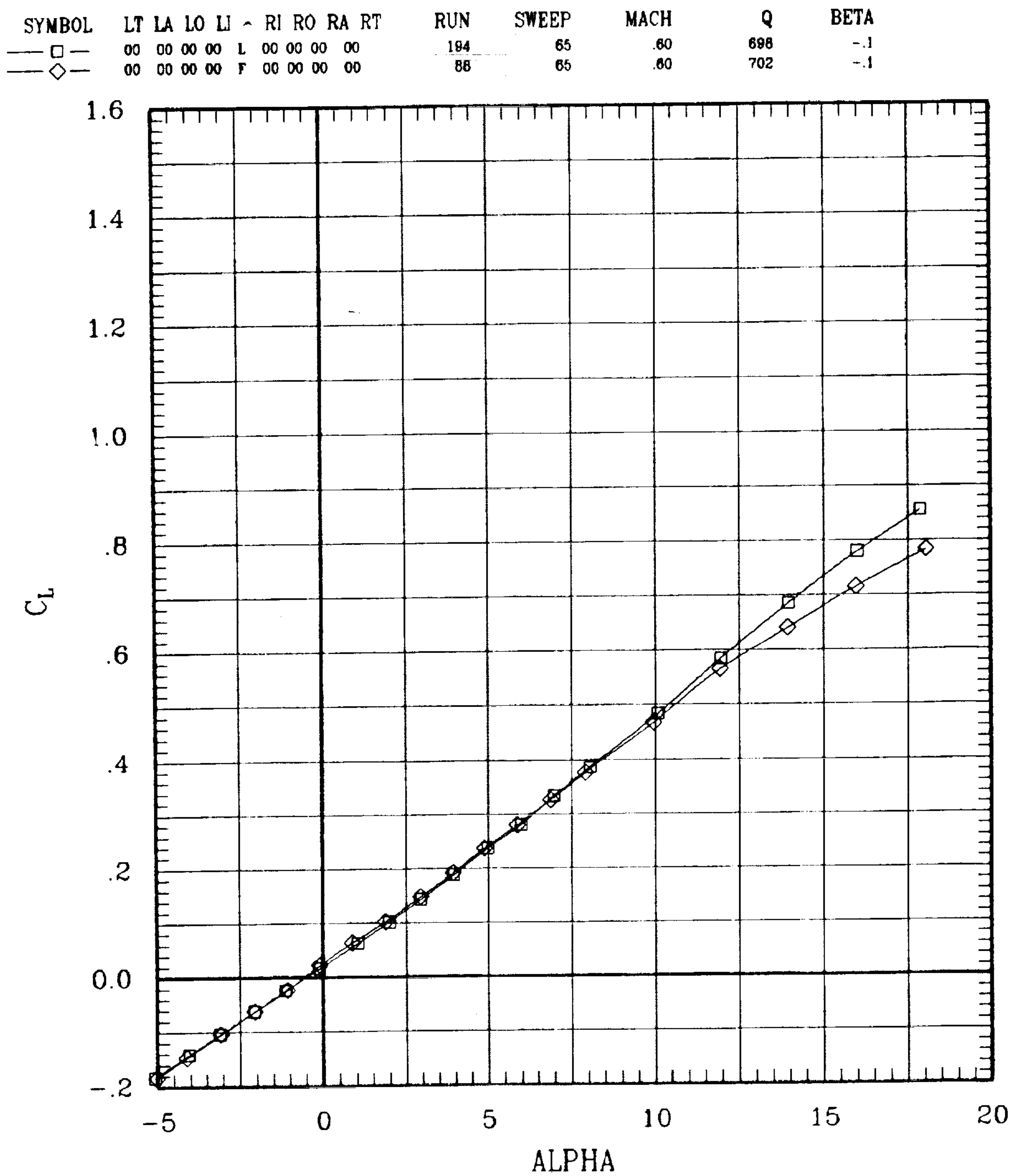

Figure 6(e). Effect of pivot height for sweep = 65 deg.

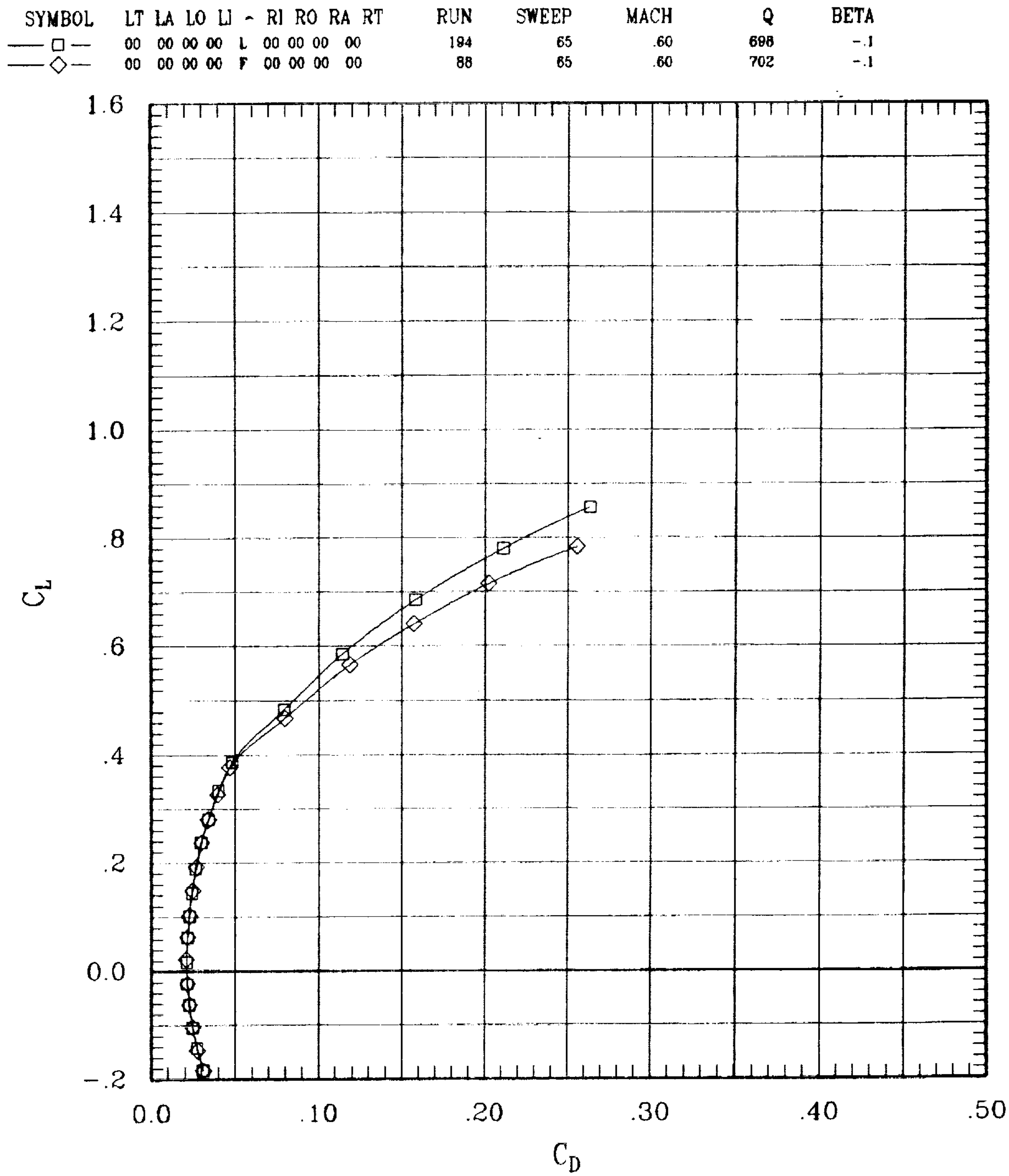

Figure 6(e). Effect of pivot height for sweep = 65 deg.

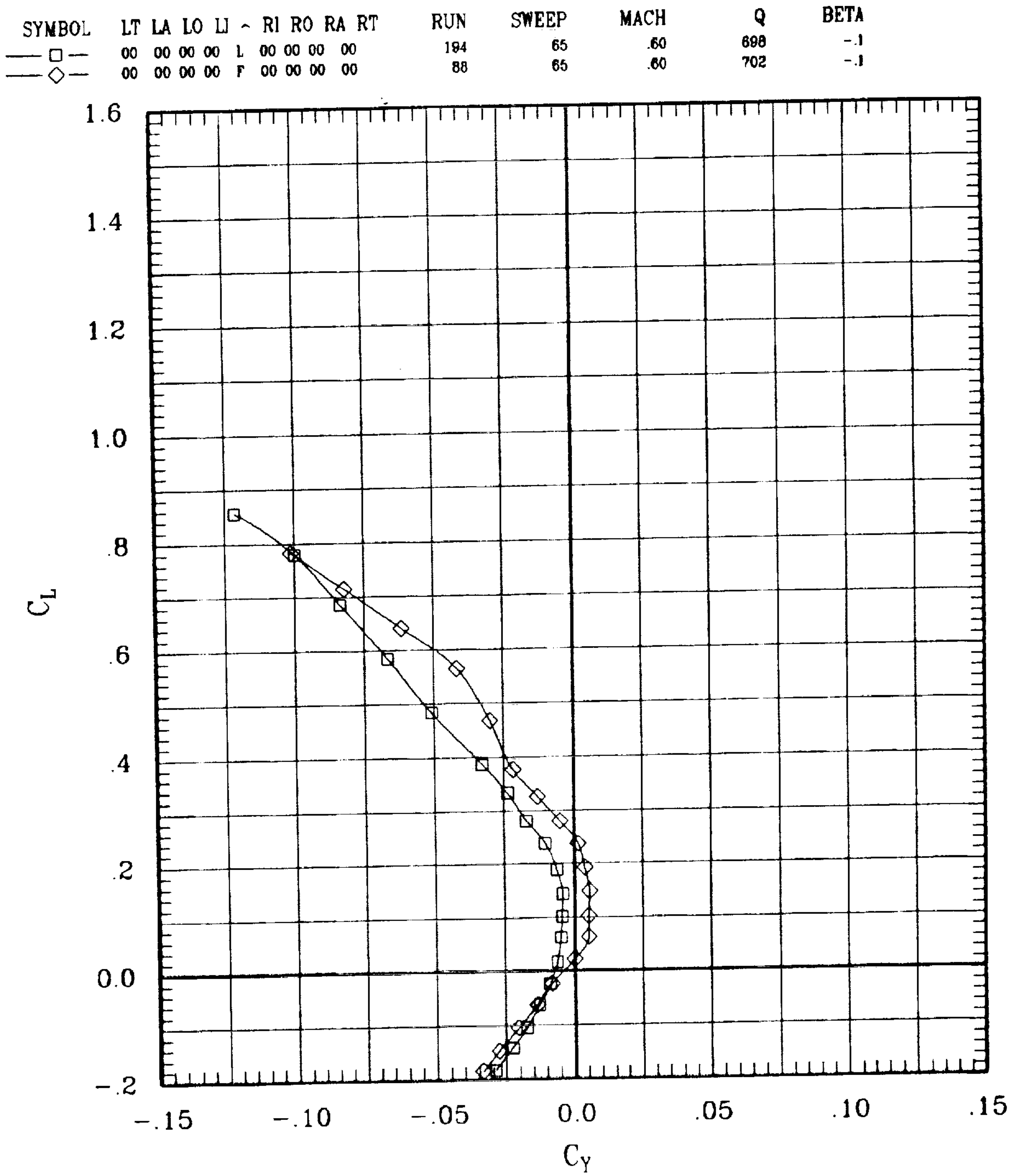

Figure 6(e). Effect of pivot height for sweep = 65 deg.

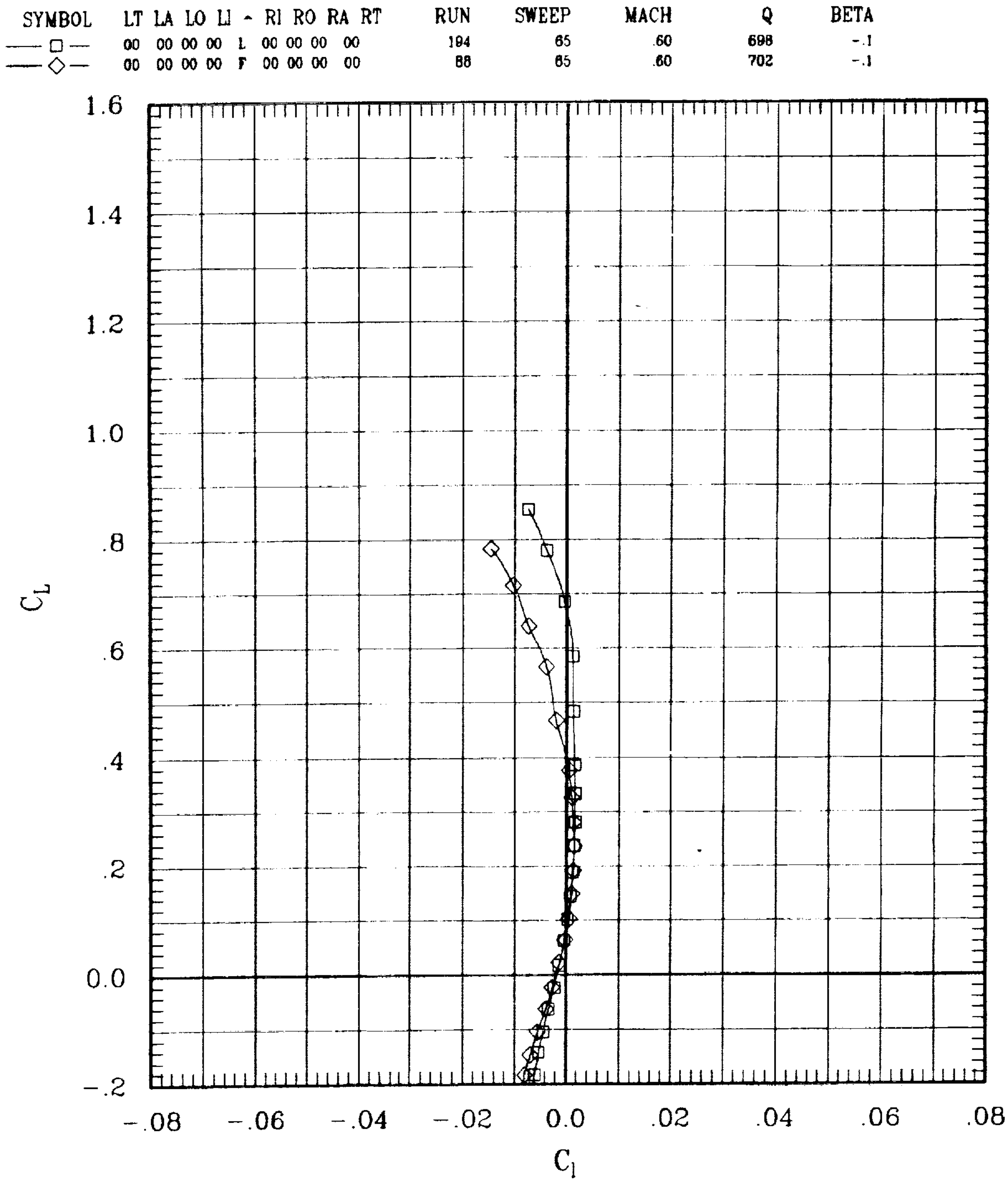

Figure 6(e). Effect of pivot height for sweep = 65 deg.

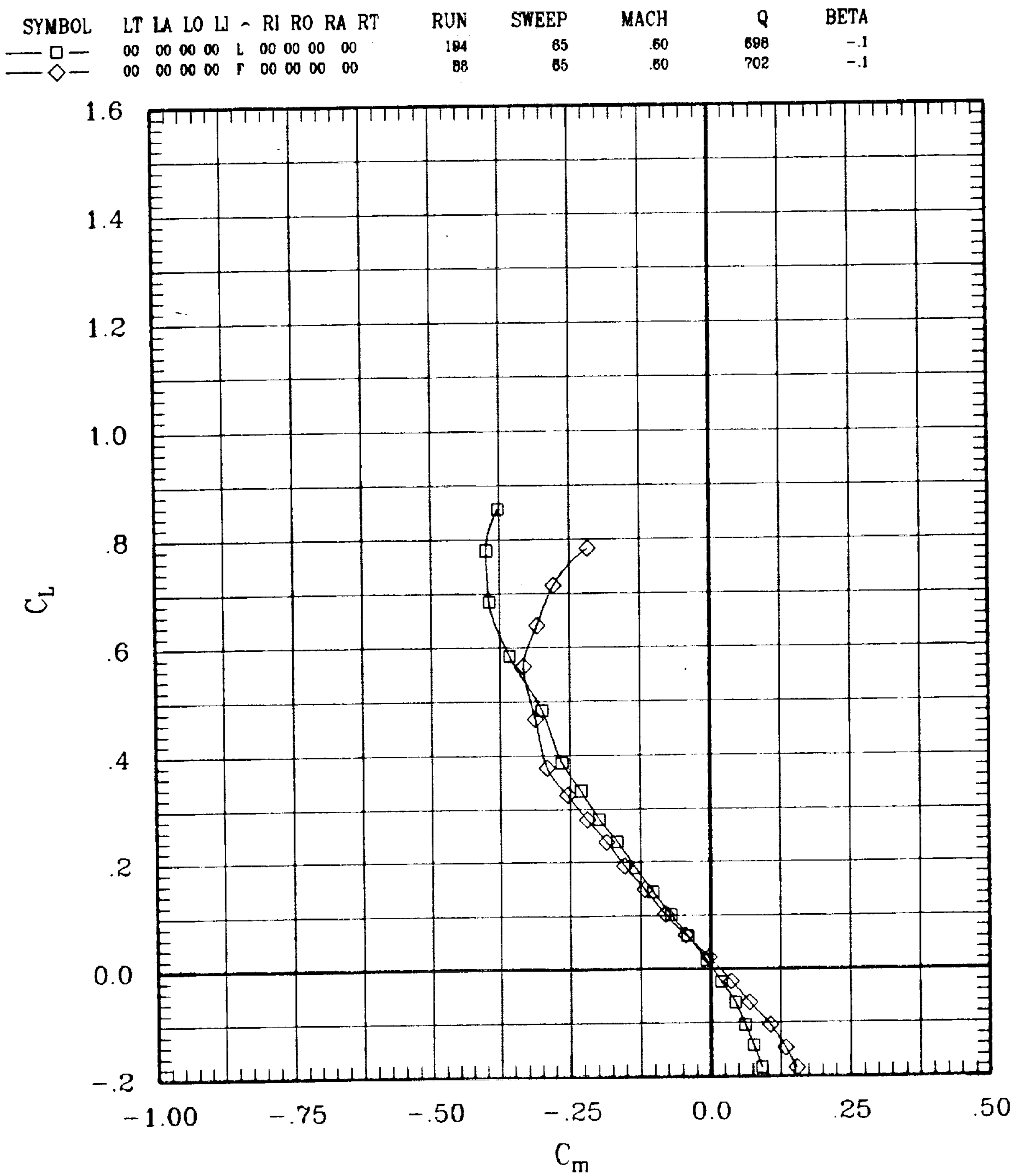

Figure 6(e). Effect of pivot height for sweep = 65 deg.

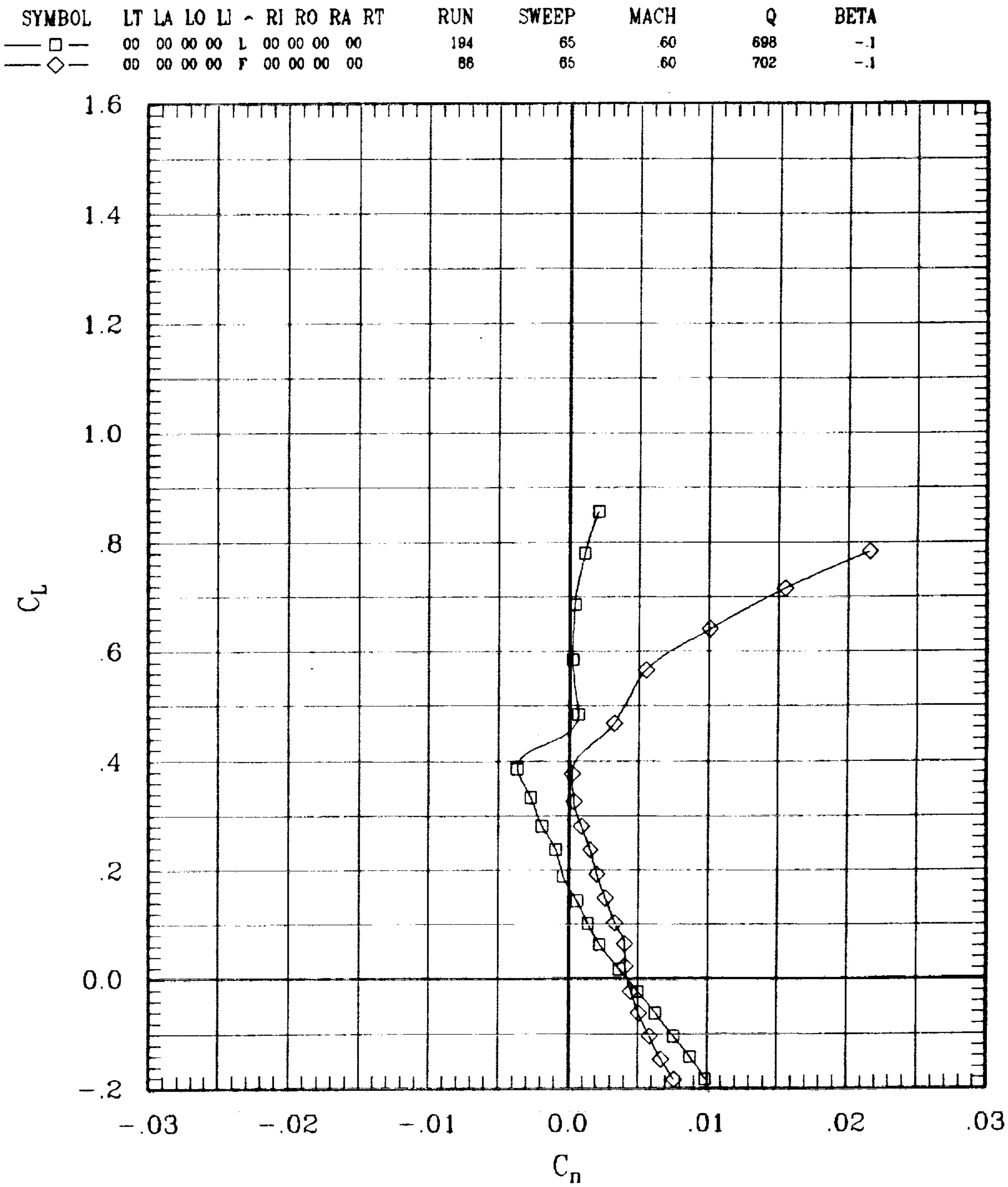

Figure 6(e). Effect of pivot height for sweep = 65 deg.

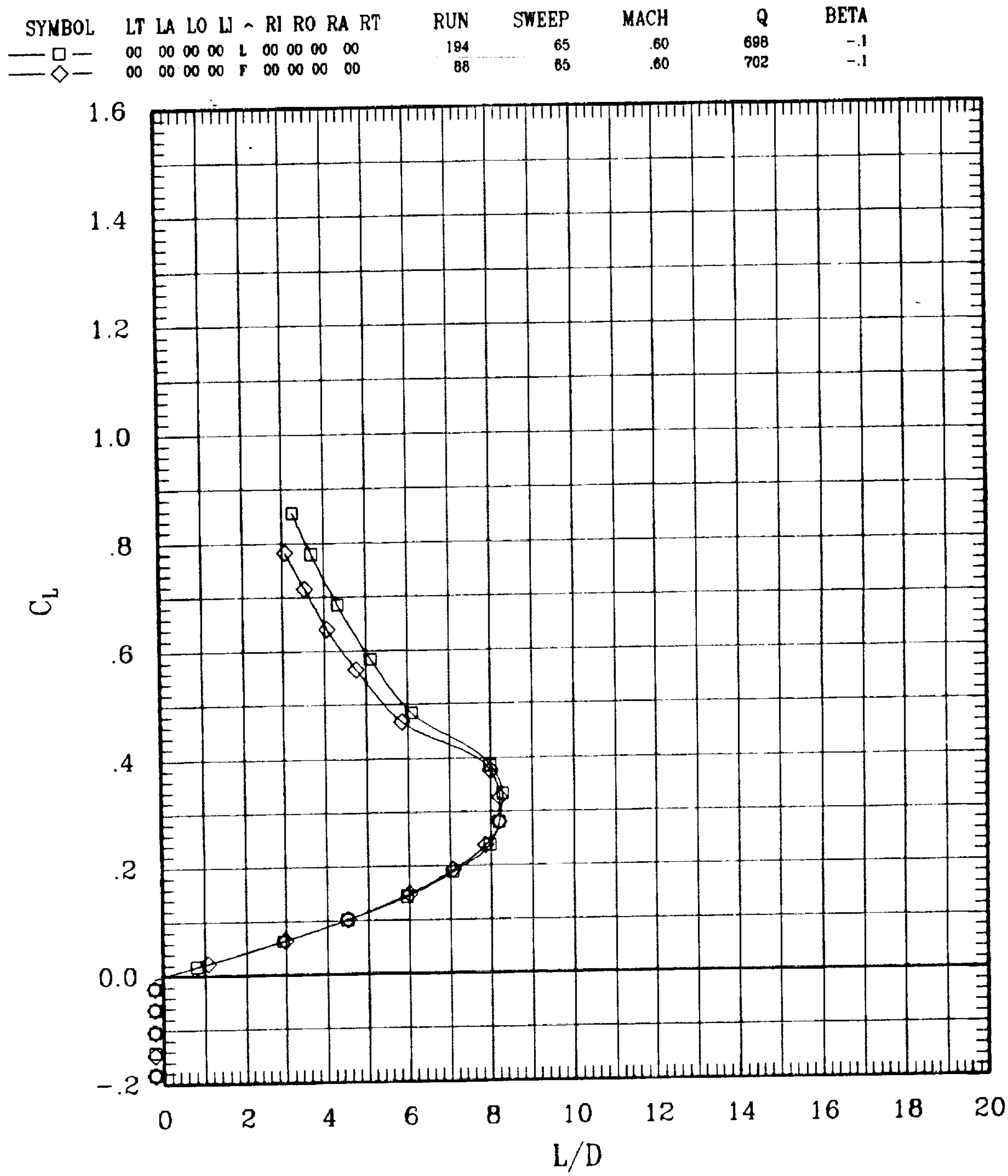

Figure 6(e). Effect of pivot height for sweep = 65 deg.

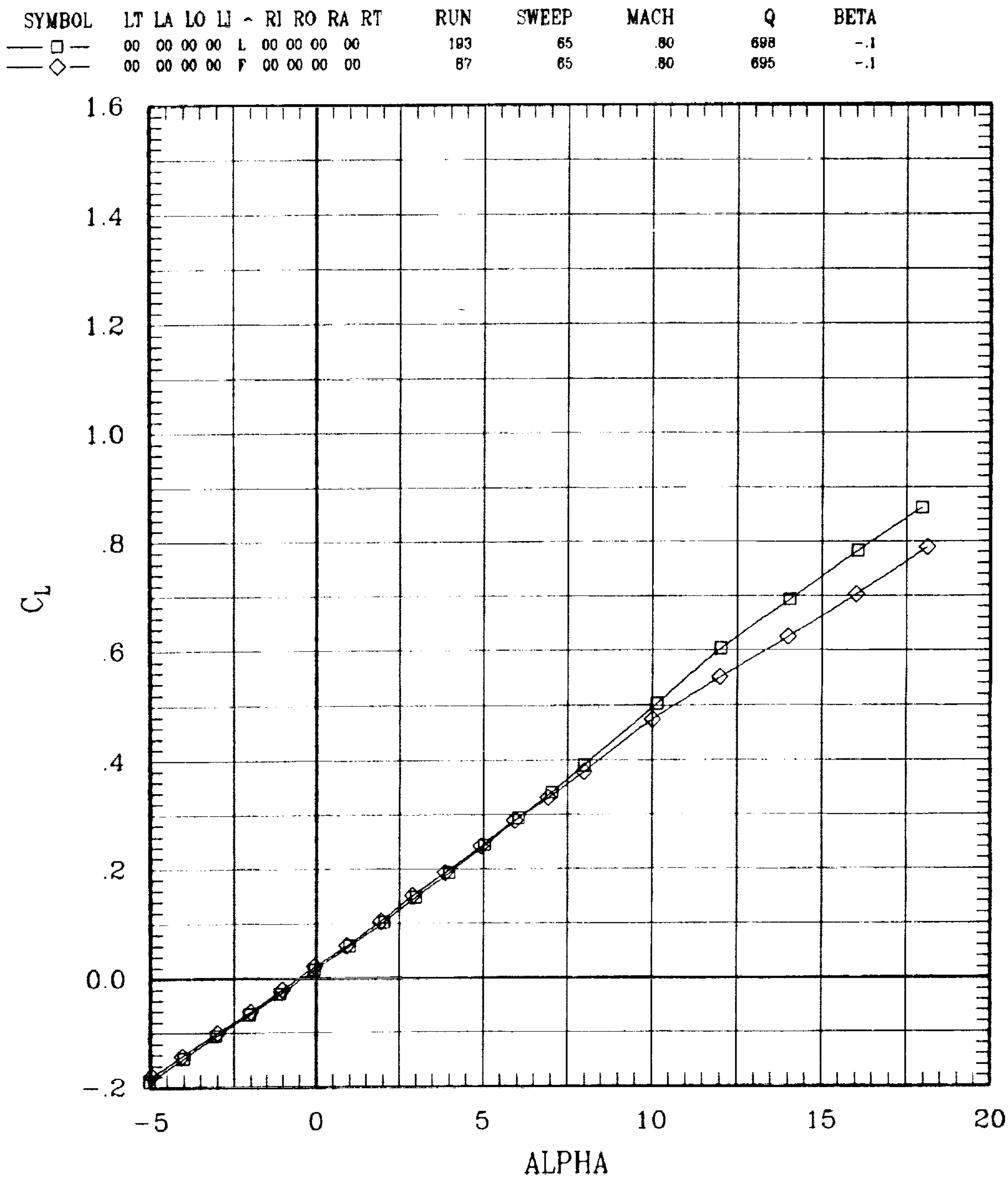

Figure 6(e). Effect of pivot height for sweep = 65 deg.

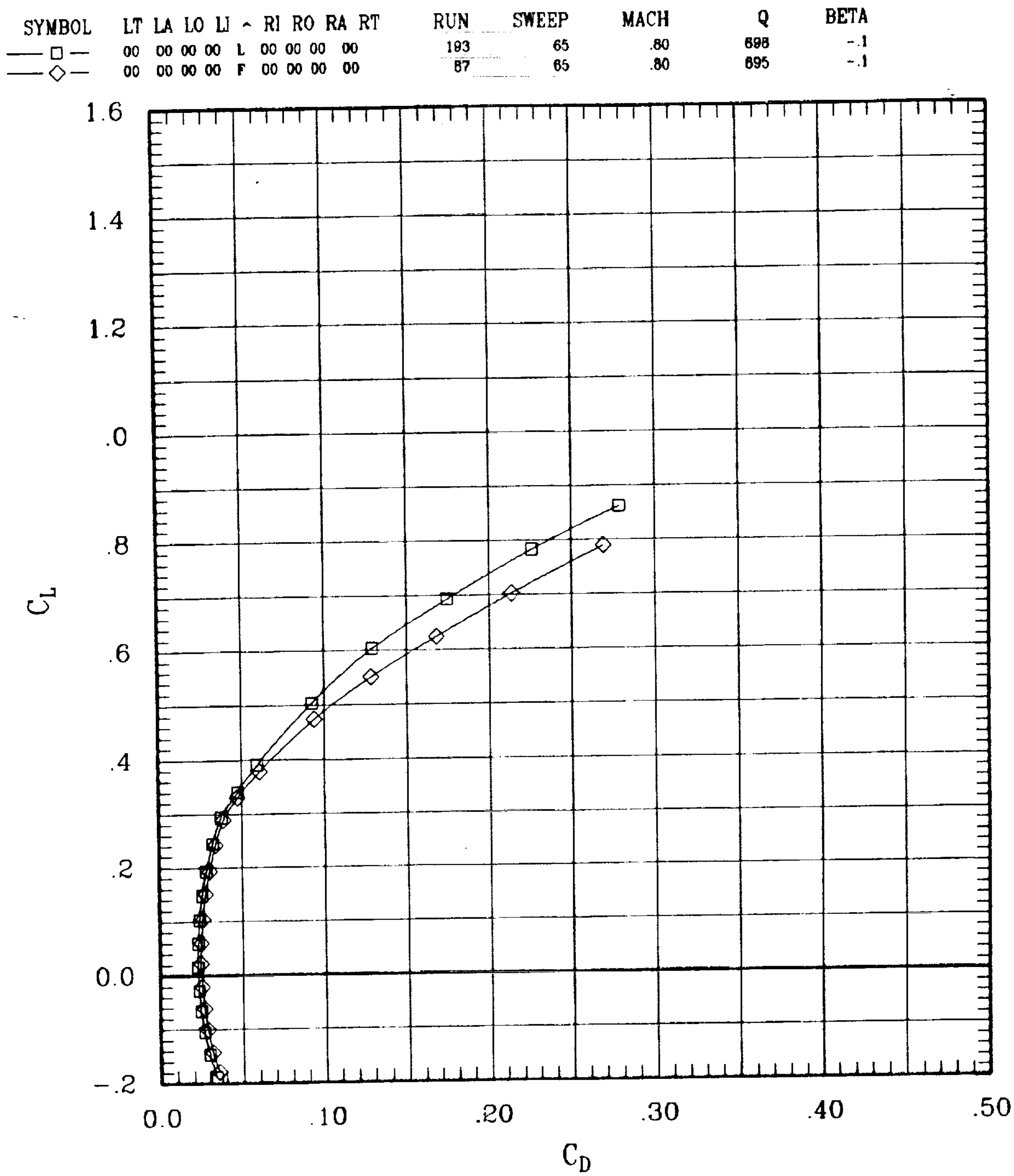

Figure 6(e). Effect of pivot height for sweep = 65 deg.

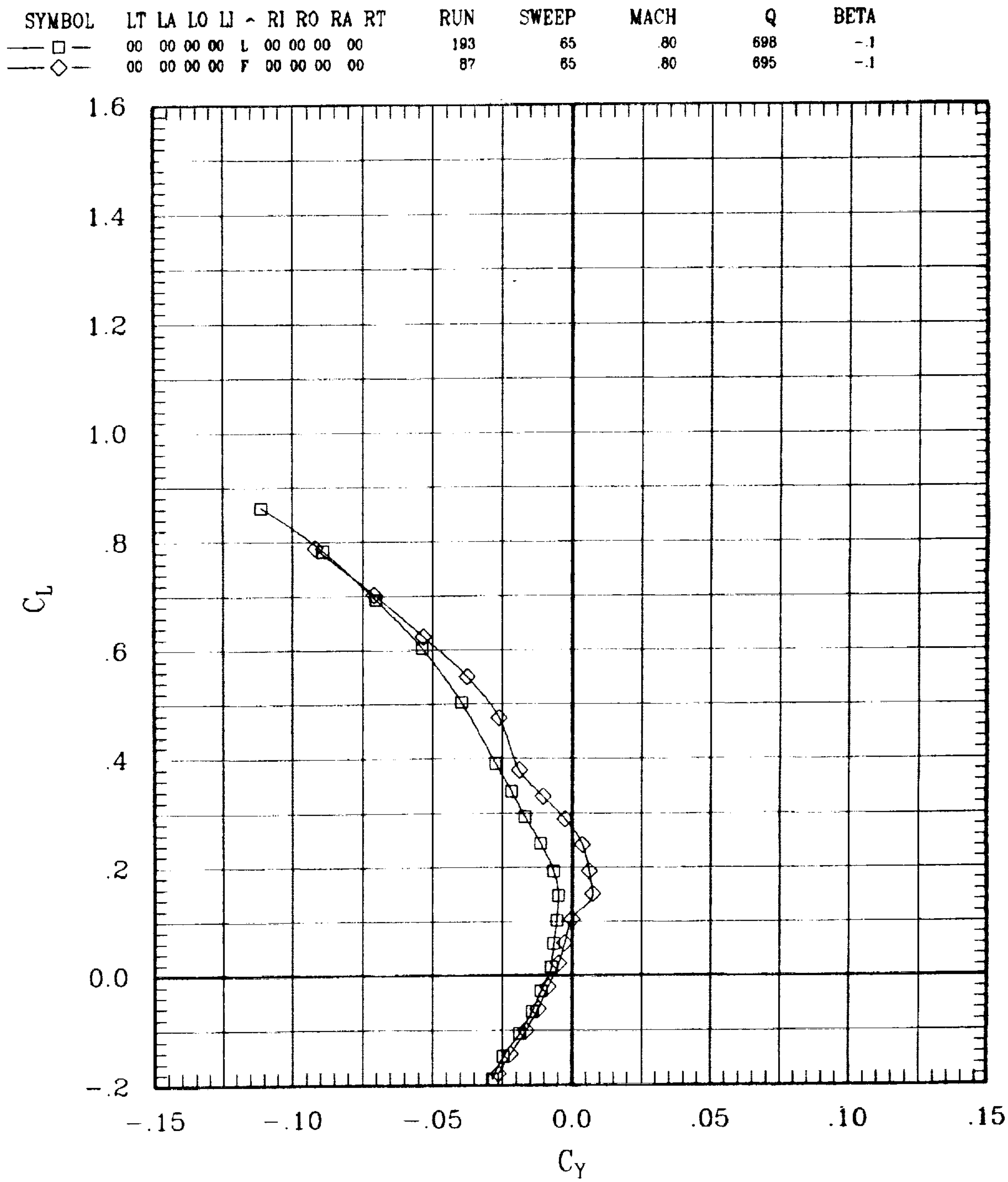

Figure 6(e). Effect of pivot height for sweep = 65 deg.

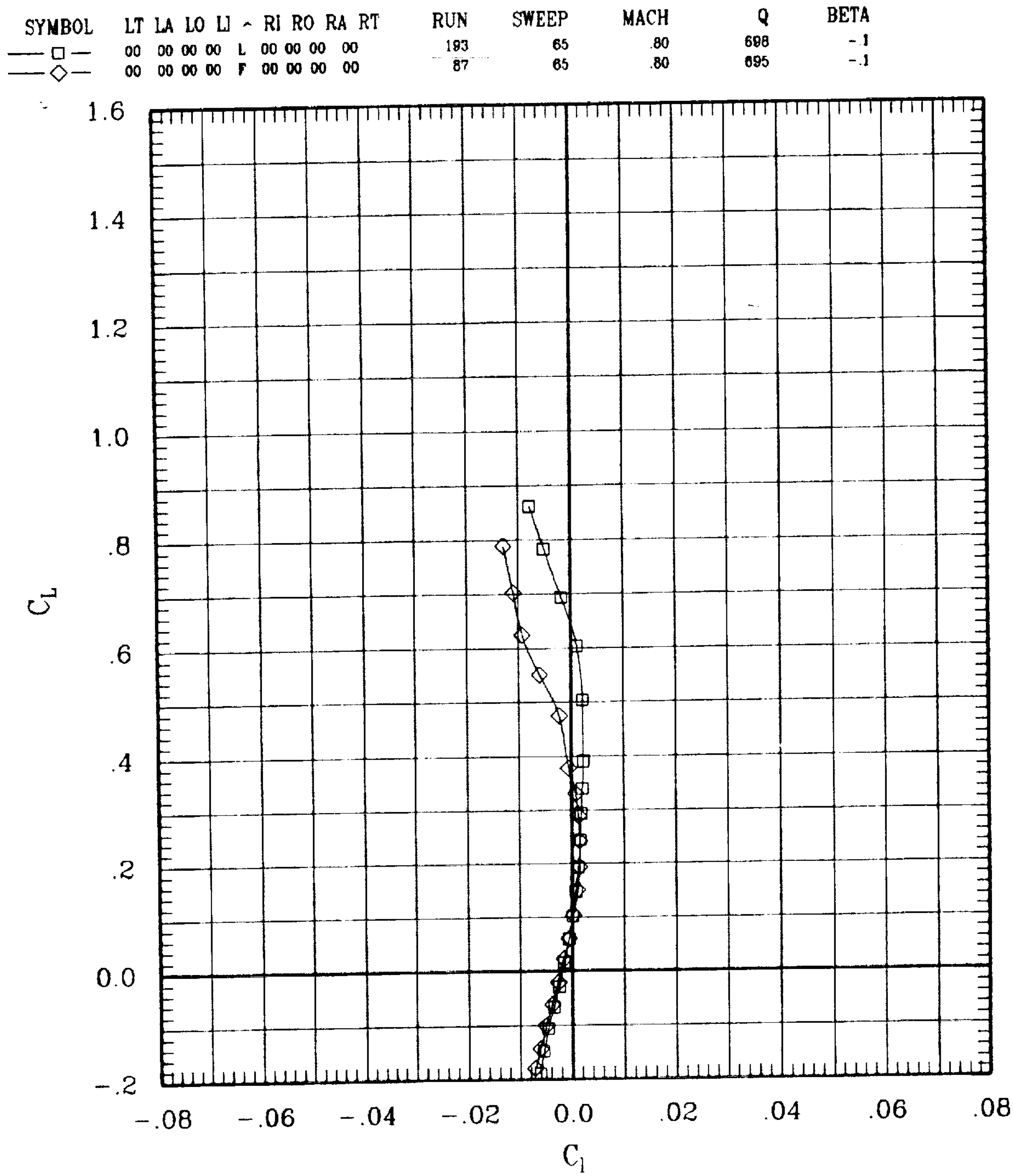

Figure 6(e). Effect of pivot height for sweep = 65 deg.

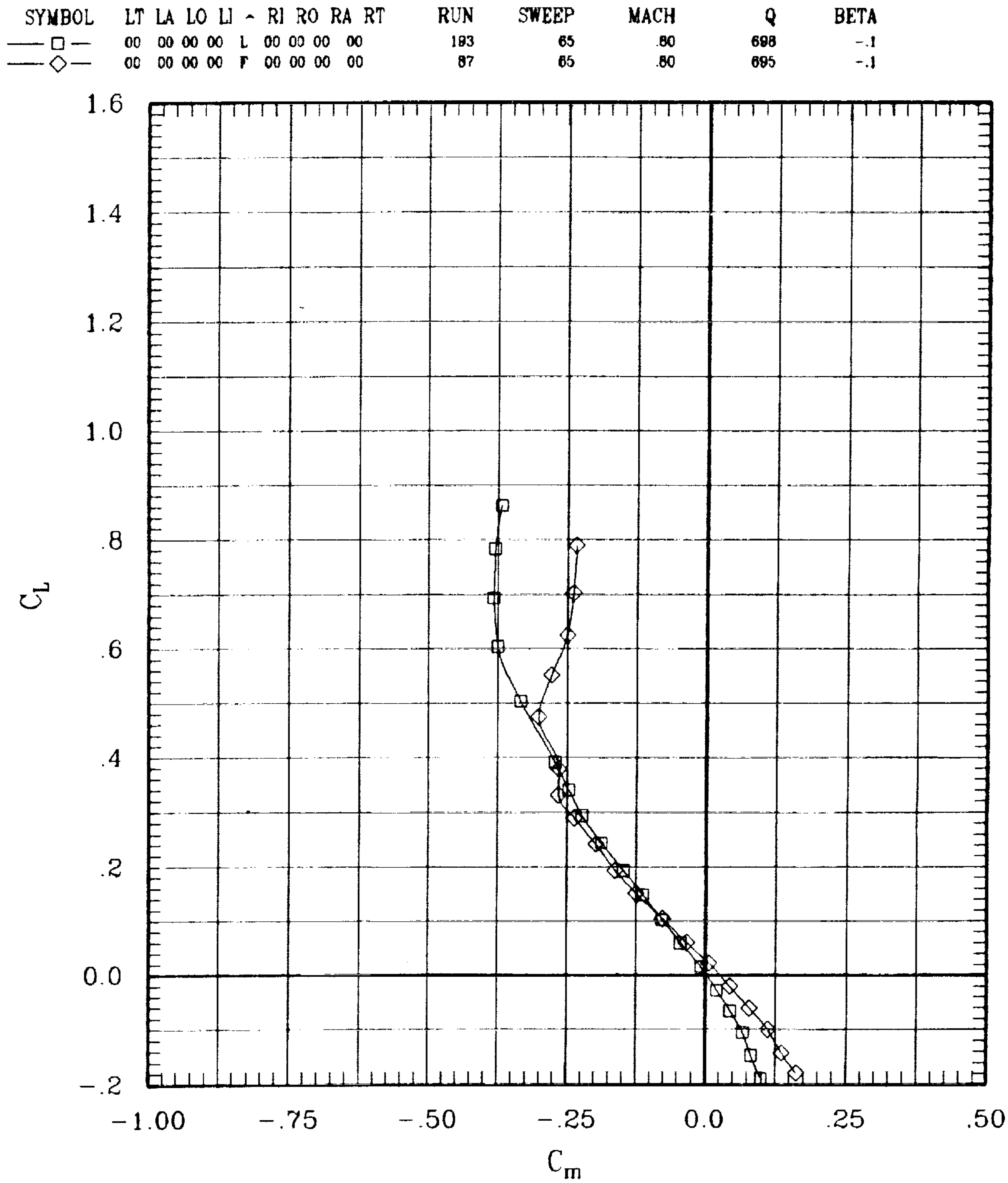

Figure 6(e). Effect of pivot height for sweep = 65 deg.

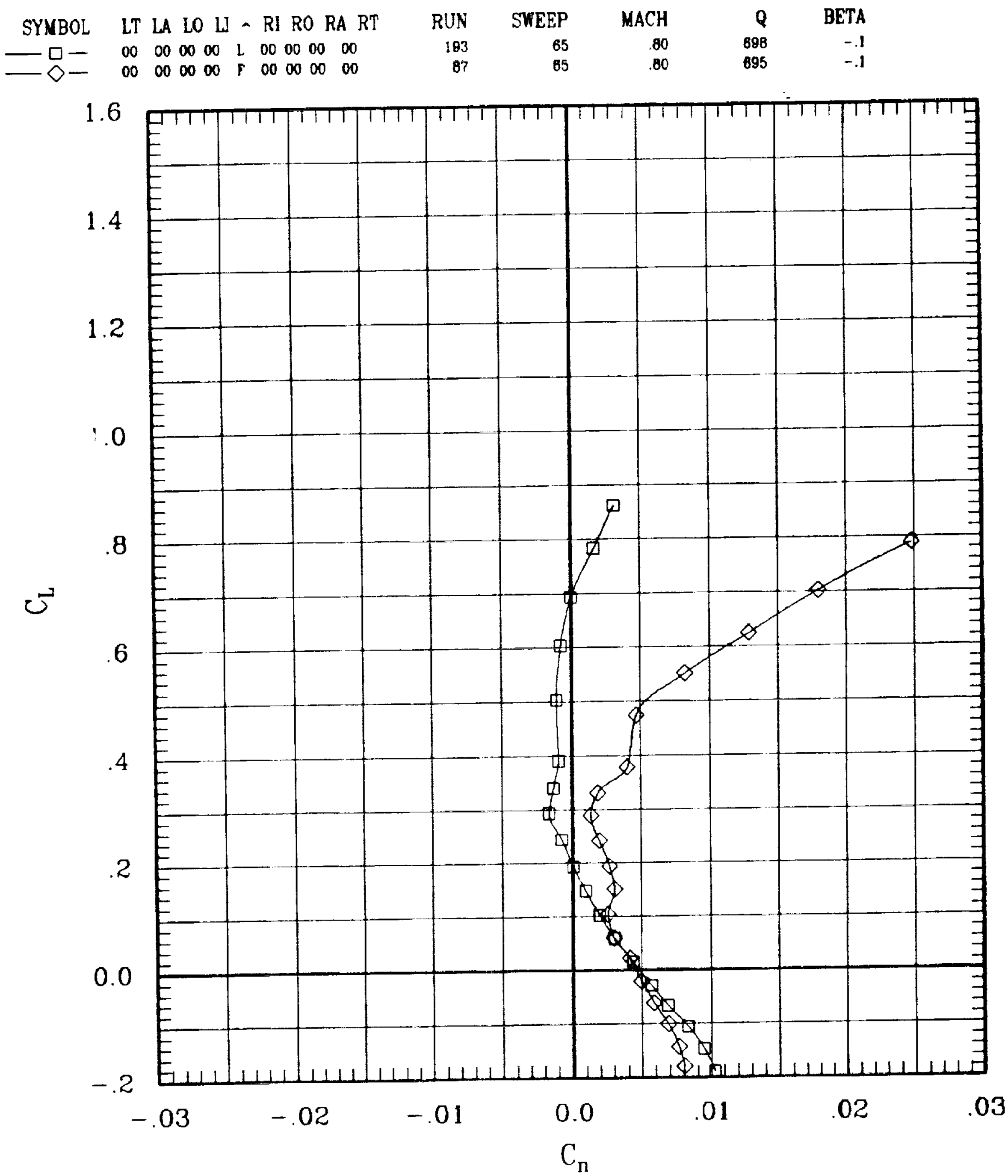

Figure 6(e). Effect of pivot height for sweep = 65 deg.

SYMBOL	LT	LA	LO	LI	-	RI	RO	RA	RT	RUN	SWEEP	MACH	Q	BETA
—□—	00	00	00	00	L	00	00	00	00	193	65	.80	698	-.1
—◇—	00	00	00	00	F	00	00	00	00	87	65	.80	695	-.1

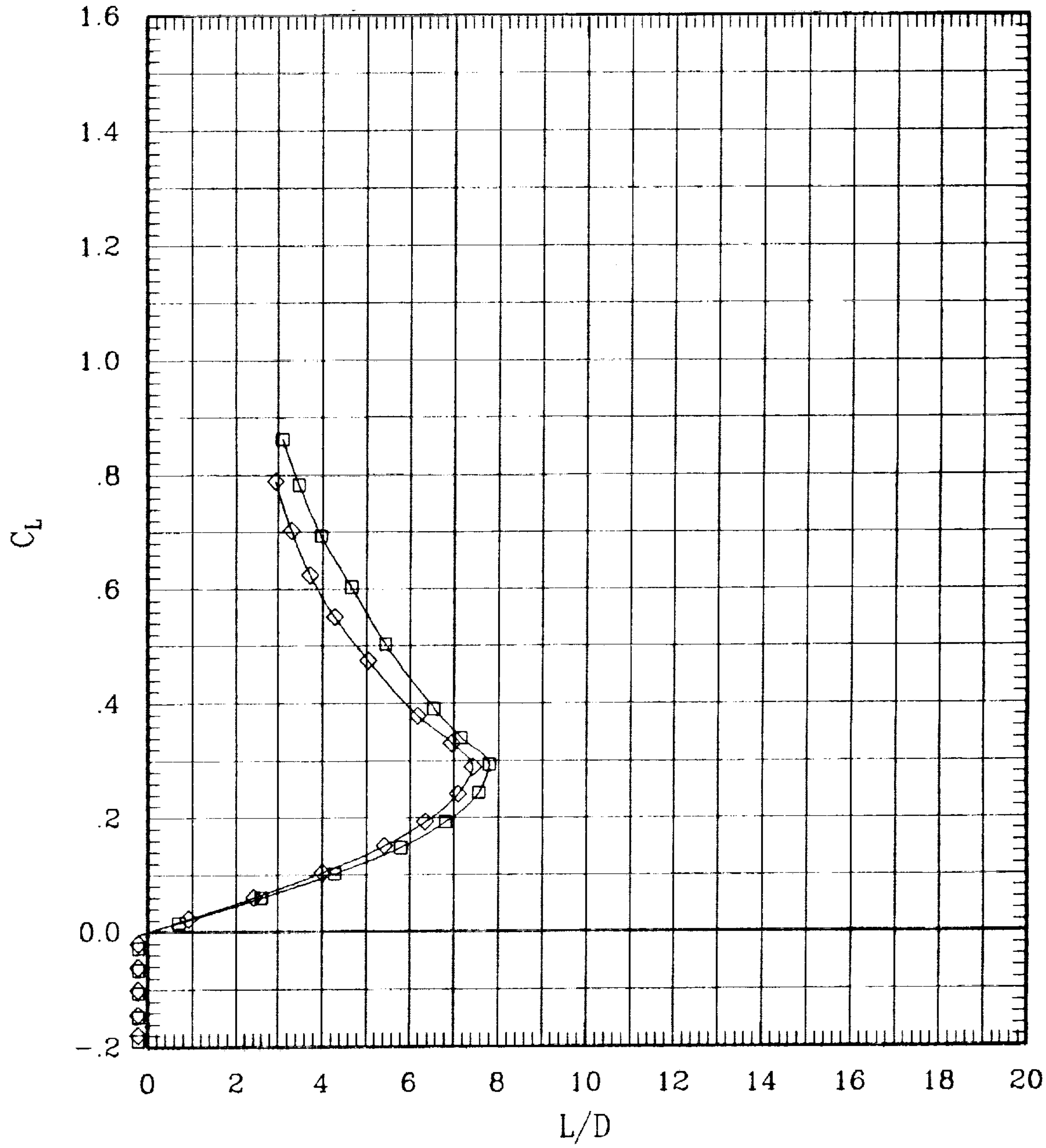

Figure 6(e). Effect of pivot height for sweep = 65 deg.

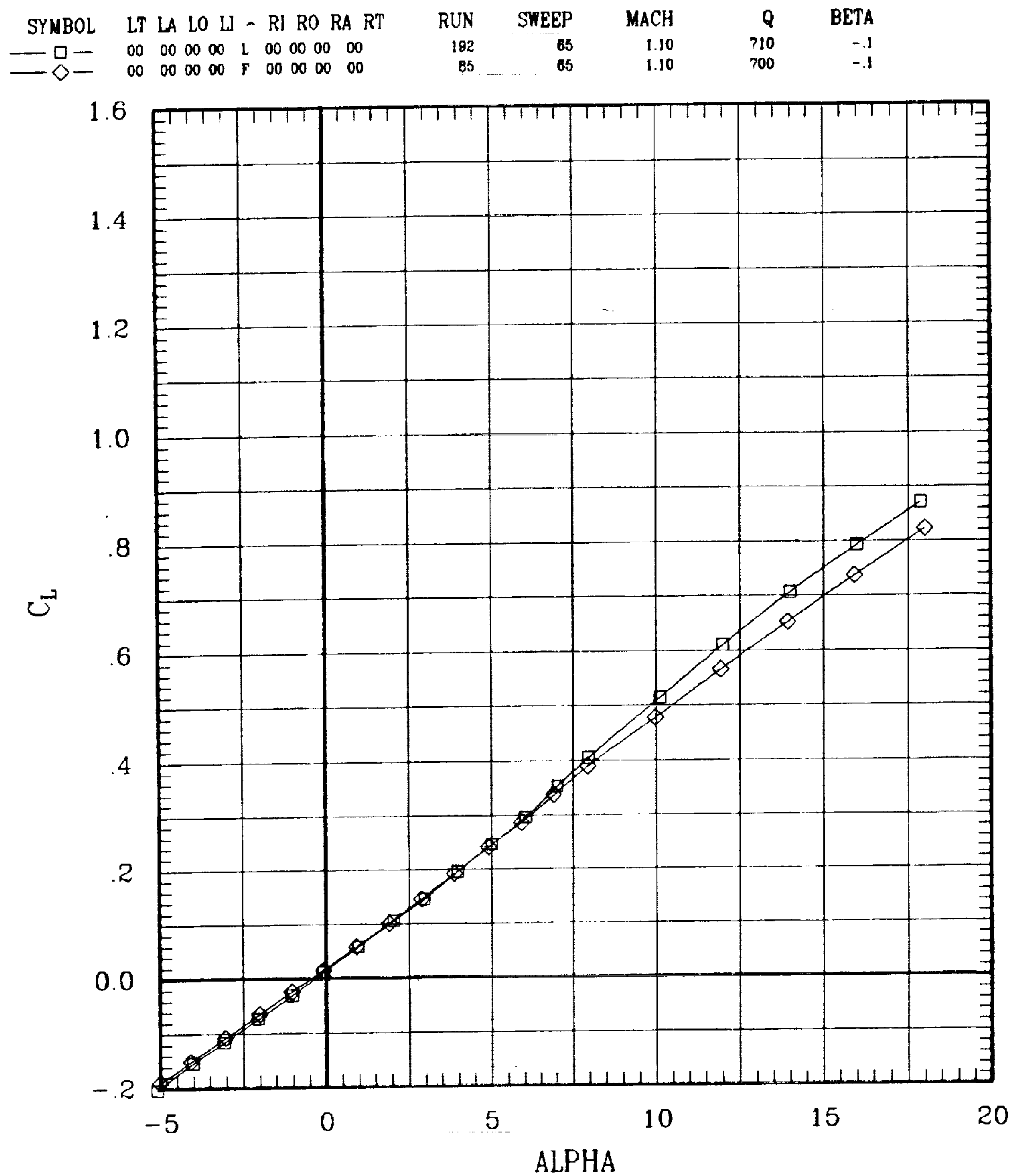

Figure 6(e). Effect of pivot height for sweep = 65 deg.

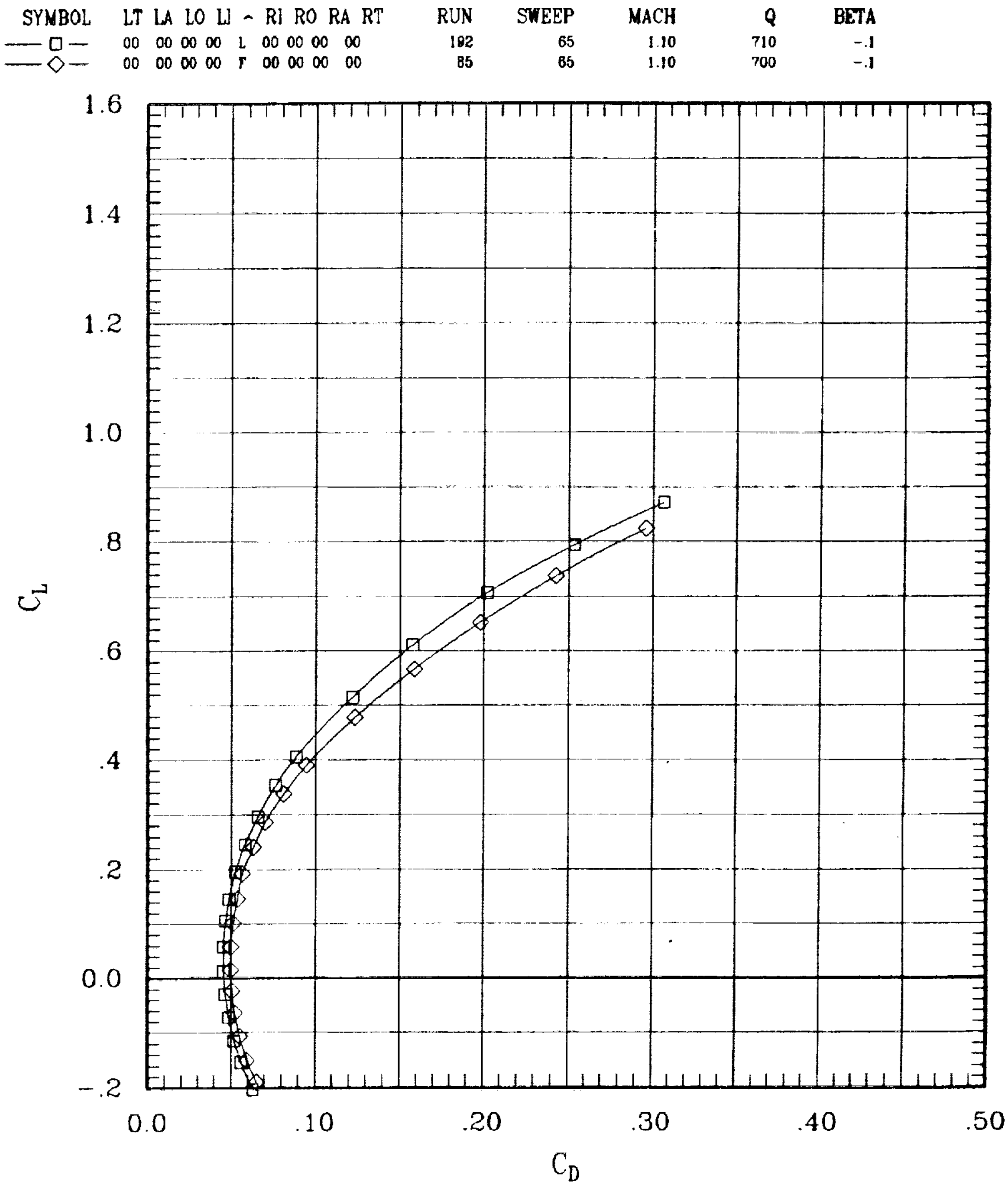

Figure 6(e). Effect of pivot height for sweep = 65 deg.

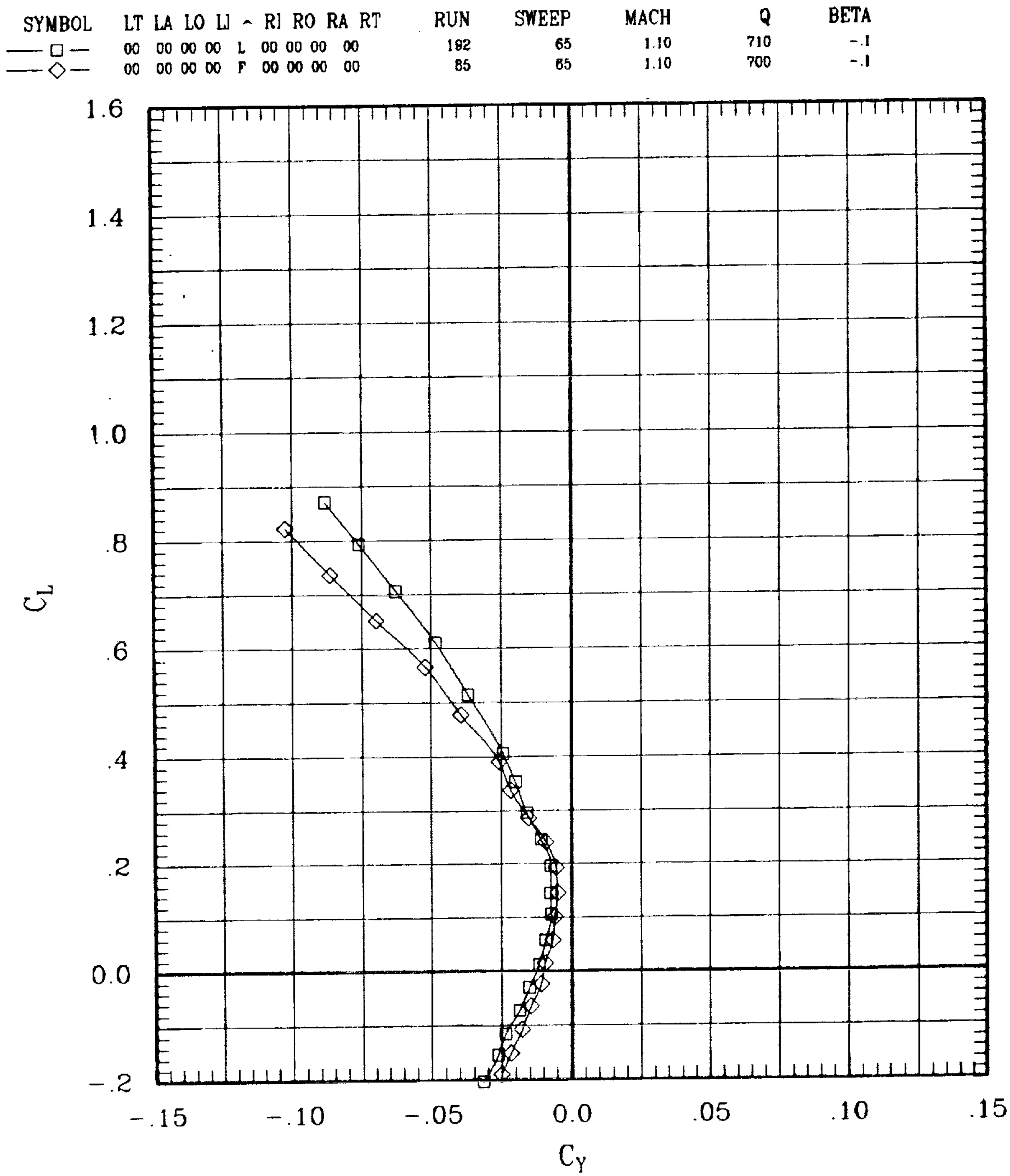

Figure 6(e). Effect of pivot height for sweep = 65 deg.

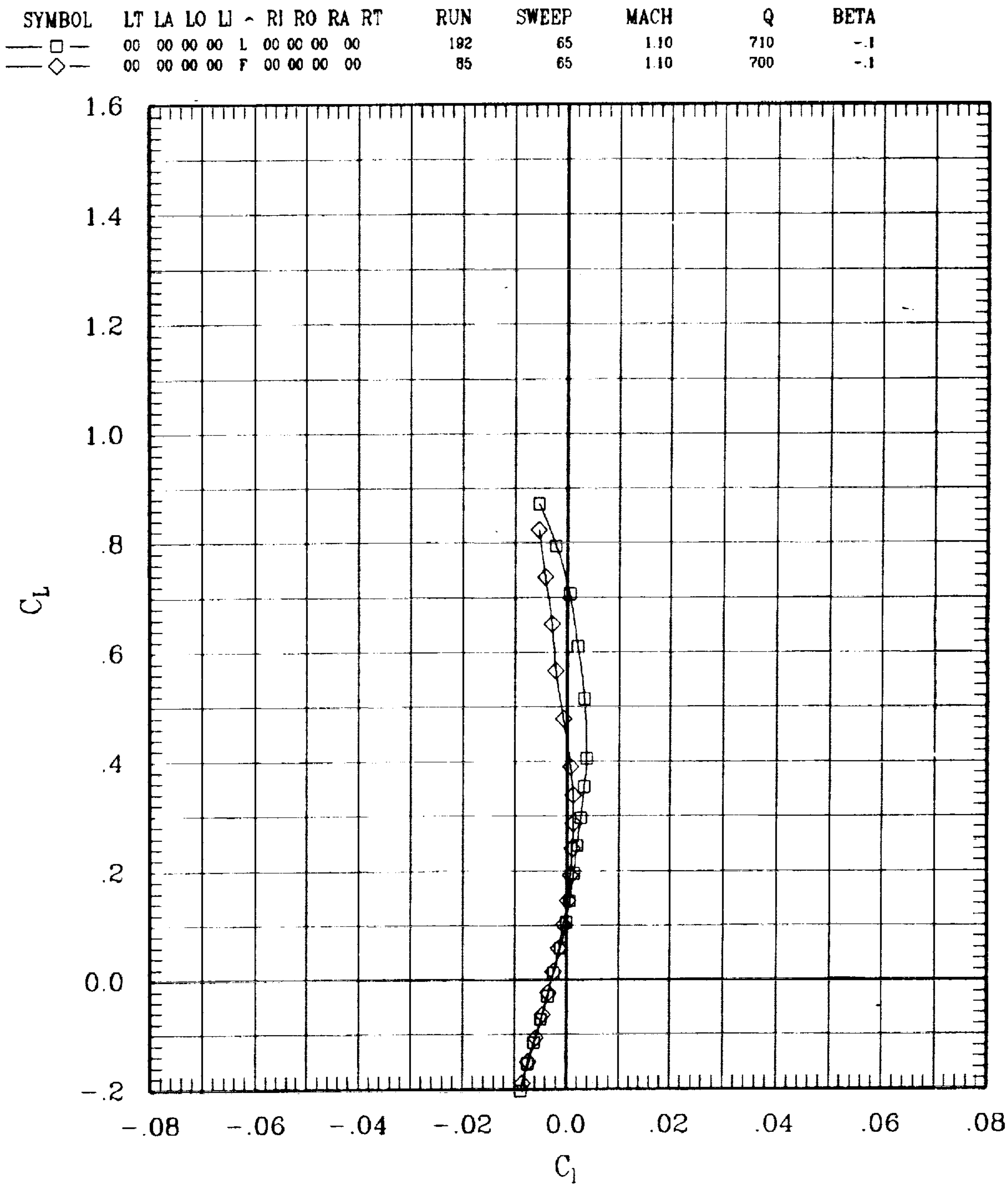

Figure 6(e). Effect of pivot height for sweep = 65 deg.

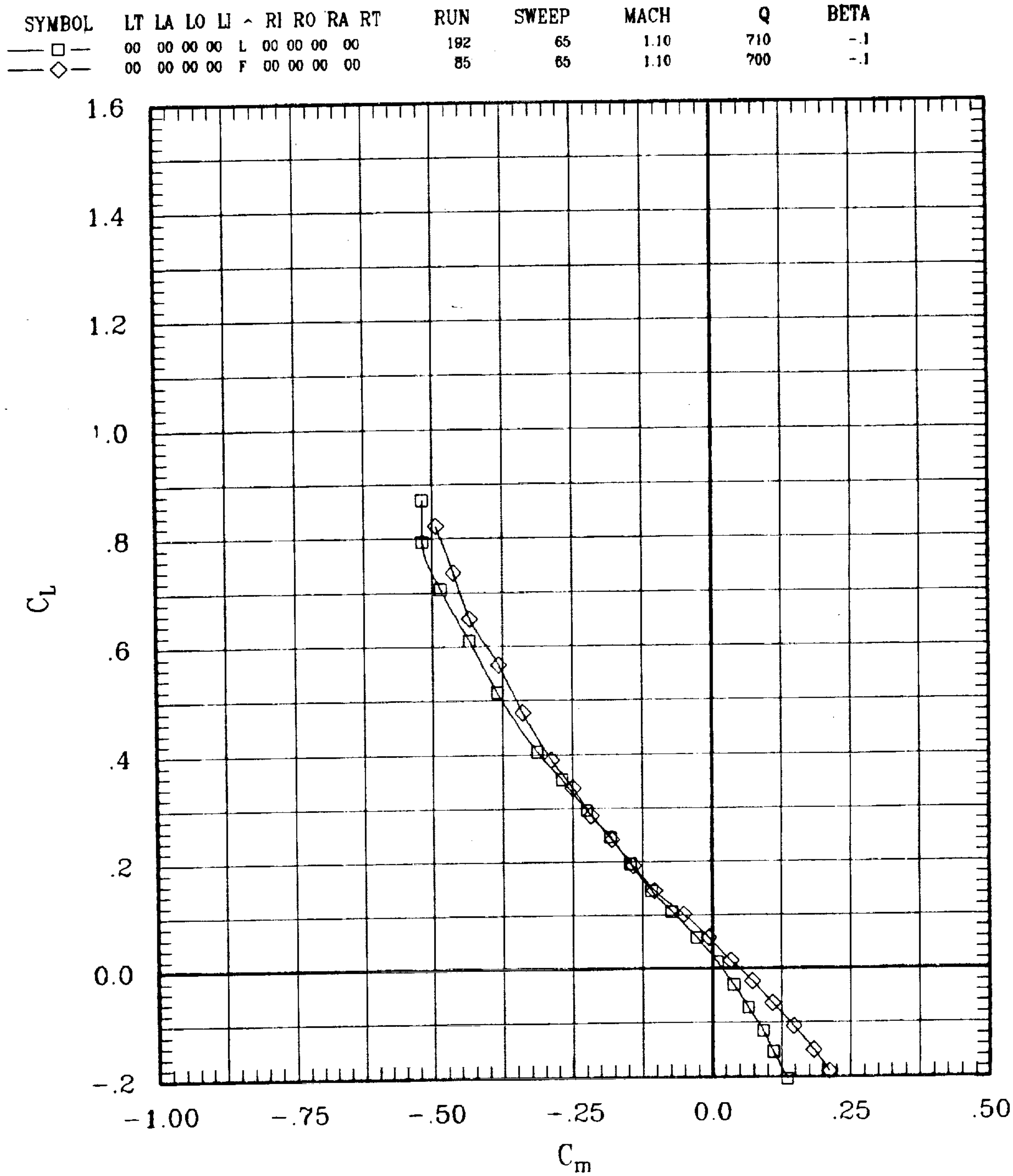

Figure 6(e). Effect of pivot height for sweep = 65 deg.

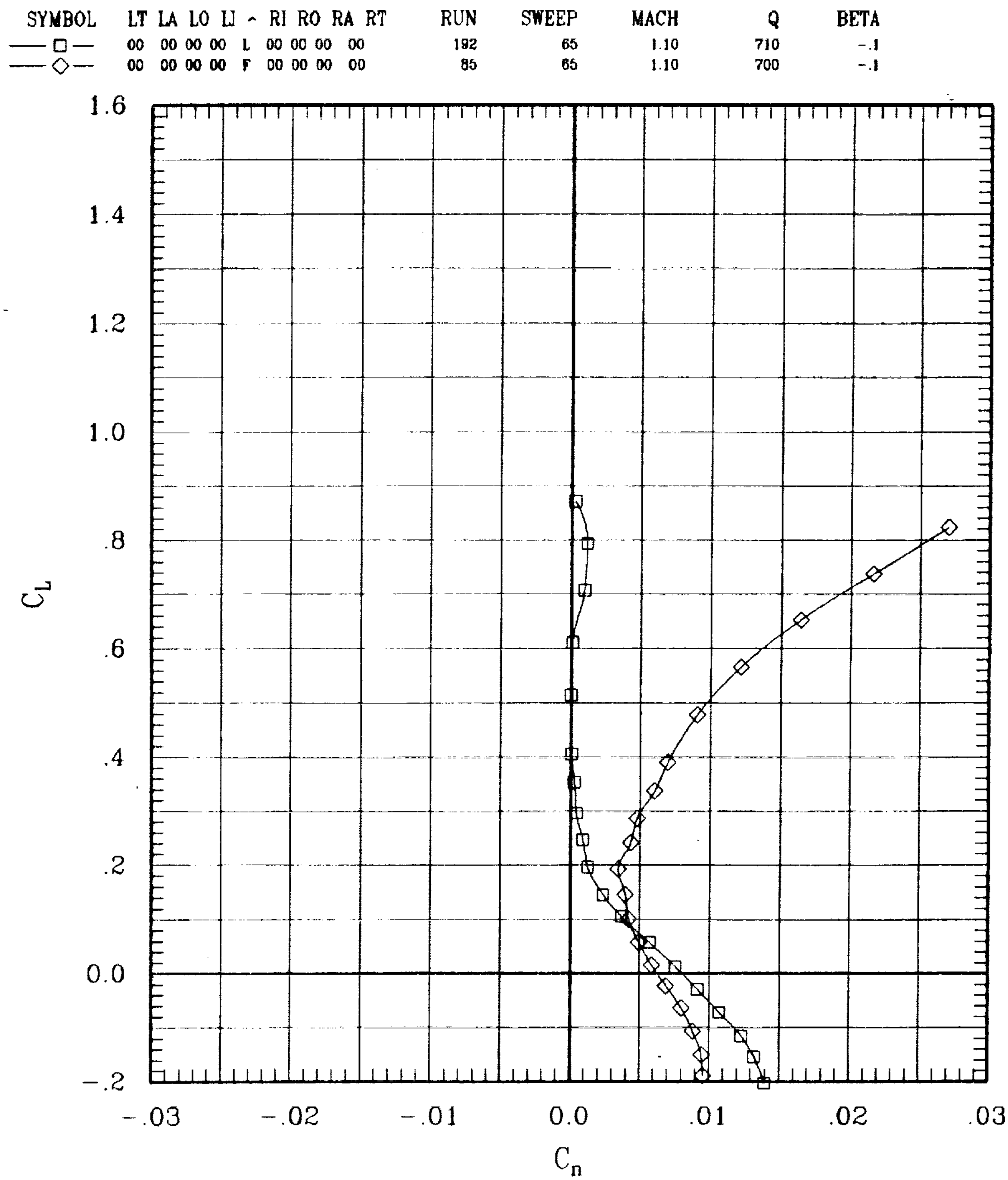

Figure 6(e). Effect of pivot height for sweep = 65 deg.

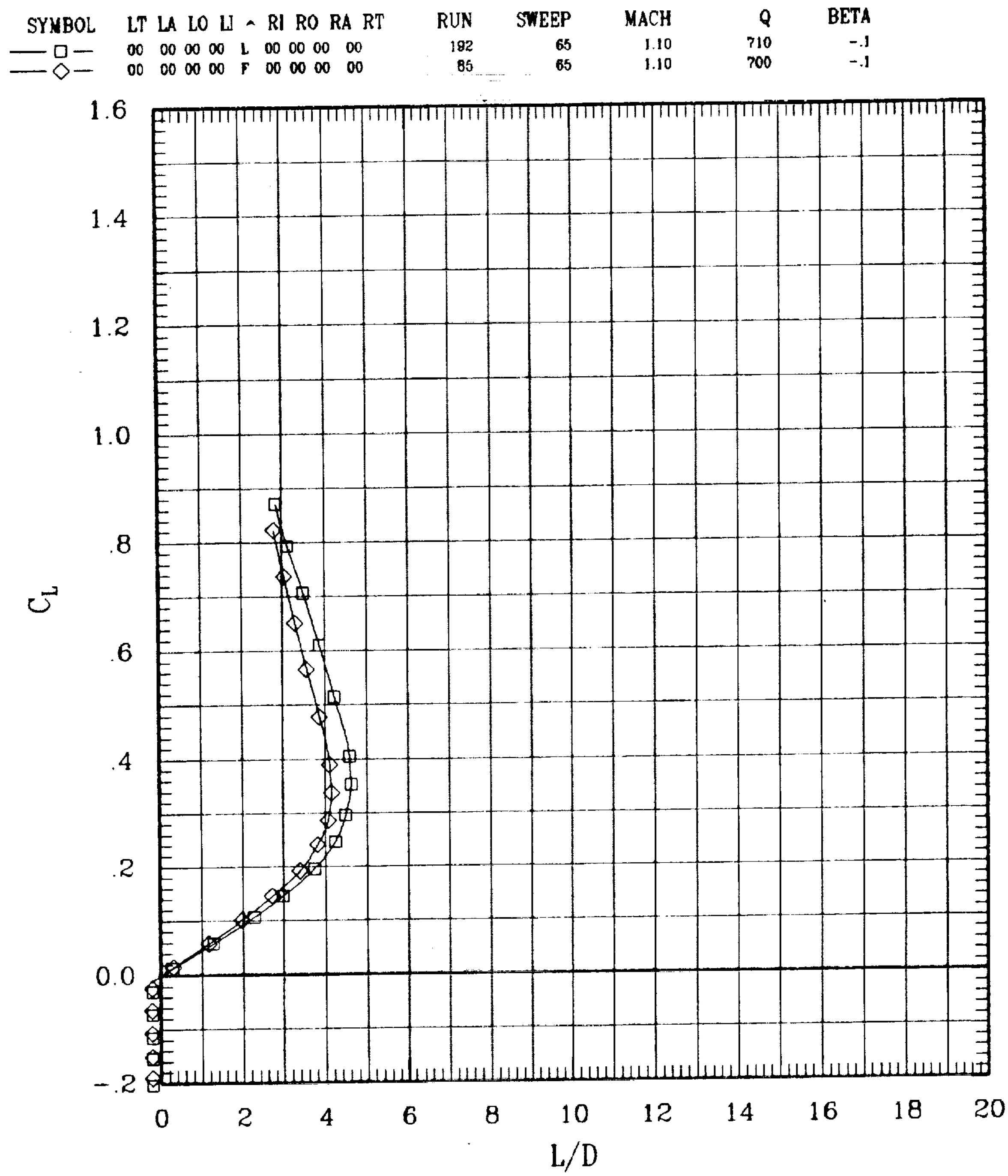

Figure 6(e). Effect of pivot height for sweep = 65 deg.

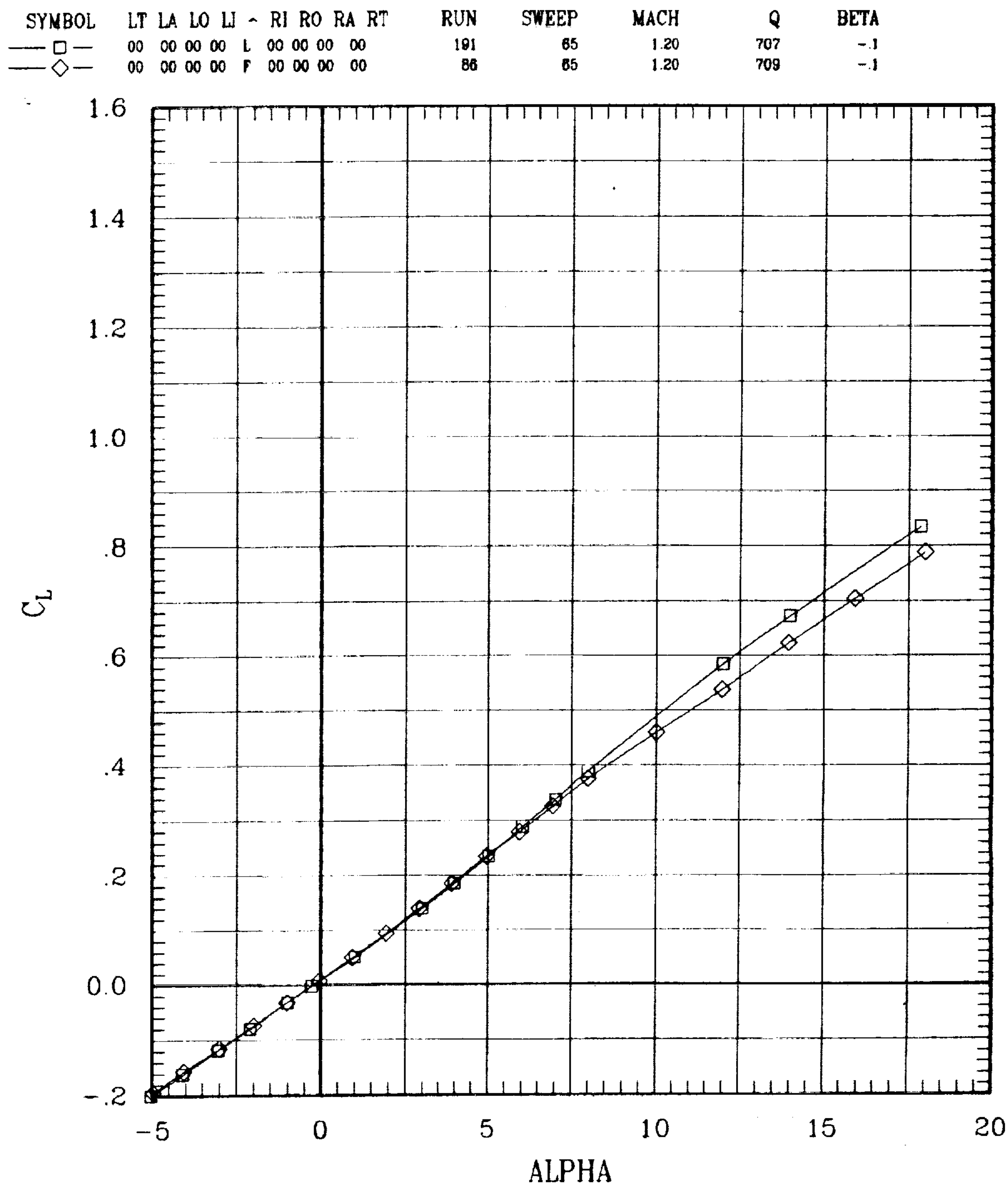

Figure 6(e). Effect of pivot height for sweep = 65 deg.

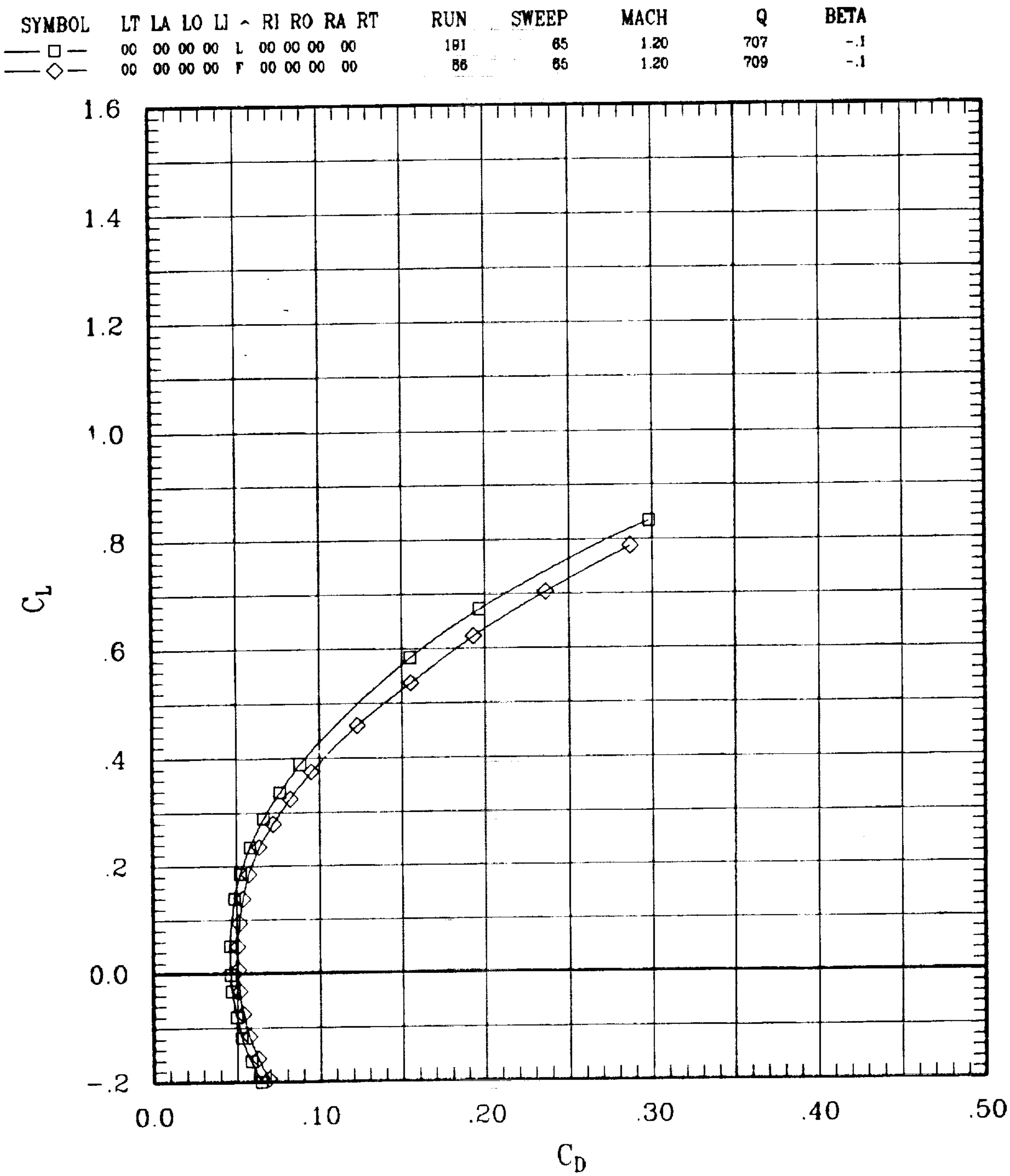

Figure 6(e). Effect of pivot height for sweep = 65 deg.

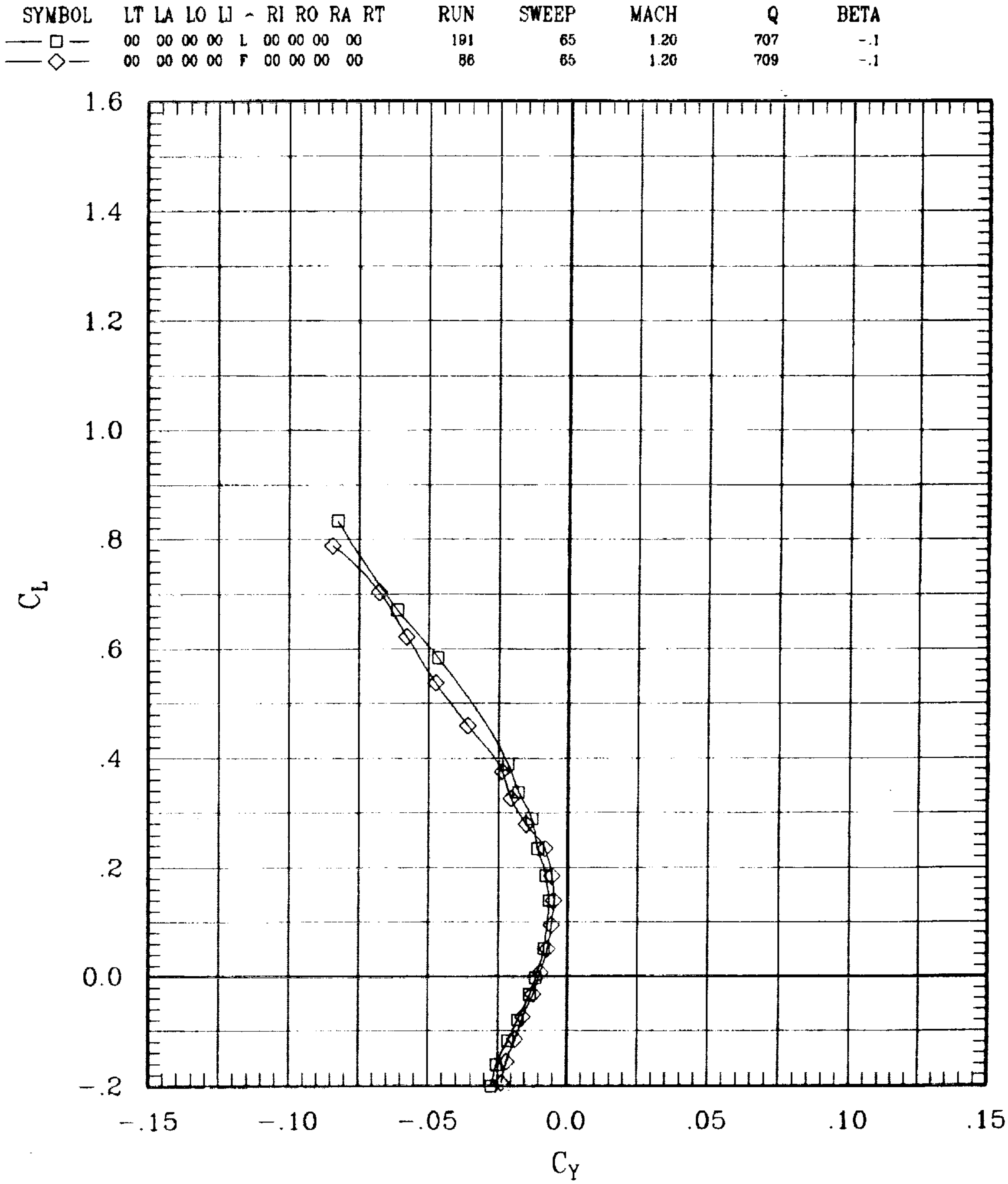

Figure 6(e). Effect of pivot height for sweep = 65 deg.

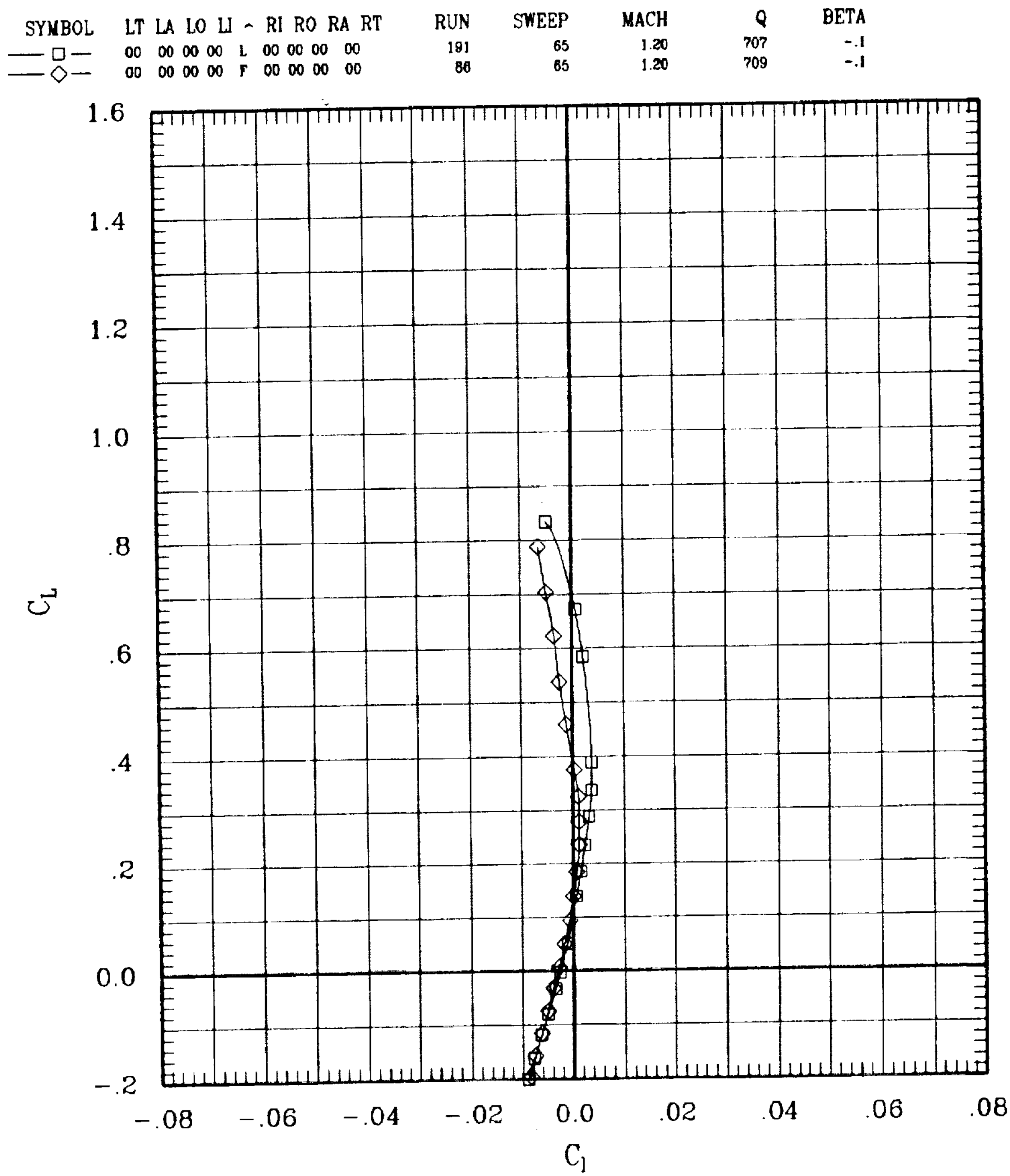

Figure 6(e). Effect of pivot height for sweep = 65 deg.

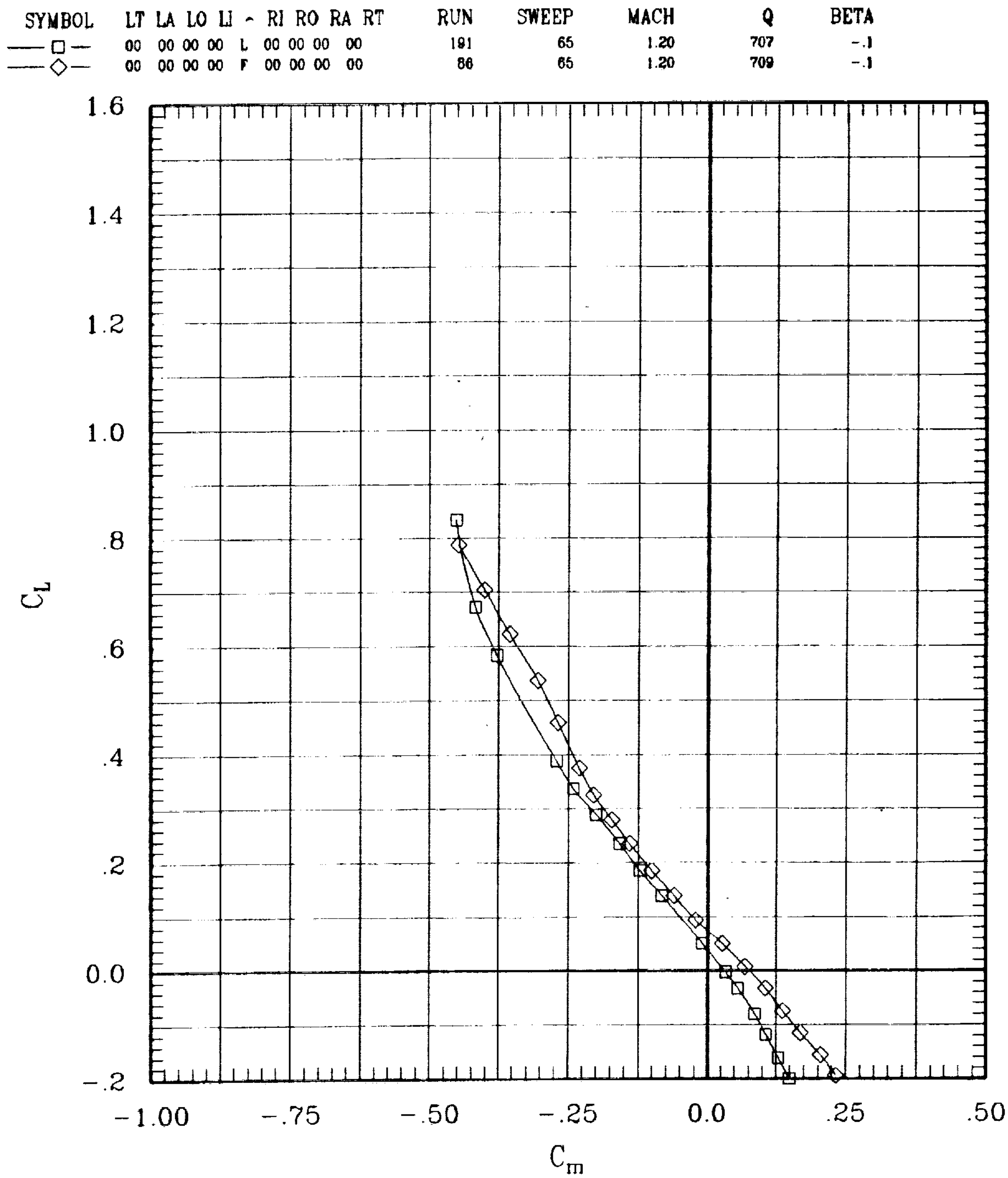

Figure 6(e). Effect of pivot height for sweep = 65 deg.

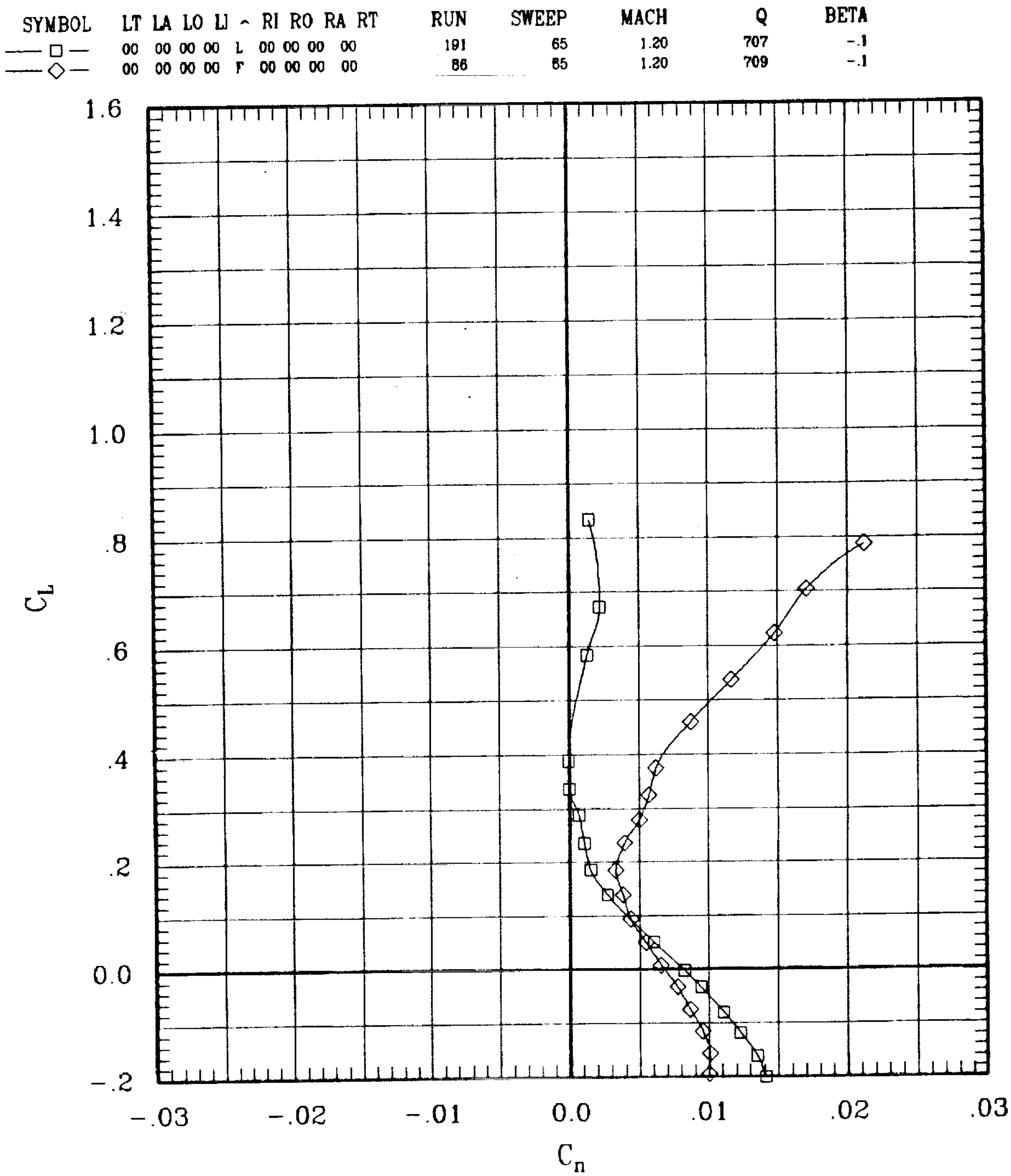

Figure 6(e). Effect of pivot height for sweep = 65 deg.

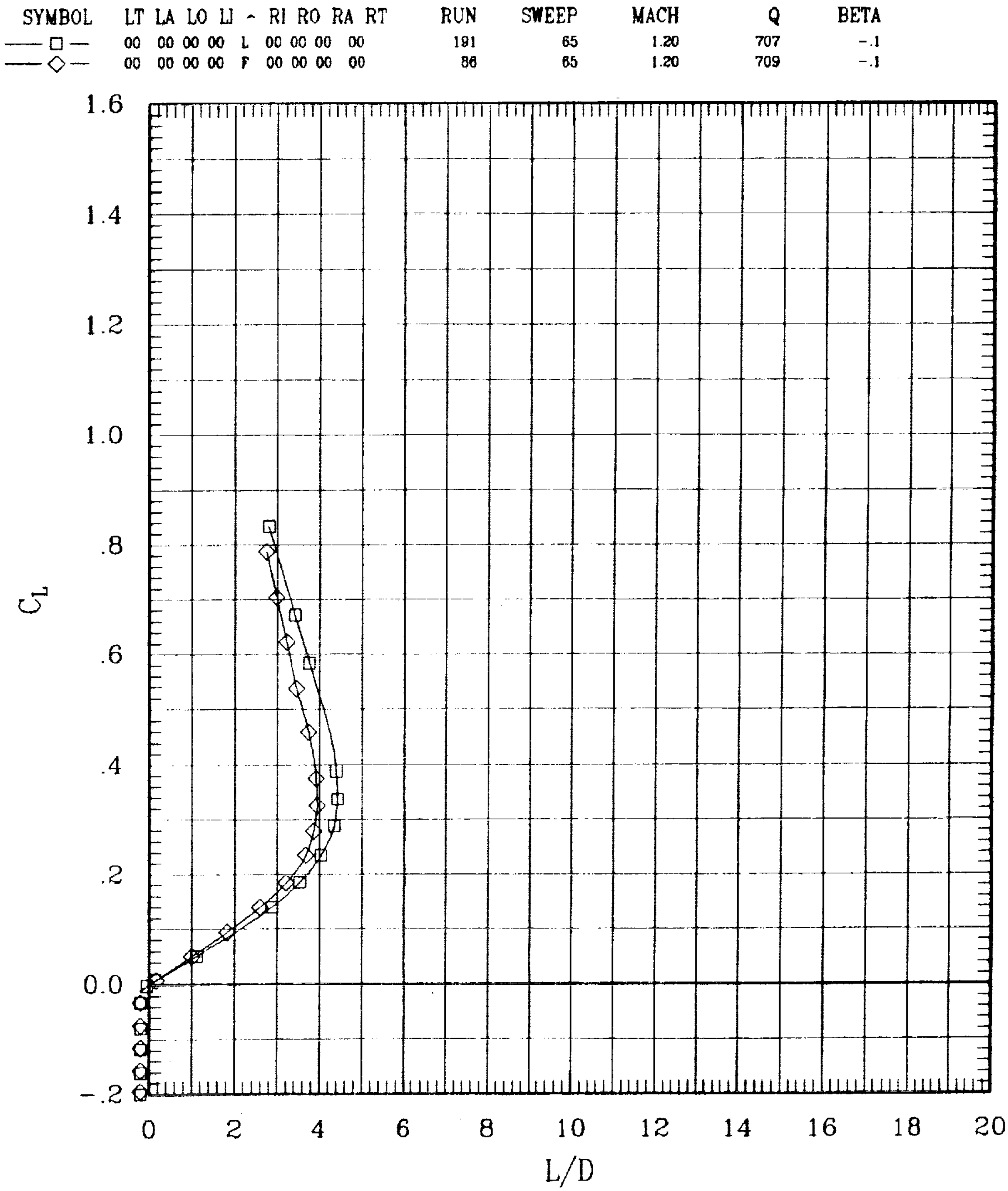

Figure 6(e). Effect of pivot height for sweep = 65 deg.

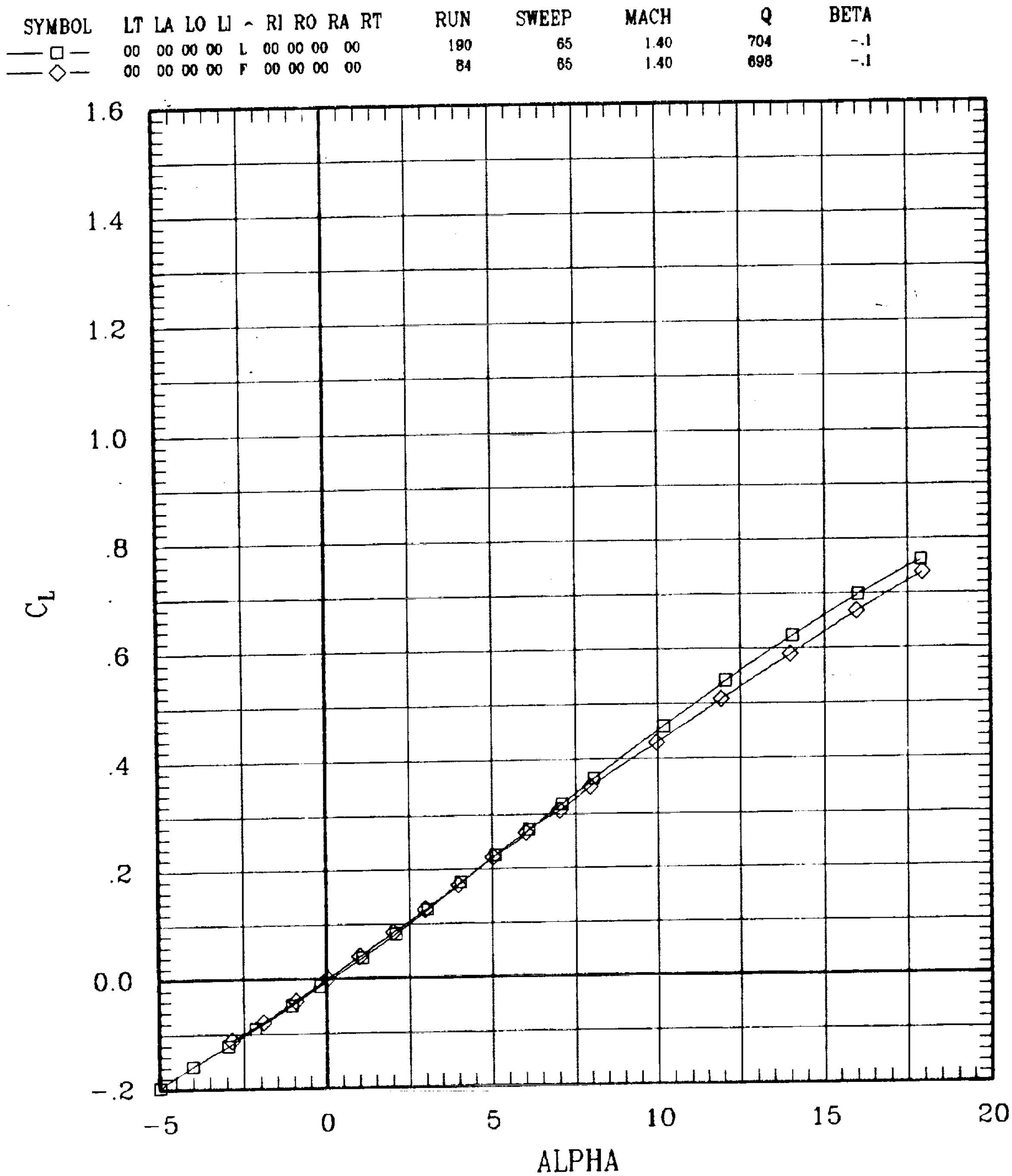

Figure 6(e). Effect of pivot height for sweep = 65 deg.

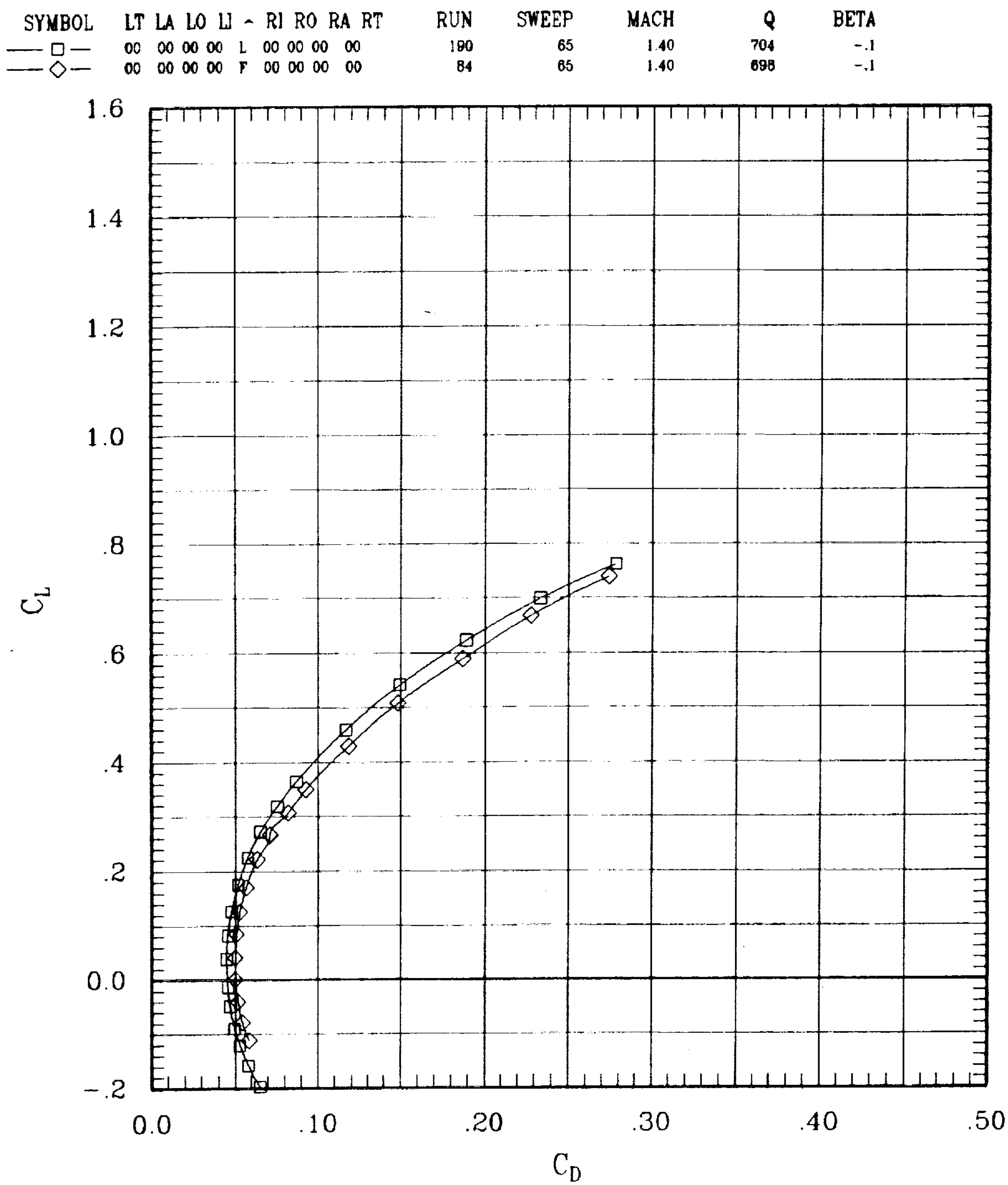

Figure 6(e). Effect of pivot height for sweep = 65 deg.

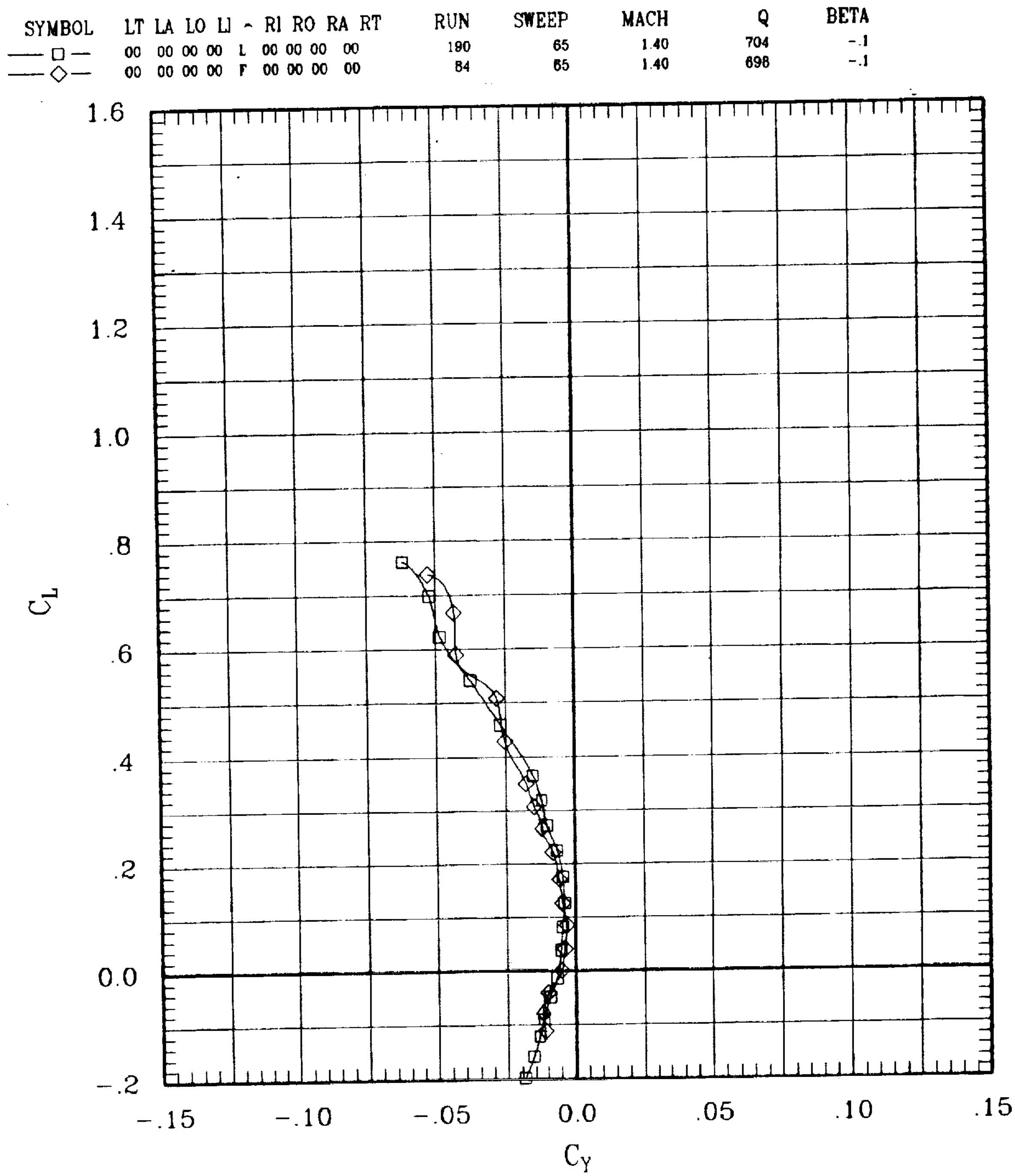

Figure 6(e). Effect of pivot height for sweep = 65 deg.

C-3

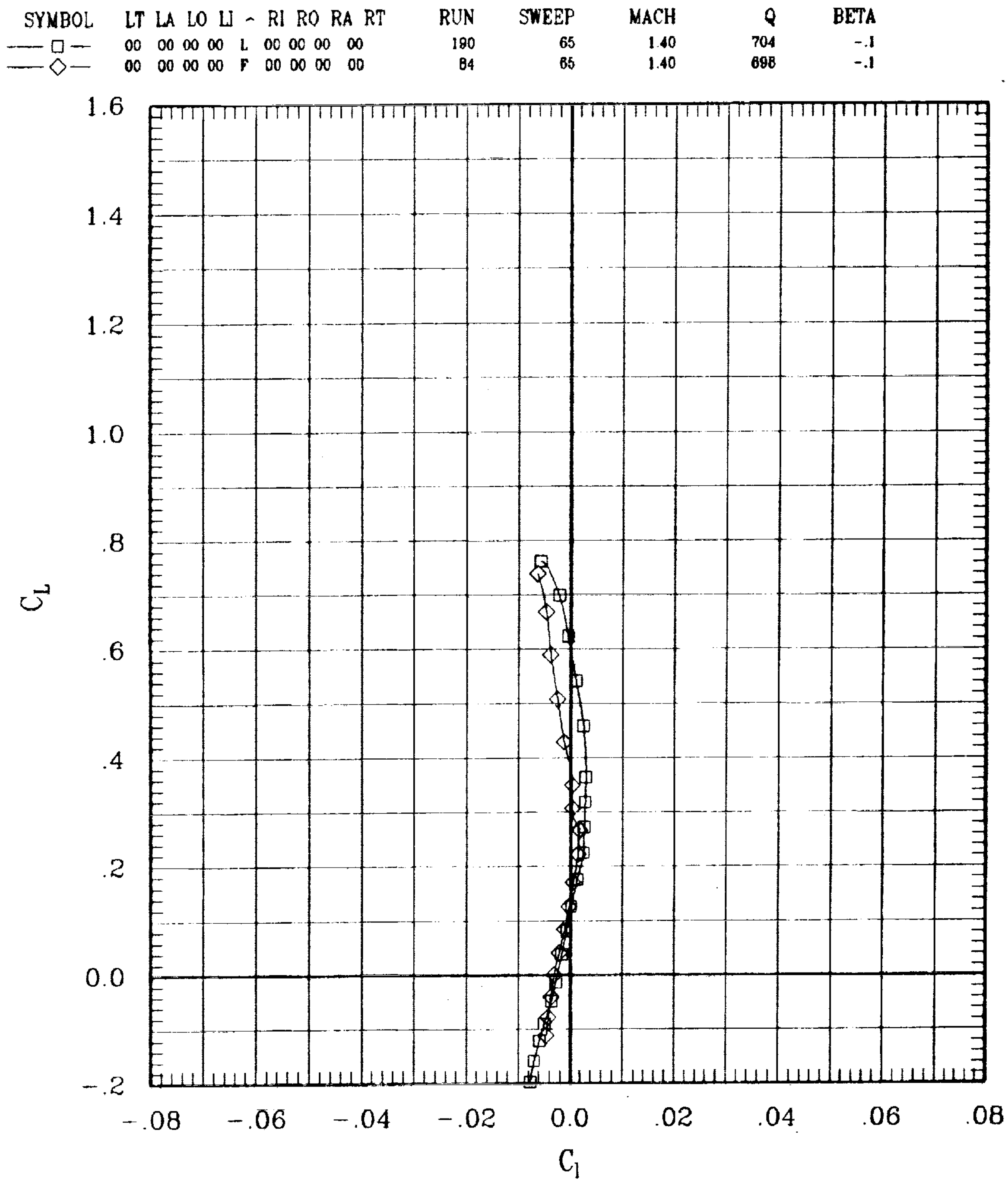

Figure 6(e). Effect of pivot height for sweep = 65 deg.

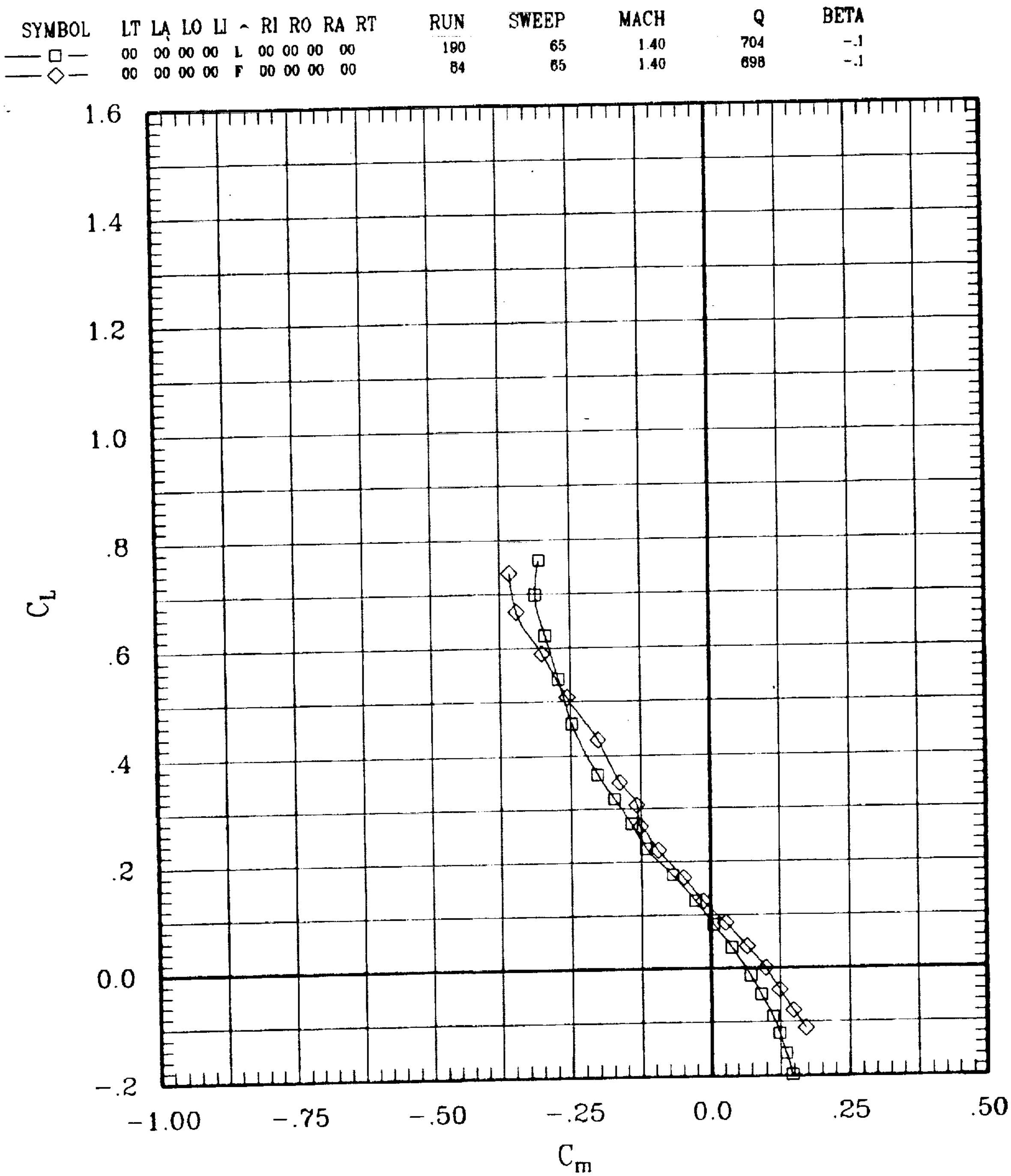

Figure 6(e). Effect of pivot height for sweep = 65 deg.

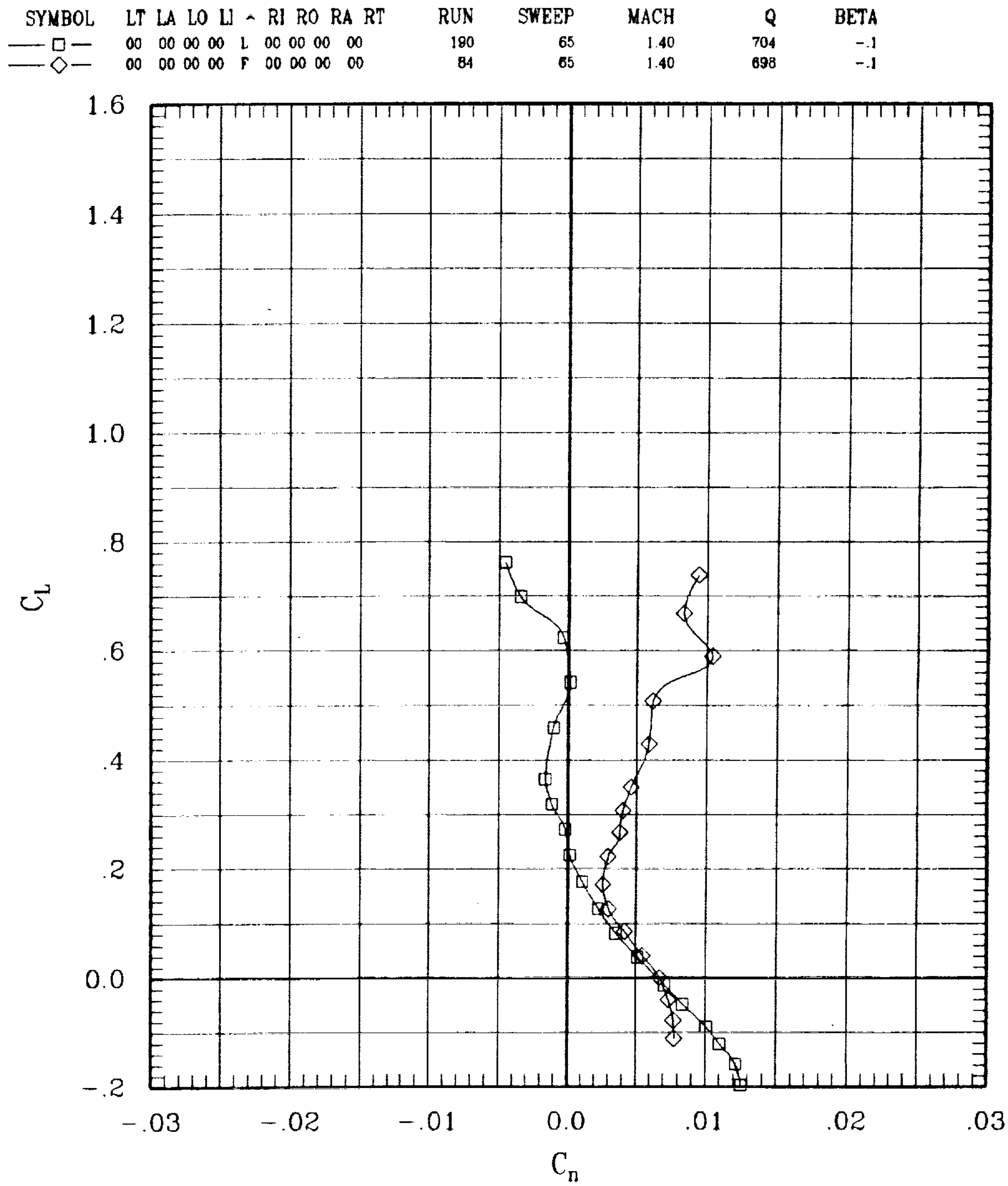

Figure 6(e). Effect of pivot height for sweep = 65 deg.

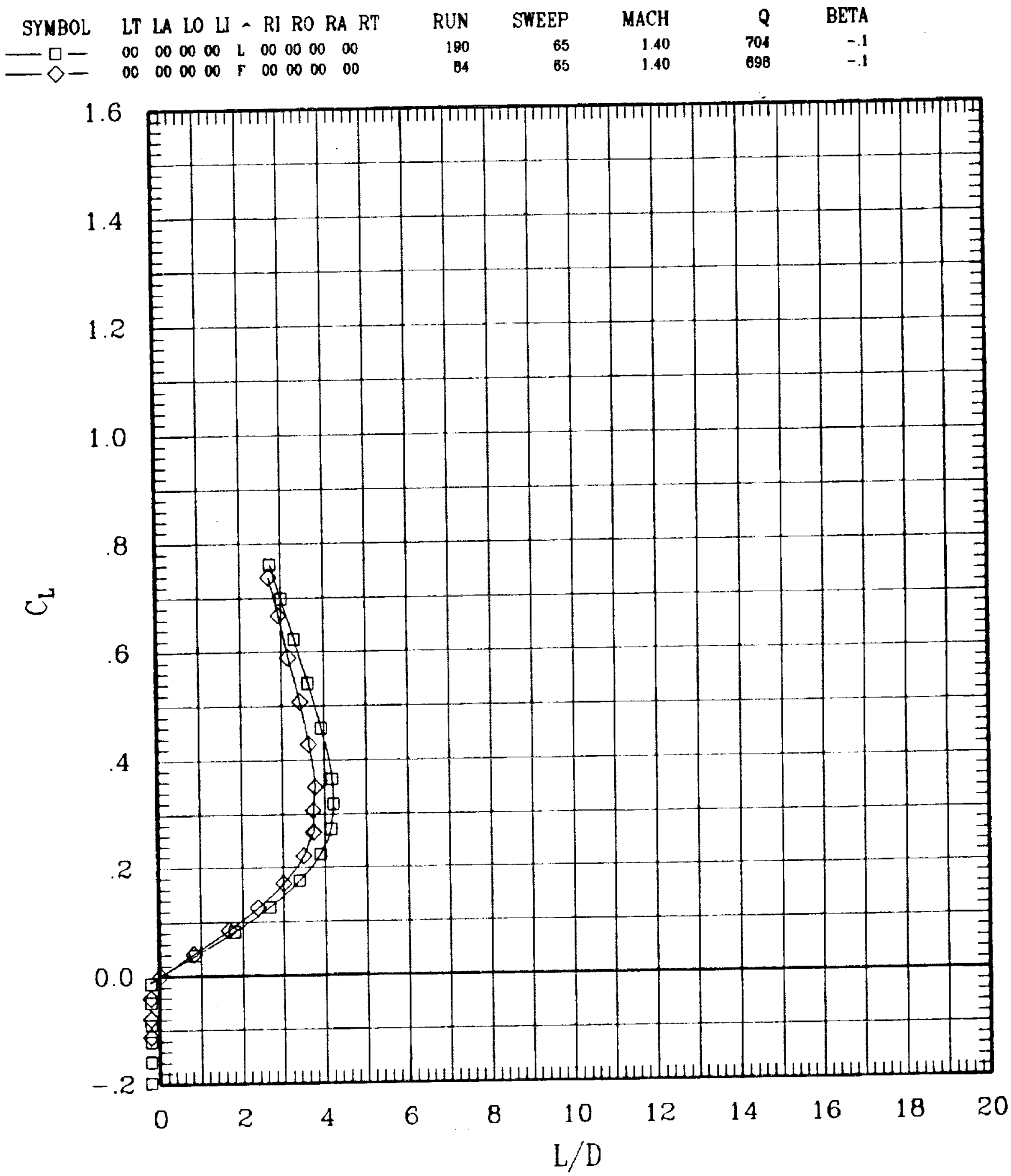

Figure 6(e). Effect of pivot height for sweep = 65 deg.

SYMBOL	LT LA LO LI ~ RI RO RA RT	RUN	SWEEP	MACH	Q	BETA
—□—	00 00 00 00 L 00 00 00 00	47	0	.60	691	-.1
—◇—	00 00 00 00 L 00 00 00 00	53	30	.60	702	-.1
—○—	00 00 00 00 L 00 00 00 00	71	45	.60	700	-.1
—△—	00 00 00 00 L 00 00 00 00	194	65	.60	698	-.1

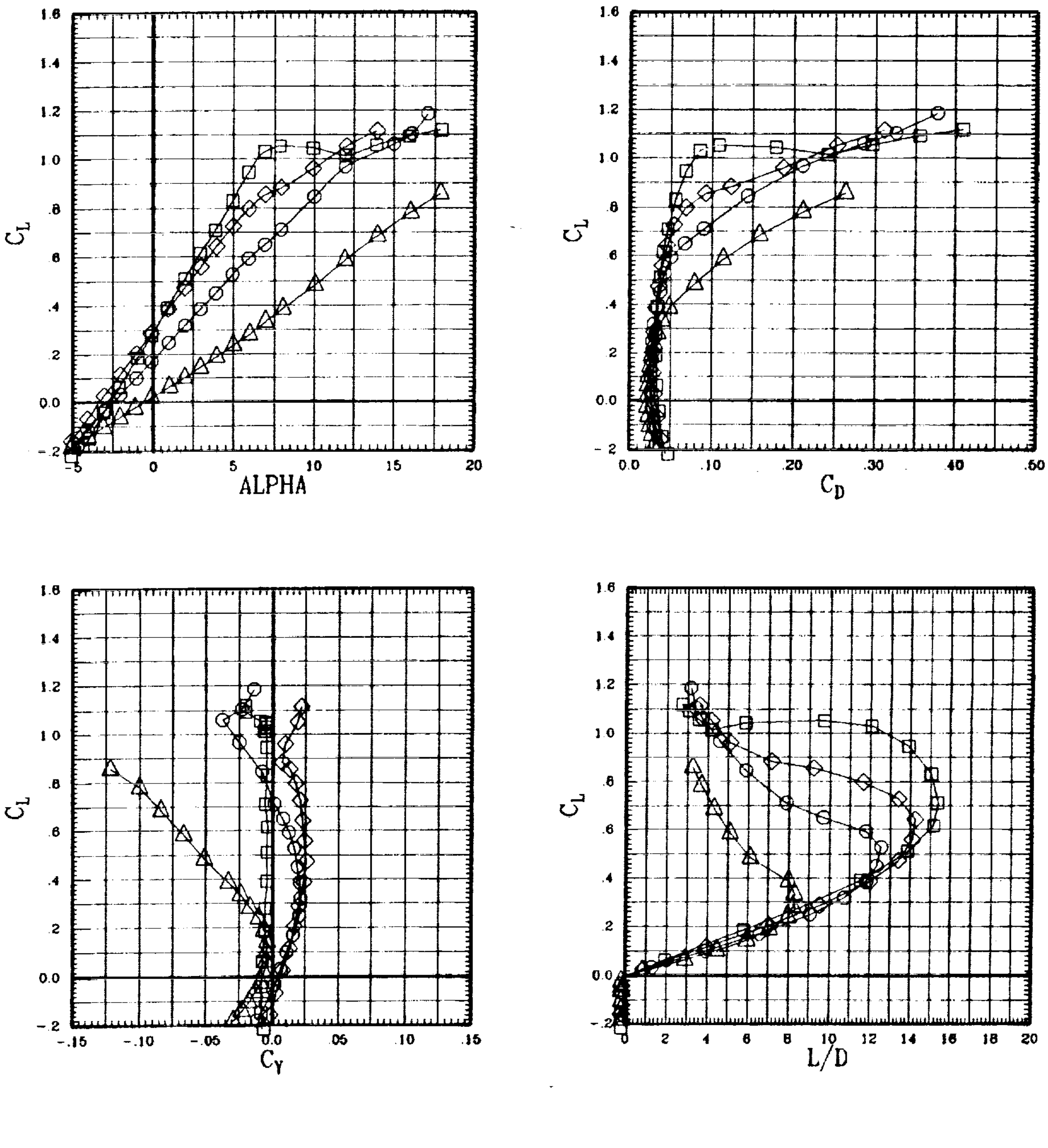

Figure 7(a). Effect of sweep for Mach 0.60 (low pivot).

SYMBOL	LT LA LO LI ~ RI RO RA RT	RUN	SWEEP	MACH	Q	BETA
—□—	00 00 00 00 L 00 00 00 00	47	0	.60	691	-.1
—◇—	00 00 00 00 L 00 00 00 00	53	30	.60	702	-.1
—○—	00 00 00 00 L 00 00 00 00	71	45	.60	700	-.1
—△—	00 00 00 00 L 00 00 00 00	194	65	.60	698	-.1

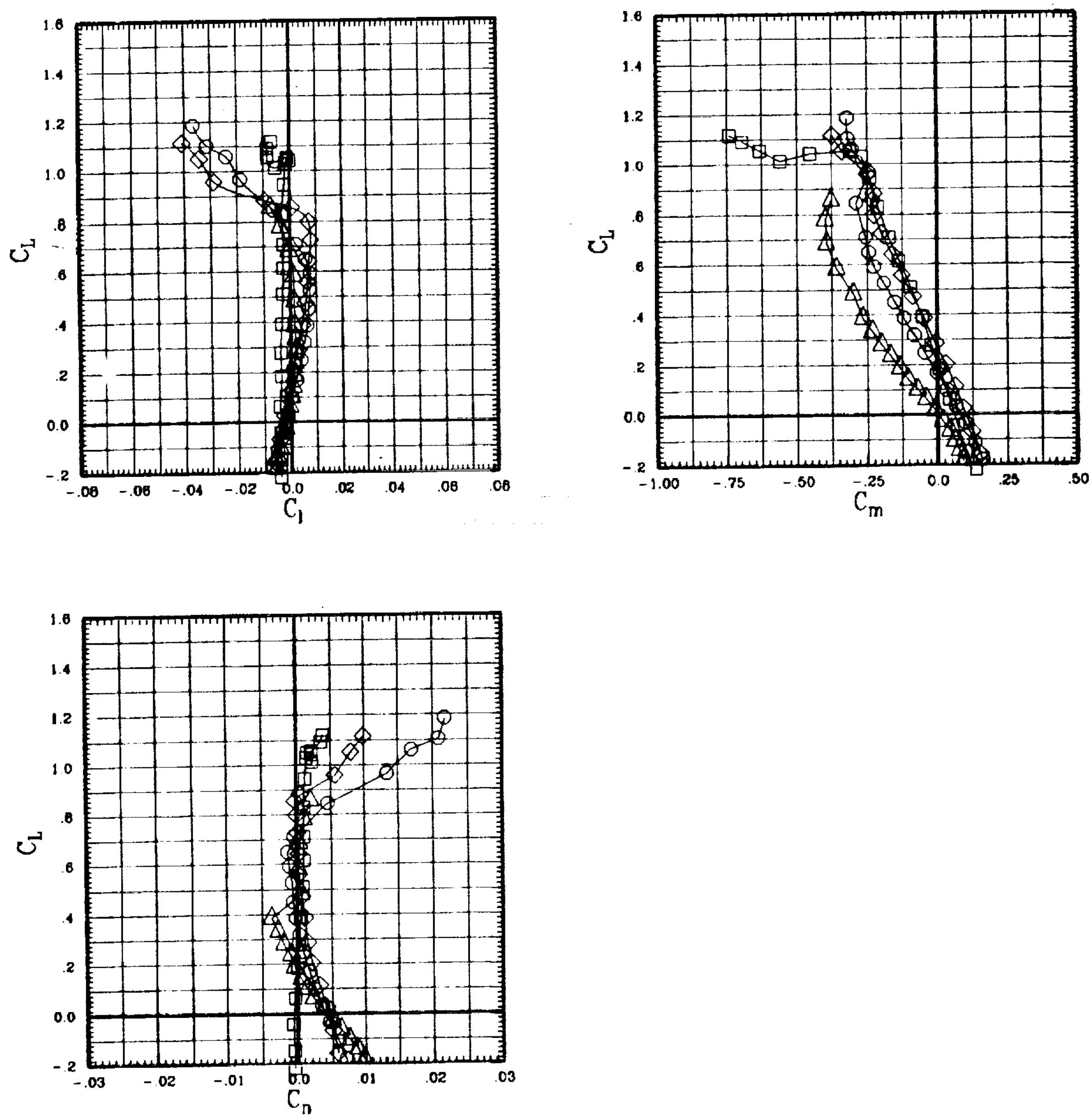

Figure 7(a). Effect of sweep for Mach 0.60 (low pivot).

SYMBOL	LT LA LO LI ⌃ RI RO RA RT	RUN	SWEEP	MACH	Q	BETA
—□—	00 00 00 00 L 00 00 00 00	45	0	.80	696	-.1
—◇—	00 00 00 00 L 00 00 00 00	51	30	.80	697	-.1
—○—	00 00 00 00 L 00 00 00 00	70	45	.80	703	-.1
—△—	00 00 00 00 L 00 00 00 00	76	60	.80	699	-.1
—▽—	00 00 00 00 L 00 00 00 00	193	65	.80	698	-.1

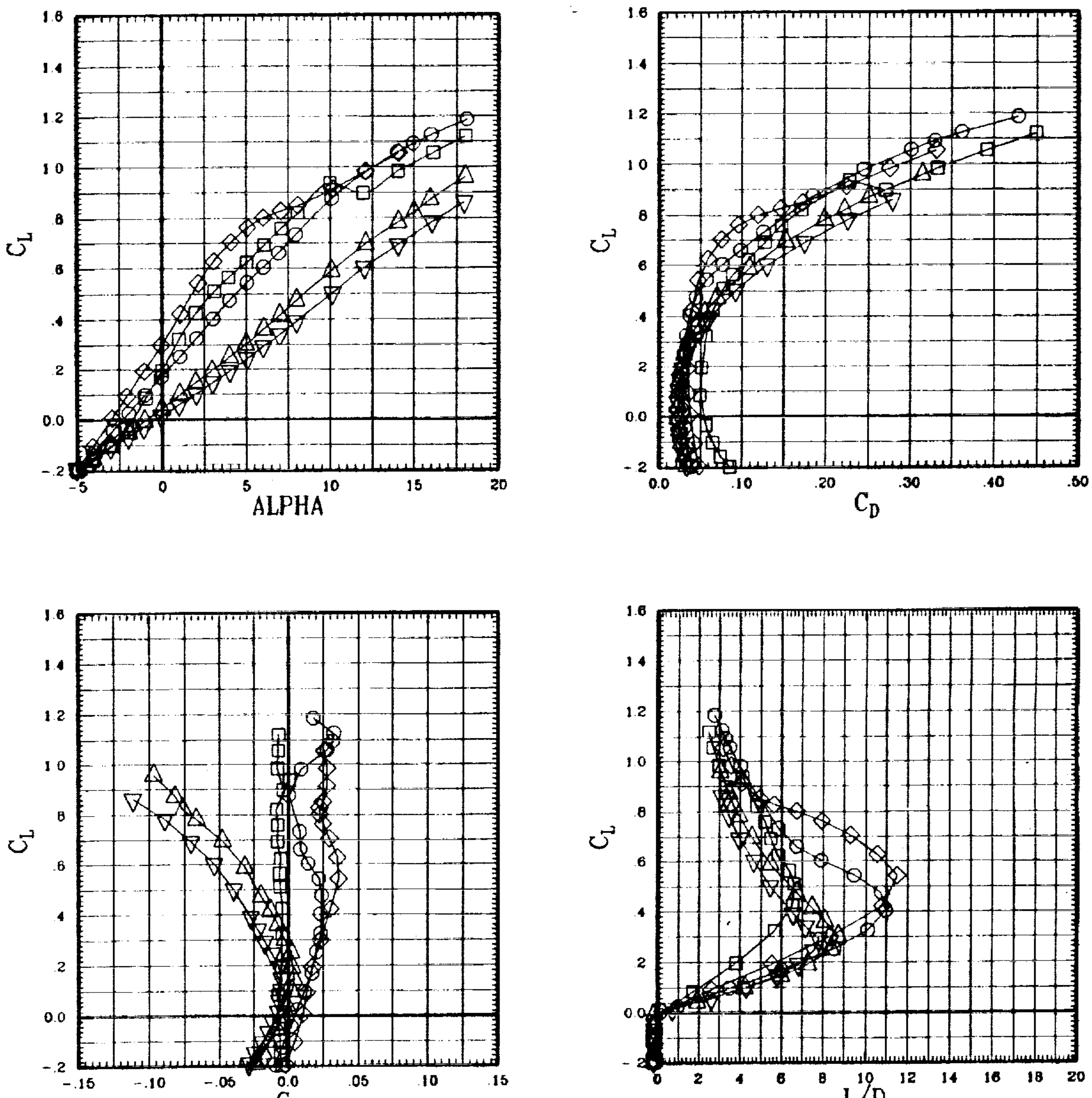

Figure 7(b). Effect of sweep for Mach 0.80 (low pivot).

SYMBOL	LT	LA	LO	LI	~	RI	RO	RA	RT	RUN	SWEEP	MACH	Q	BETA
—□—	00	00	00	00	L	00	00	00	00	45	0	.80	696	-.1
—◇—	00	00	00	00	L	00	00	00	00	51	30	.80	697	-.1
—○—	00	00	00	00	L	00	00	00	00	70	45	.80	703	-.1
—△—	00	00	00	00	L	00	00	00	00	76	60	.80	699	-.1
—▽—	00	00	00	00	L	00	00	00	00	193	65	.80	698	-.1

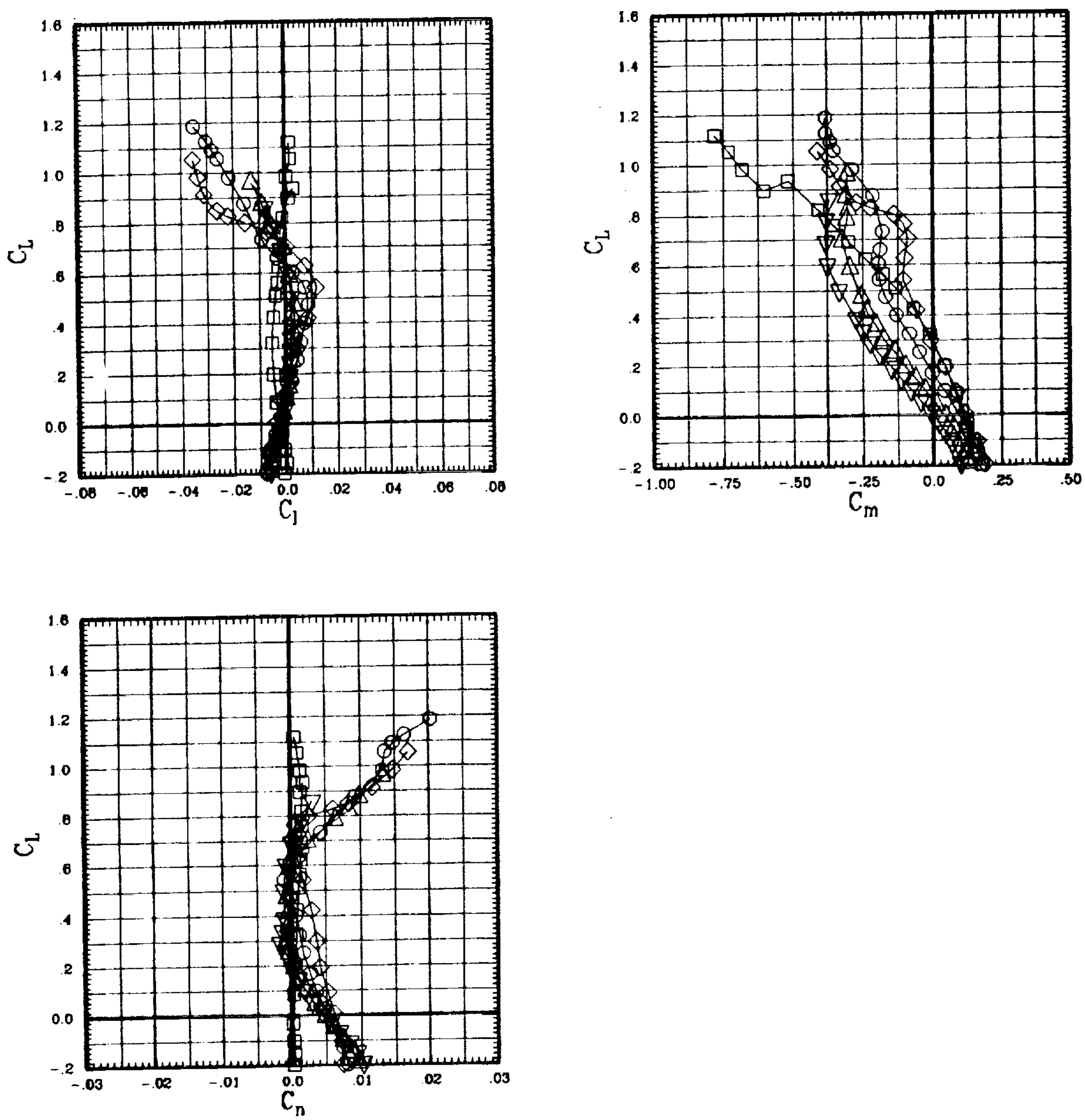

Figure 7(b). Effect of sweep for Mach 0.80 (low pivot).

SYMBOL	LT LA LO LI ^ RI RO RA RT	RUN	SWEEP	MACH	Q	BETA
—□—	00 00 00 00 L 00 00 00 00	66	45	1.20	703	-.2
—◇—	00 00 00 00 L 00 00 00 00	73	60	1.20	705	-.2
—○—	00 00 00 00 L 00 00 00 00	191	65	1.20	707	-.1

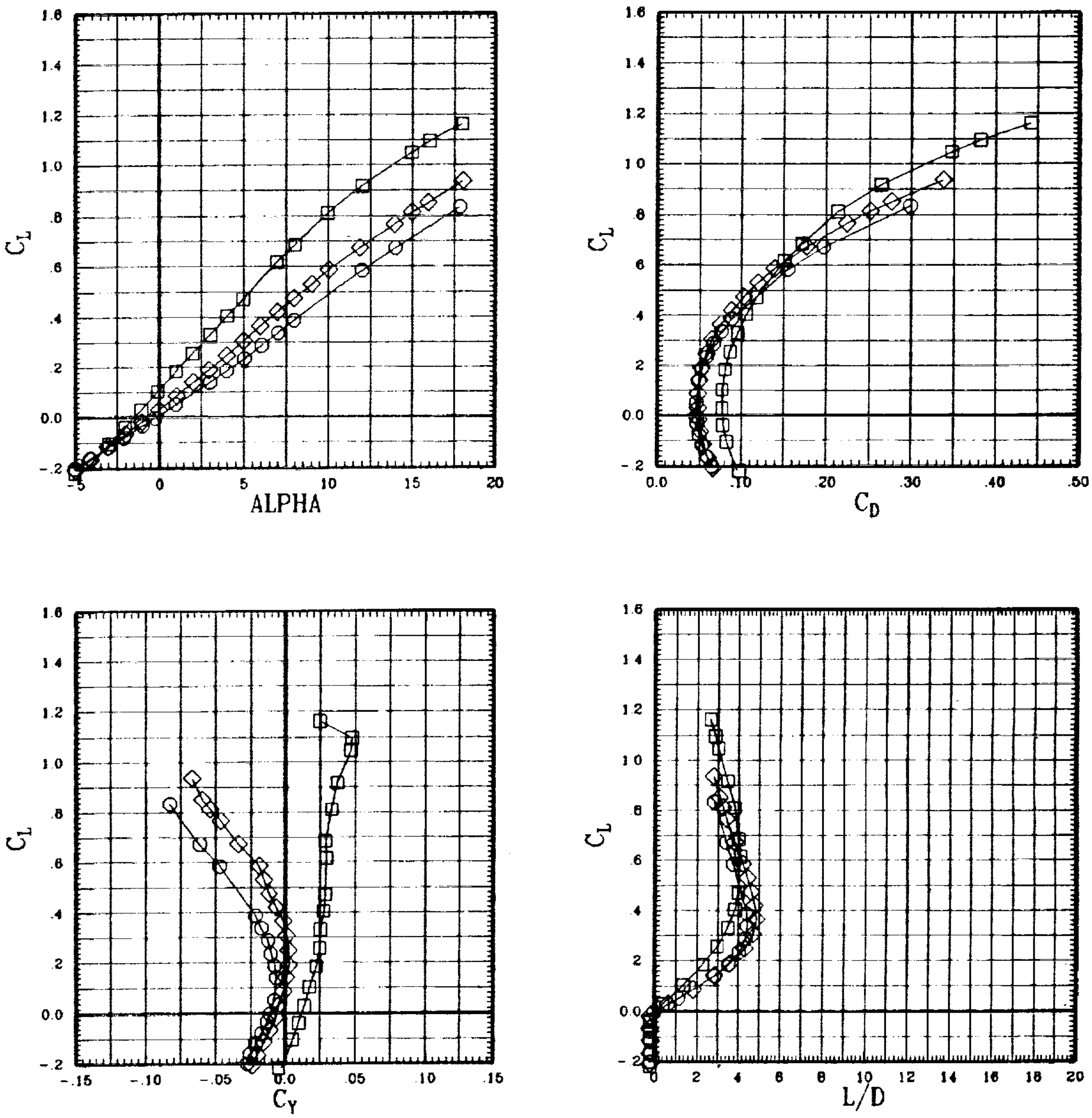

Figure 7(c). Effect of sweep for Mach 1.20 (low pivot).

SYMBOL	LT	LA	LO	LI	^	RI	RO	RA	RT	RUN	SWEEP	MACH	Q	BETA
—□—	00	00	00	00	L	00	00	00	00	66	45	1.20	703	-.2
—◇—	00	00	00	00	L	00	00	00	00	73	60	1.20	705	-.2
—○—	00	00	00	00	L	00	00	00	00	191	65	1.20	707	-.1

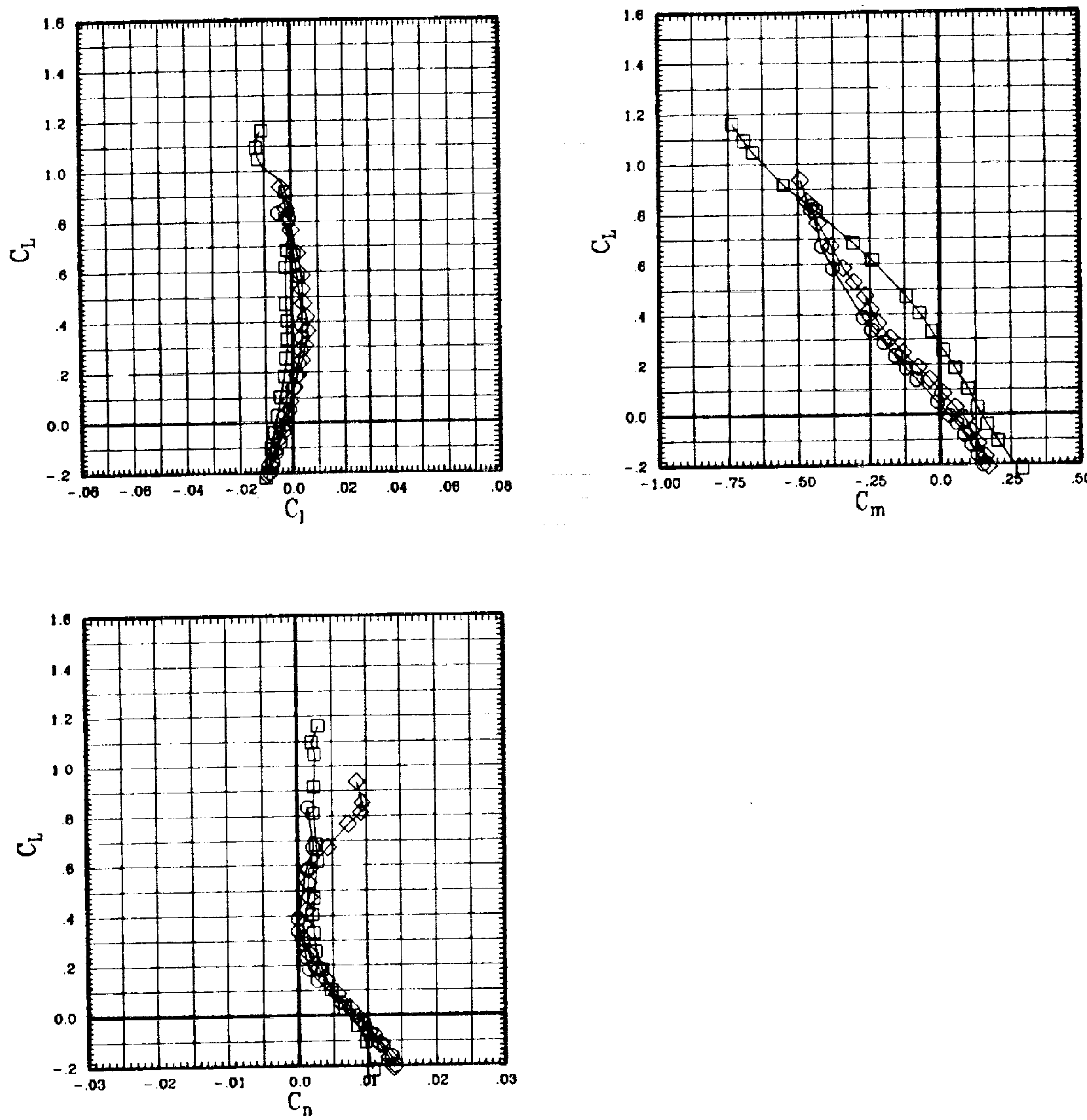

Figure 7(c). Effect of sweep for Mach 1.20 (low pivot).

SYMBOL	LT	LA	LO	LI	^	RI	RO	RA	RT	RUN	SWEEP	MACH	Q	BETA
—□—	00	00	00	00	L	00	00	00	00	48	0	.30	240	-.1
—◇—	00	00	00	00	L	00	00	00	00	49	0	.40	425	-.1
—○—	00	00	00	00	L	00	00	00	00	124	0	.50	678	-.1
—△—	00	00	00	00	L	00	00	00	00	47	0	.60	691	-.1
—▽—	00	00	00	00	L	00	00	00	00	46	0	.70	704	-.1
—▷—	00	00	00	00	L	00	00	00	00	45	0	.80	696	-.1

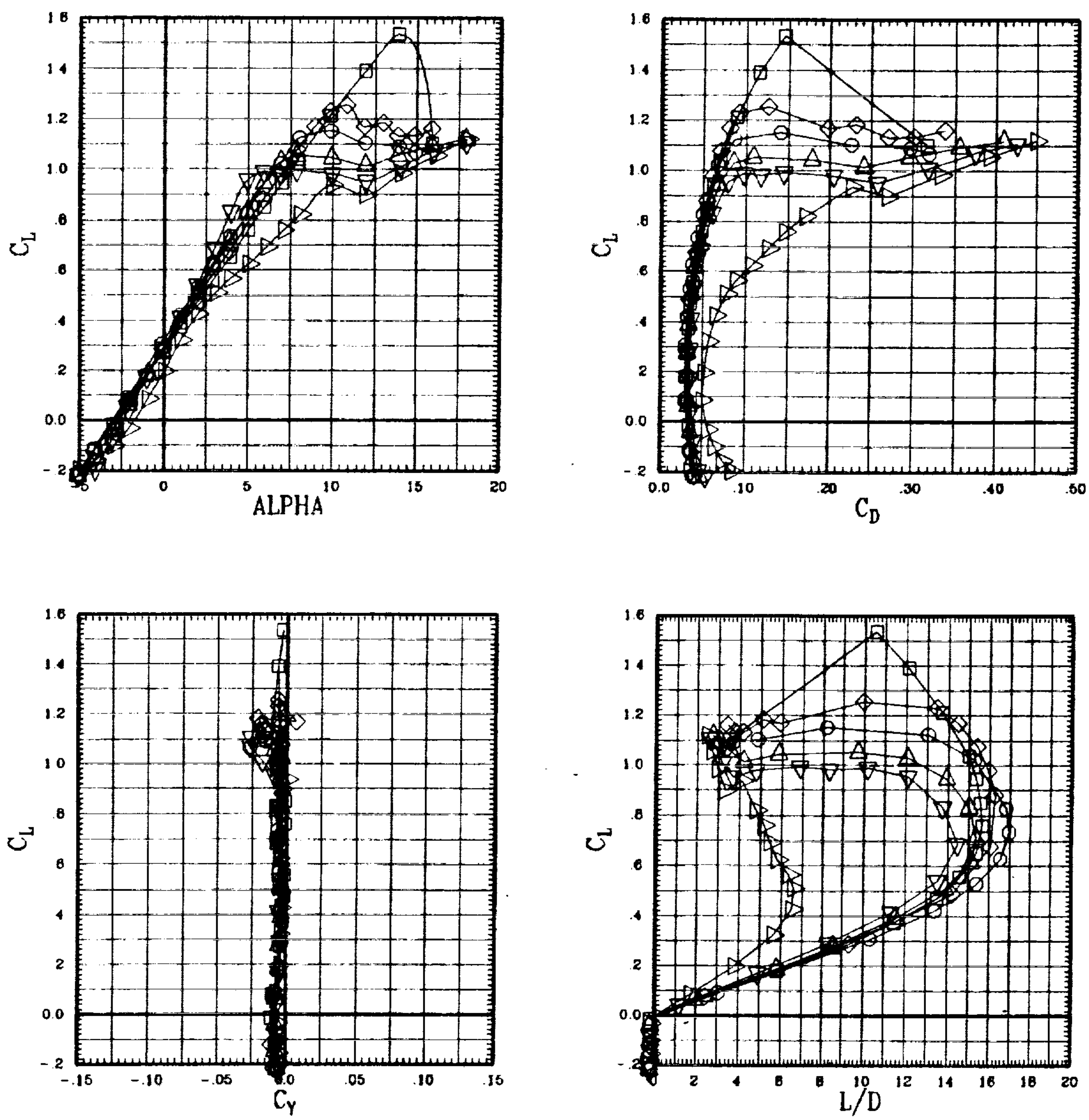

Figure 8(a). Effect of Mach number for sweep = 0 deg (low pivot).

SYMBOL	LT	LA	LO	LI	^	RI	RO	RA	RT	RUN	SWEEP	MACH	Q	BETA
—□—	00	00	00	00	L	00	00	00	00	48	0	.30	240	-.1
—◇—	00	00	00	00	L	00	00	00	00	49	0	.40	425	-.1
—○—	00	00	00	00	L	00	00	00	00	124	0	.50	678	-.1
—△—	00	00	00	00	L	00	00	00	00	47	0	.60	691	-.1
—▽—	00	00	00	00	L	00	00	00	00	46	0	.70	704	-.1
—▷—	00	00	00	00	L	00	00	00	00	45	0	.80	696	-.1

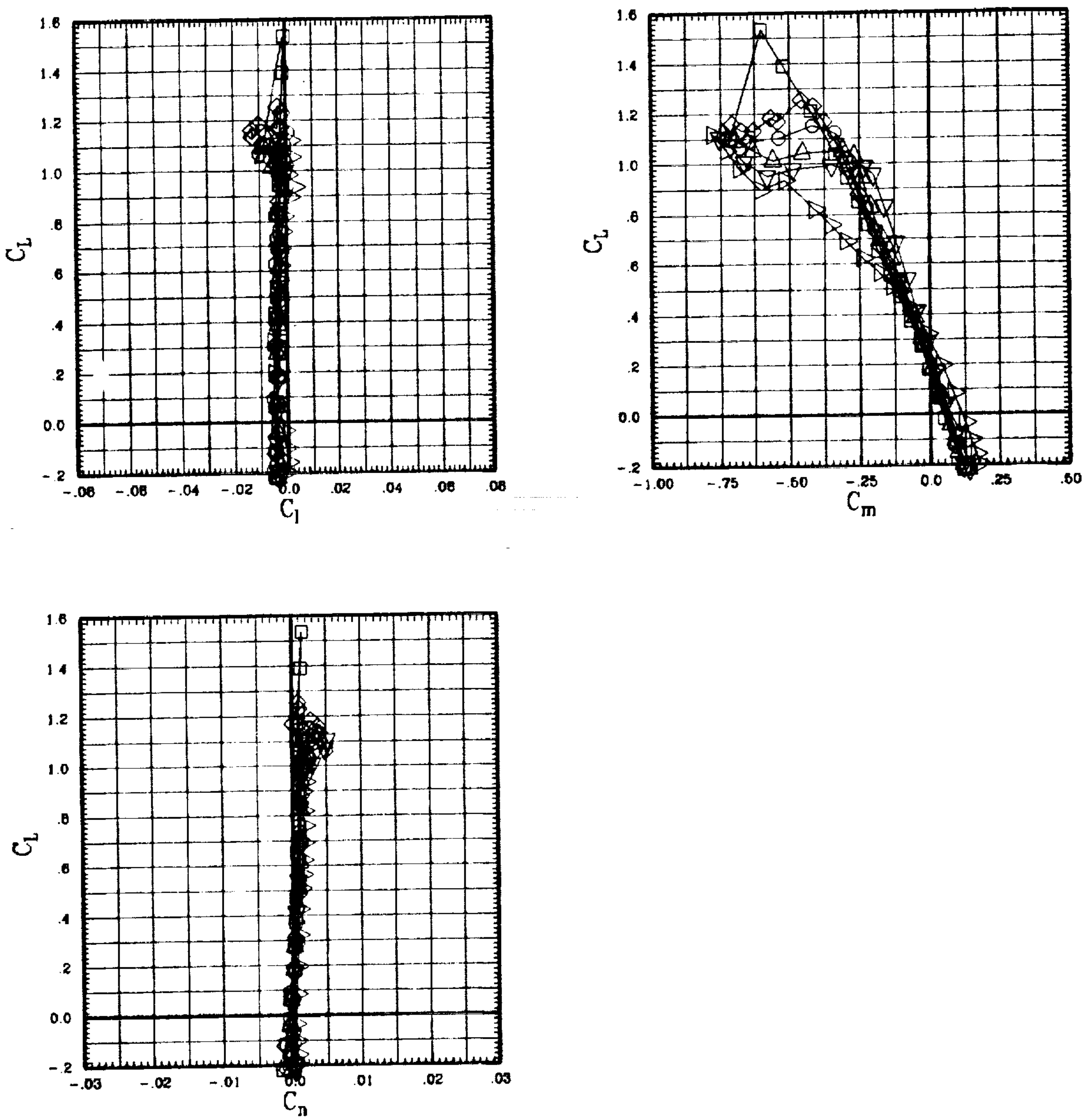

Figure 8(a). Effect of Mach number for sweep = 0 deg (low pivot).

SYMBOL	LT LA LO LI ~ RI RO RA RT	RUN	SWEEP	MACH	Q	BETA
—□—	00 00 00 00 L 00 00 00 00	53	30	.60	702	-.1
—◇—	00 00 00 00 L 00 00 00 00	52	30	.70	699	-.1
—○—	00 00 00 00 L 00 00 00 00	51	30	.80	697	-.1
—△—	00 00 00 00 L 00 00 00 00	228	30	.85	708	-.1
—▽—	00 00 00 00 L 00 00 00 00	50	30	.90	698	-.1

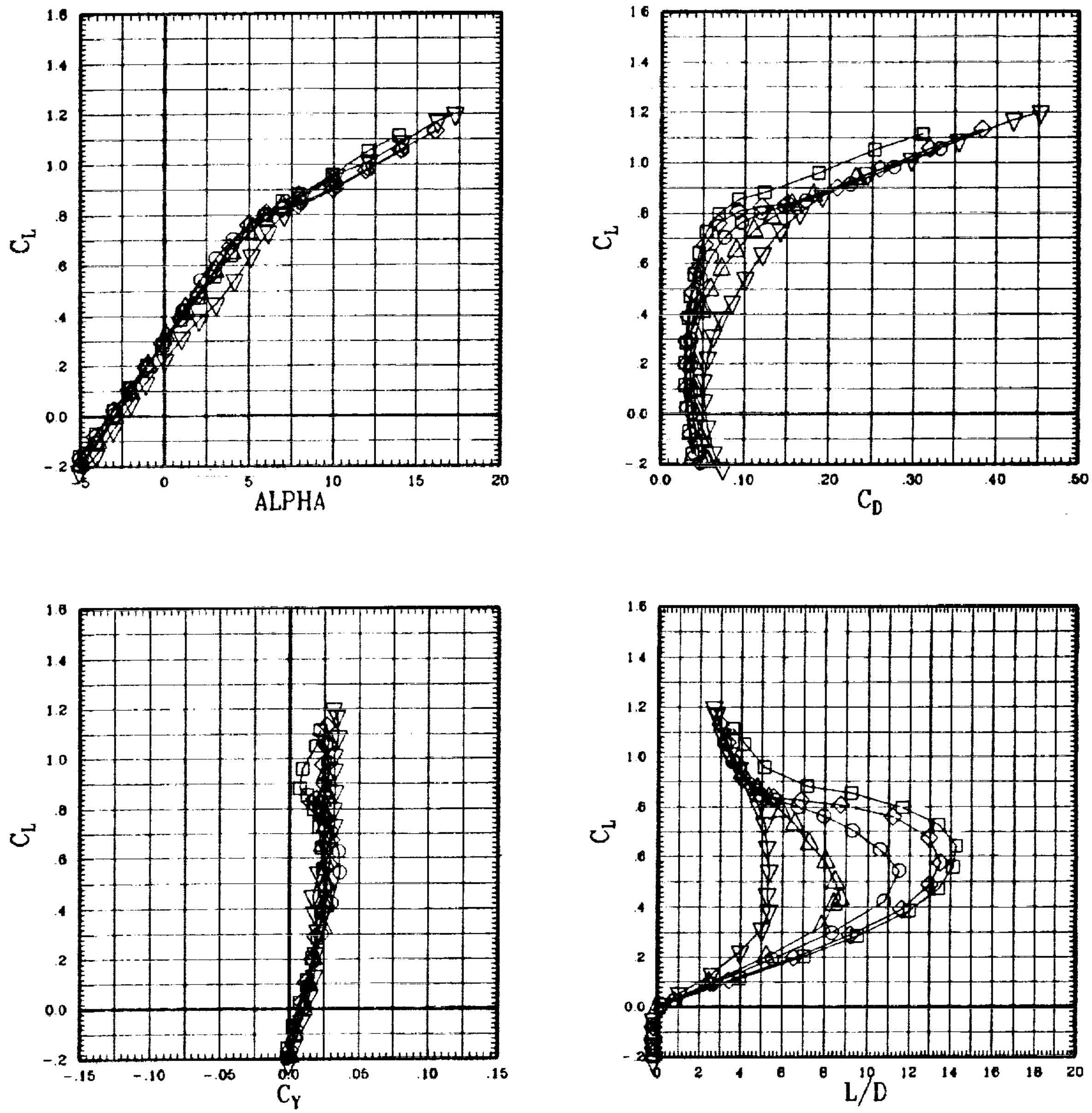

Figure 8(b). Effect of Mach number for sweep = 30 deg (low pivot).

SYMBOL	LT	LA	LO	LI	^	RI	RO	RA	RT	RUN	SWEEP	MACH	Q	BETA
—□—	00	00	00	00	L	00	00	00	00	53	30	.60	702	-.1
—◇—	00	00	00	00	L	00	00	00	00	52	30	.70	699	-.1
—○—	00	00	00	00	L	00	00	00	00	51	30	.80	697	-.1
—△—	00	00	00	00	L	00	00	00	00	228	30	.85	708	-.1
—▽—	00	00	00	00	L	00	00	00	00	50	30	.90	698	-.1

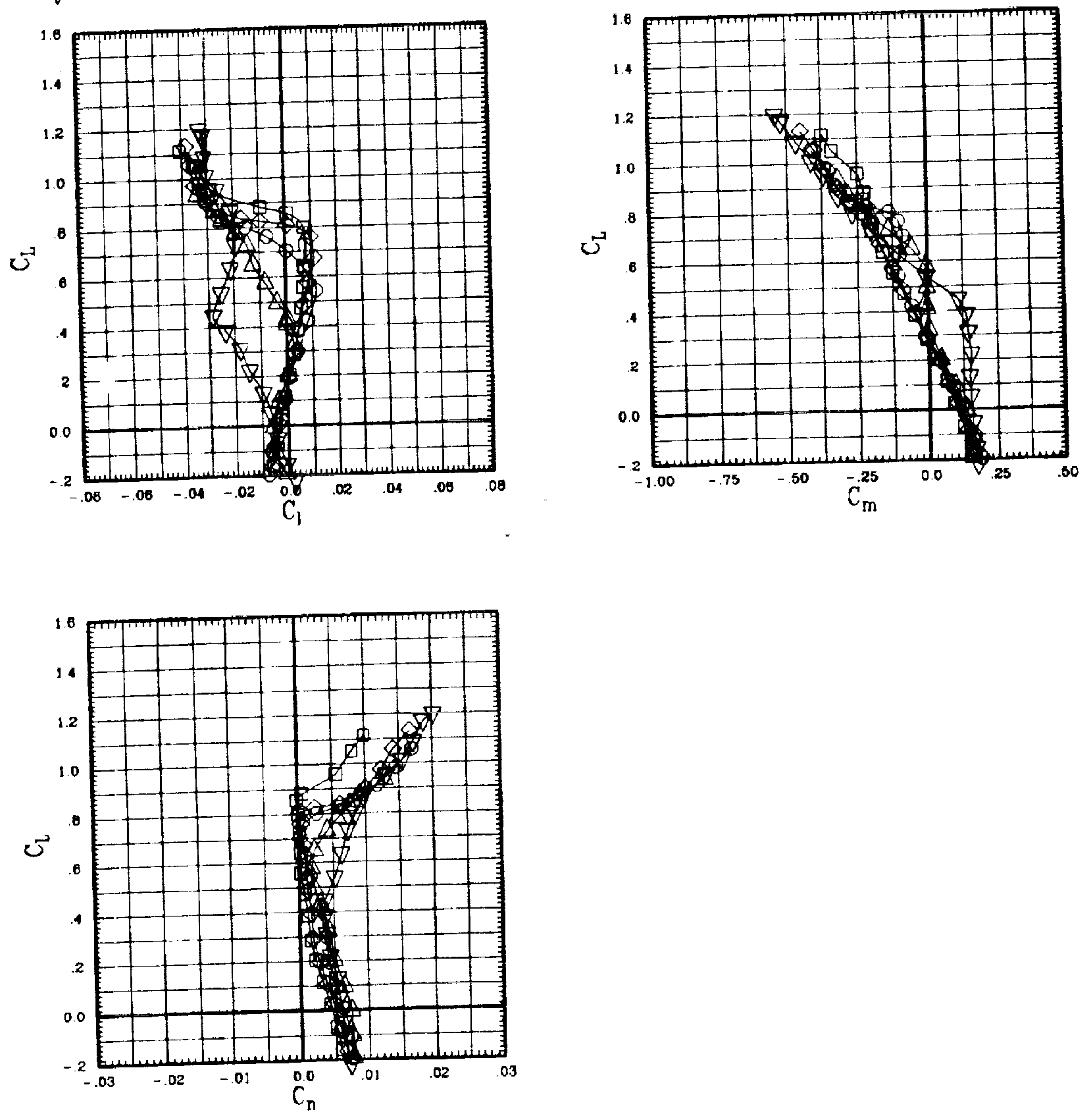

Figure 8(b). Effect of Mach number for sweep = 30 deg (low pivot).

SYMBOL	LT	LA	LO	LI	^	RI	RO	RA	RT	RUN	SWEEP	MACH	Q	BETA
□	00	00	00	00	L	00	00	00	00	71	45	.60	700	-.1
◇	00	00	00	00	L	00	00	00	00	70	45	.80	703	-.1
○	00	00	00	00	L	00	00	00	00	69	45	.90	704	-.1
△	00	00	00	00	L	00	00	00	00	68	45	.95	700	-.1
▽	00	00	00	00	L	00	00	00	00	67	45	1.10	691	-.2
▷	00	00	00	00	L	00	00	00	00	66	45	1.20	703	-.2

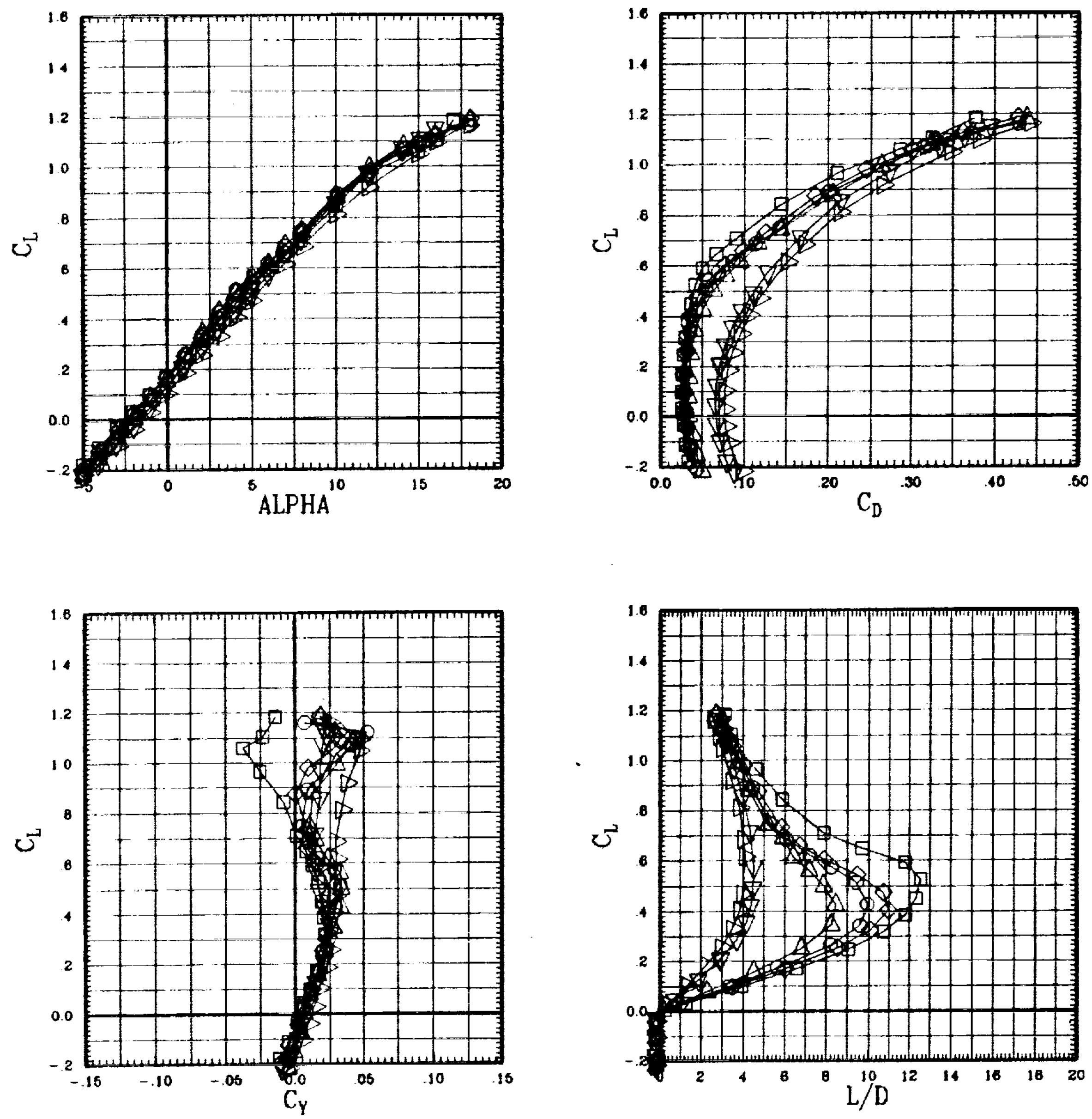

Figure 8(c). Effect of Mach number for sweep = 45 deg (low pivot).

SYMBOL	LT	LA	LO	LI	^	RI	RO	RA	RT	RUN	SWEEP	MACH	Q	BETA
—□—	00	00	00	00	L	00	00	00	00	71	45	.60	700	-.1
—◇—	00	00	00	00	L	00	00	00	00	70	45	.80	703	-.1
—○—	00	00	00	00	L	00	00	00	00	69	45	.90	704	-.1
—△—	00	00	00	00	L	00	00	00	00	68	45	.95	700	-.1
—▽—	00	00	00	00	L	00	00	00	00	67	45	1.10	691	-.2
—▷—	00	00	00	00	L	00	00	00	00	66	45	1.20	703	-.2

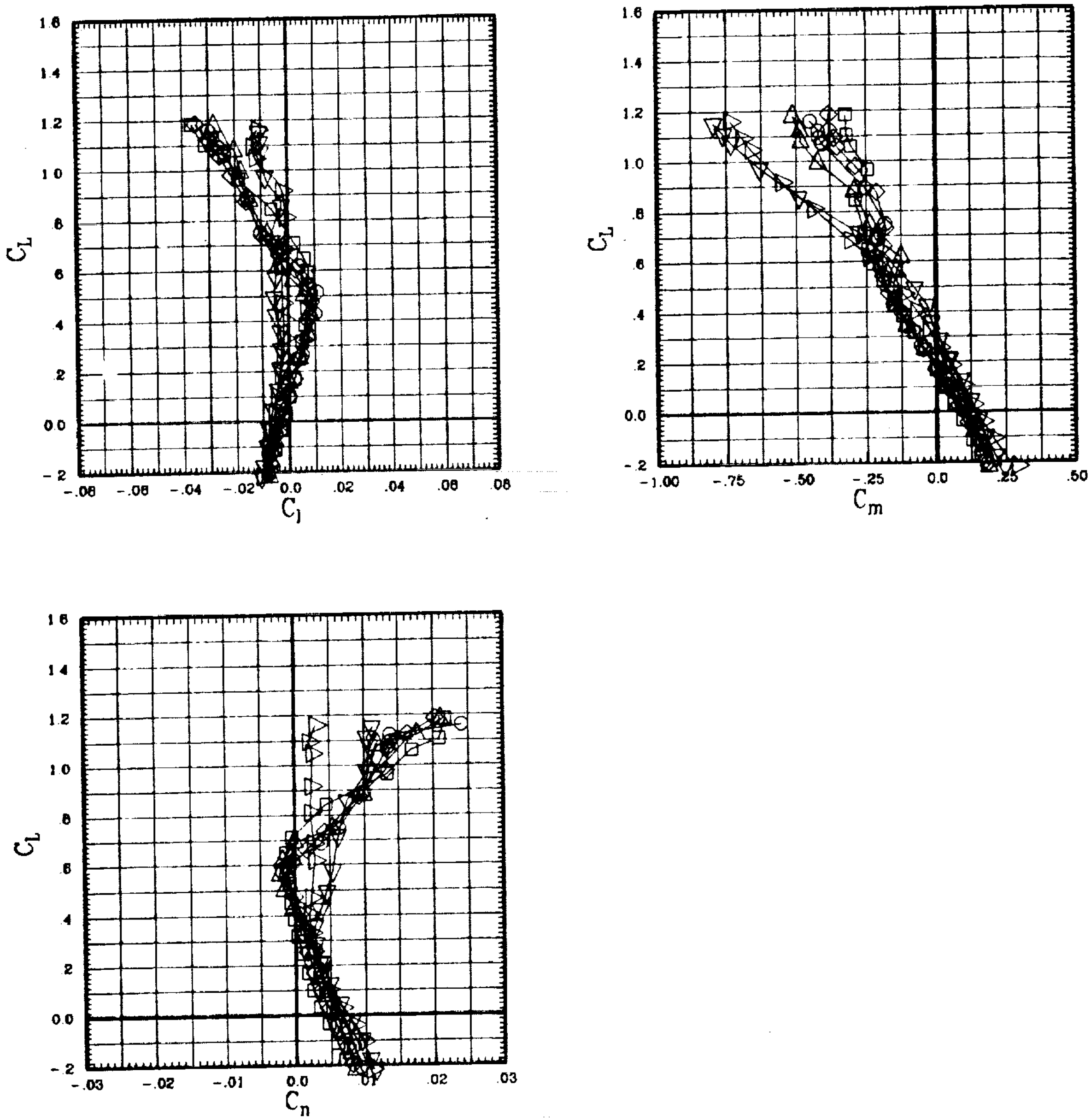

Figure 8(c). Effect of Mach number for sweep = 45 deg (low pivot).

SYMBOL	LT LA LO LI ^ RI RO RA RT	RUN	SWEEP	MACH	Q	BETA
—□—	00 00 00 00 L 00 00 00 00	77	60	.70	702	-.1
—◇—	00 00 00 00 L 00 00 00 00	76	60	.80	699	-.1
—○—	00 00 00 00 L 00 00 00 00	75	60	.95	701	-.1
—△—	00 00 00 00 L 00 00 00 00	74	60	1.10	702	-.1
—▽—	00 00 00 00 L 00 00 00 00	73	60	1.20	705	-.2
—▷—	00 00 00 00 L 00 00 00 00	72	60	1.40	700	0.0

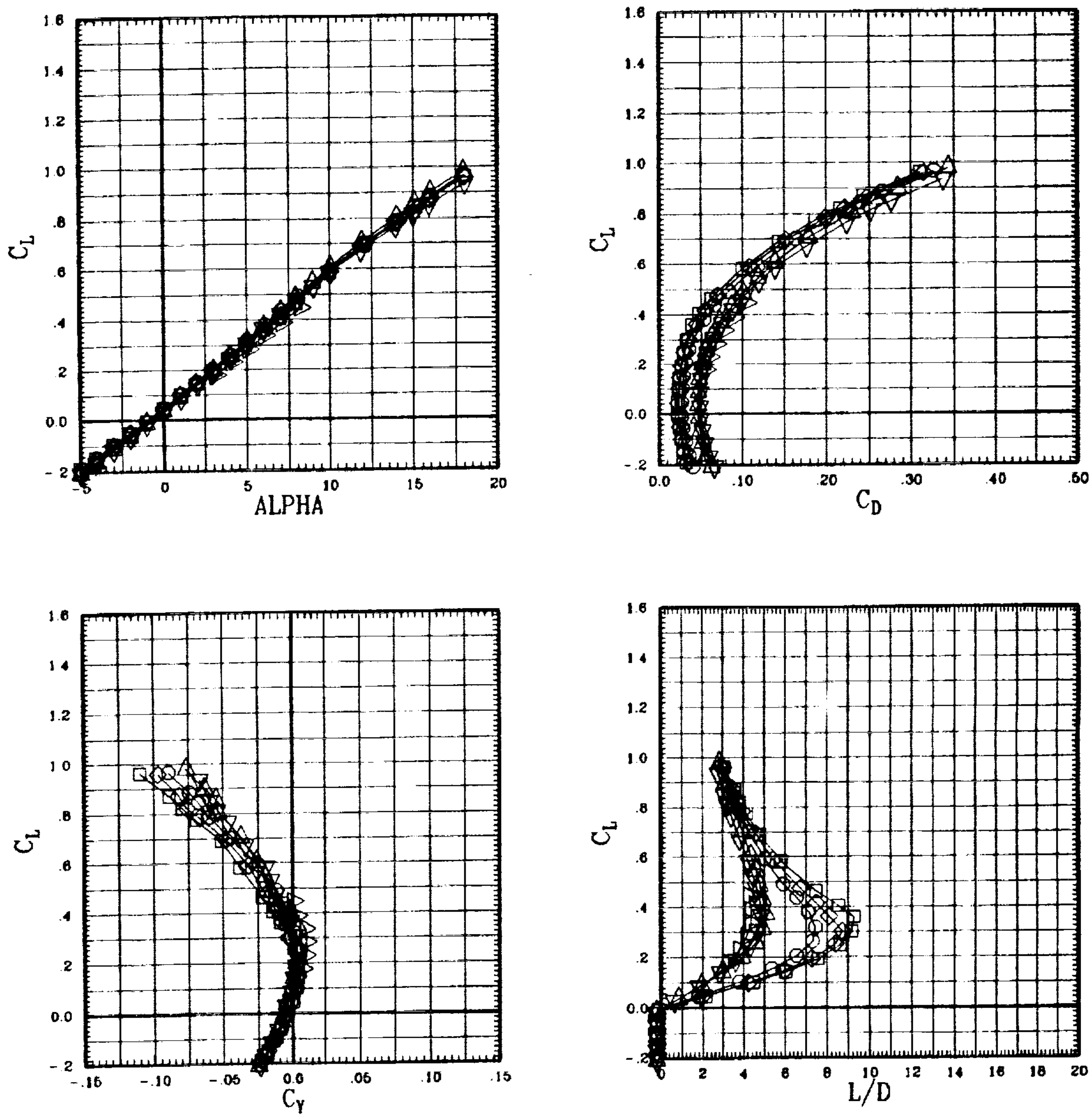

Figure 8(d). Effect of Mach number for sweep = 60 deg (low pivot).

SYMBOL	LT	LA	LO	LI	^	RI	RO	RA	RT	RUN	SWEEP	MACH	Q	BETA
—□—	00	00	00	00	L	00	00	00	00	77	60	.70	702	-.1
—◇—	00	00	00	00	L	00	00	00	00	76	60	.80	699	-.1
—○—	00	00	00	00	L	00	00	00	00	75	60	.95	701	-.1
—△—	00	00	00	00	L	00	00	00	00	74	60	1.10	702	-.1
—▽—	00	00	00	00	L	00	00	00	00	73	60	1.20	705	-.2
—▷—	00	00	00	00	L	00	00	00	00	72	60	1.40	700	0.0

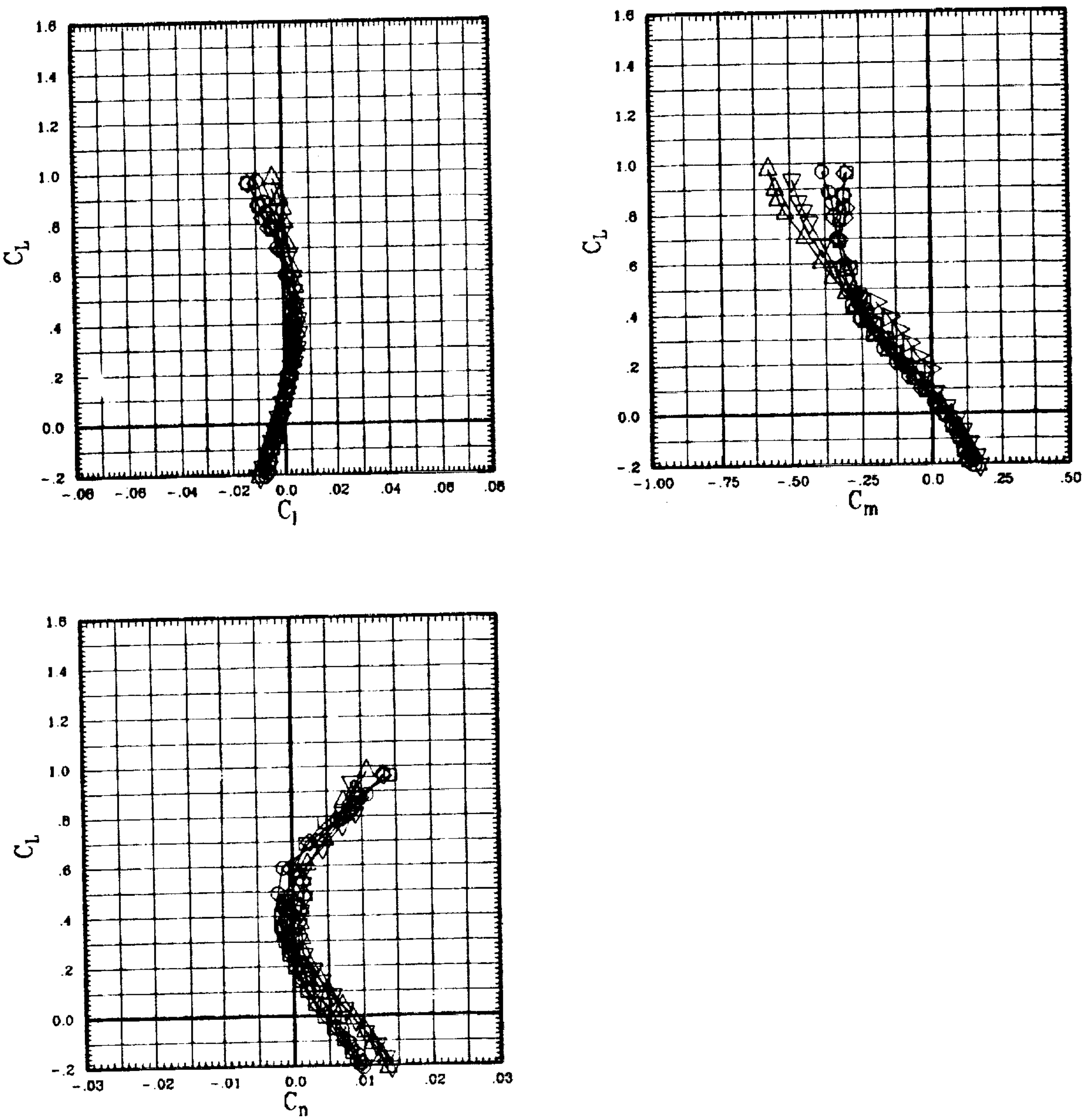

Figure 8(d). Effect of Mach number for sweep = 60 deg (low pivot).

SYMBOL	LT	LA	LO	LI	^	RI	RO	RA	RT	RUN	SWEEP	MACH	Q	BETA
—□—	00	00	00	00	L	00	00	00	00	194	65	.60	698	-.1
—◇—	00	00	00	00	L	00	00	00	00	193	65	.80	698	-.1
—○—	00	00	00	00	L	00	00	00	00	192	65	1.10	710	-.1
—△—	00	00	00	00	L	00	00	00	00	191	65	1.20	707	-.1
—▽—	00	00	00	00	L	00	00	00	00	190	65	1.40	704	-.1

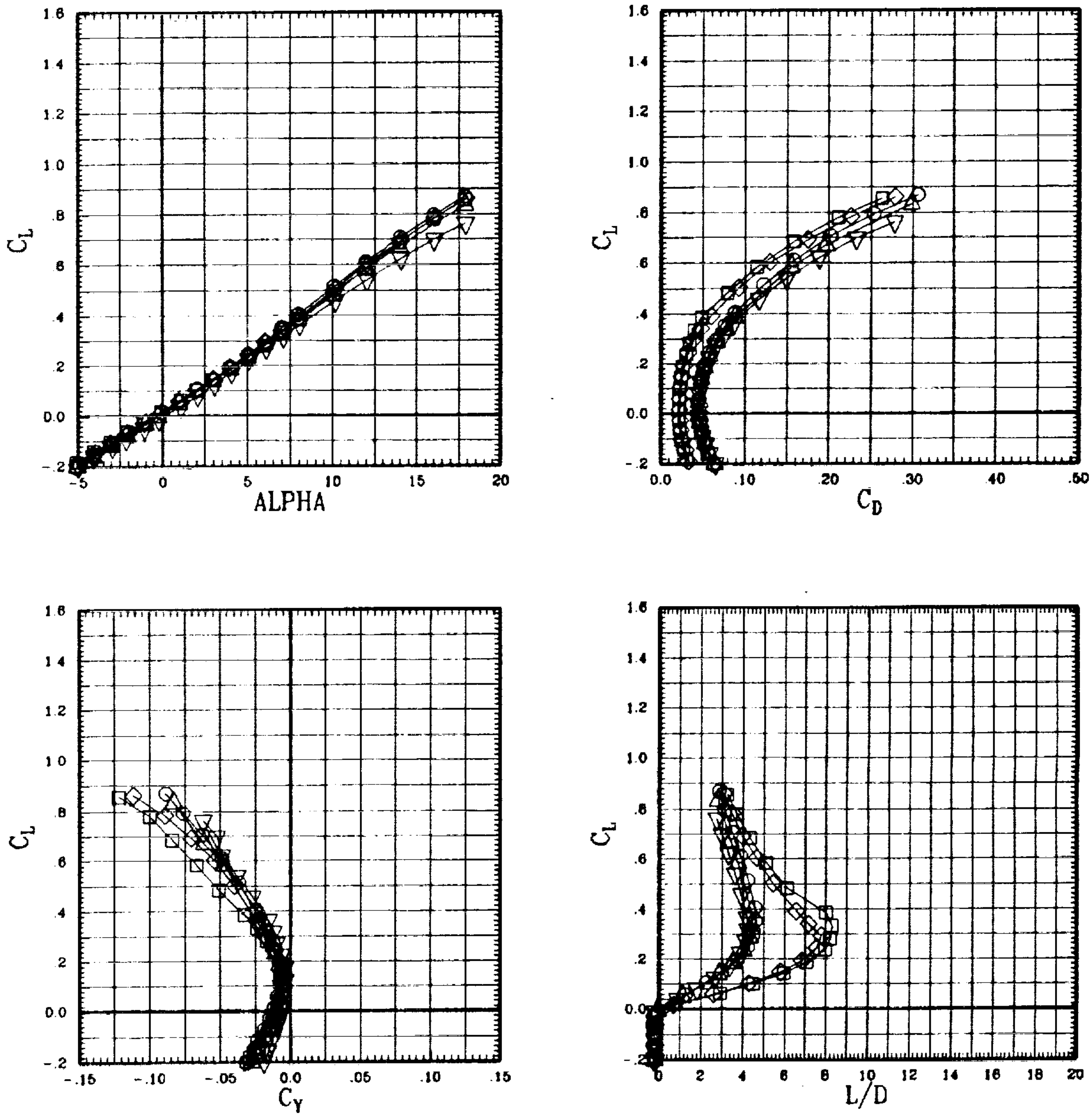

Figure 8(e). Effect of Mach number for sweep = 65 deg (low pivot).

SYMBOL	LT LA LO LI ~ RI RO RA RT	RUN	SWEEP	MACH	Q	BETA
—□—	00 00 00 00 L 00 00 00 00	194	65	.60	698	-.1
—◇—	00 00 00 00 L 00 00 00 00	193	65	.80	698	-.1
—○—	00 00 00 00 L 00 00 00 00	192	65	1.10	710	-.1
—△—	00 00 00 00 L 00 00 00 00	191	65	1.20	707	-.1
—▽—	00 00 00 00 L 00 00 00 00	190	65	1.40	704	-.1

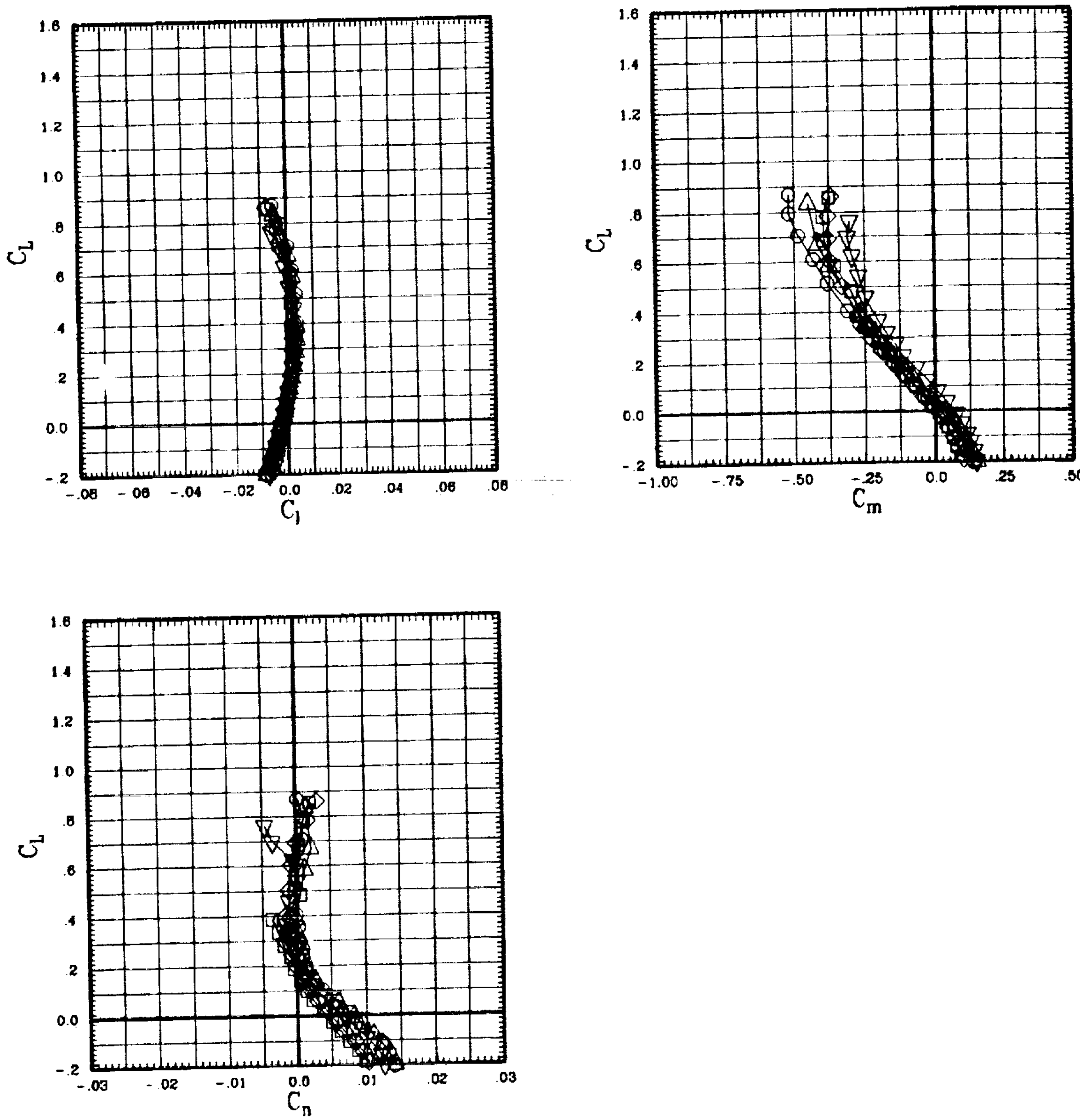

Figure 8(e). Effect of Mach number for sweep = 65 deg (low pivot).

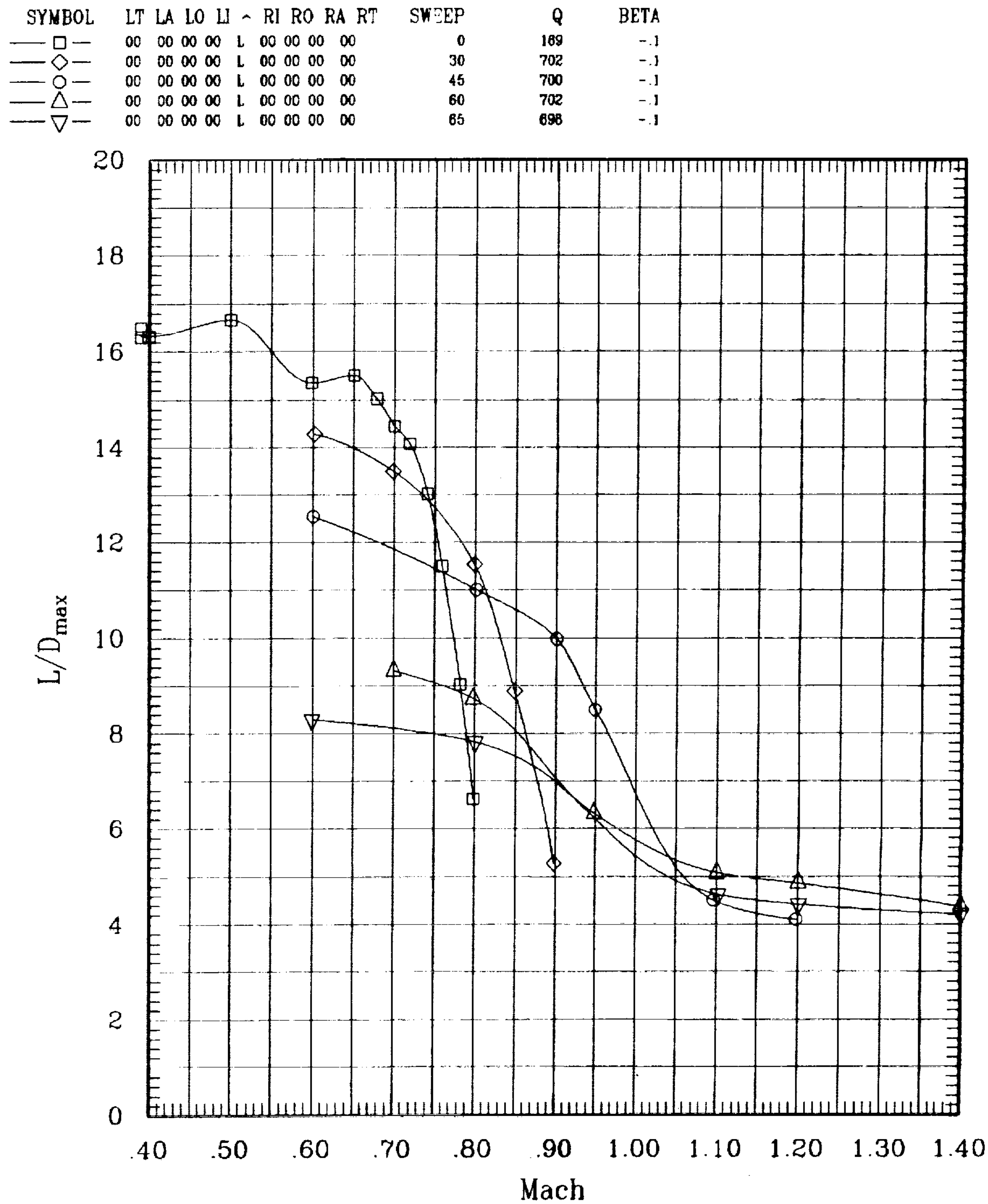

Figure 9. Summary of derived aerodynamic parameters (low pivot).

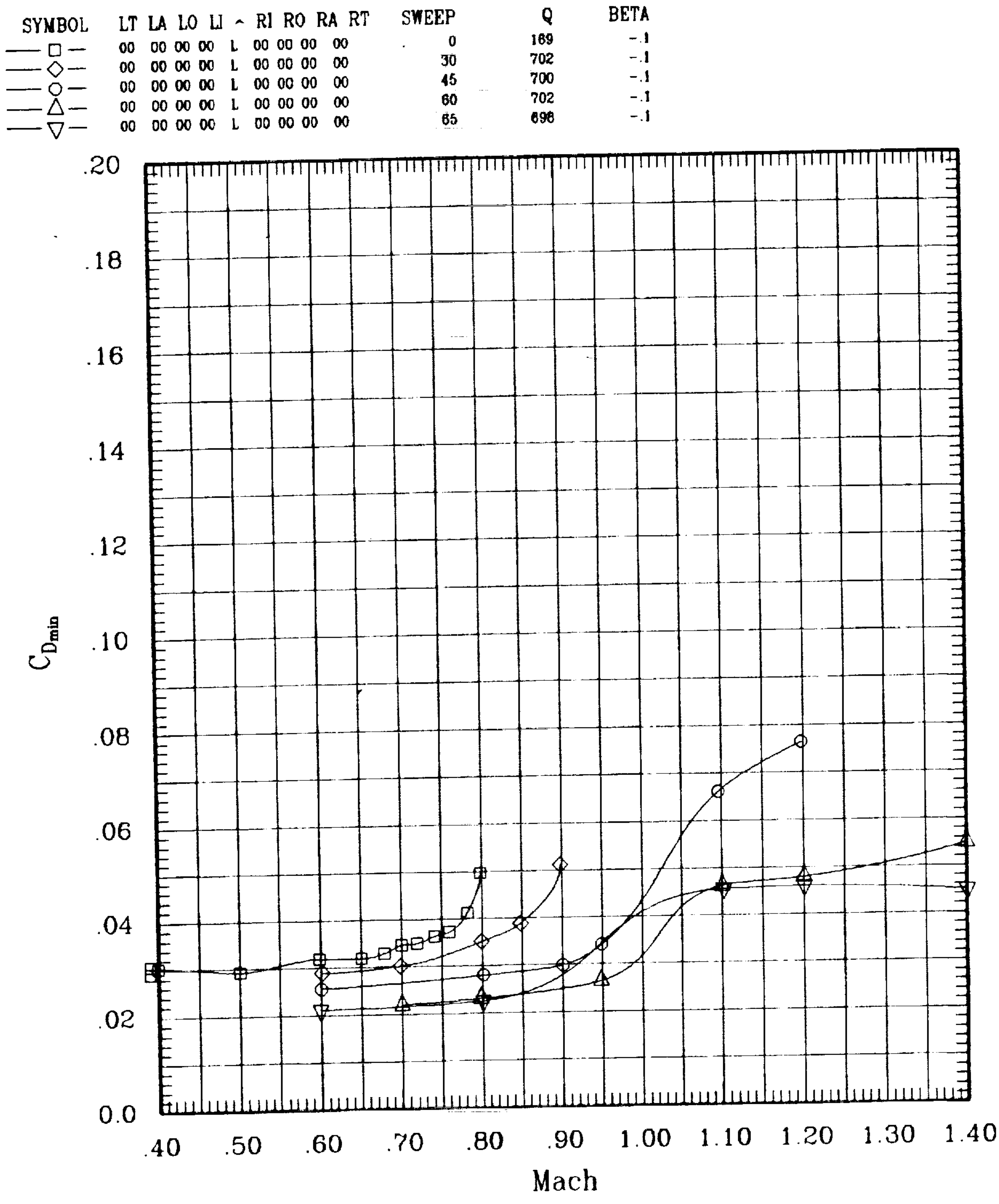

Figure 9. Summary of derived aerodynamic parameters (low pivot).

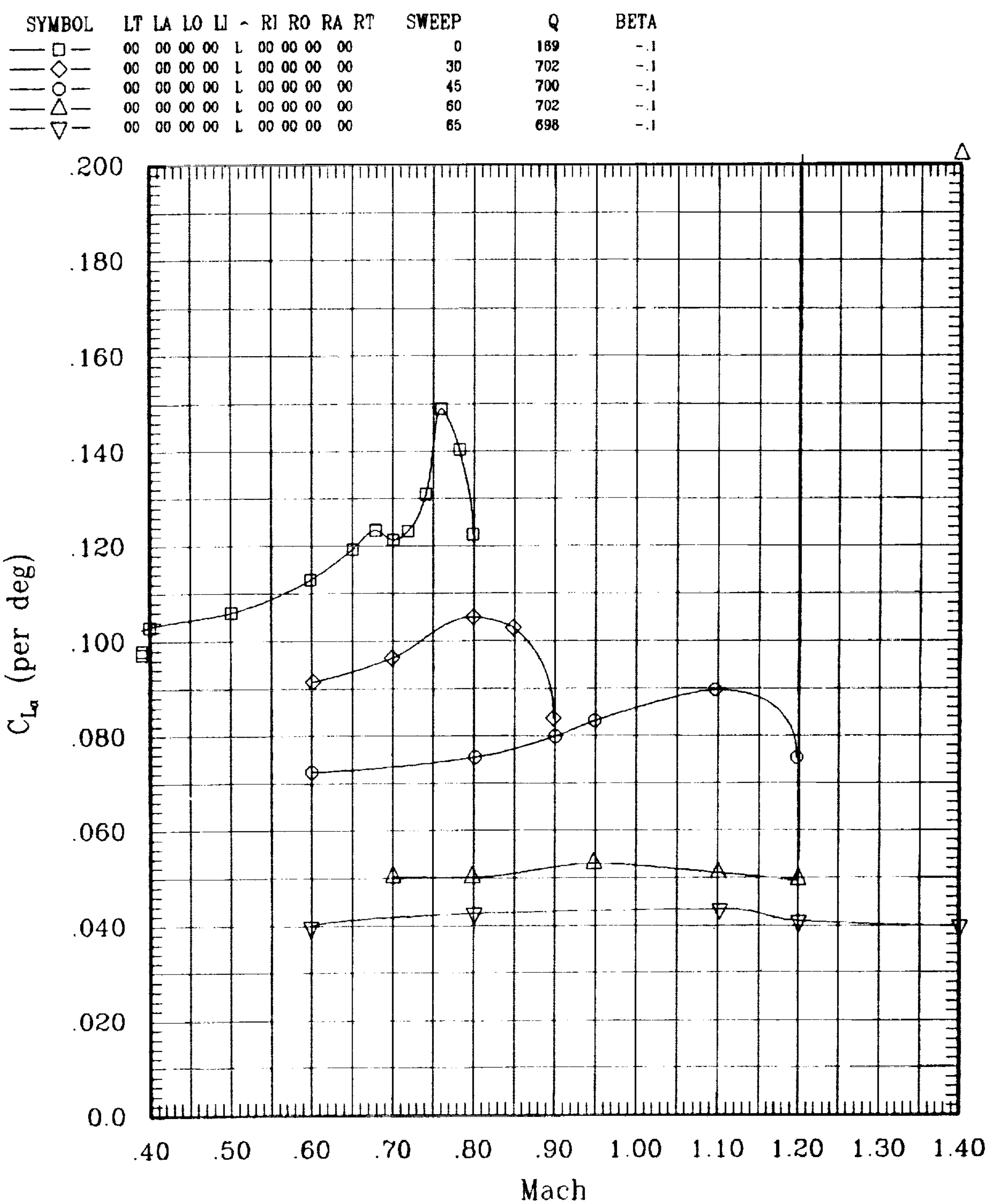

Figure 9. Summary of derived aerodynamic parameters (low pivot).

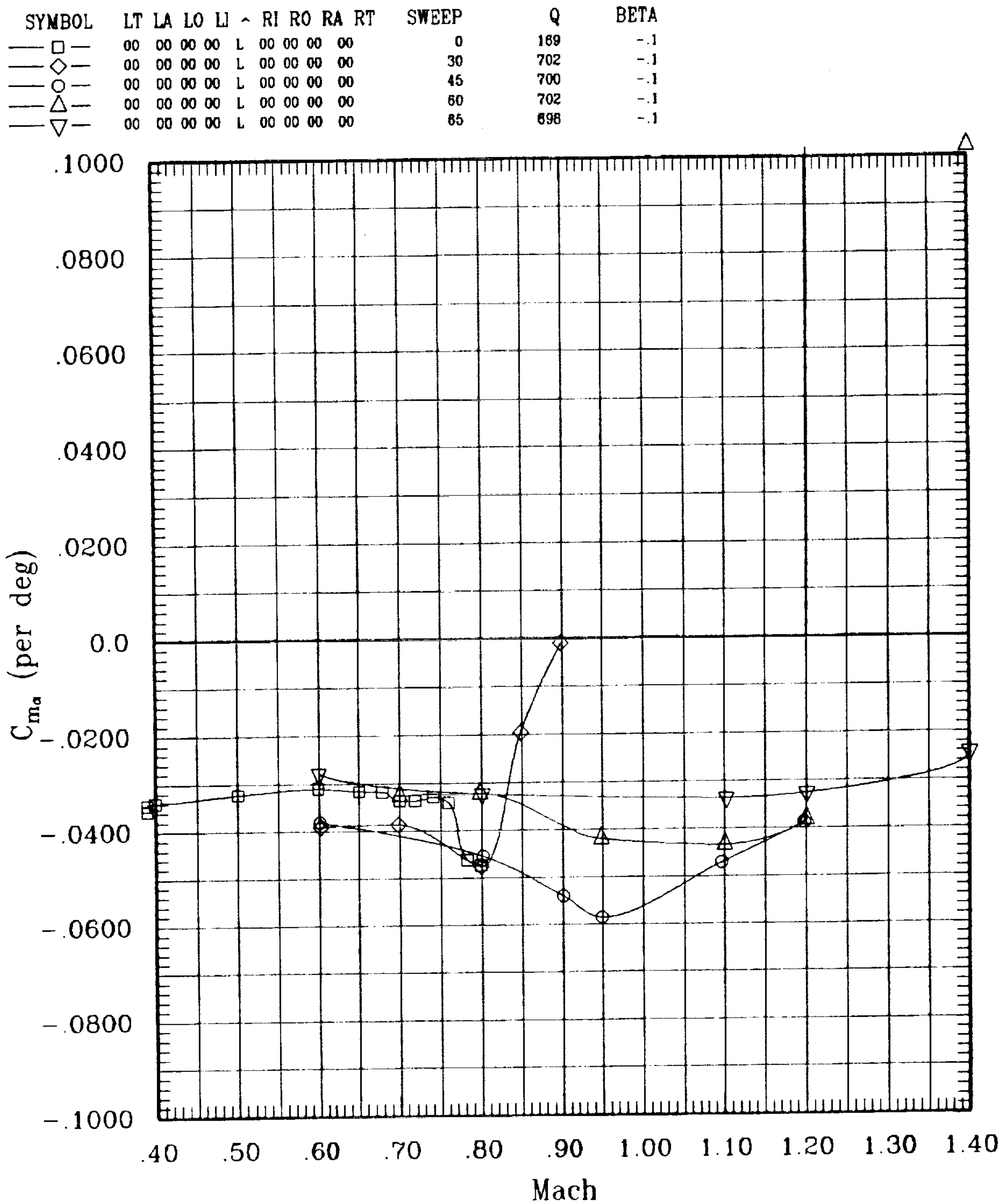

Figure 9. Summary of derived aerodynamic parameters (low pivot).

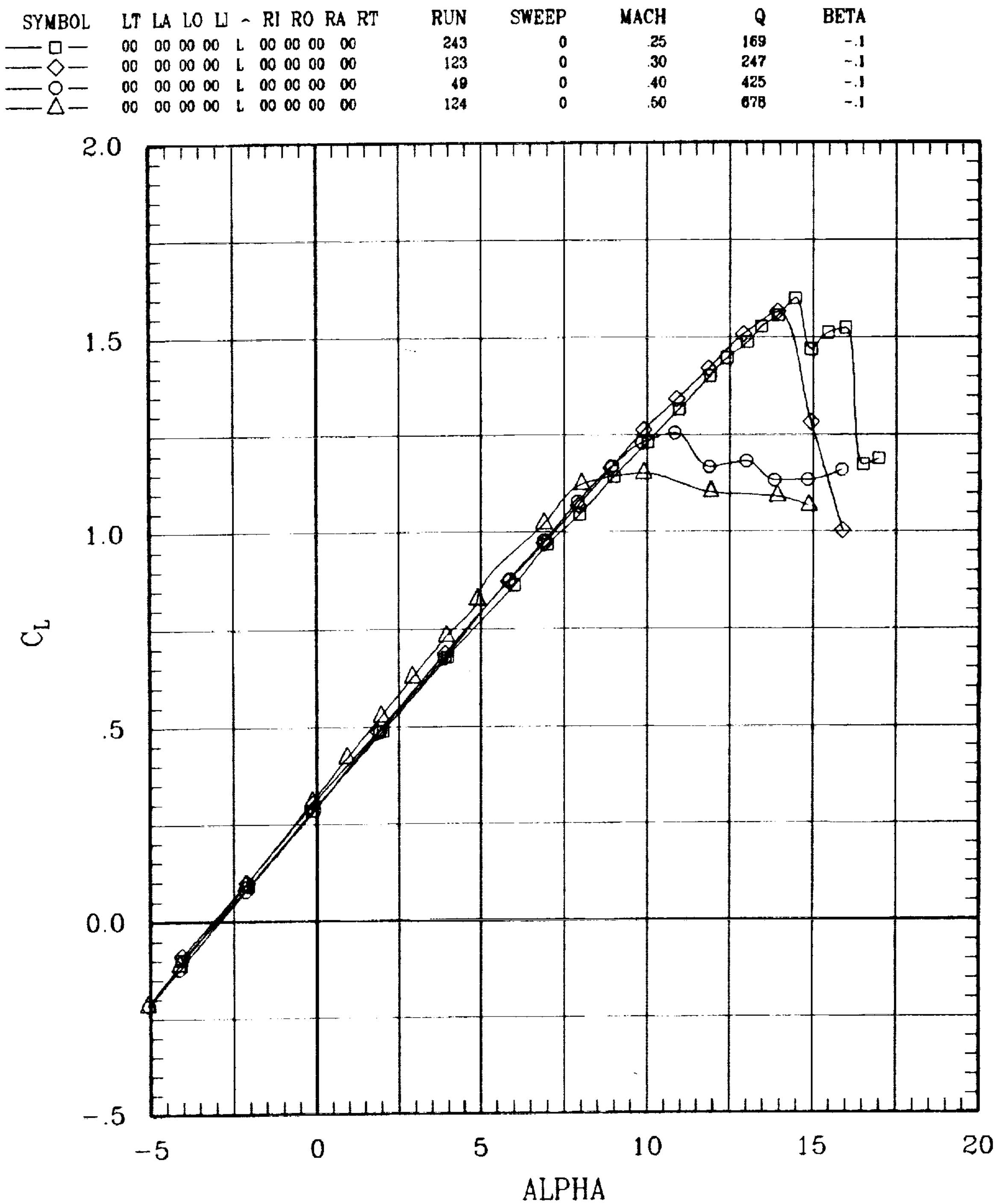

Figure 10. Effect of Mach on stall behavior (low pivot).

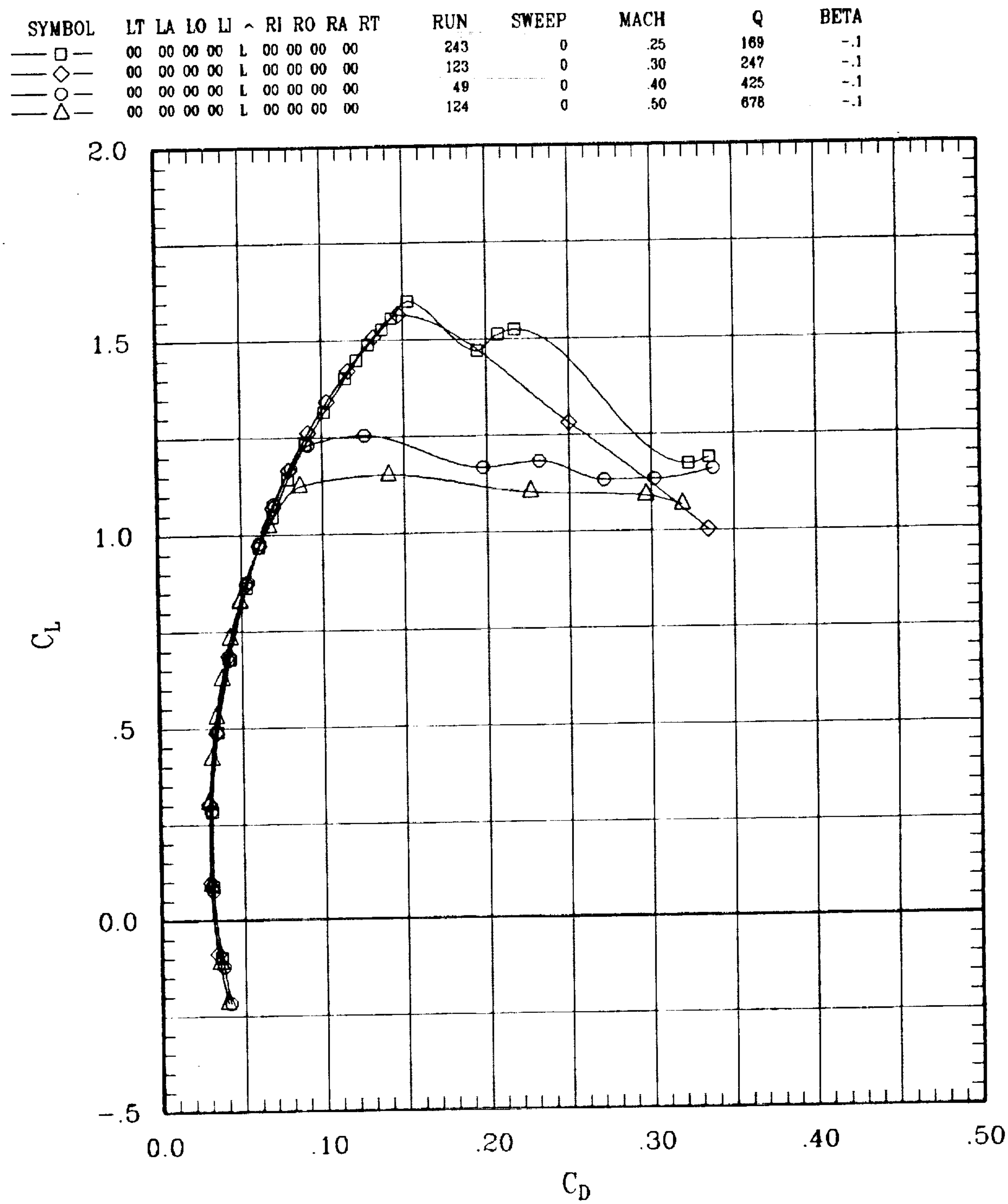

Figure 10. Effect of Mach on stall behavior (low pivot).

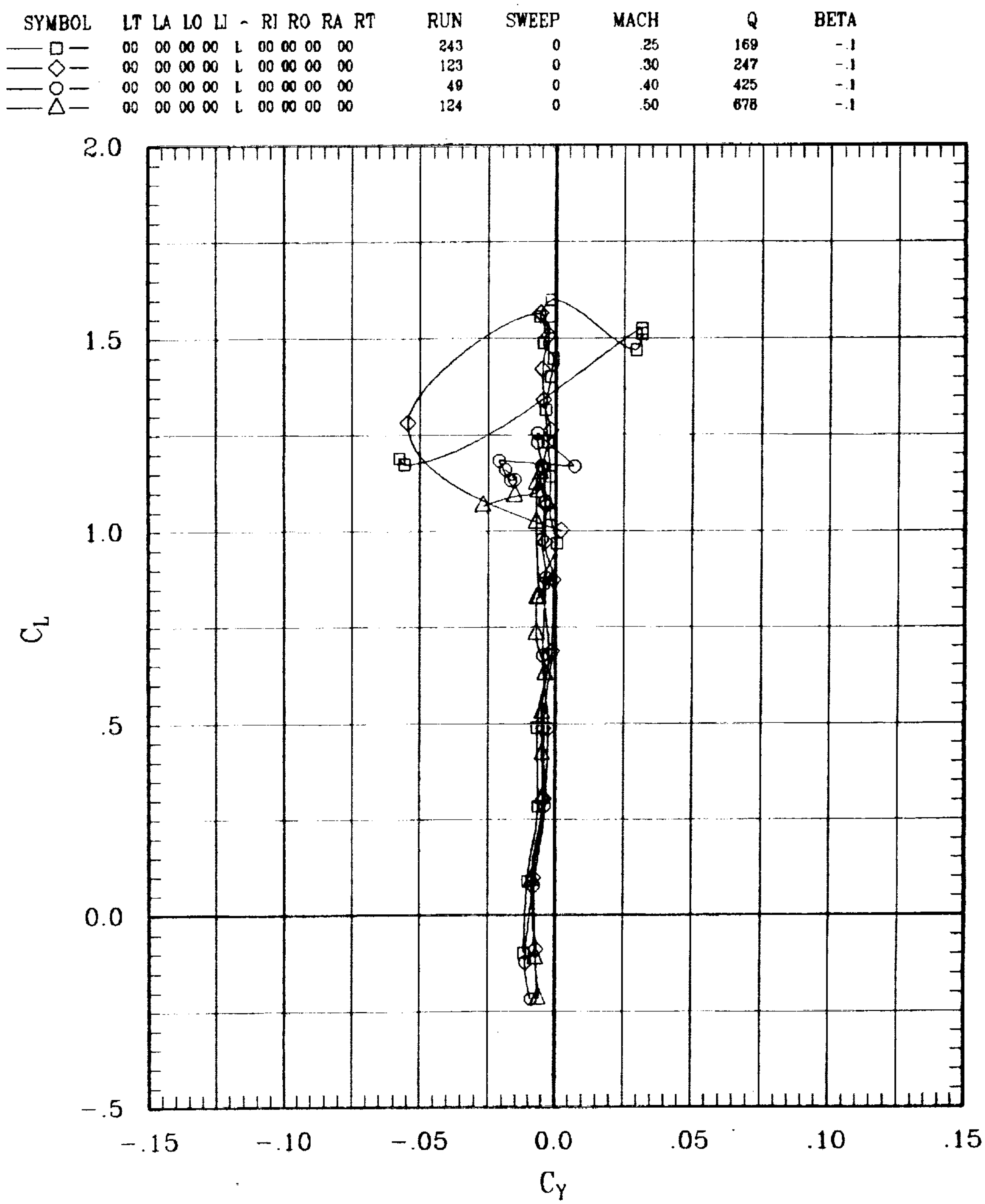

Figure 10. Effect of Mach on stall behavior (low pivot).

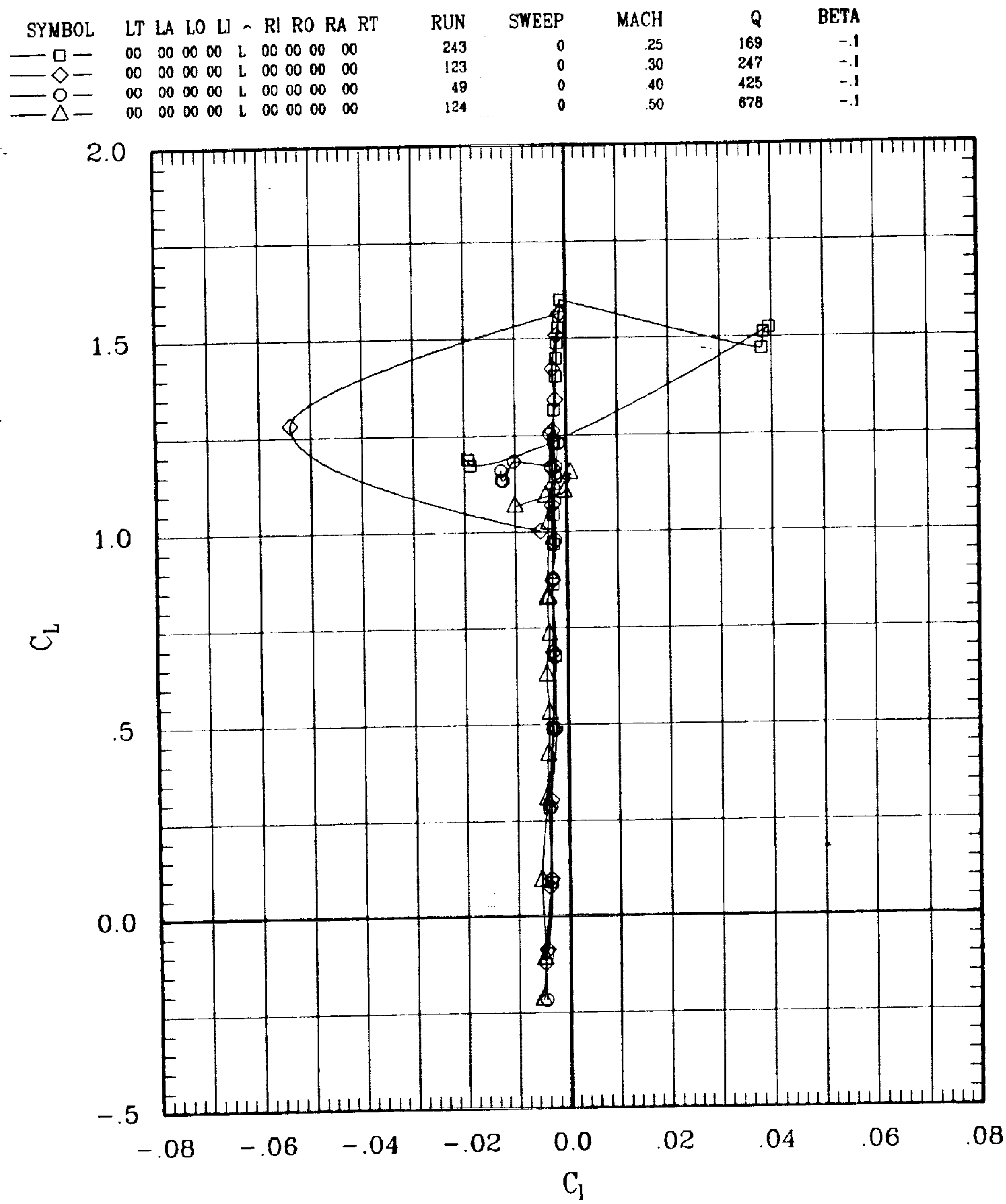

Figure 10. Effect of Mach on stall behavior (low pivot).

SYMBOL	LT	LA	LO	LI	^	RI	RO	RA	RT	RUN	SWEEP	MACH	Q	BETA
—□—	00	00	00	00	L	00	00	00	00	243	0	.25	169	-.1
—◇—	00	00	00	00	L	00	00	00	00	123	0	.30	247	-.1
—○—	00	00	00	00	L	00	00	00	00	49	0	.40	425	-.1
—△—	00	00	00	00	L	00	00	00	00	124	0	.50	678	-.1

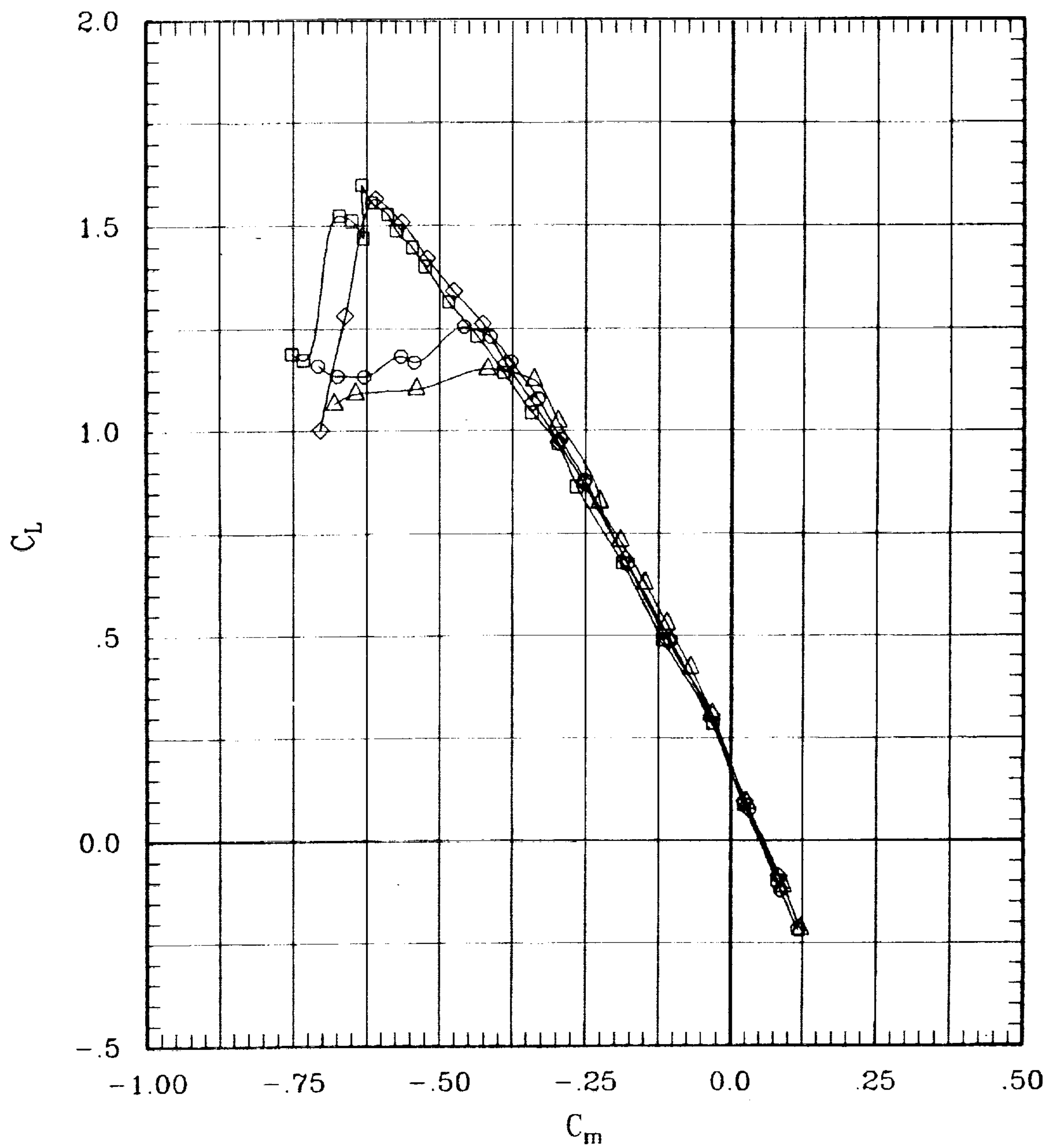

Figure 10. Effect of Mach on stall behavior (low pivot).

SYMBOL	LT LA LO LI ~ RI RO RA RT	RUN	SWEEP	MACH	Q	BETA
—□—	00 00 00 00 L 00 00 00 00	243	0	.25	169	-.1
—◇—	00 00 00 00 L 00 00 00 00	123	0	.30	247	-.1
—○—	00 00 00 00 L 00 00 00 00	49	0	.40	425	-.1
—△—	00 00 00 00 L 00 00 00 00	124	0	.50	678	-.1

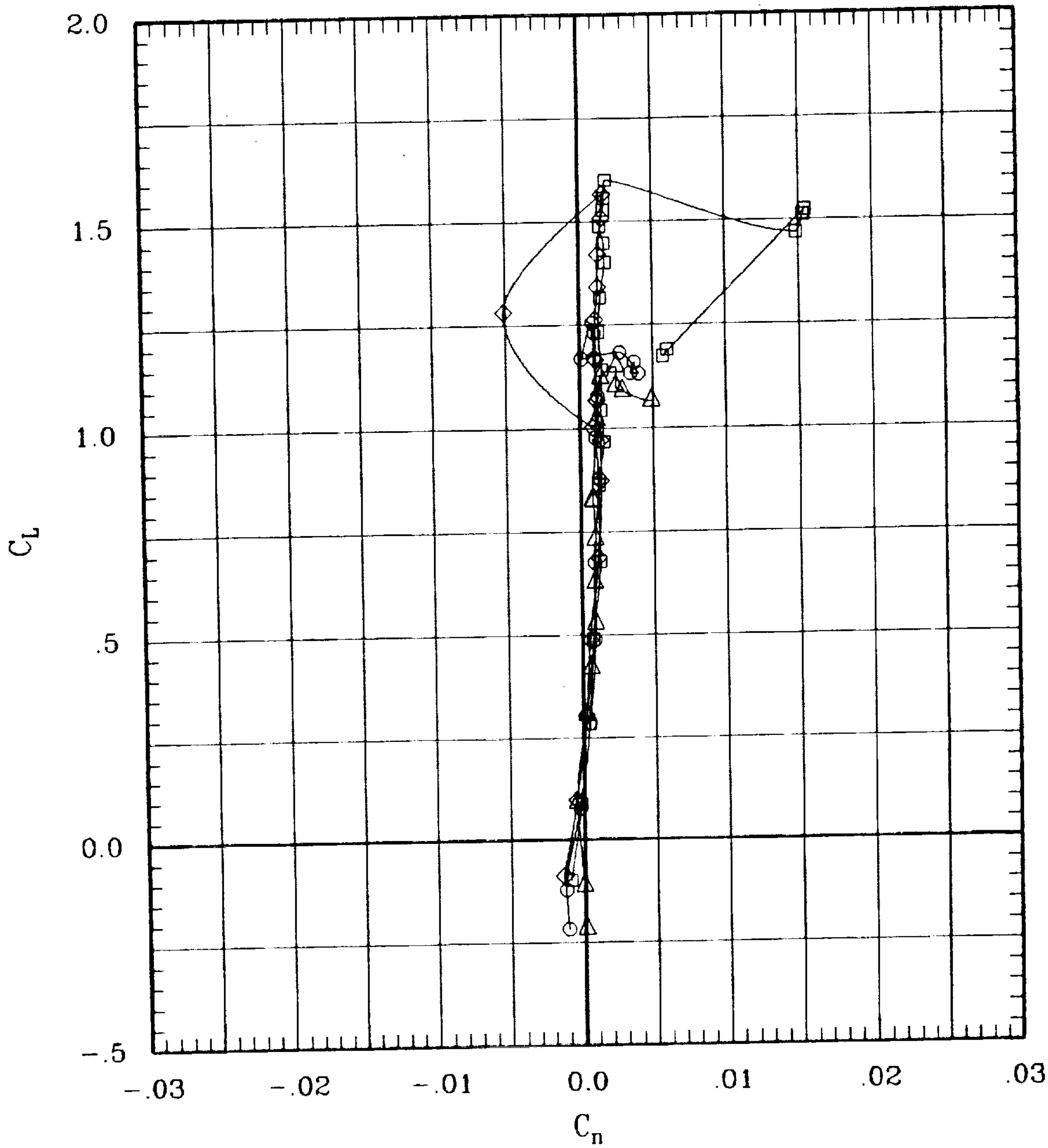

Figure 10. Effect of Mach on stall behavior (low pivot).

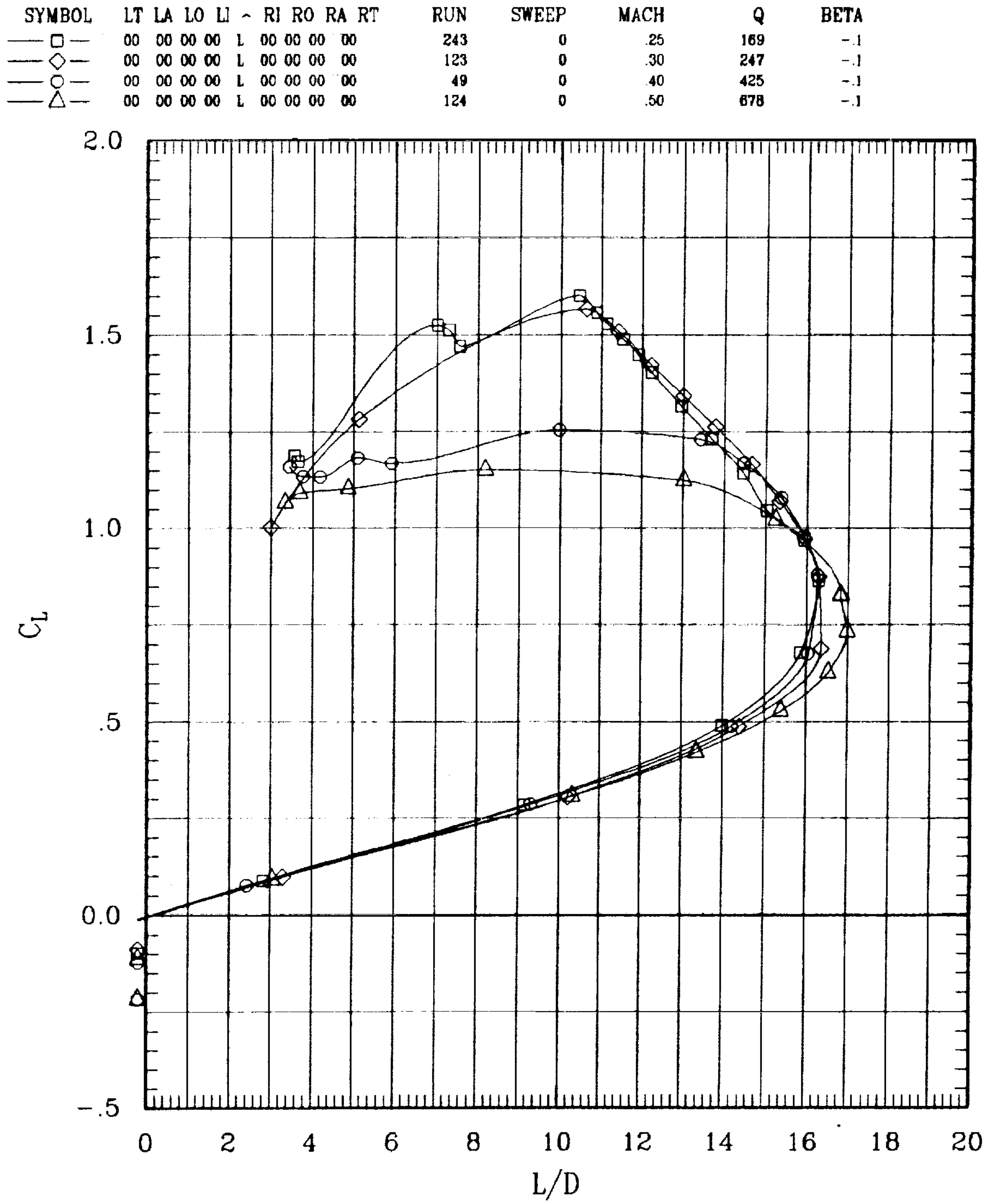

Figure 10. Effect of Mach on stall behavior (low pivot).

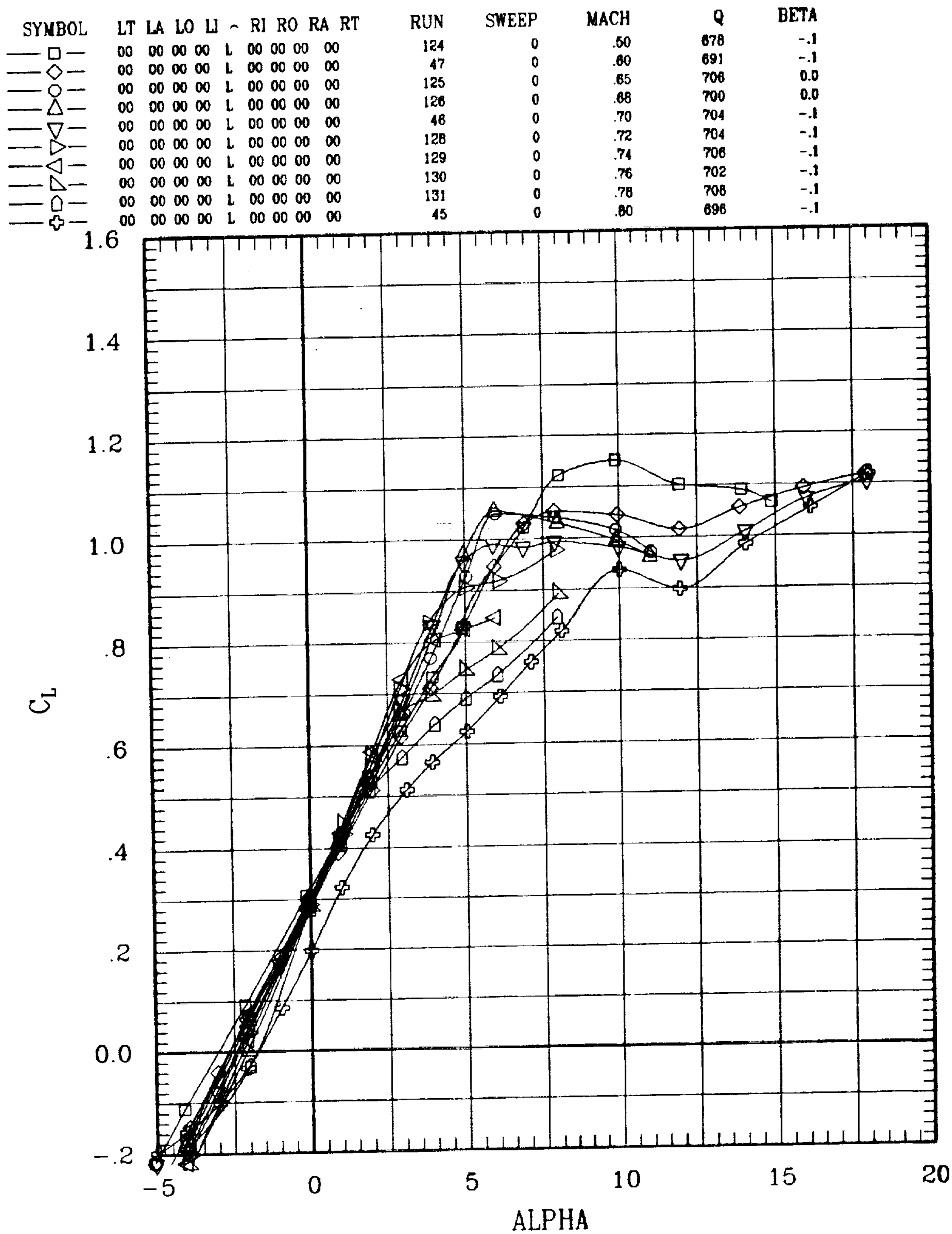

Figure 11. Transonic aerodynamic characteristics for sweep = 0 deg.

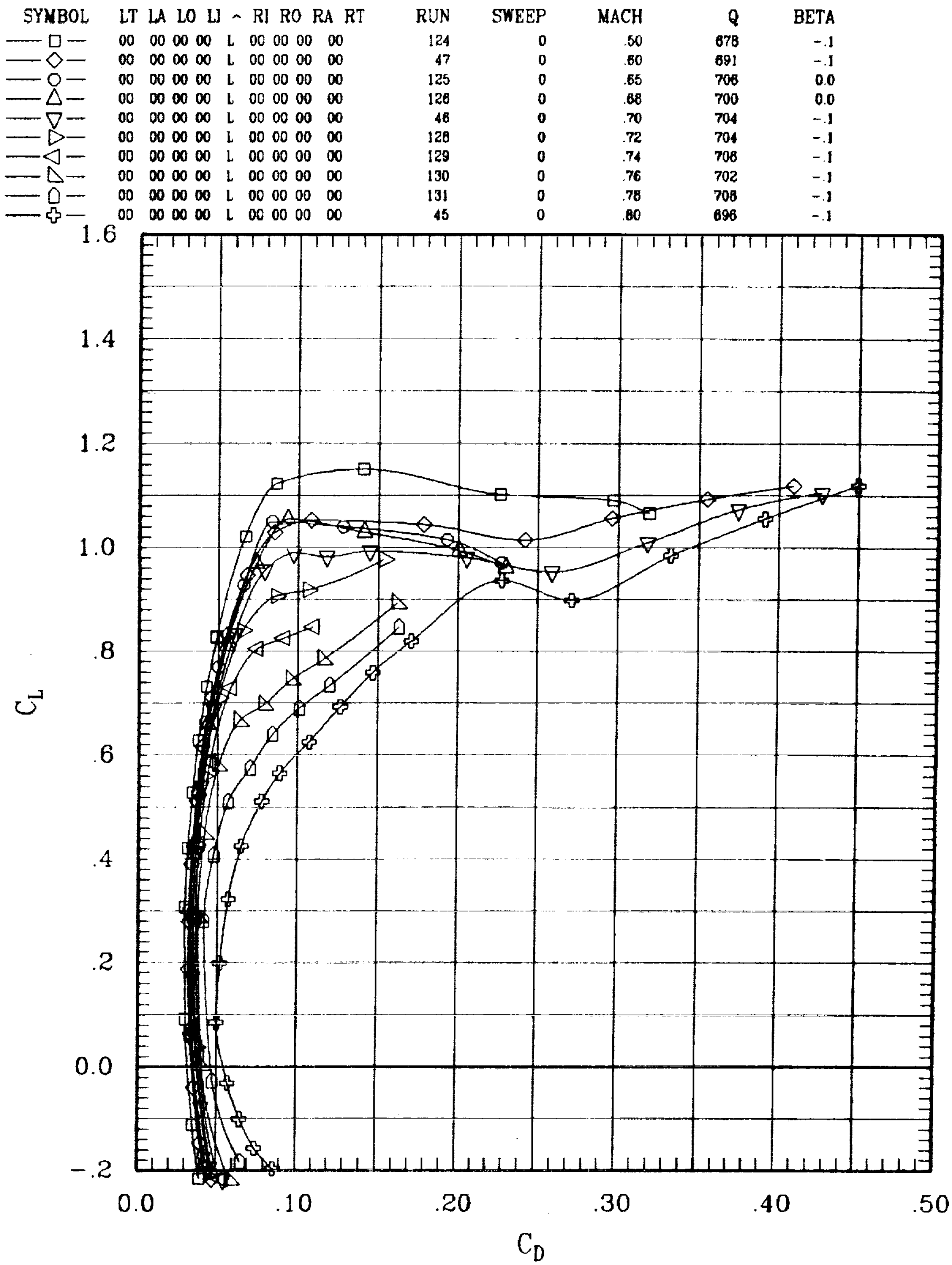

Figure 11. Transonic aerodynamic characteristics for sweep = 0 deg.

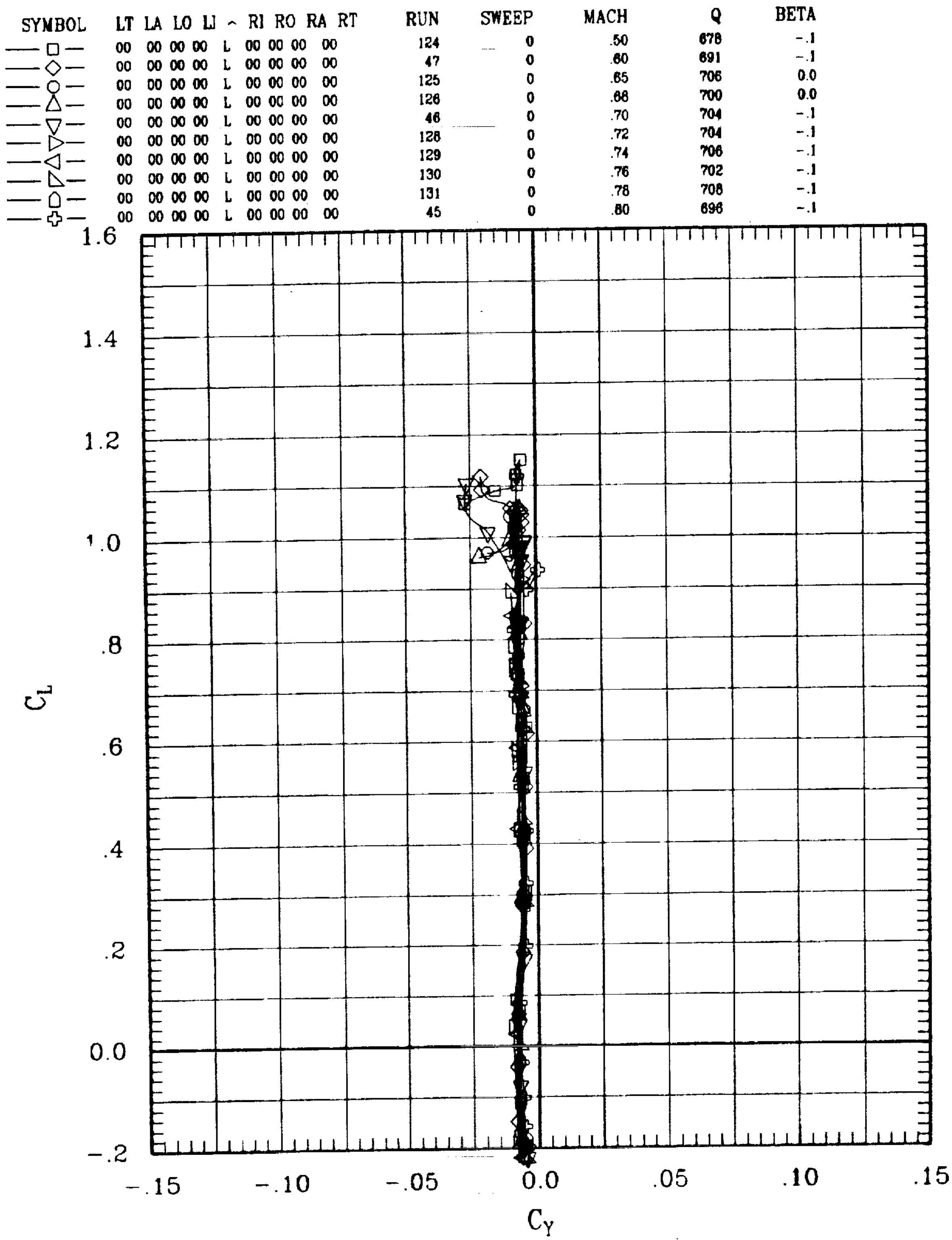

Figure 11. Transonic aerodynamic characteristics for sweep = 0 deg.

SYMBOL	LT	LA	LO	LI	~	RI	RO	RA	RT	RUN	SWEEP	MACH	Q	BETA
□	00	00	00	00	L	00	00	00	00	124	0	.60	678	-.1
◇	00	00	00	00	L	00	00	00	00	47	0	.60	691	-.1
○	00	00	00	00	L	00	00	00	00	125	0	.65	706	0.0
△	00	00	00	00	L	00	00	00	00	126	0	.68	700	0.0
▽	00	00	00	00	L	00	00	00	00	46	0	.70	704	-.1
▷	00	00	00	00	L	00	00	00	00	128	0	.72	704	-.1
◁	00	00	00	00	L	00	00	00	00	129	0	.74	706	-.1
◺	00	00	00	00	L	00	00	00	00	130	0	.76	702	-.1
⌂	00	00	00	00	L	00	00	00	00	131	0	.78	708	-.1
✢	00	00	00	00	L	00	00	00	00	45	0	.80	696	-.1

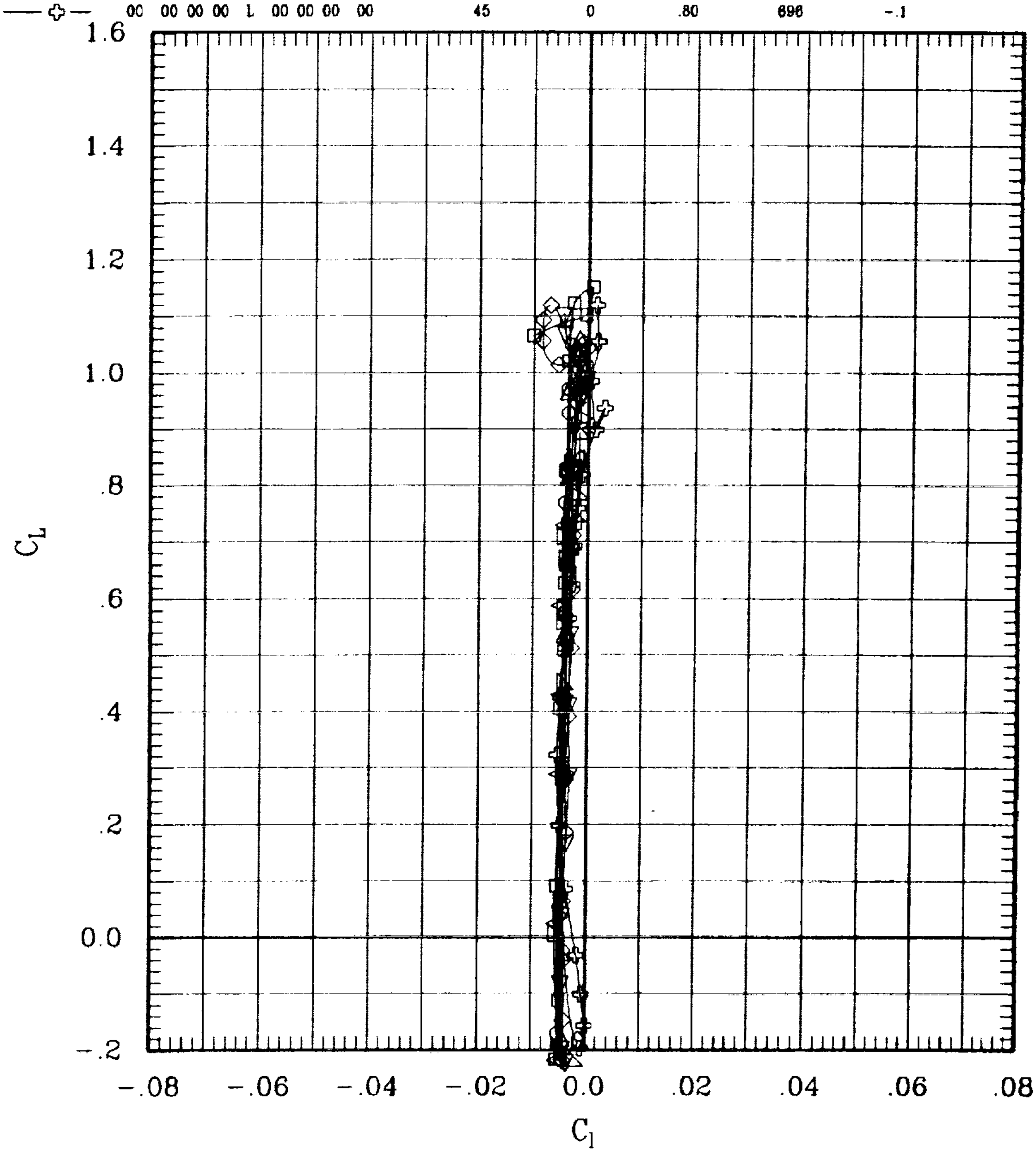

Figure 11. Transonic aerodynamic characteristics for sweep = 0 deg.

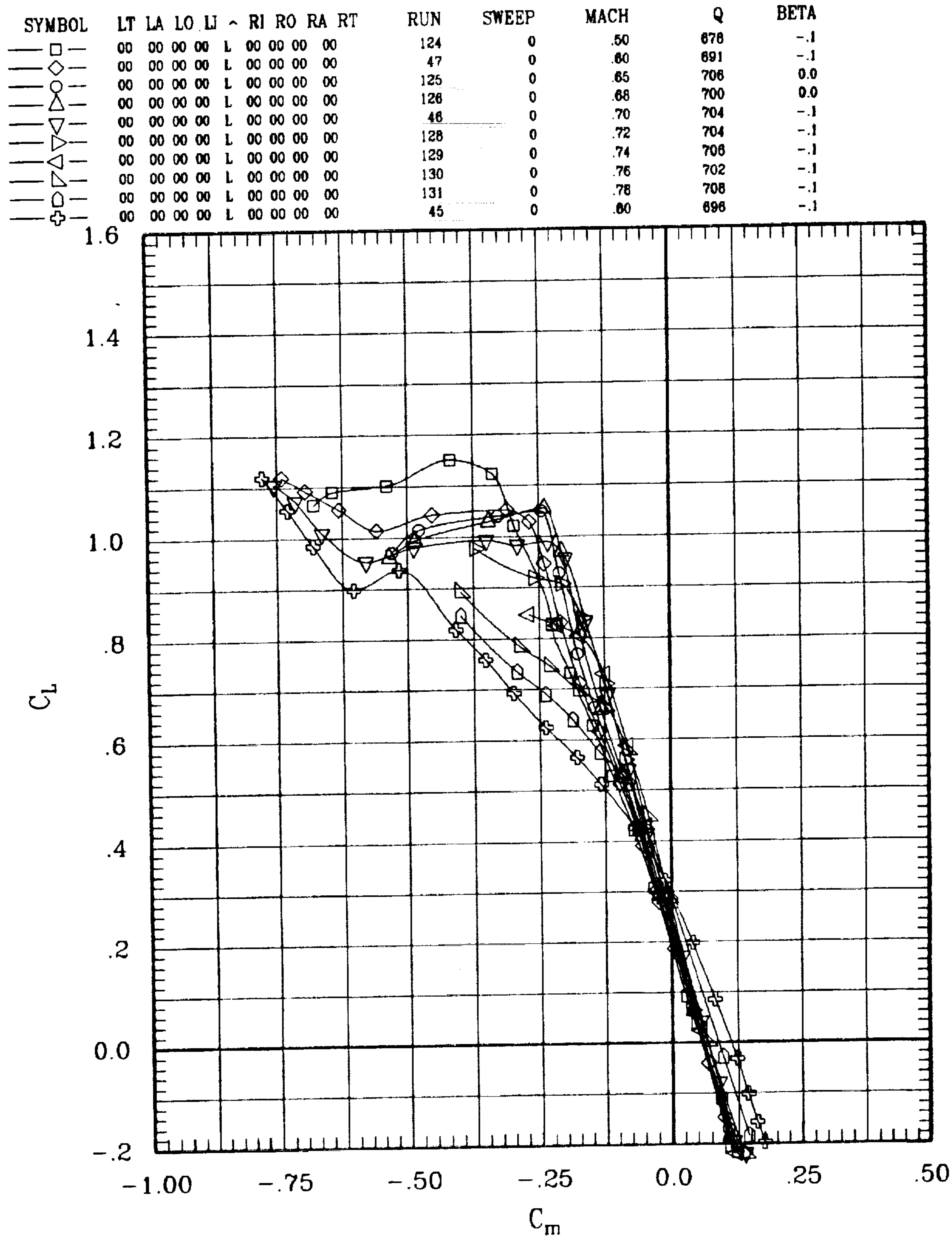

Figure 11. Transonic aerodynamic characteristics for sweep = 0 deg.

SYMBOL	LT	LA	LO	LI	⌢	RI	RO	RA	RT	RUN	SWEEP	MACH	Q	BETA
□	00	00	00	00	L	00	00	00	00	124	0	.50	678	-.1
◇	00	00	00	00	L	00	00	00	00	47	0	.60	691	-.1
○	00	00	00	00	L	00	00	00	00	125	0	.65	706	0.0
△	00	00	00	00	L	00	00	00	00	126	0	.68	700	0.0
▽	00	00	00	00	L	00	00	00	00	48	0	.70	704	-.1
▷	00	00	00	00	L	00	00	00	00	128	0	.72	704	-.1
◁	00	00	00	00	L	00	00	00	00	129	0	.74	706	-.1
◺	00	00	00	00	L	00	00	00	00	130	0	.76	702	-.1
⌂	00	00	00	00	L	00	00	00	00	131	0	.78	708	-.1
✚	00	00	00	00	L	00	00	00	00	45	0	.80	696	-.1

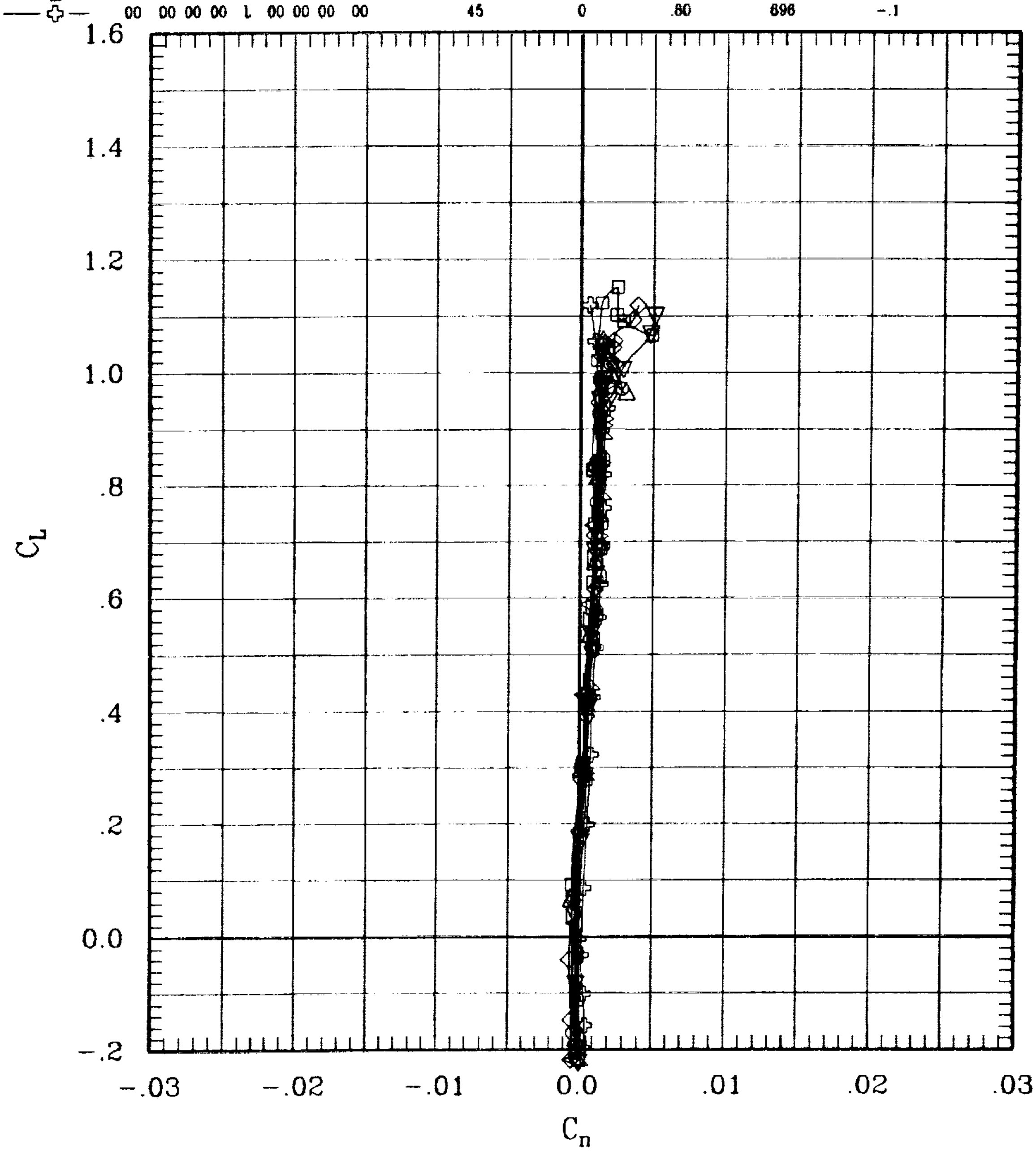

Figure 11. Transonic aerodynamic characteristics for sweep = 0 deg.

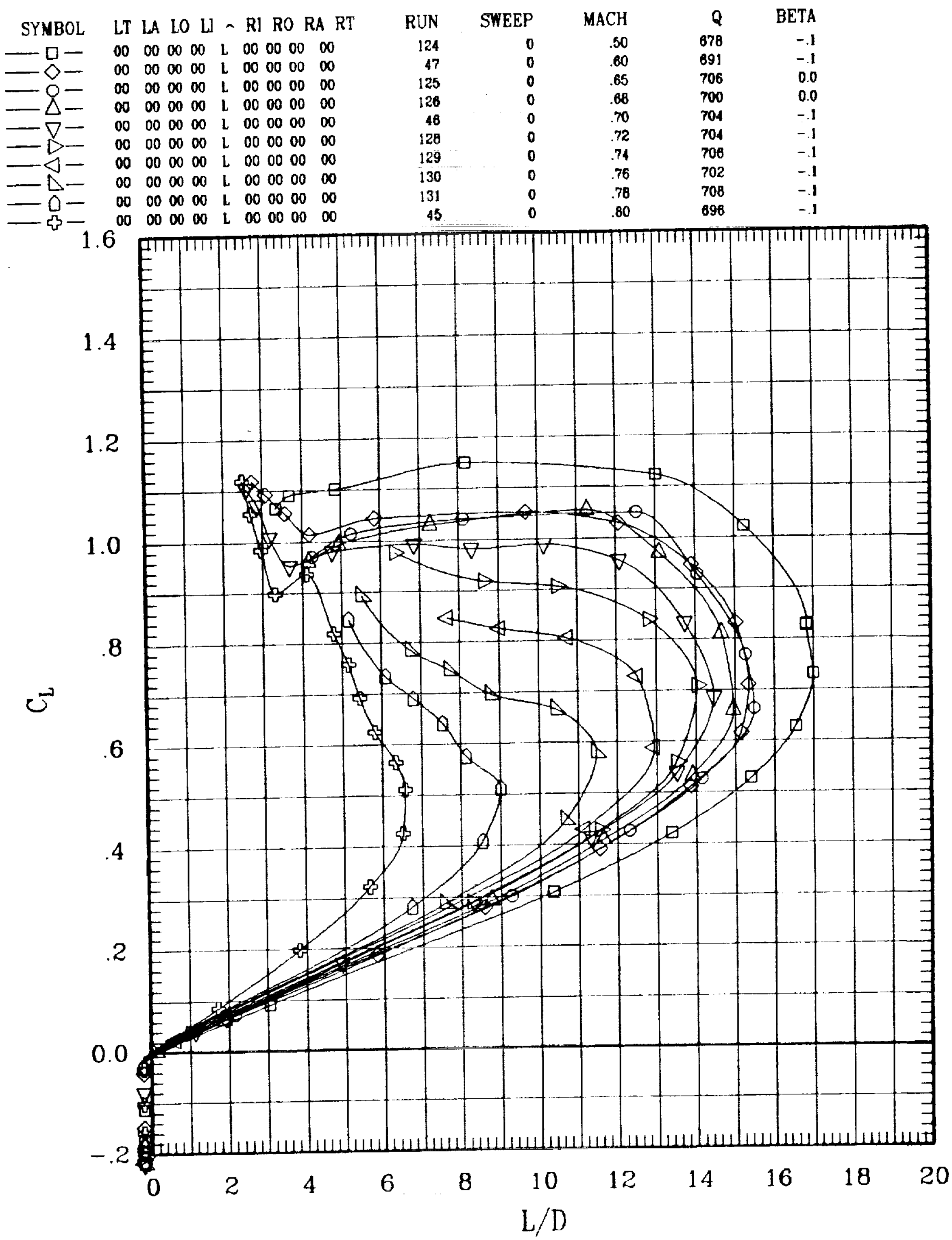

Figure 11. Transonic aerodynamic characteristics for sweep = 0 deg.

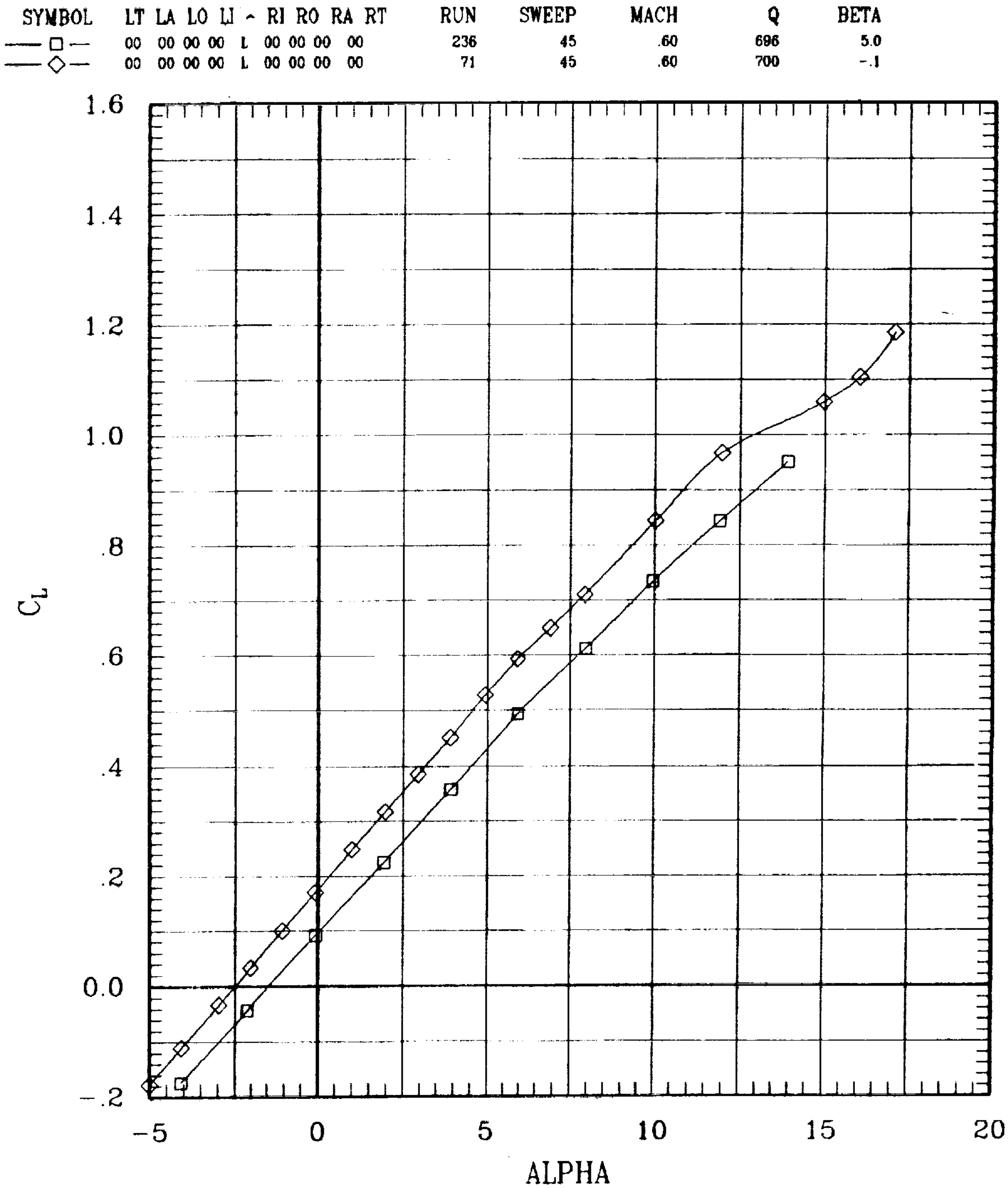

Figure 12. Effect of sideslip for sweep = 45 deg.

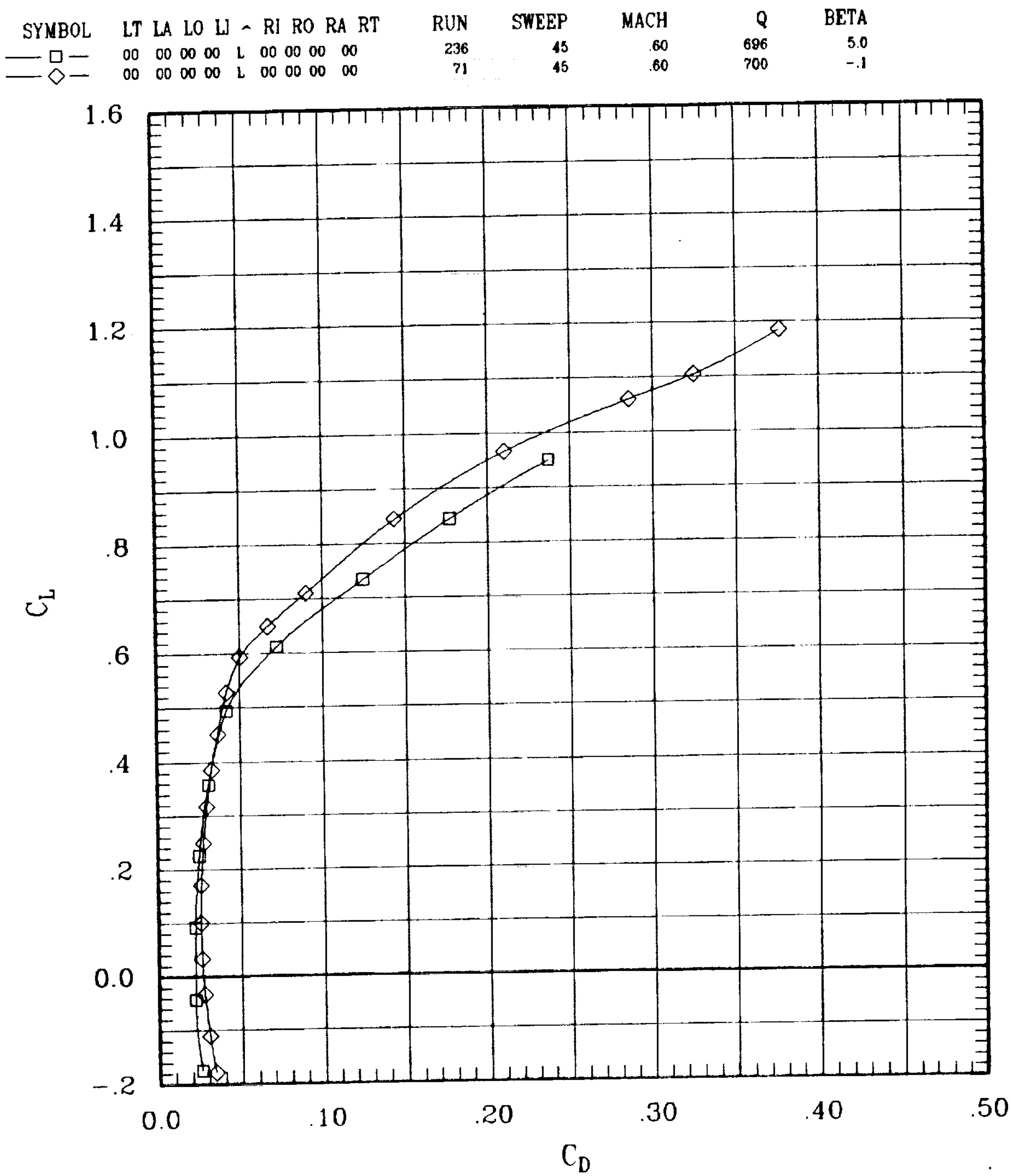

Figure 12. Effect of sideslip for sweep = 45 deg.

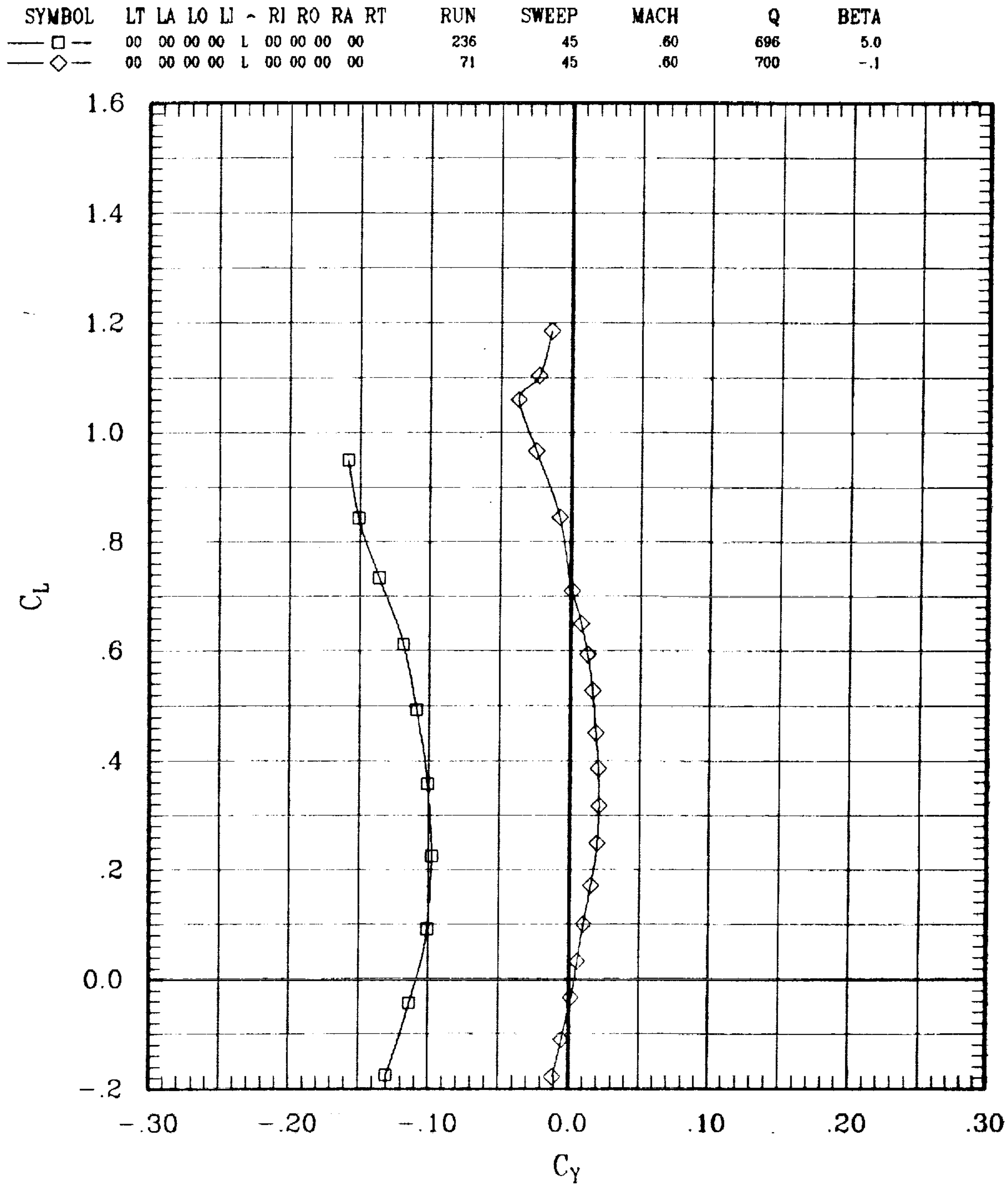

Figure 12. Effect of sideslip for sweep = 45 deg.

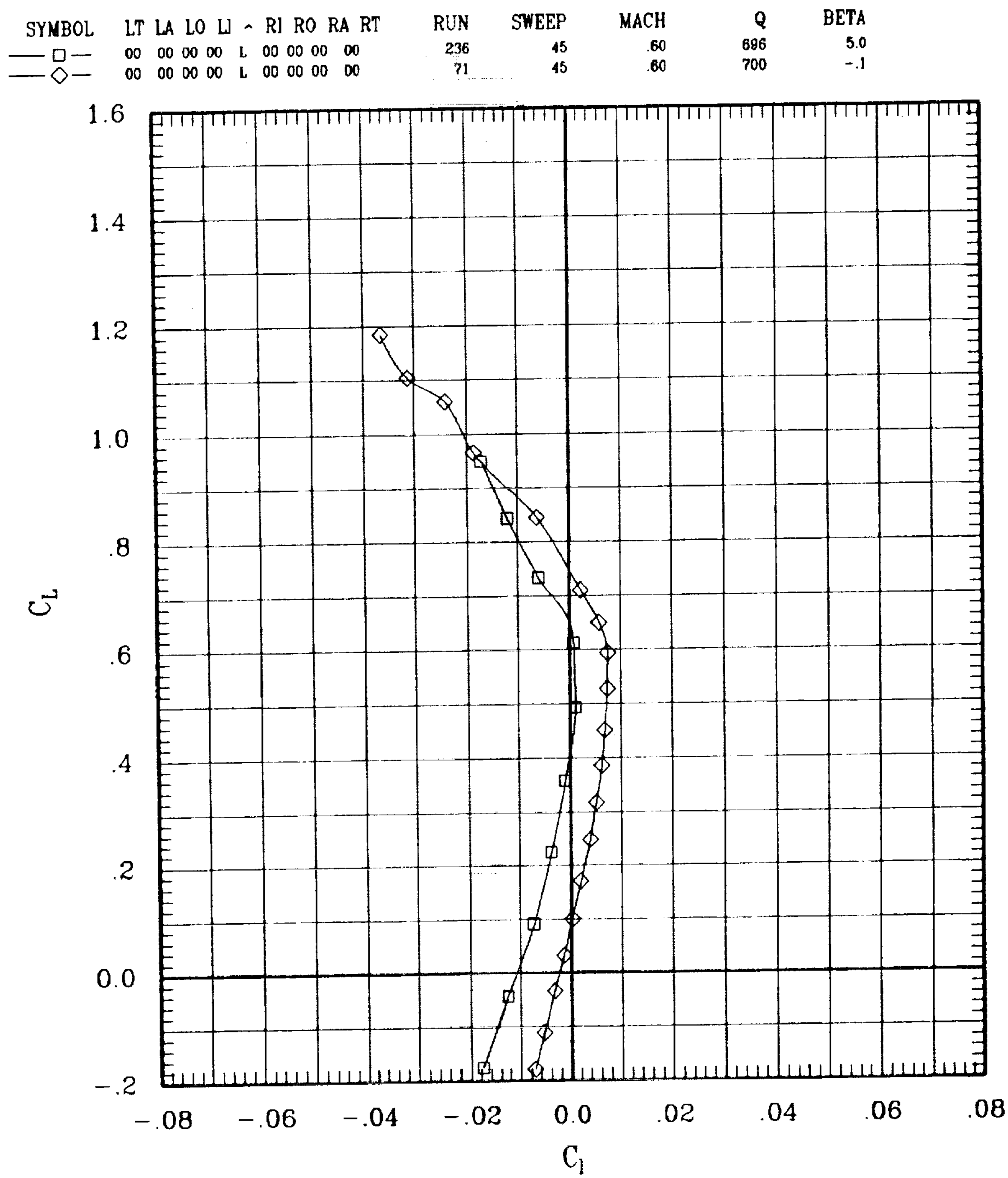

Figure 12. Effect of sideslip for sweep = 45 deg.

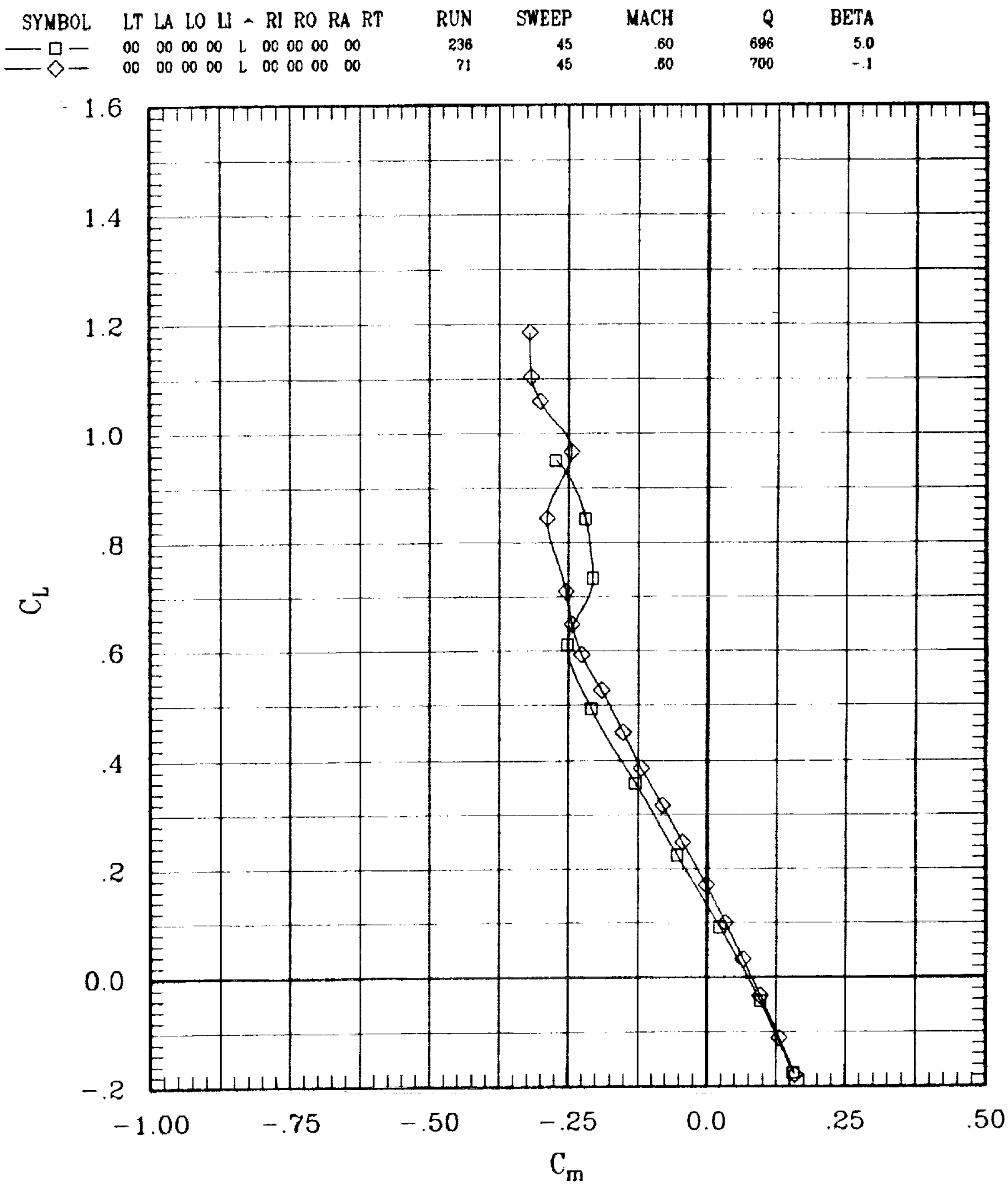

Figure 12. Effect of sideslip for sweep = 45 deg.

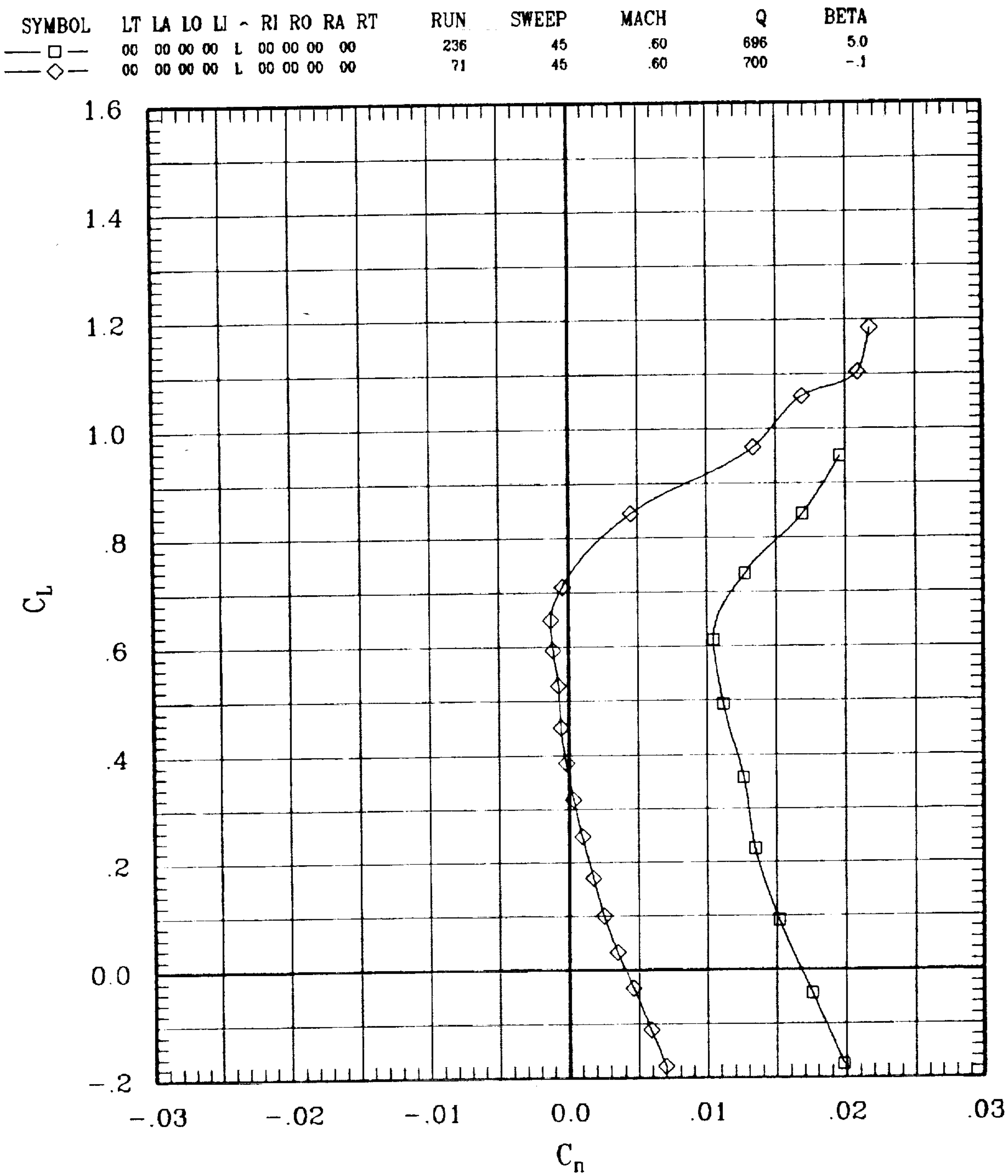

Figure 12. Effect of sideslip for sweep = 45 deg.

SYMBOL	LT LA LO LI - RI RO RA RT	RUN	SWEEP	MACH	Q	BETA
—□—	00 00 00 00 L 00 00 00 00	236	45	.60	696	5.0
—◇—	00 00 00 00 L 00 00 00 00	71	45	.60	700	-.1

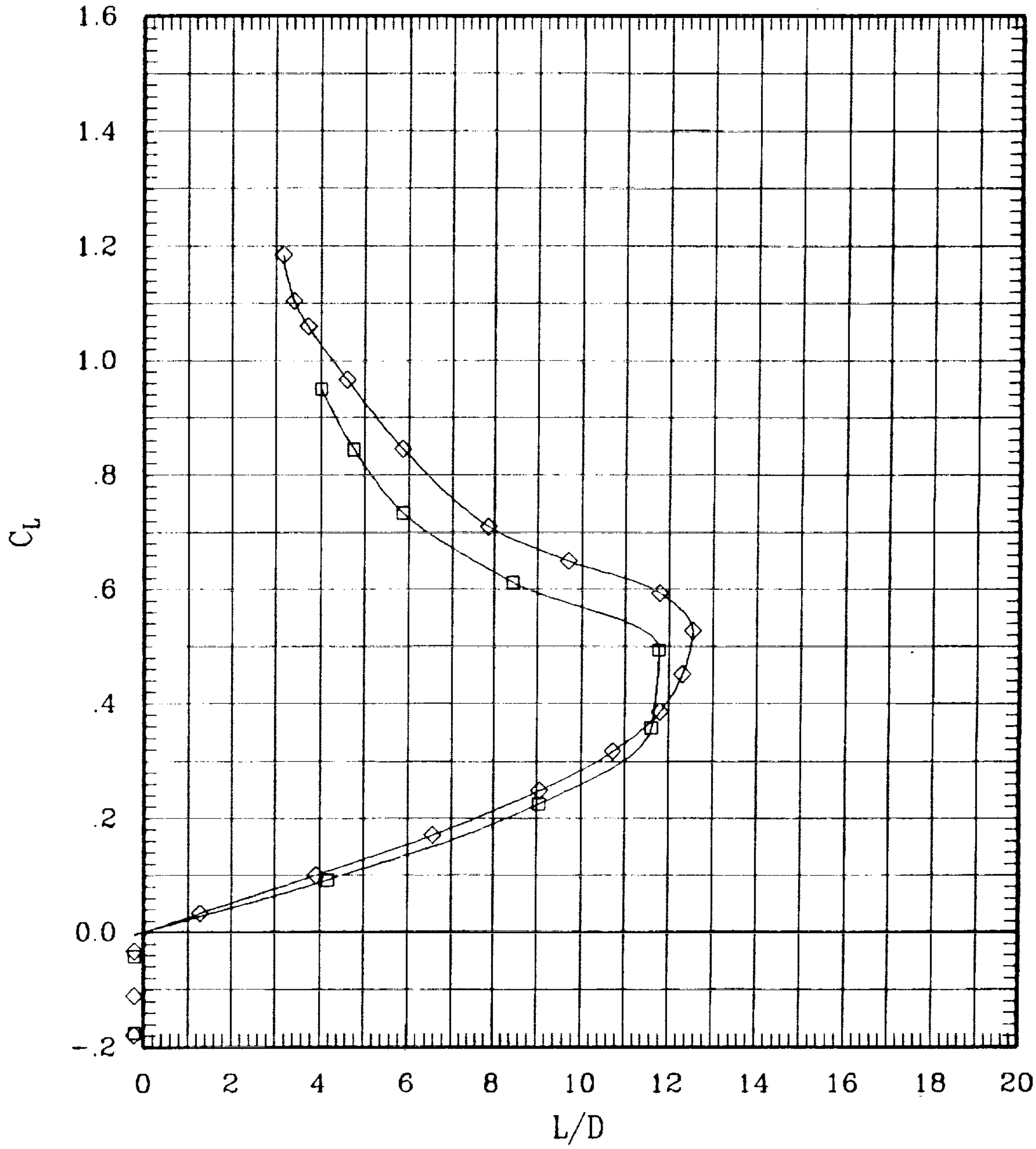

Figure 12. Effect of sideslip for sweep = 45 deg.

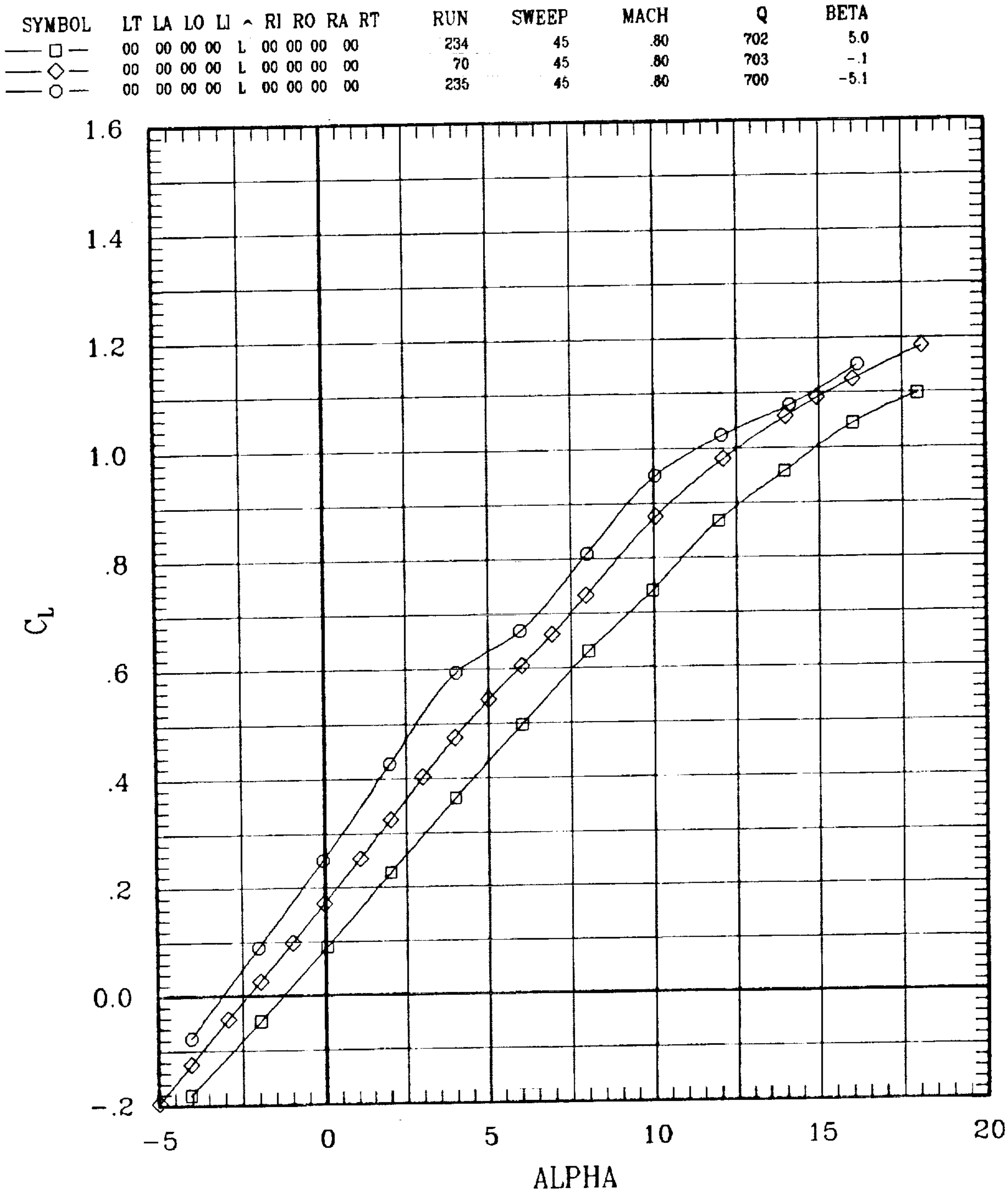

Figure 12. Effect of sideslip for sweep = 45 deg.

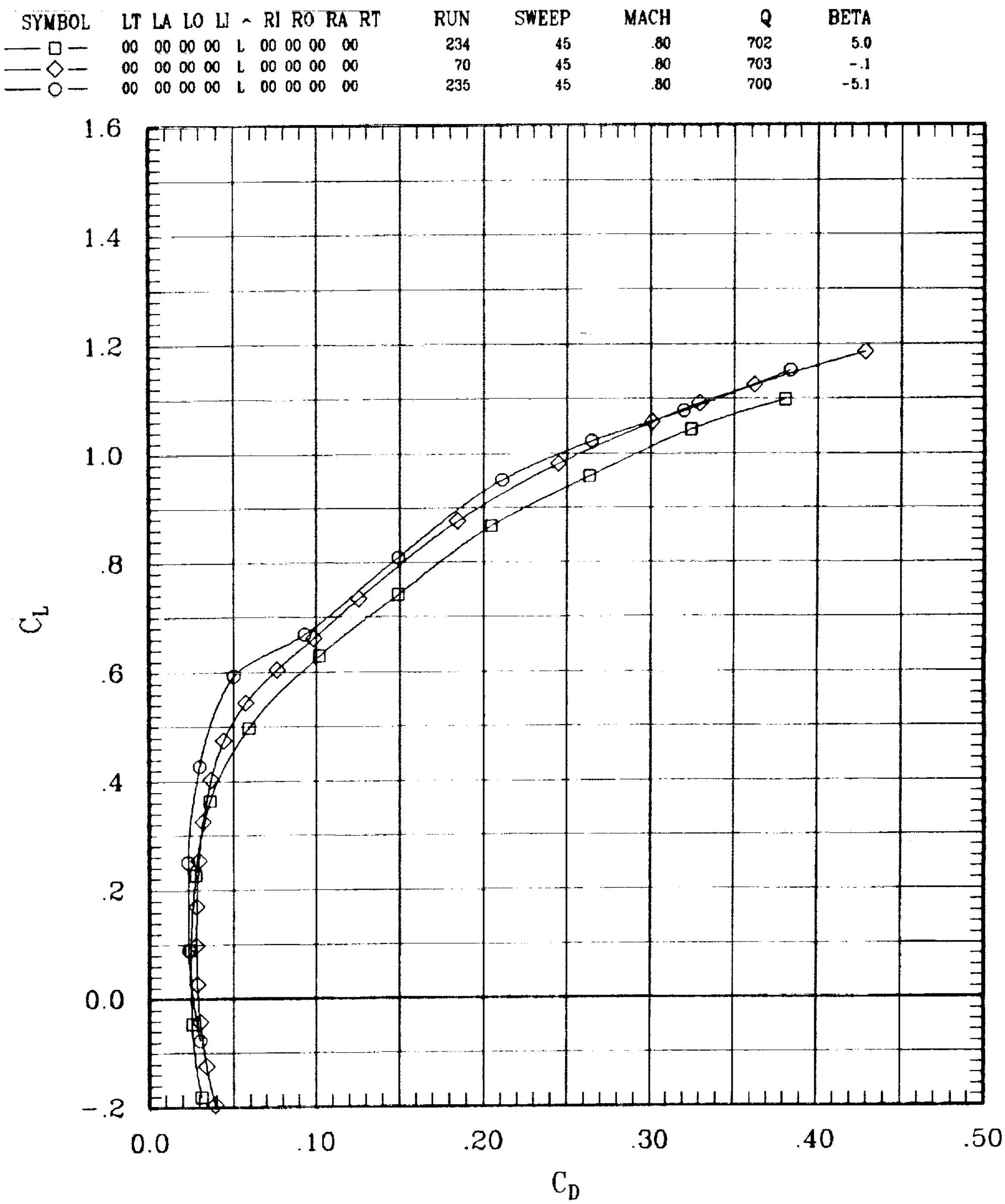

Figure 12. Effect of sideslip for sweep = 45 deg.

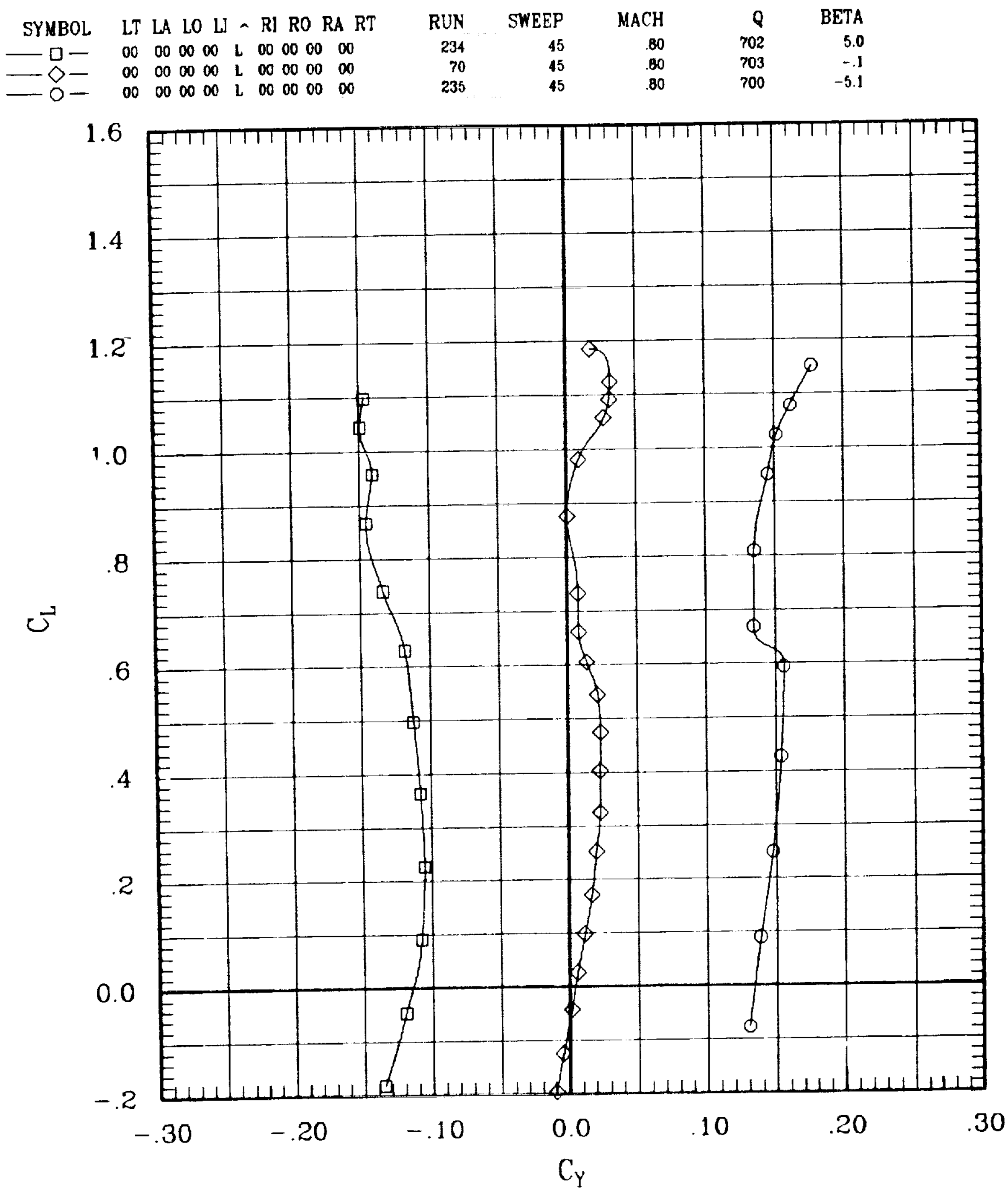

Figure 12. Effect of sideslip for sweep = 45 deg.

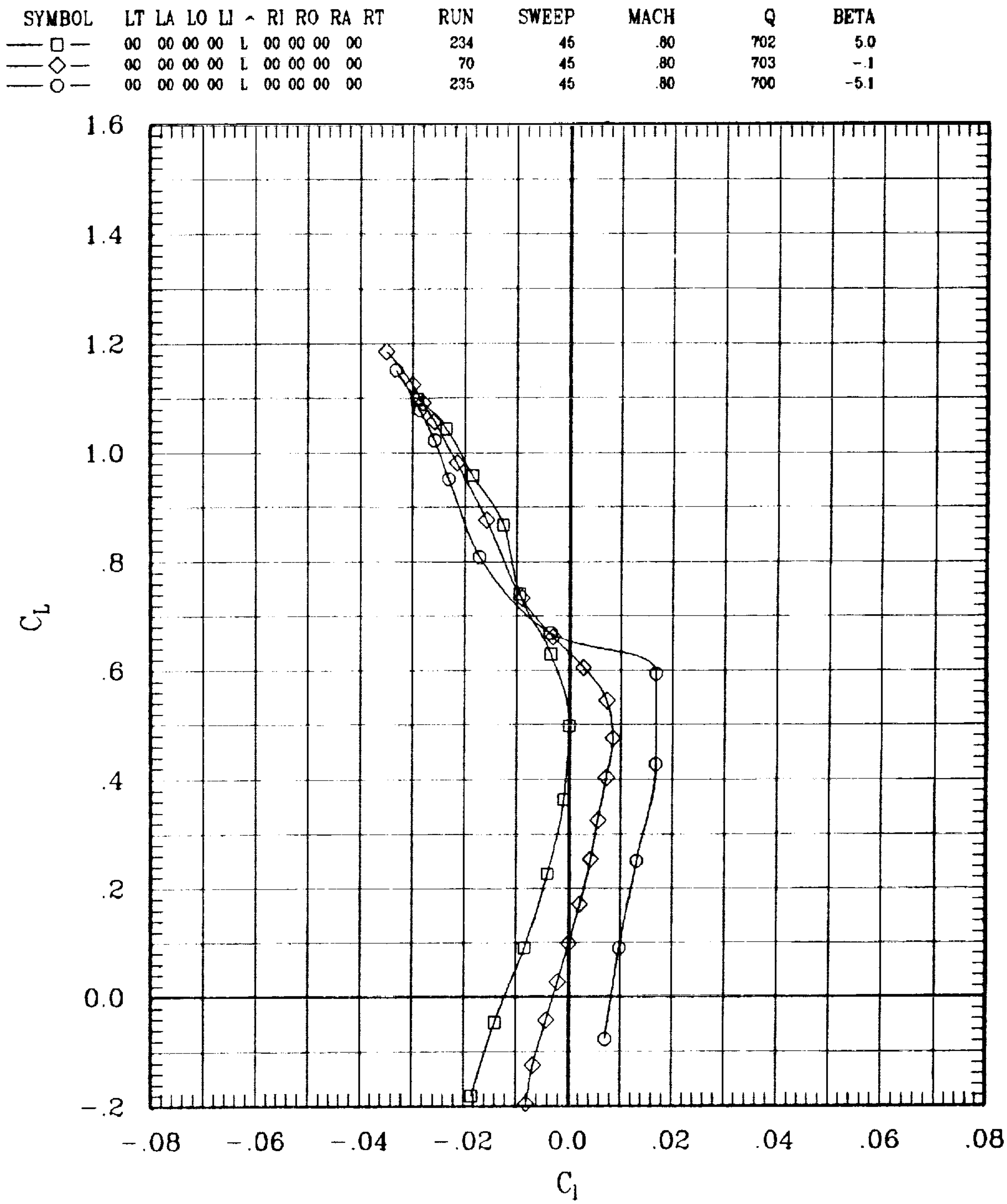

Figure 12. Effect of sideslip for sweep = 45 deg.

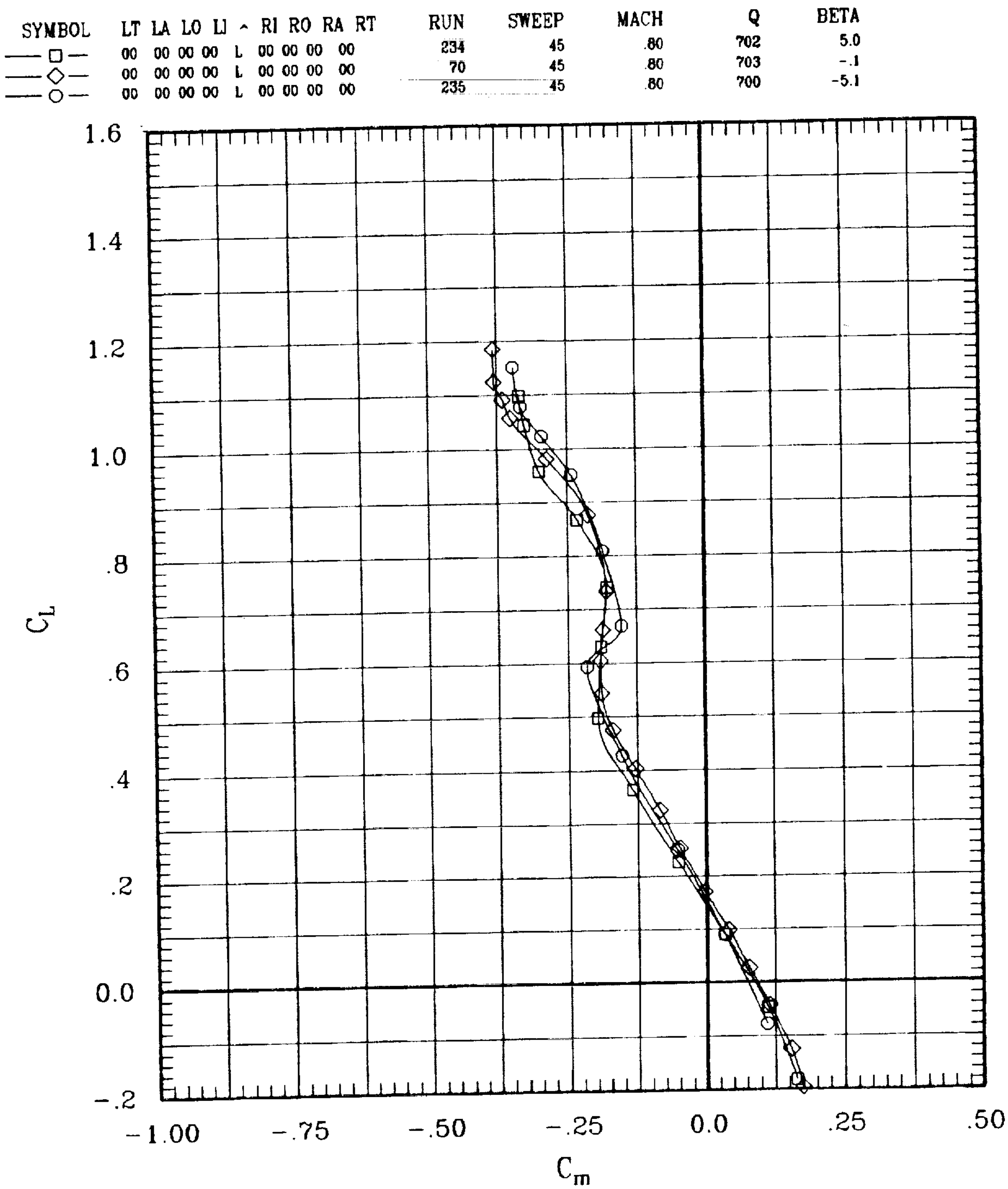

Figure 12. Effect of sideslip for sweep = 45 deg.

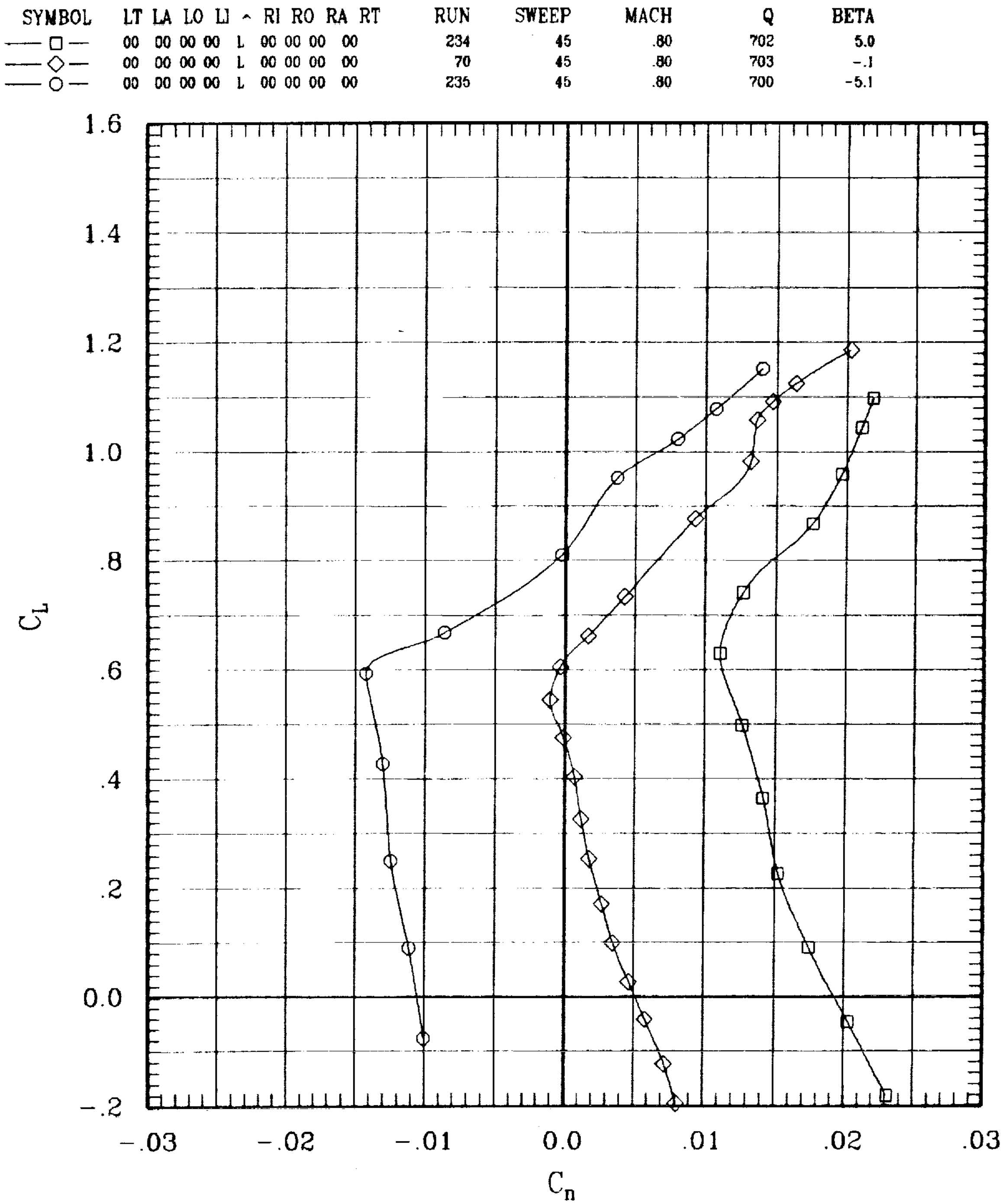

Figure 12. Effect of sideslip for sweep = 45 deg.

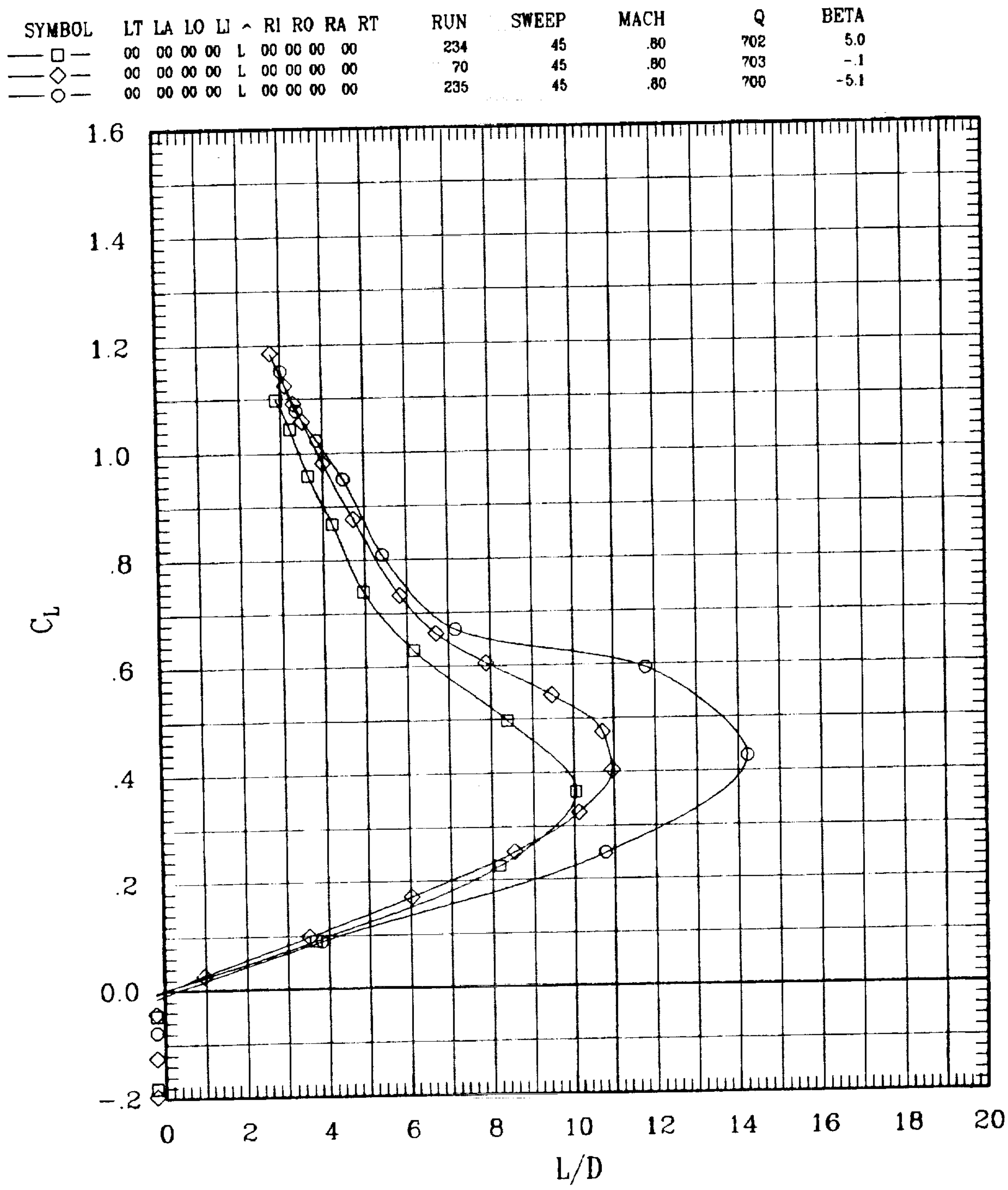

Figure 12. Effect of sideslip for sweep = 45 deg.

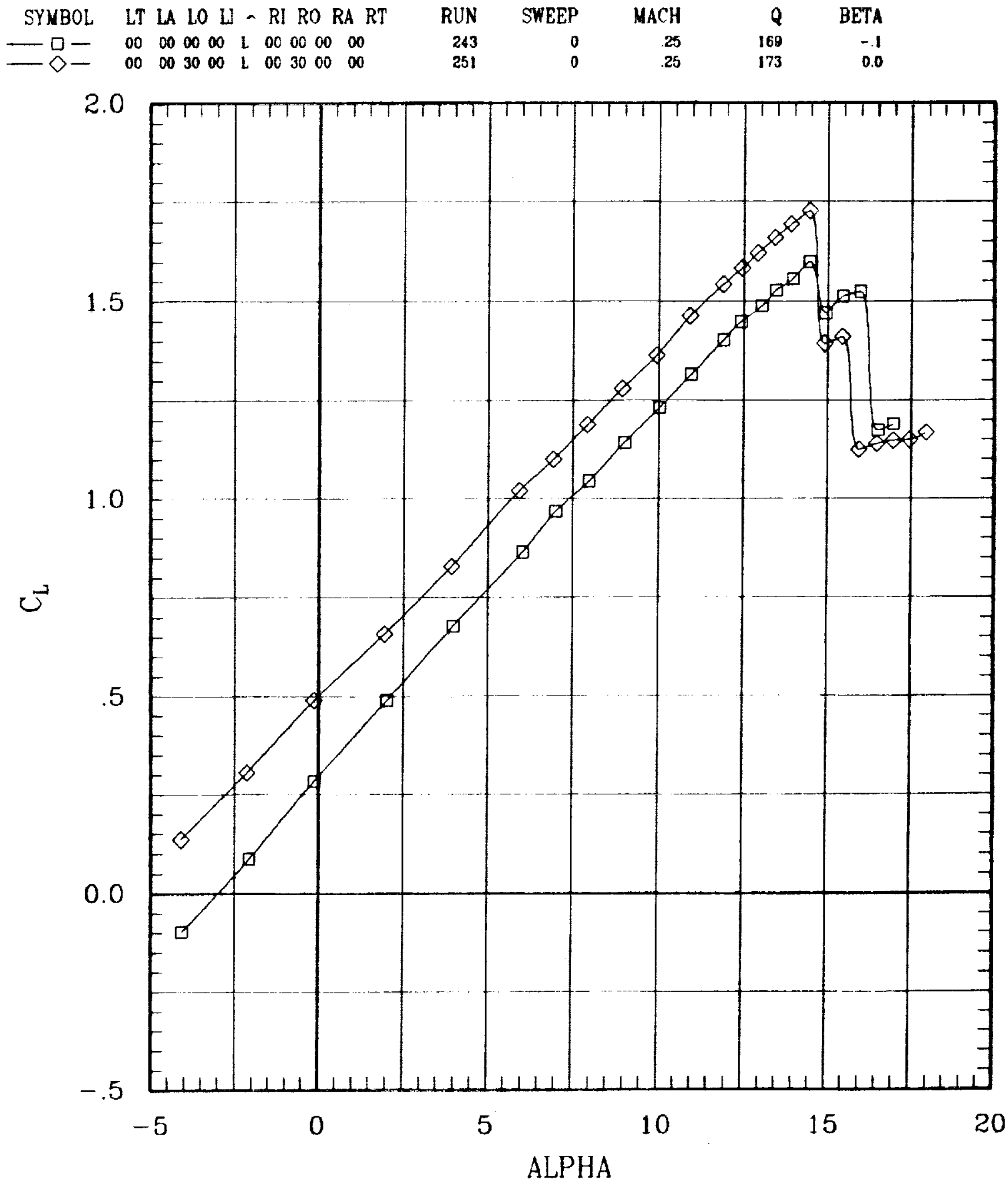

Figure 13. Effect of flap deflection.

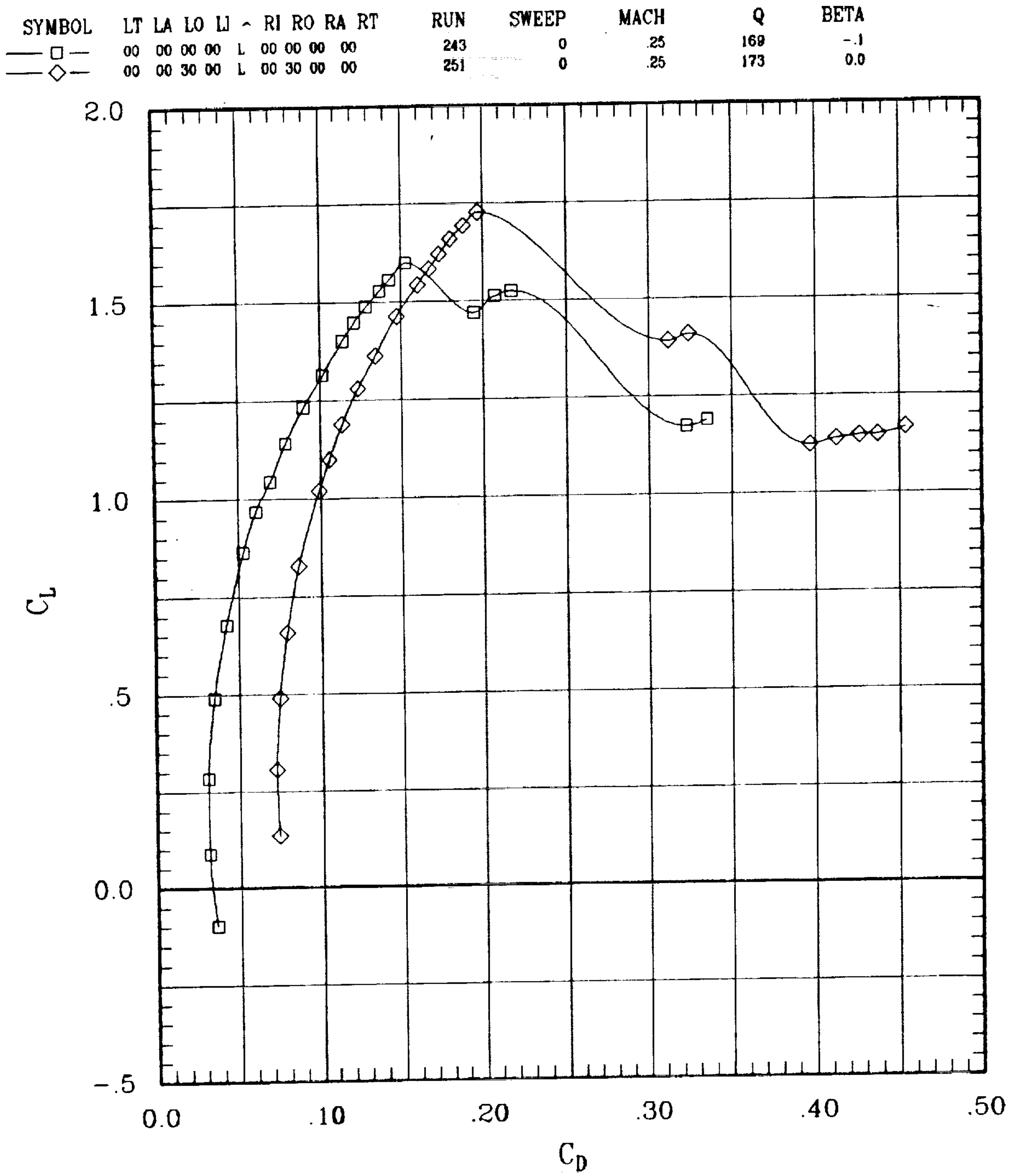

Figure 13. Effect of flap deflection.

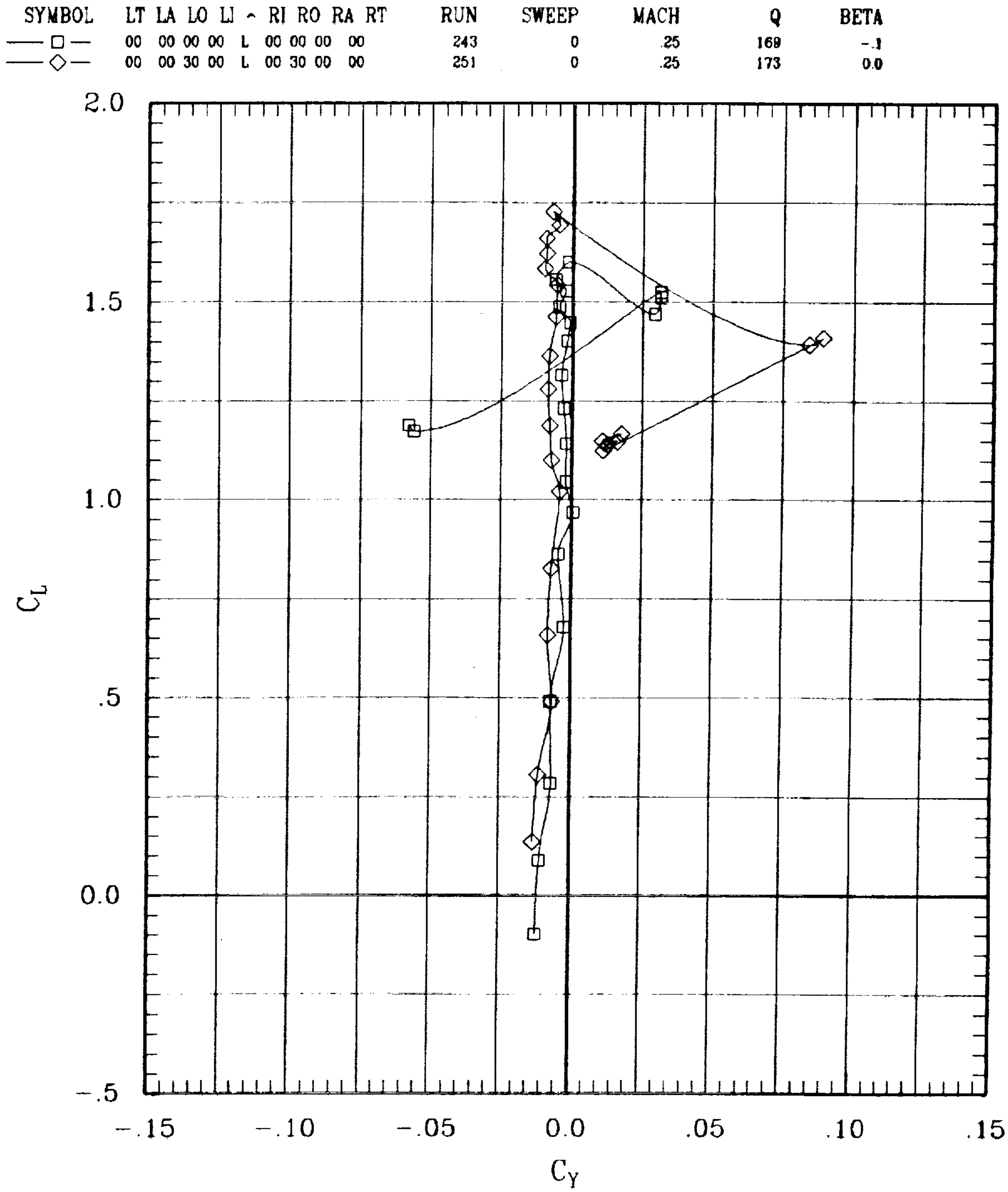

Figure 13. Effect of flap deflection.

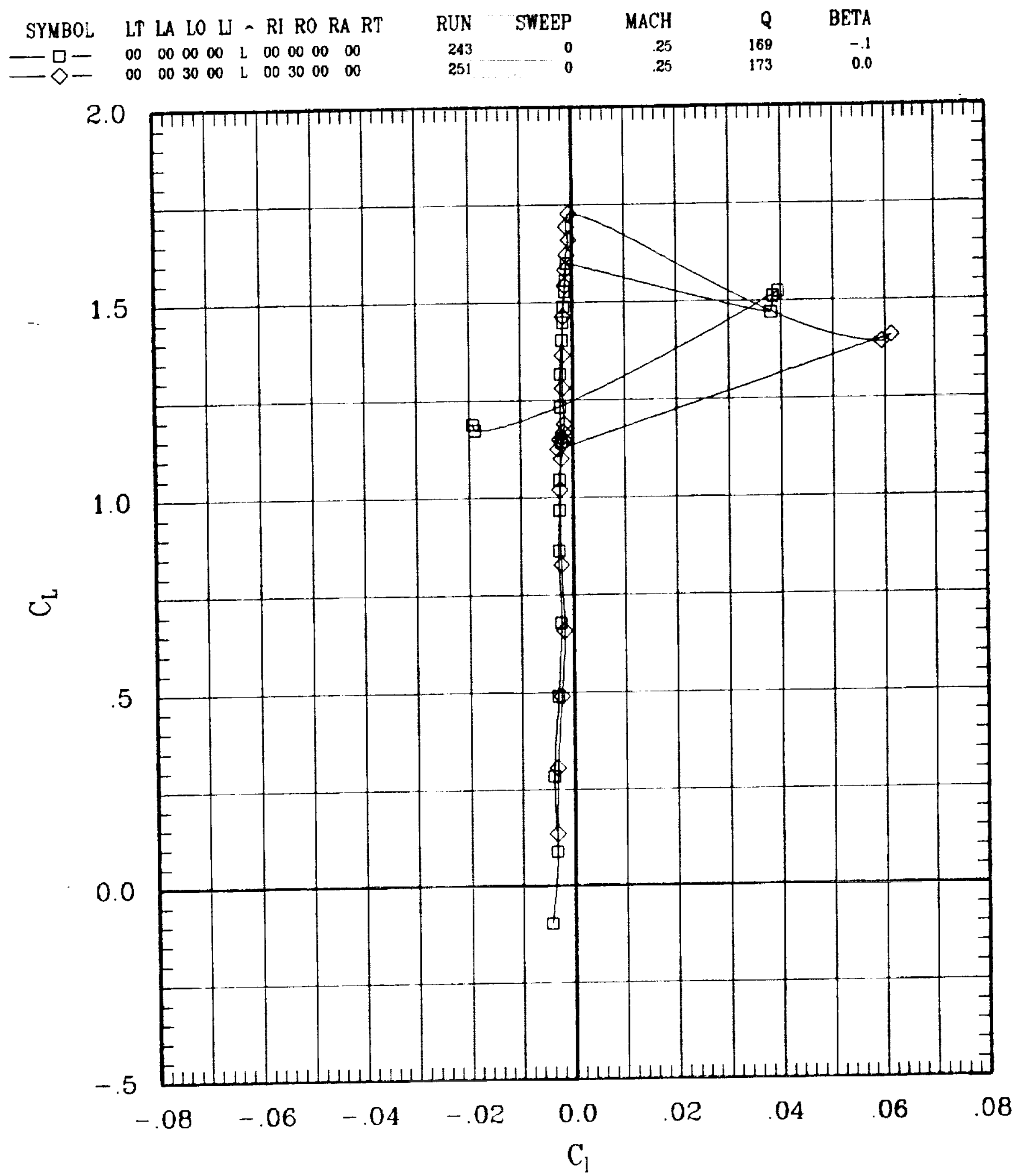

Figure 13. Effect of flap deflection.

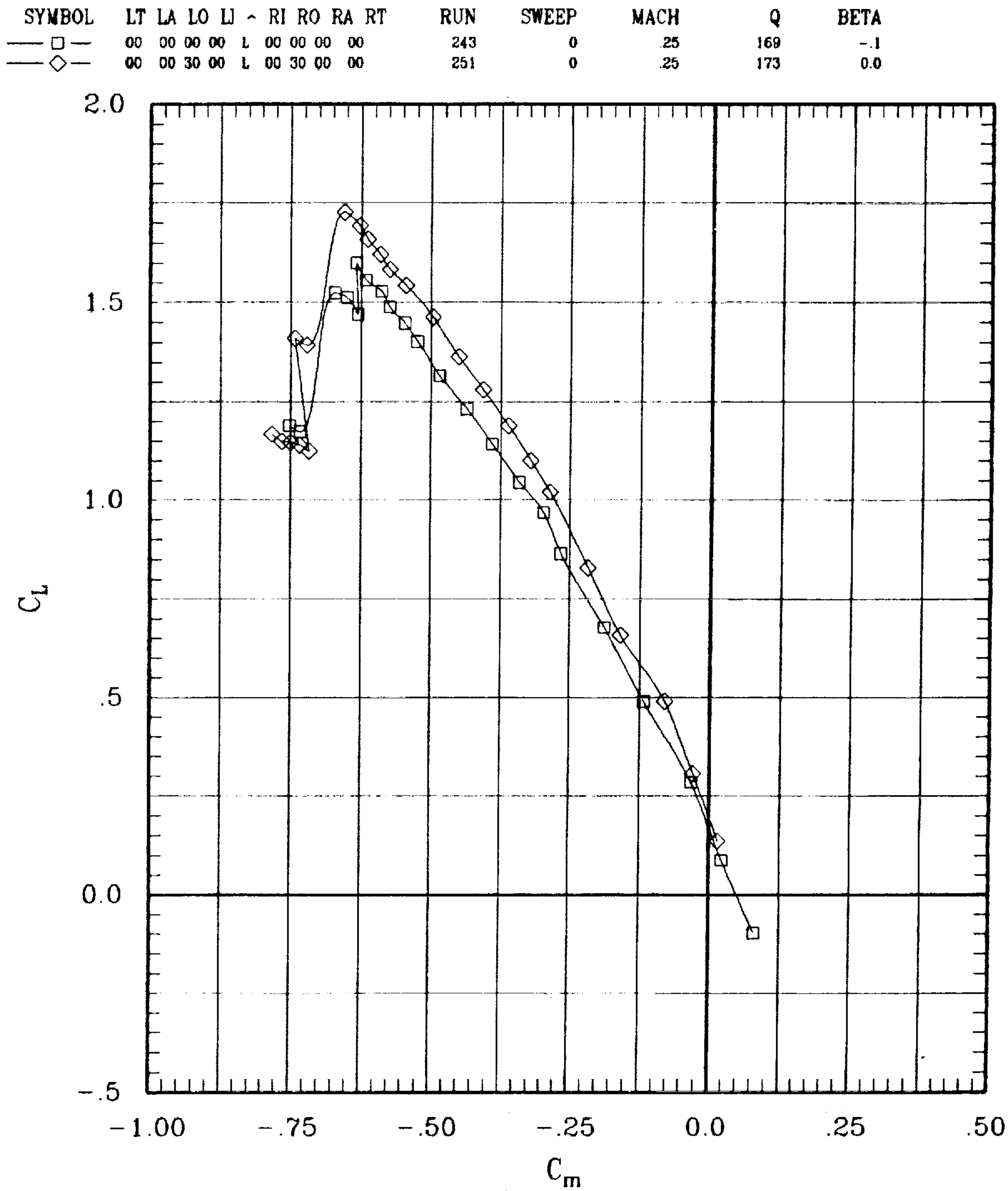

Figure 13. Effect of flap deflection.

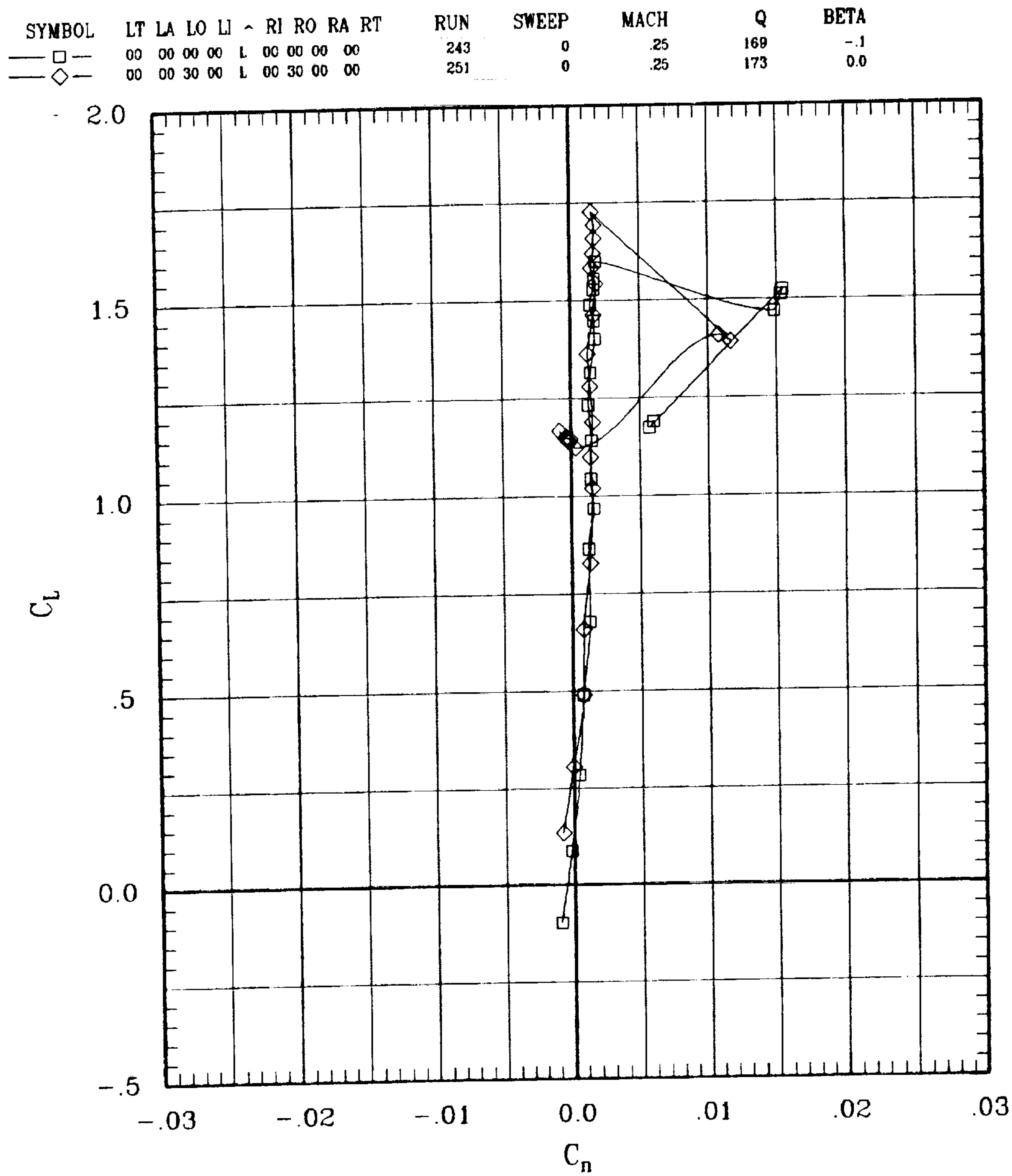

Figure 13. Effect of flap deflection.

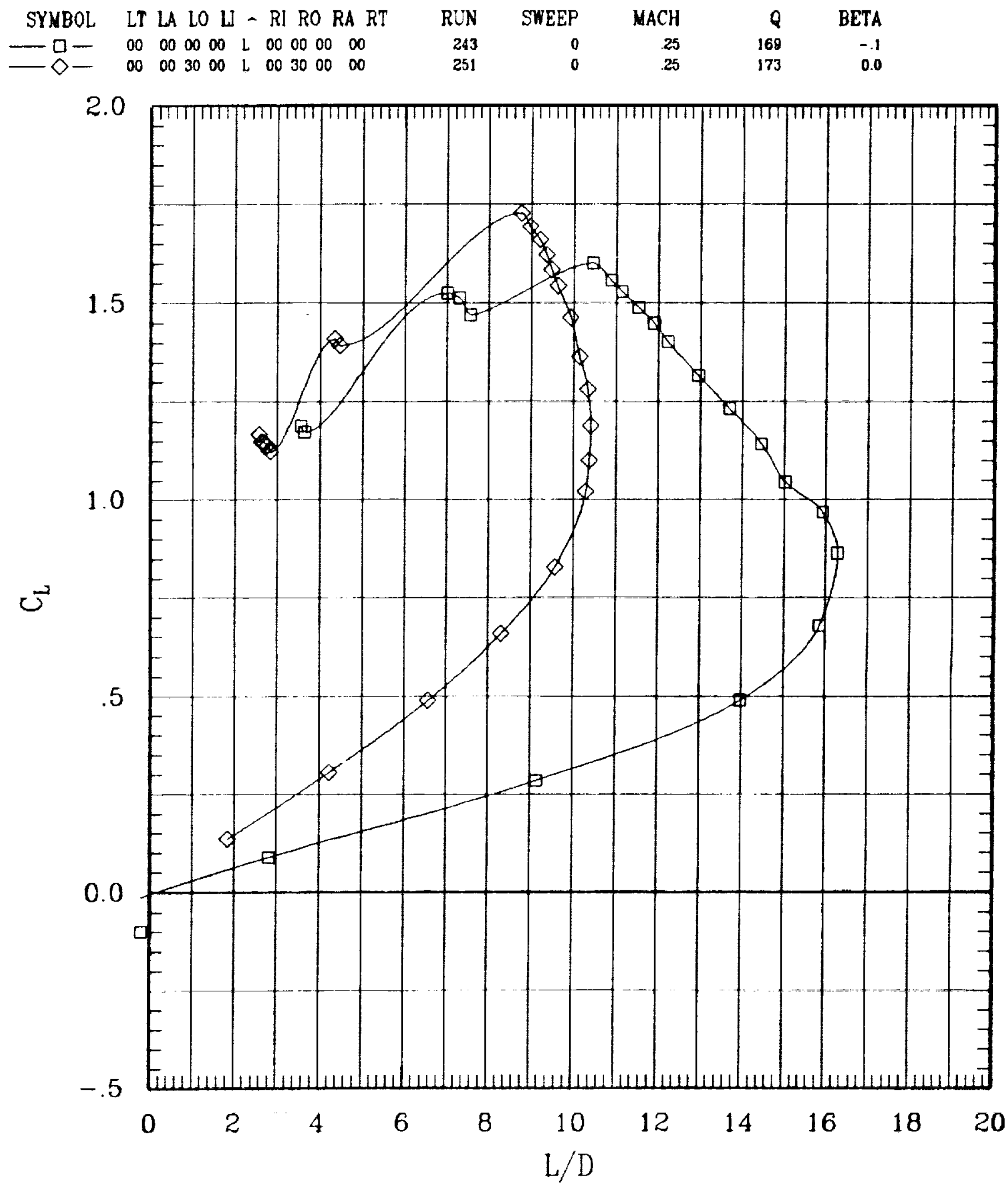

Figure 13. Effect of flap deflection.

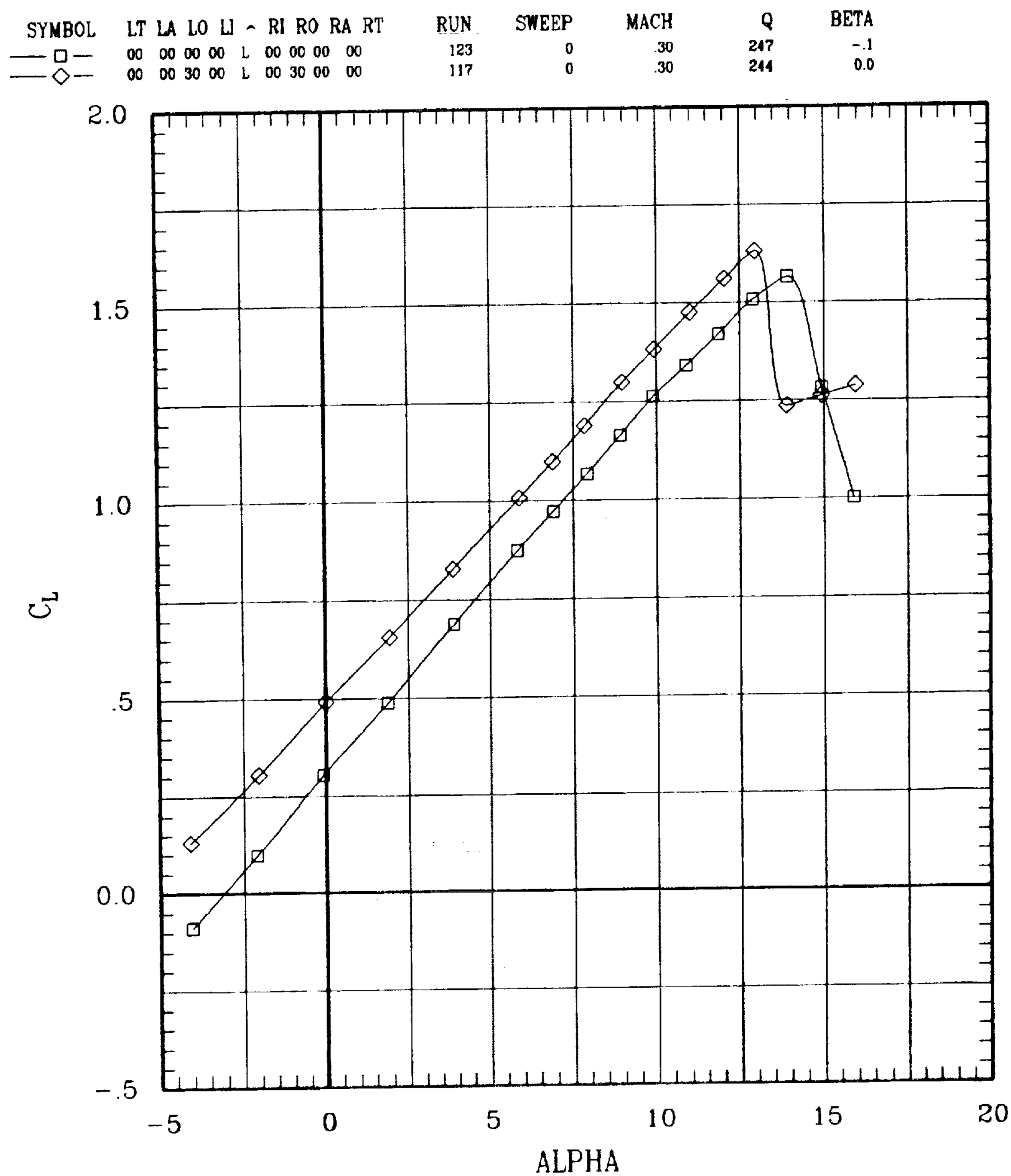

Figure 13. Effect of flap deflection.

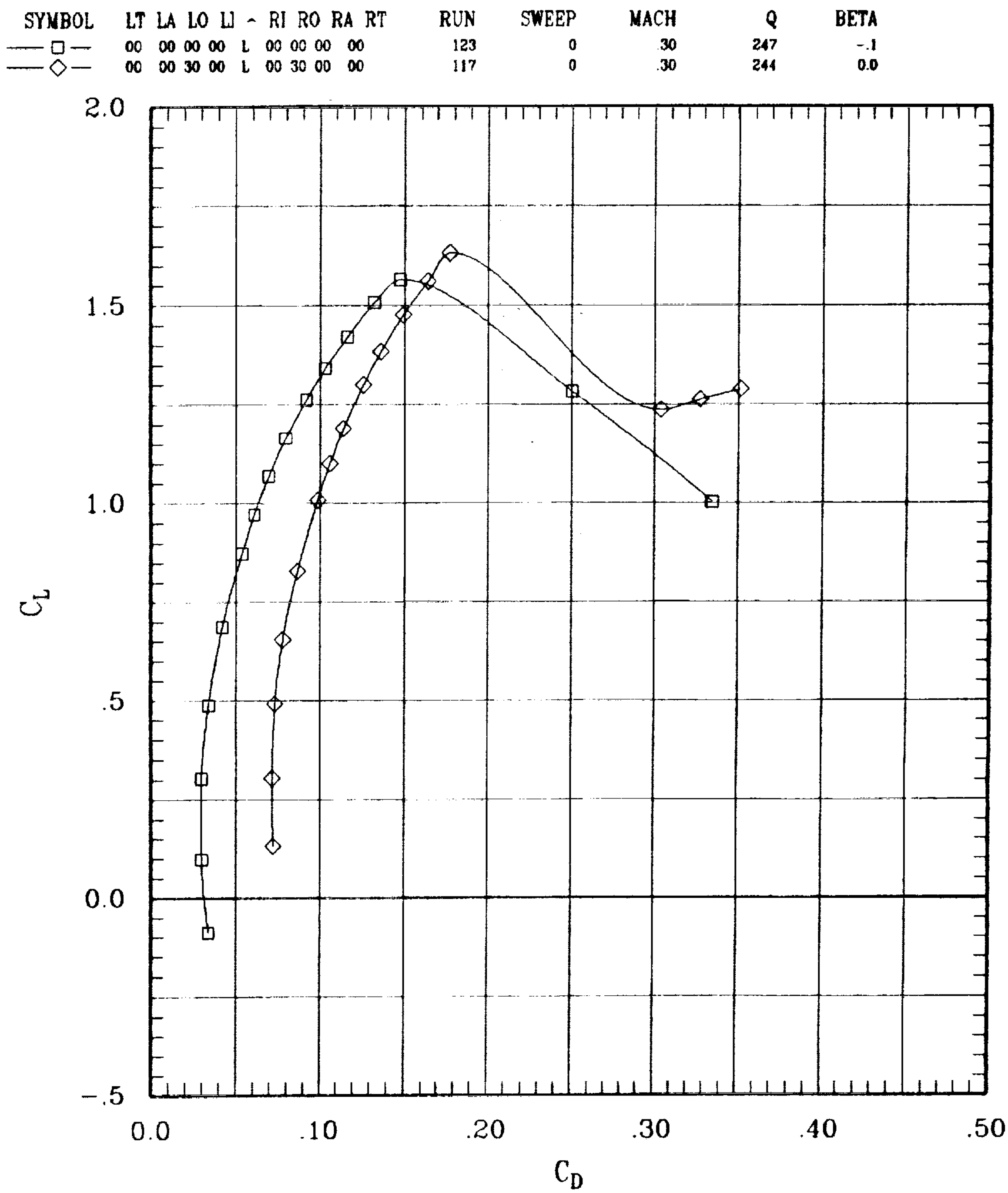

Figure 13. Effect of flap deflection.

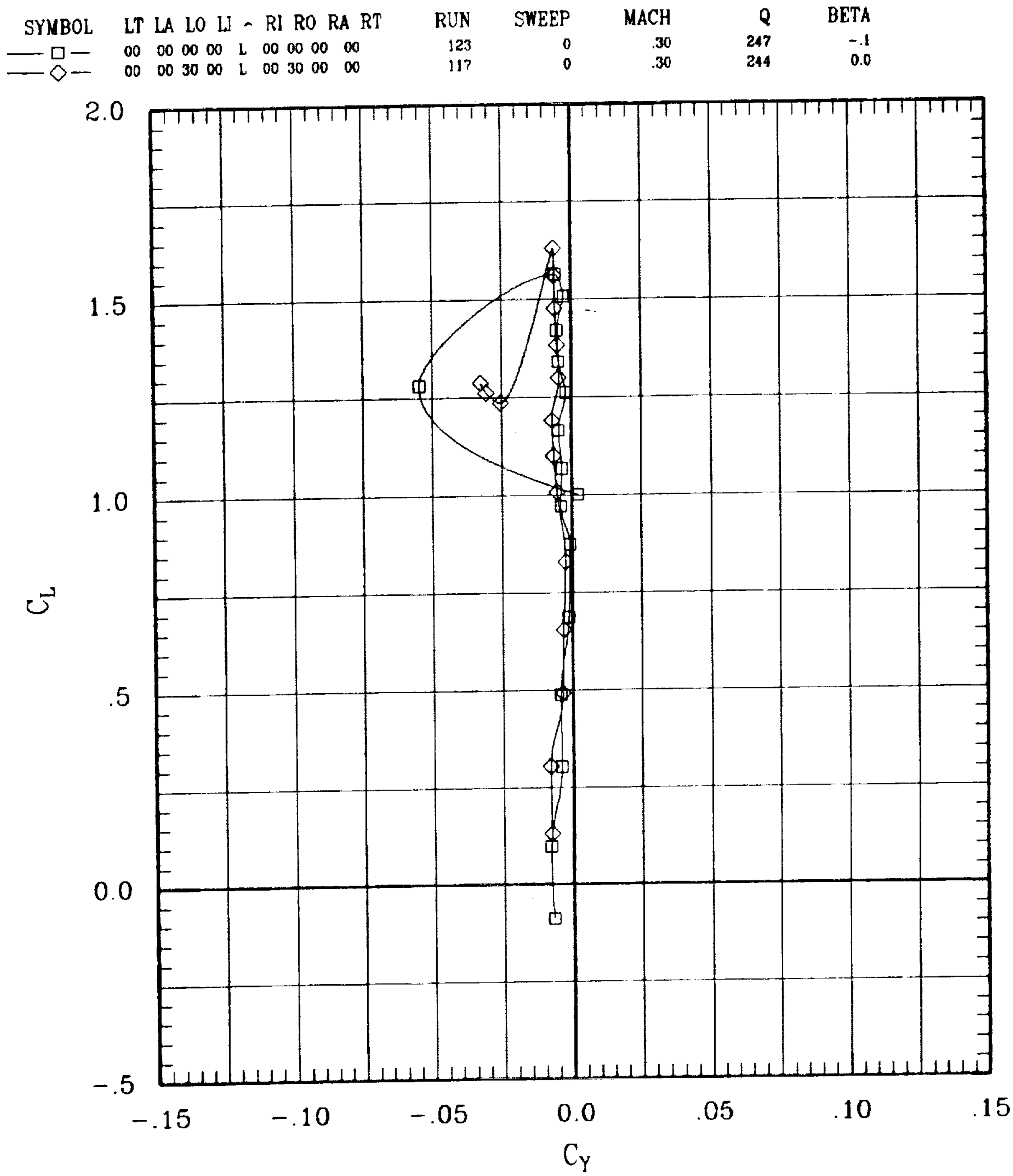

Figure 13. Effect of flap deflection.

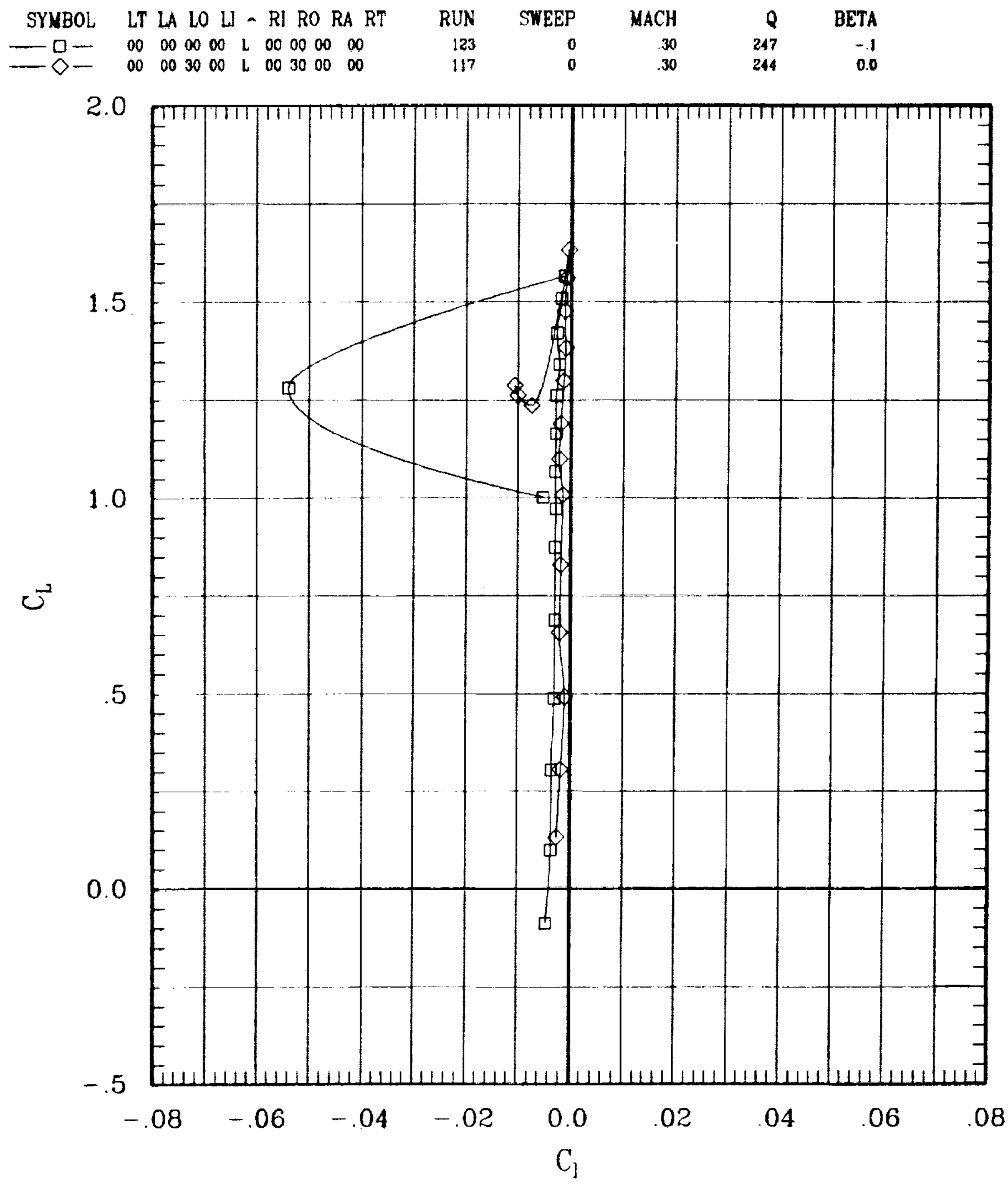

Figure 13. Effect of flap deflection.

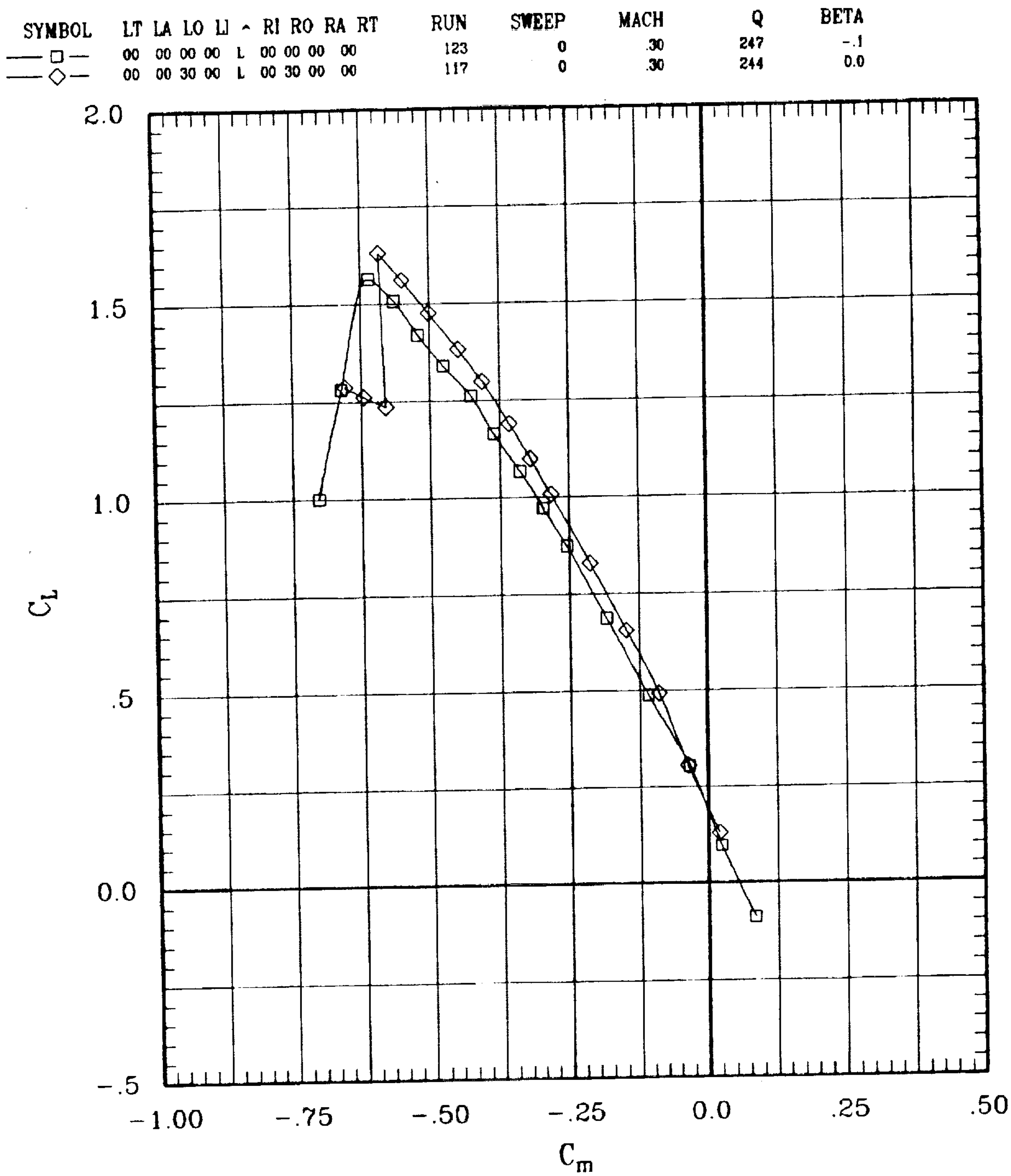

Figure 13. Effect of flap deflection.

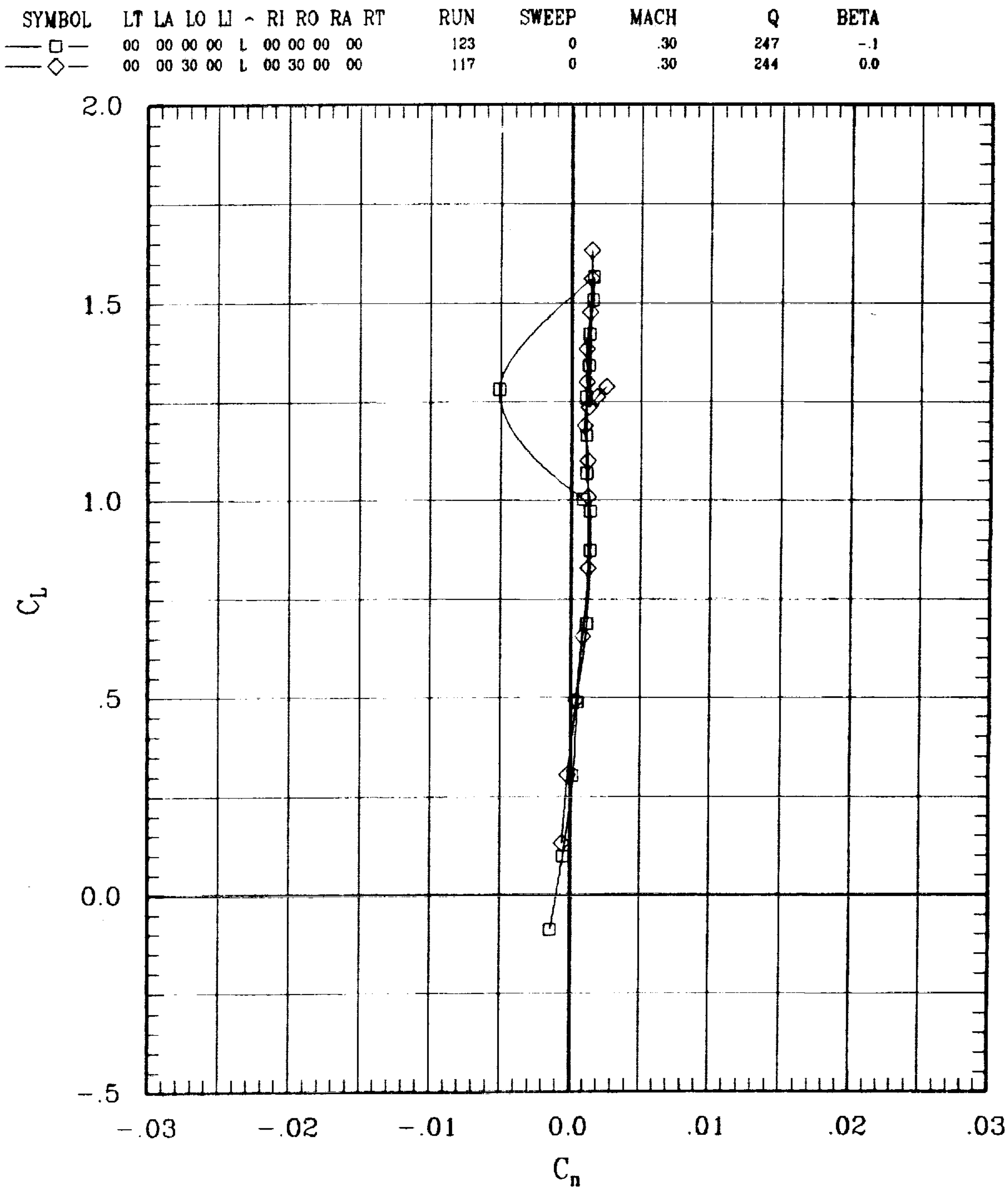

Figure 13. Effect of flap deflection.

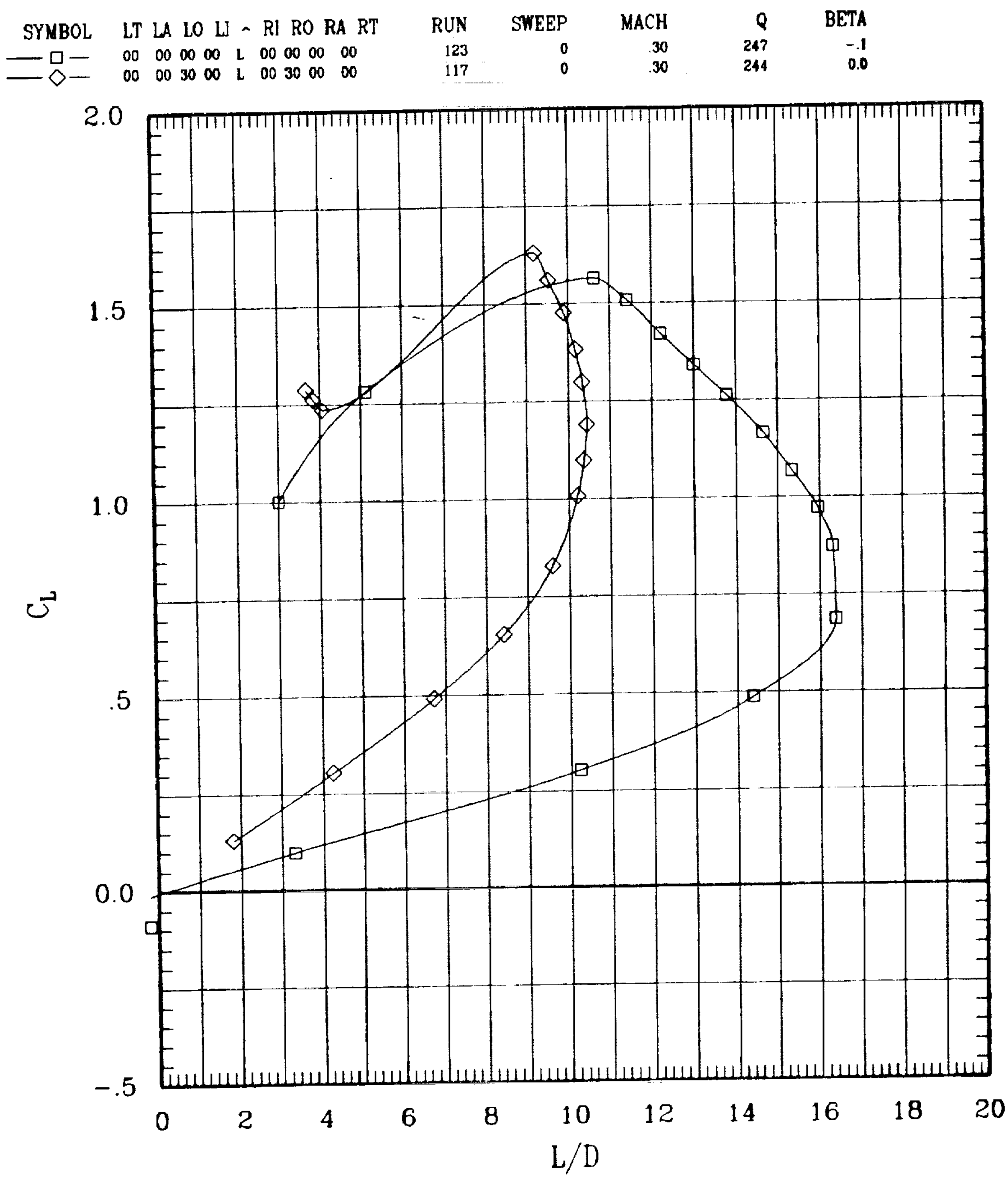

Figure 13. Effect of flap deflection.

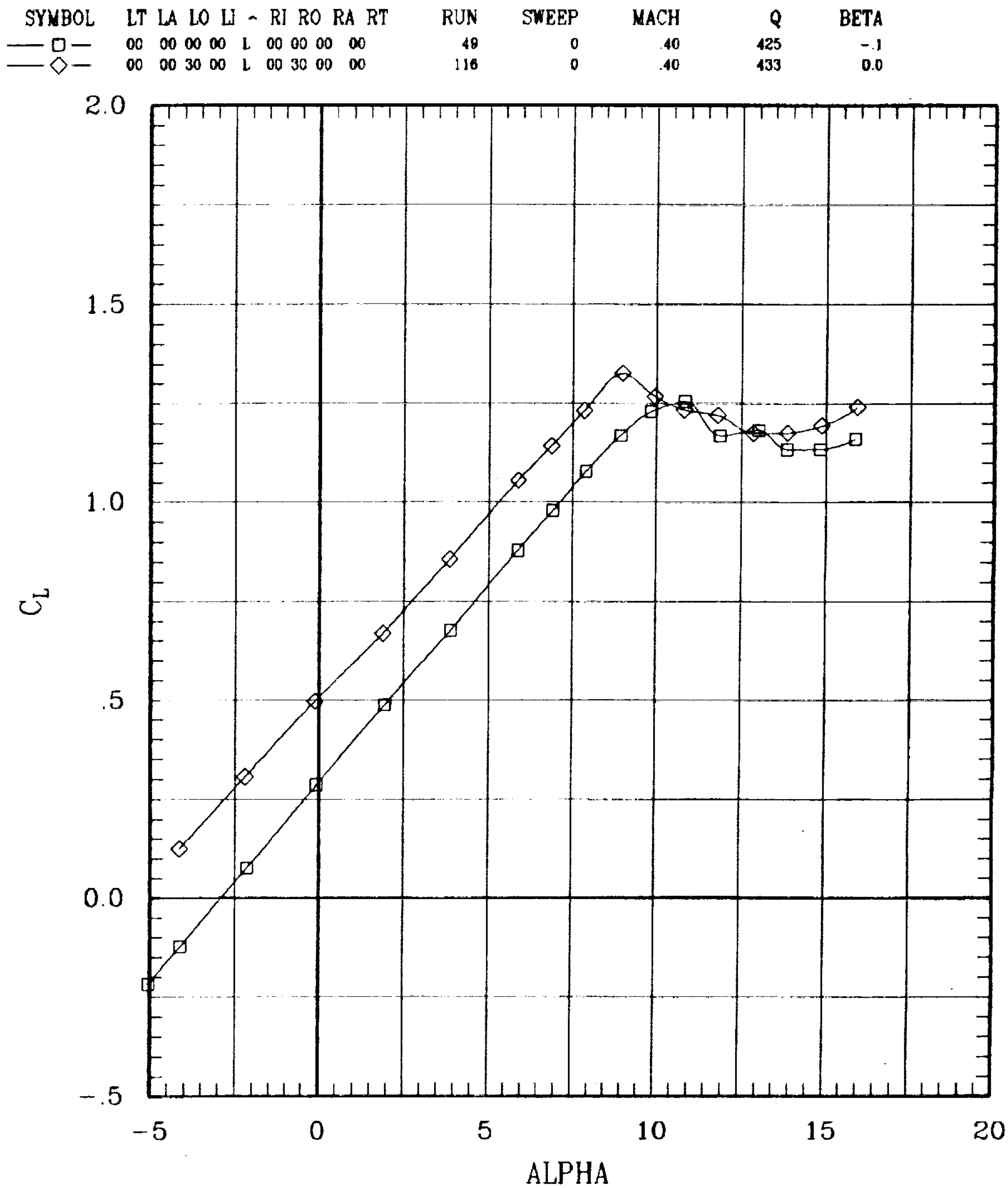

Figure 13. Effect of flap deflection.

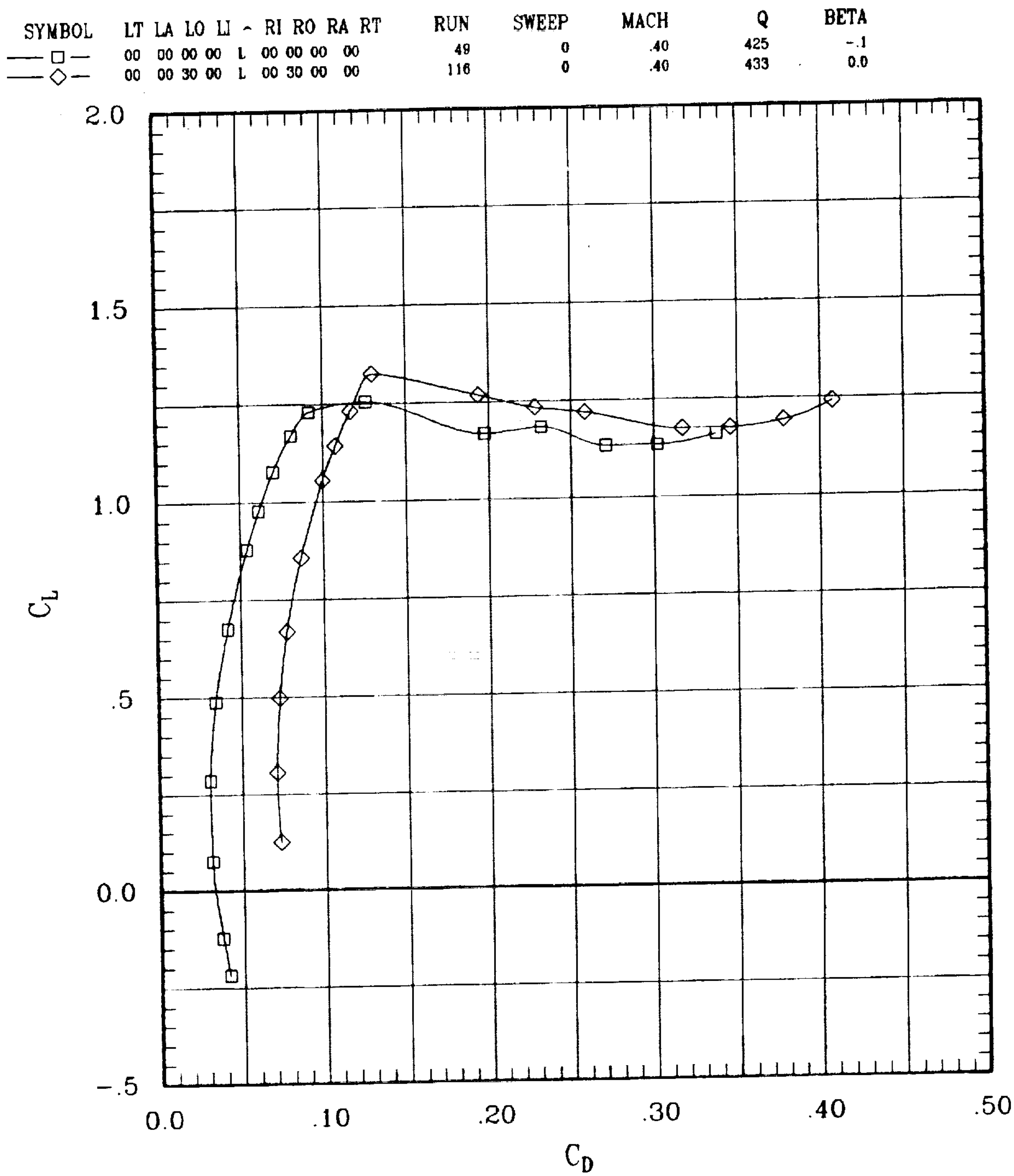

Figure 13. Effect of flap deflection.

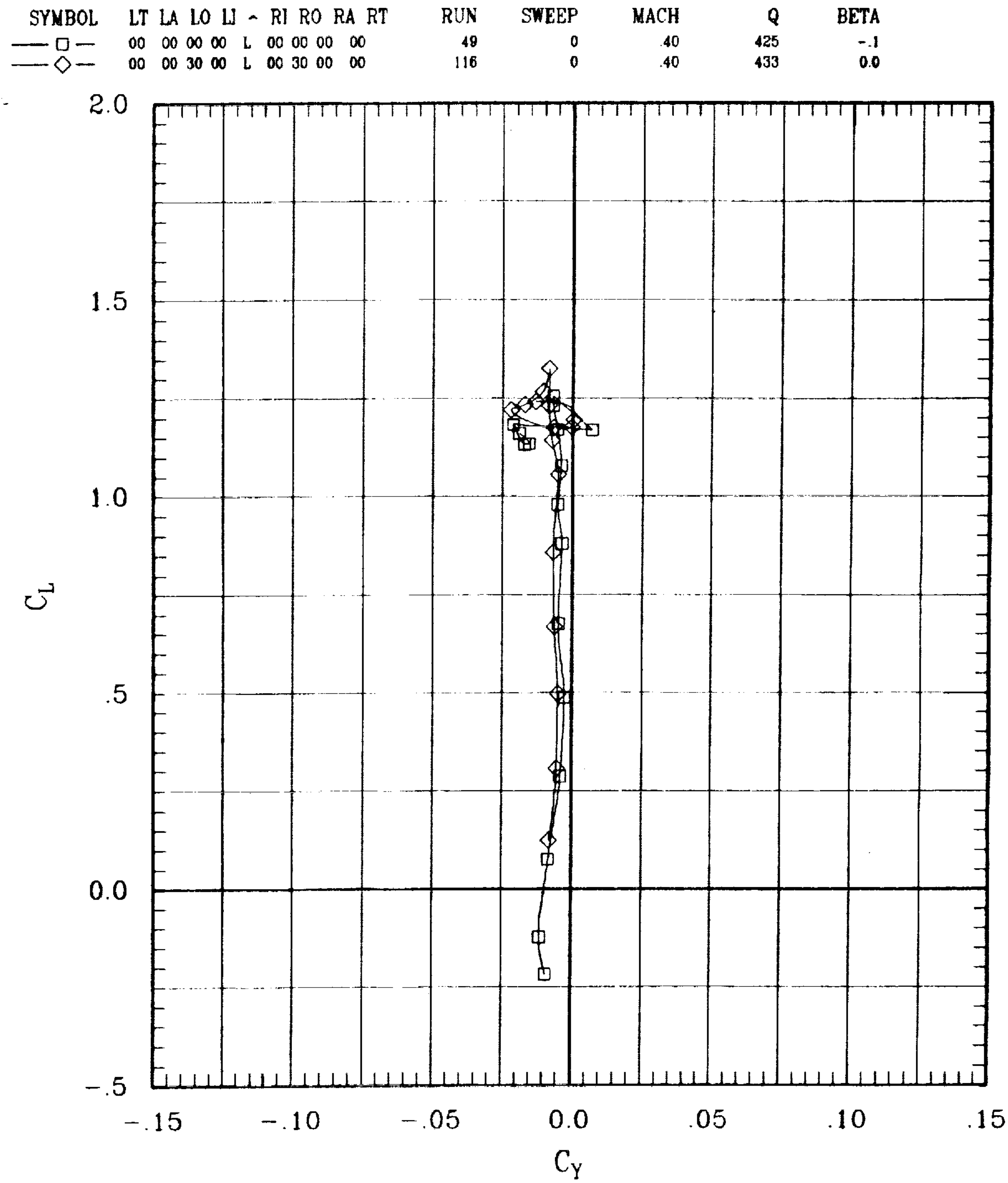

Figure 13. Effect of flap deflection.

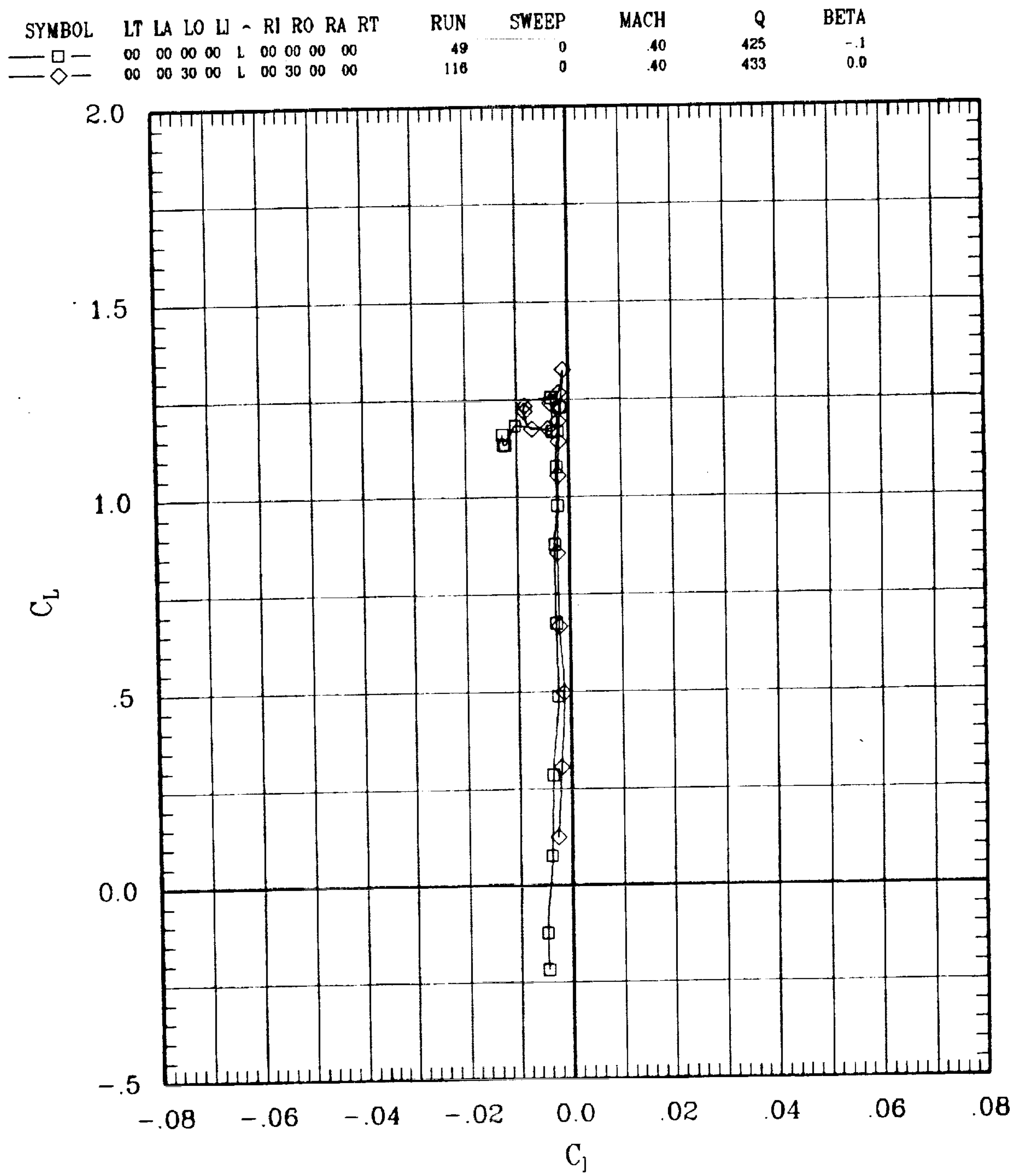

Figure 13. Effect of flap deflection.

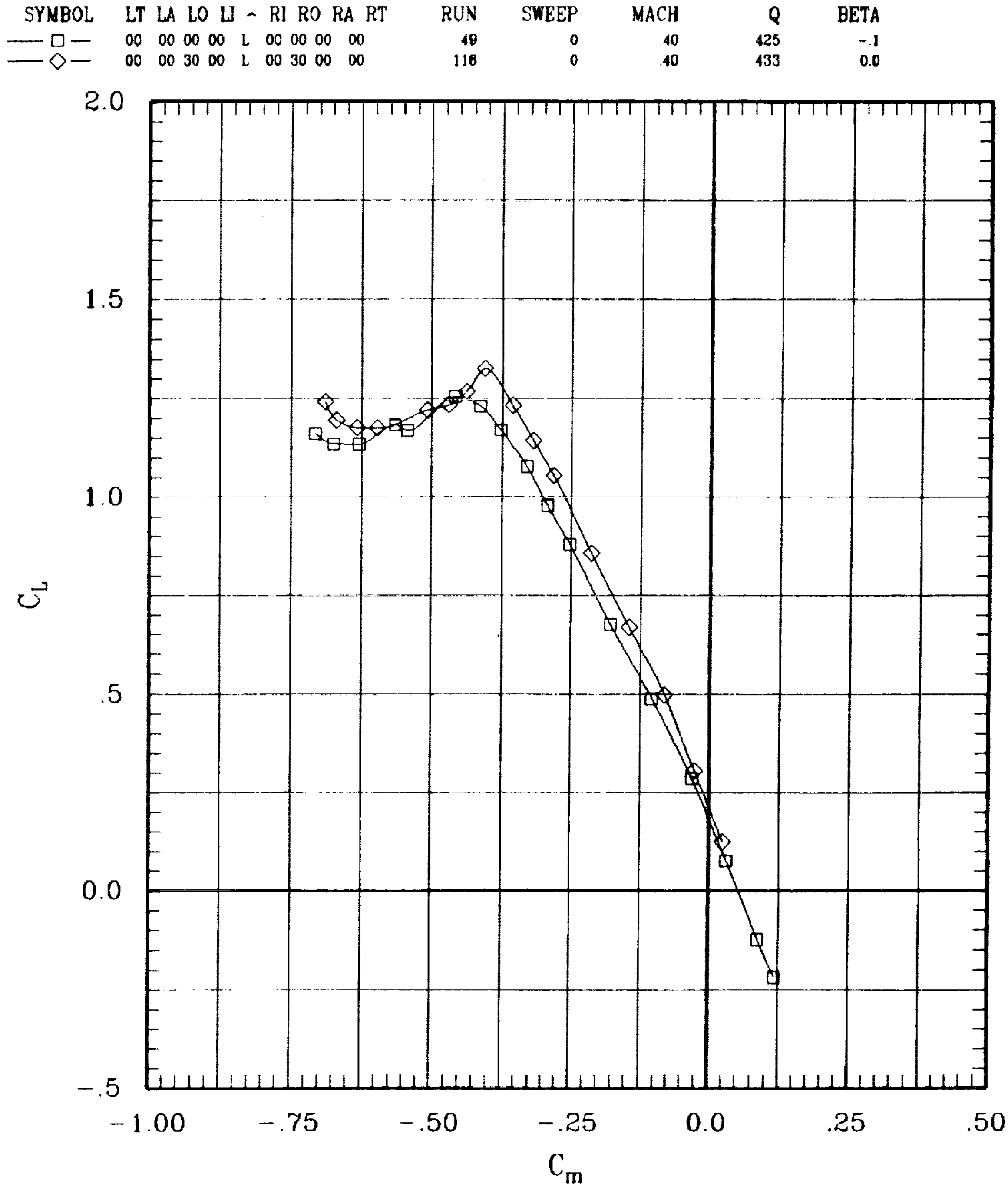

Figure 13. Effect of flap deflection.

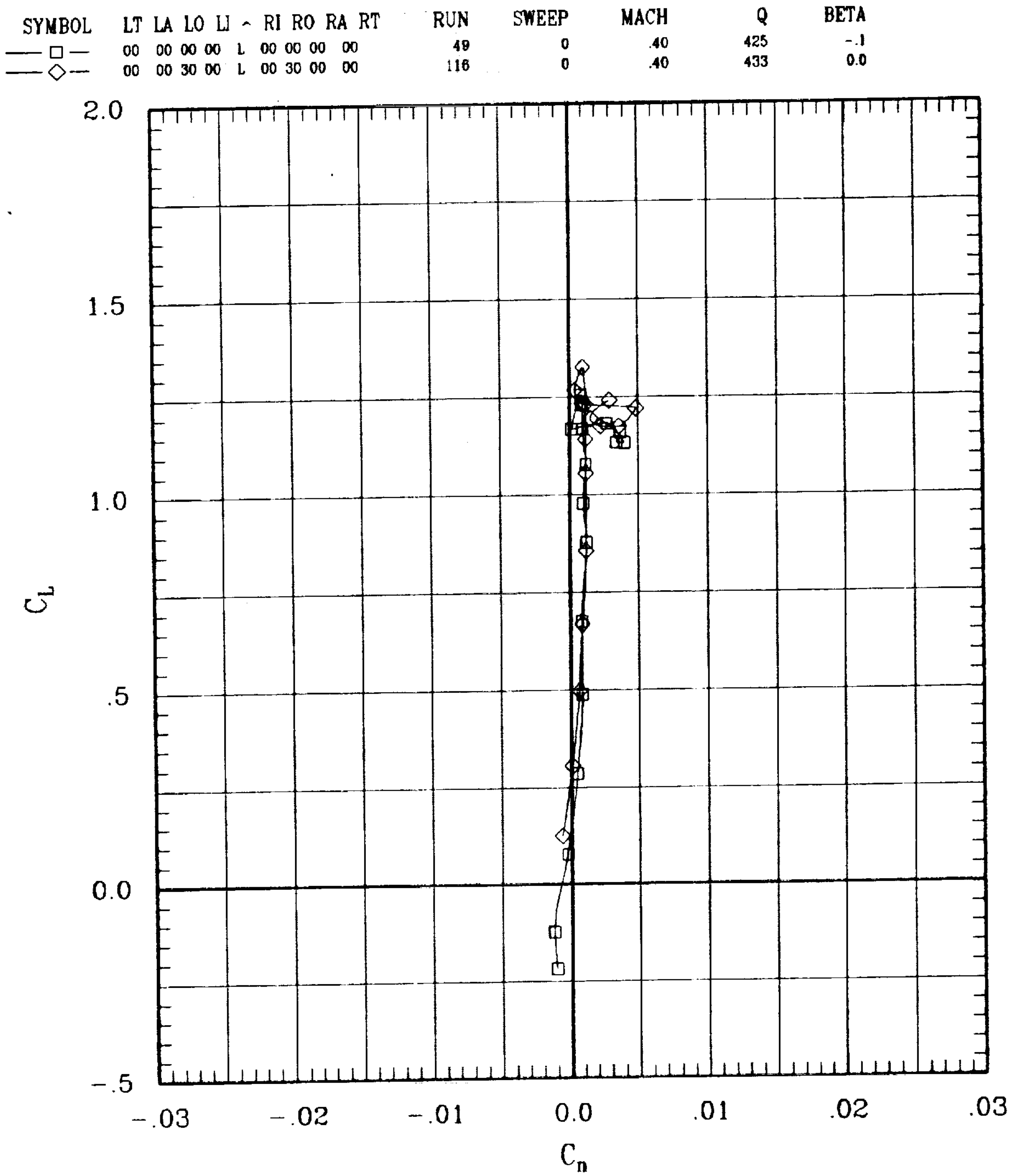

Figure 13. Effect of flap deflection.

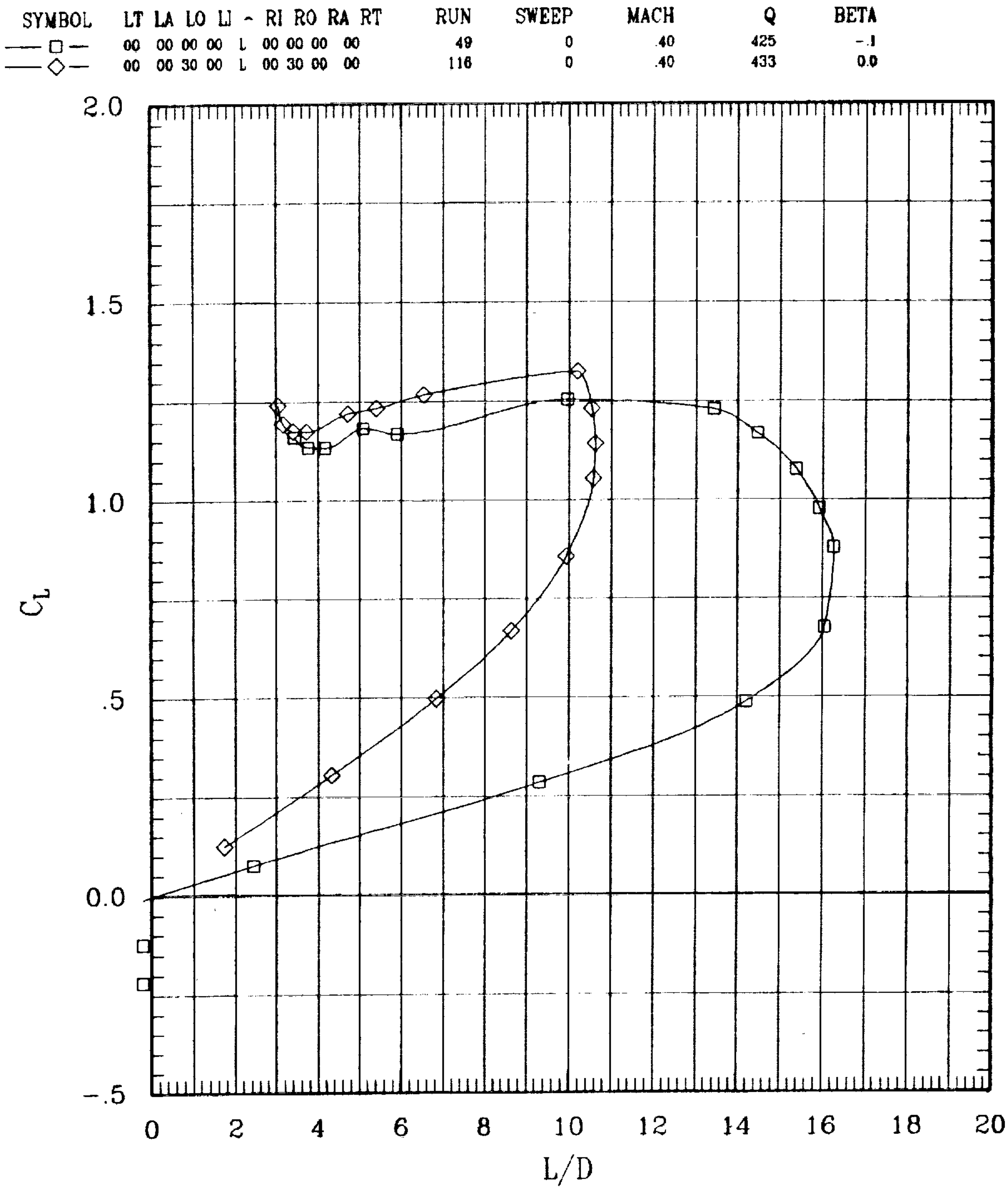

Figure 13. Effect of flap deflection.

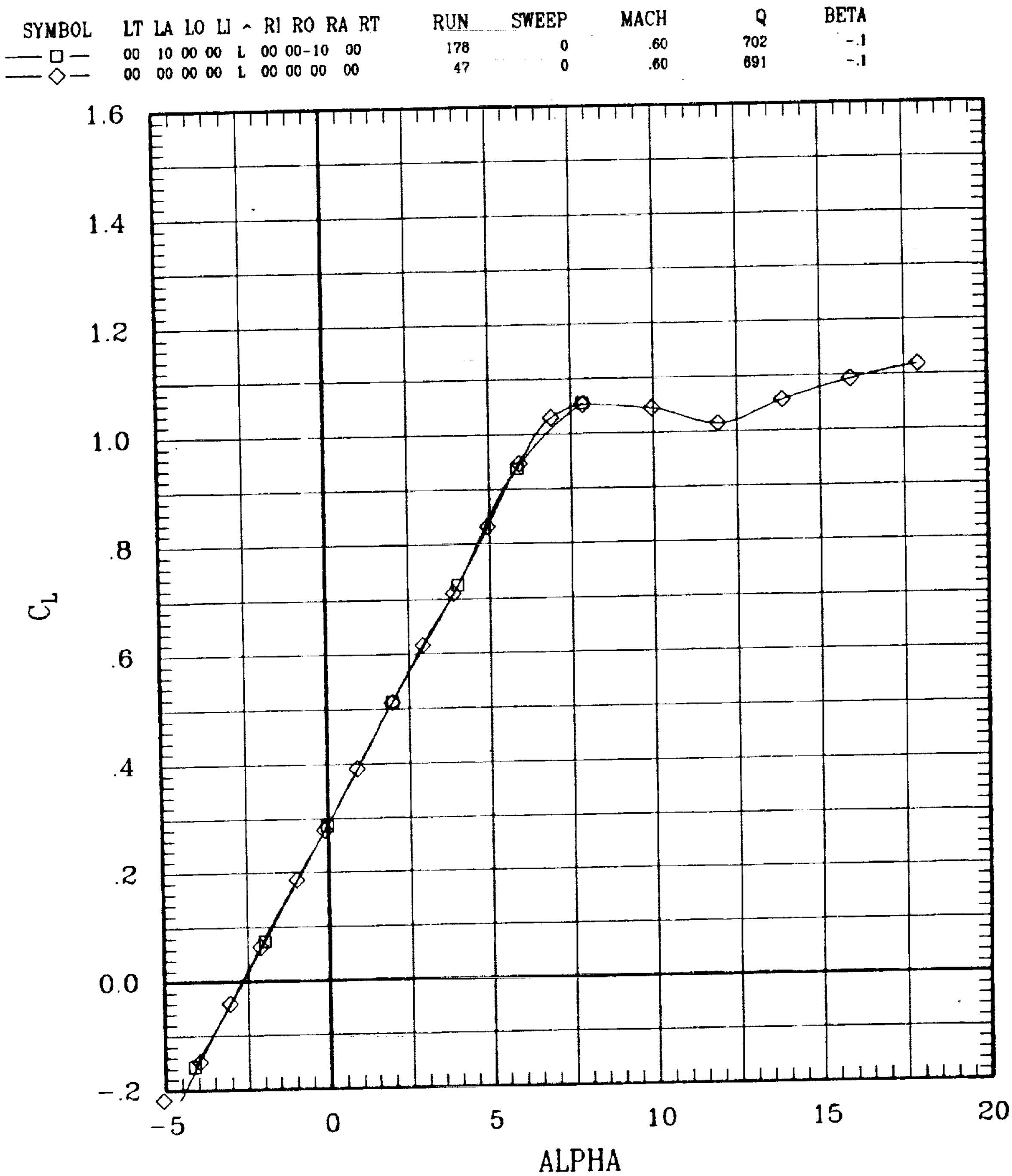

Figure 14(a). Effect of aileron deflection for sweep = 0 deg.

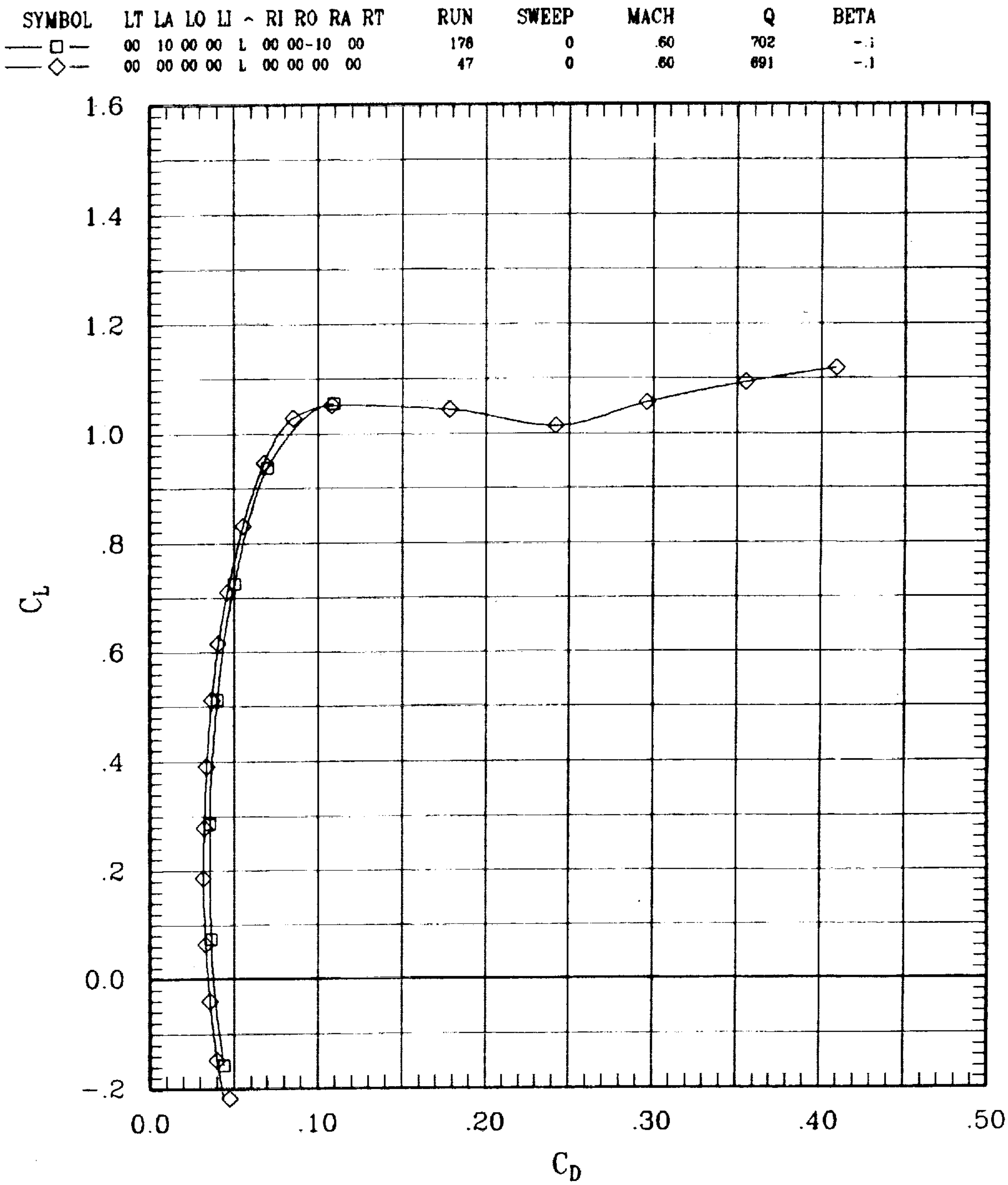

Figure 14(a). Effect of aileron deflection for sweep = 0 deg.

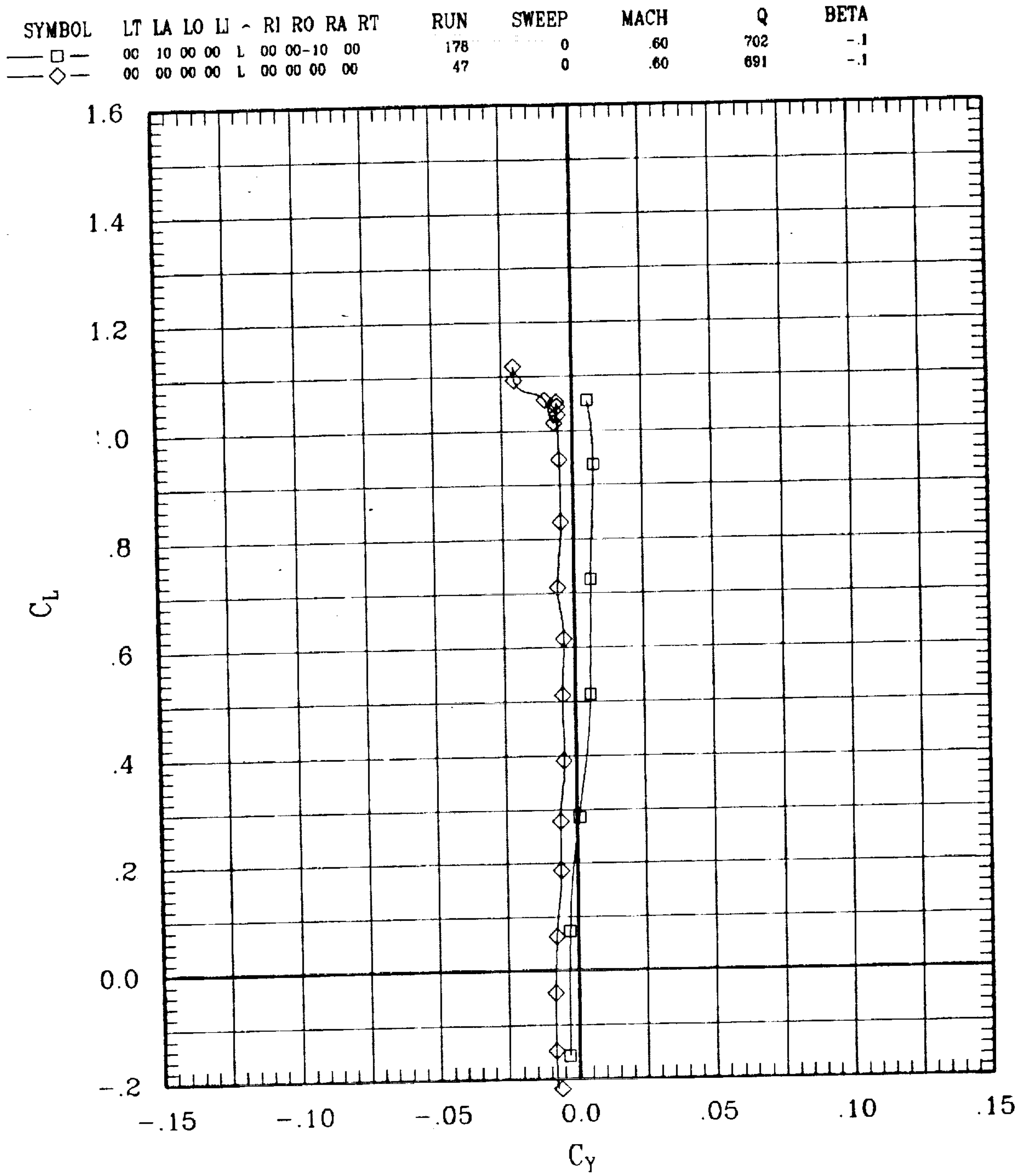

Figure 14(a). Effect of aileron deflection for sweep = 0 deg.

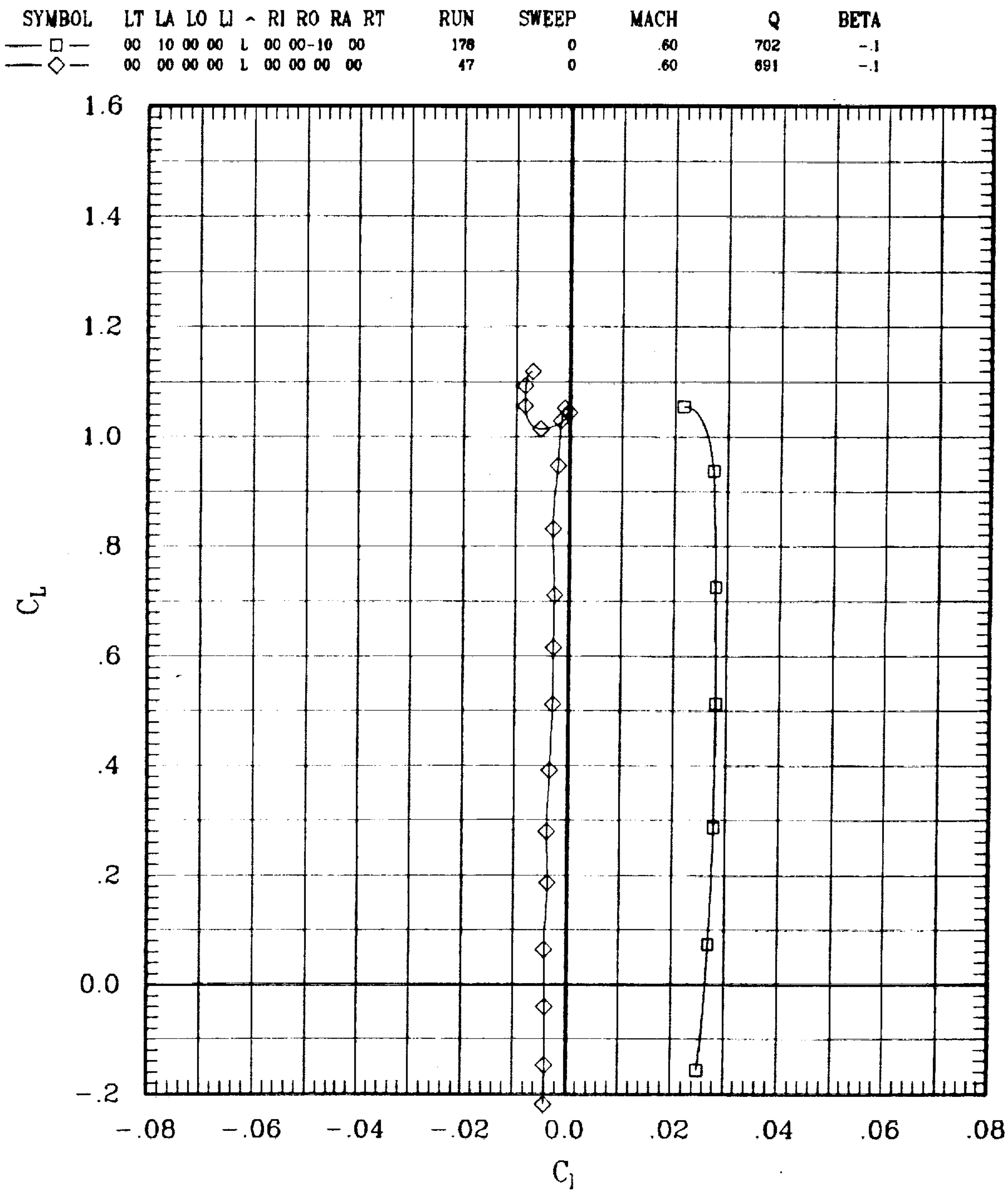

Figure 14(a). Effect of aileron deflection for sweep = 0 deg.

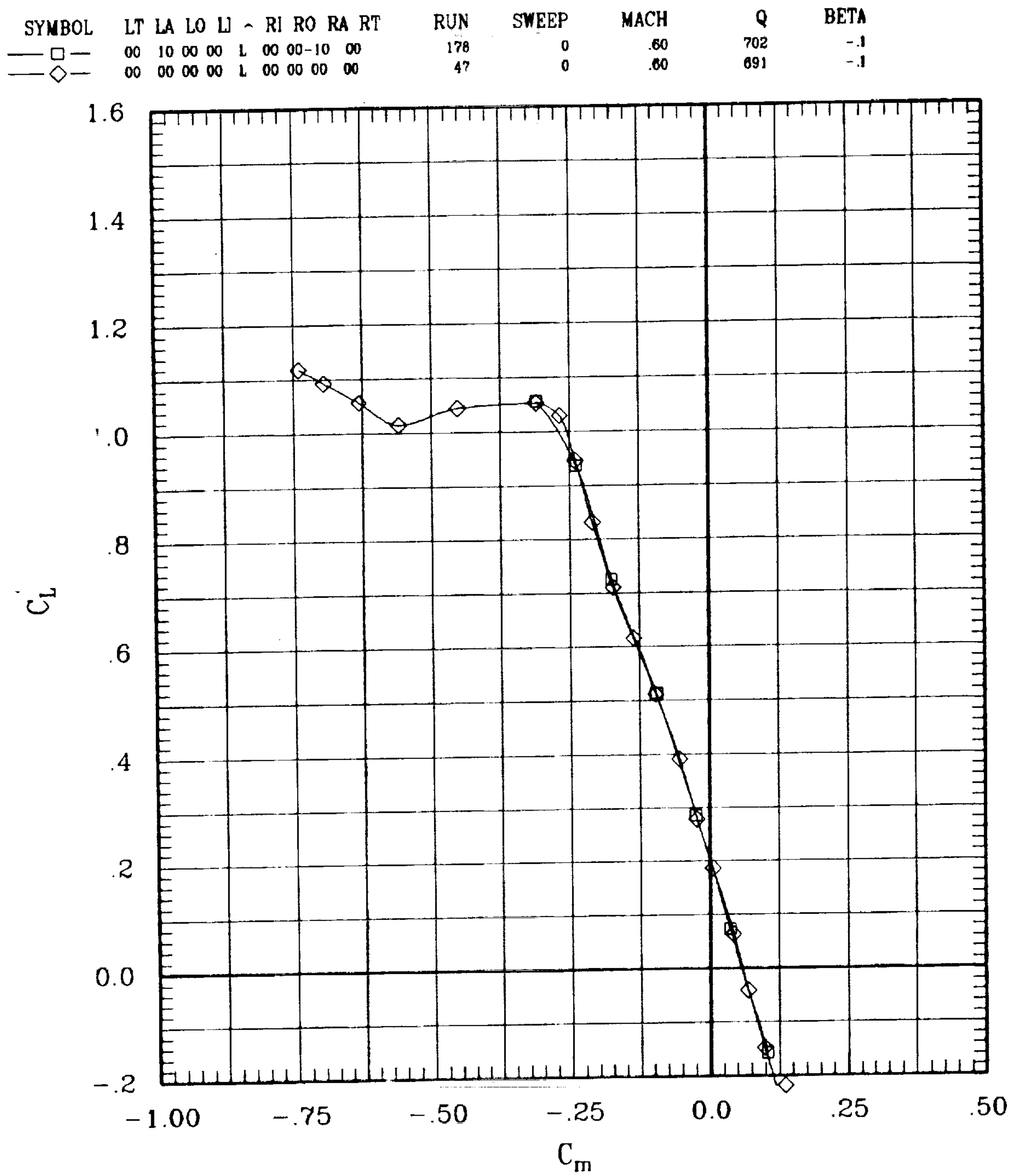

Figure 14(a). Effect of aileron deflection for sweep = 0 deg.

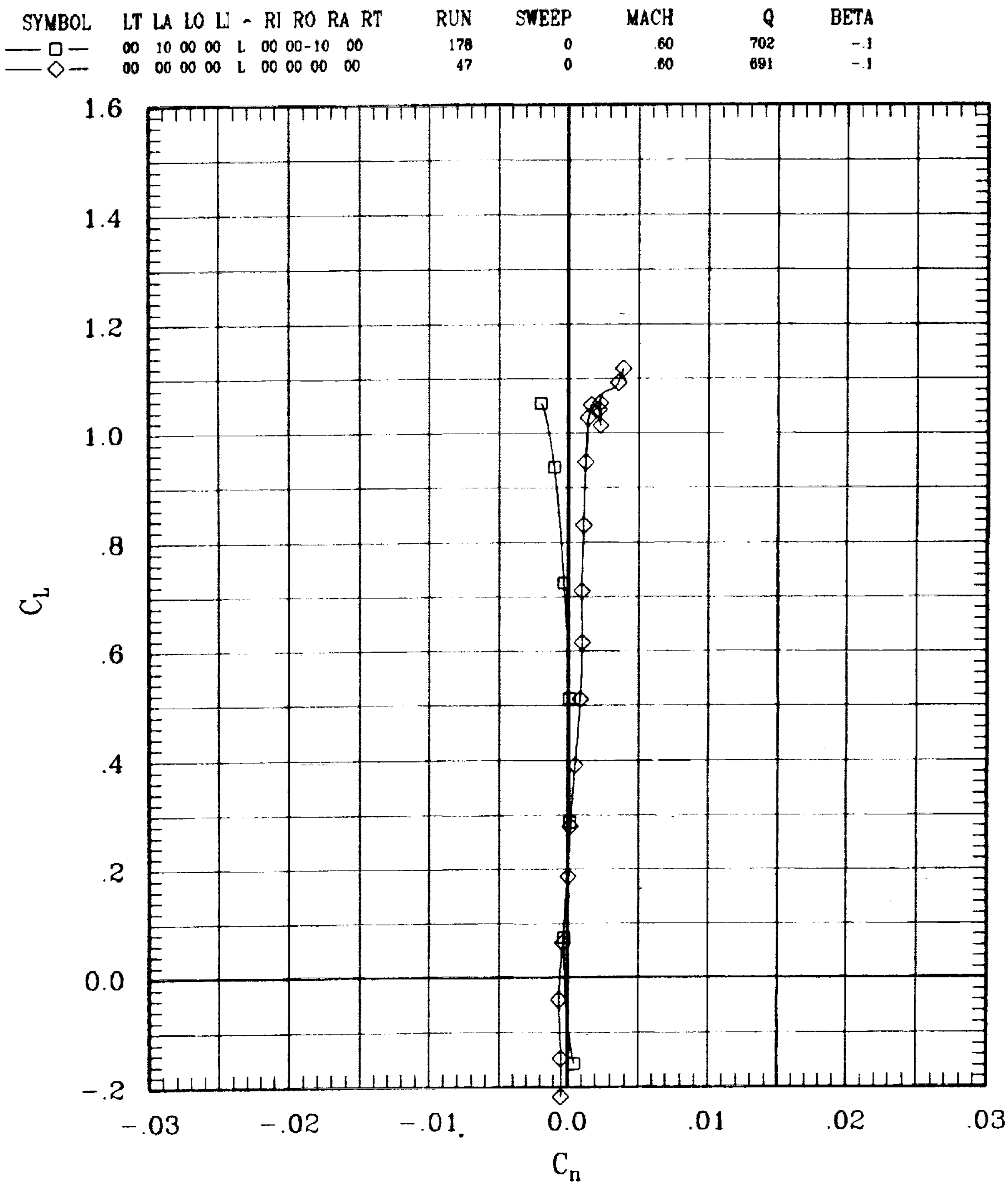

Figure 14(a). Effect of aileron deflection for sweep = 0 deg.

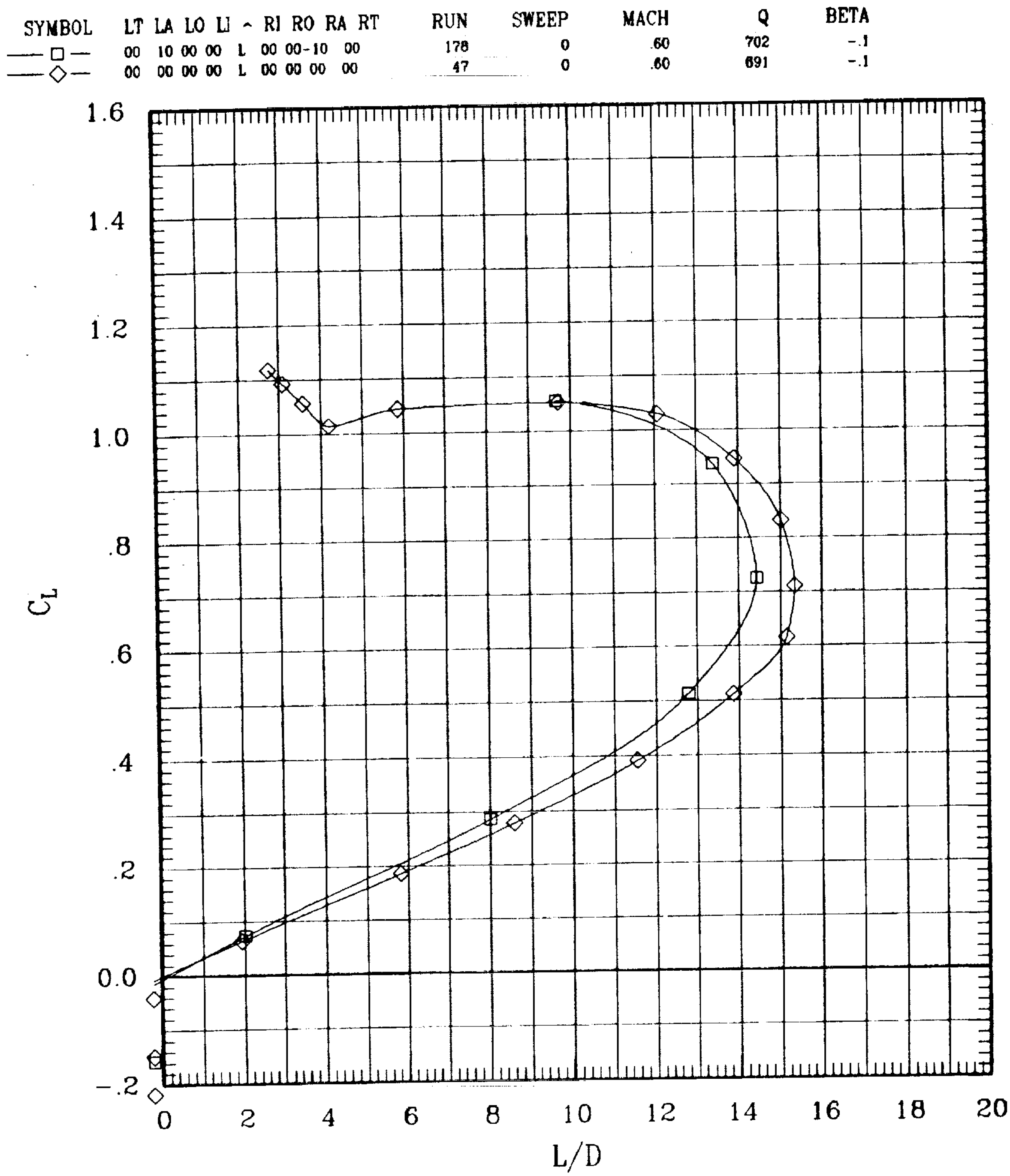

Figure 14(a). Effect of aileron deflection for sweep = 0 deg.

SYMBOL	LT LA LO LI - RI RO RA RT	RUN	SWEEP	MACH	Q	BETA
—□—	00 10 00 00 L 00 00-10 00	177	0	.80	705	-.1
—◇—	00 00 00 00 L 00 00 00 00	45	0	.80	696	-.1

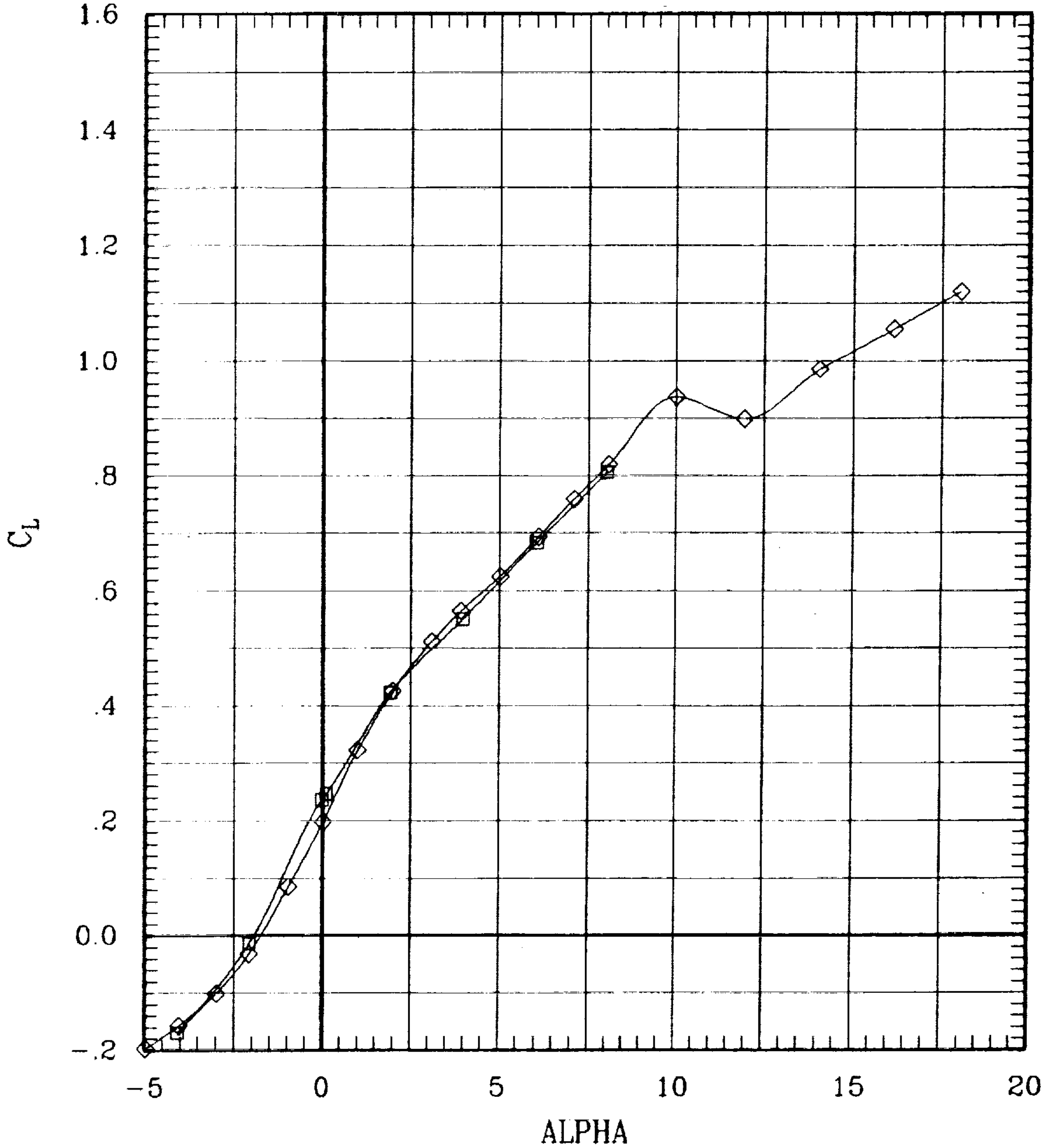

Figure 14(a). Effect of aileron deflection for sweep = 0 deg.

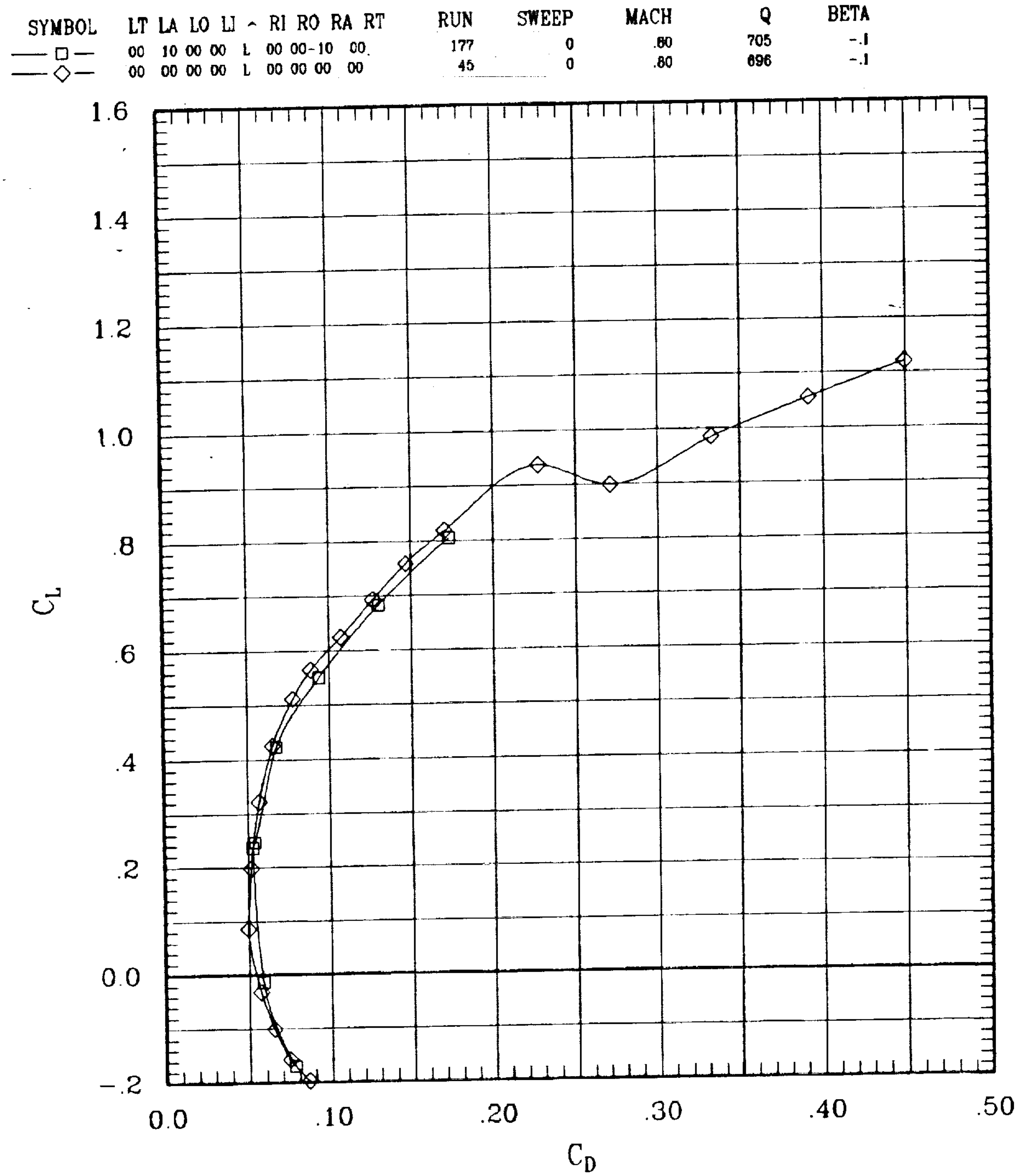

Figure 14(a). Effect of aileron deflection for sweep = 0 deg.

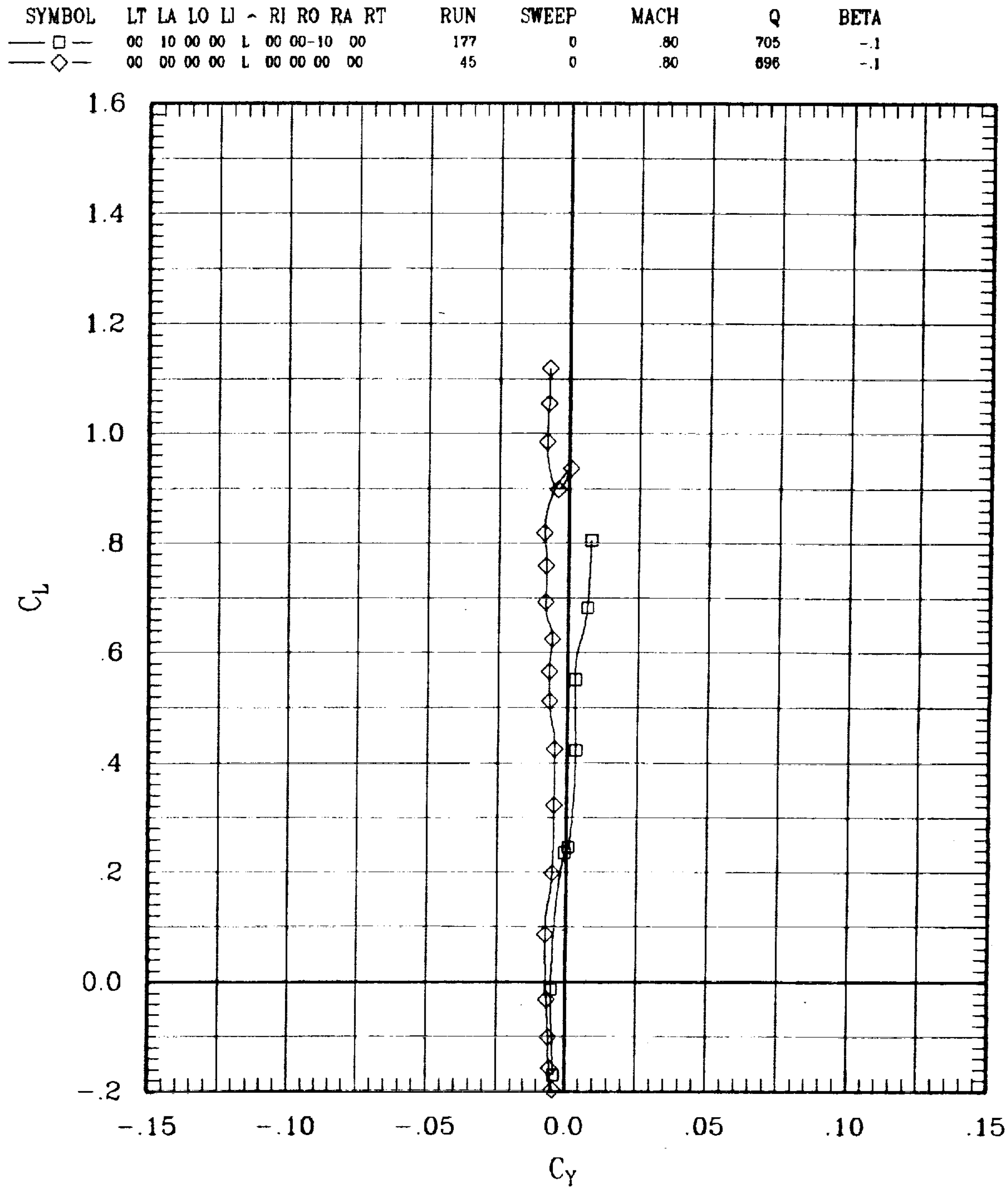

Figure 14(a). Effect of aileron deflection for sweep = 0 deg.

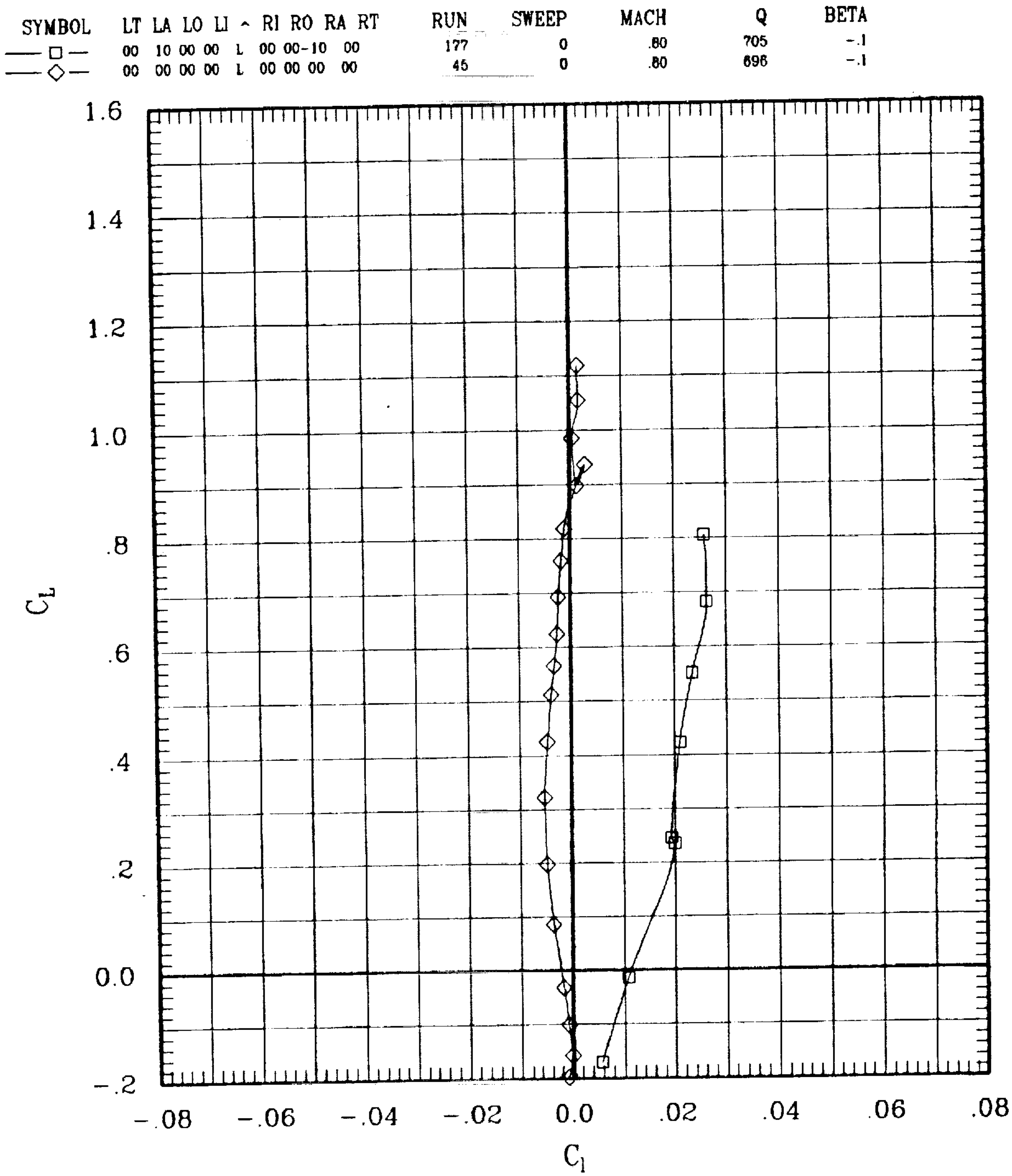

Figure 14(a). Effect of aileron deflection for sweep = 0 deg.

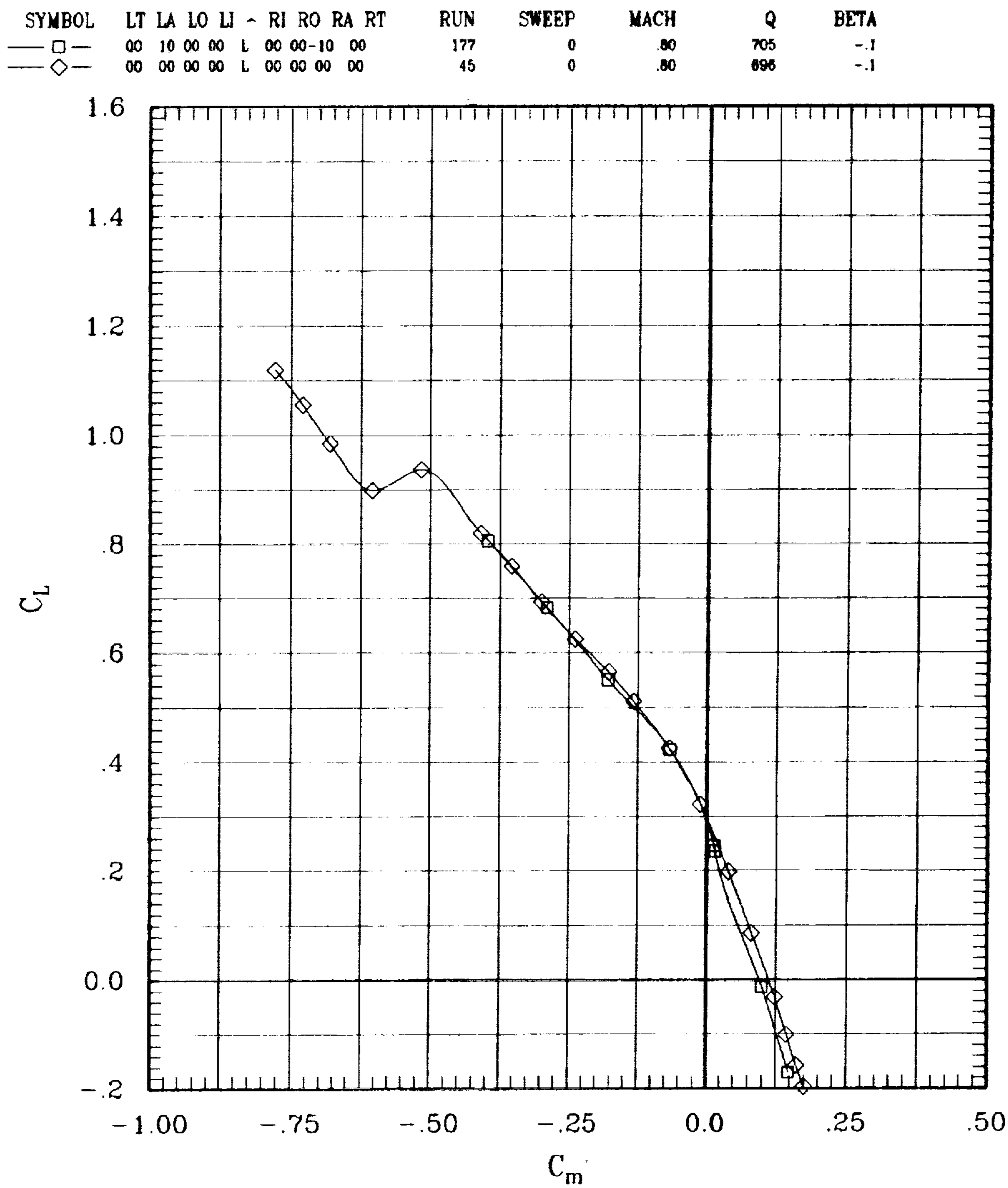

Figure 14(a). Effect of aileron deflection for sweep = 0 deg.

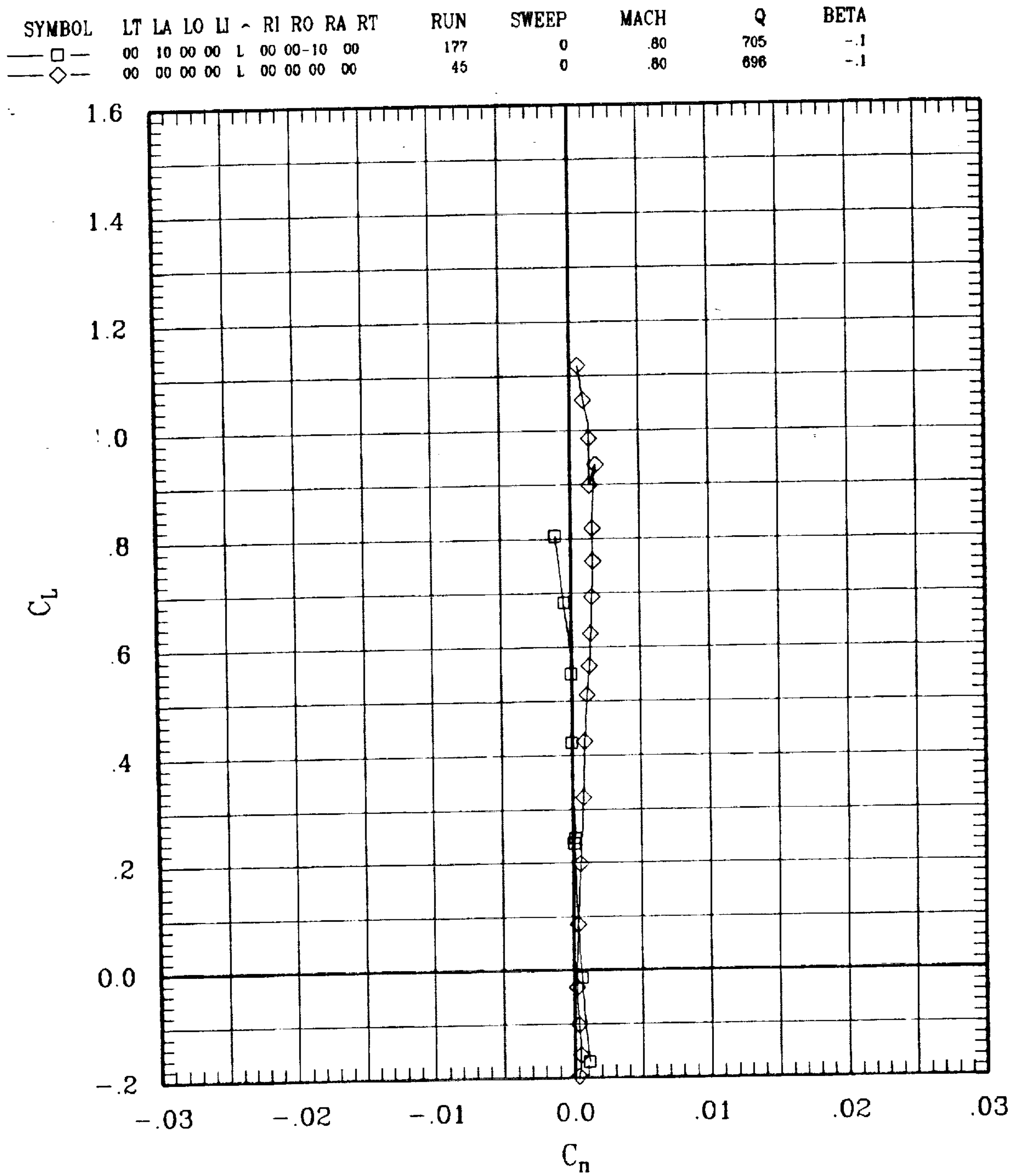

Figure 14(a). Effect of aileron deflection for sweep = 0 deg.

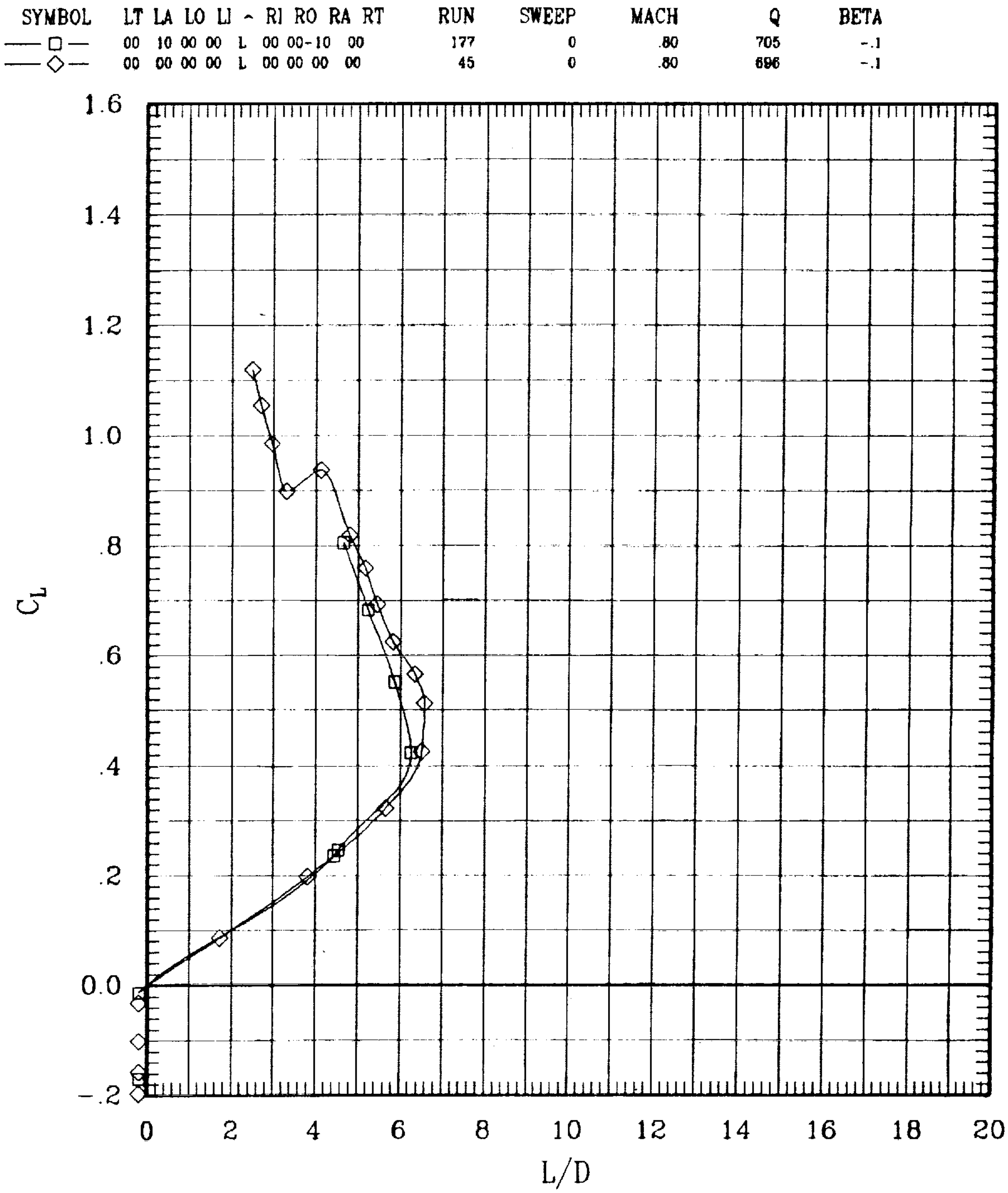

Figure 14(a). Effect of aileron deflection for sweep = 0 deg.

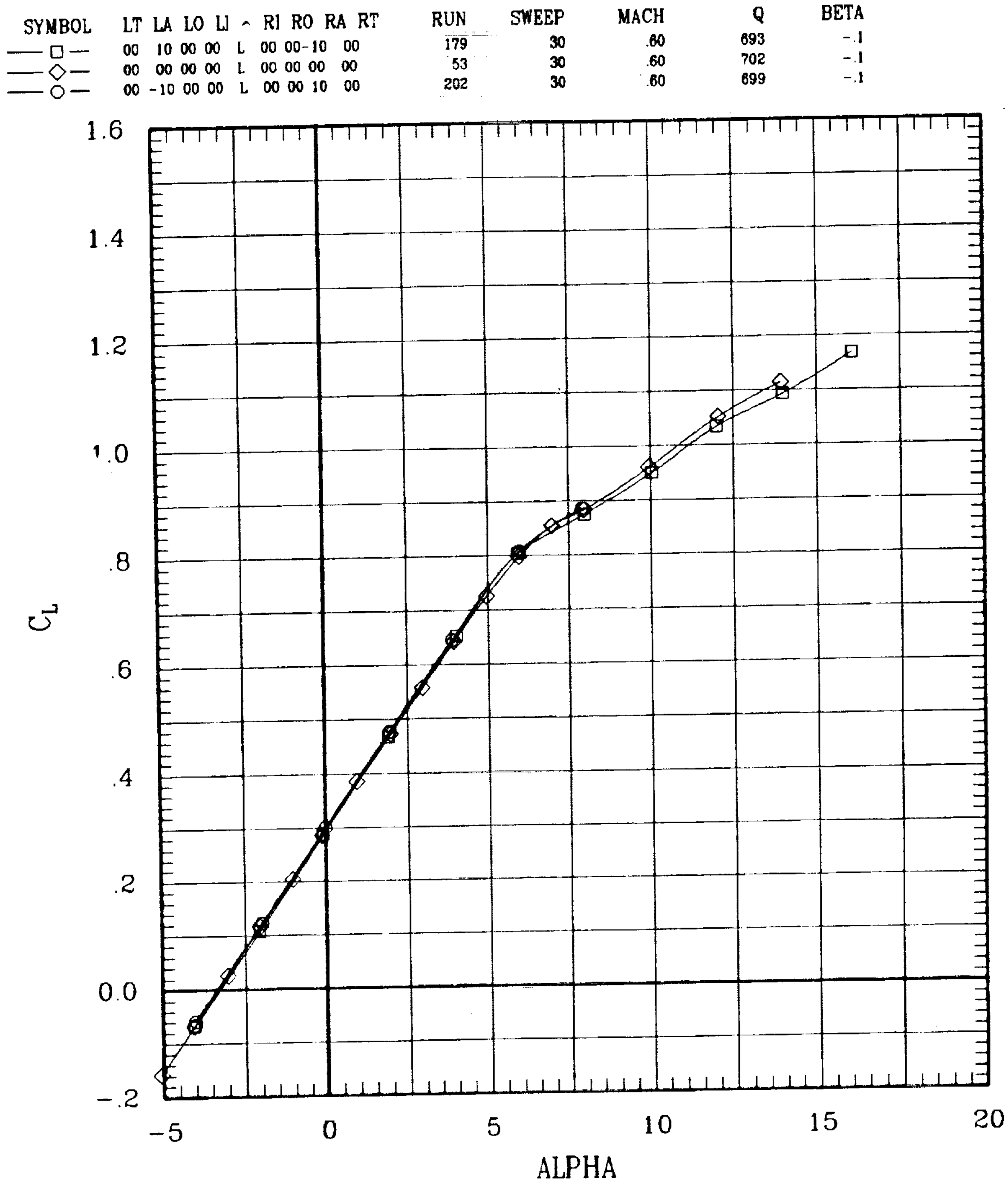

Figure 14(b). Effect of aileron deflection for sweep = 30 deg.

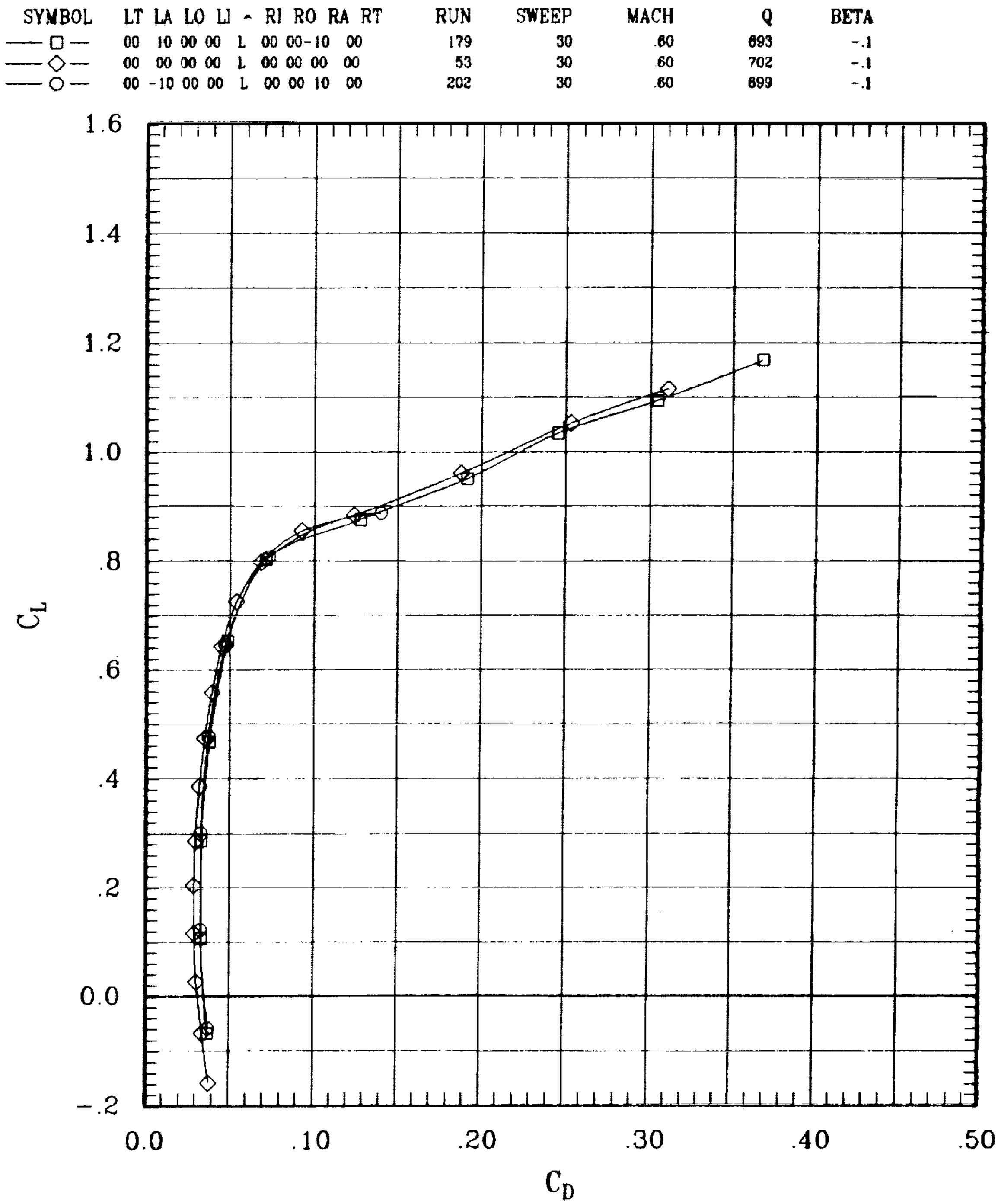

Figure 14(b). Effect of aileron deflection for sweep = 30 deg.

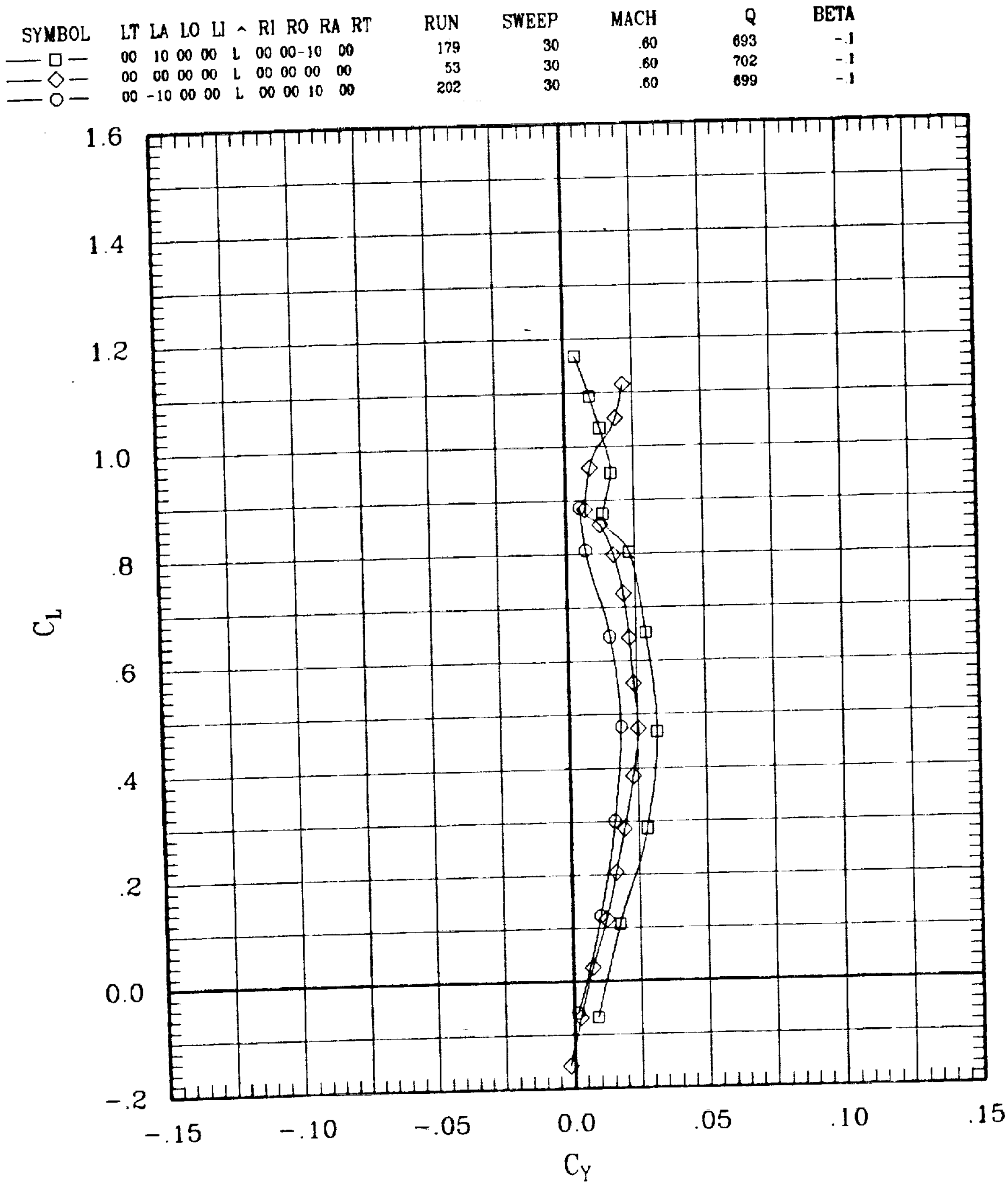

Figure 14(b). Effect of aileron deflection for sweep = 30 deg.

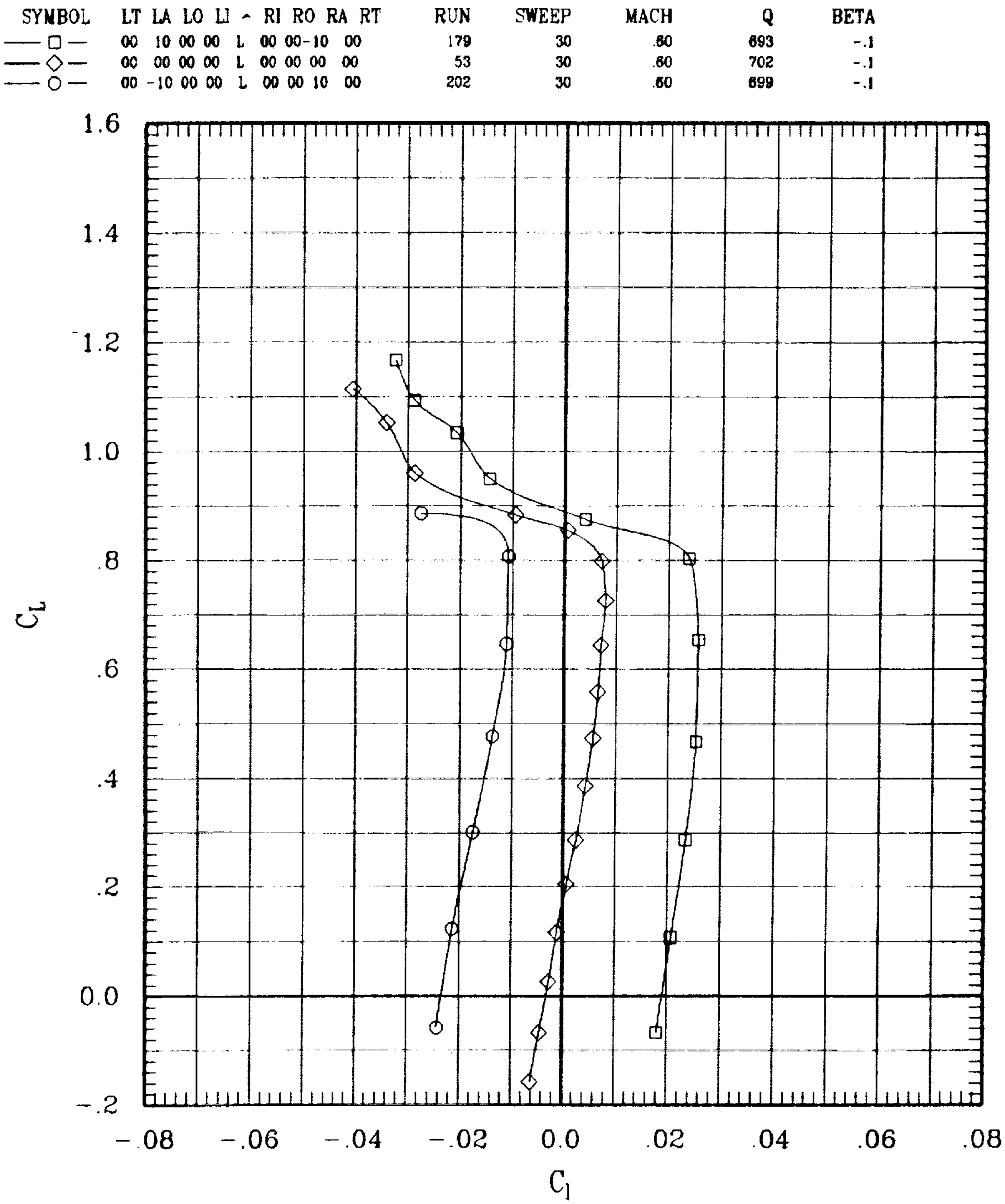

Figure 14(b). Effect of aileron deflection for sweep = 30 deg.

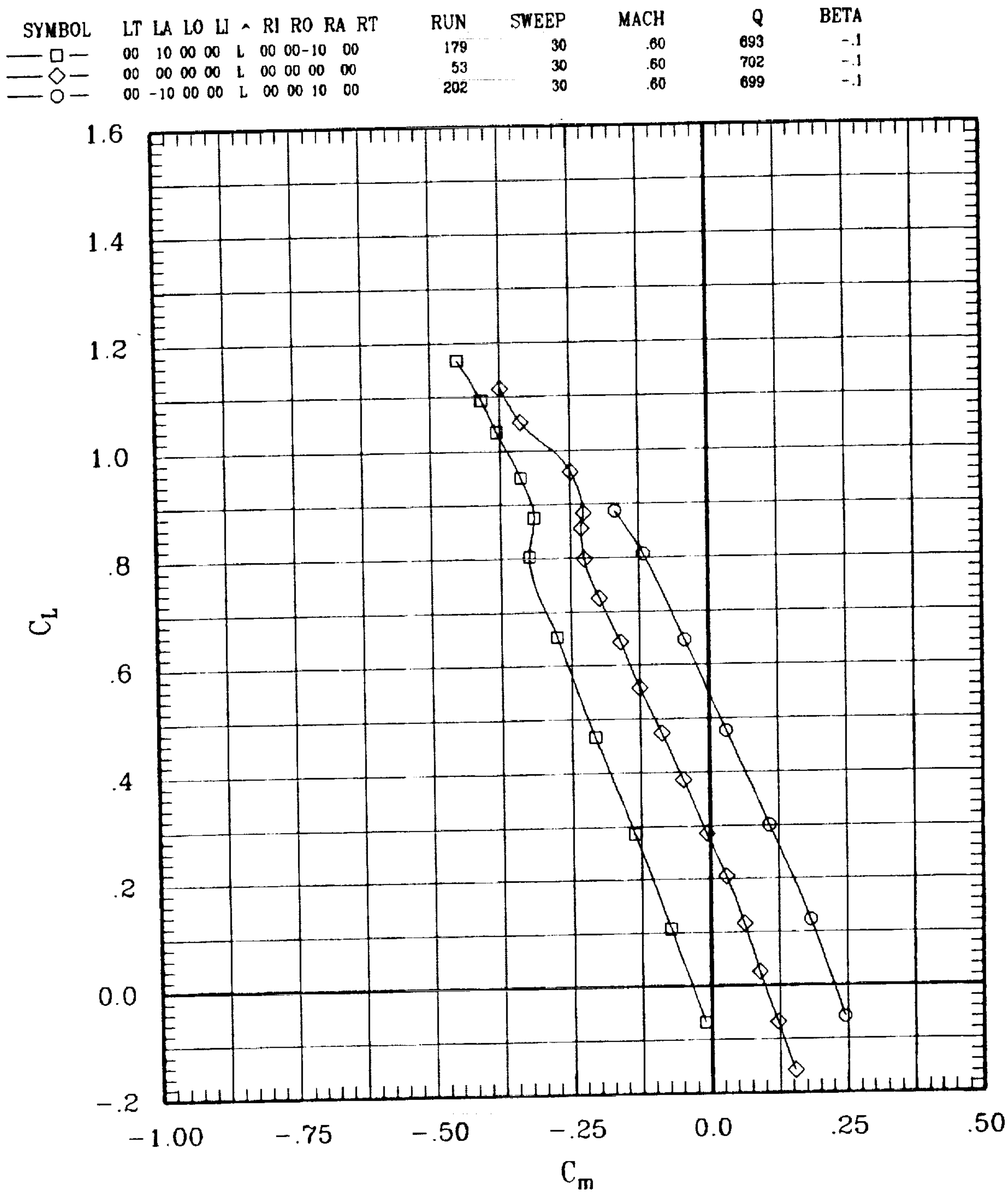

Figure 14(b). Effect of aileron deflection for sweep = 30 deg.

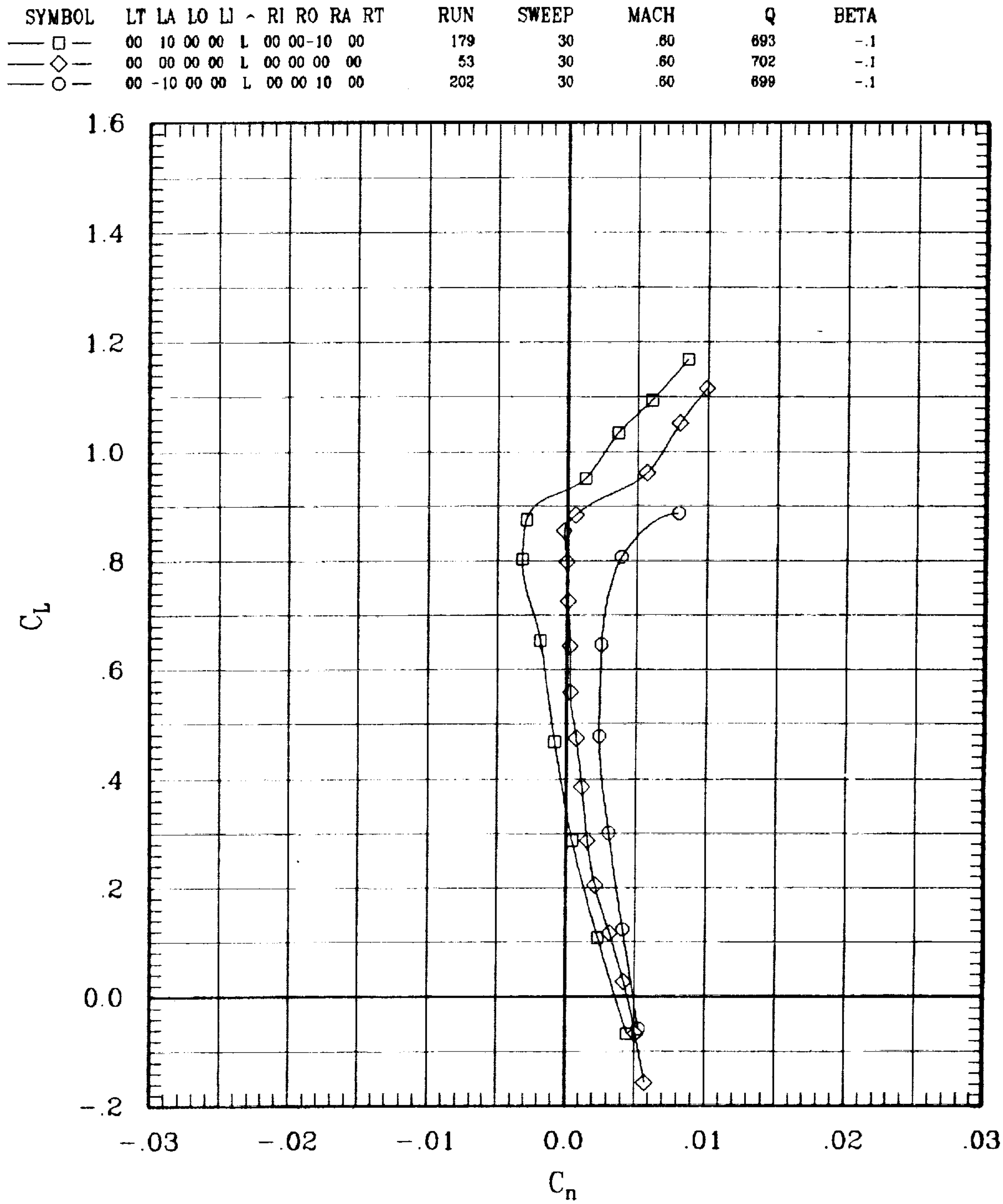

Figure 14(b). Effect of aileron deflection for sweep = 30 deg.

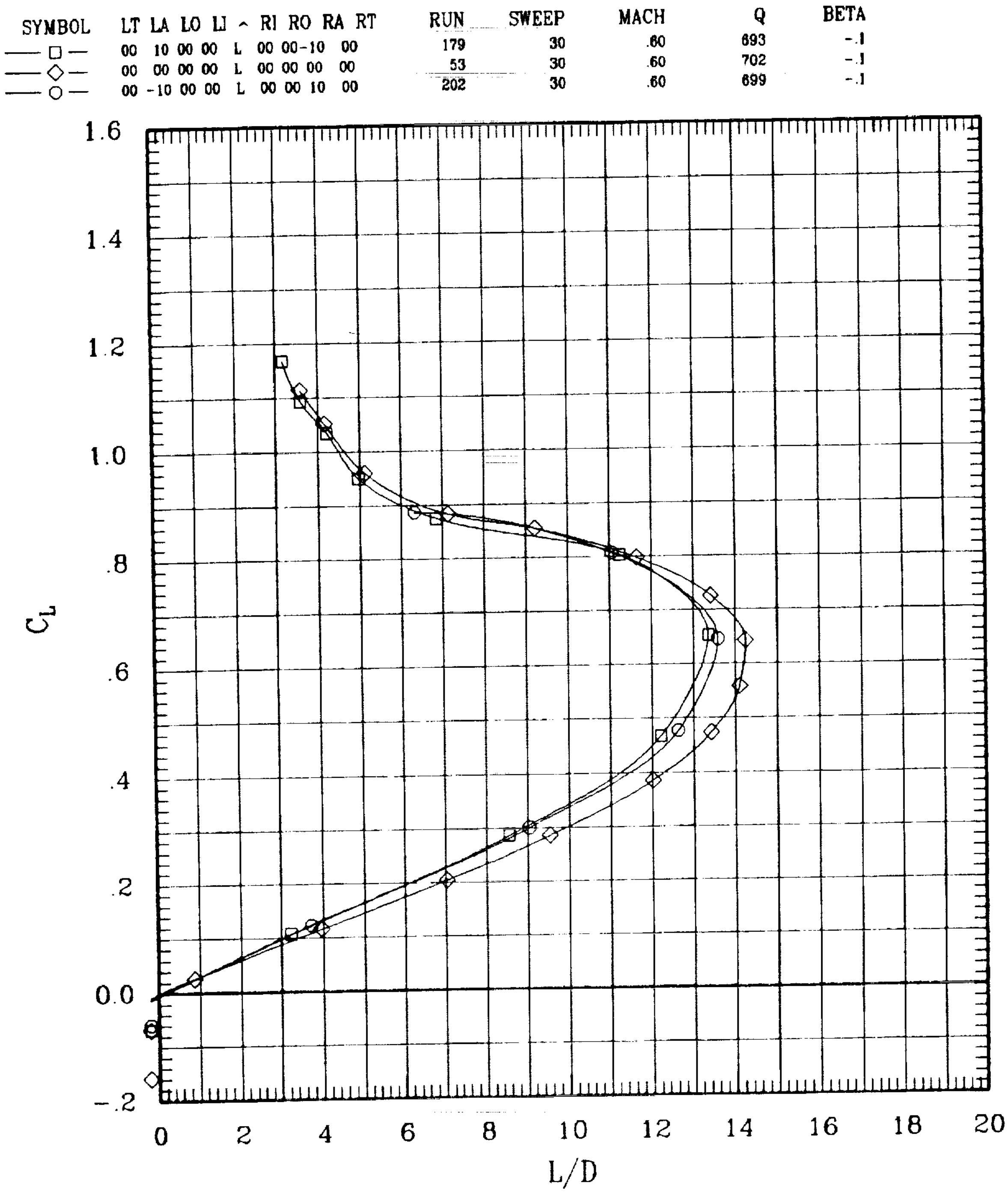

Figure 14(b). Effect of aileron deflection for sweep = 30 deg.

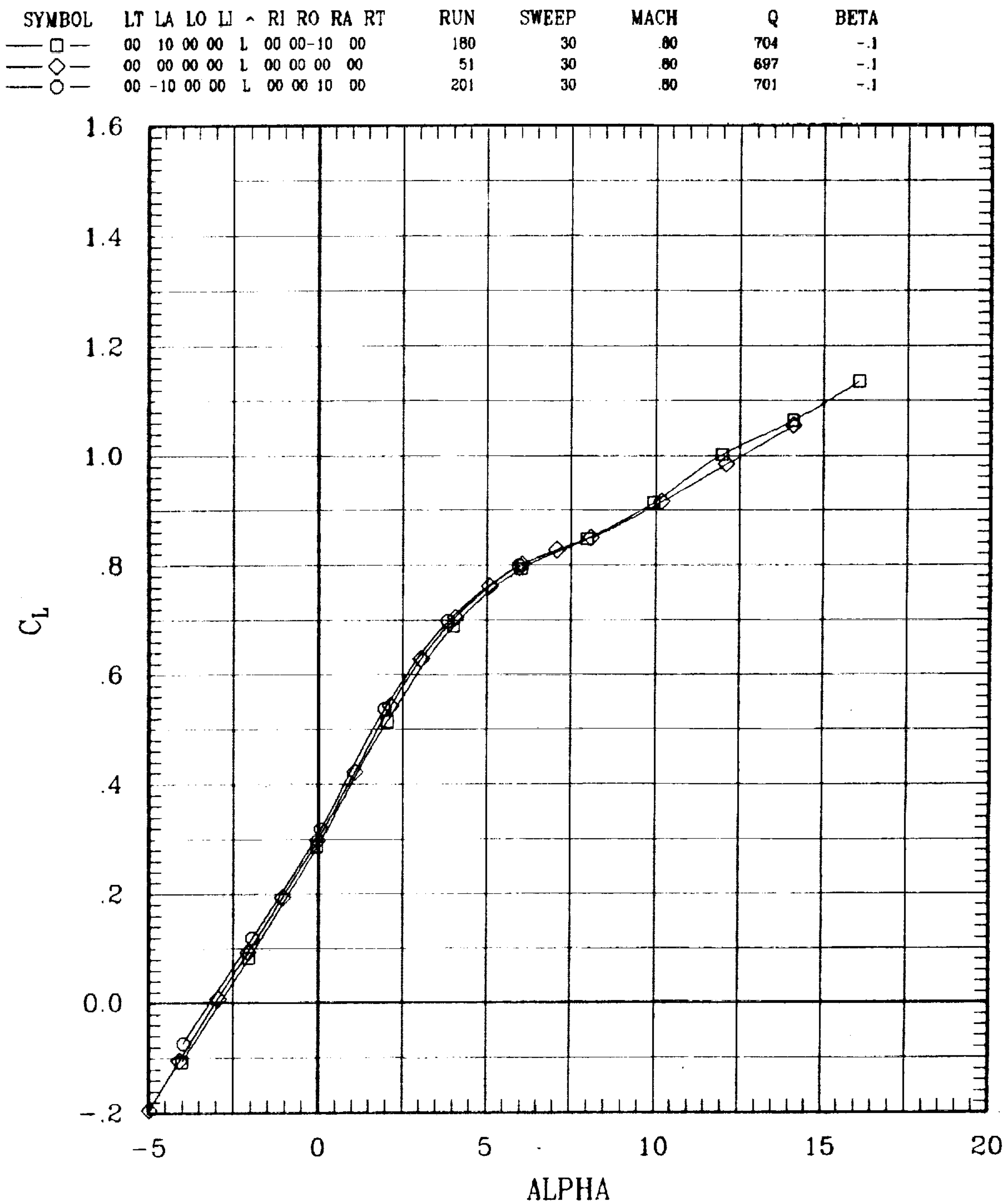

Figure 14(b). Effect of aileron deflection for sweep = 30 deg.

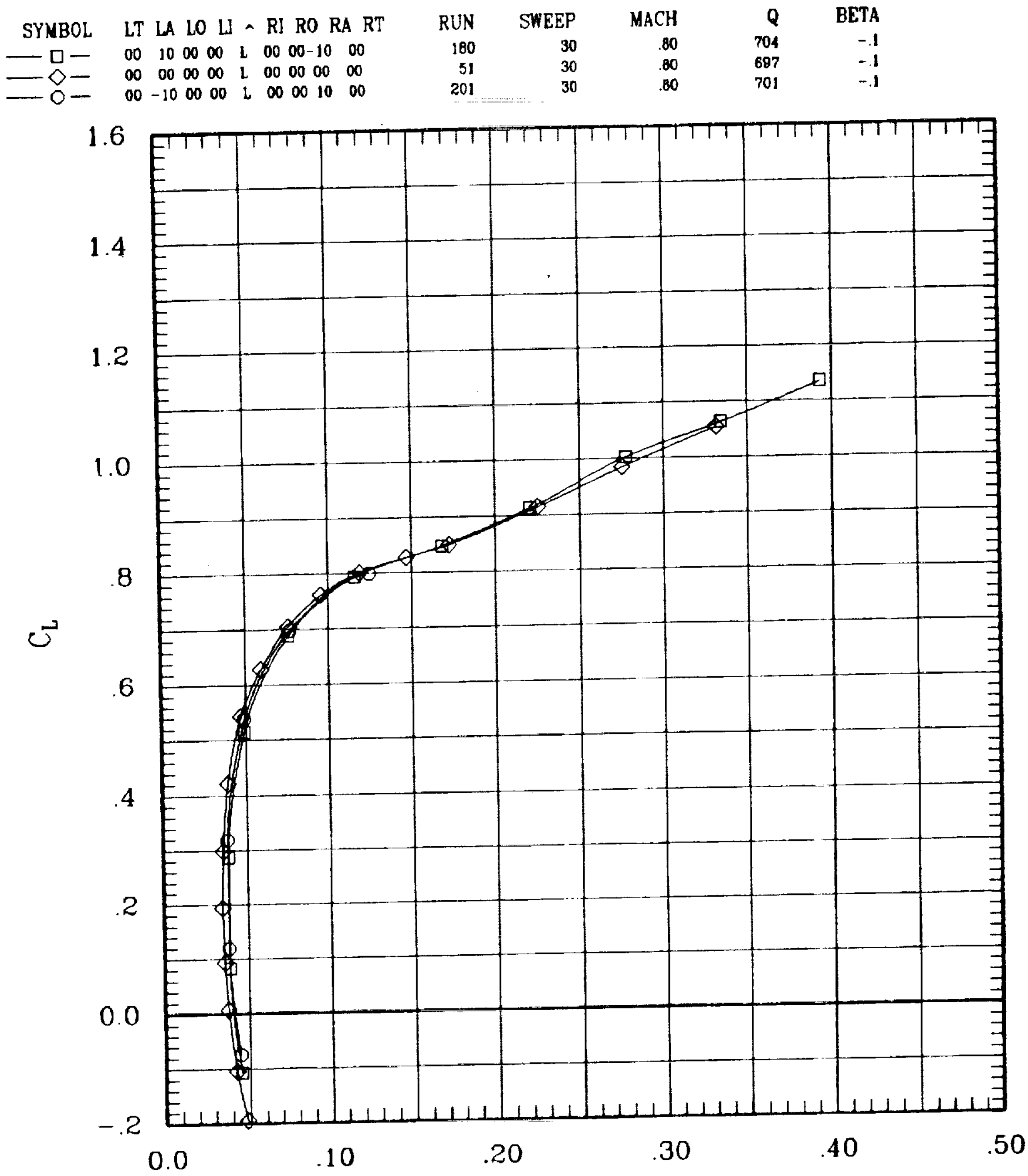

Figure 14(b). Effect of aileron deflection for sweep = 30 deg.

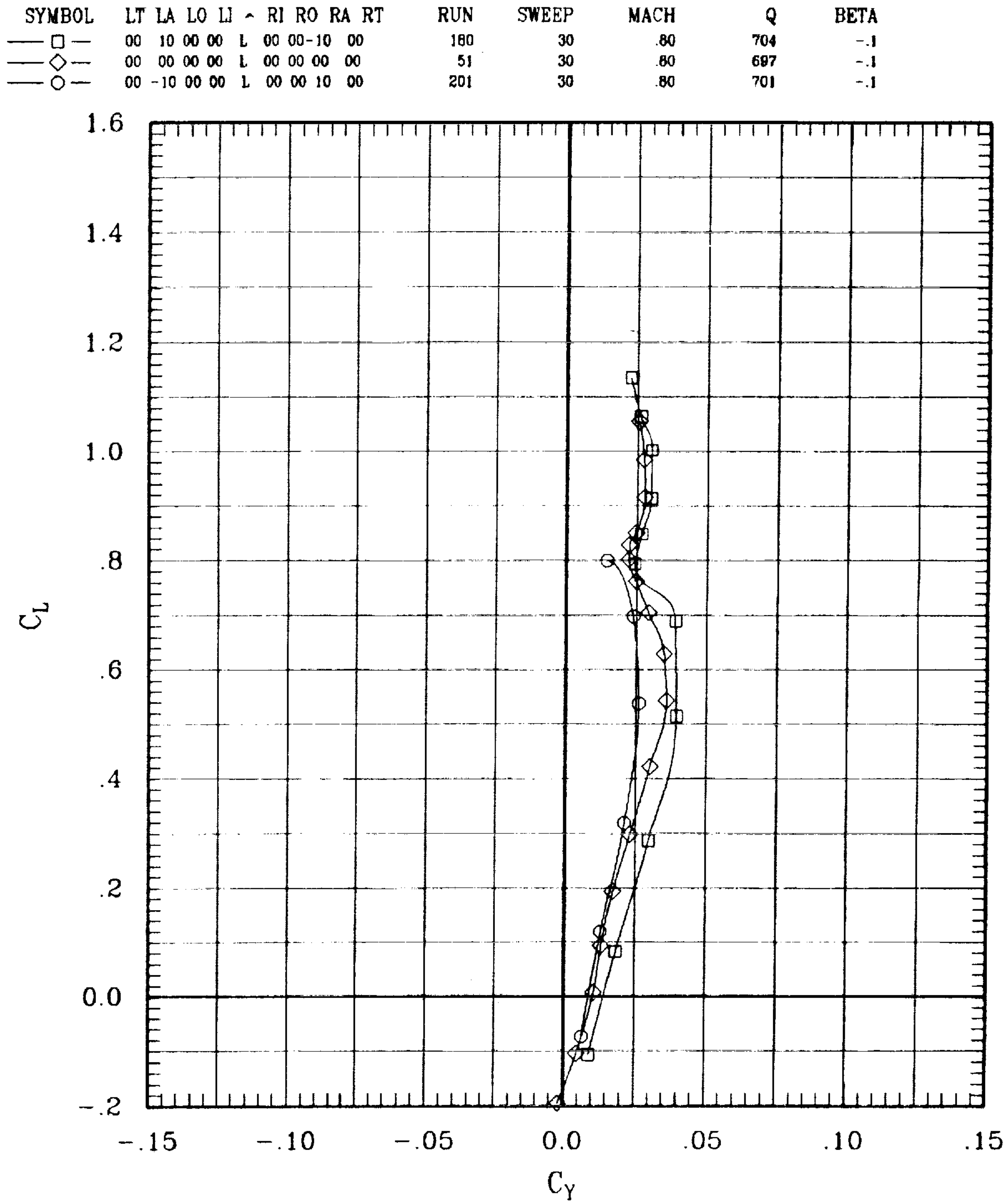

Figure 14(b). Effect of aileron deflection for sweep = 30 deg.

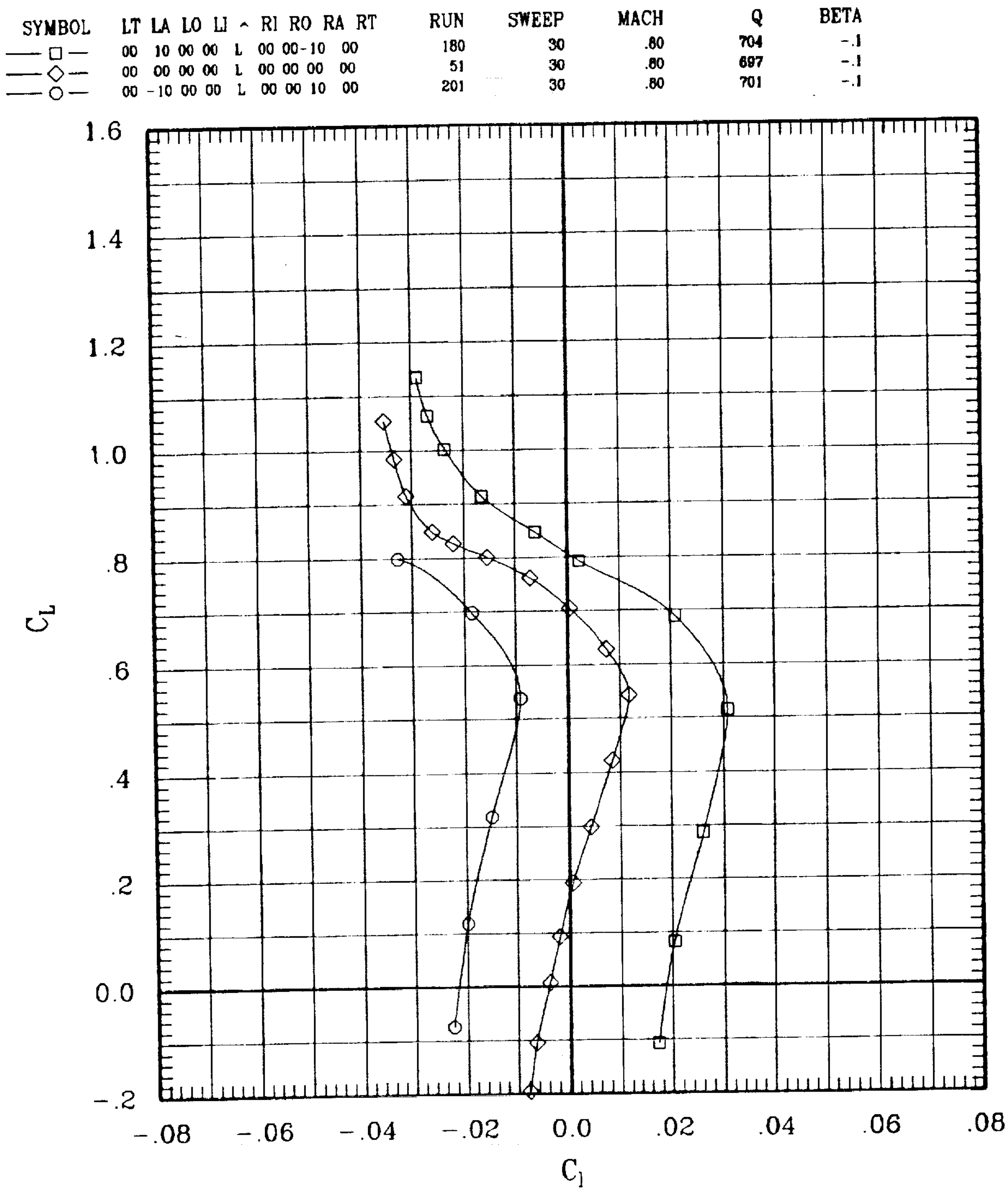

Figure 14(b). Effect of aileron deflection for sweep = 30 deg.

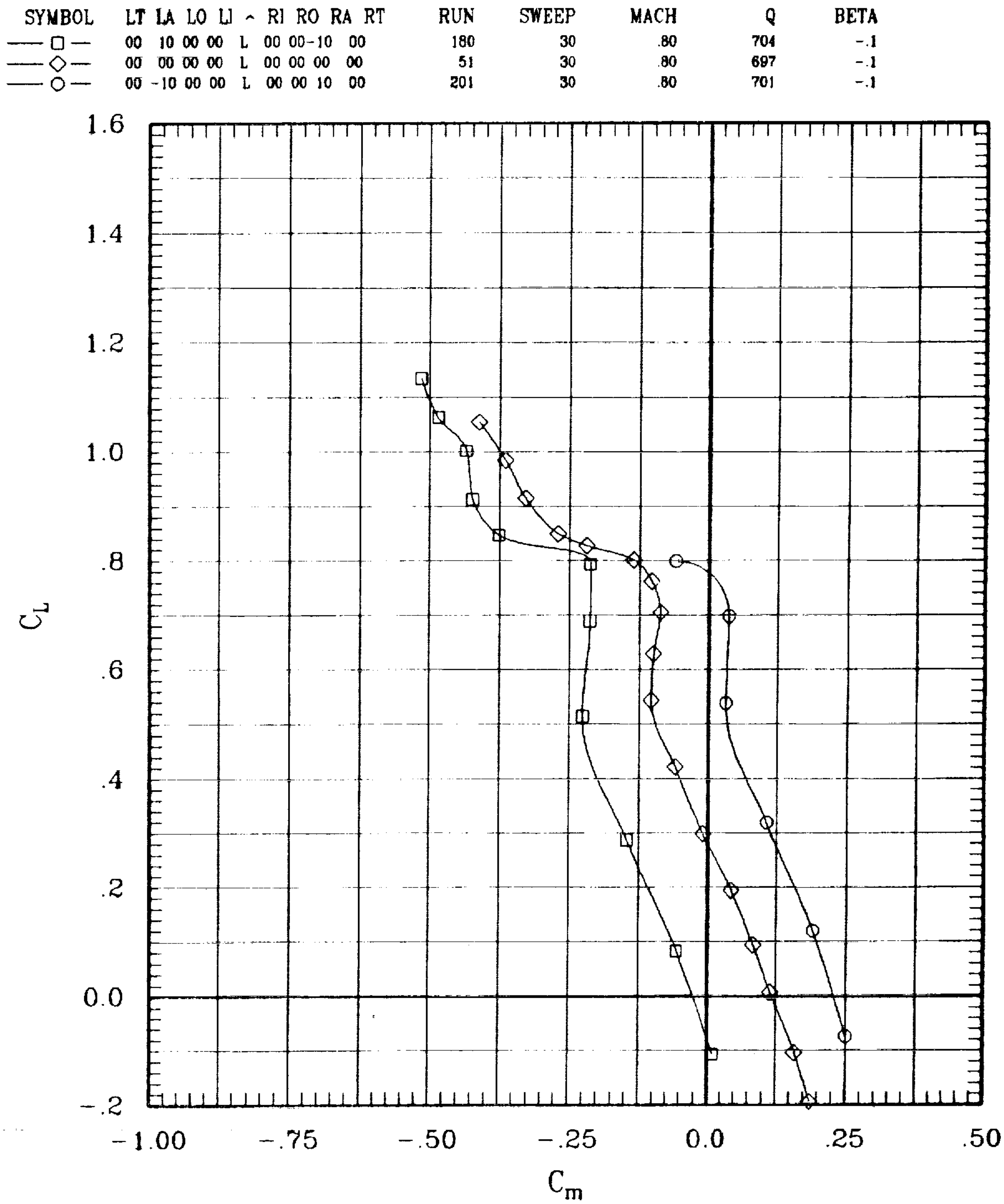

Figure 14(b). Effect of aileron deflection for sweep = 30 deg.

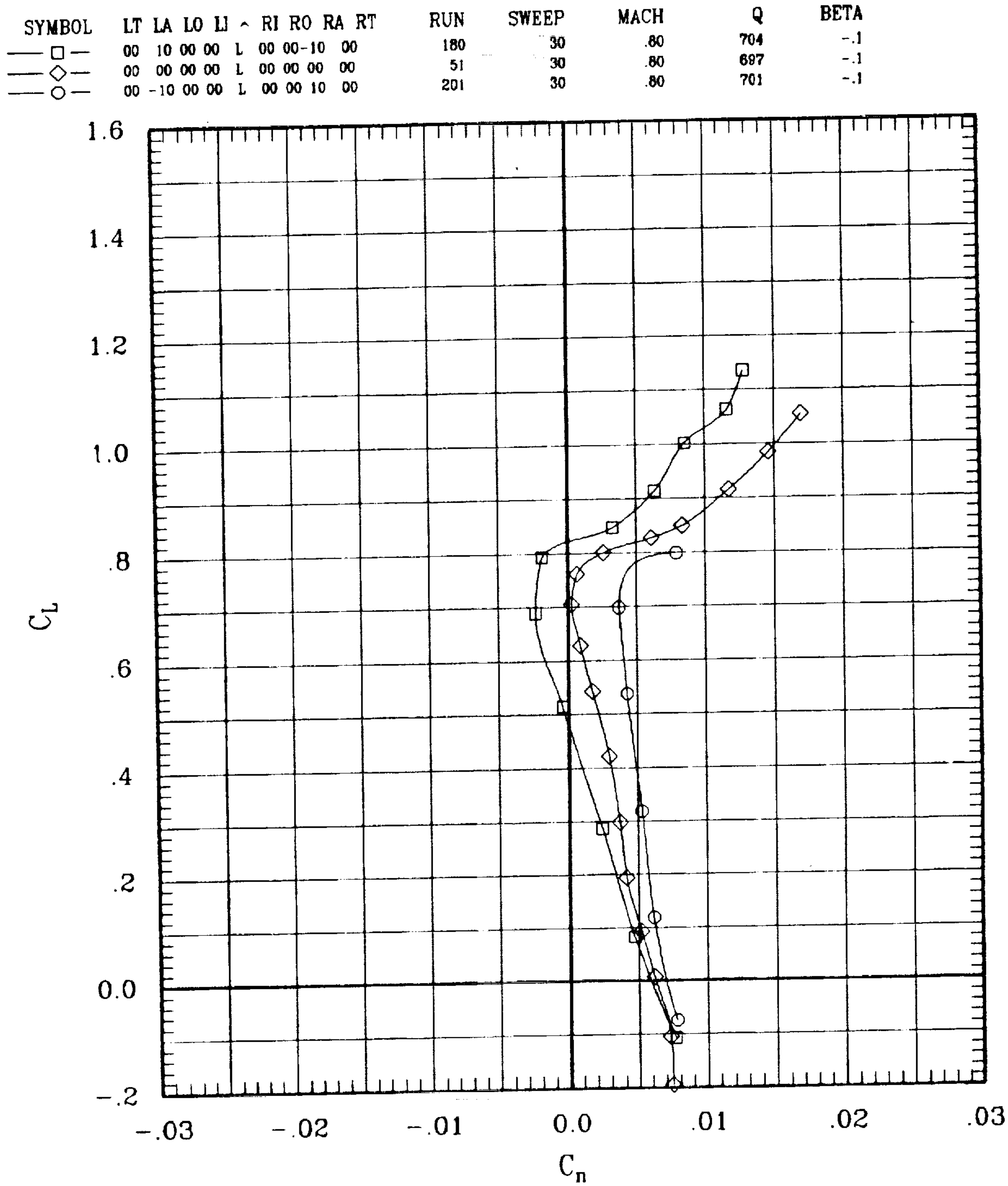

Figure 14(b). Effect of aileron deflection for sweep = 30 deg.

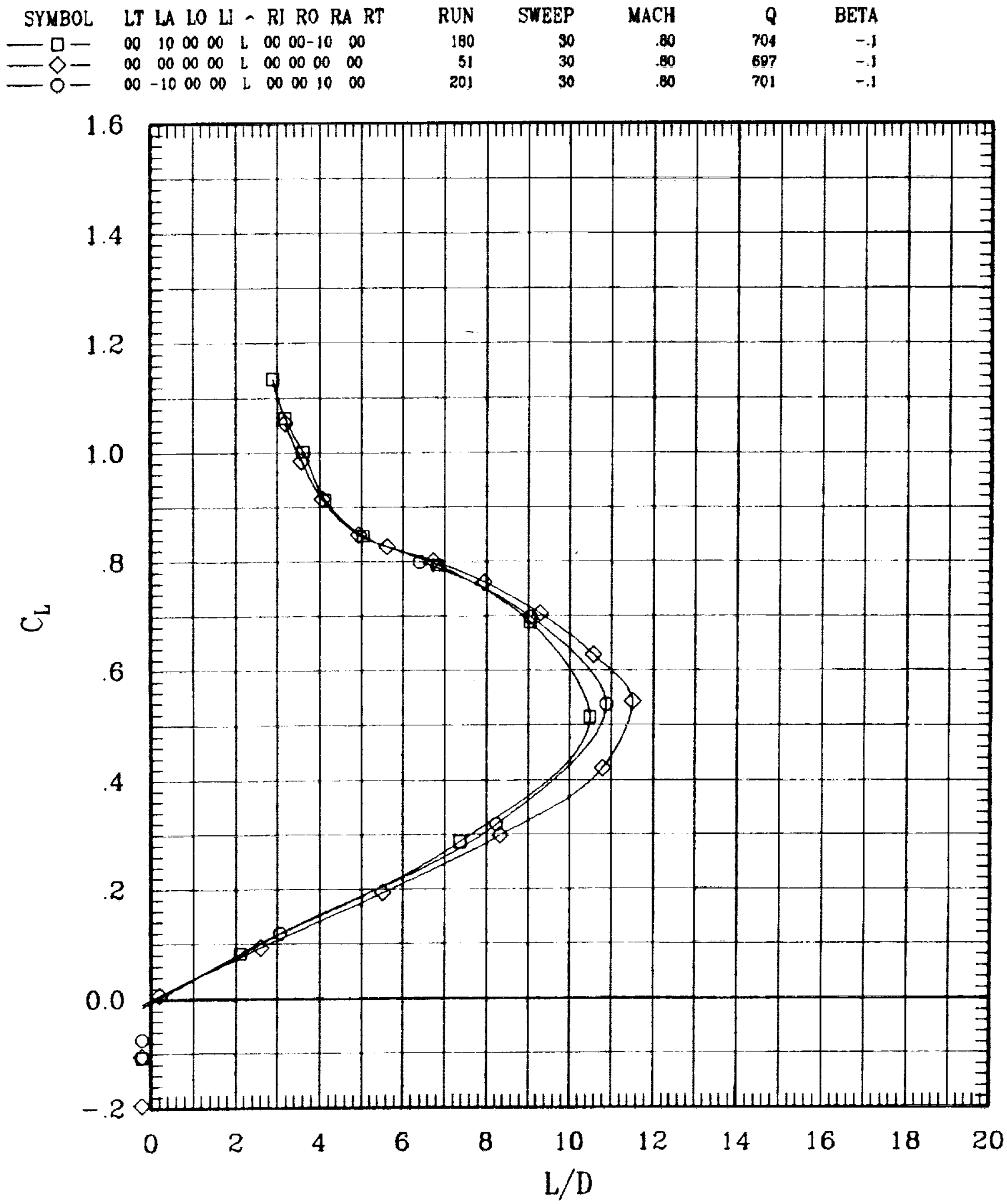

Figure 14(b). Effect of aileron deflection for sweep = 30 deg.

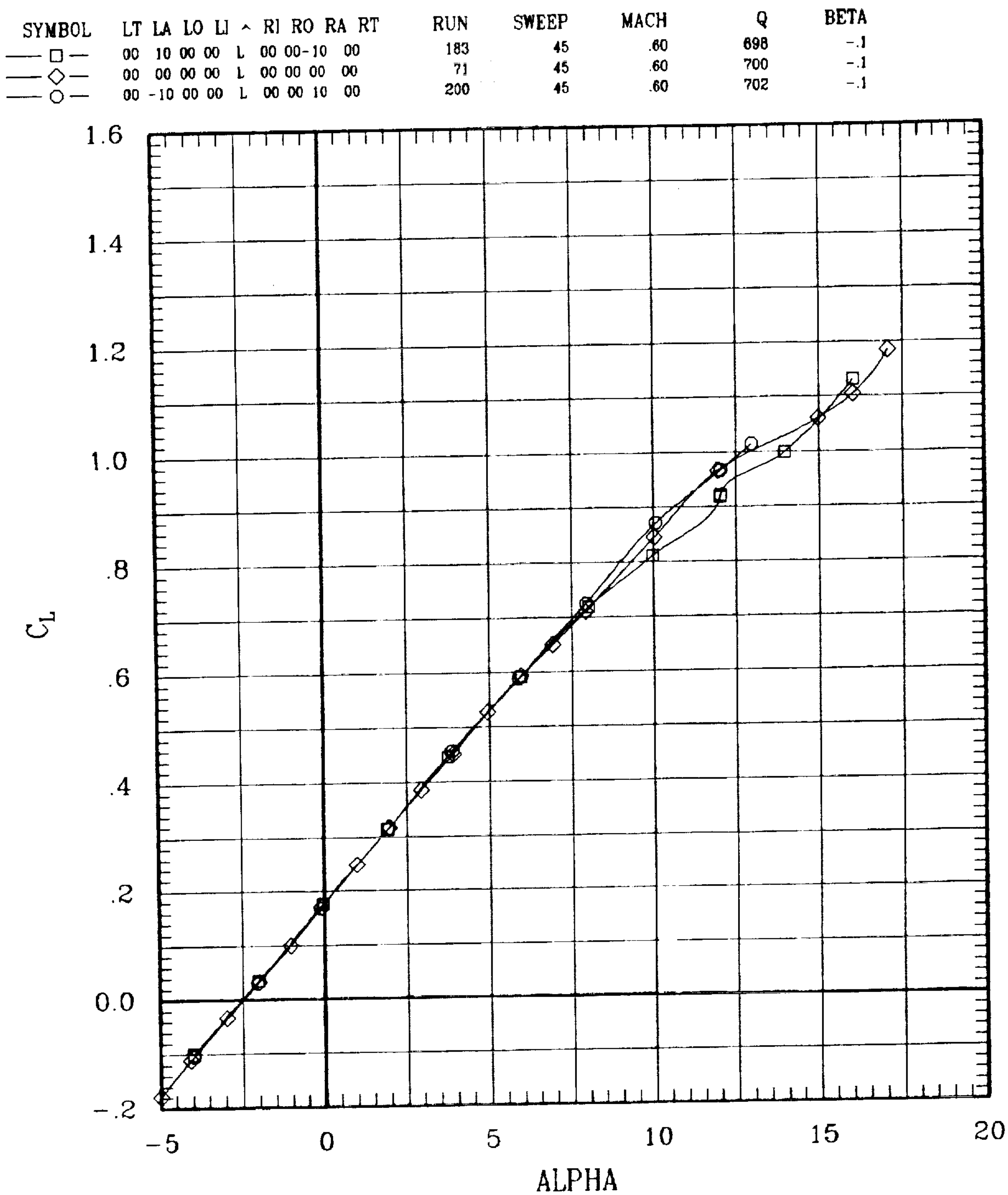

Figure 14(c). Effect of aileron deflection for sweep = 45 deg.

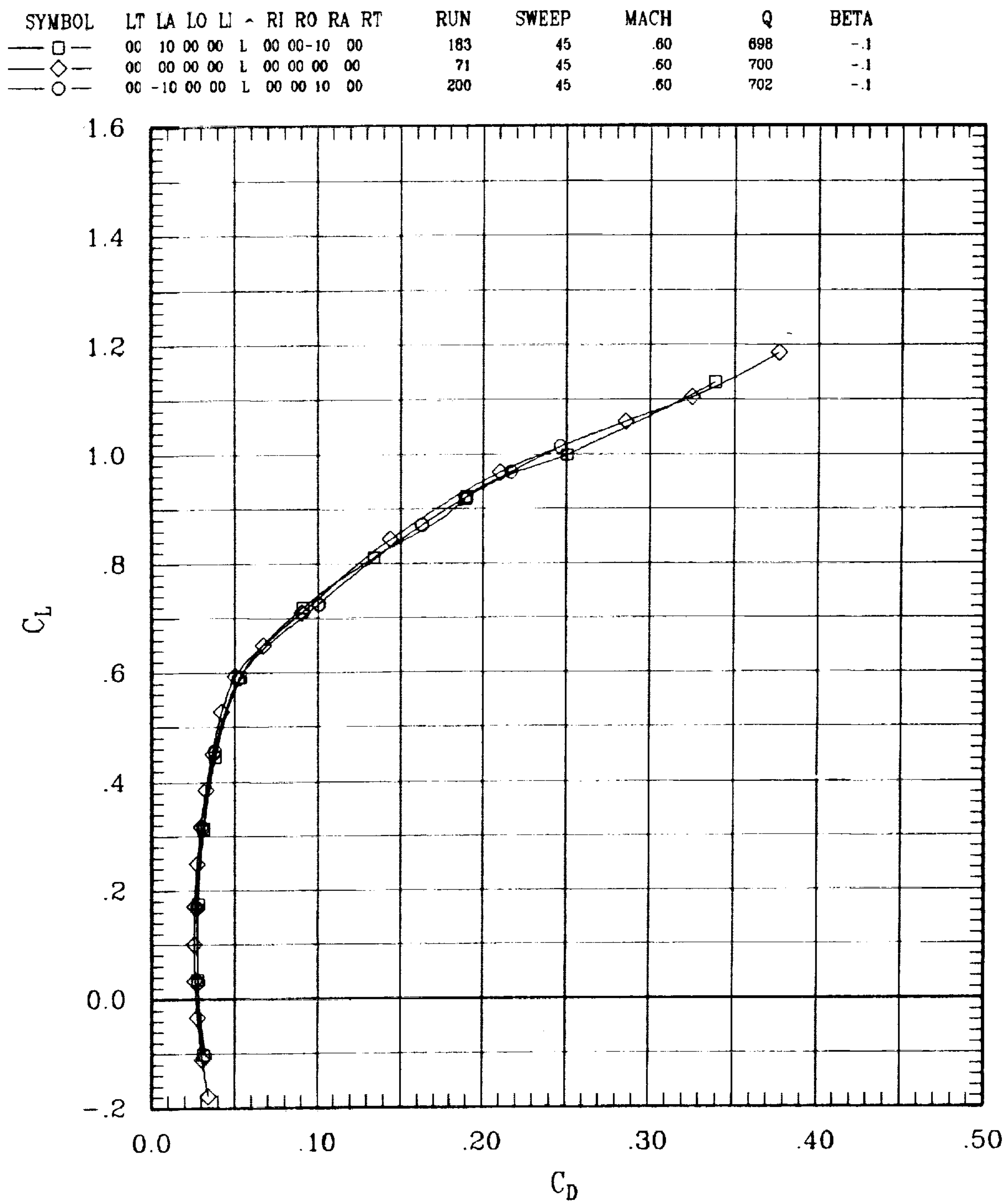

Figure 14(c). Effect of aileron deflection for sweep = 45 deg.

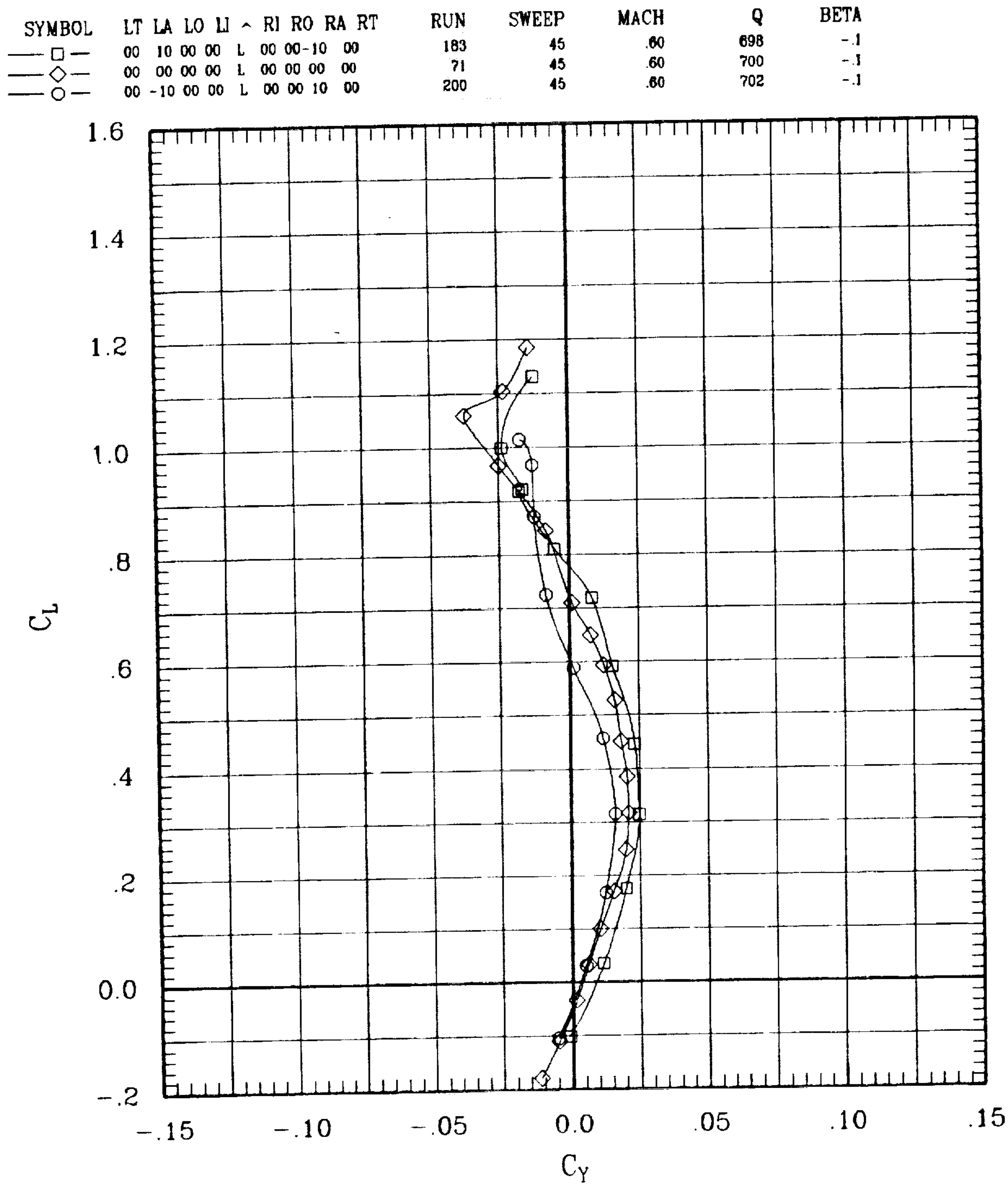

Figure 14(c). Effect of aileron deflection for sweep = 45 deg.

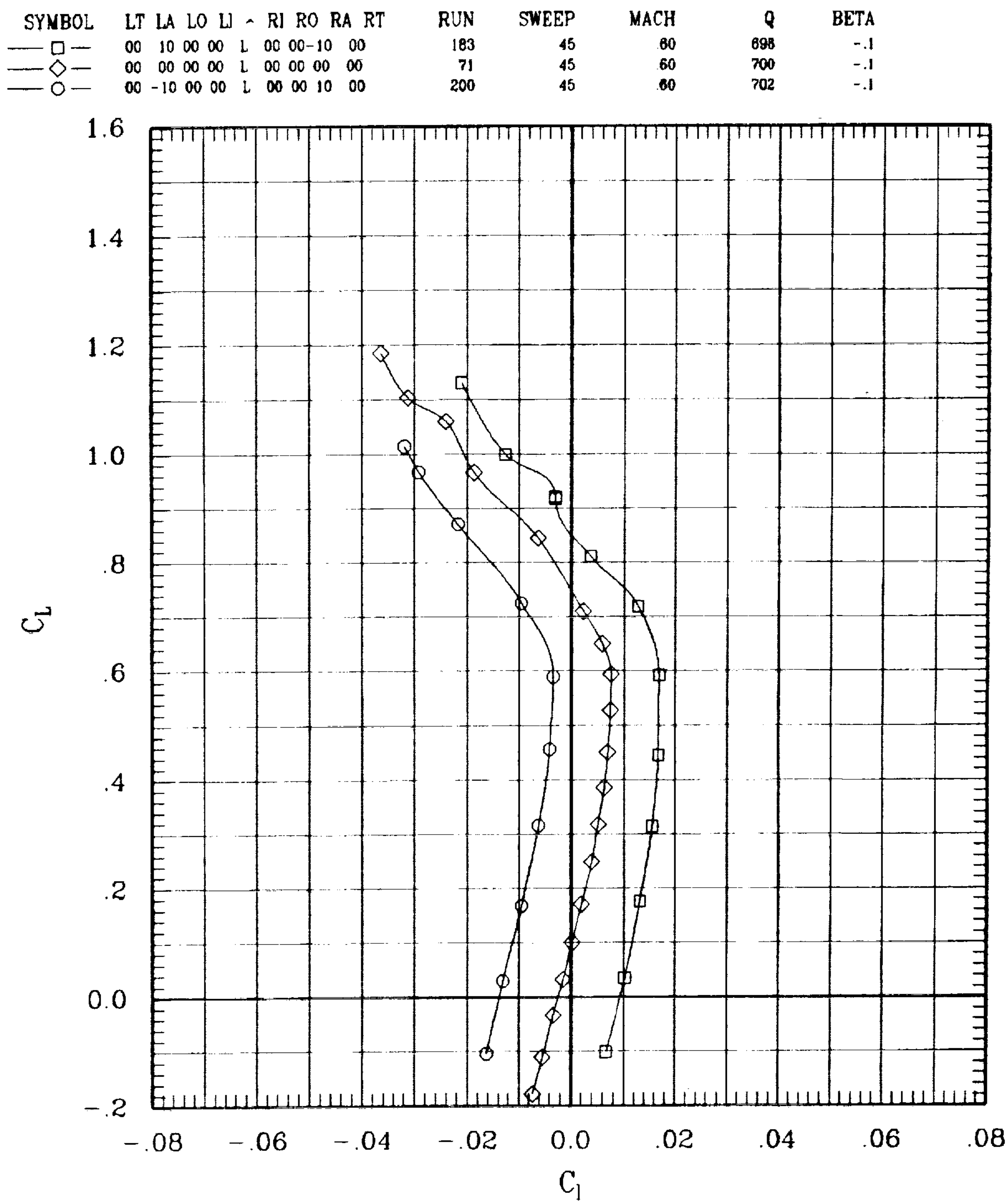

Figure 14(c). Effect of aileron deflection for sweep = 45 deg.

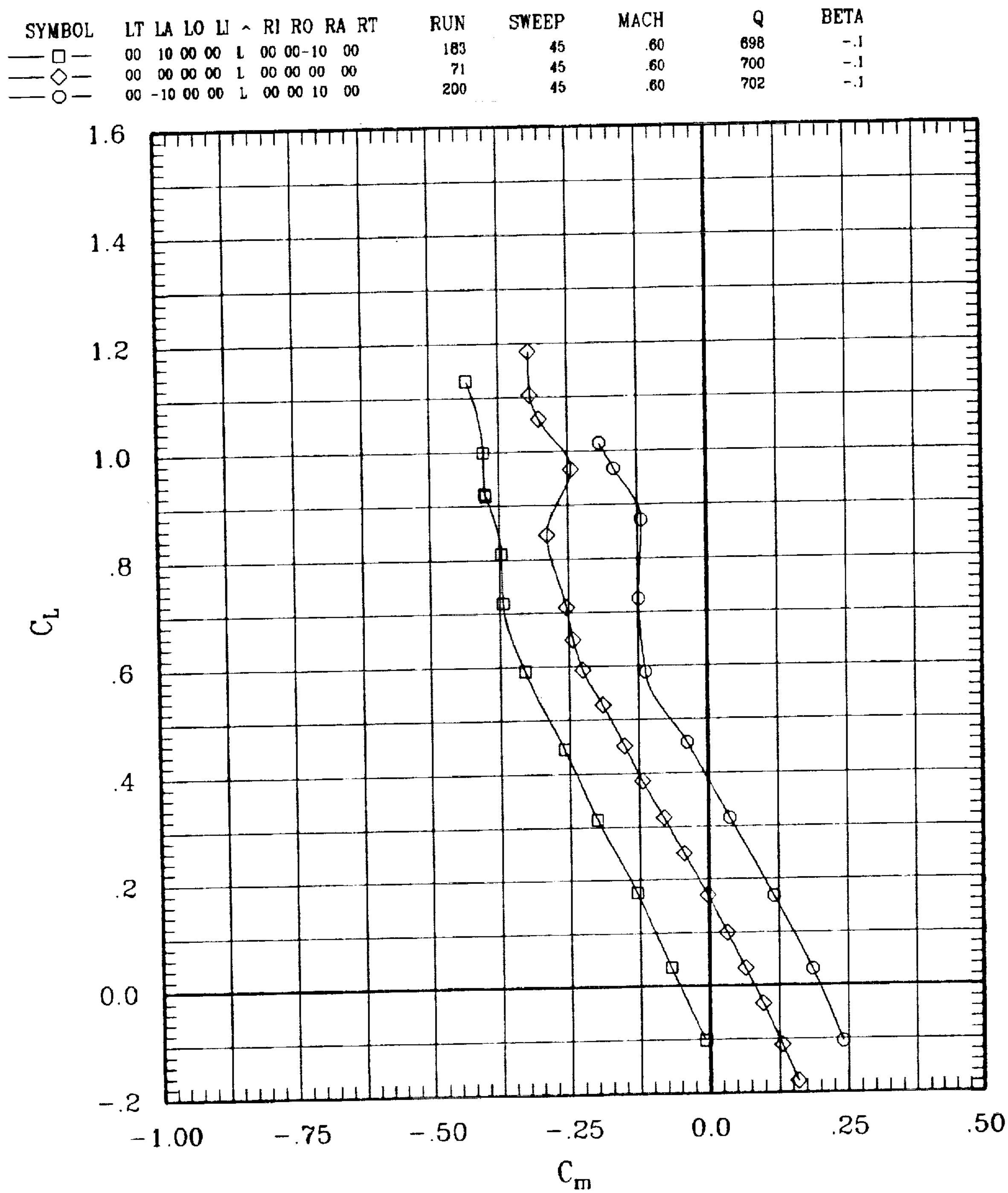

Figure 14(c). Effect of aileron deflection for sweep = 45 deg.

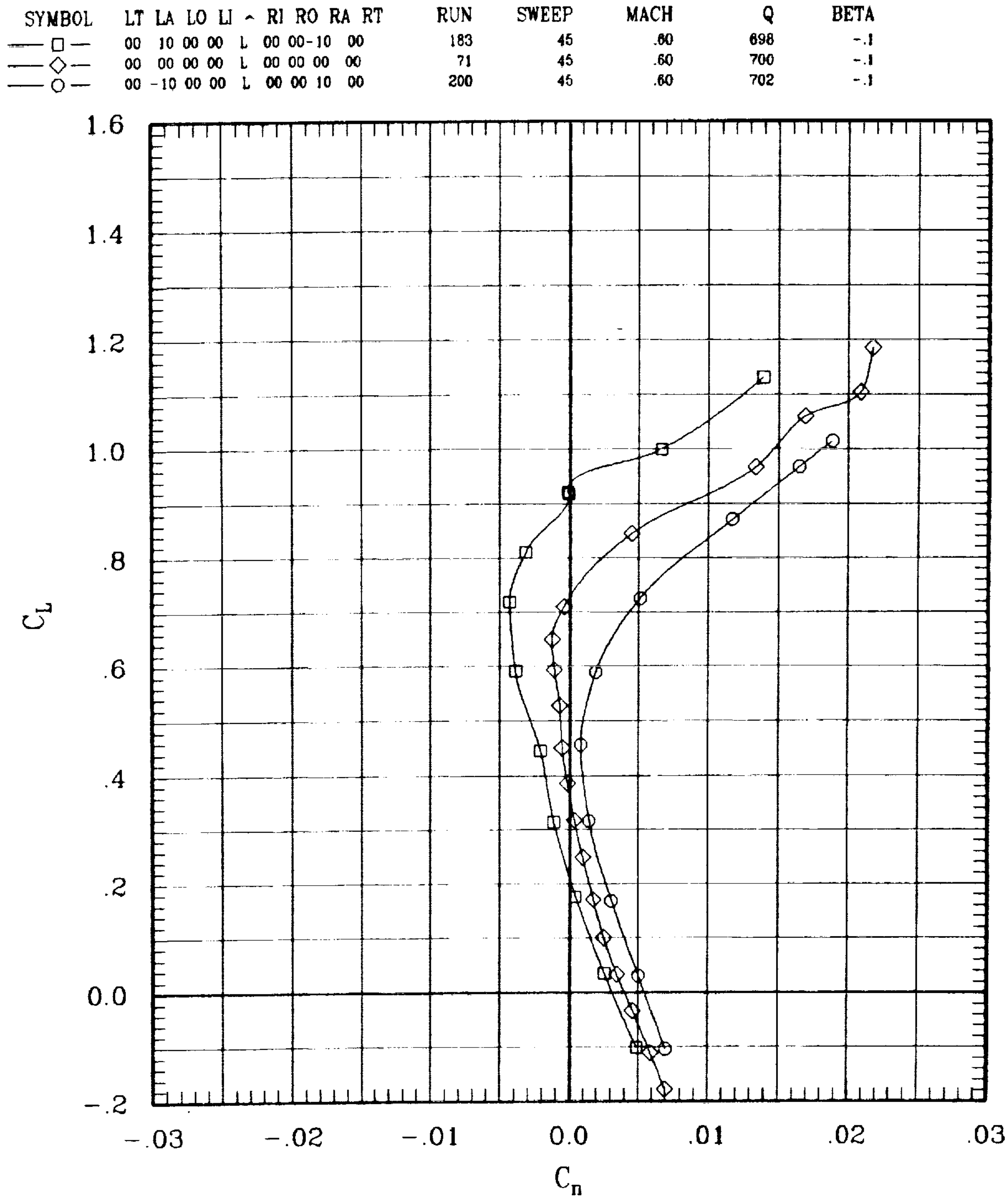

Figure 14(c). Effect of aileron deflection for sweep = 45 deg.

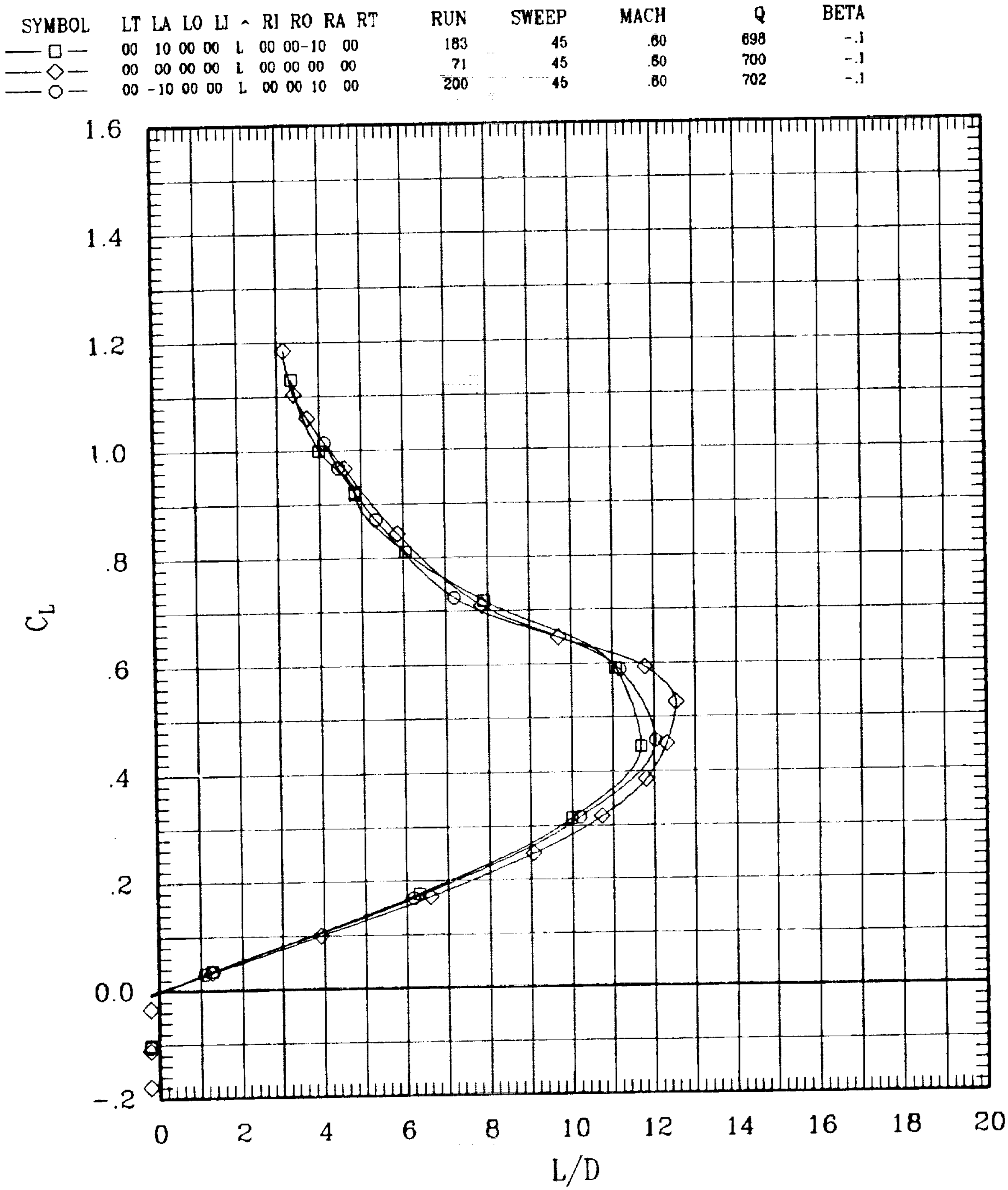

Figure 14(c). Effect of aileron deflection for sweep = 45 deg.

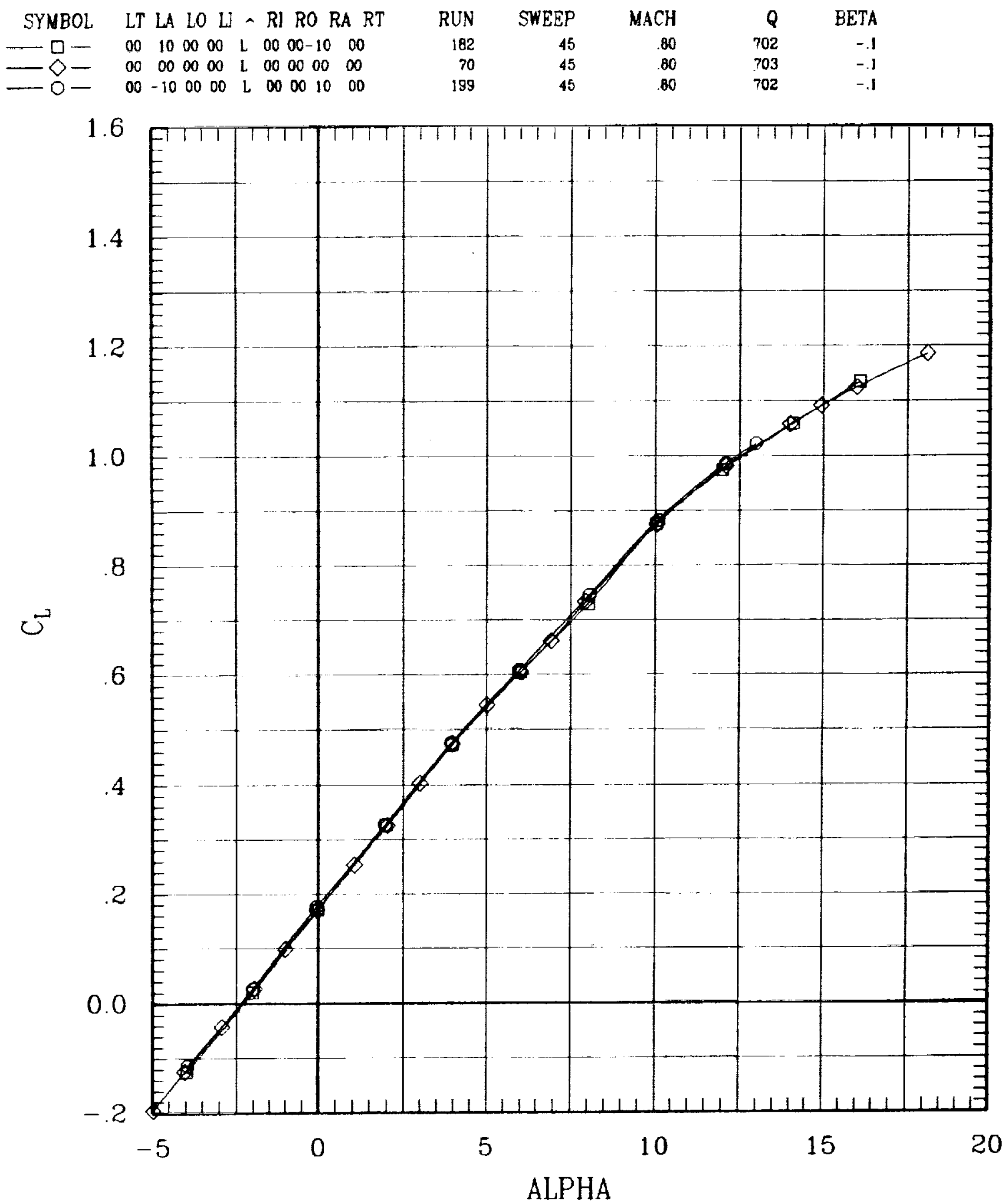

Figure 14(c). Effect of aileron deflection for sweep = 45 deg.

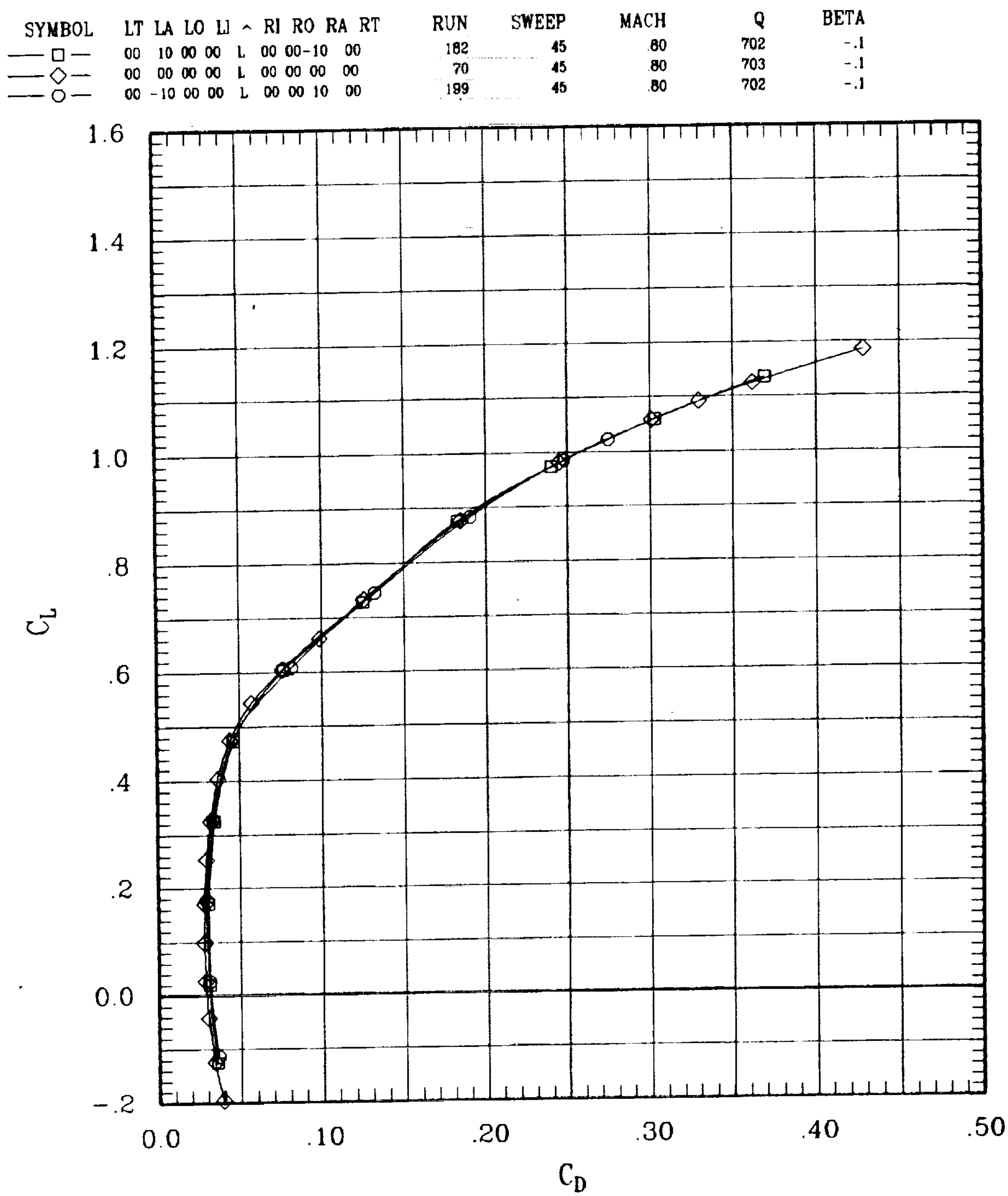

Figure 14(c). Effect of aileron deflection for sweep = 45 deg.

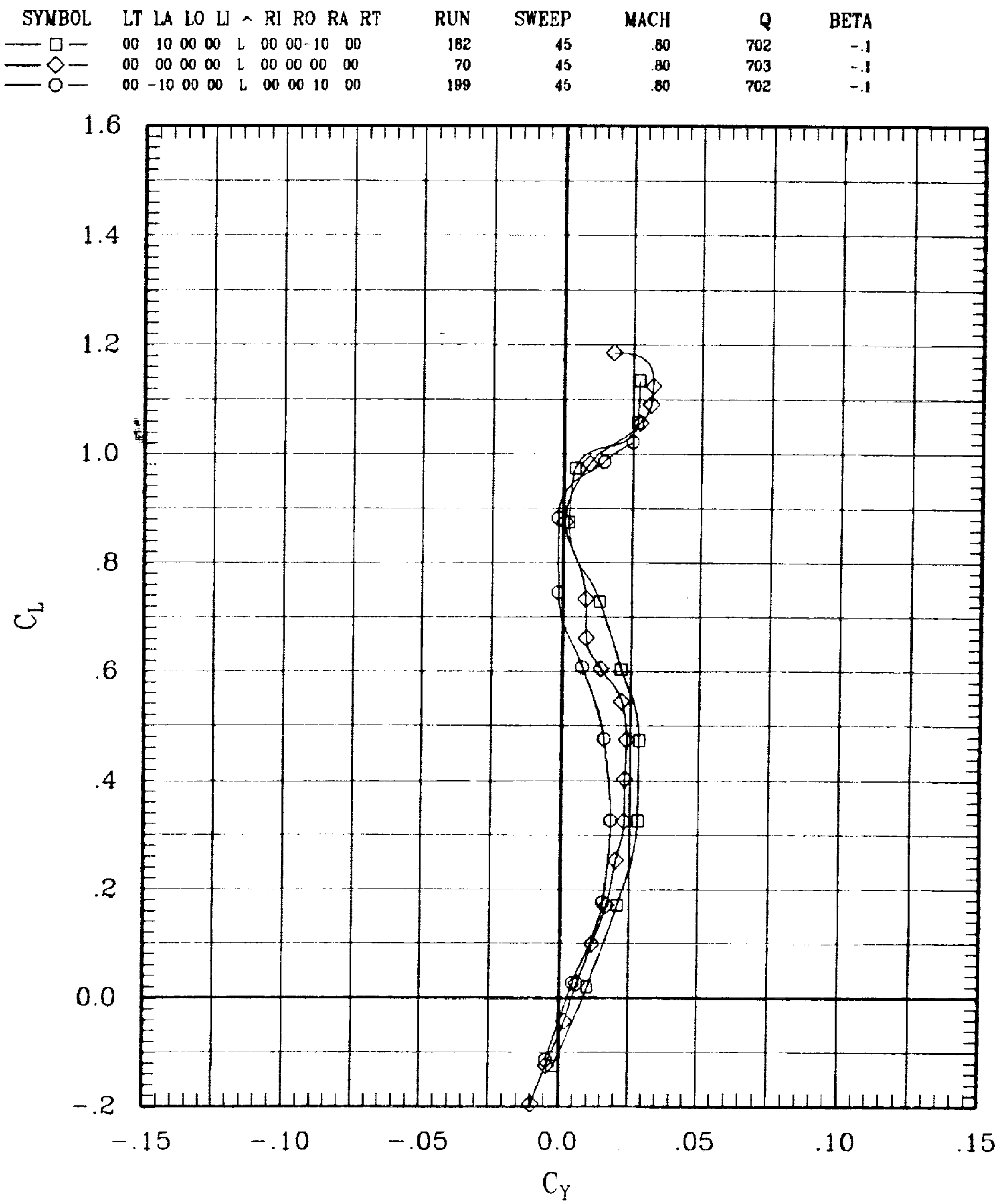

Figure 14(c). Effect of aileron deflection for sweep = 45 deg.

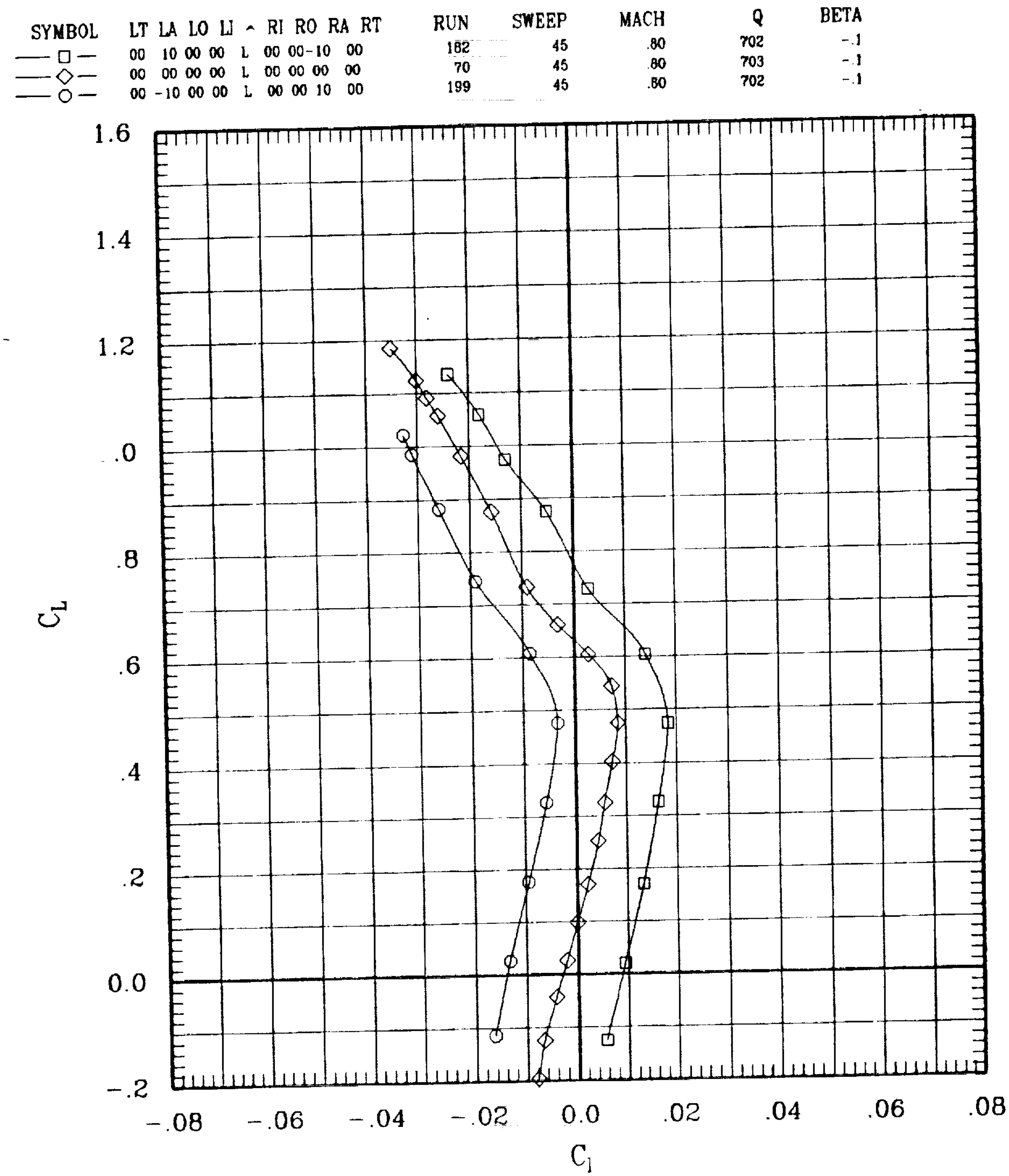

Figure 14(c). Effect of aileron deflection for sweep = 45 deg.

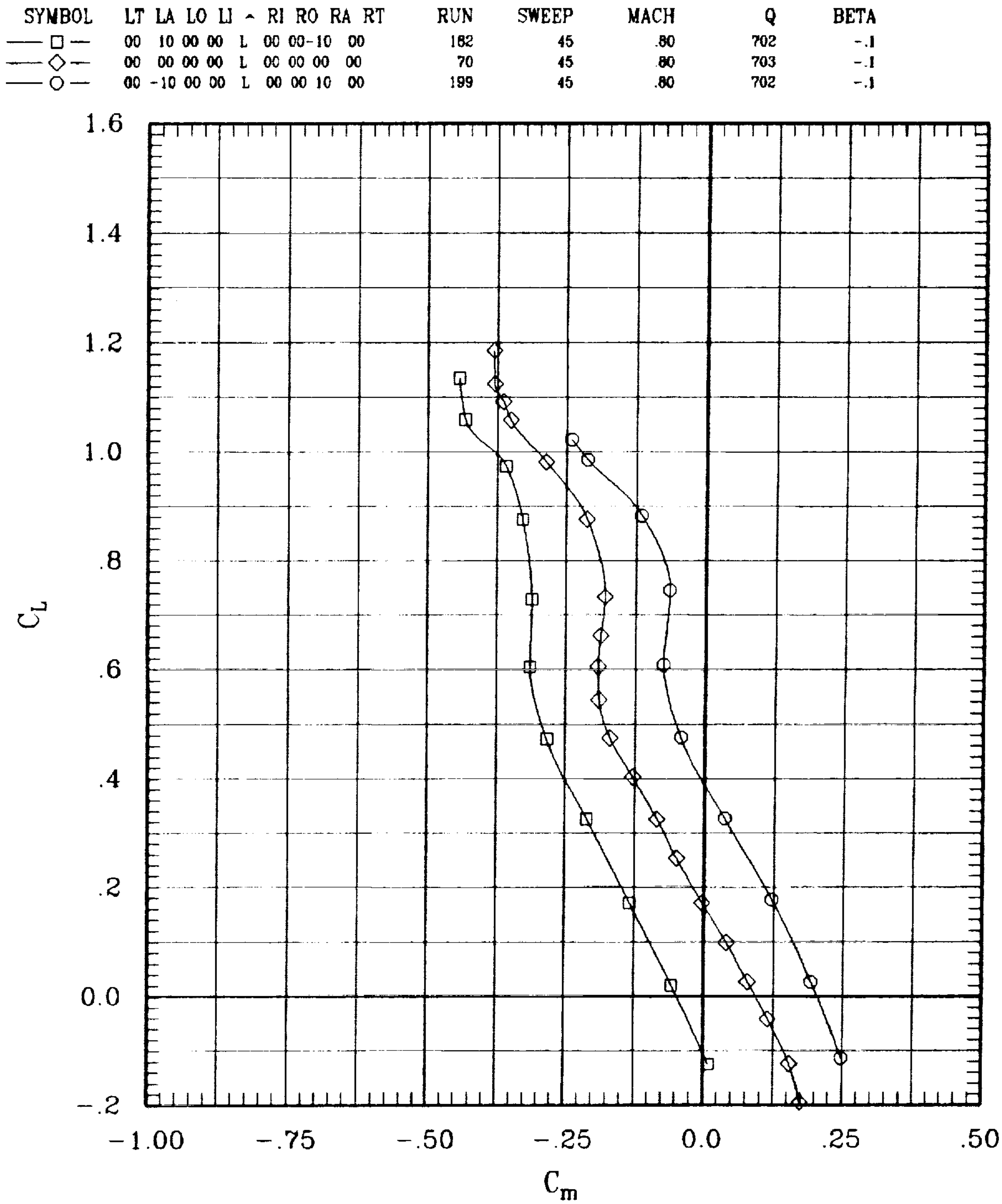

Figure 14(c). Effect of aileron deflection for sweep = 45 deg.

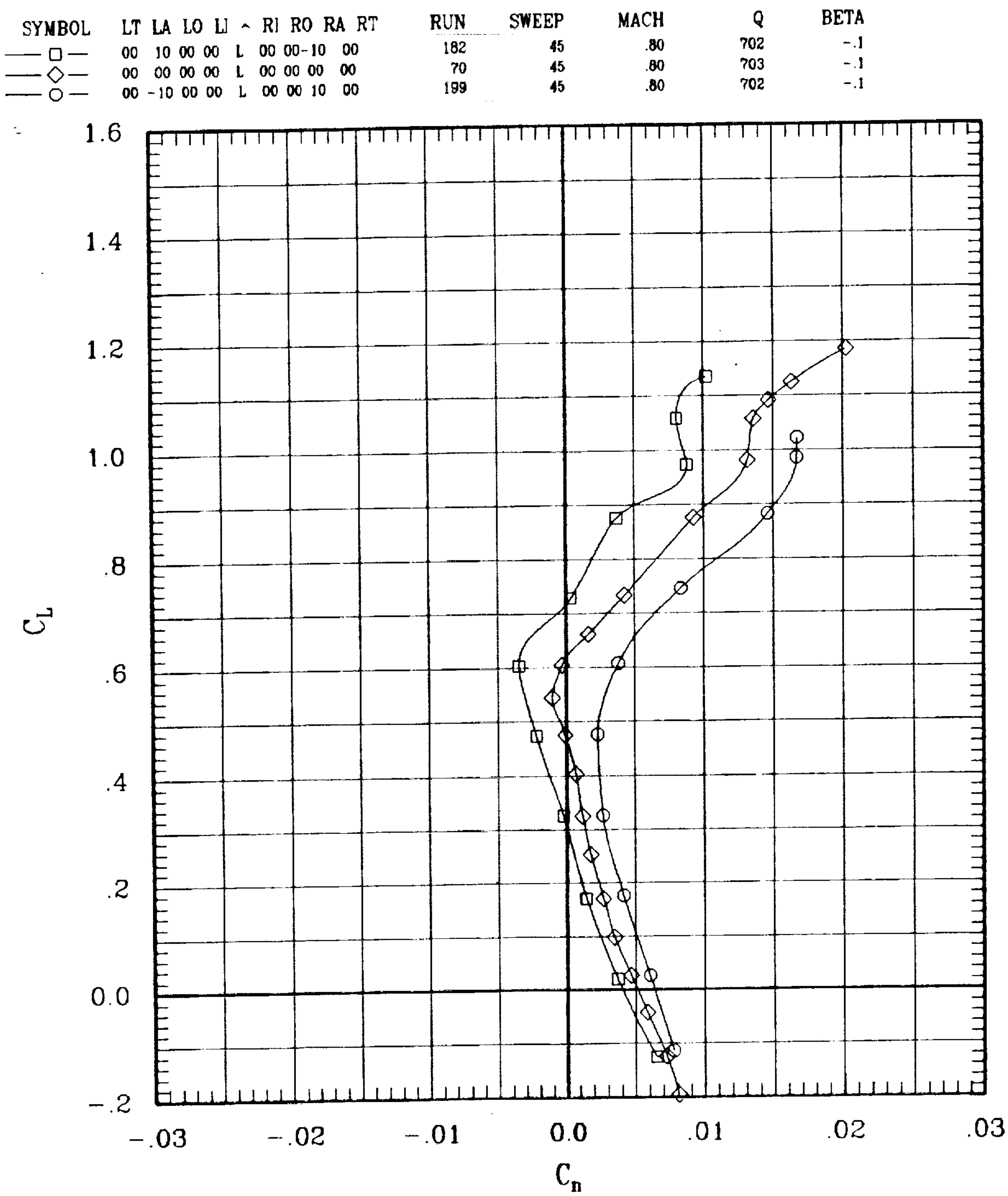

Figure 14(c). Effect of aileron deflection for sweep = 45 deg.

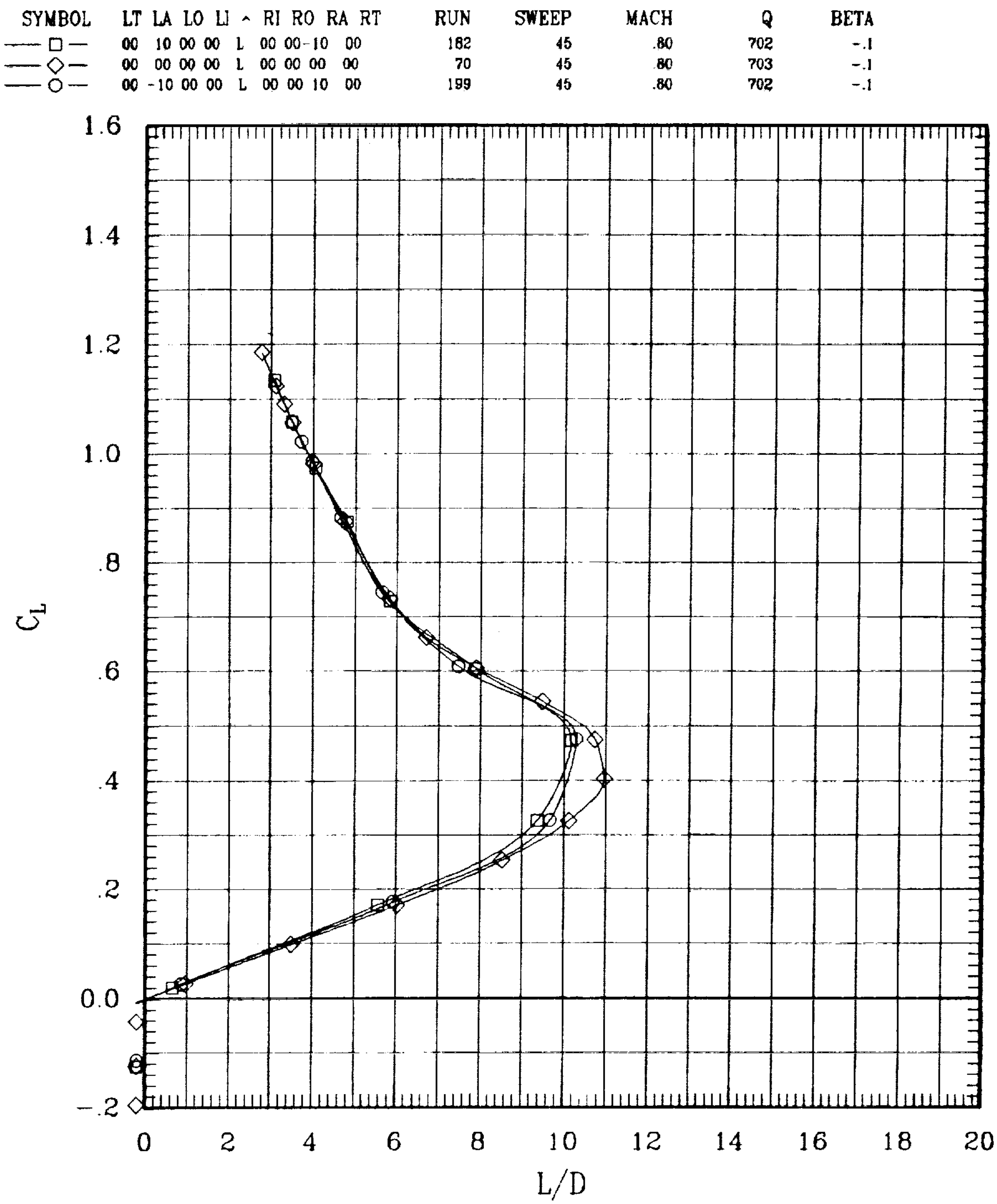

Figure 14(c). Effect of aileron deflection for sweep = 45 deg.

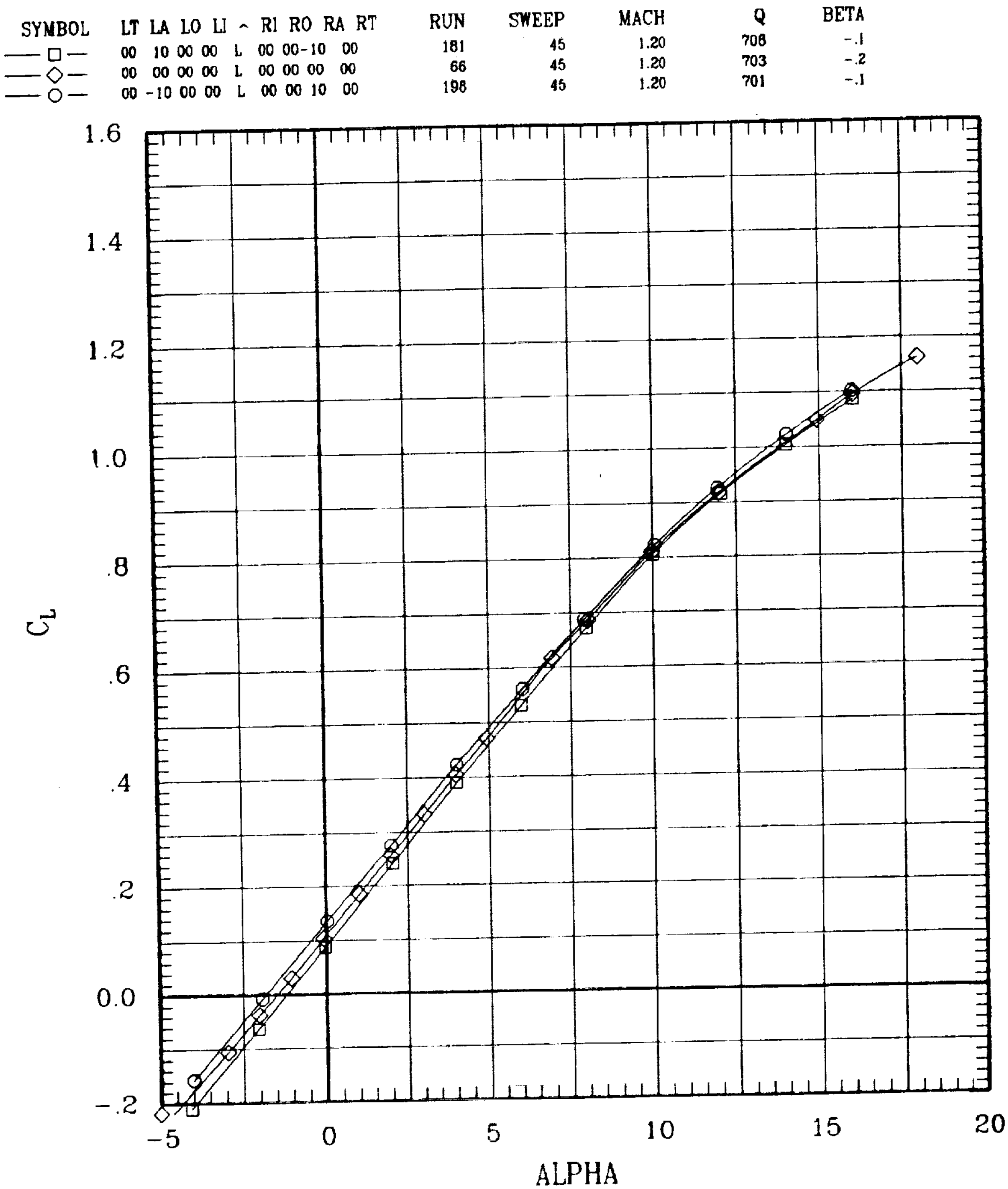

Figure 14(c). Effect of aileron deflection for sweep = 45 deg.

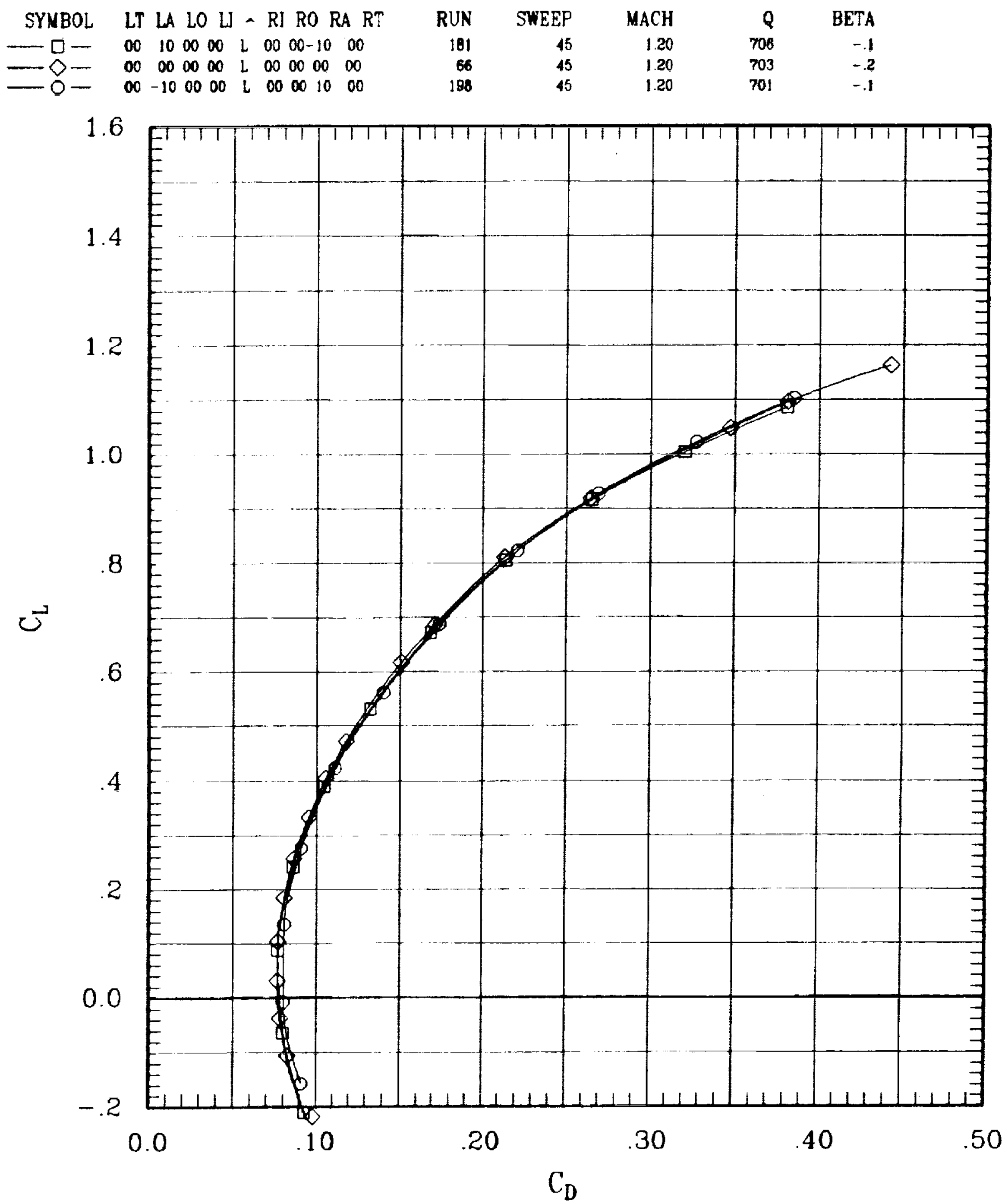

Figure 14(c). Effect of aileron deflection for sweep = 45 deg.

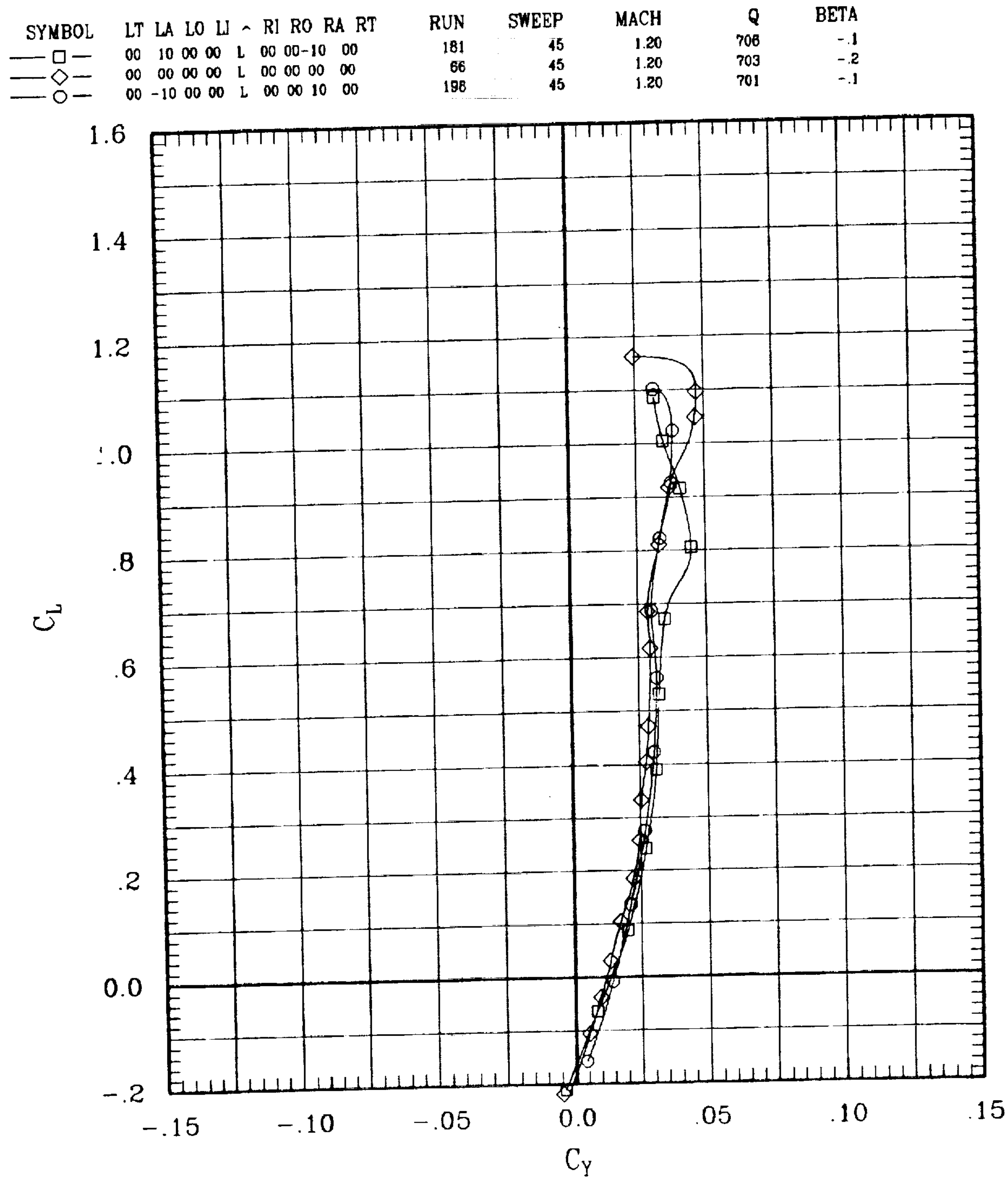

Figure 14(c). Effect of aileron deflection for sweep = 45 deg.

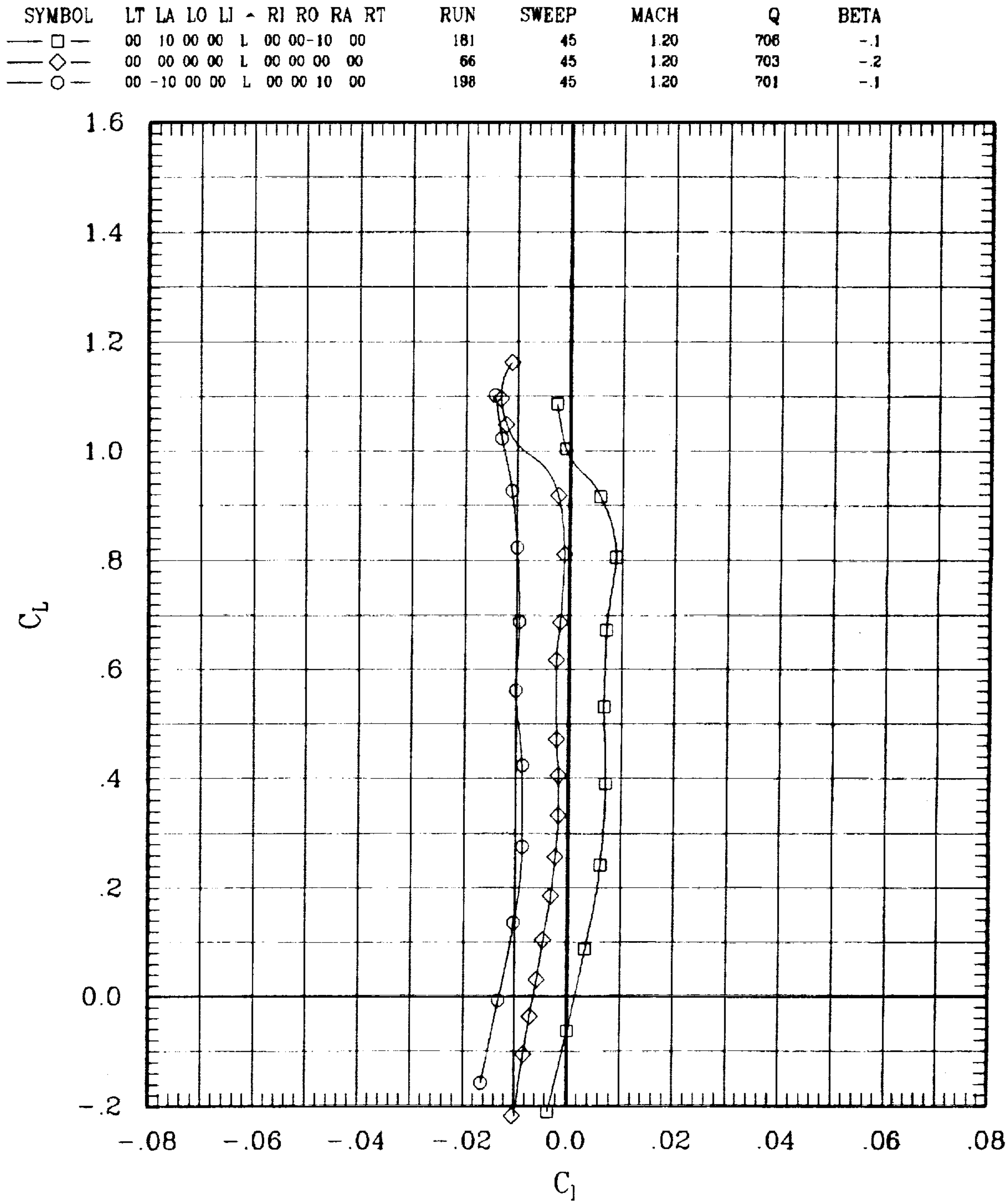

Figure 14(c). Effect of aileron deflection for sweep = 45 deg.

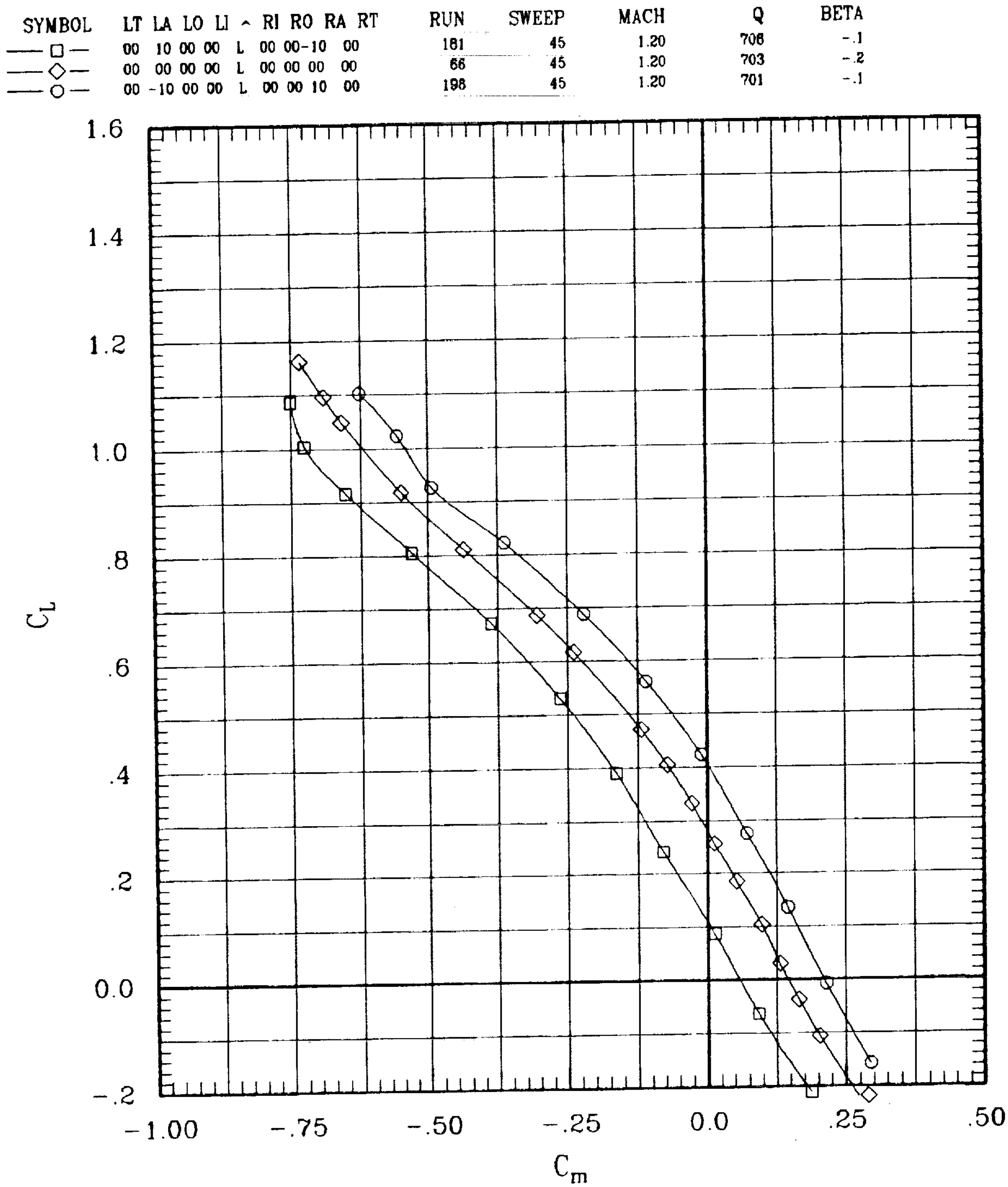

Figure 14(c). Effect of aileron deflection for sweep = 45 deg.

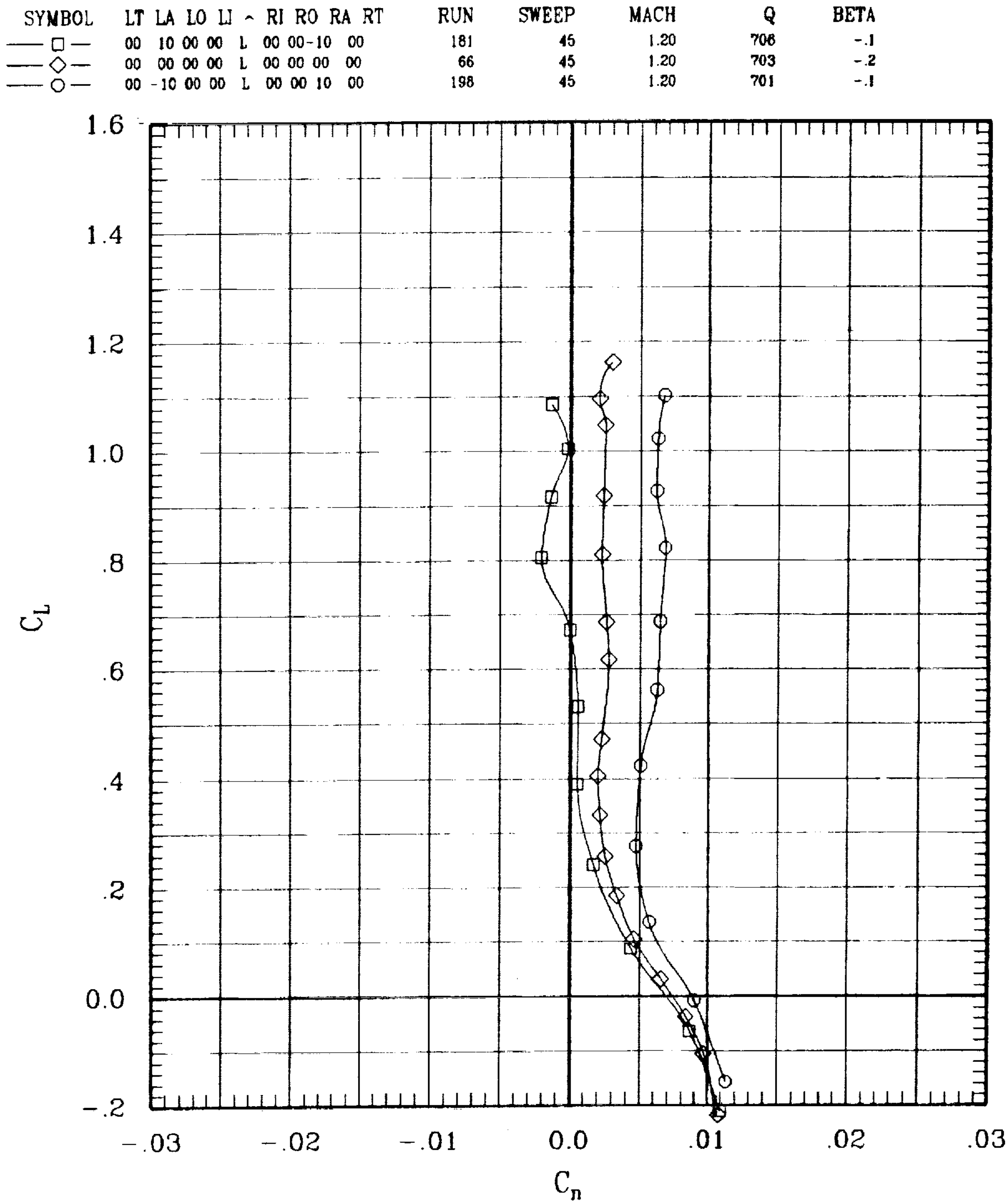

Figure 14(c). Effect of aileron deflection for sweep = 45 deg.

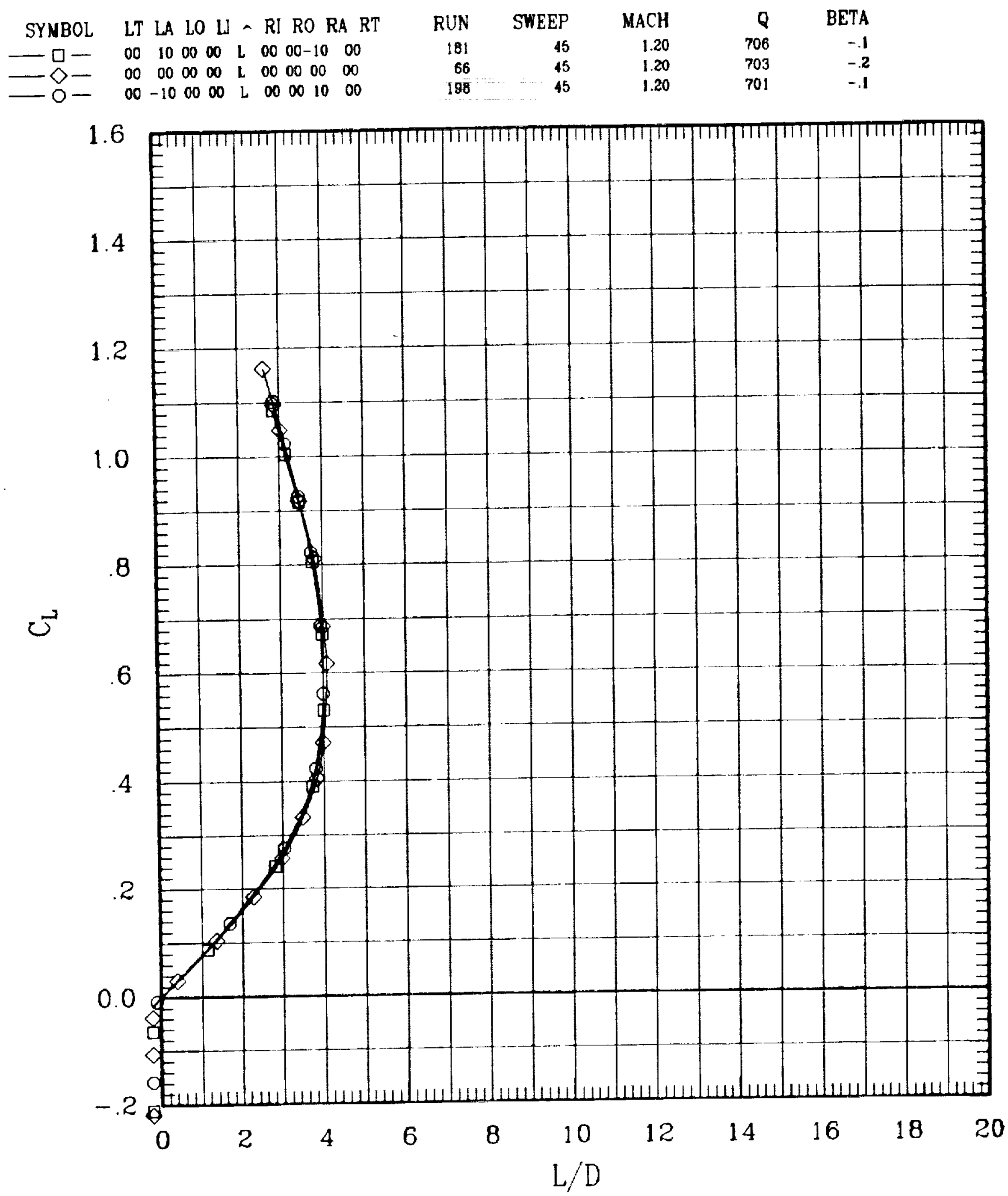

Figure 14(c). Effect of aileron deflection for sweep = 45 deg.

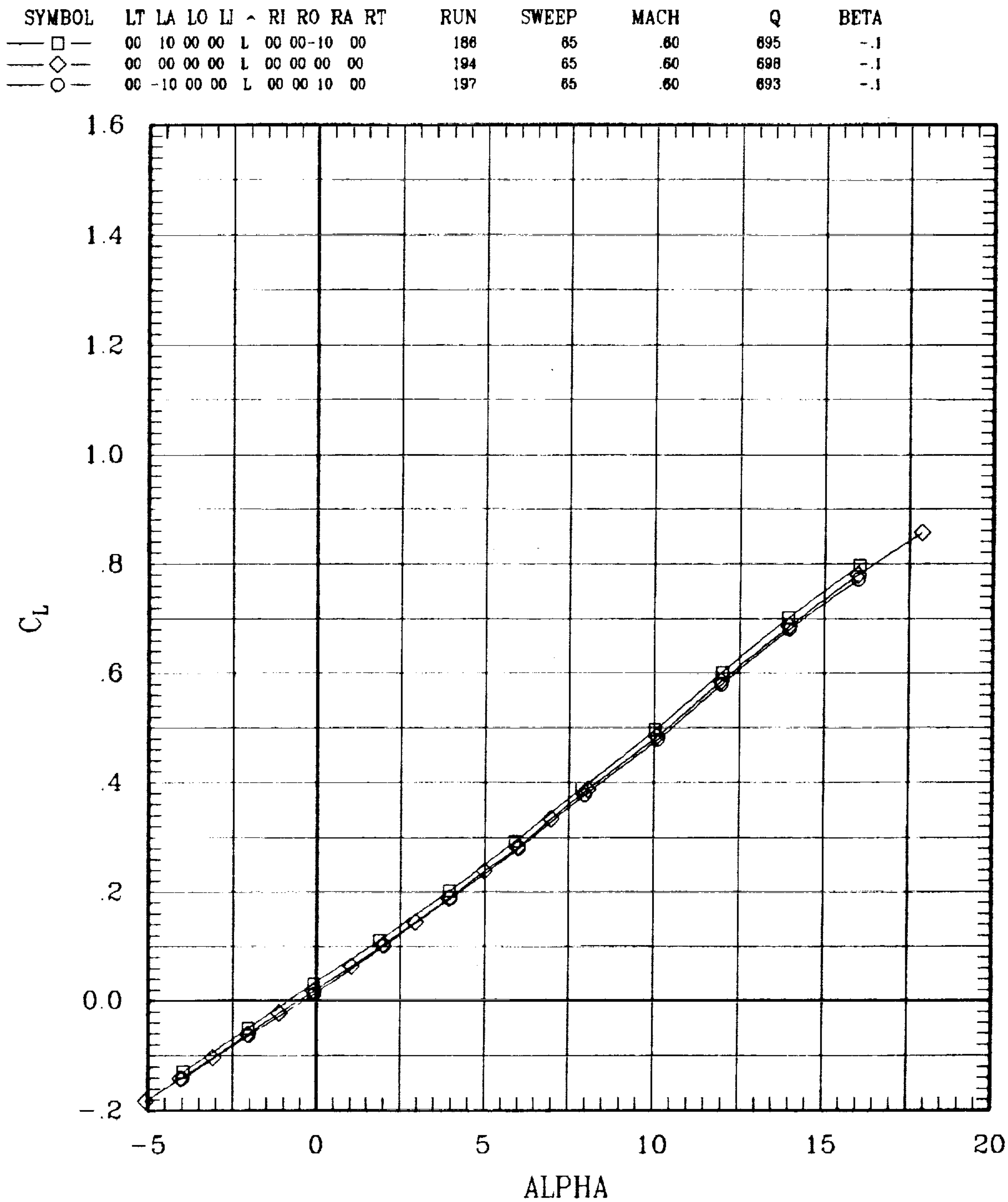

Figure 14(d). Effect of aileron deflection for sweep = 65 deg.

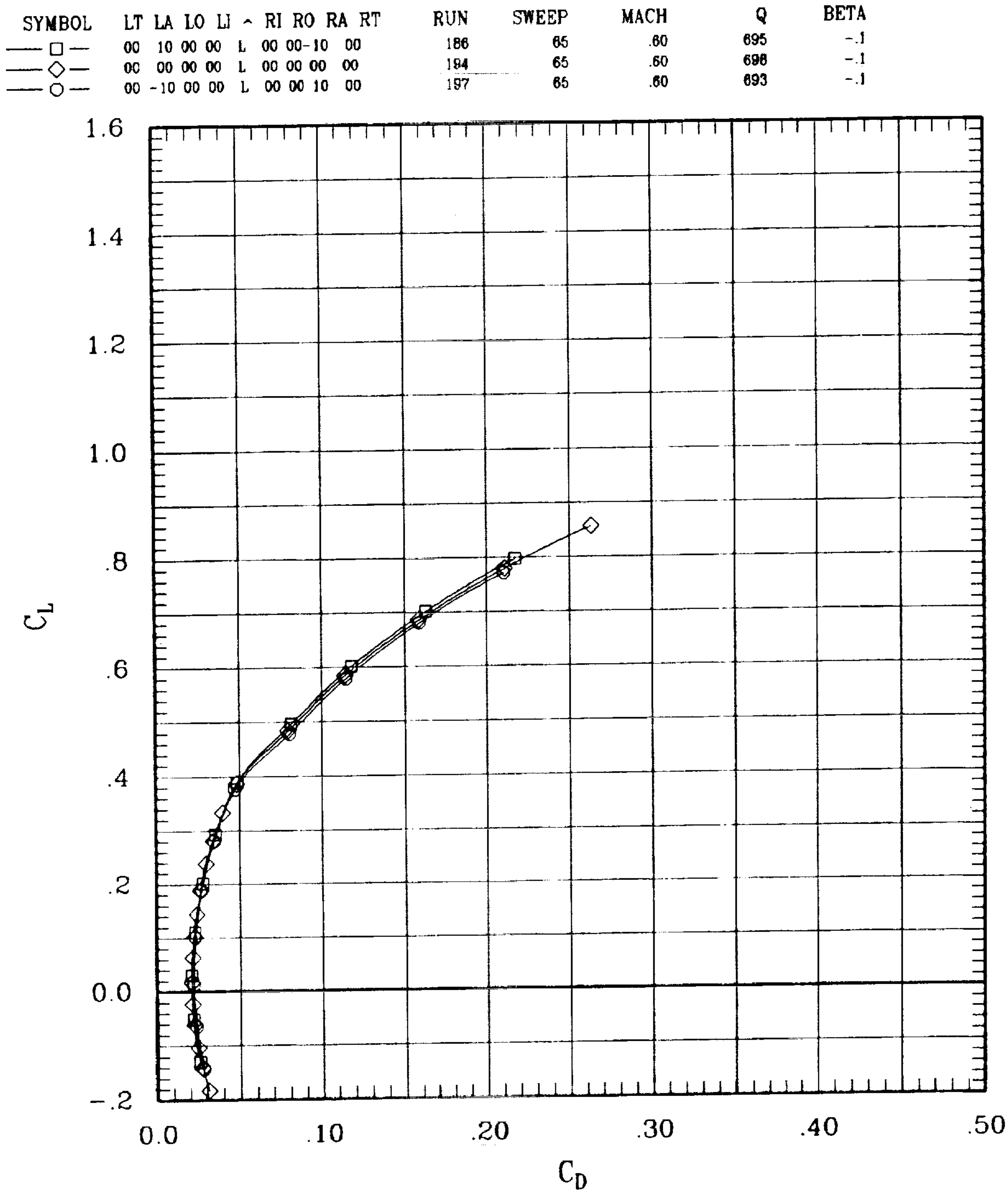

Figure 14(d). Effect of aileron deflection for sweep = 65 deg.

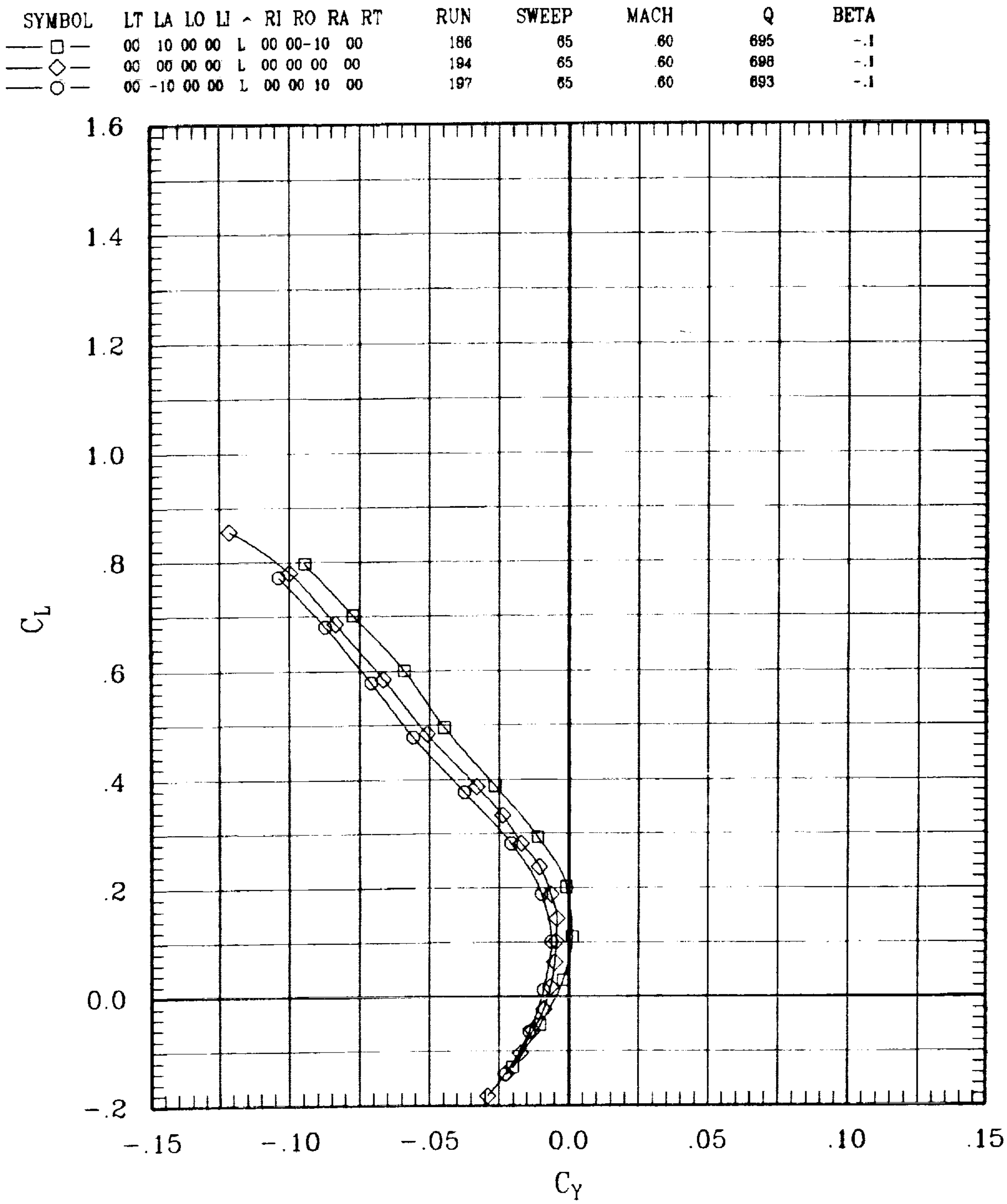

Figure 14(d). Effect of aileron deflection for sweep = 65 deg.

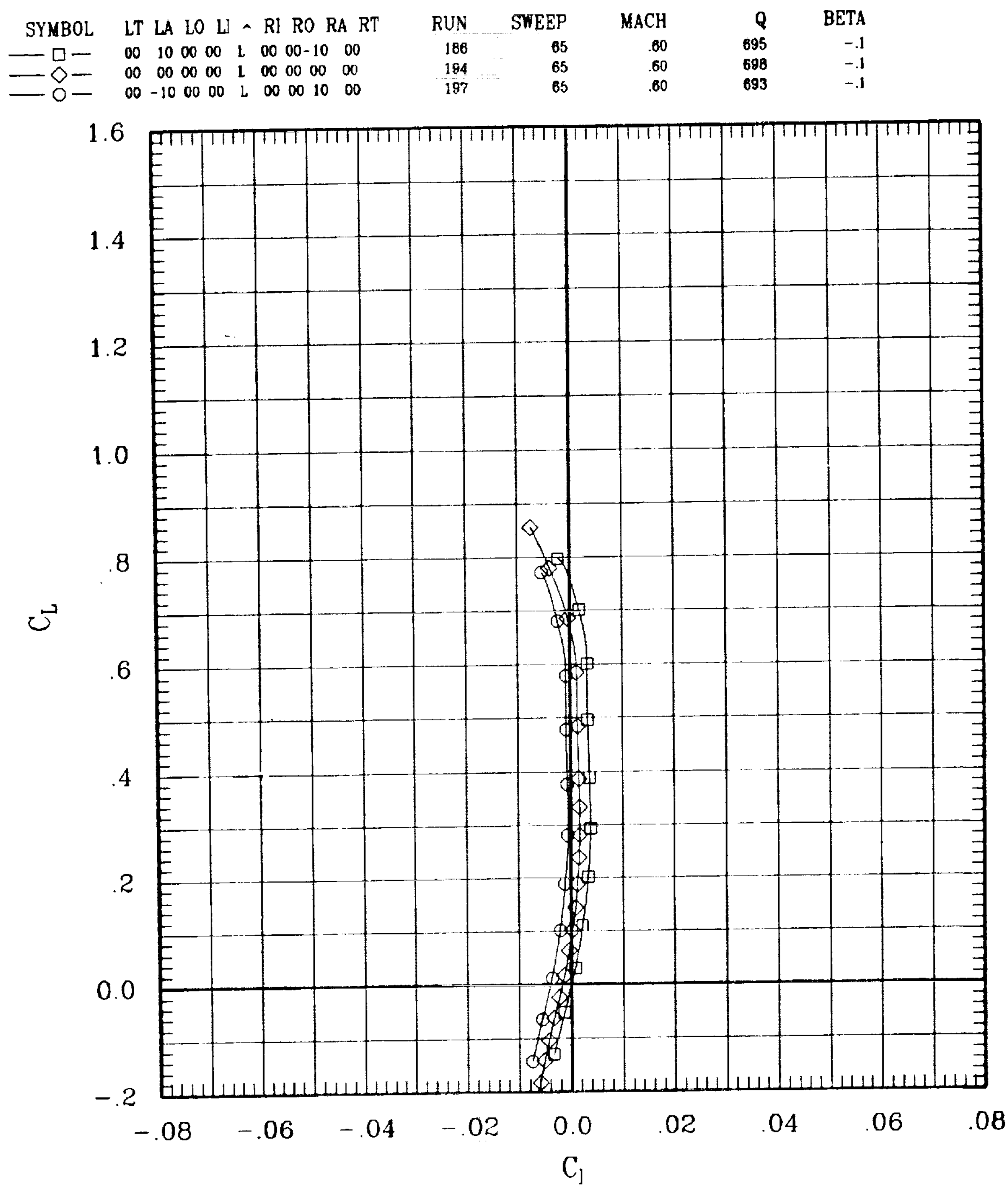

Figure 14(d). Effect of aileron deflection for sweep = 65 deg.

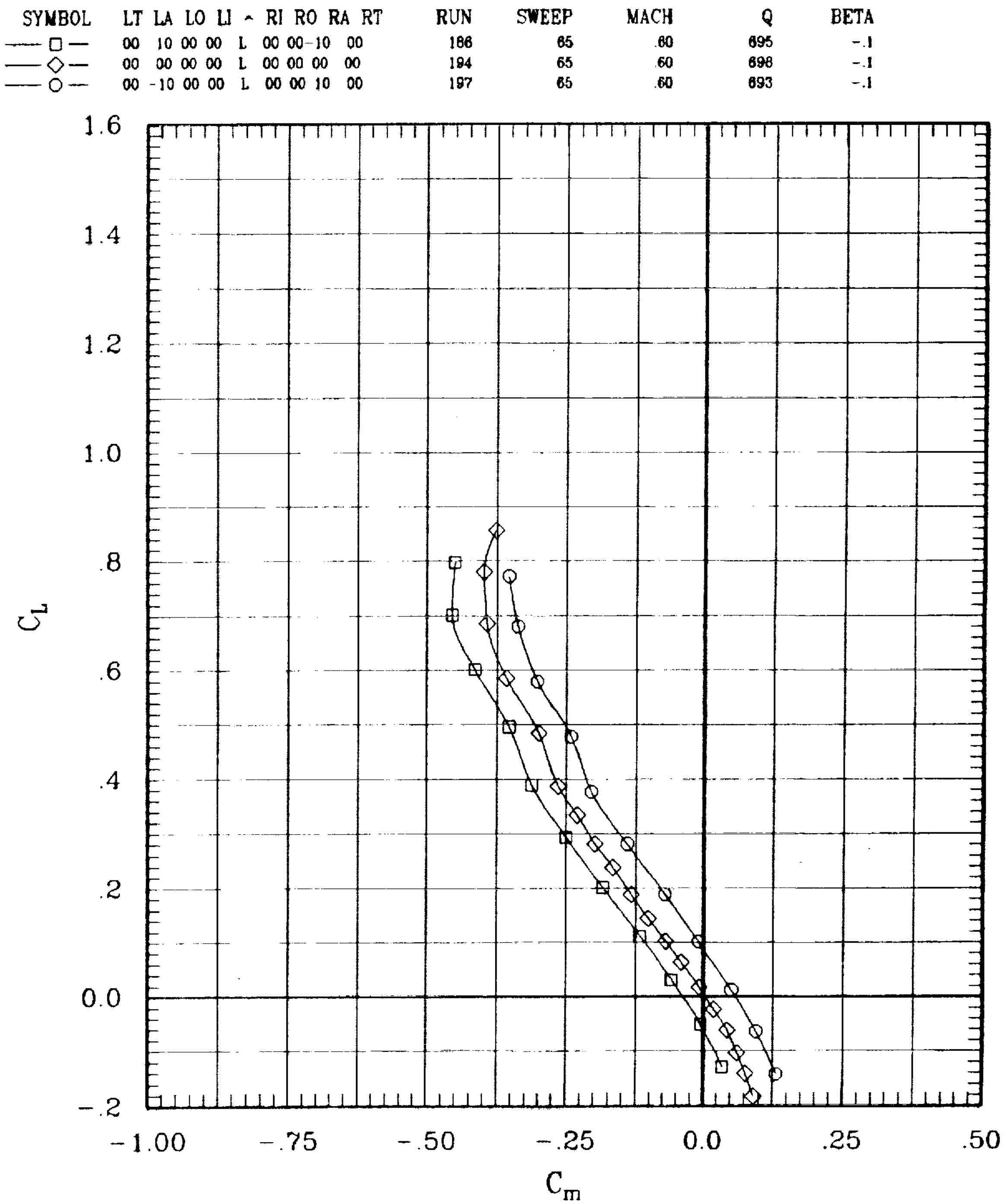

Figure 14(d). Effect of aileron deflection for sweep = 65 deg.

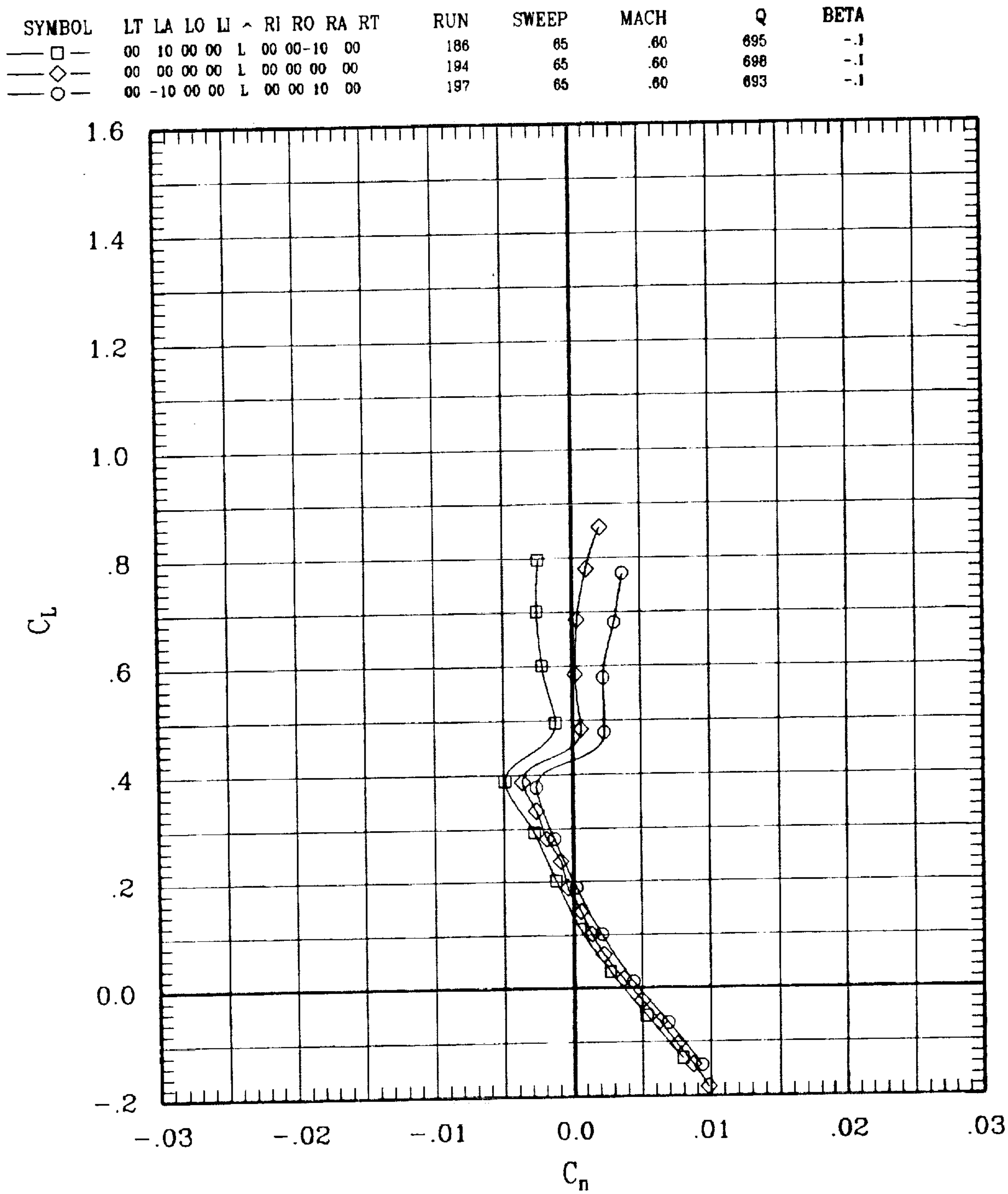

Figure 14(d). Effect of aileron deflection for sweep = 65 deg.

SYMBOL	LT LA LO LI ^ RI RO RA RT	RUN	SWEEP	MACH	Q	BETA
—□—	00 10 00 00 L 00 00 -10 00	186	65	.60	695	-.1
—◇—	00 00 00 00 L 00 00 00 00	194	65	.60	698	-.1
—○—	00 -10 00 00 L 00 00 10 00	197	65	.60	693	-.1

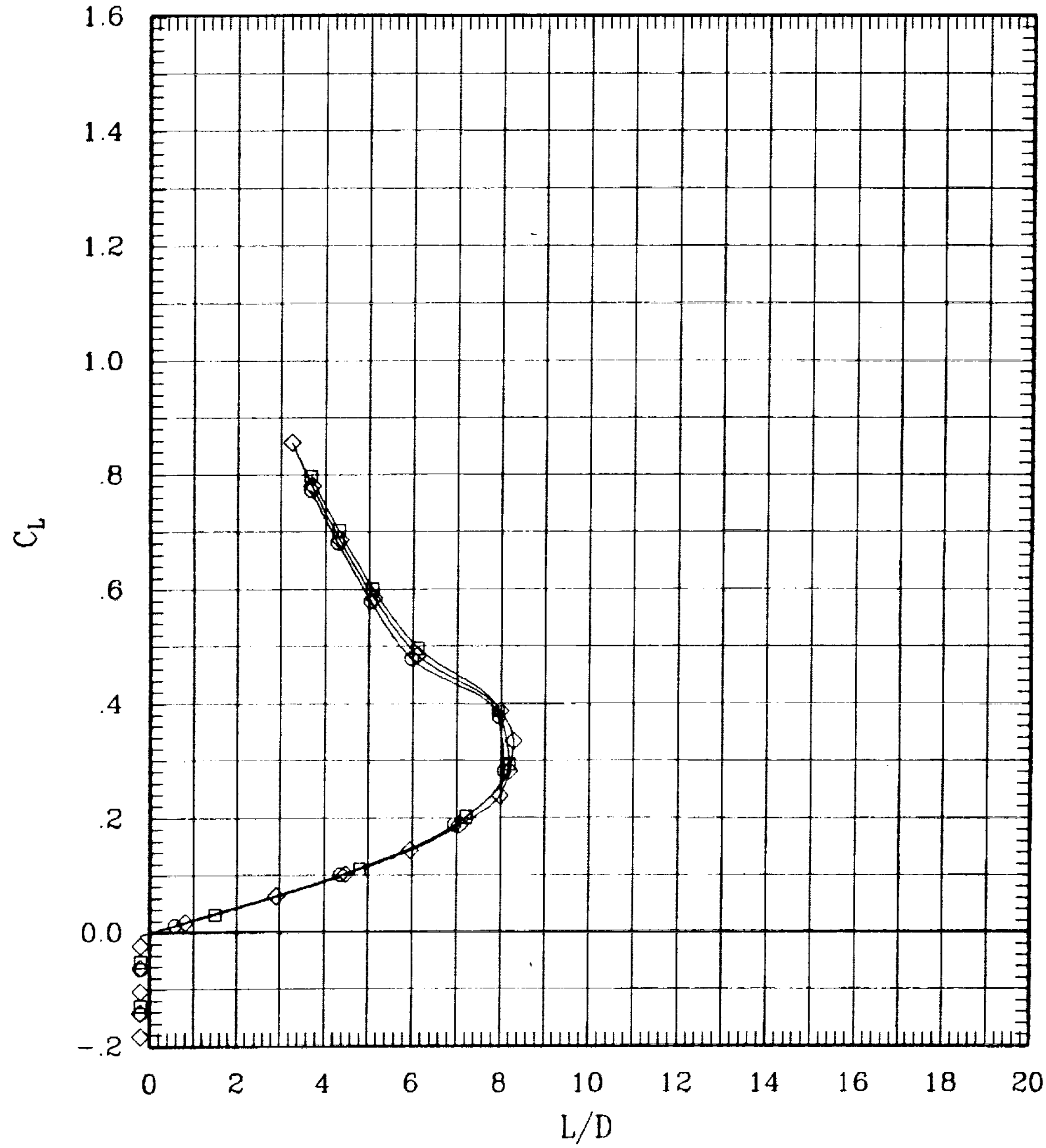

Figure 14(d). Effect of aileron deflection for sweep = 65 deg.

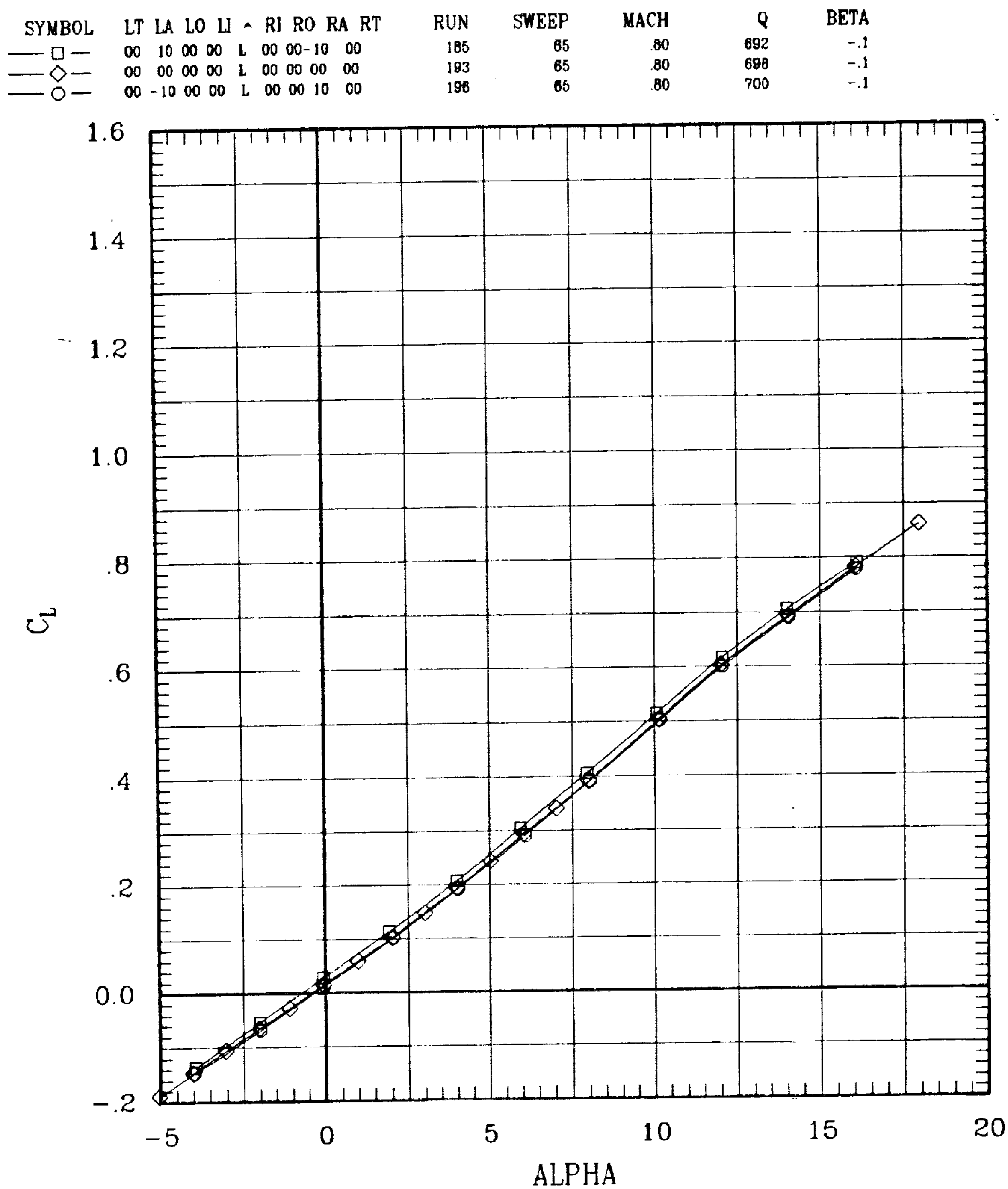

Figure 14(d). Effect of aileron deflection for sweep = 65 deg.

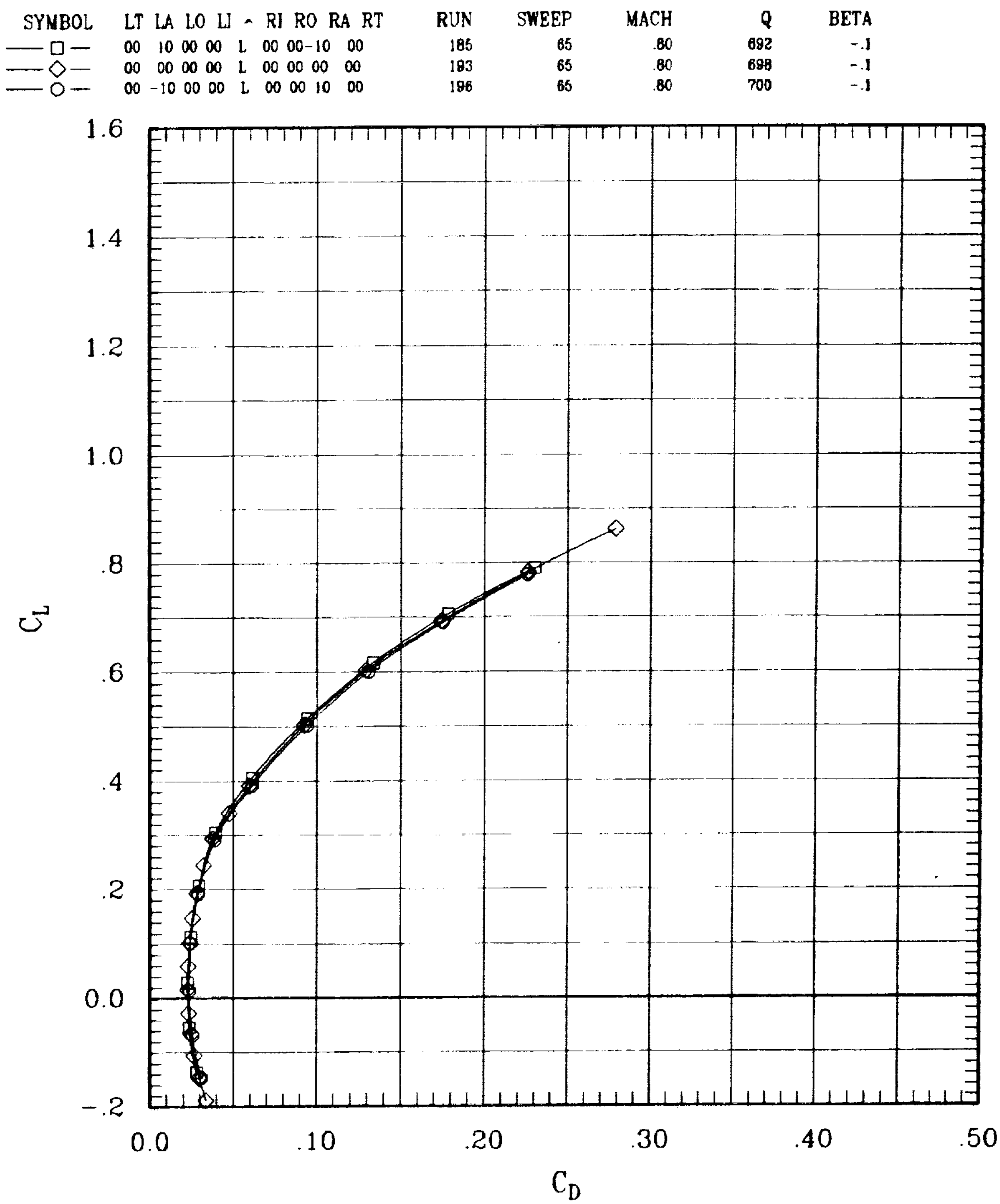

Figure 14(d). Effect of aileron deflection for sweep = 65 deg.

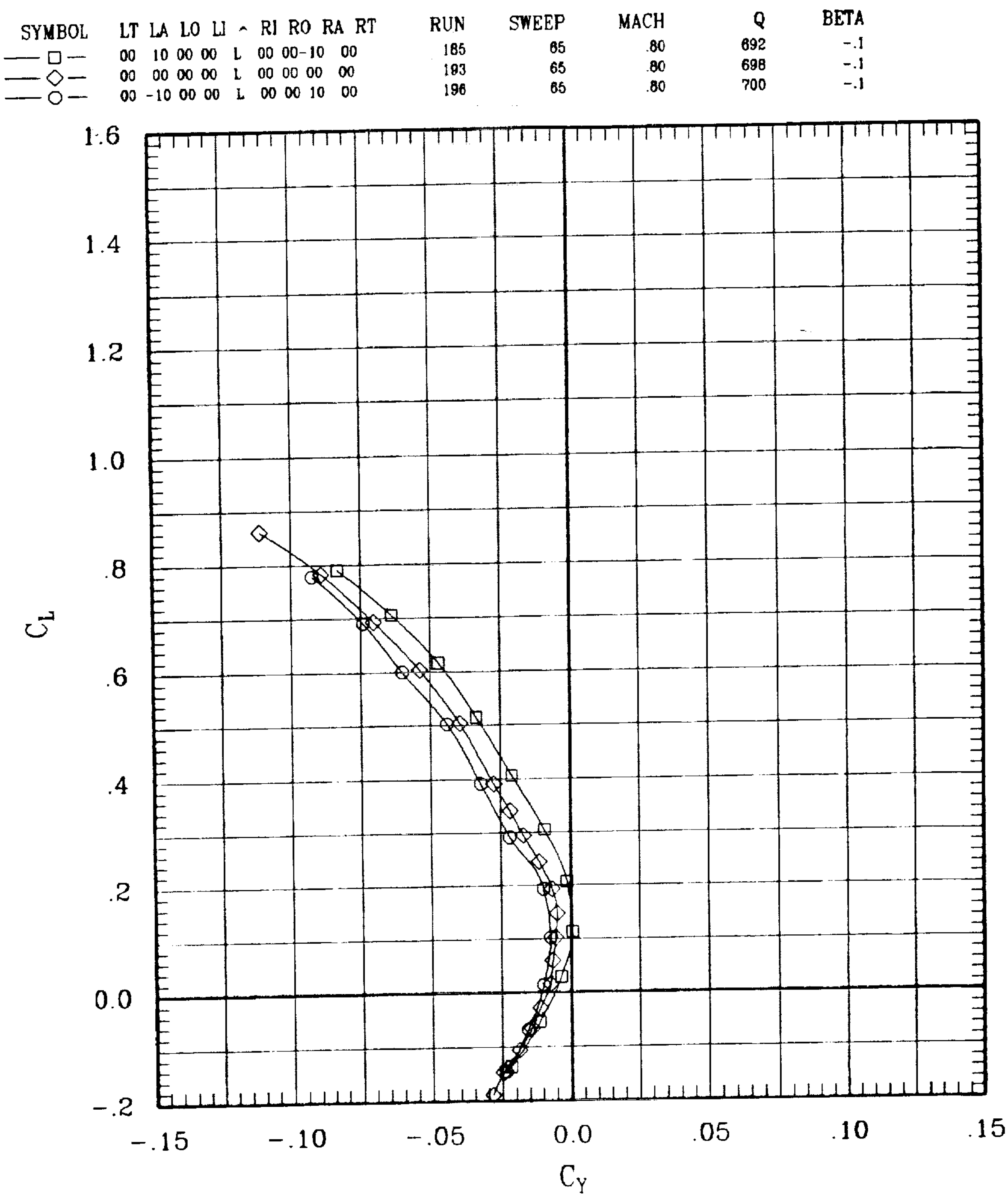

Figure 14(d). Effect of aileron deflection for sweep = 65 deg.

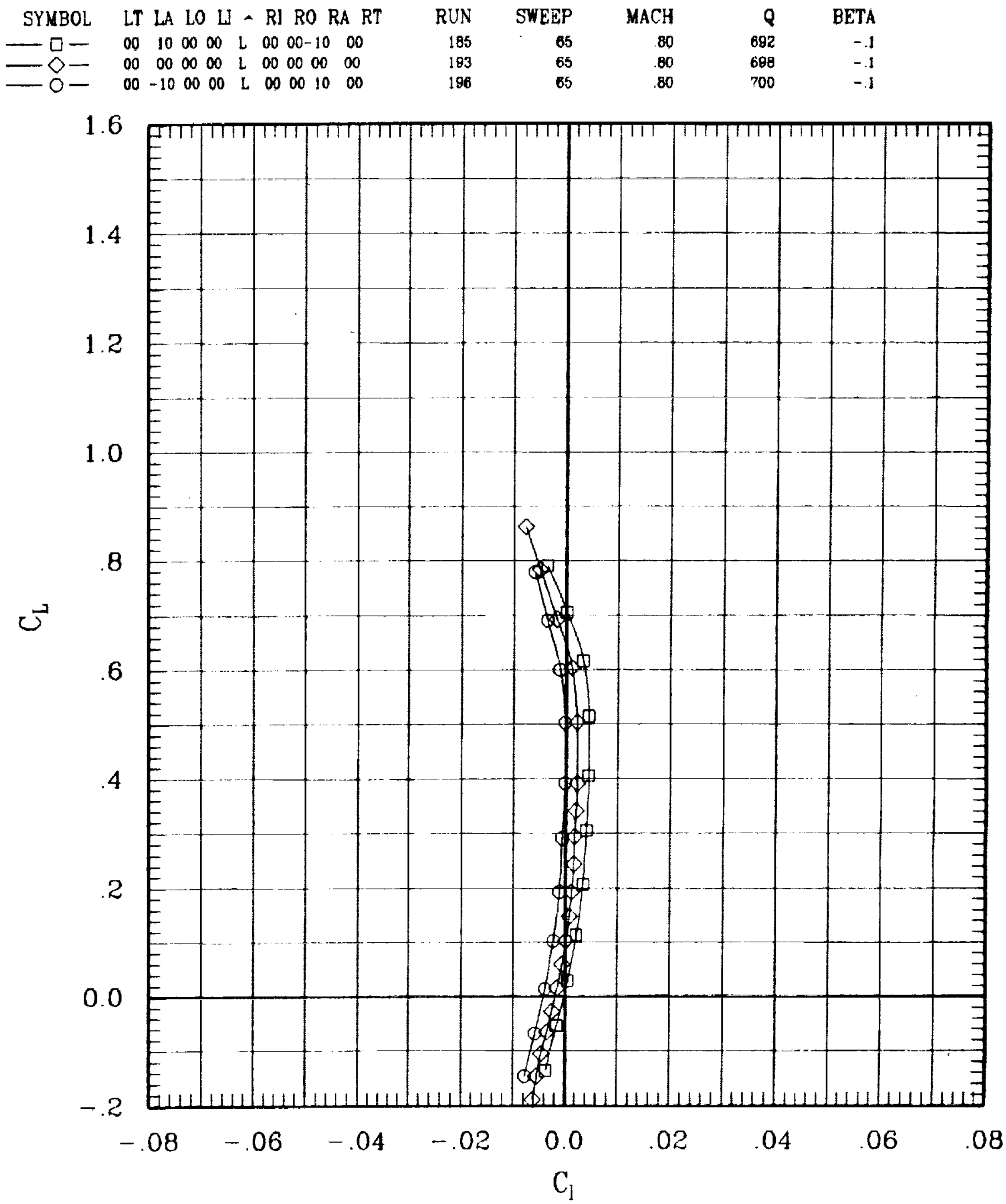

Figure 14(d). Effect of aileron deflection for sweep = 65 deg.

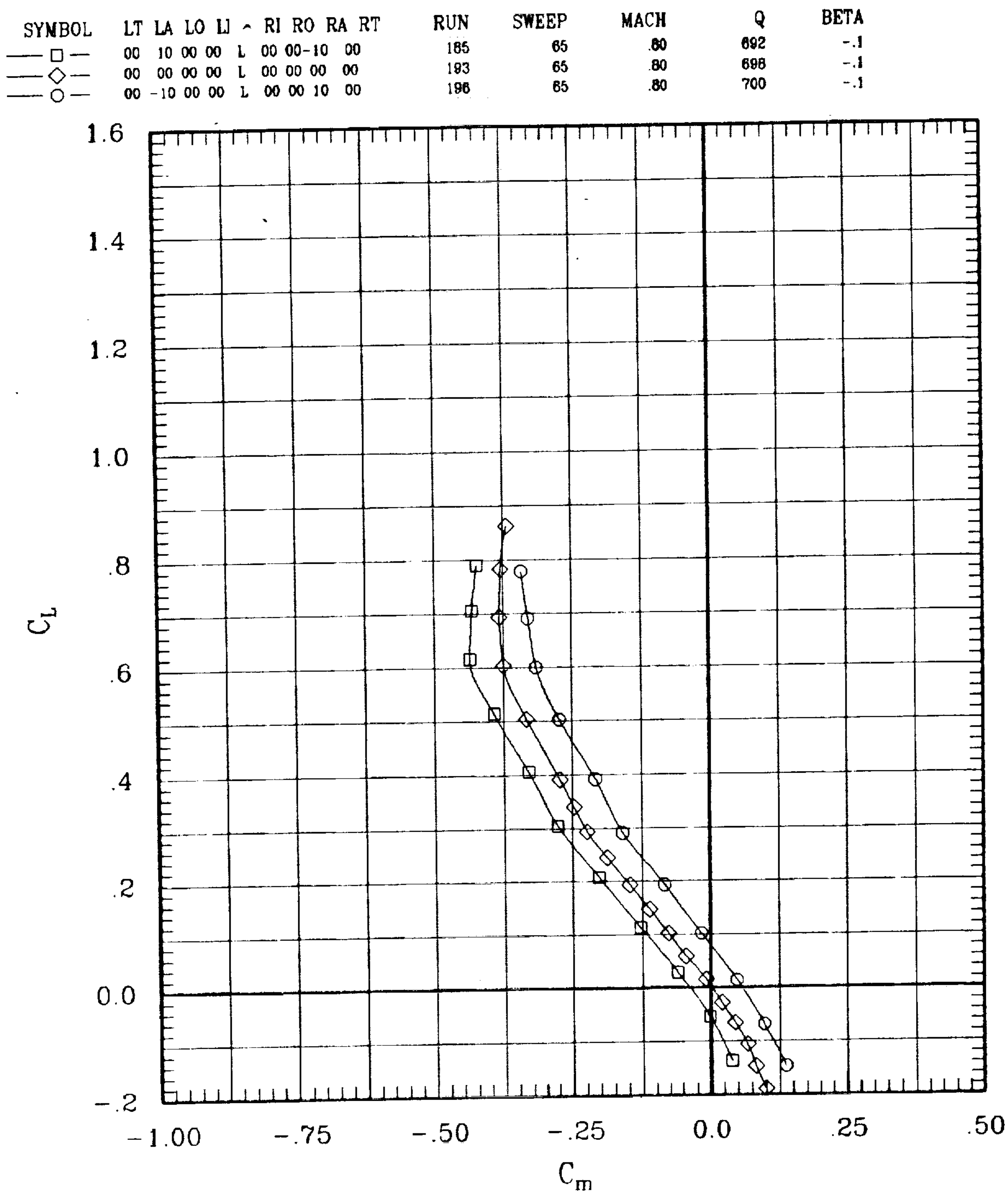

Figure 14(d). Effect of aileron deflection for sweep = 65 deg.

SYMBOL	LT LA LO LI ^ RI RO RA RT	RUN	SWEEP	MACH	Q	BETA
—□—	00 10 00 00 L 00 00-10 00	185	65	.80	692	-.1
—◇—	00 00 00 00 L 00 00 00 00	193	65	.80	698	-.1
—○—	00 -10 00 00 L 00 00 10 00	196	65	.80	700	-.1

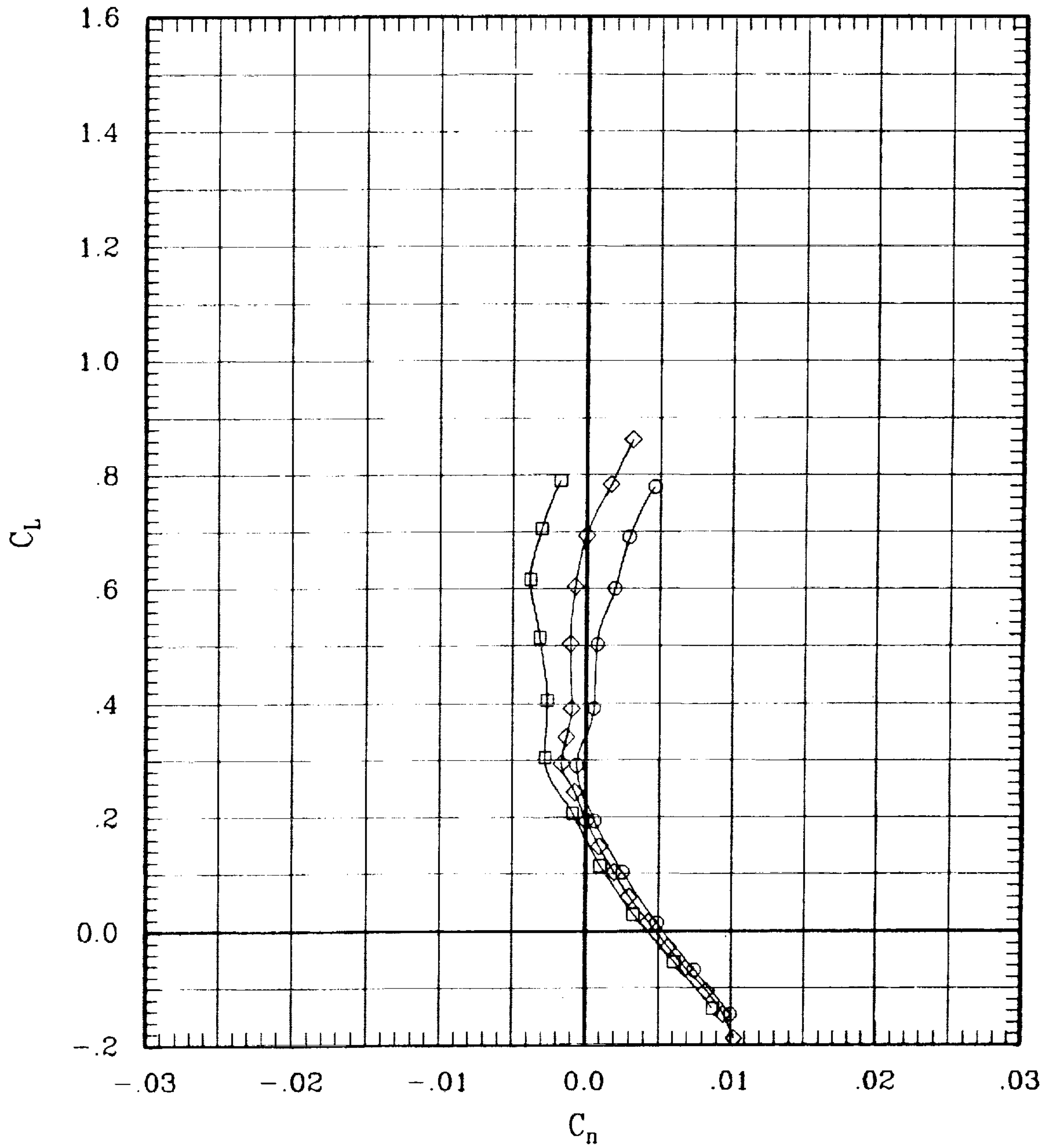

Figure 14(d). Effect of aileron deflection for sweep = 65 deg.

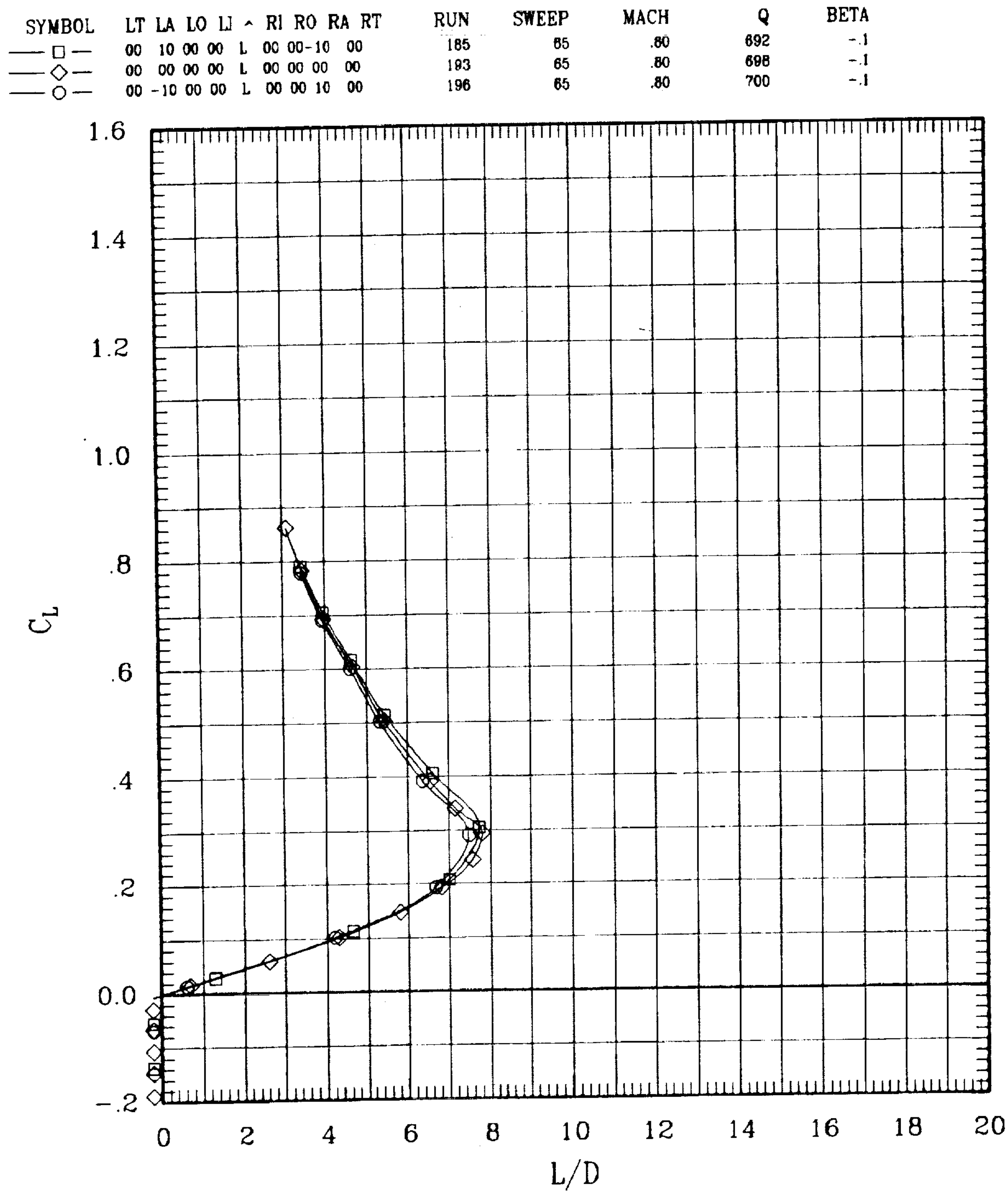

Figure 14(d). Effect of aileron deflection for sweep = 65 deg.

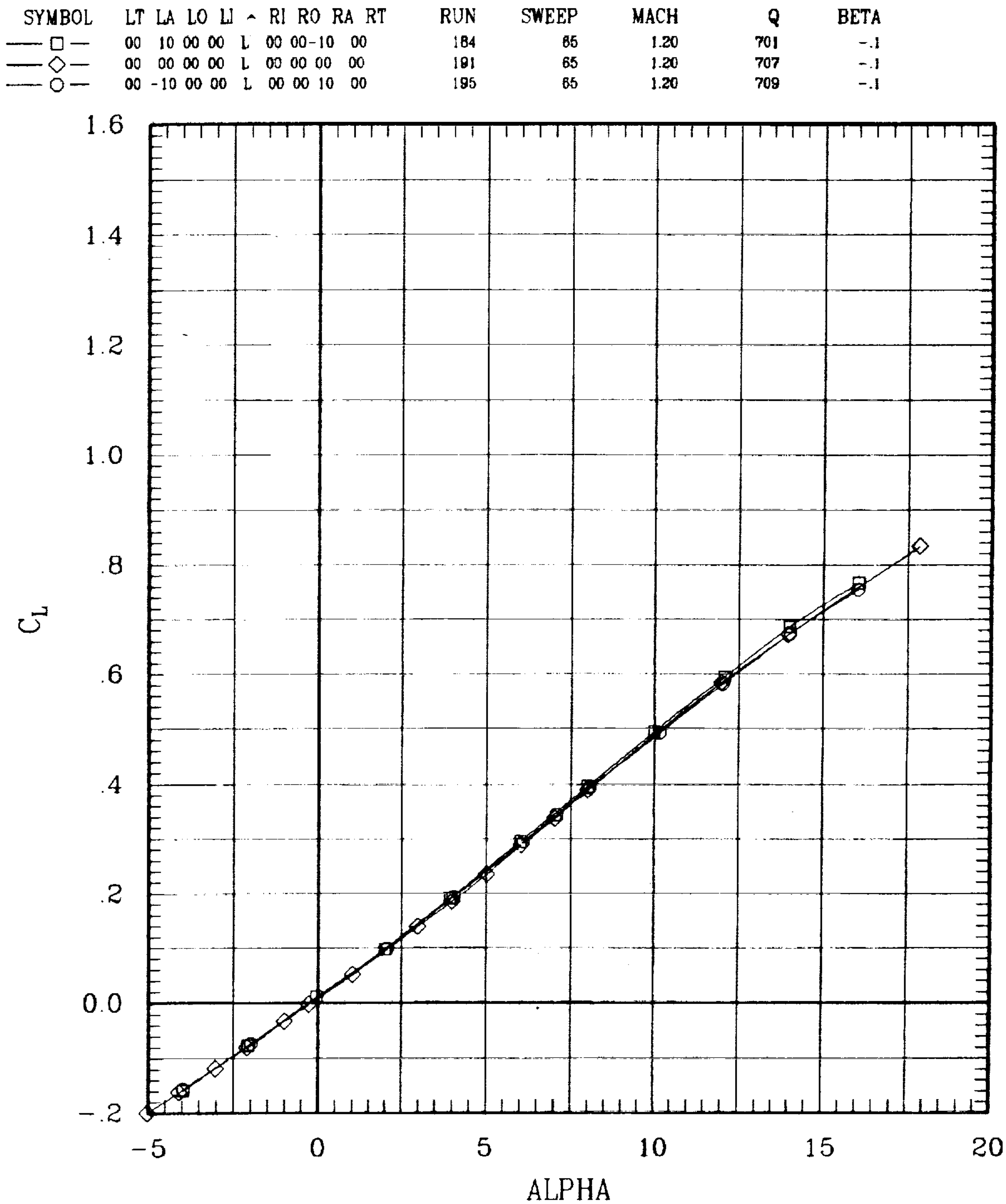

Figure 14(d). Effect of aileron deflection for sweep = 65 deg.

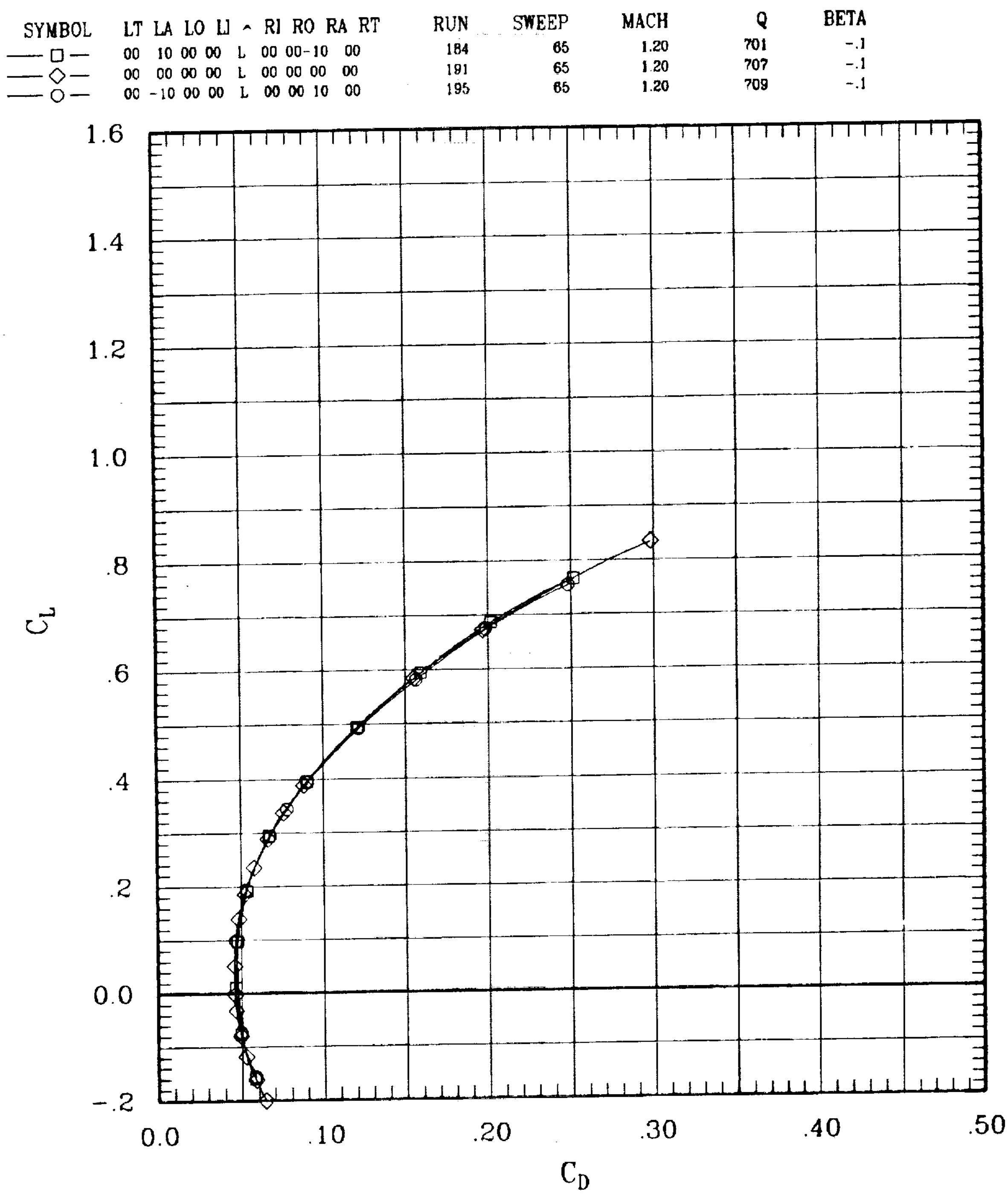

Figure 14(d). Effect of aileron deflection for sweep = 65 deg.

SYMBOL	LT LA LO LI ^ RI RO RA RT	RUN	SWEEP	MACH	Q	BETA
—□—	00 10 00 00 L 00 00 -10 00	184	65	1.20	701	-.1
—◇—	00 00 00 00 L 00 00 00 00	191	65	1.20	707	-.1
—○—	00 -10 00 00 L 00 00 10 00	195	65	1.20	709	-.1

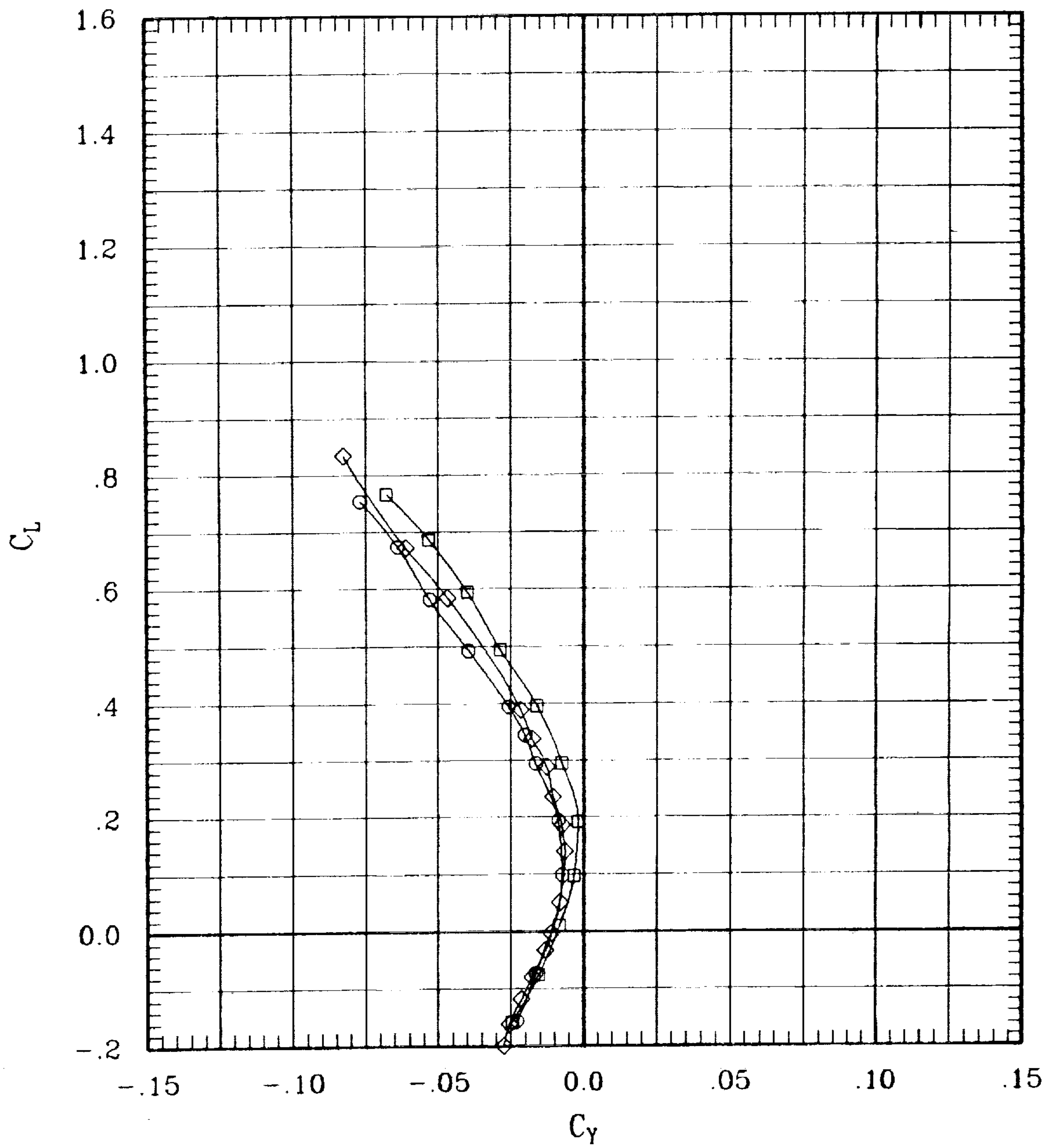

Figure 14(d). Effect of aileron deflection for sweep = 65 deg.

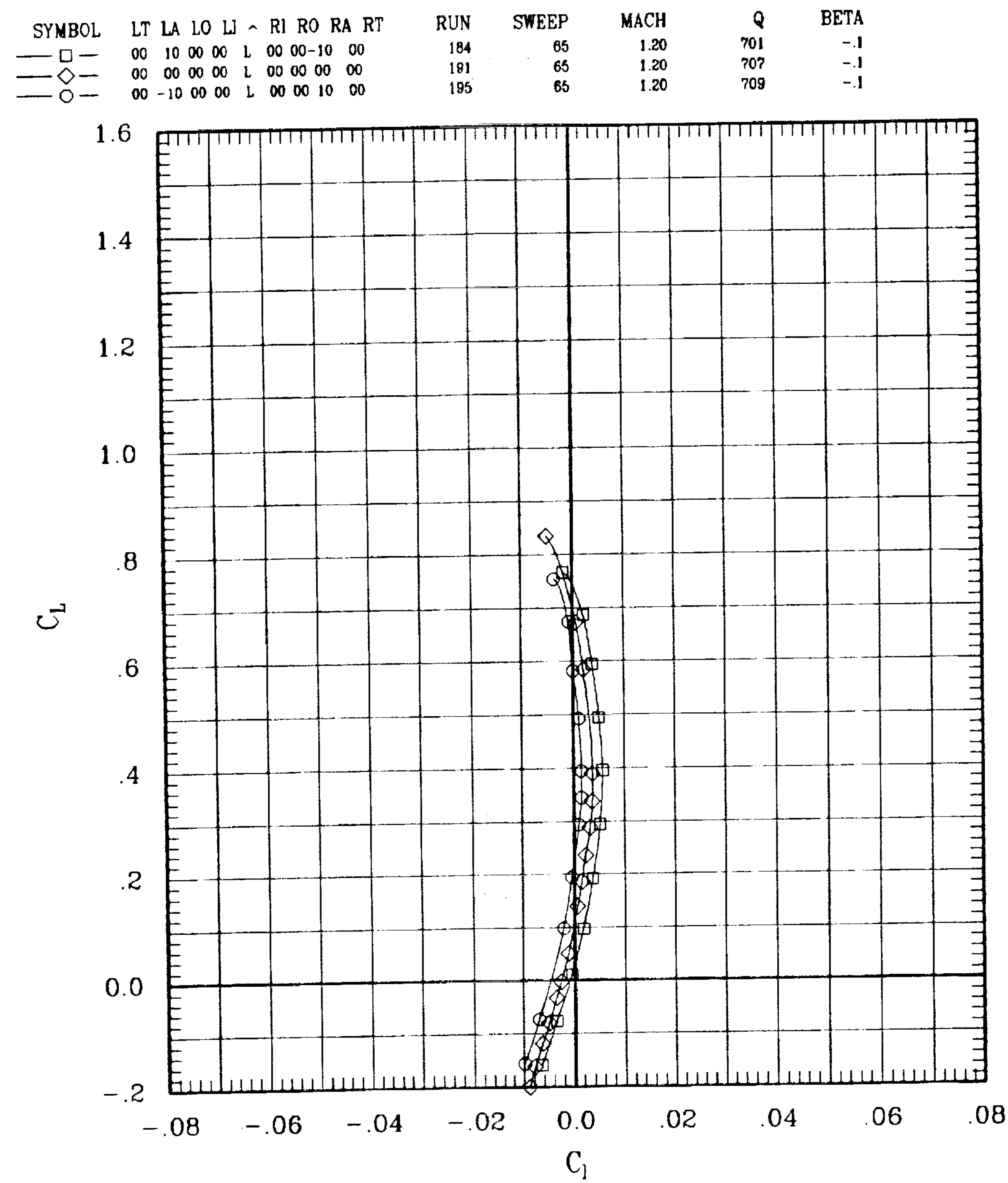

Figure 14(d). Effect of aileron deflection for sweep = 65 deg.

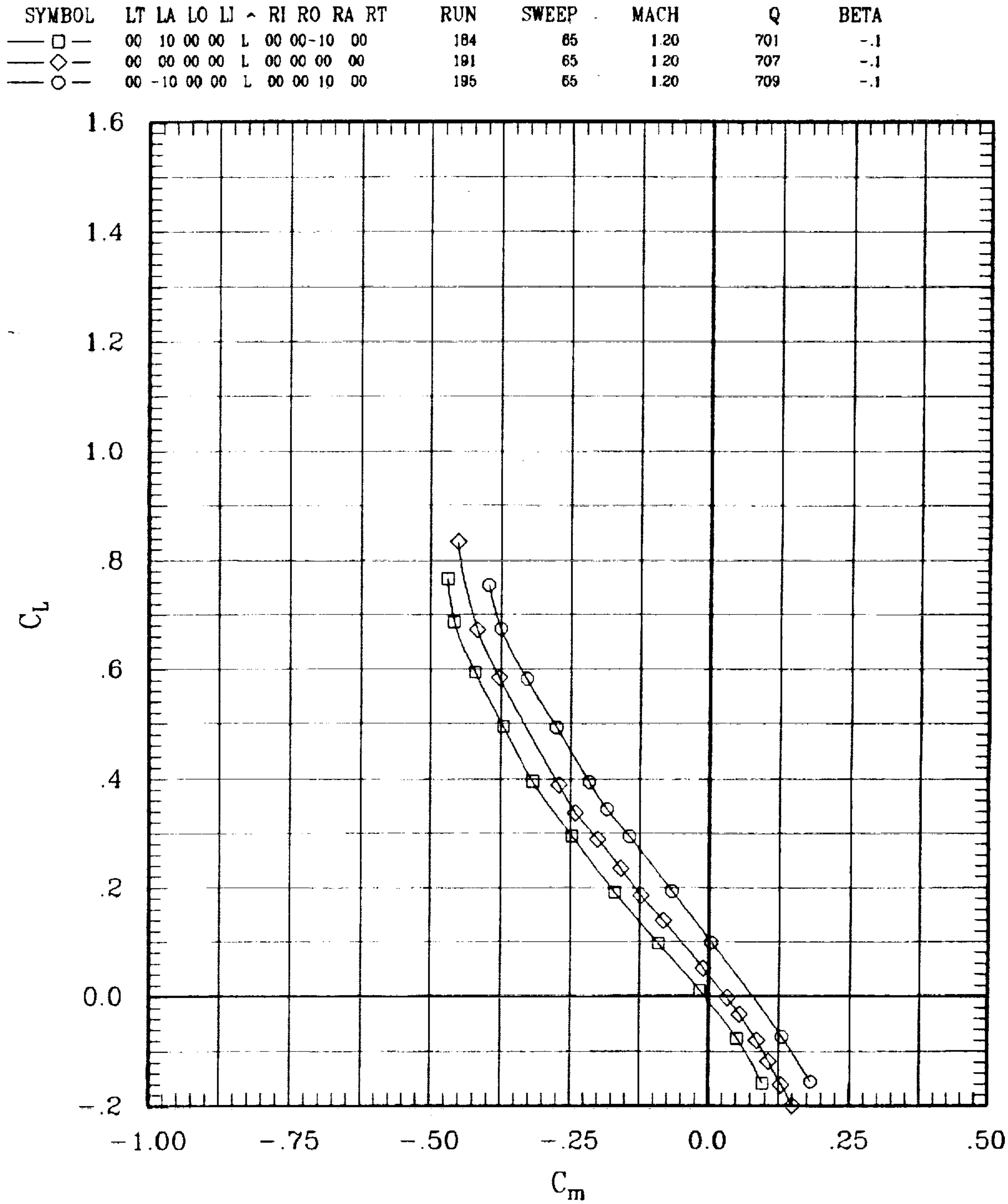

Figure 14(d). Effect of aileron deflection for sweep = 65 deg.

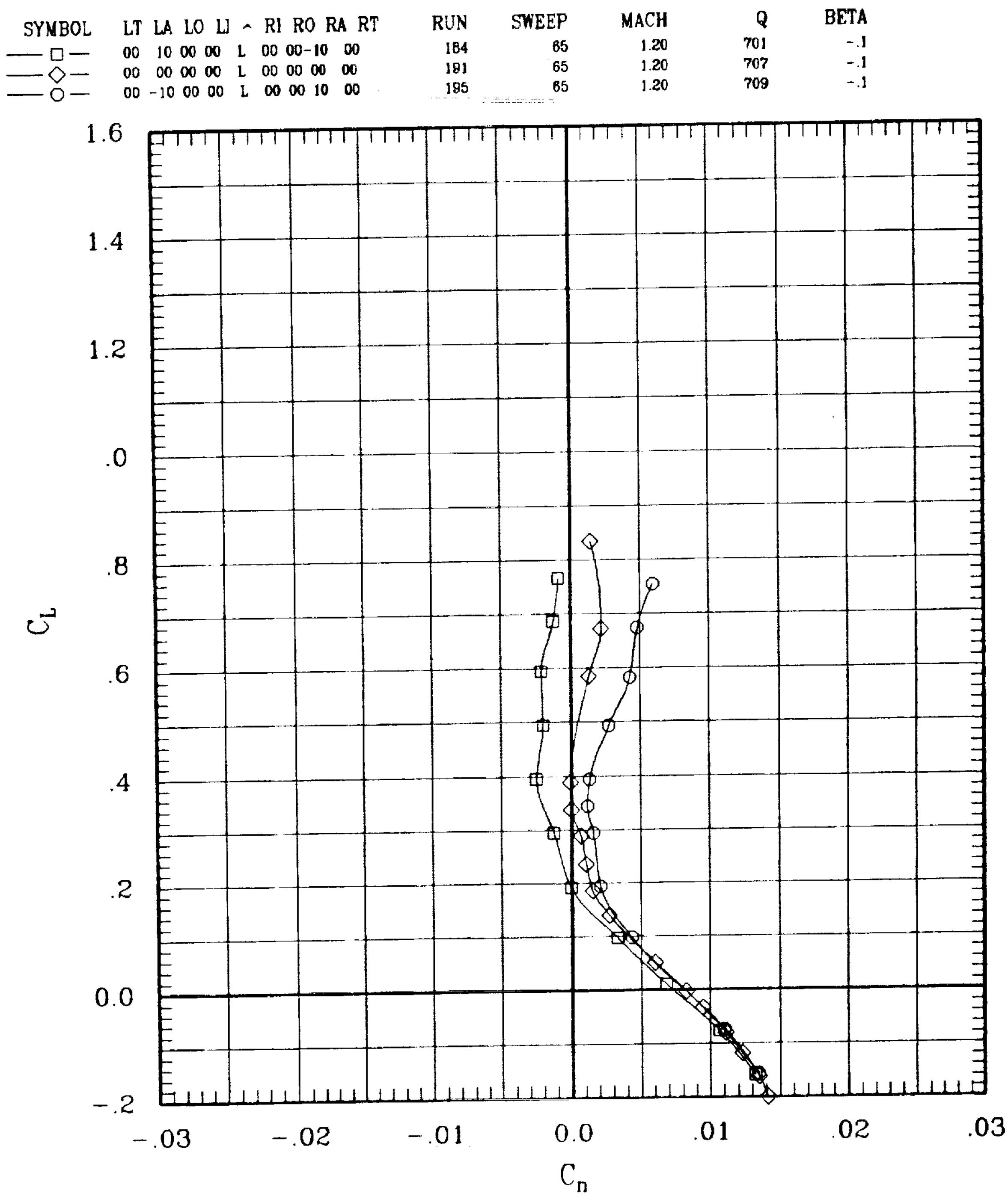

Figure 14(d). Effect of aileron deflection for sweep = 65 deg.

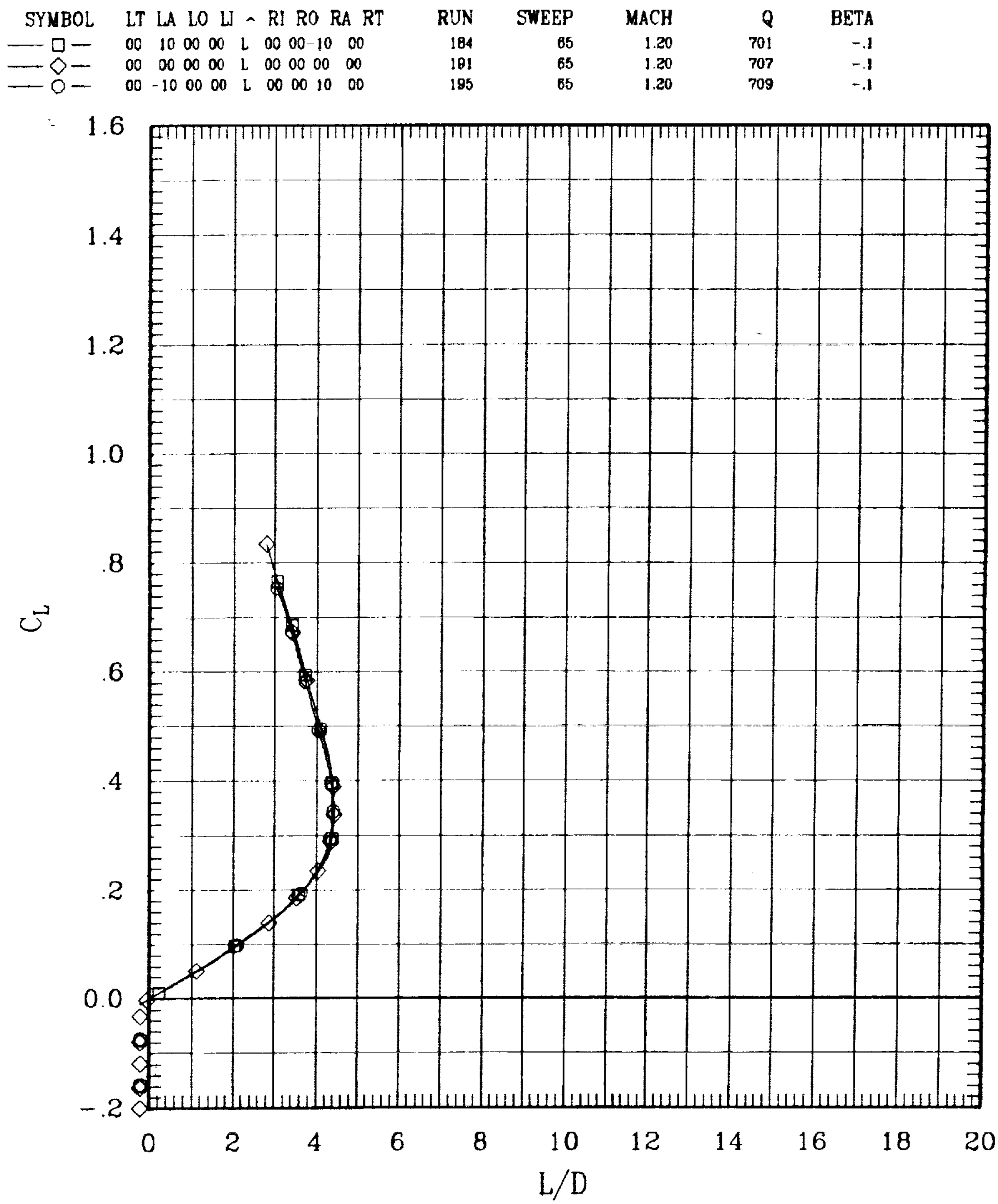

Figure 14(d). Effect of aileron deflection for sweep = 65 deg.

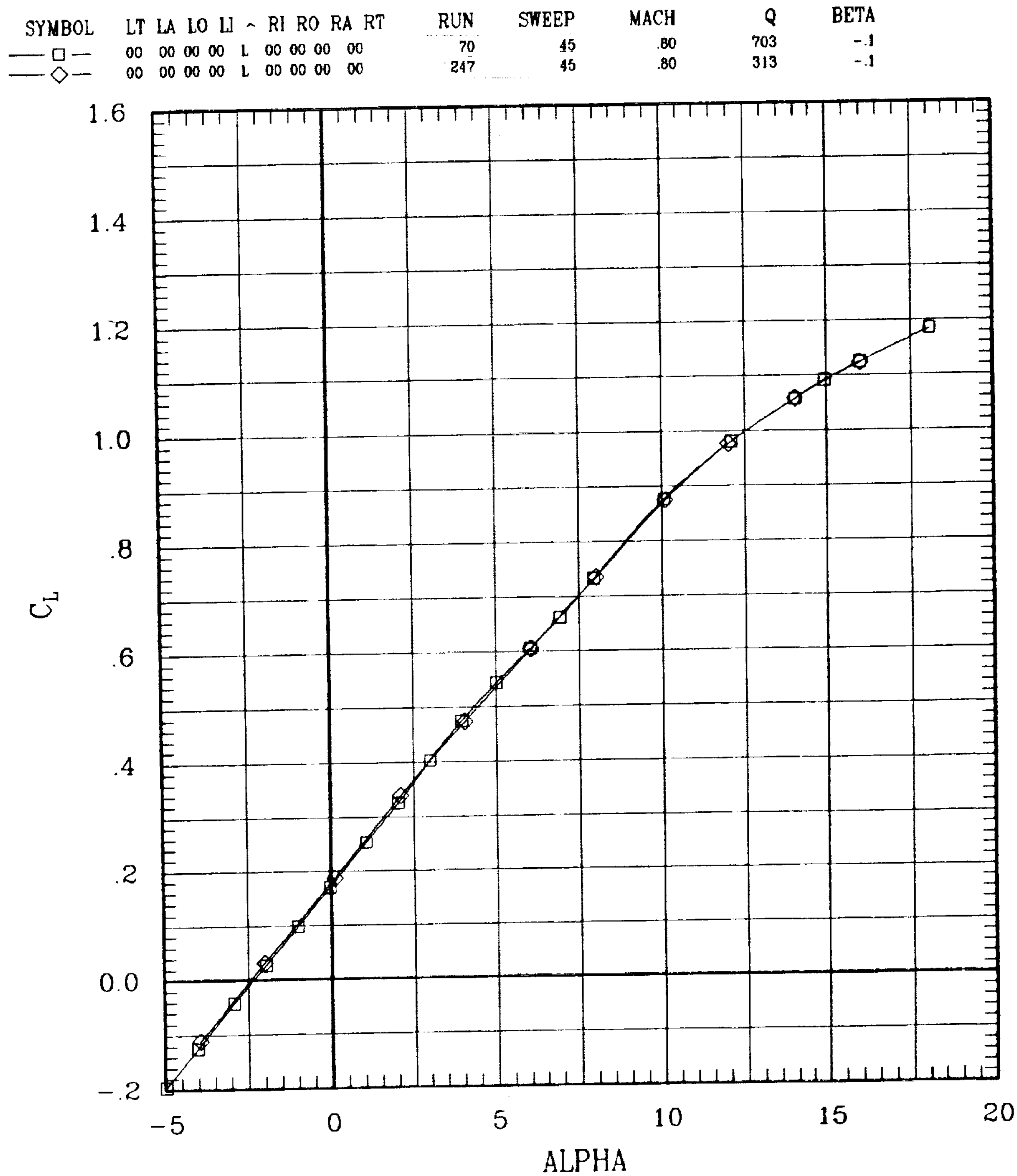

Figure 15. Effect of reduced dynamic pressure.

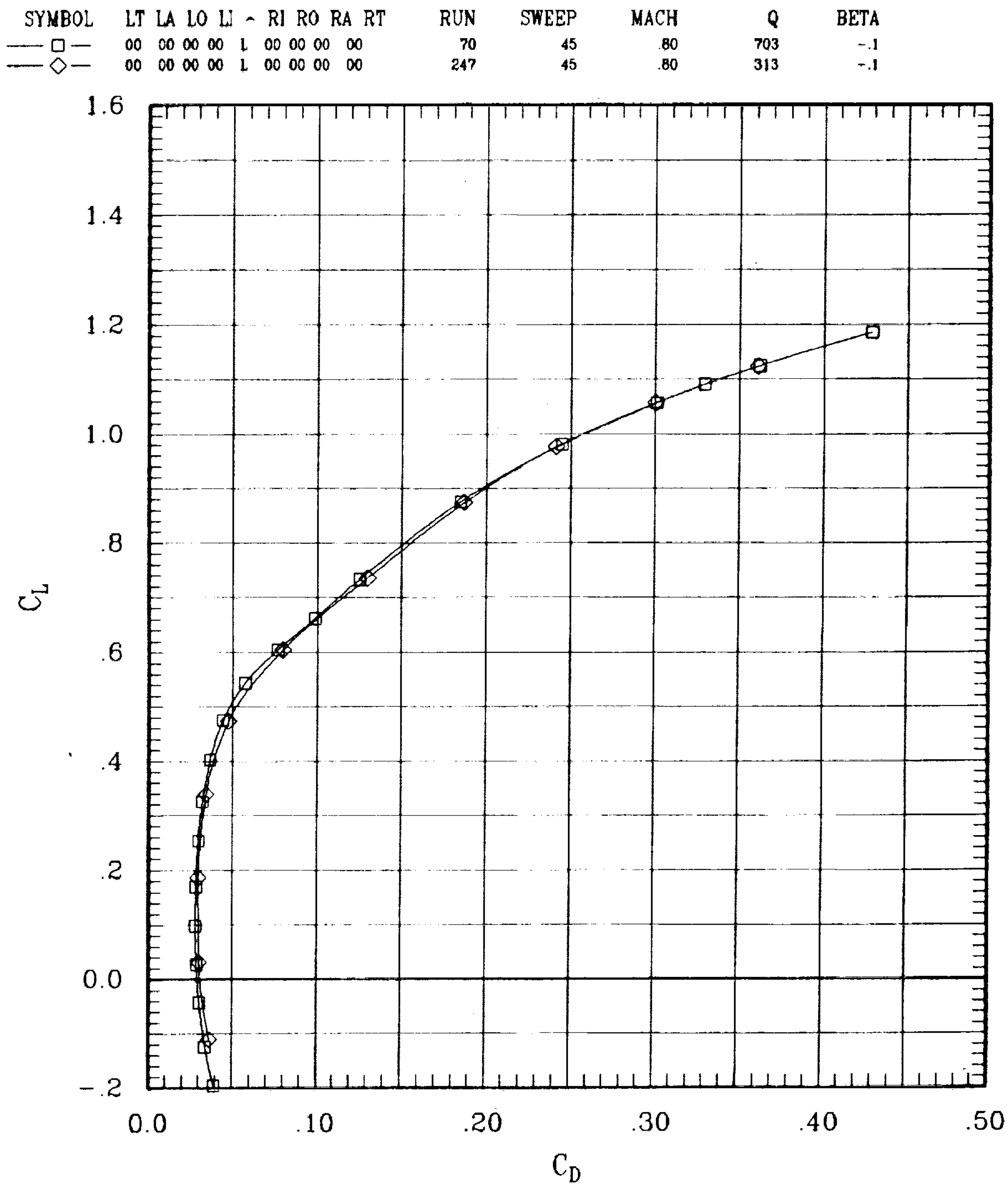

Figure 15. Effect of reduced dynamic pressure.

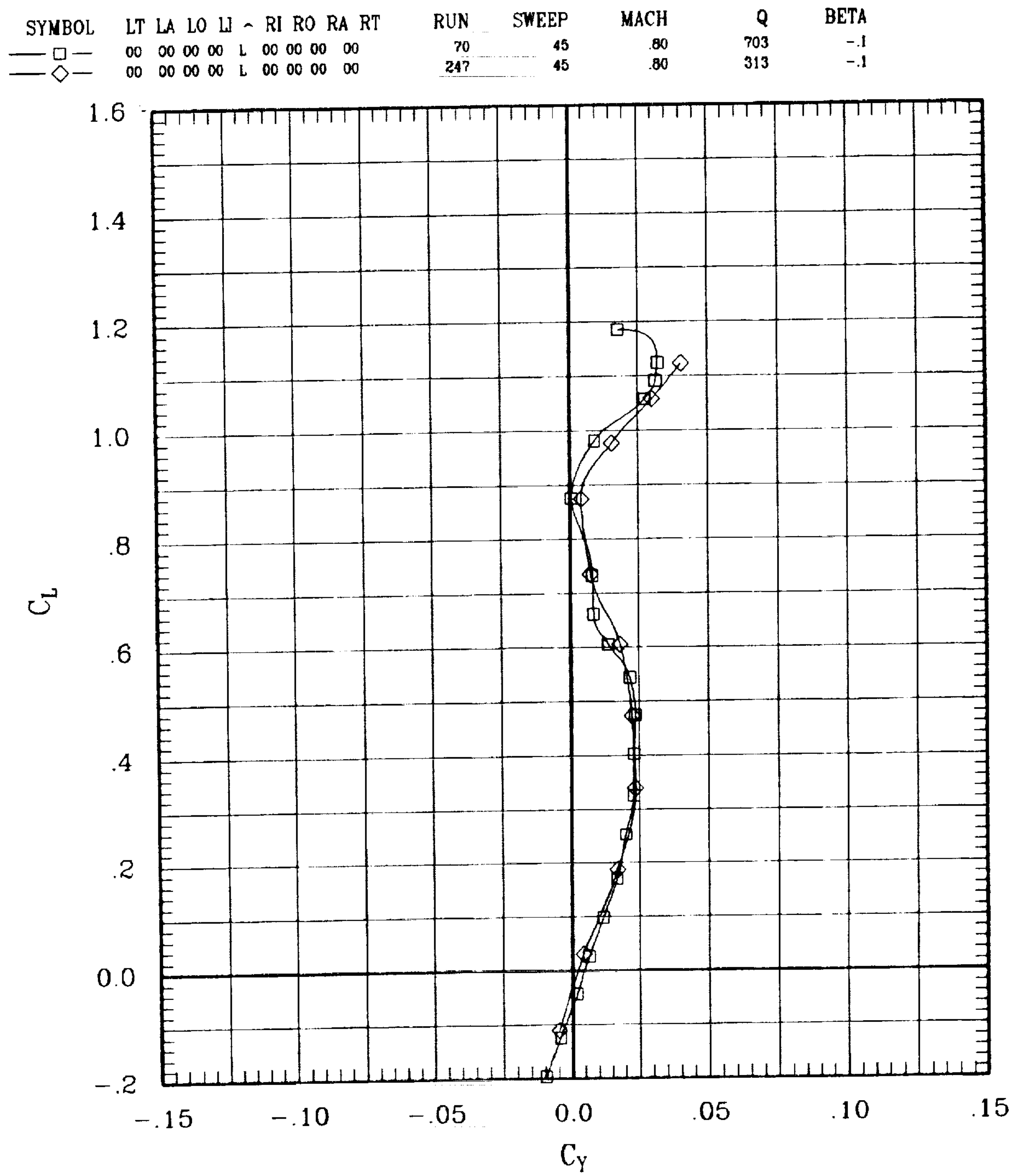

Figure 15. Effect of reduced dynamic pressure.

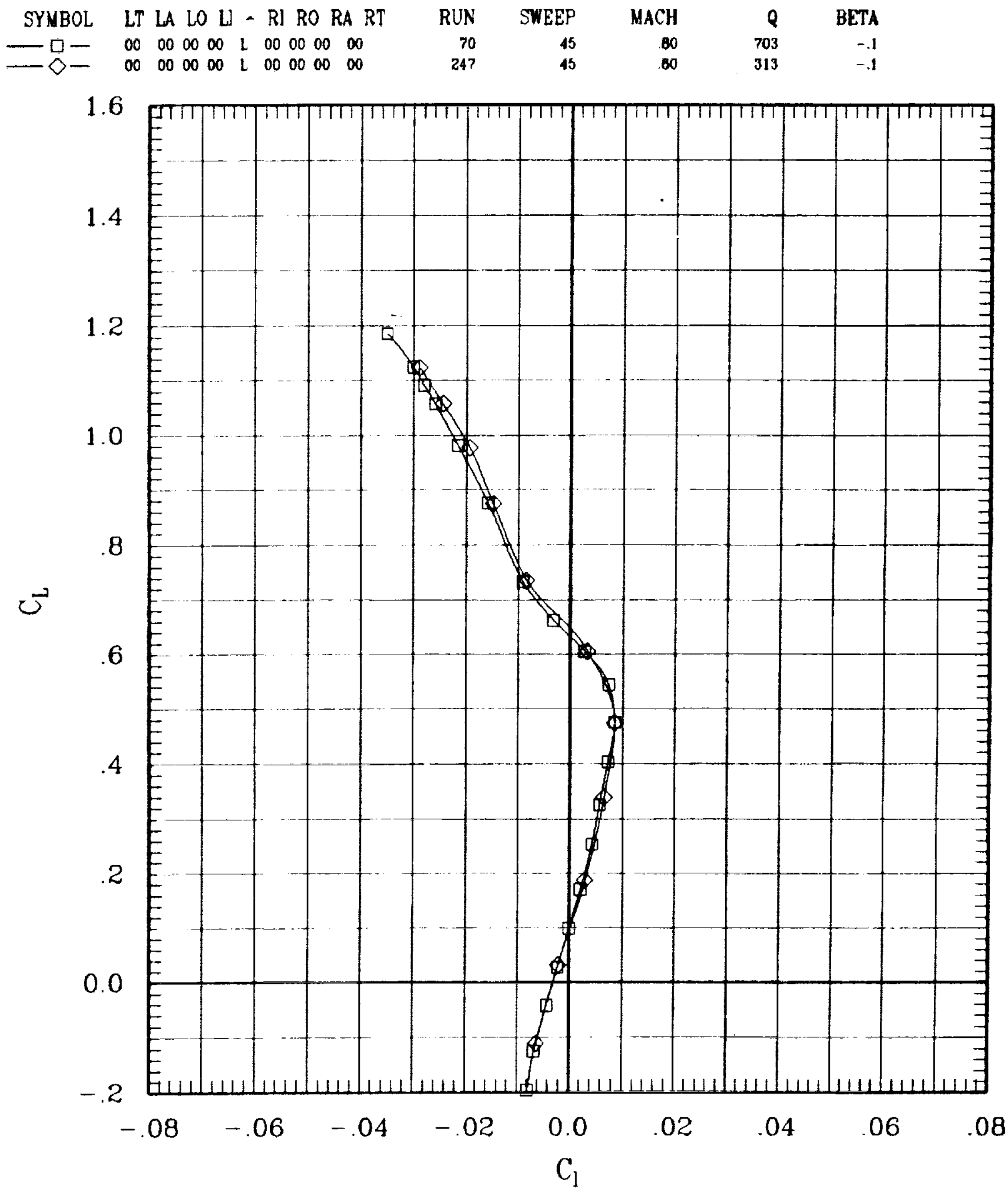

Figure 15. Effect of reduced dynamic pressure.

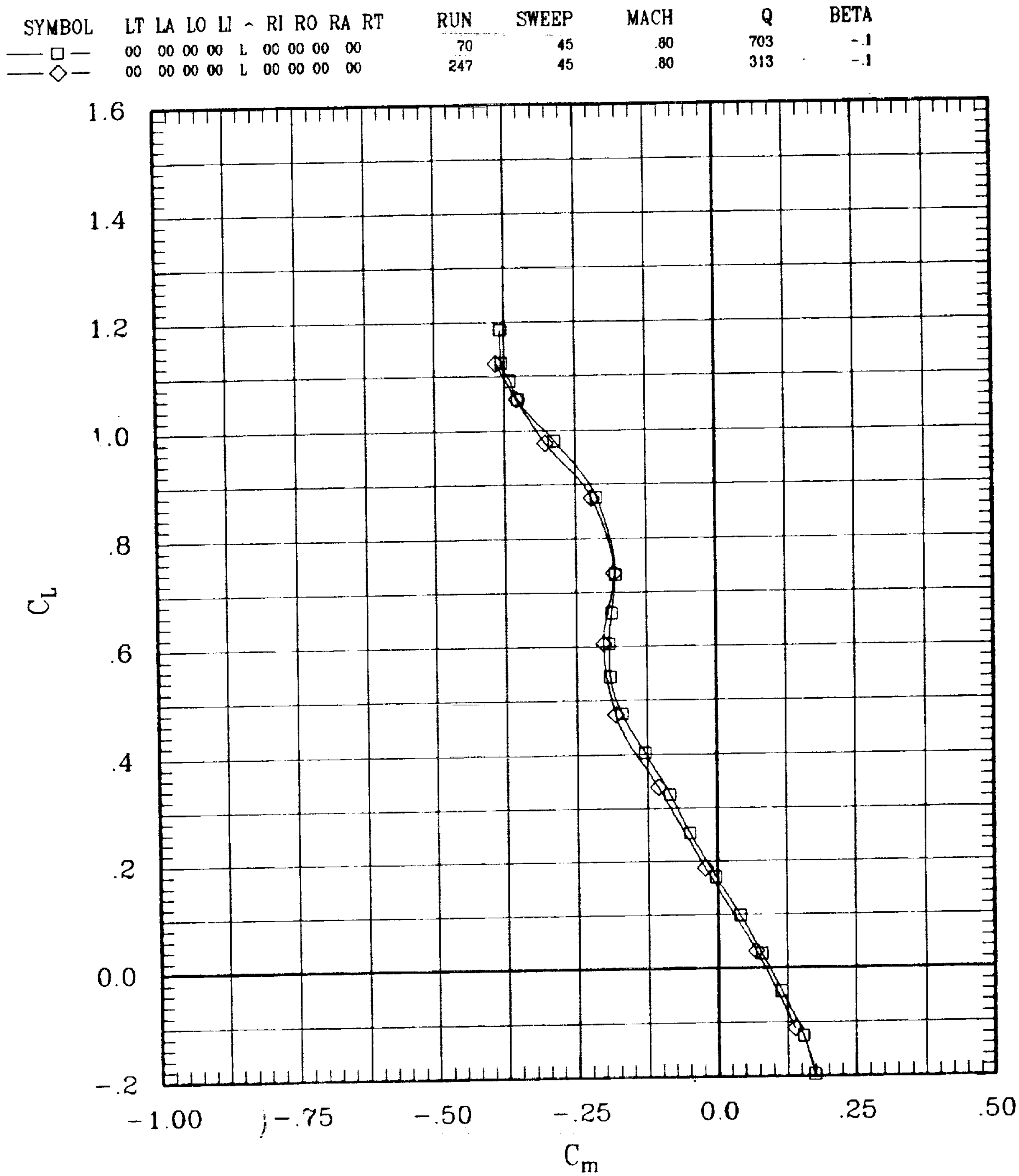

Figure 15. Effect of reduced dynamic pressure.

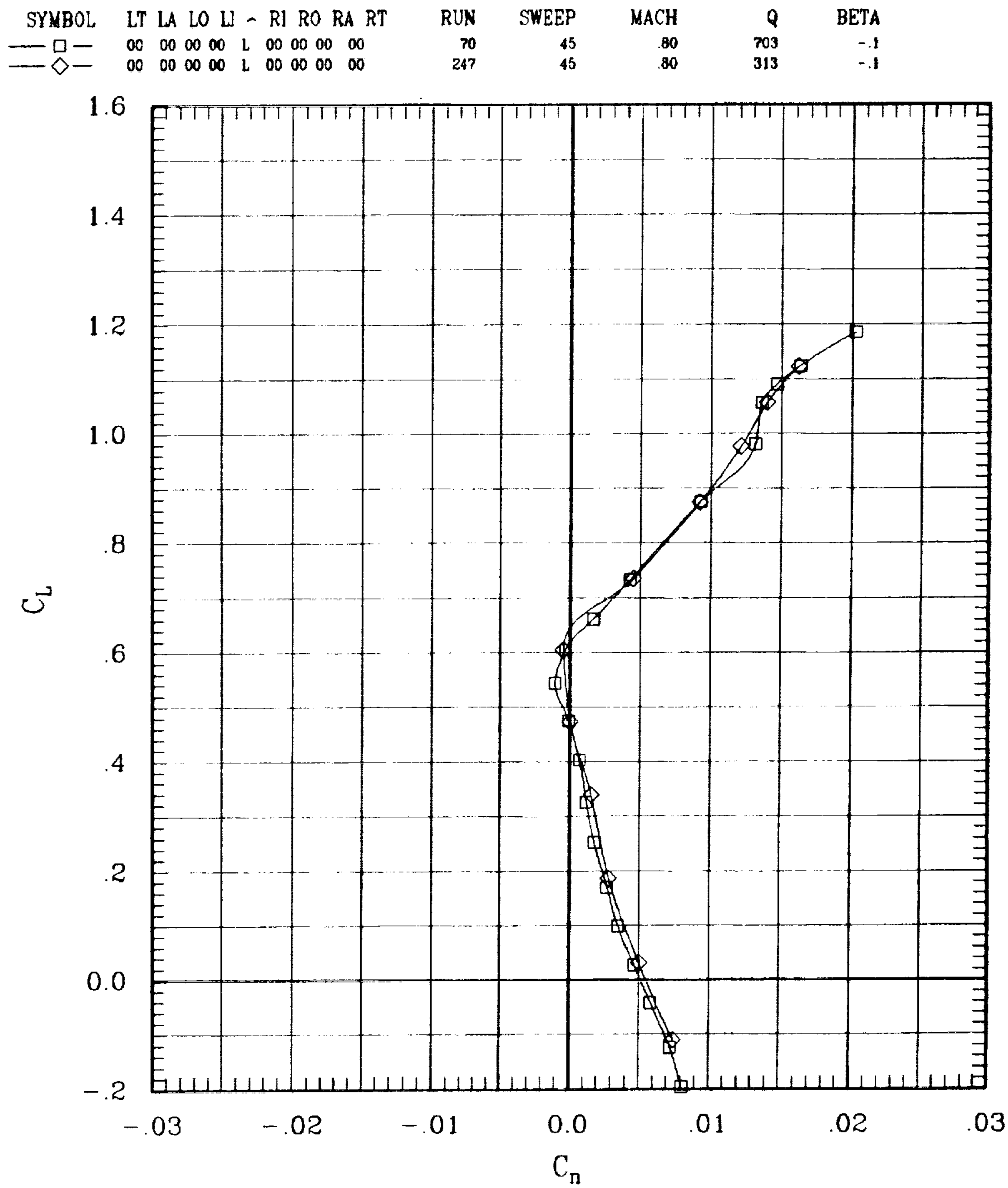

Figure 15. Effect of reduced dynamic pressure.

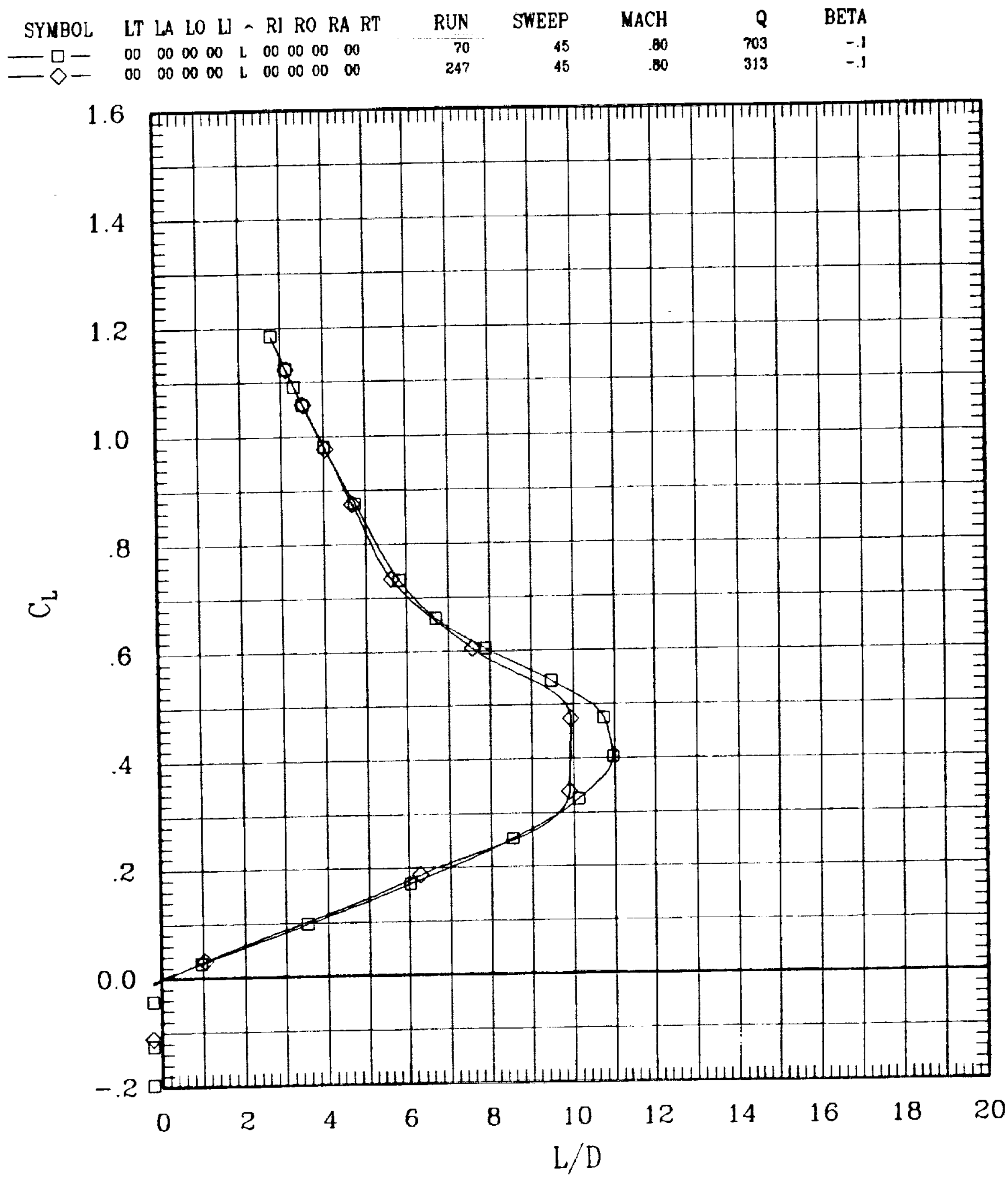

Figure 15. Effect of reduced dynamic pressure.

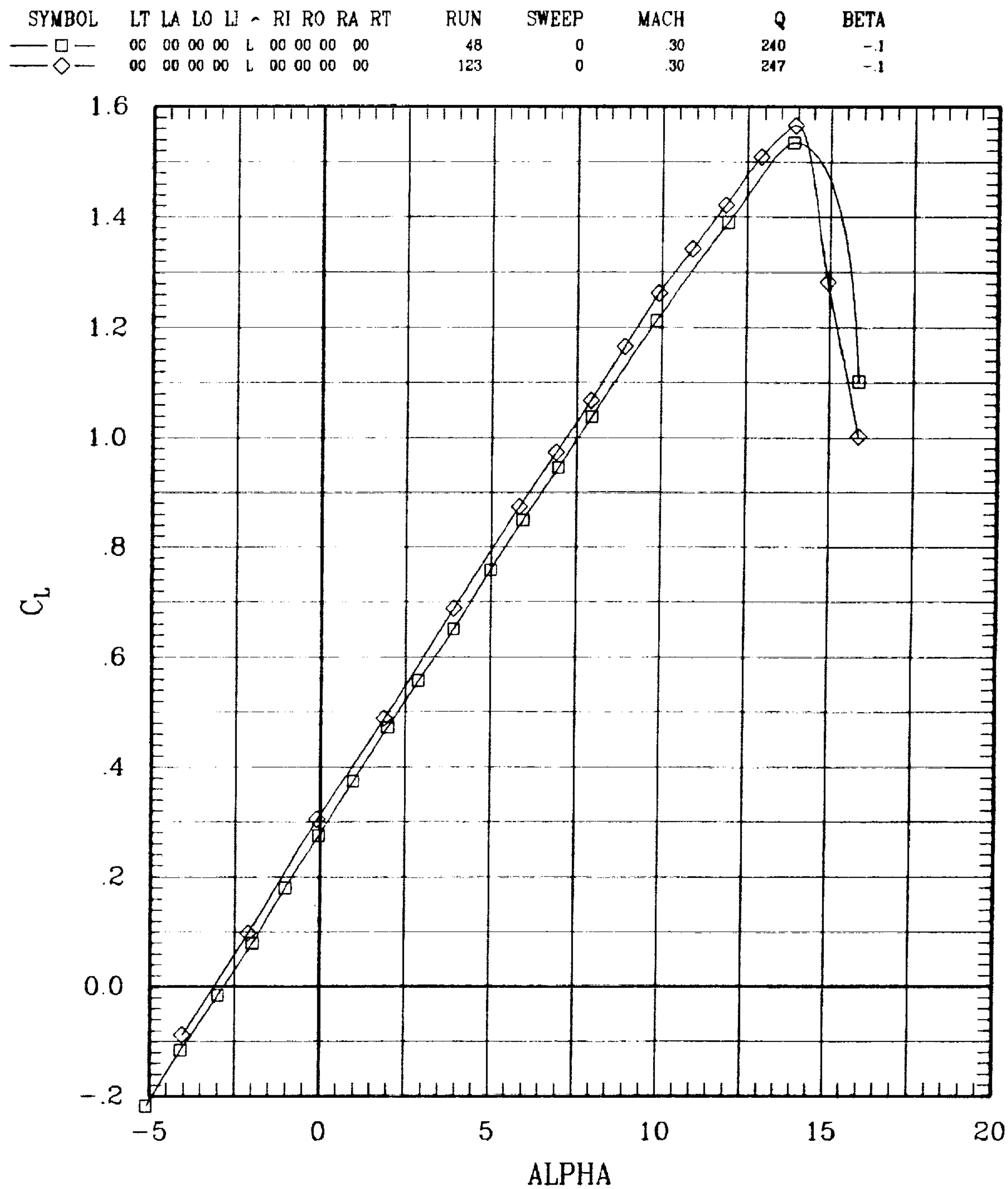

Figure 16. Repeat runs.

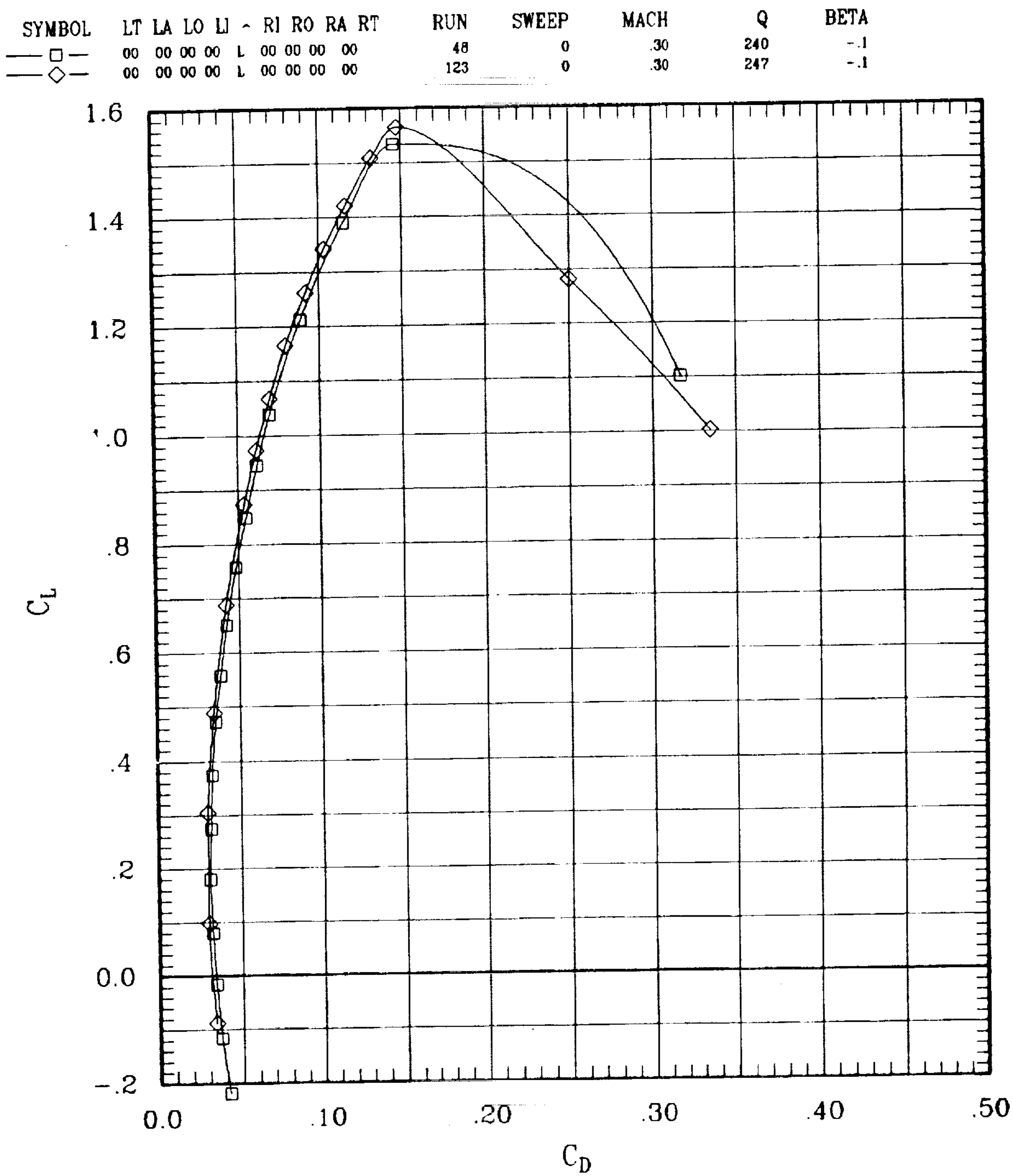

Figure 16. Repeat runs.

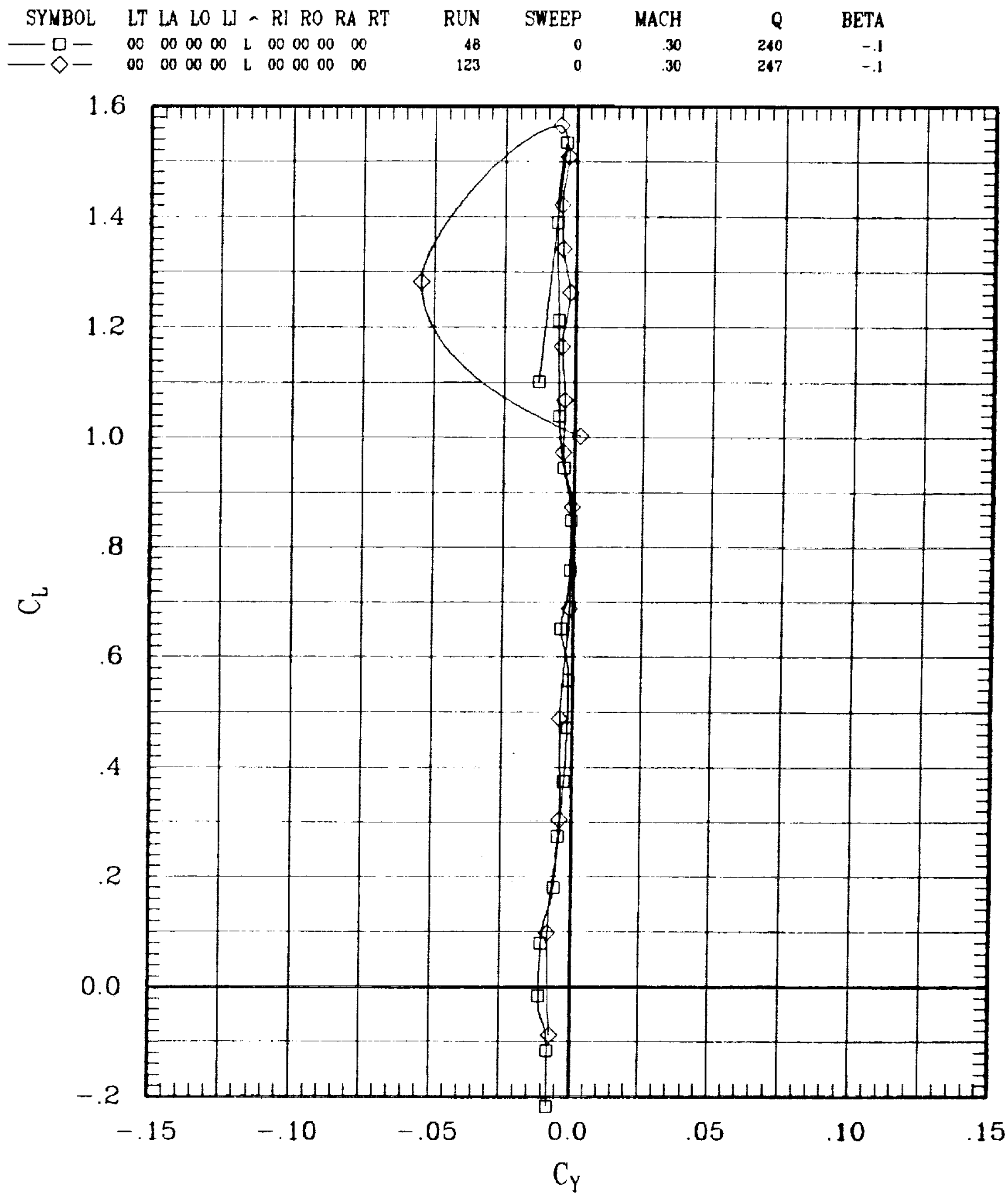

Figure 16. Repeat runs.

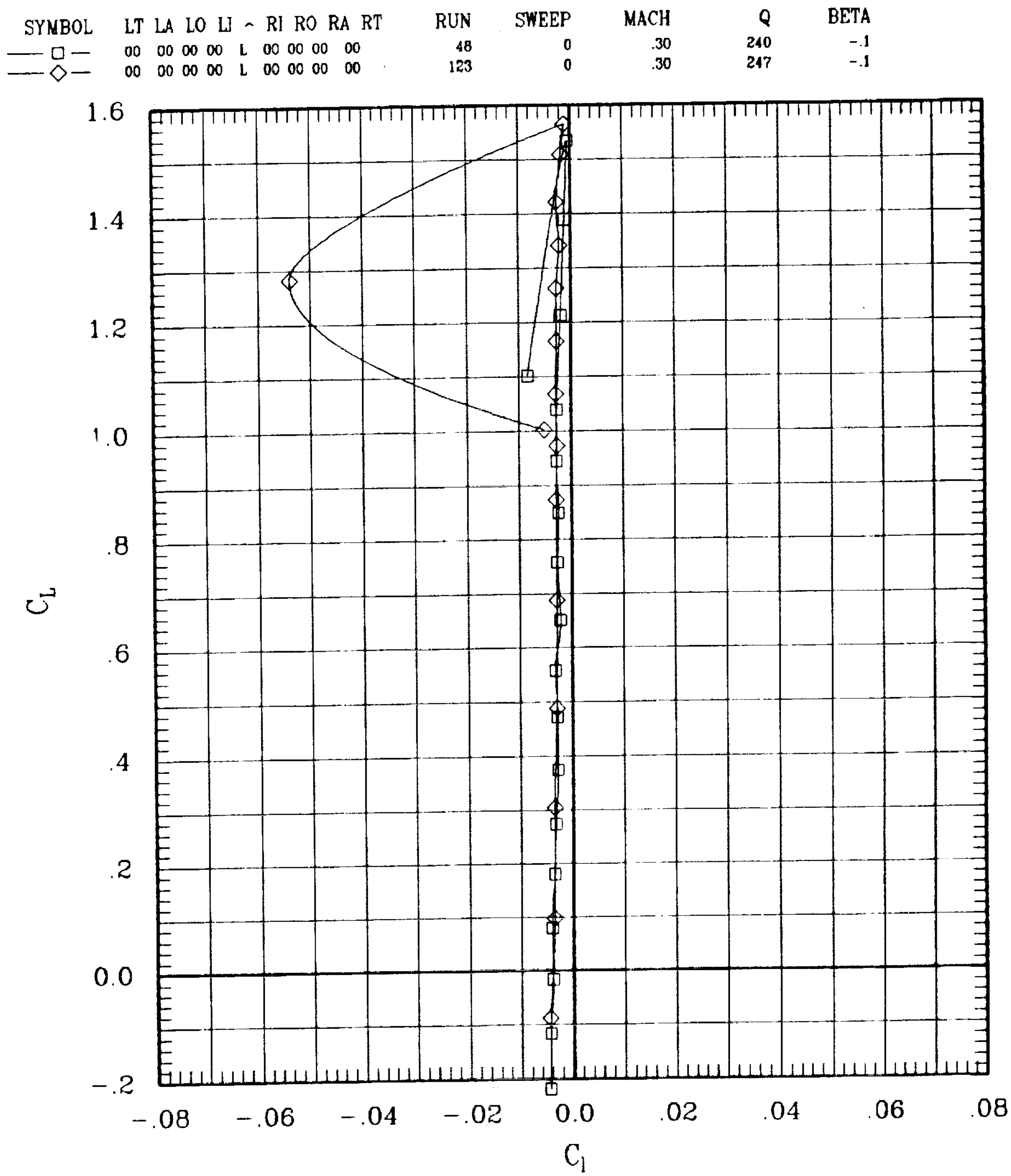

Figure 16. Repeat runs.

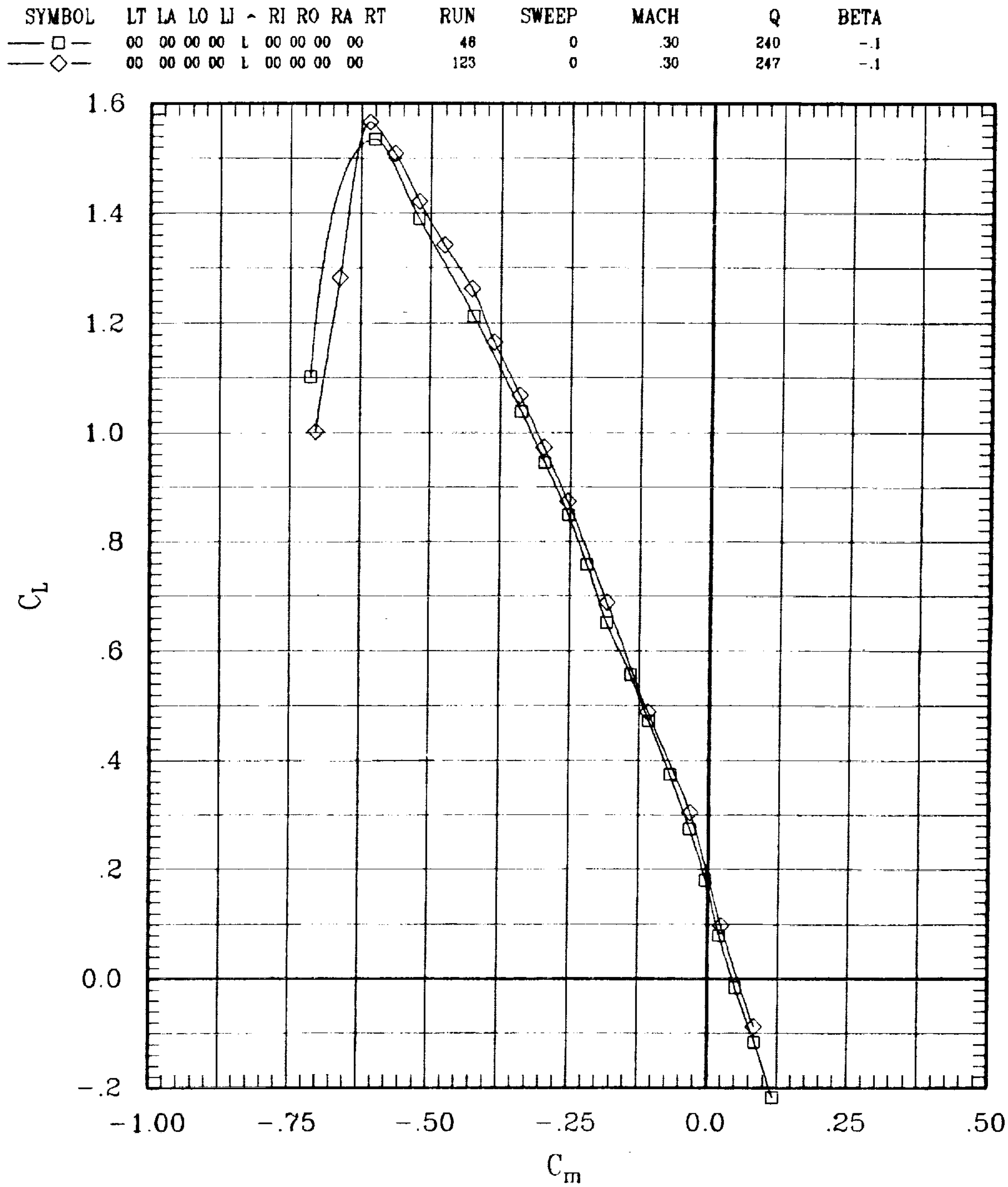

Figure 16. Repeat runs.

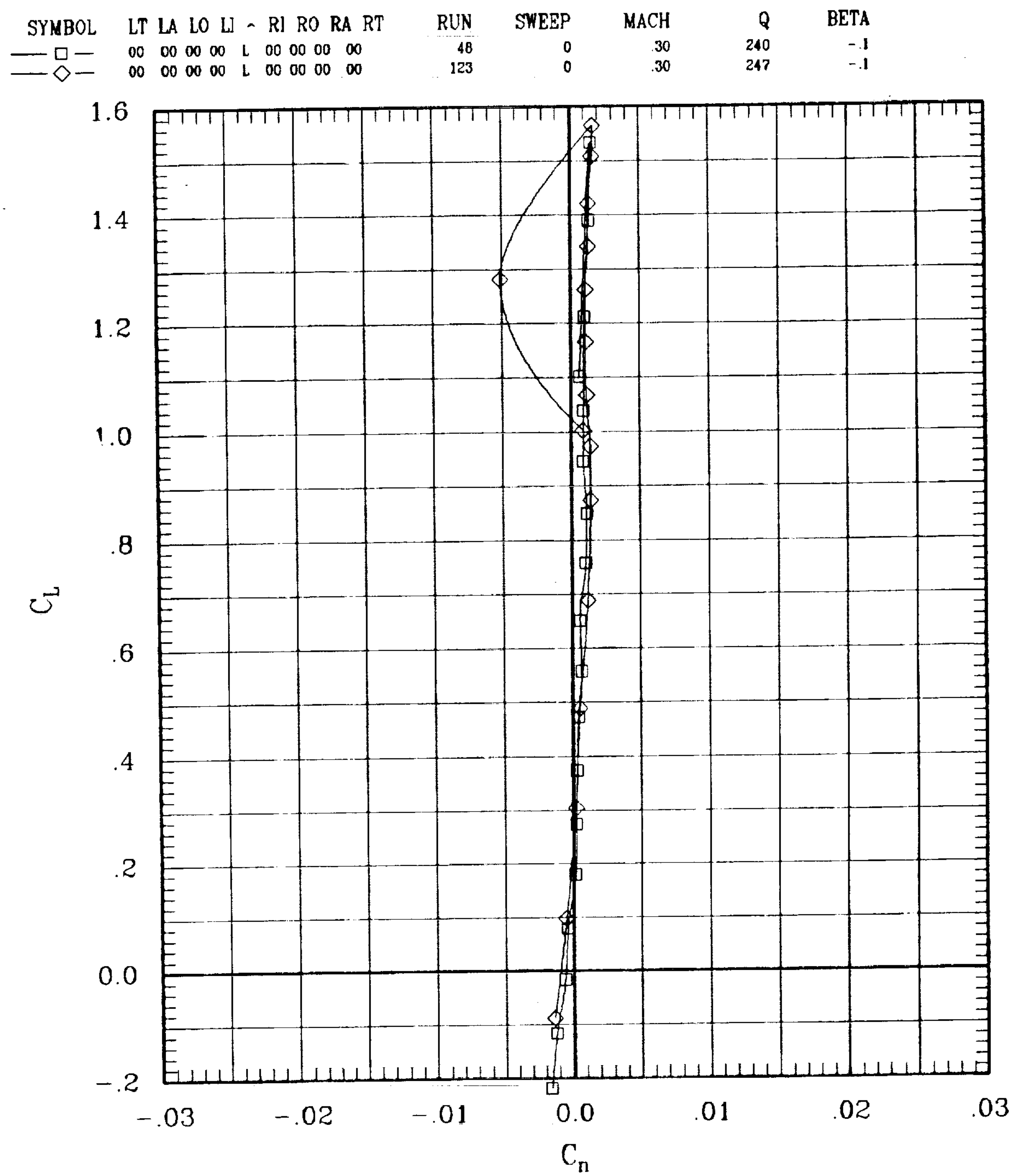

Figure 16. Repeat runs.

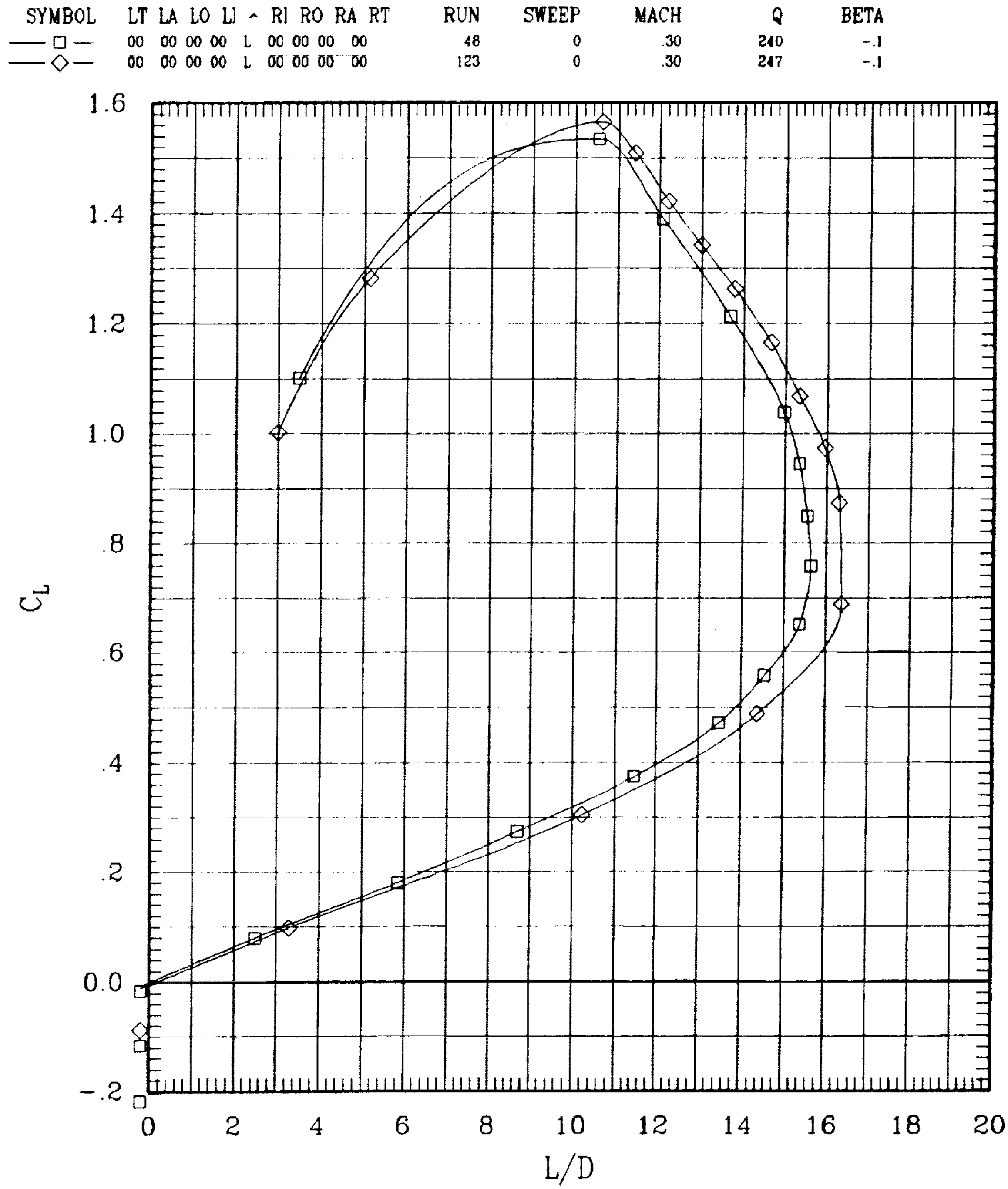

Figure 16. Repeat runs.

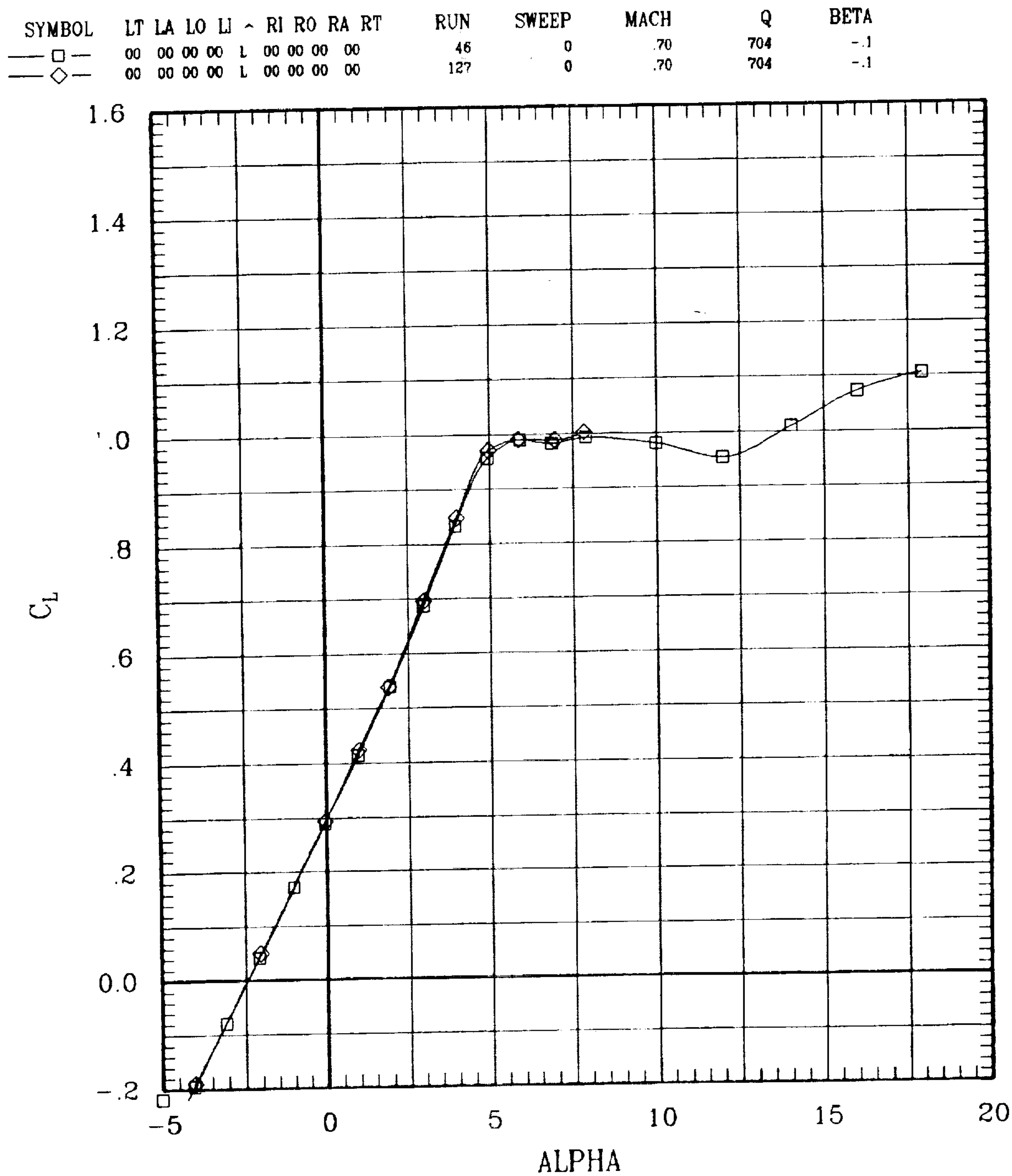

Figure 16. Repeat runs.

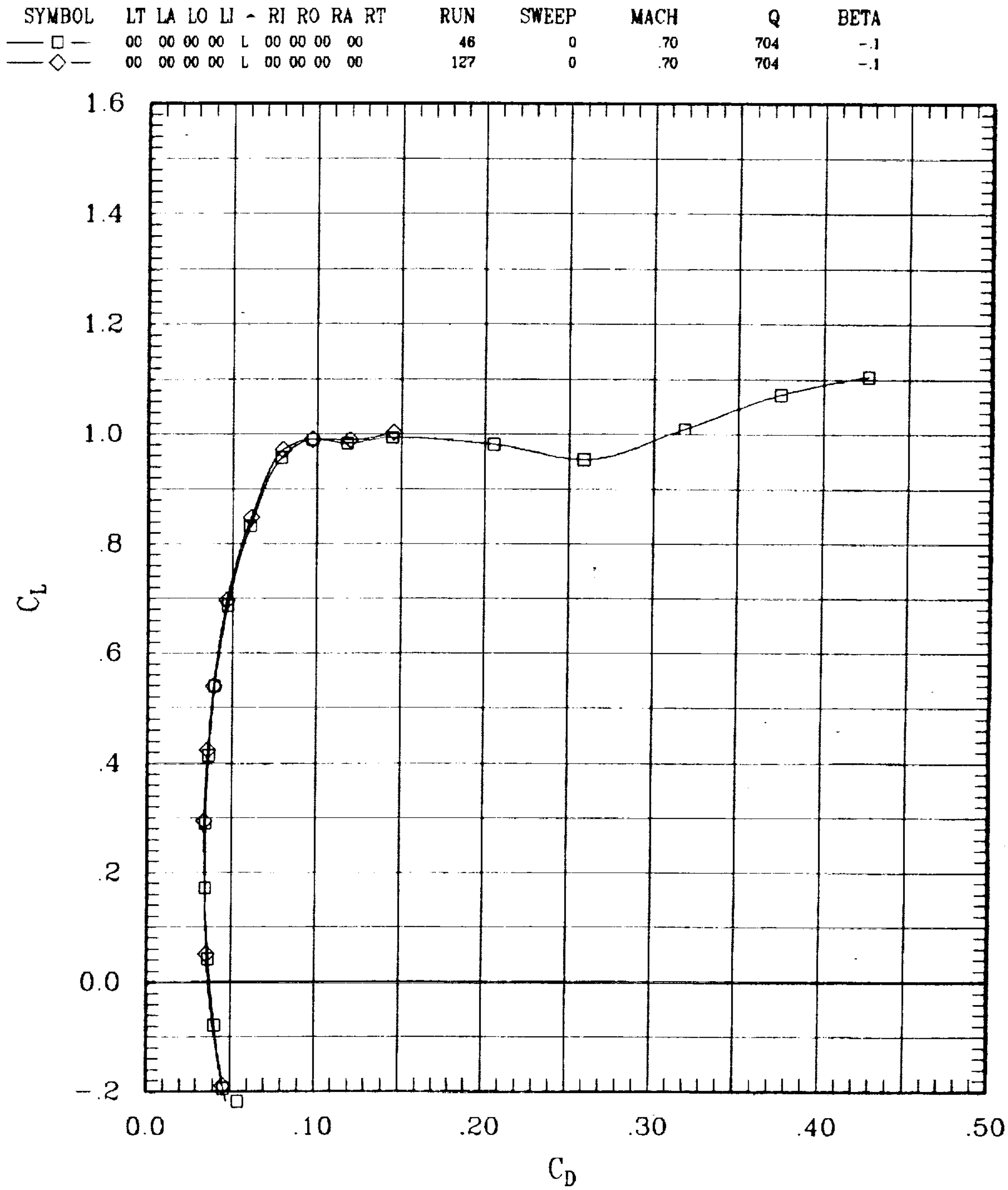

Figure 16. Repeat runs.

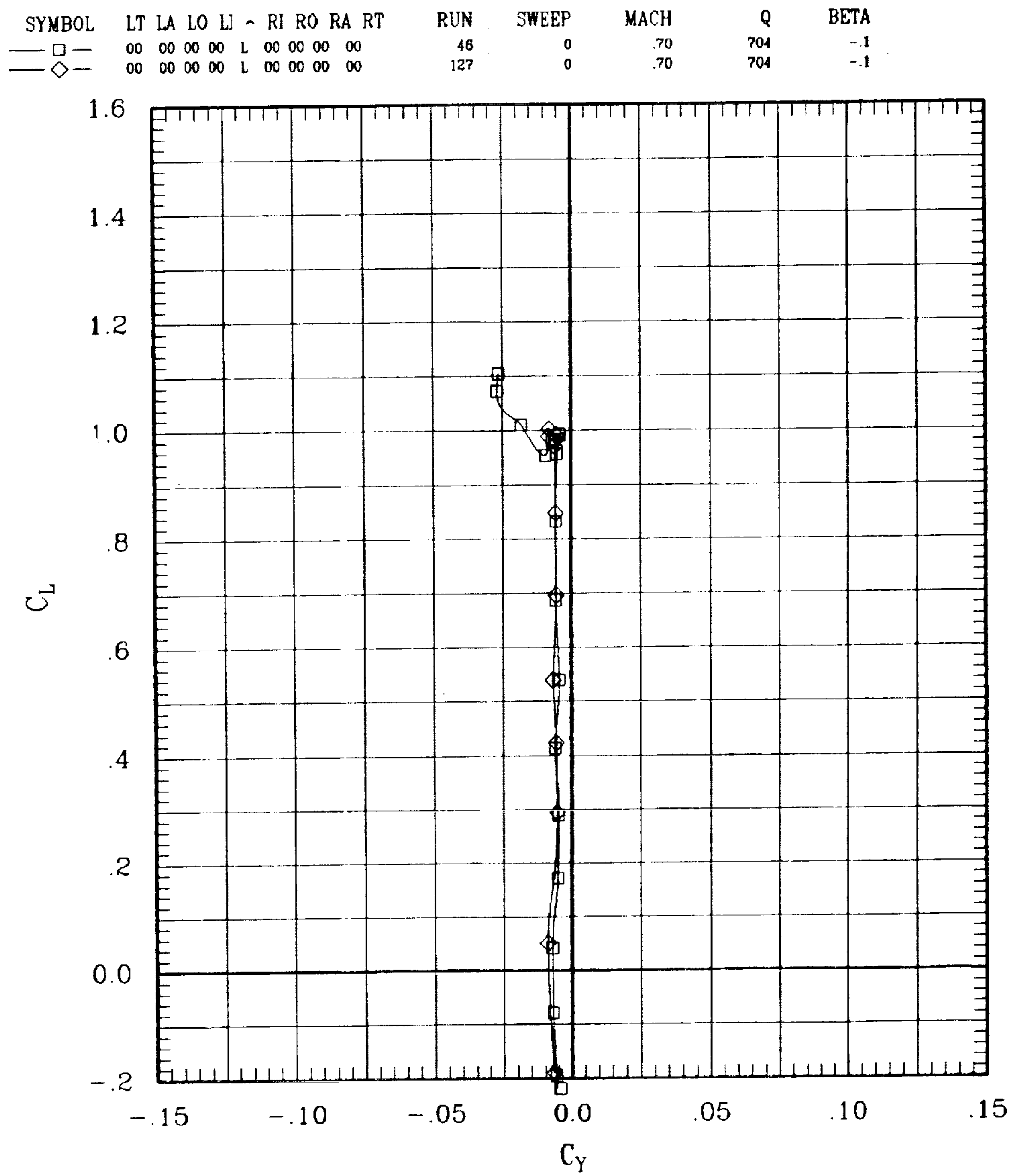

Figure 16. Repeat runs.

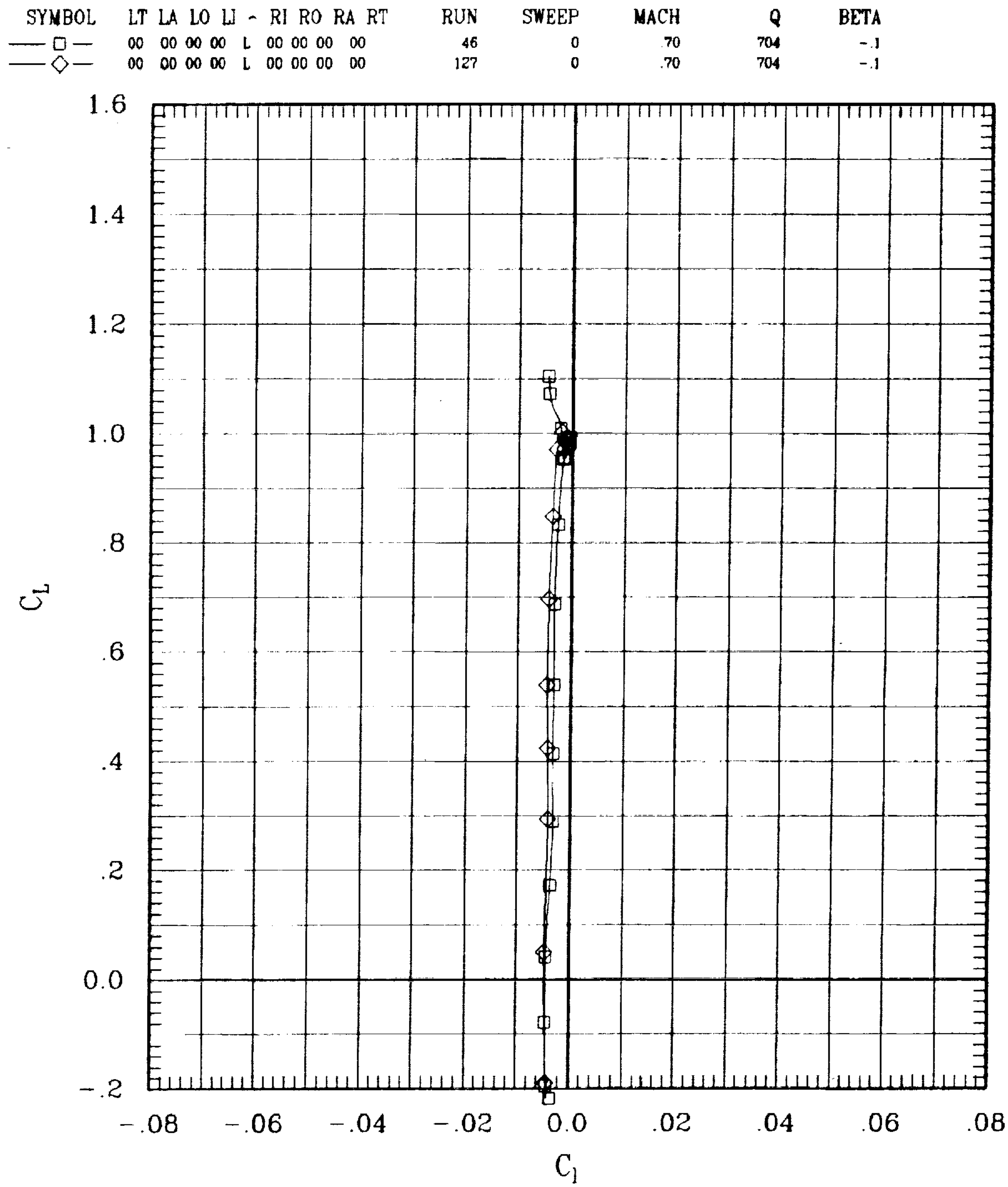

Figure 16. Repeat runs.

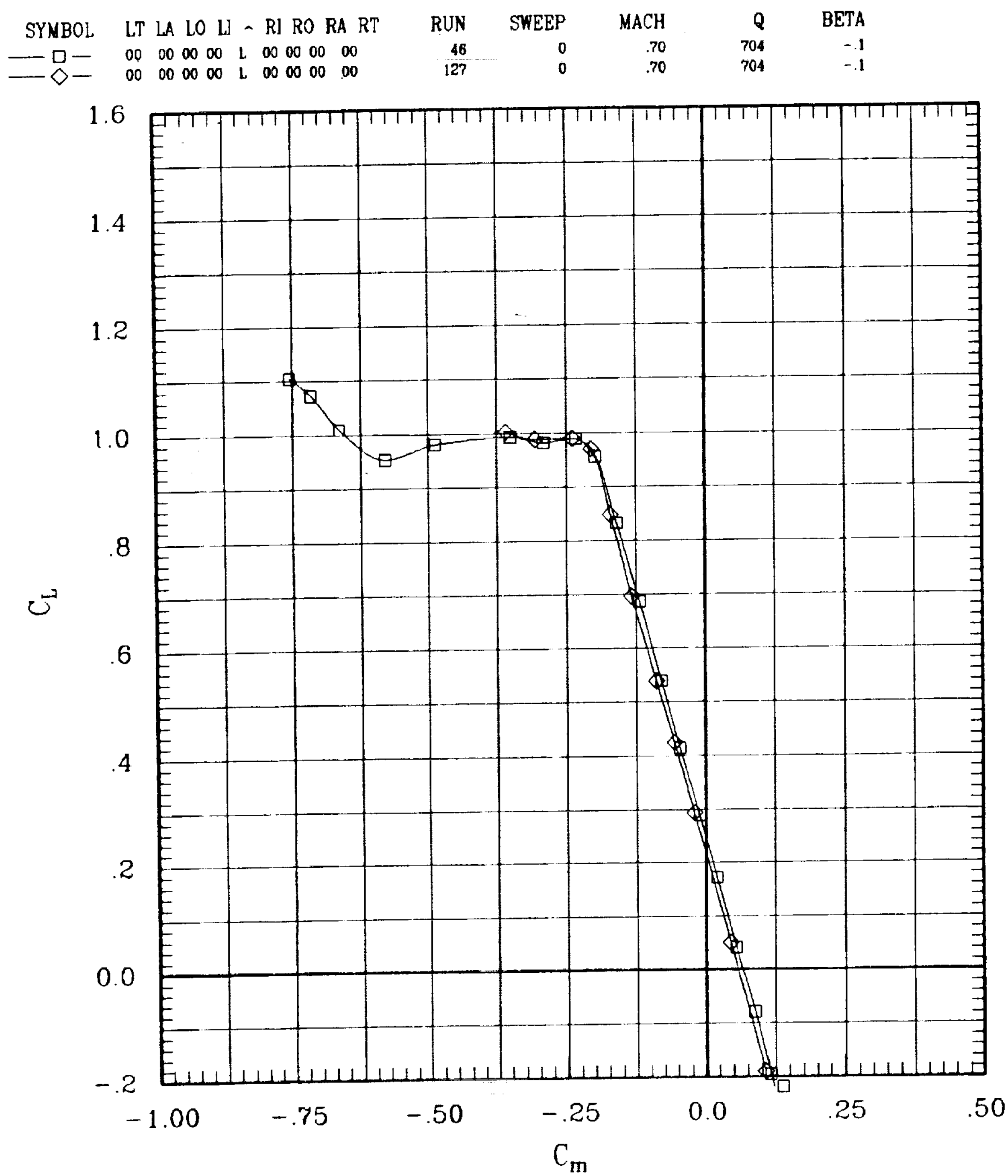

Figure 16. Repeat runs.

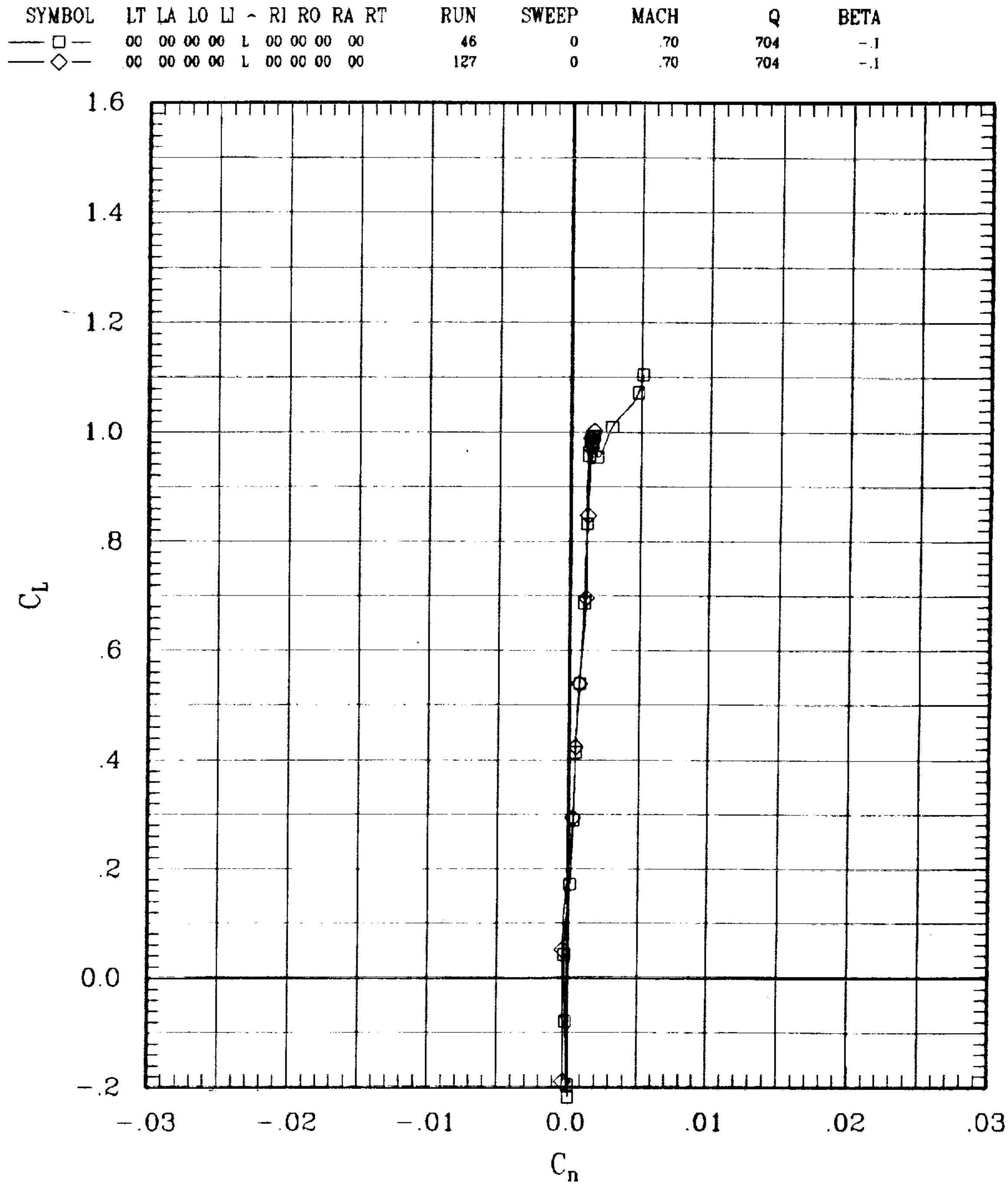

Figure 16. Repeat runs.

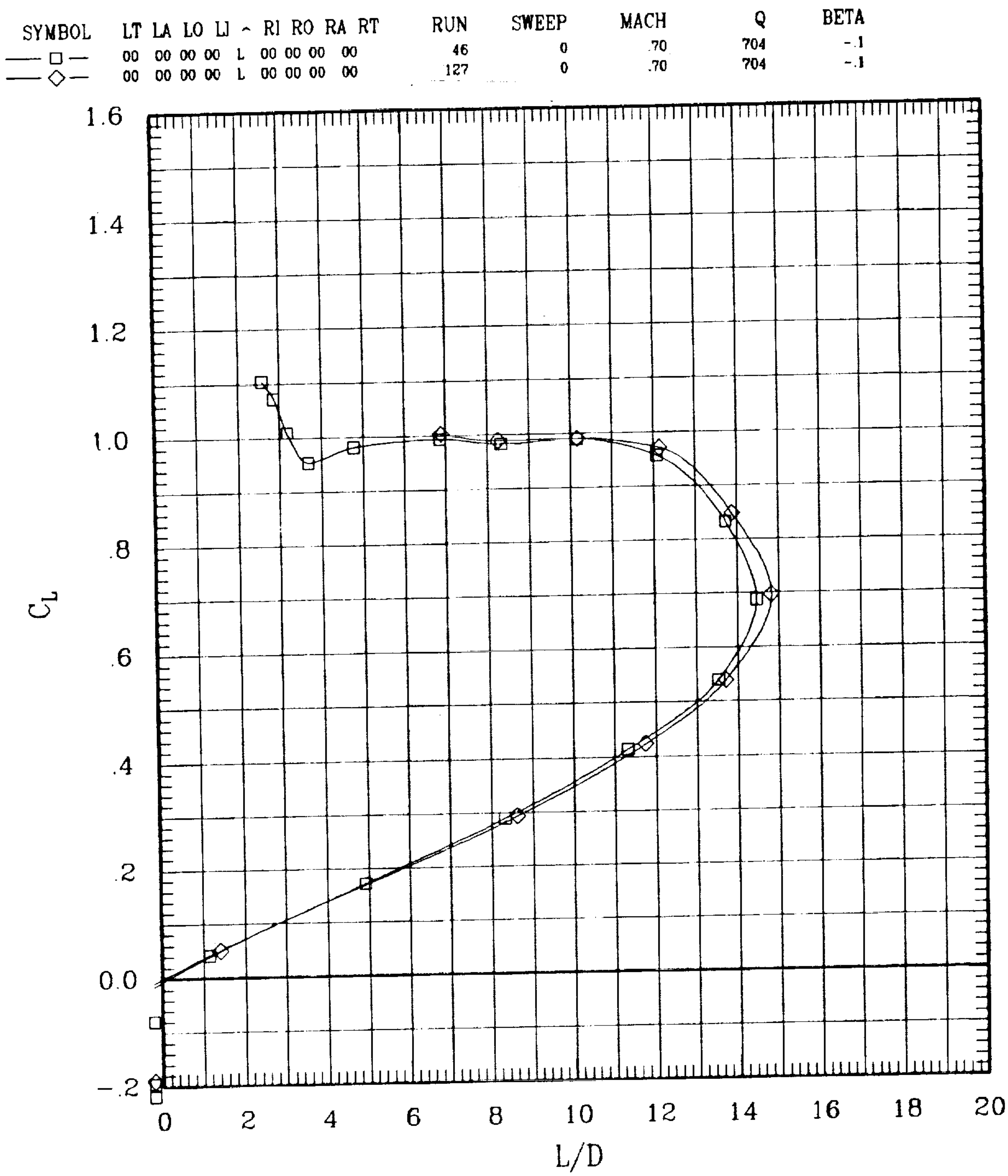

Figure 16. Repeat runs.

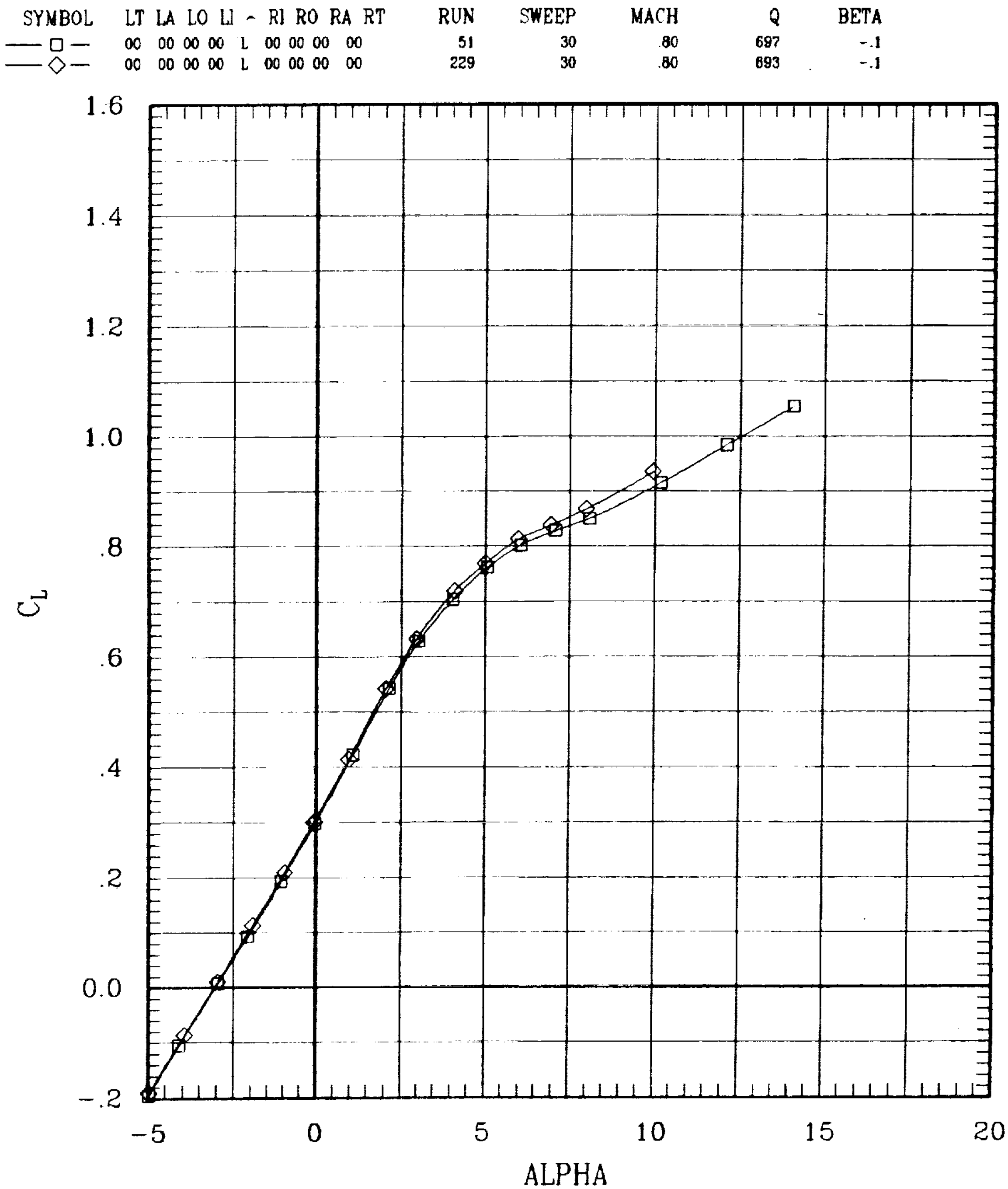

Figure 16. Repeat runs.

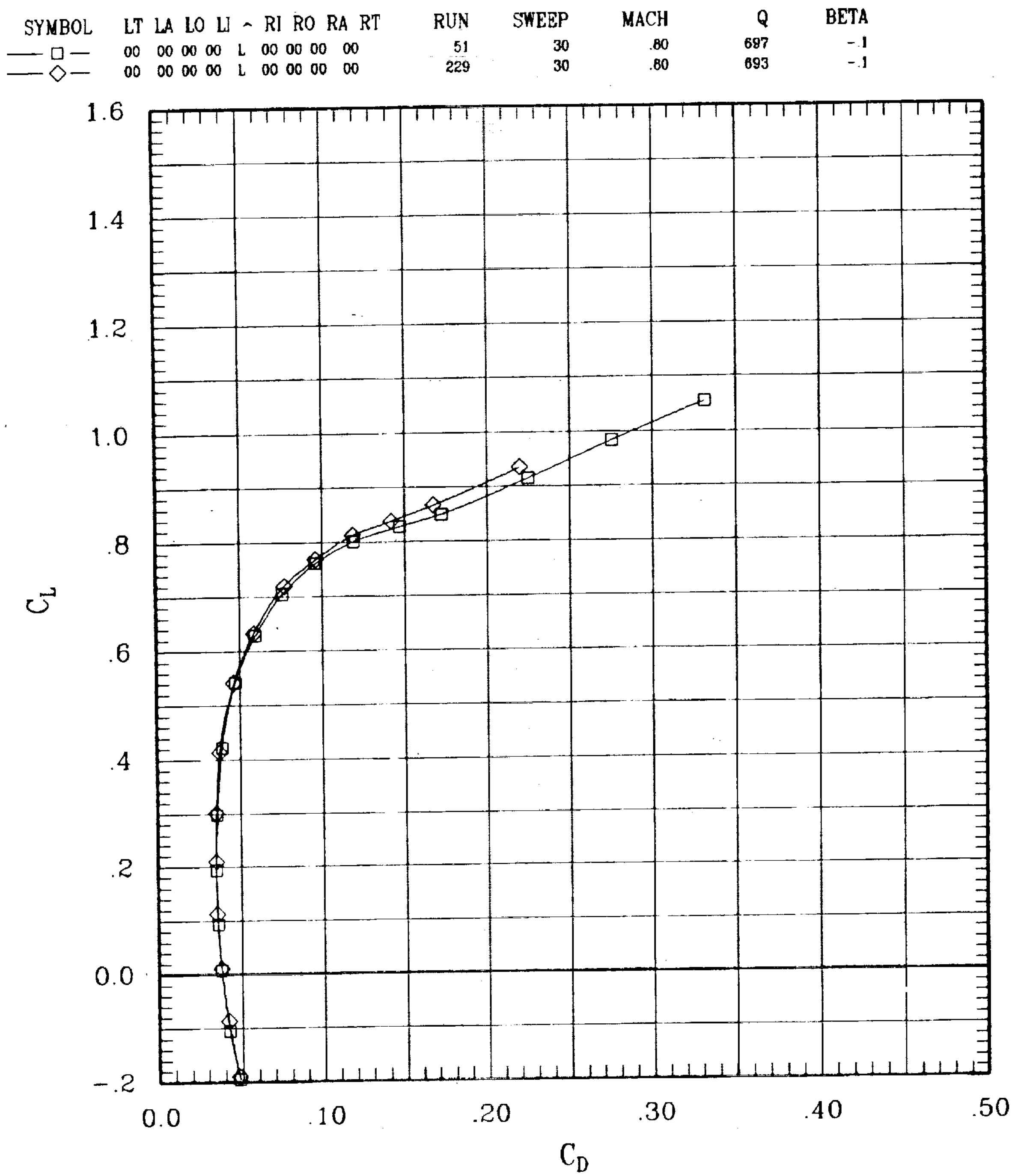

Figure 16. Repeat runs.

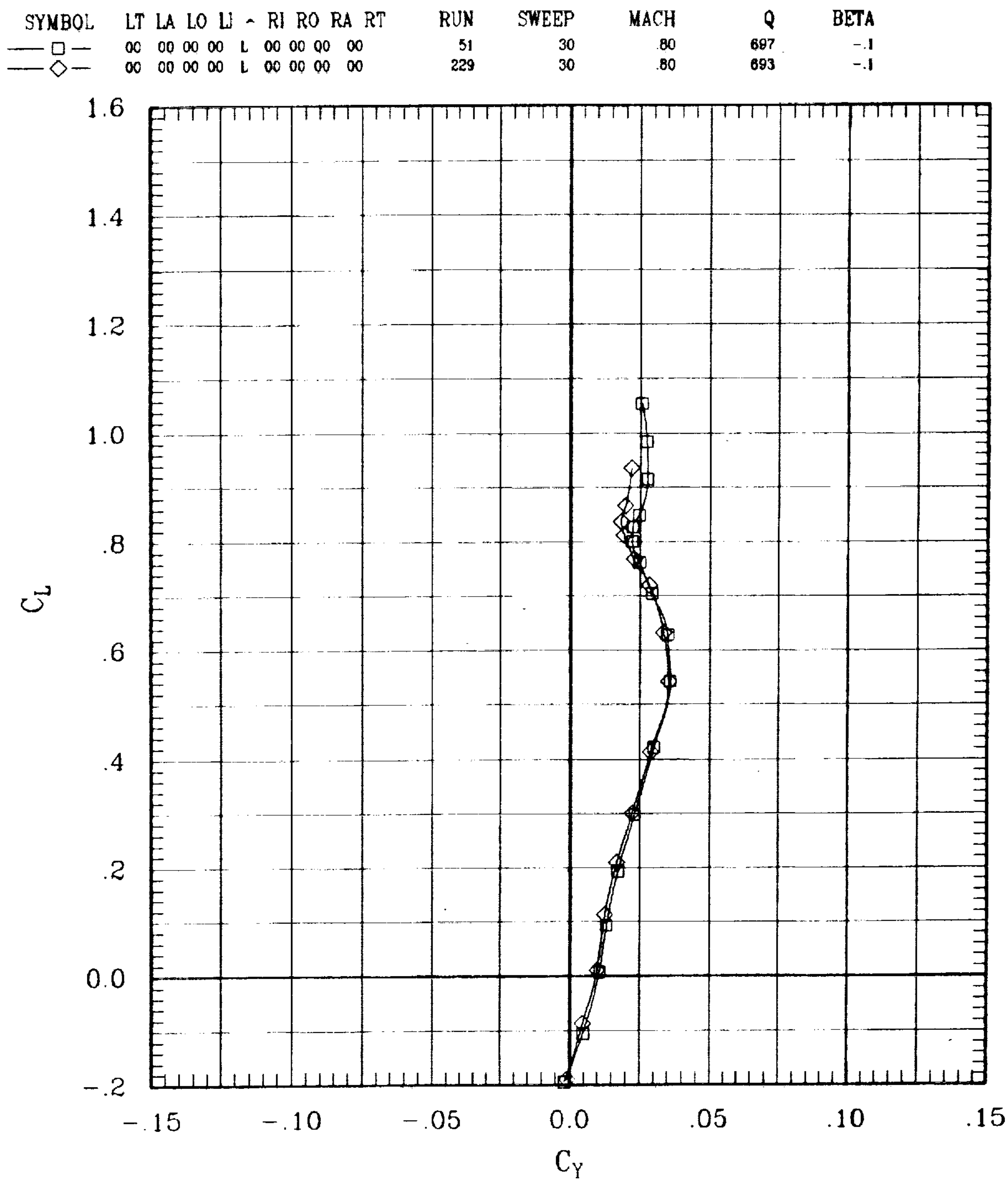

Figure 16. Repeat runs.

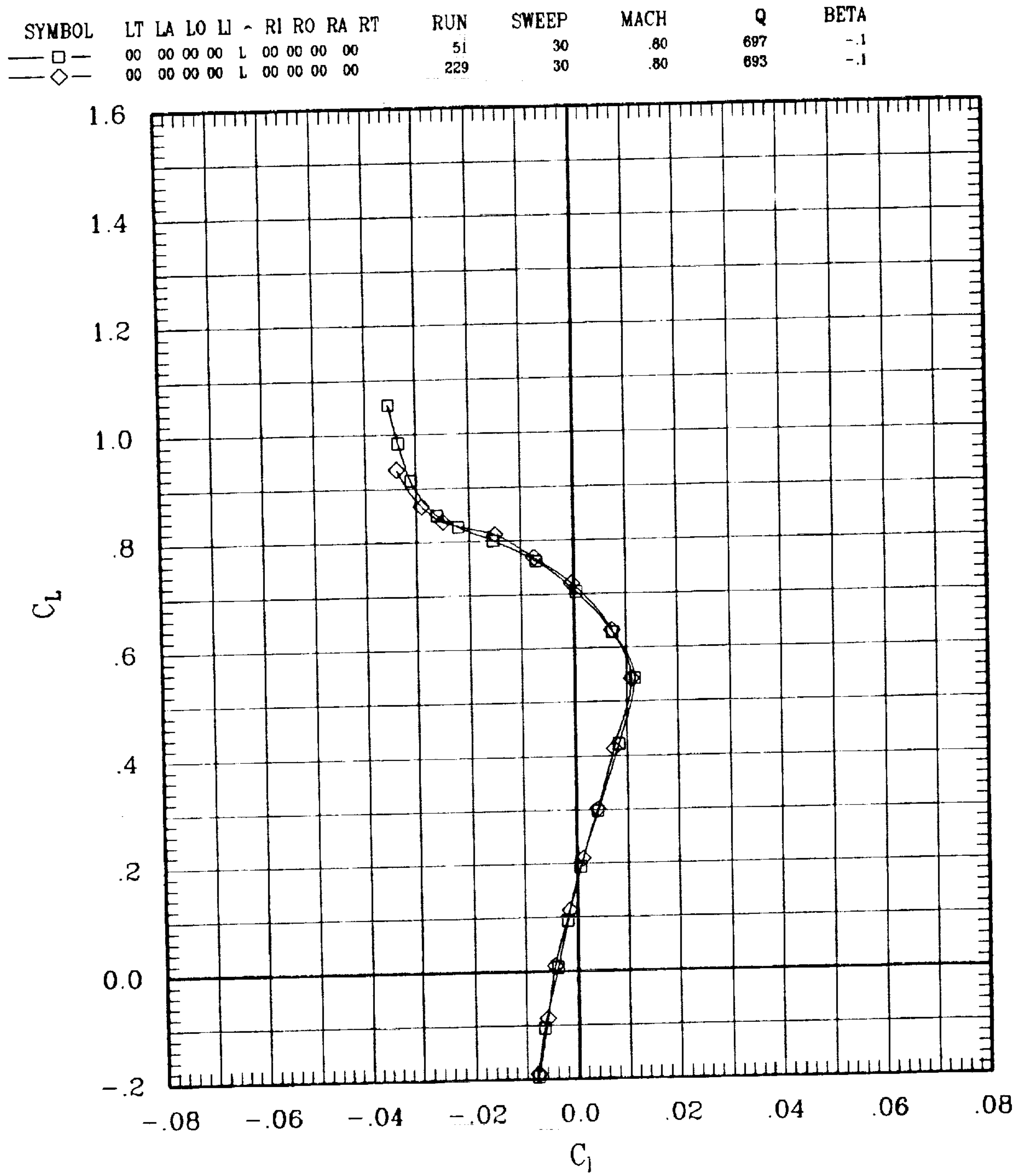

Figure 16. Repeat runs.

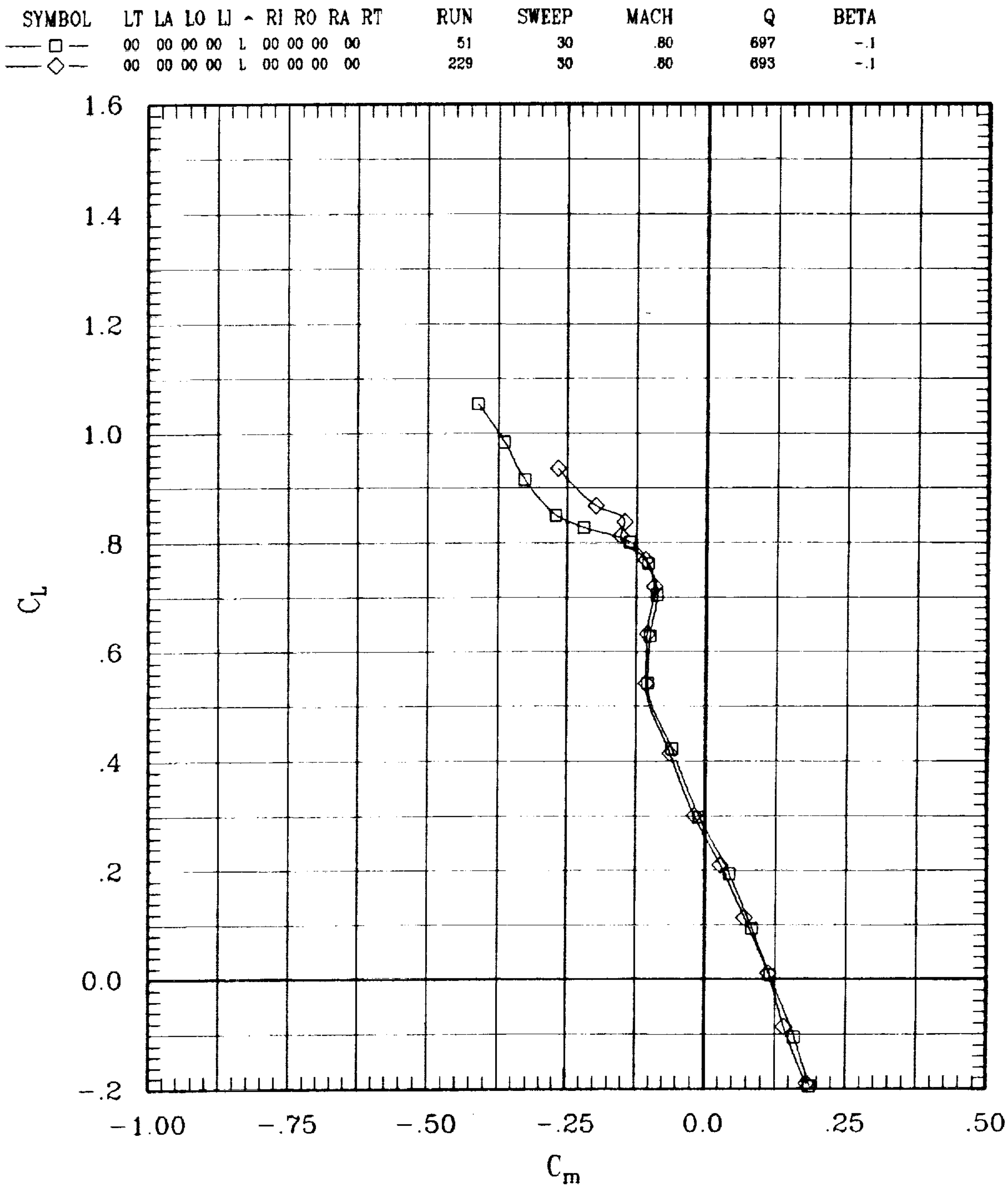

Figure 16. Repeat runs.

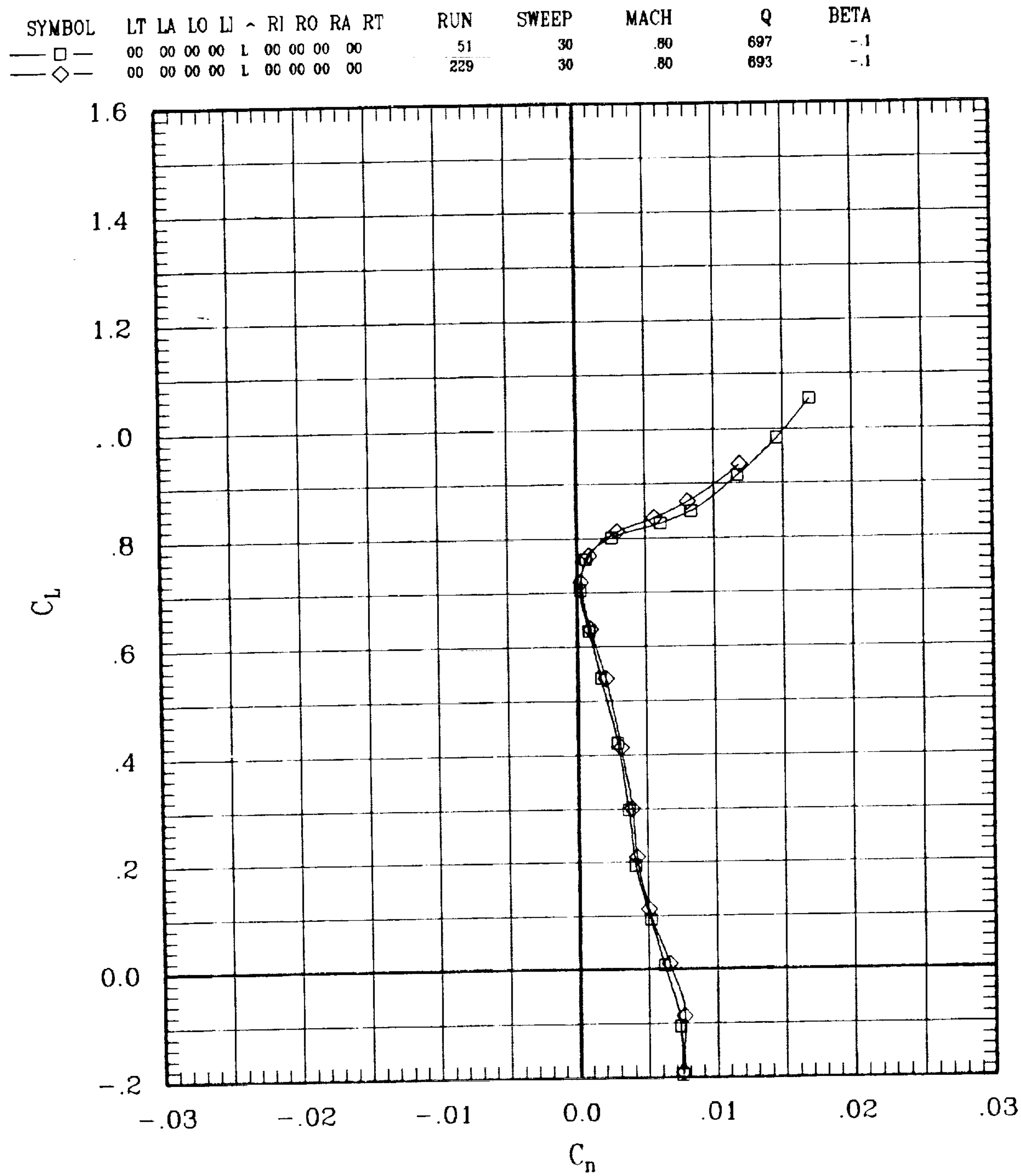

Figure 16. Repeat runs.

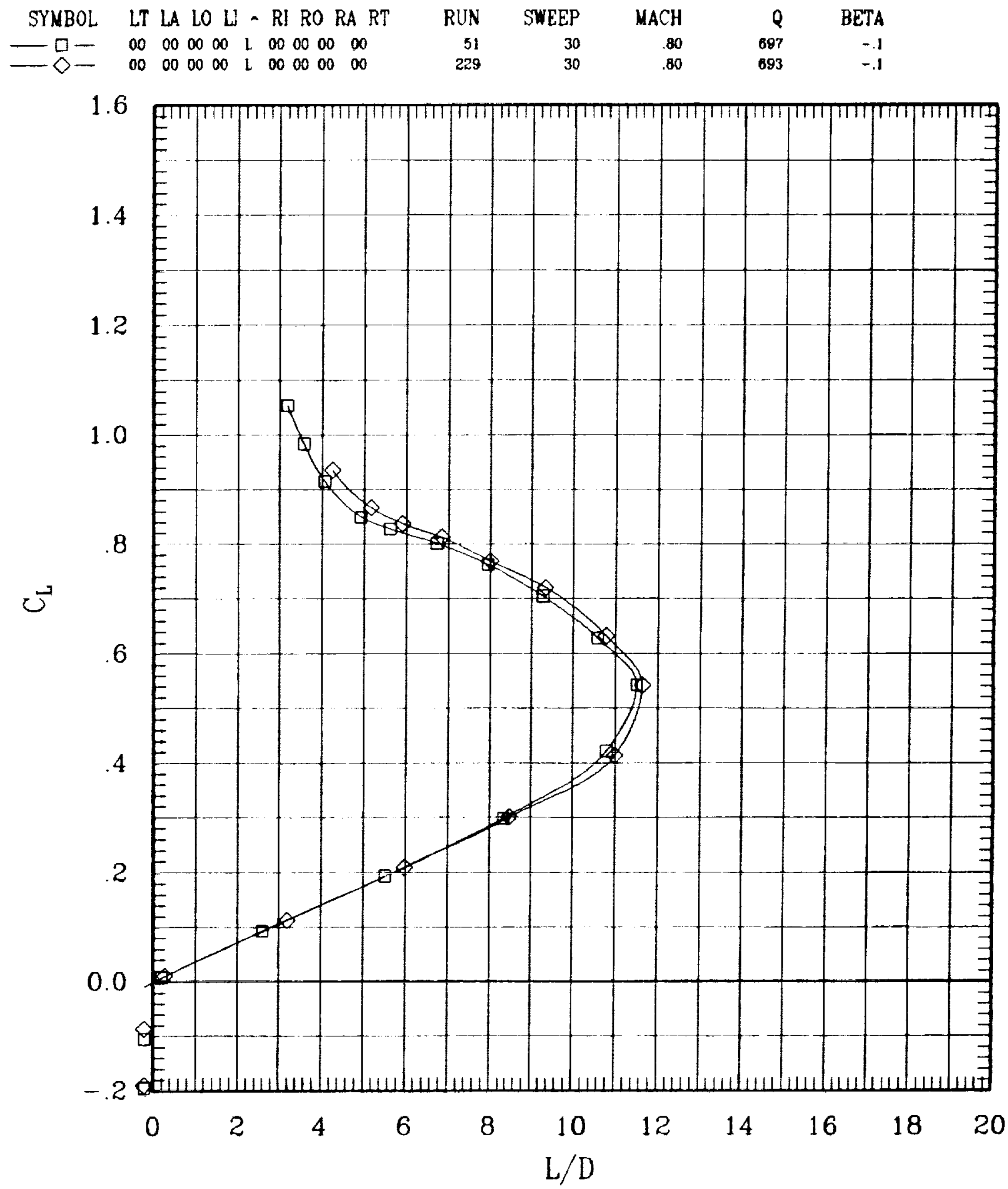

Figure 16. Repeat runs.

SYMBOL	CONFIGURATION	TEST	RUN	SWEEP	MACH	Q	BETA
—□—	Rockwell	100	48	0	.30	240	-.1
—◇—	NASA Ames	100	115	0	.30	246	-.1

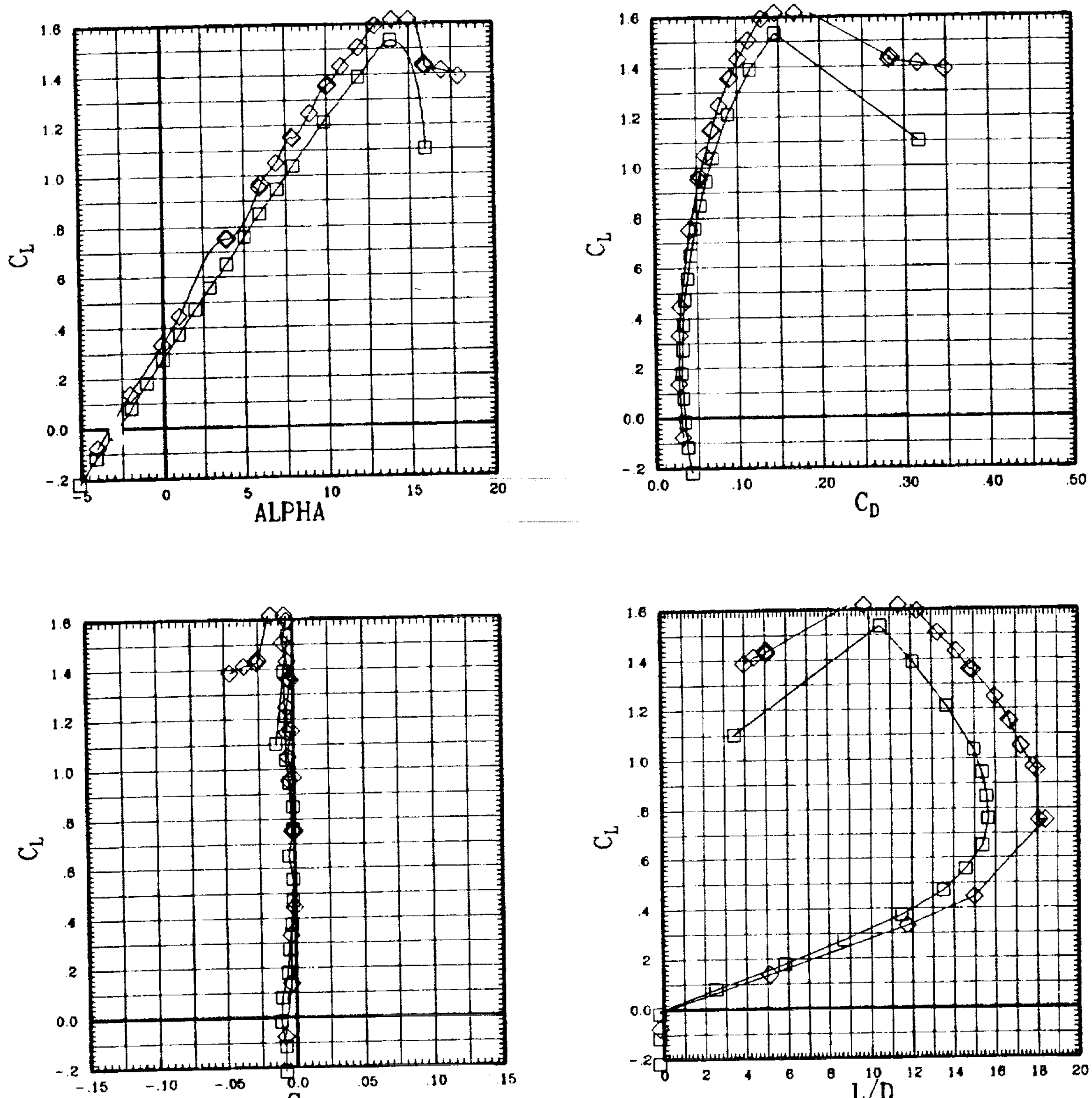

Figure A-1(a). Rockwell and NASA Ames wings for sweep = 0 deg.

SYMBOL	CONFIGURATION	TEST	RUN	SWEEP	MACH	Q	BETA
—□—	Rockwell	100	48	0	.30	240	-.1
—◇—	NASA Ames	100	115	0	.30	246	-.1

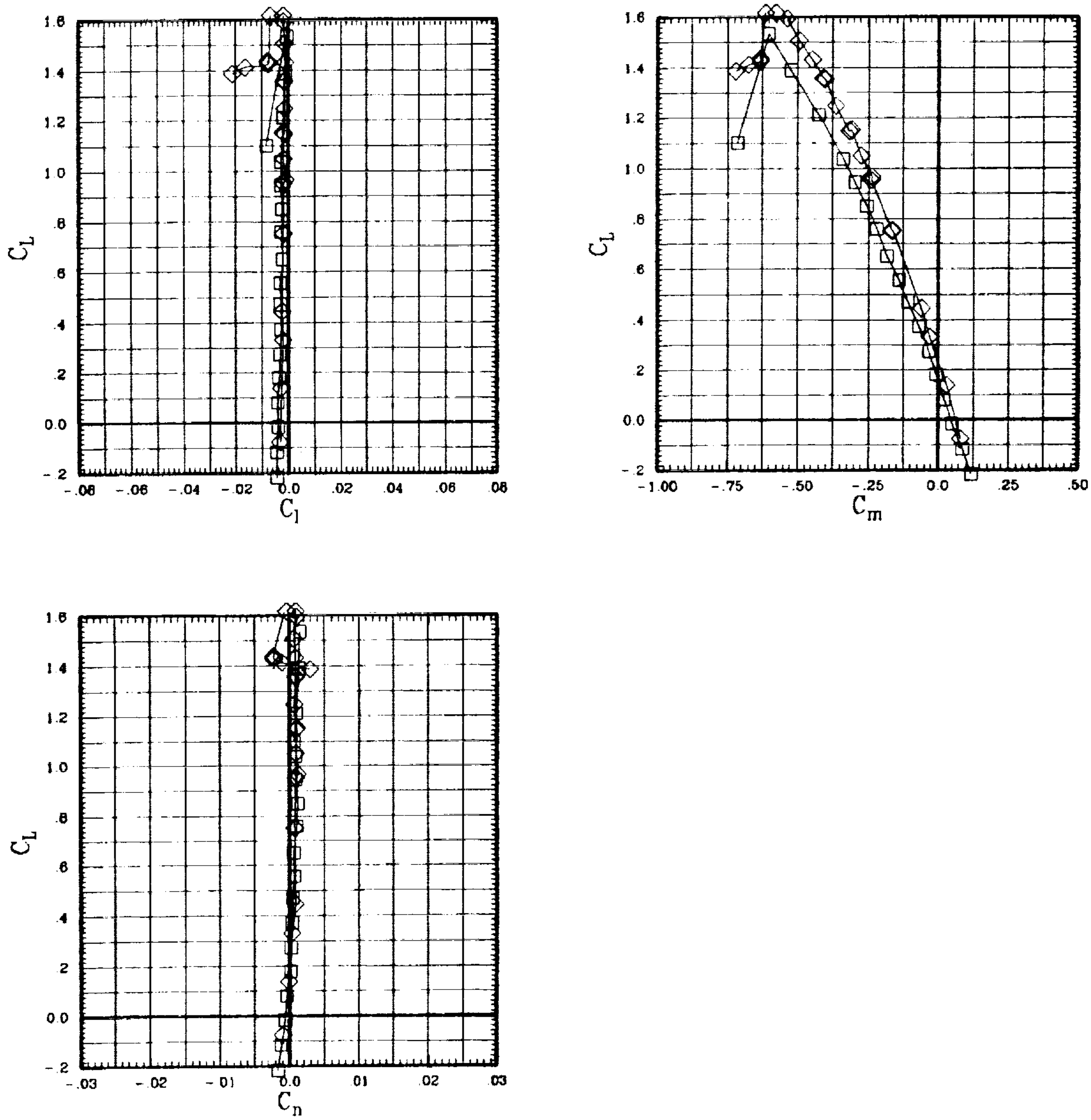

Figure A-1(a). Rockwell and NASA Ames wings for sweep = 0 deg.

SYMBOL	CONFIGURATION	TEST	RUN	SWEEP	MACH	Q	BETA
—□—	Rockwell	100	49	0	.40	425	-.1
—◇—	NASA Ames	100	17	0	.40	429	-.1

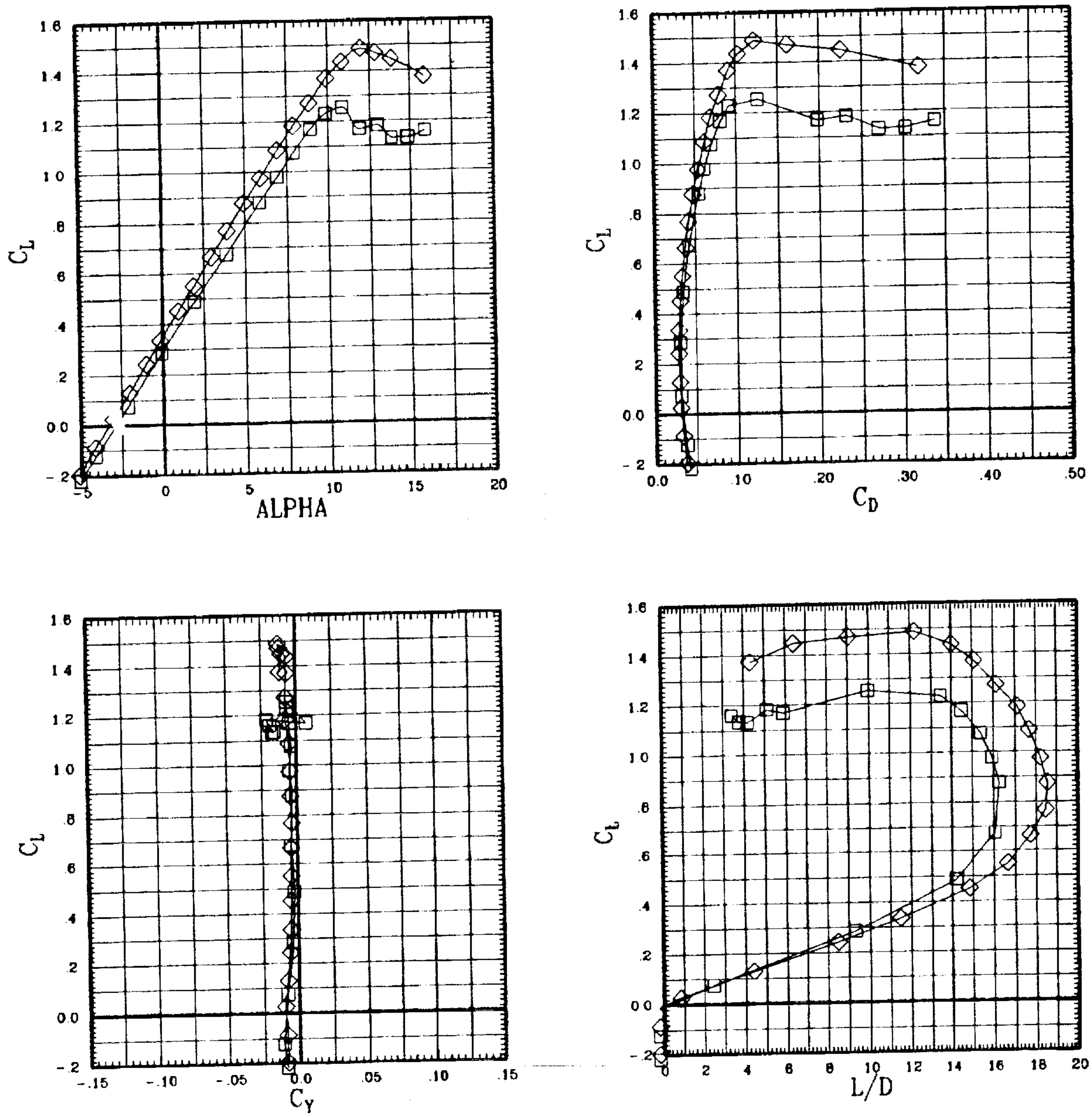

Figure A-1(a). Rockwell and NASA Ames wings for sweep = 0 deg.

SYMBOL	CONFIGURATION	TEST	RUN	SWEEP	MACH	Q	BETA
—□—	Rockwell	100	49	0	.40	425	-.1
—◇—	NASA Ames	100	17	0	.40	429	-.1

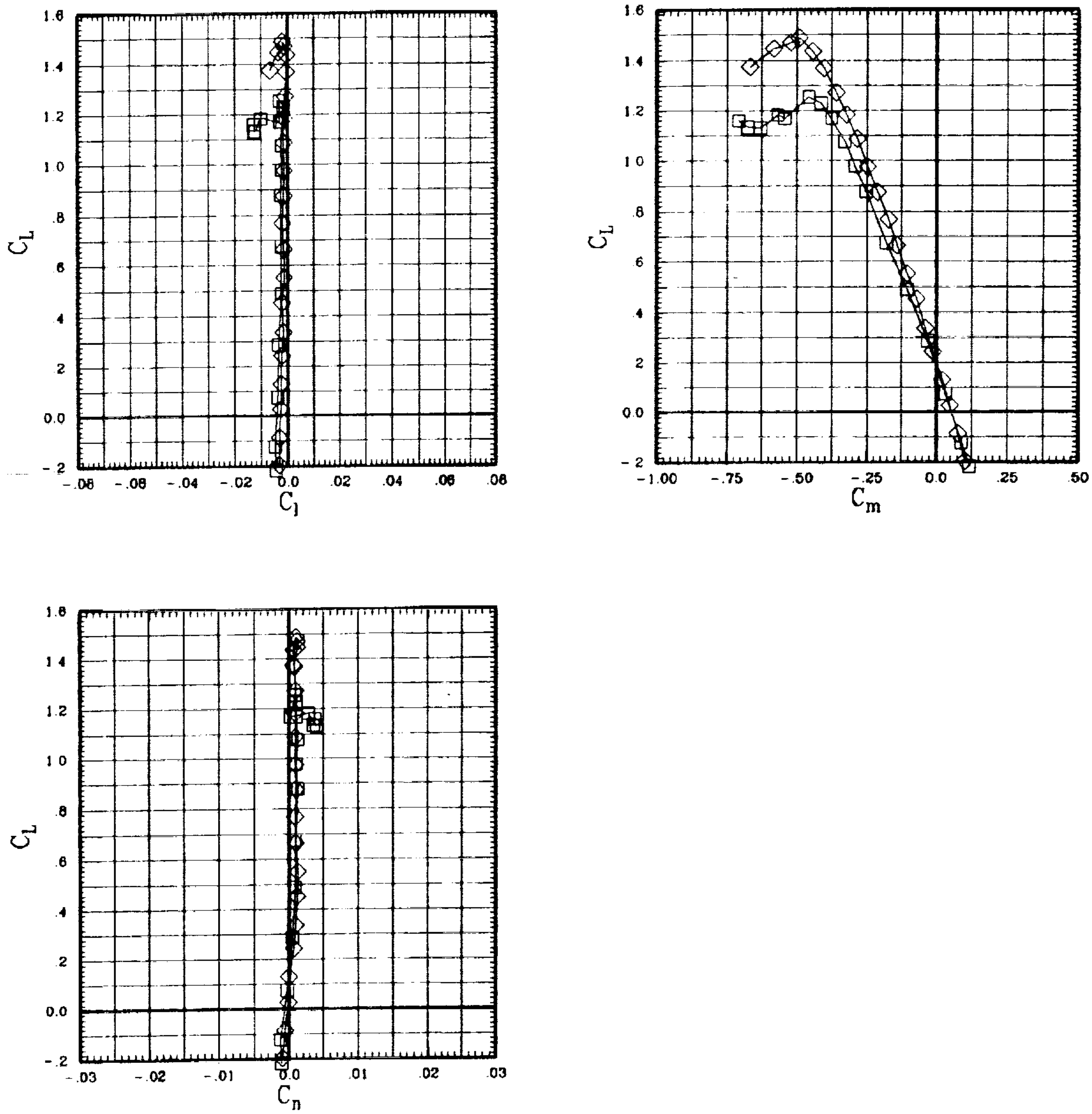

Figure A-1(a). Rockwell and NASA Ames wings for sweep = 0 deg.

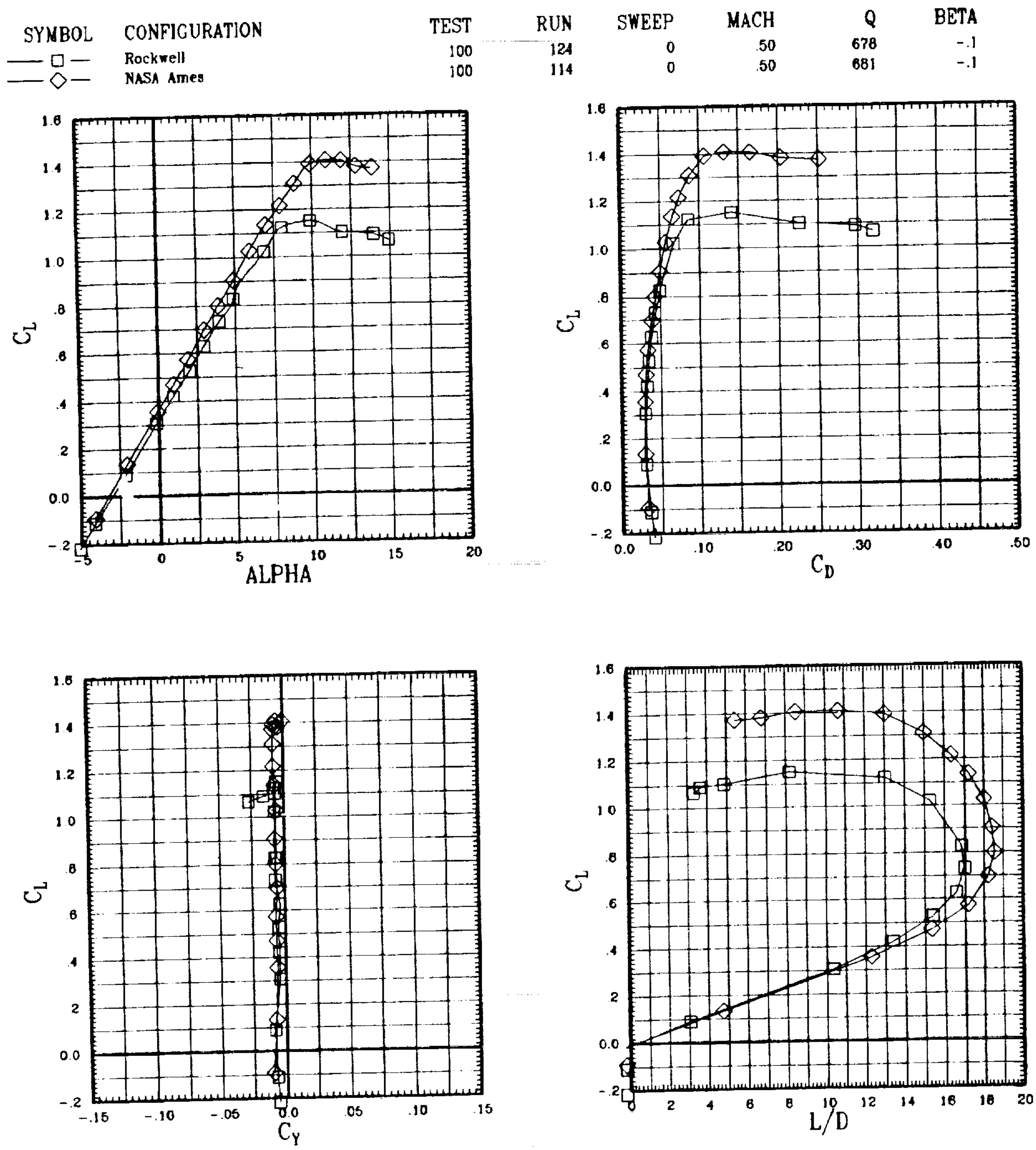

Figure A-1(a). Rockwell and NASA Ames wings for sweep = 0 deg.

SYMBOL	CONFIGURATION	TEST	RUN	SWEEP	MACH	Q	BETA
—□—	Rockwell	100	124	0	.50	678	-.1
—◇—	NASA Ames	100	114	0	.50	681	-.1

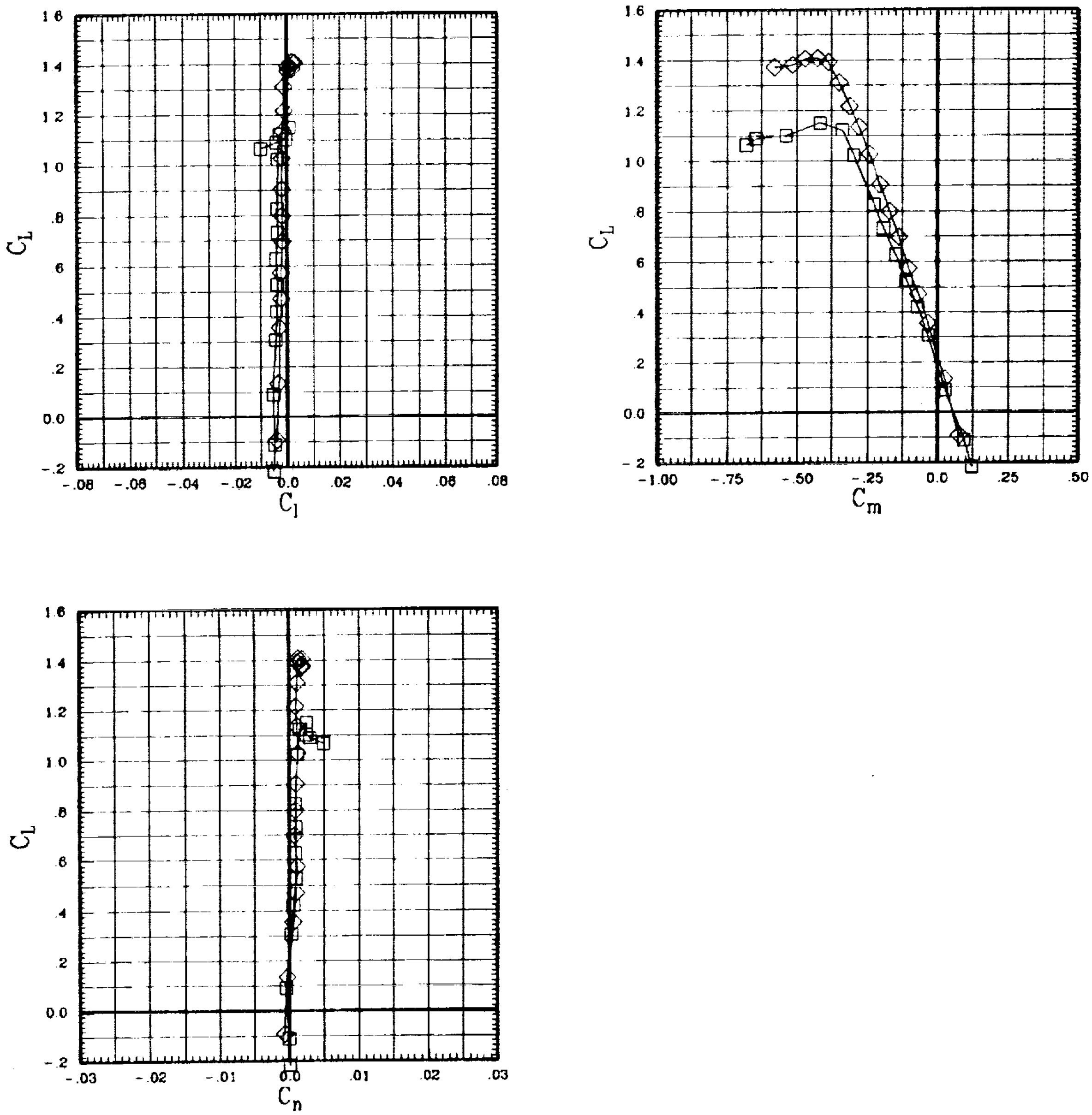

Figure A-1(a). Rockwell and NASA Ames wings for sweep = 0 deg.

SYMBOL	CONFIGURATION	TEST	RUN	SWEEP	MACH	Q	BETA
—□—	Rockwell	100	47	0	.60	691	-.1
—◇—	NASA Ames	100	15	0	.60	700	-.1

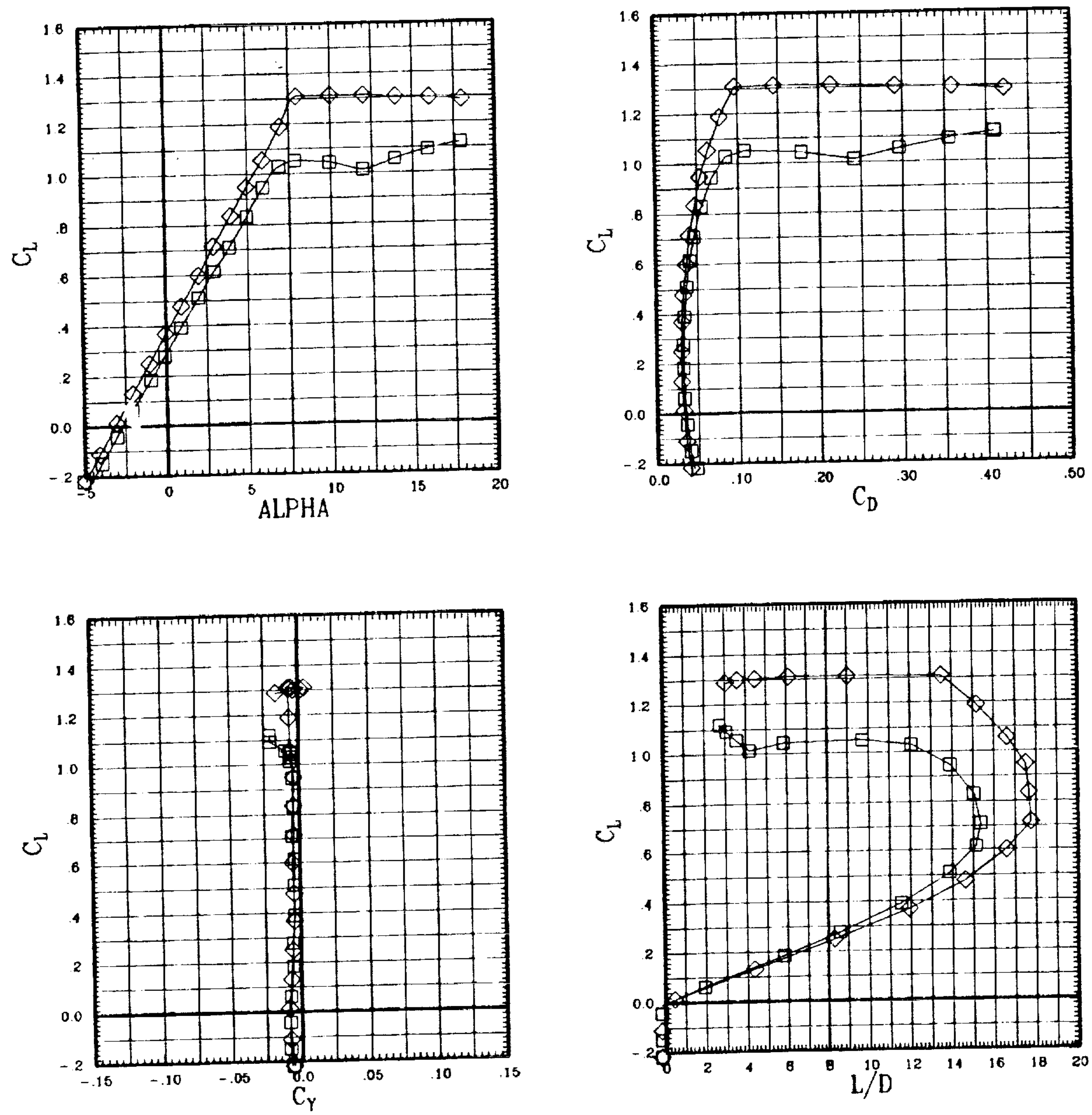

Figure A-1(a). Rockwell and NASA Ames wings for sweep = 0 deg.

SYMBOL	CONFIGURATION	TEST	RUN	SWEEP	MACH	Q	BETA
—□—	Rockwell	100	47	0	.60	691	-.1
—◇—	NASA Ames	100	15	0	.60	700	-.1

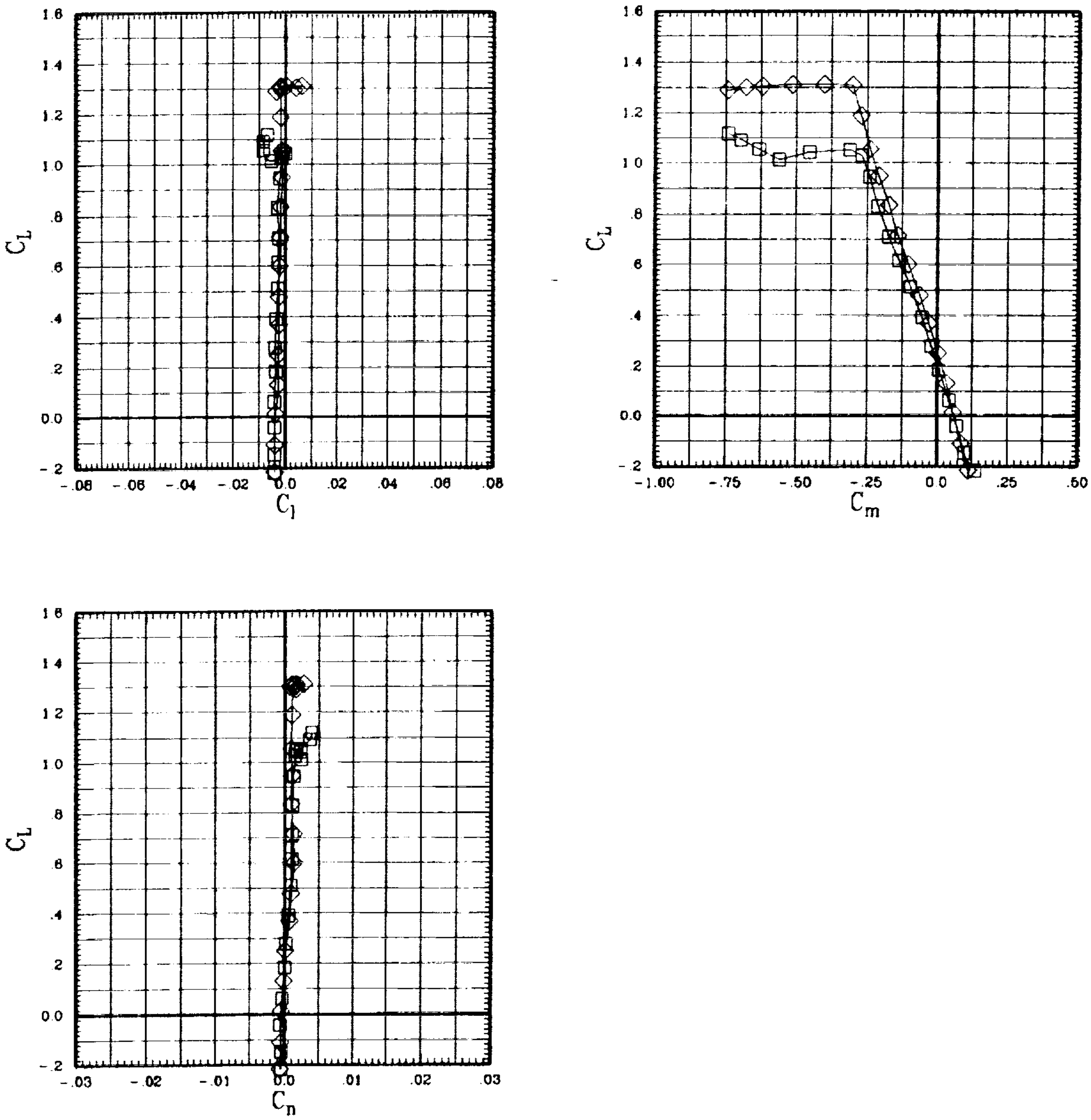

Figure A-1(a). Rockwell and NASA Ames wings for sweep = 0 deg.

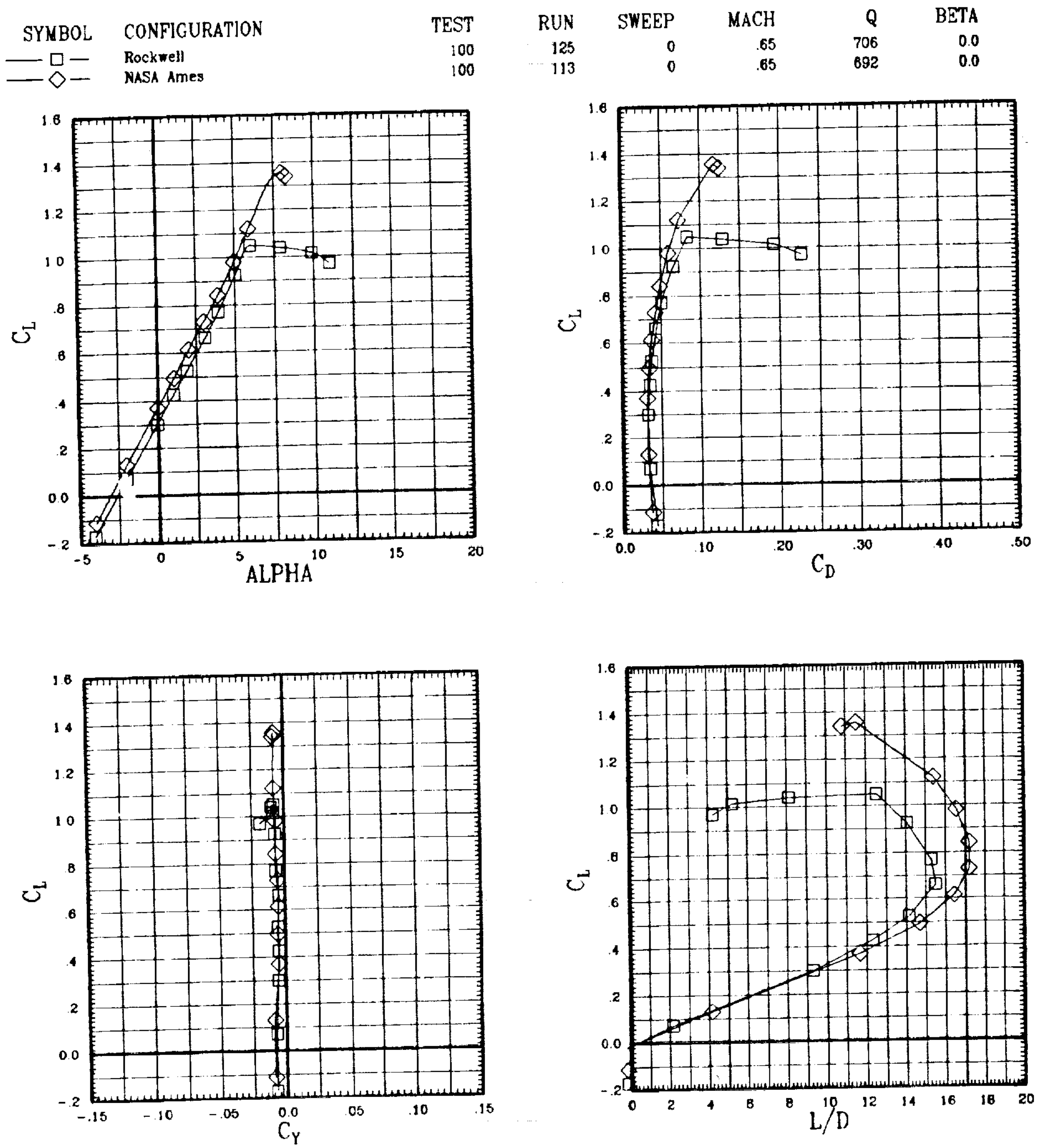

Figure A-1(a). Rockwell and NASA Ames wings for sweep = 0 deg.

SYMBOL	CONFIGURATION	TEST	RUN	SWEEP	MACH	Q	BETA
—□—	Rockwell	100	125	0	.65	706	0.0
—◇—	NASA Ames	100	113	0	.65	692	0.0

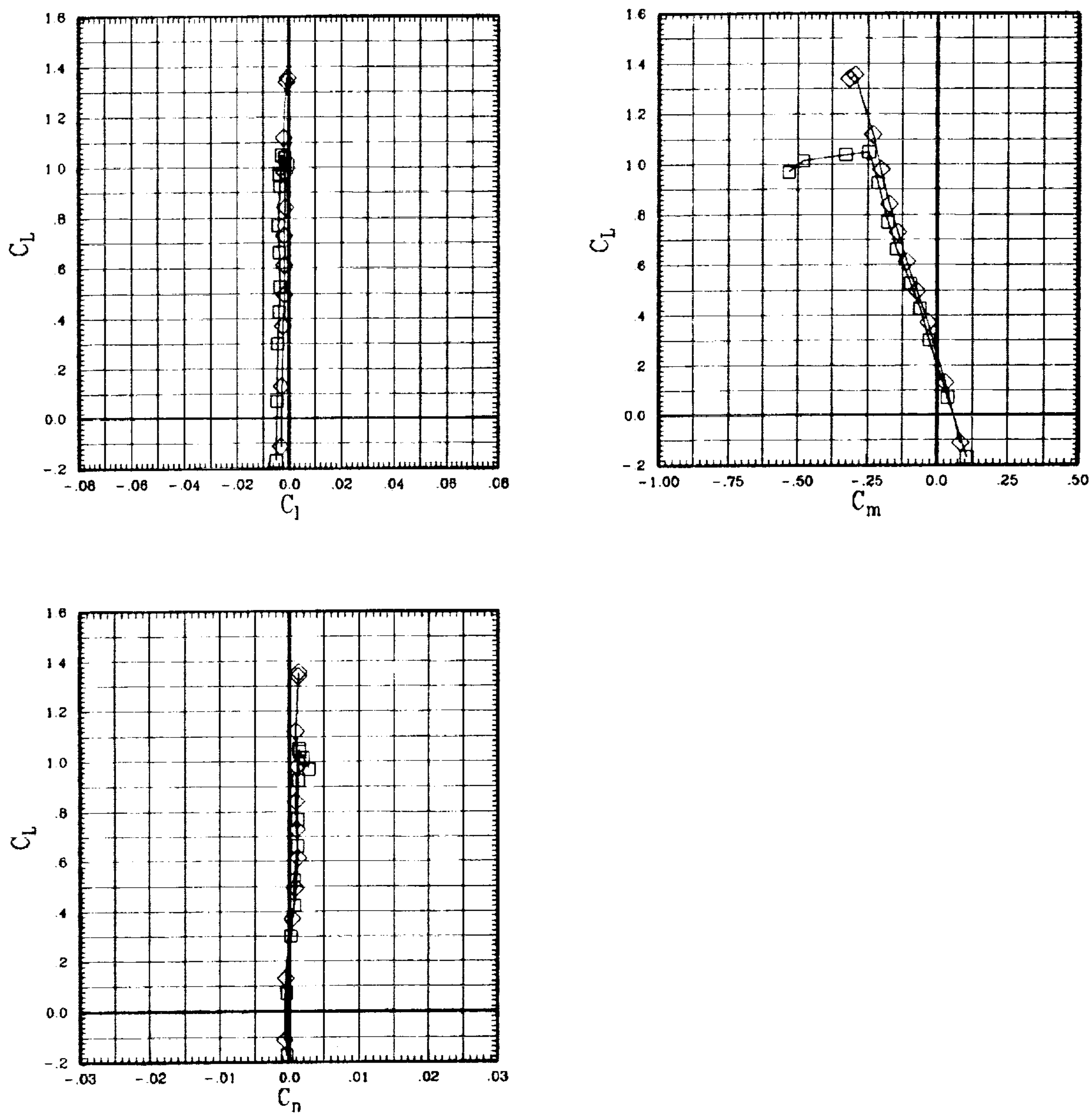

Figure A-1(a). Rockwell and NASA Ames wings for sweep = 0 deg.

SYMBOL	CONFIGURATION	TEST	RUN	SWEEP	MACH	Q	BETA
—□—	Rockwell	100	126	0	.68	700	0.0
—◇—	NASA Ames	100	112	0	.68	700	-.1

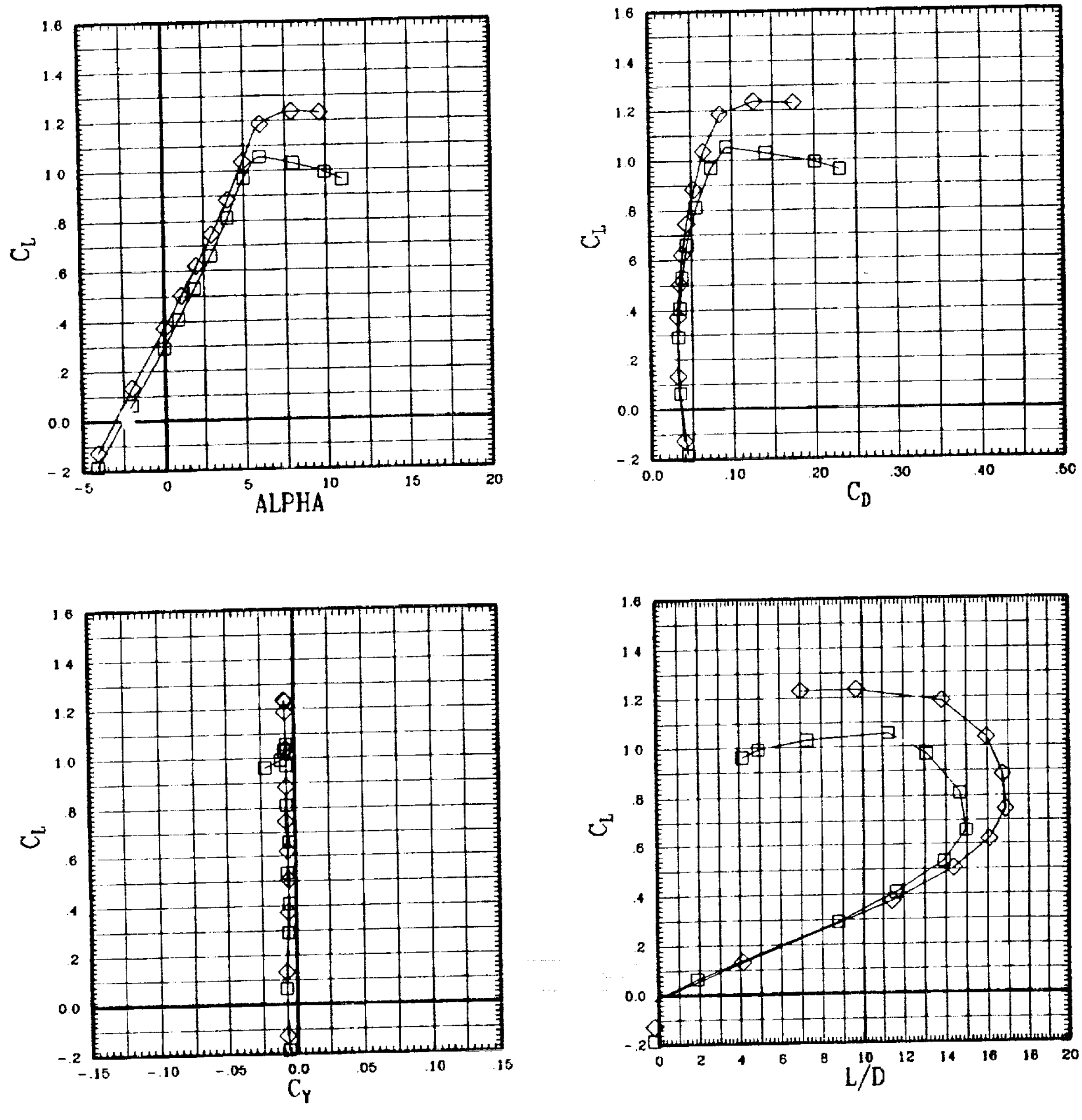

Figure A-1(a). Rockwell and NASA Ames wings for sweep = 0 deg.

SYMBOL	CONFIGURATION	TEST	RUN	SWEEP	MACH	Q	BETA
—□—	Rockwell	100	126	0	.68	700	0.0
—◇—	NASA Ames	100	112	0	.68	700	-.1

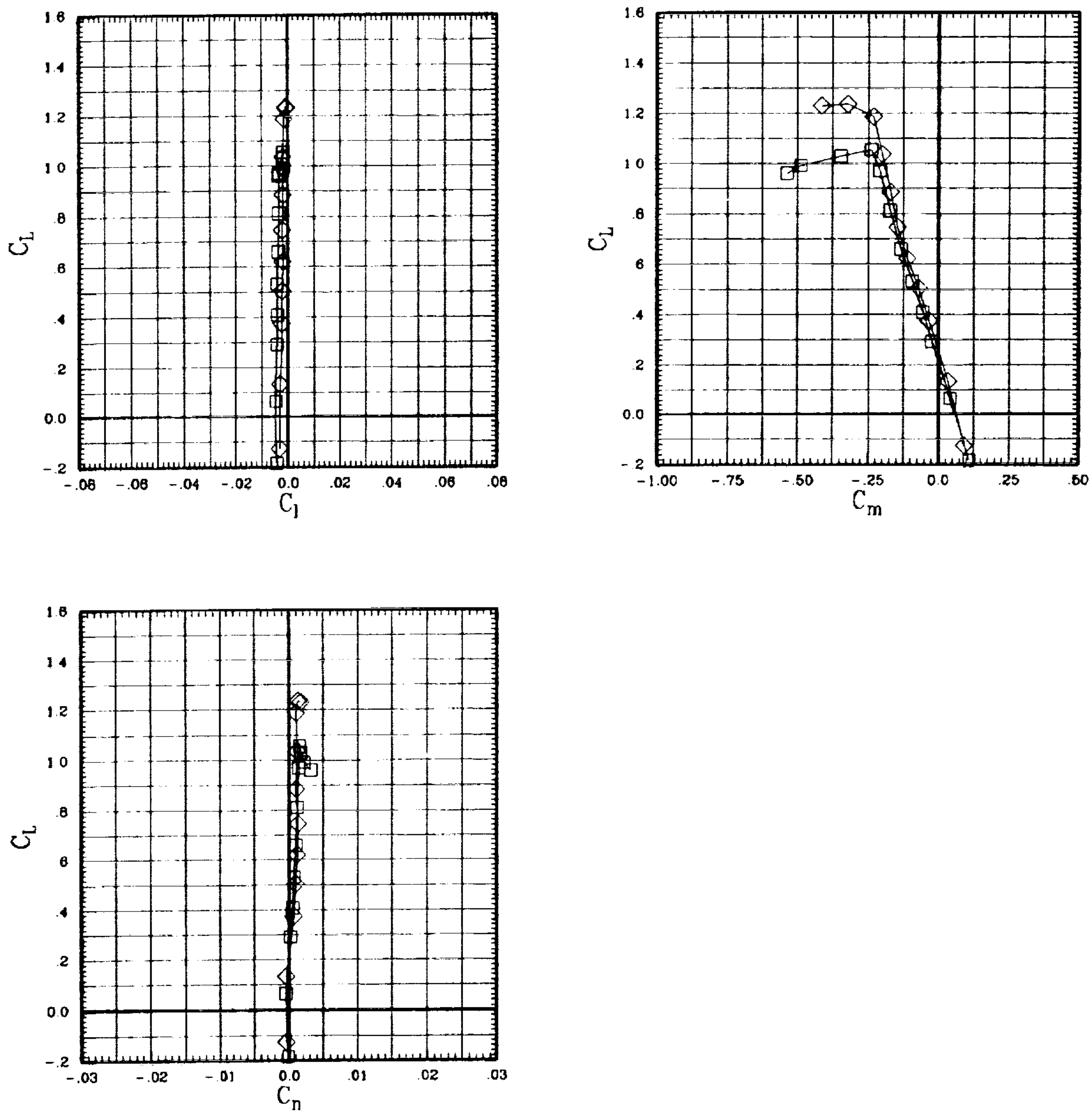

Figure A-1(a). Rockwell and NASA Ames wings for sweep = 0 deg.

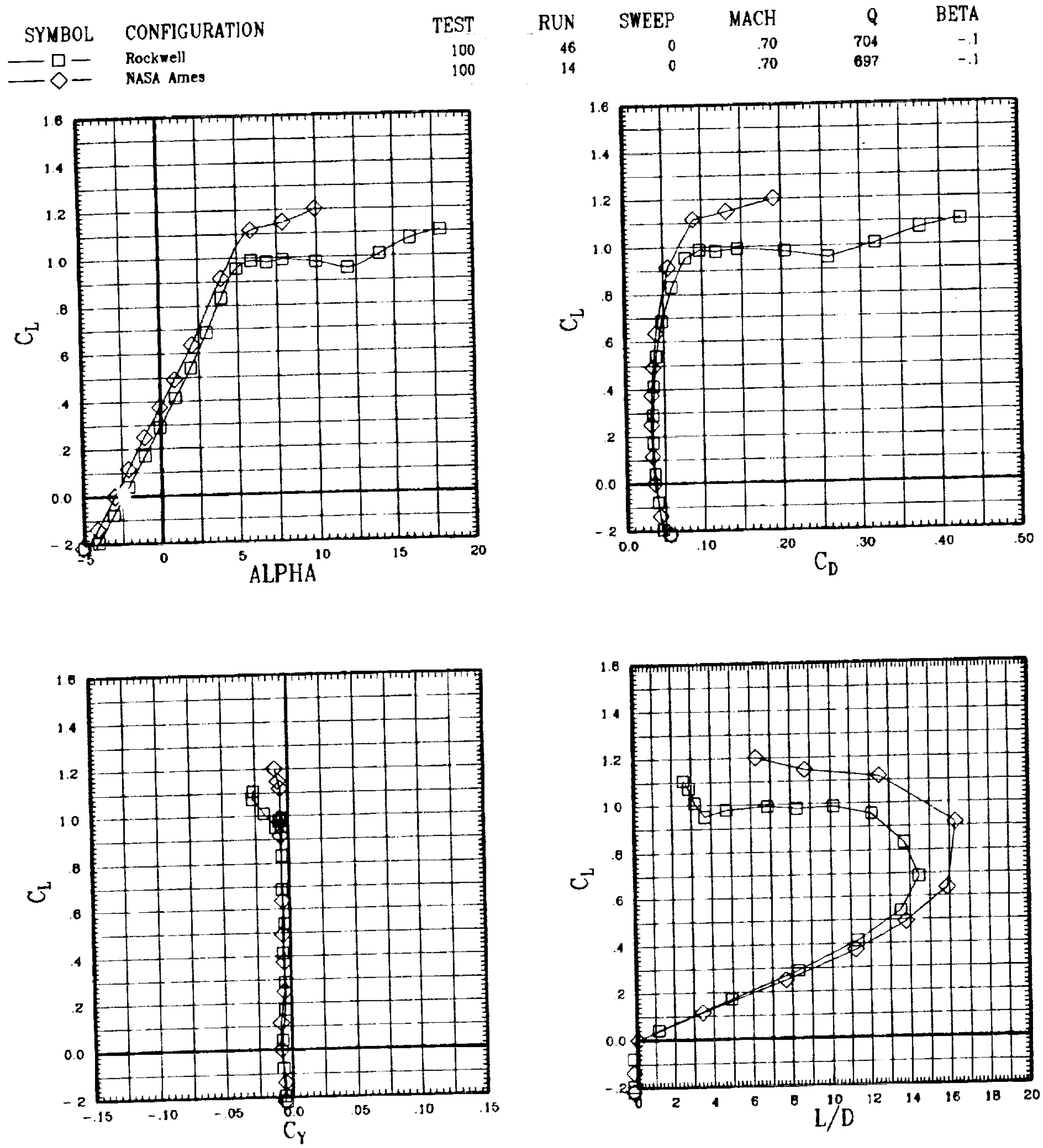

Figure A-1(a). Rockwell and NASA Ames wings for sweep = 0 deg.

SYMBOL	CONFIGURATION	TEST	RUN	SWEEP	MACH	Q	BETA
—□—	Rockwell	100	46	0	.70	704	-.1
—◇—	NASA Ames	100	14	0	.70	697	-.1

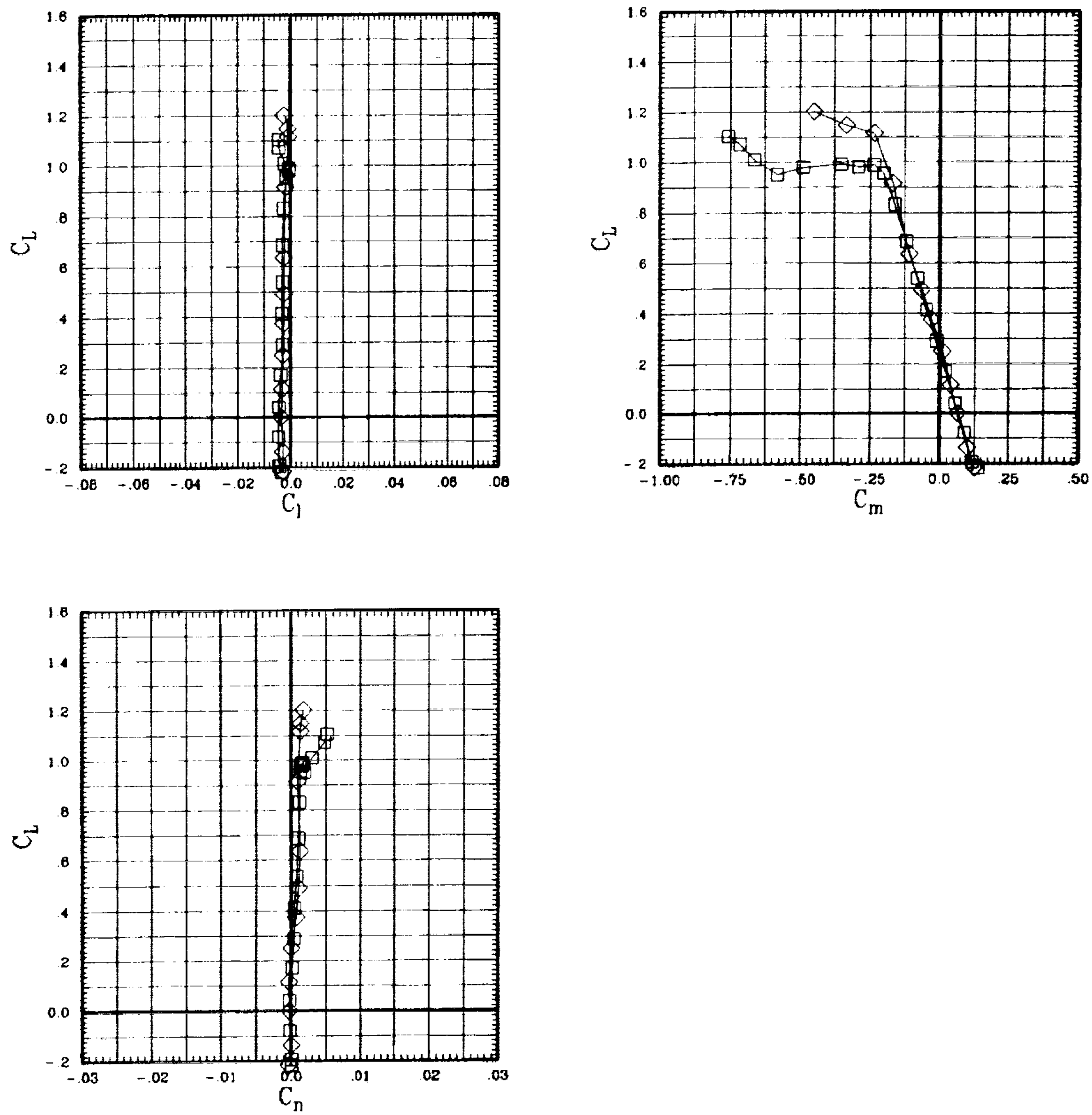

Figure A-1(a). Rockwell and NASA Ames wings for sweep = 0 deg.

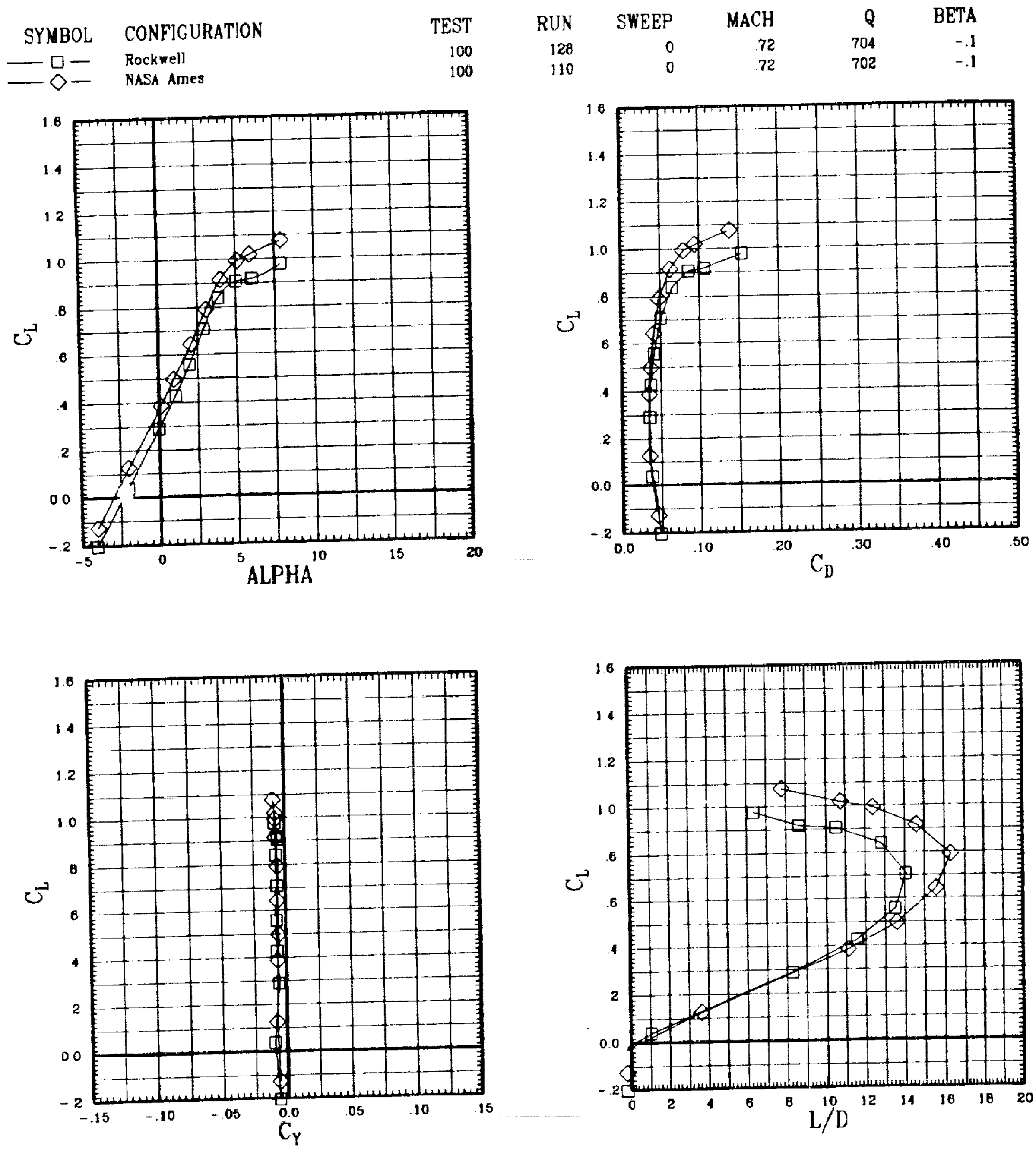

Figure A-1(a). Rockwell and NASA Ames wings for sweep = 0 deg.

SYMBOL	CONFIGURATION	TEST	RUN	SWEEP	MACH	Q	BETA
—□—	Rockwell	100	128	0	.72	704	-.1
—◇—	NASA Ames	100	110	0	.72	702	-.1

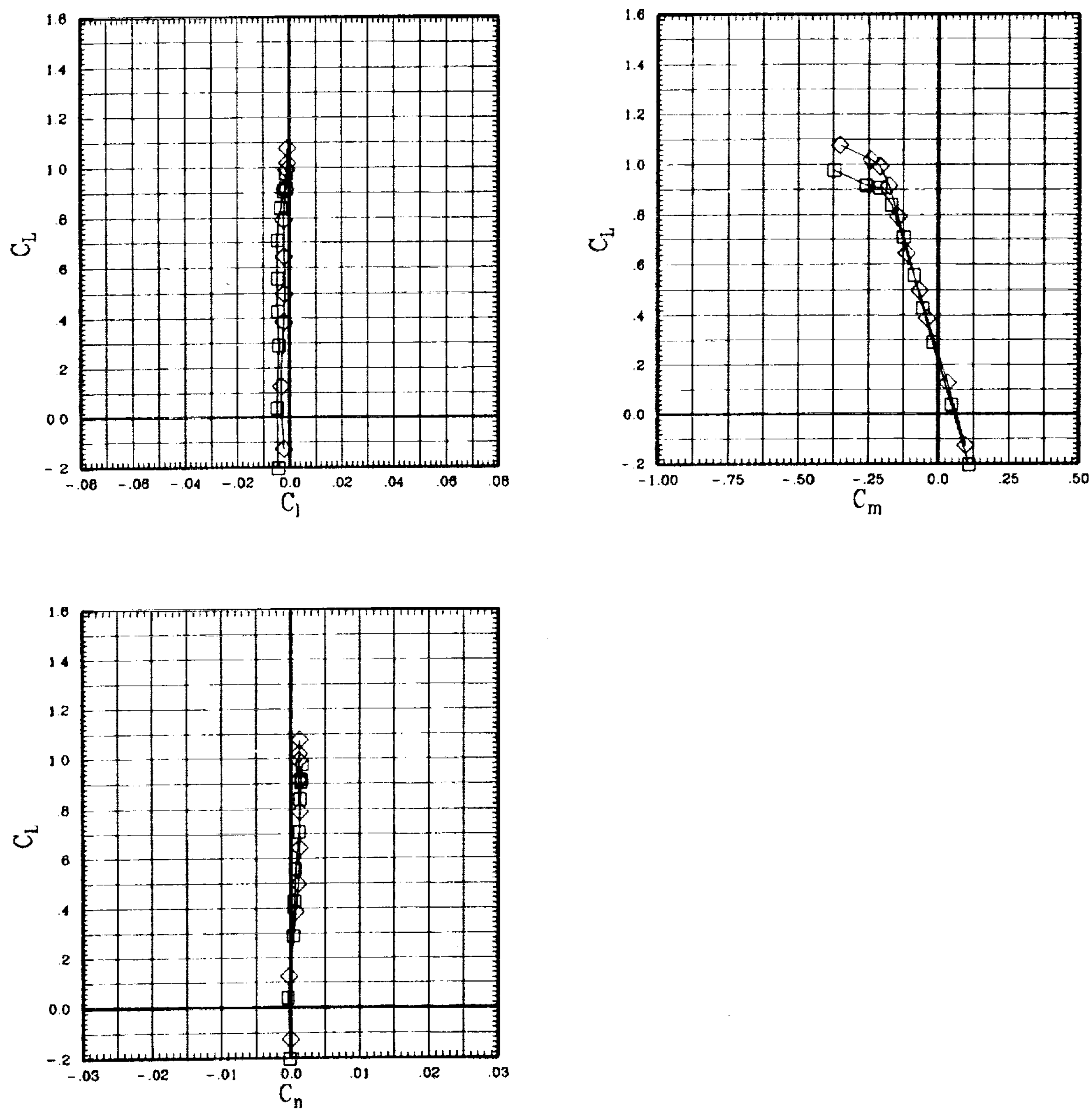

Figure A-1(a). Rockwell and NASA Ames wings for sweep = 0 deg.

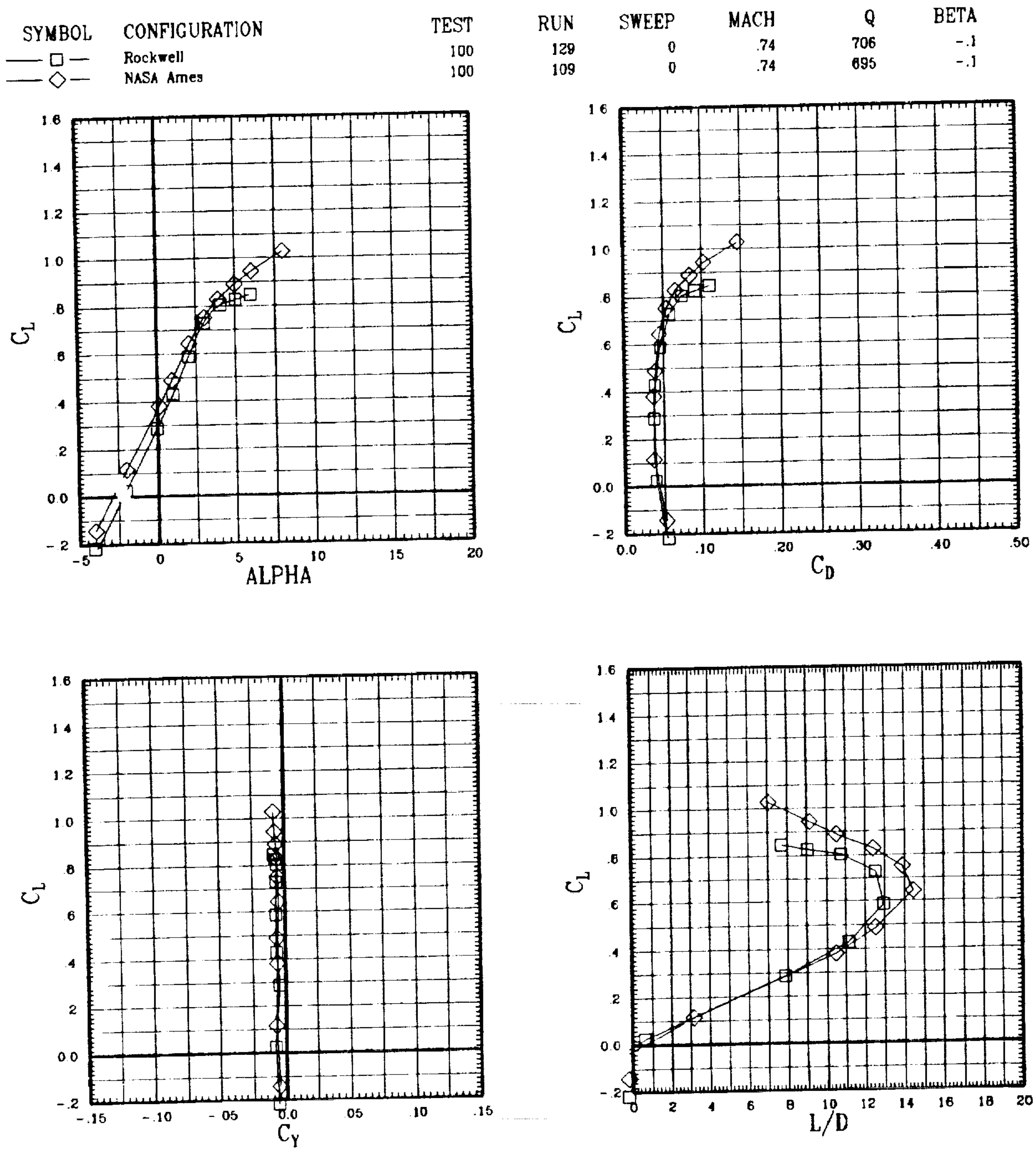

Figure A-1(a). Rockwell and NASA Ames wings for sweep = 0 deg.

SYMBOL	CONFIGURATION	TEST	RUN	SWEEP	MACH	Q	BETA
—□—	Rockwell	100	129	0	.74	706	-.1
—◇—	NASA Ames	100	109	0	.74	695	-.1

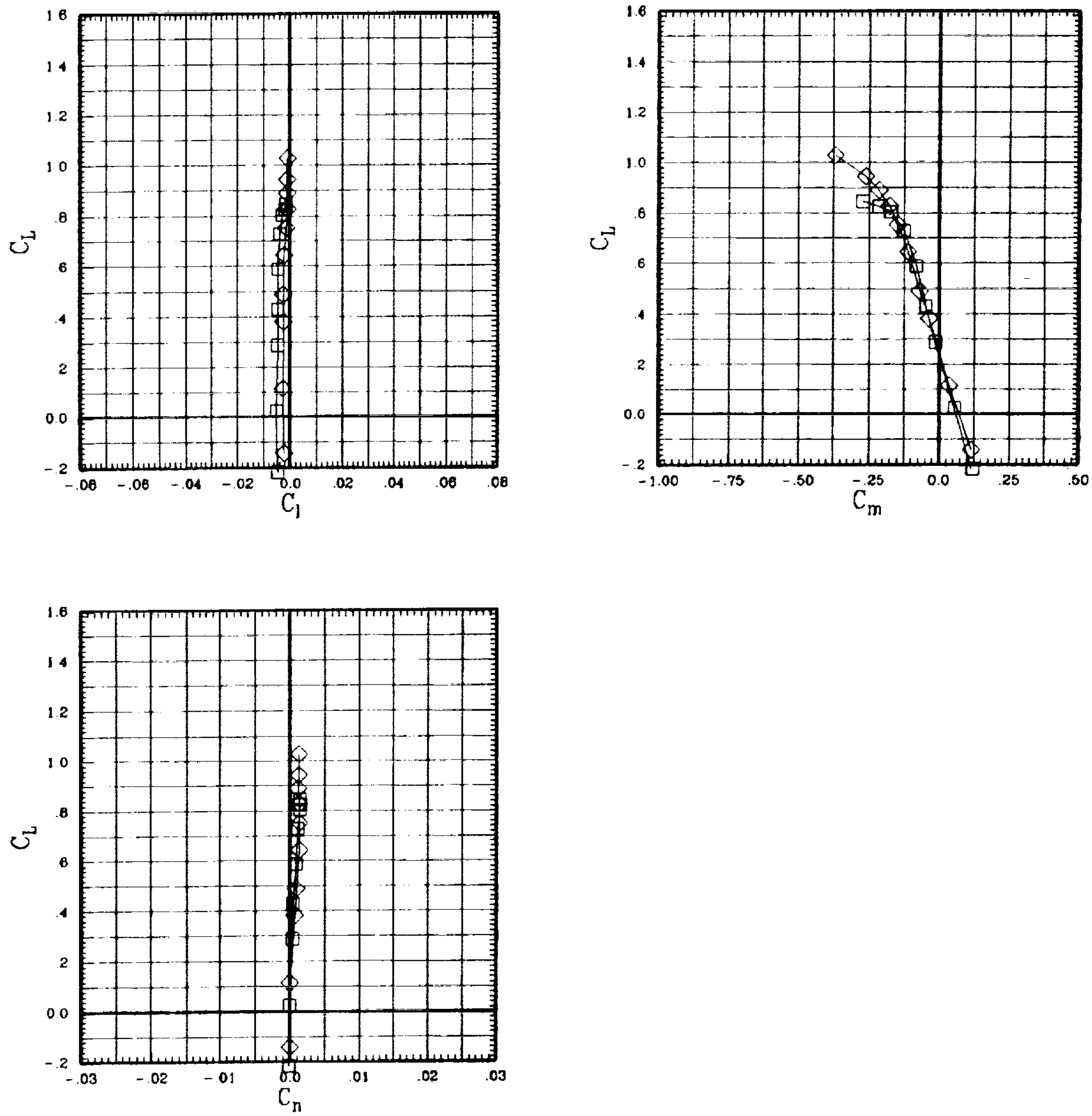

Figure A-1(a). Rockwell and NASA Ames wings for sweep = 0 deg.

SYMBOL	CONFIGURATION	TEST	RUN	SWEEP	MACH	Q	BETA
—□—	Rockwell	100	130	0	.76	702	-.1
—◇—	NASA Ames	100	108	0	.76	693	-.1

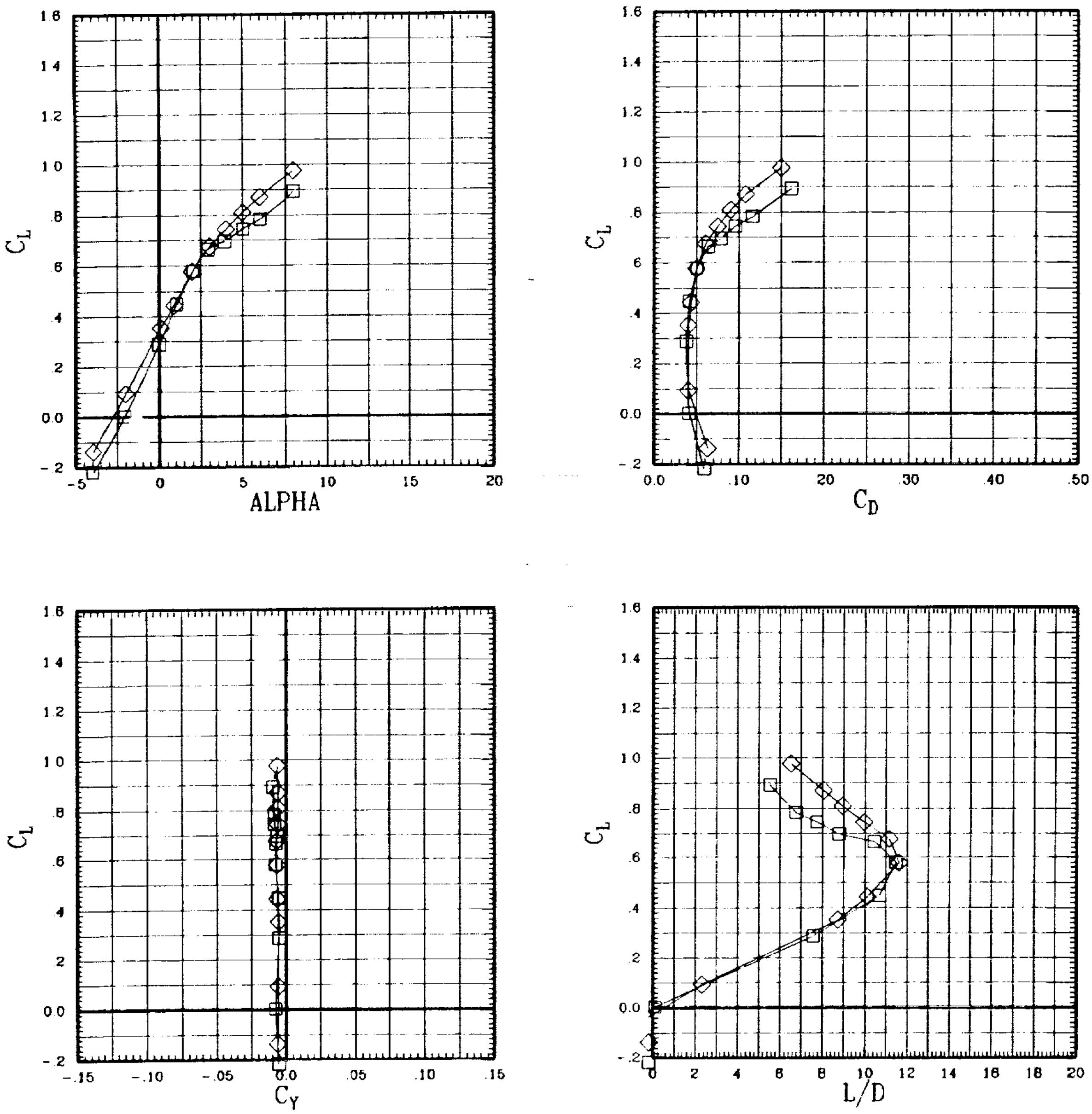

Figure A-1(a). Rockwell and NASA Ames wings for sweep = 0 deg.

SYMBOL	CONFIGURATION	TEST	RUN	SWEEP	MACH	Q	BETA
—□—	Rockwell	100	130	0	.76	702	-.1
—◇—	NASA Ames	100	108	0	.76	693	-.1

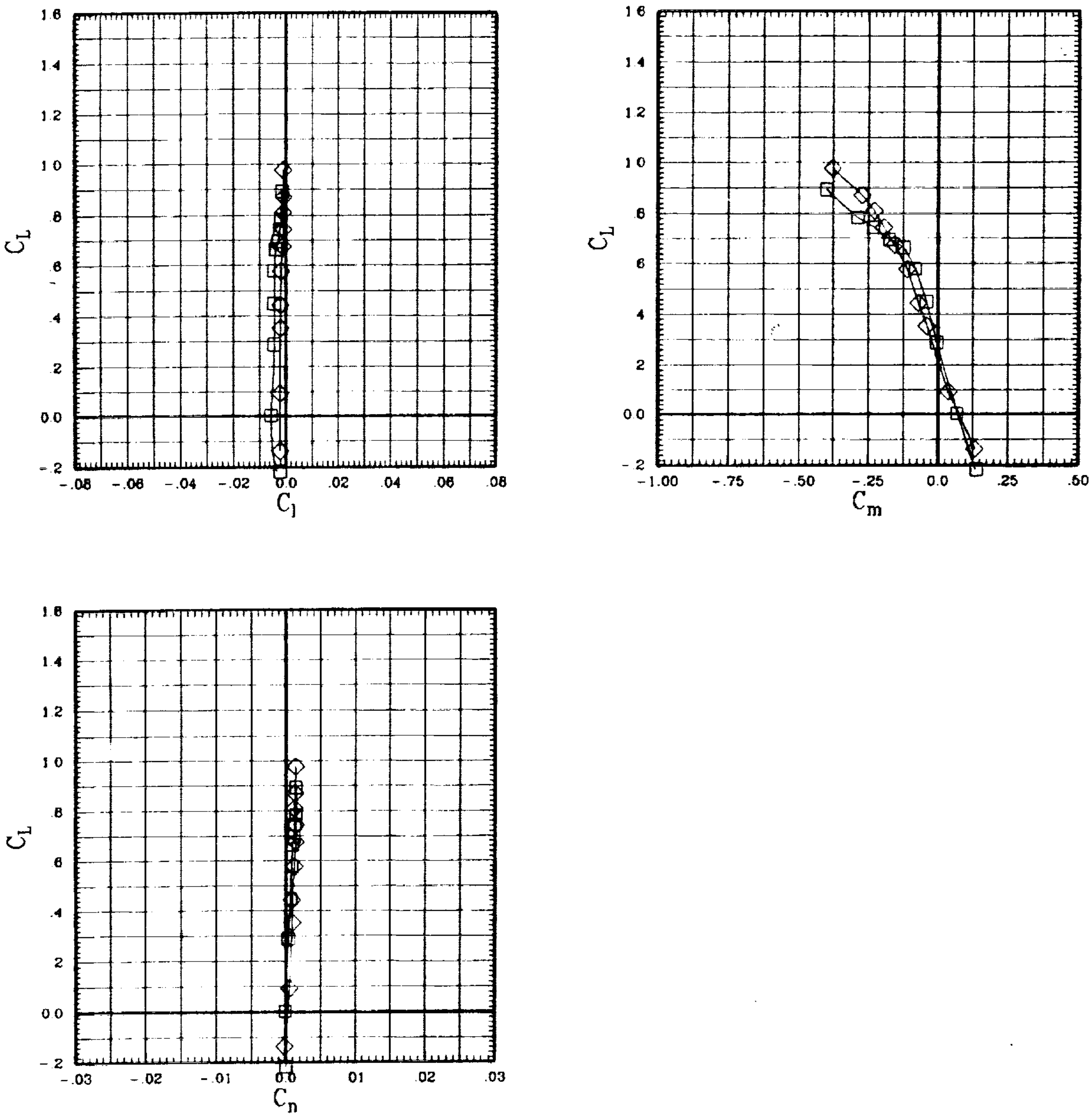

Figure A-1(a). Rockwell and NASA Ames wings for sweep = 0 deg.

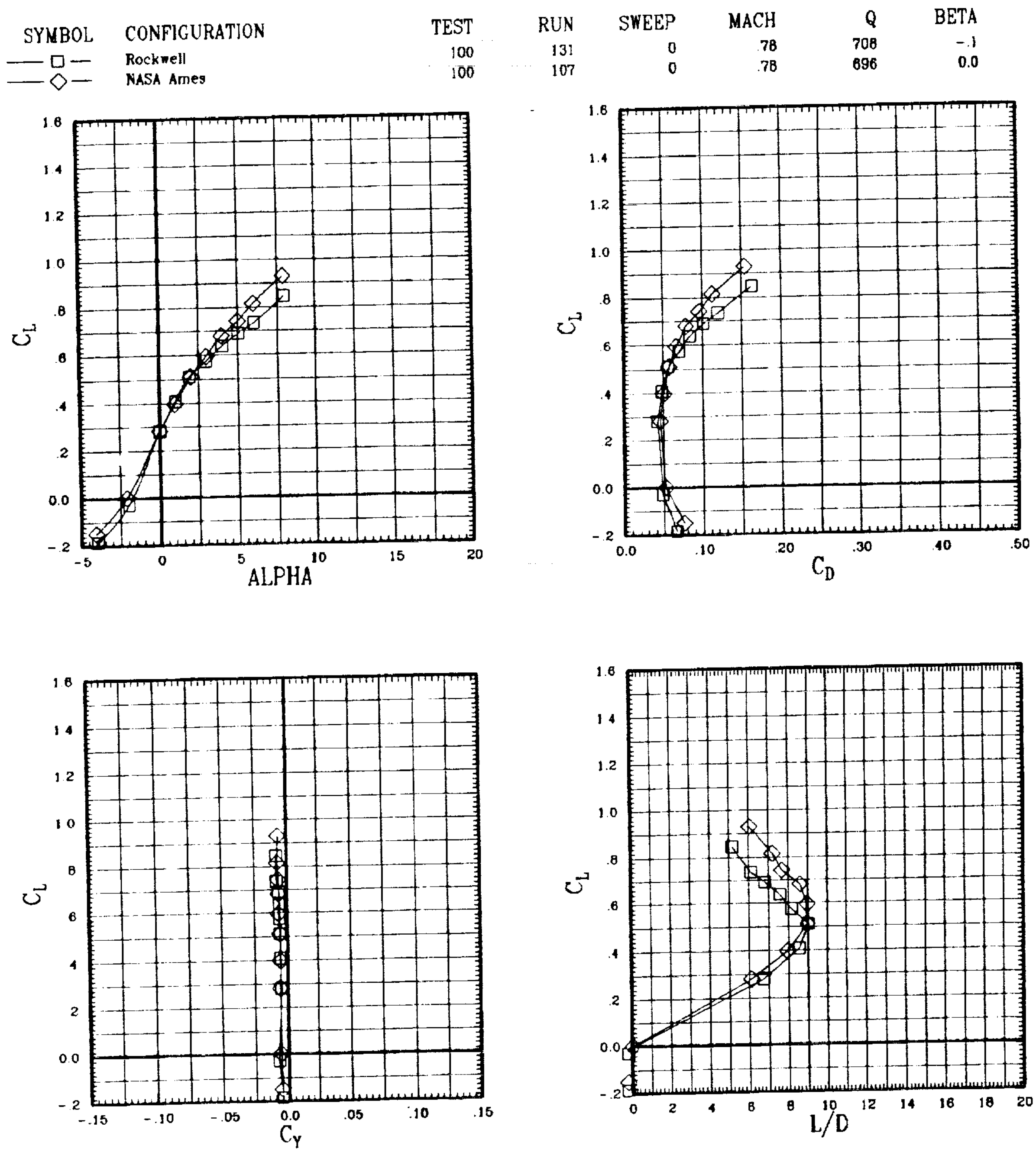

Figure A-1(a). Rockwell and NASA Ames wings for sweep = 0 deg.

SYMBOL	CONFIGURATION	TEST	RUN	SWEEP	MACH	Q	BETA
—□—	Rockwell	100	131	0	.78	708	-.1
—◇—	NASA Ames	100	107	0	.78	696	0.0

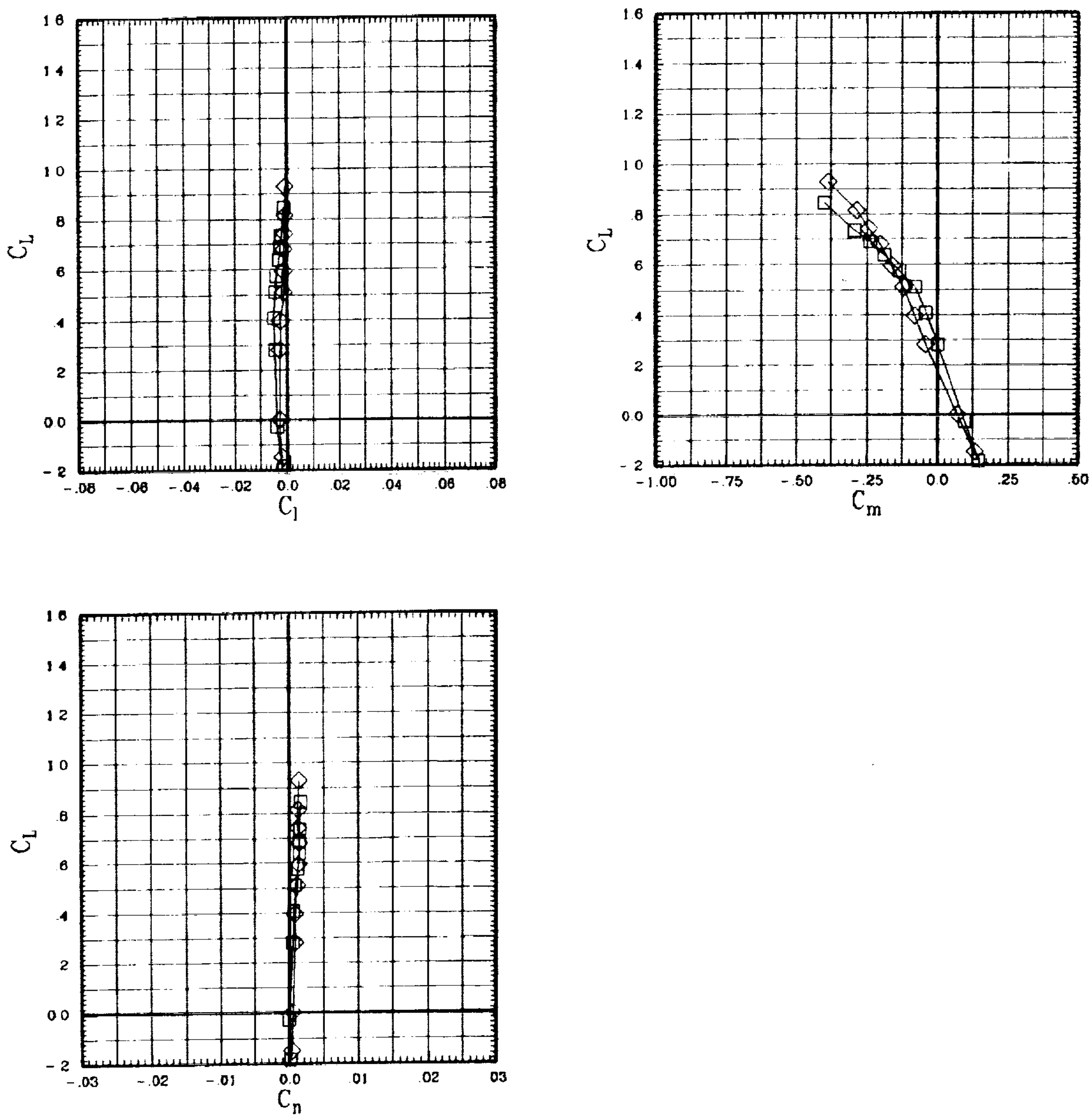

Figure A-1(a). Rockwell and NASA Ames wings for sweep = 0 deg.

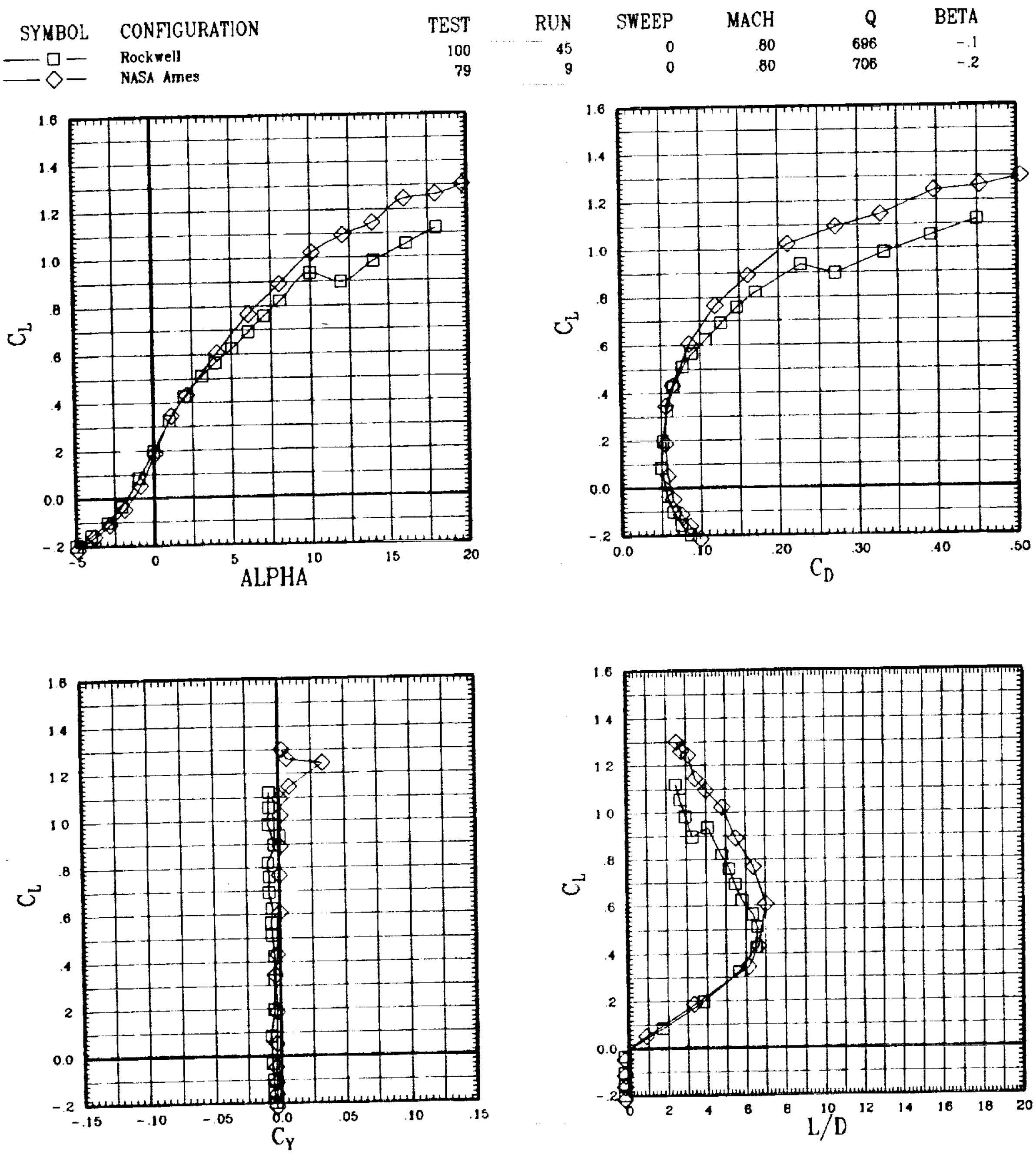

Figure A-1(a). Rockwell and NASA Ames wings for sweep = 0 deg.

C-5

SYMBOL	CONFIGURATION	TEST	RUN	SWEEP	MACH	Q	BETA
—□—	Rockwell	100	45	0	.80	696	-.1
—◇—	NASA Ames	79	9	0	.80	706	-.2

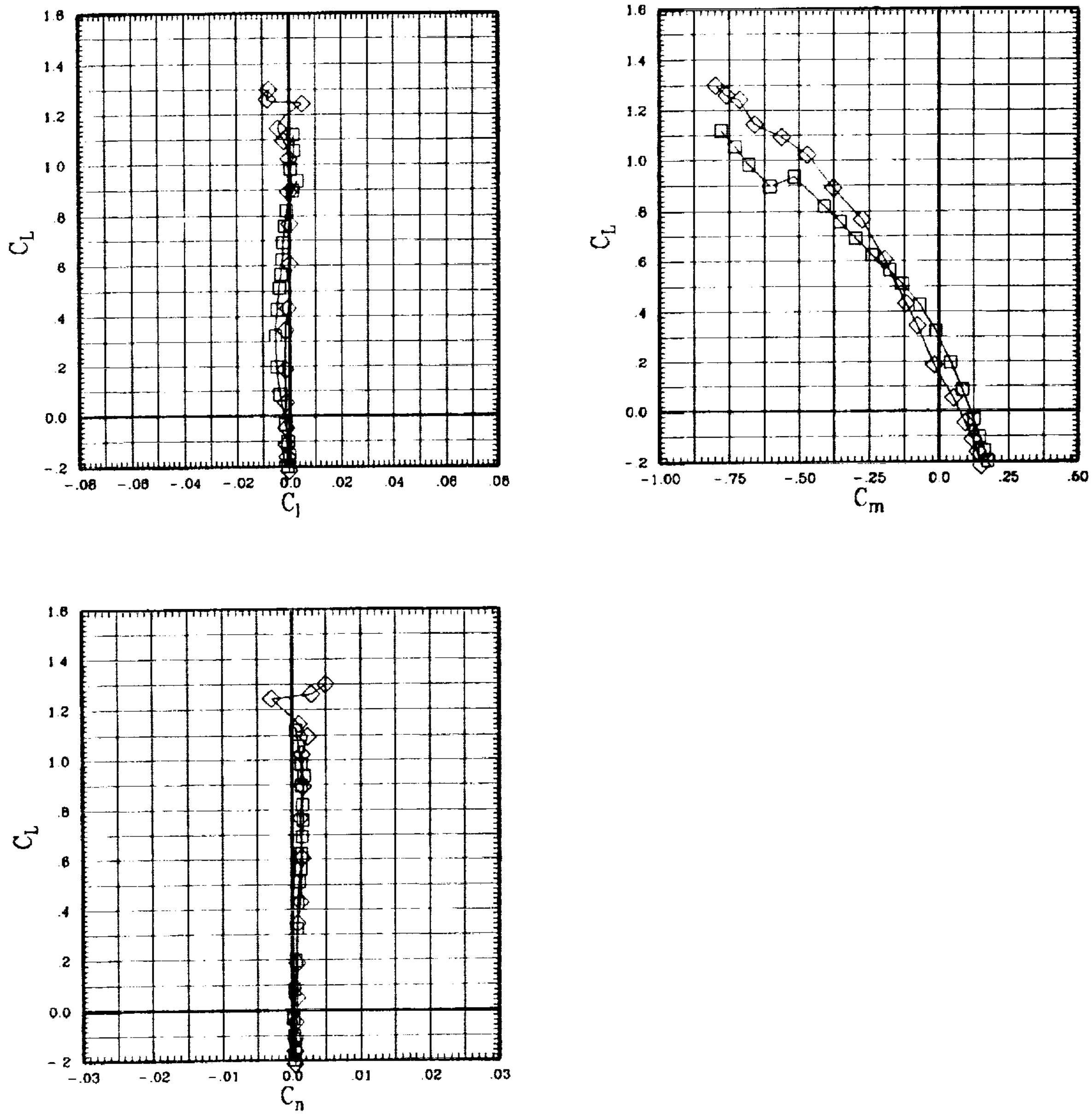

Figure A-1(a). Rockwell and NASA Ames wings for sweep = 0 deg.

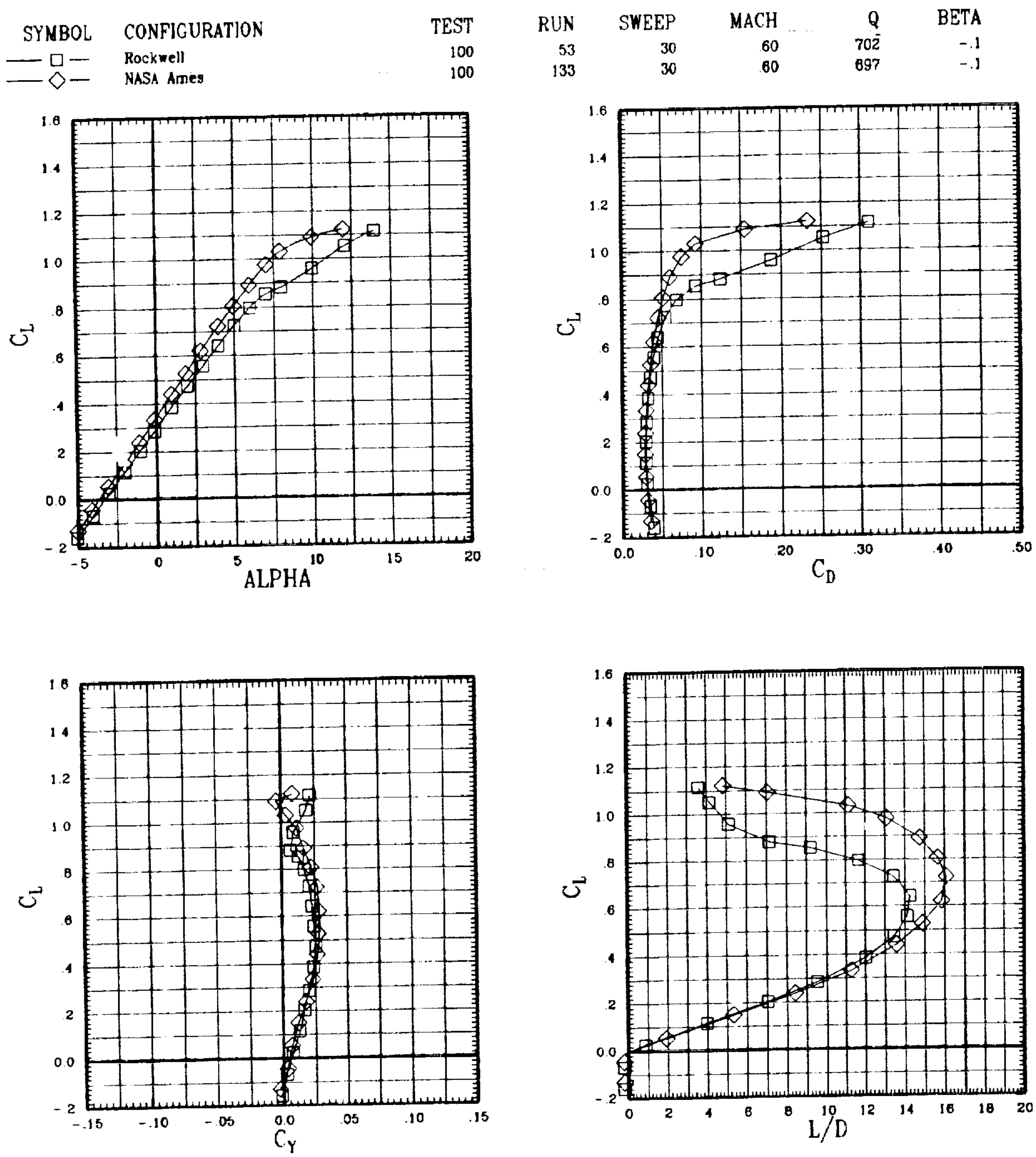

Figure A-1(b). Rockwell and NASA Ames wings for sweep = 30 deg.

SYMBOL	CONFIGURATION	TEST	RUN	SWEEP	MACH	Q	BETA
—□—	Rockwell	100	53	30	.60	702	-.1
—◇—	NASA Ames	100	133	30	.60	697	-.1

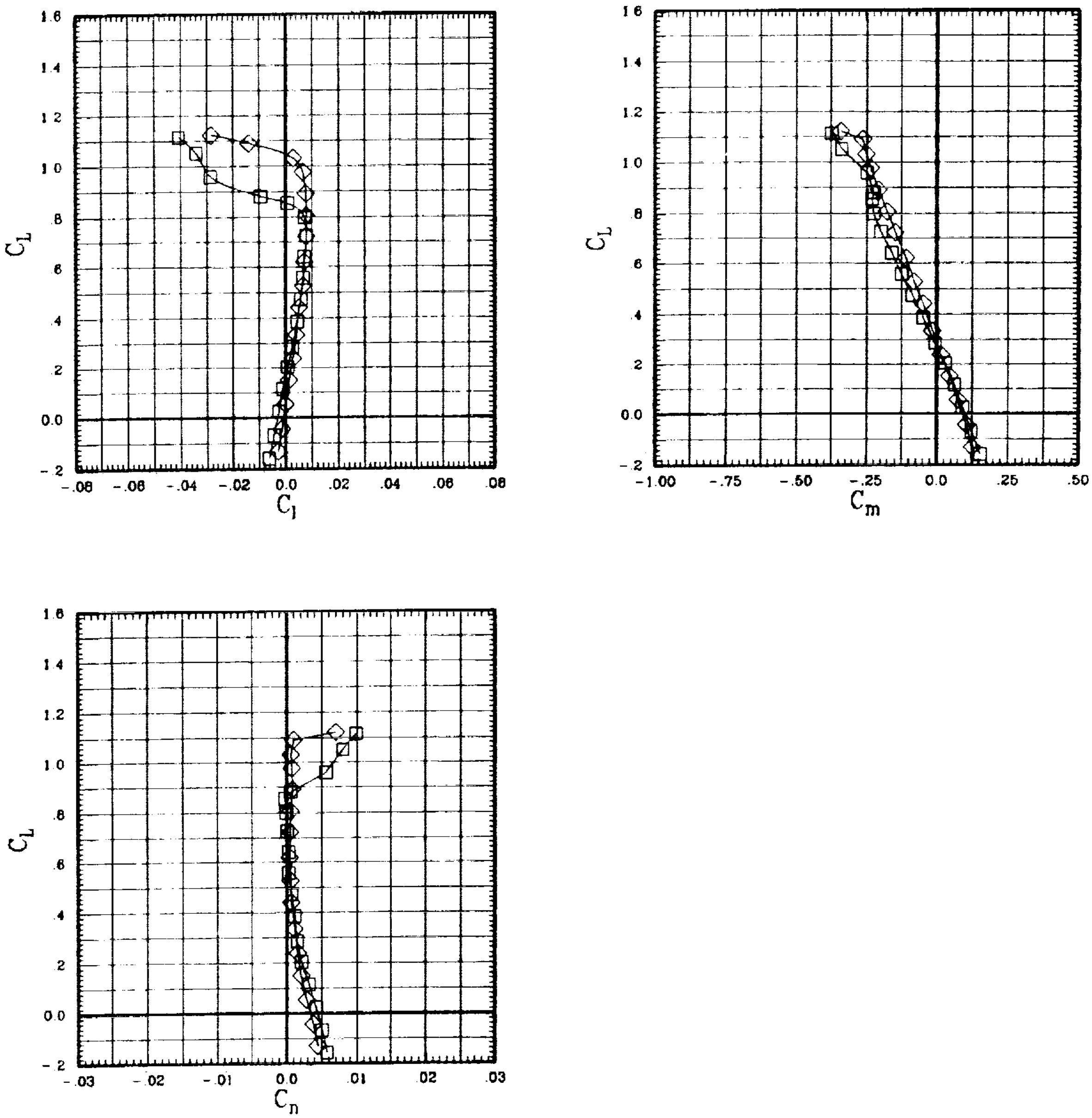

Figure A-1(b). Rockwell and NASA Ames wings for sweep = 30 deg.

SYMBOL	CONFIGURATION	TEST	RUN	SWEEP	MACH	Q	BETA
—□—	Rockwell	100	52	30	.70	699	-.1
—◇—	NASA Ames	100	132	30	.70	711	-.1

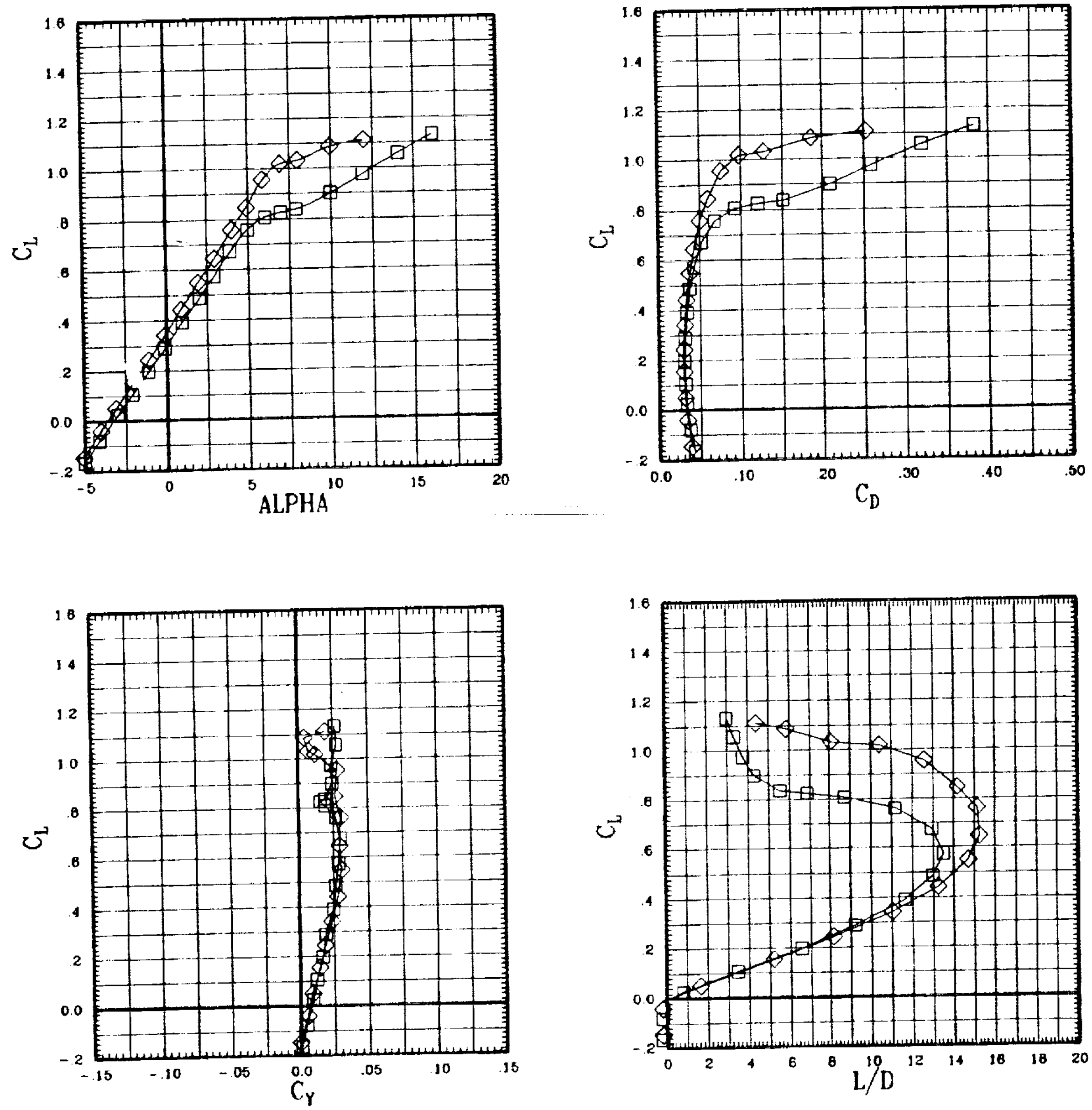

Figure A-1(b). Rockwell and NASA Ames wings for sweep = 30 deg.

SYMBOL	CONFIGURATION	TEST	RUN	SWEEP	MACH	Q	BETA
—□—	Rockwell	100	52	30	.70	699	-.1
—◇—	NASA Ames	100	132	30	.70	711	-.1

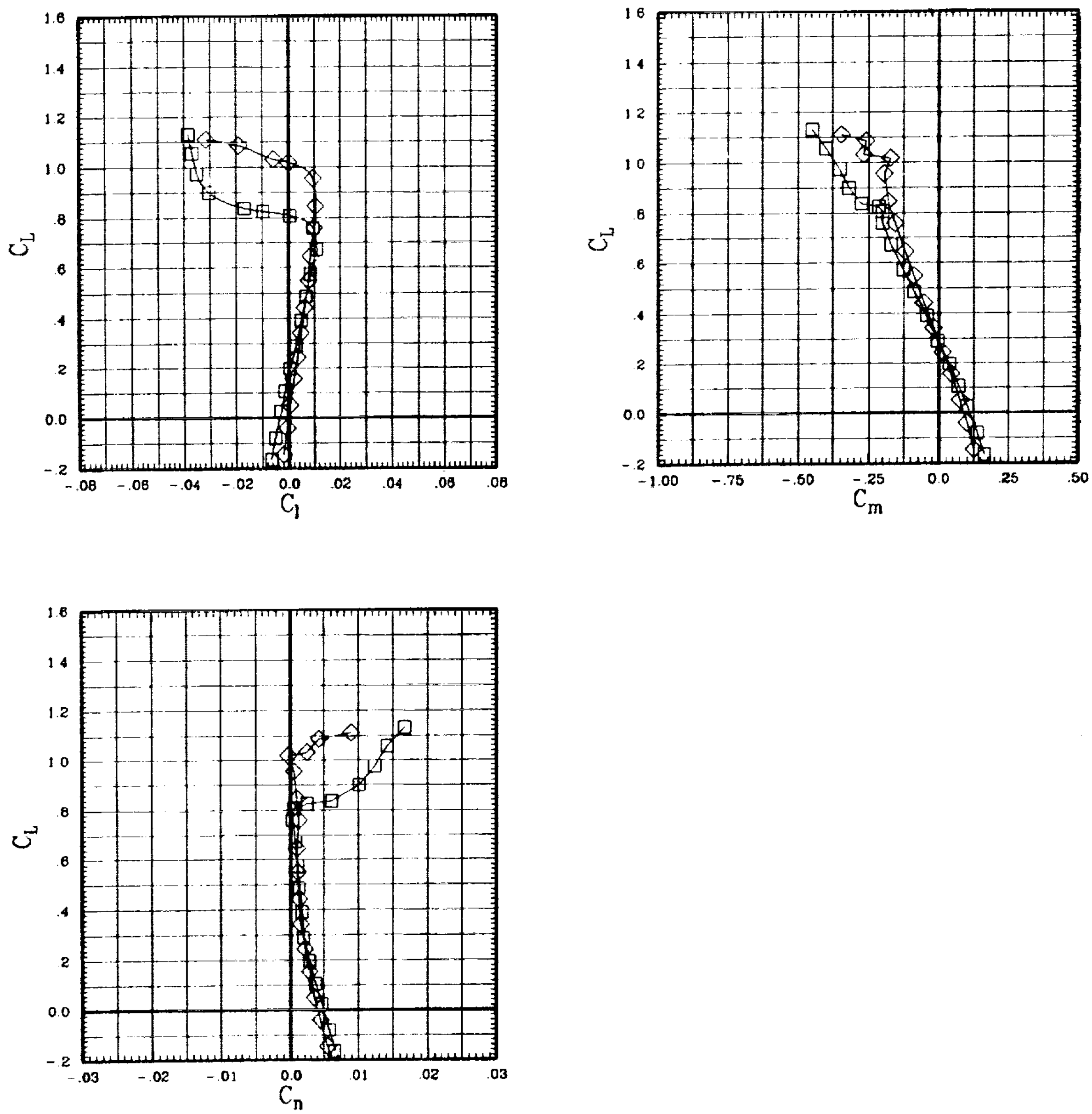

Figure A-1(b). Rockwell and NASA Ames wings for sweep = 30 deg.

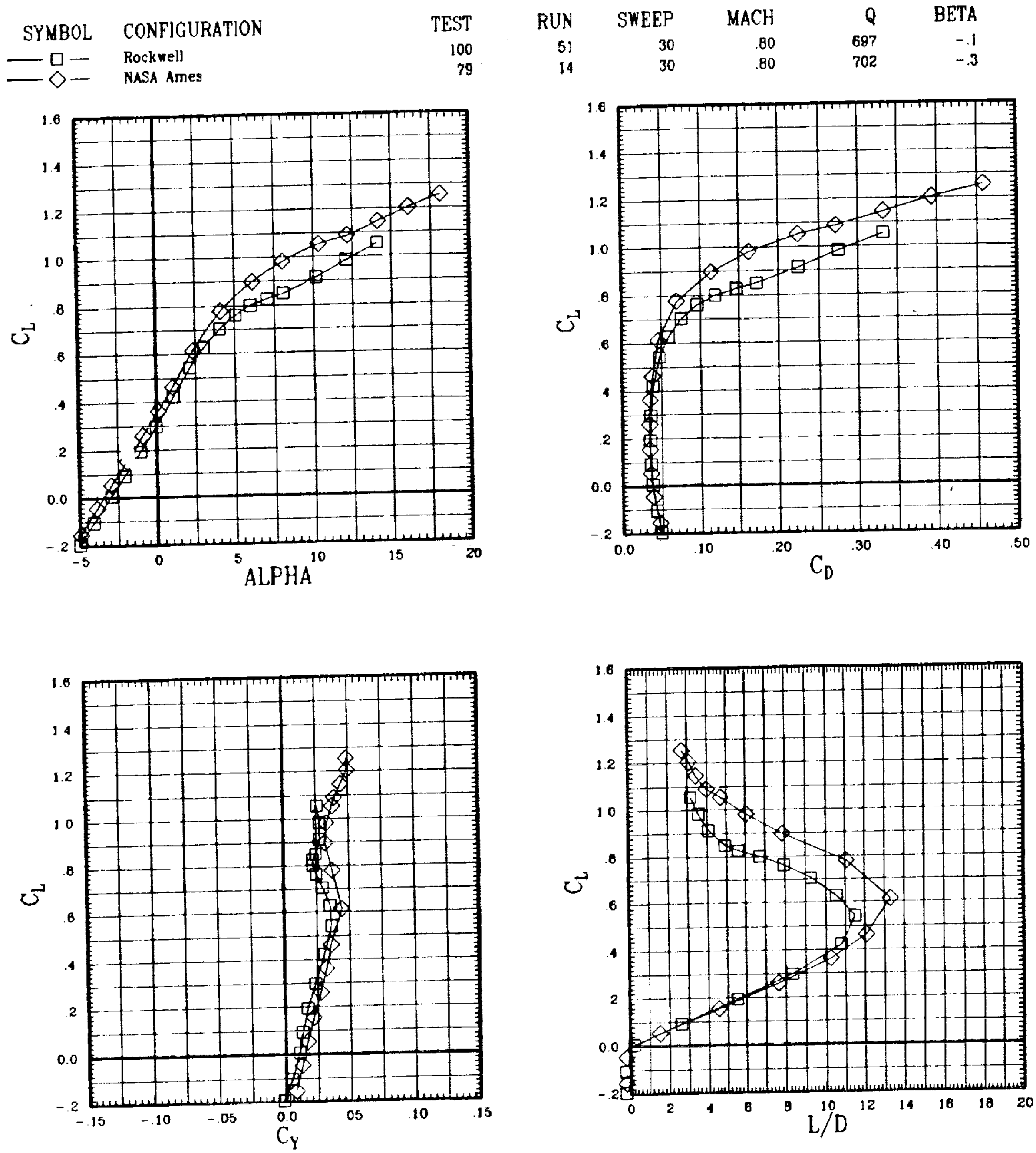

Figure A-1(b). Rockwell and NASA Ames wings for sweep = 30 deg.

SYMBOL	CONFIGURATION	TEST	RUN	SWEEP	MACH	Q	BETA
—□—	Rockwell	100	51	30	.80	697	-.1
—◇—	NASA Ames	79	14	30	.80	702	-.3

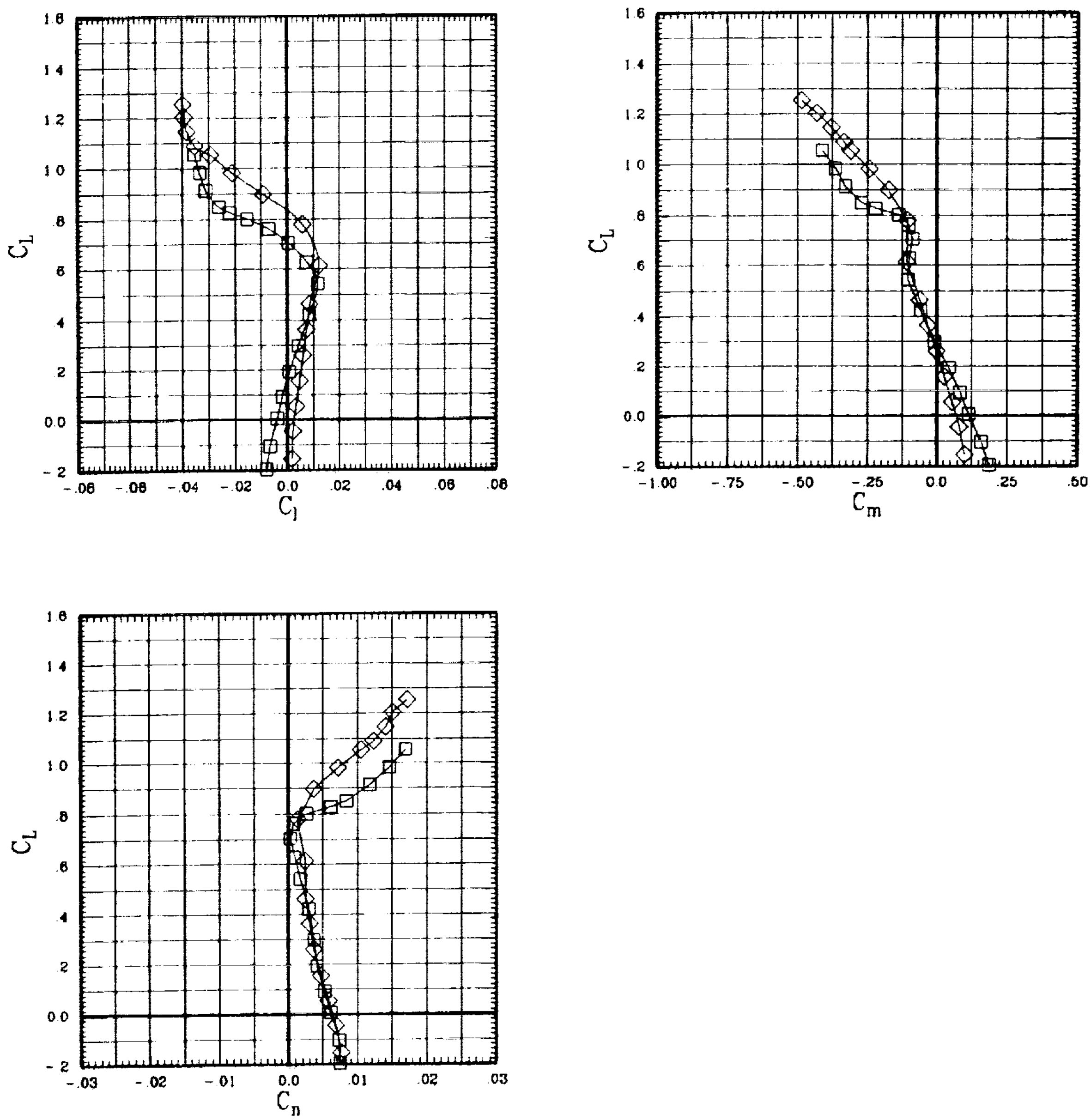

Figure A-1(b). Rockwell and NASA Ames wings for sweep = 30 deg.

SYMBOL	CONFIGURATION	TEST	RUN	SWEEP	MACH	Q	BETA
—□—	Rockwell	100	50	30	.90	698	-.1
—◇—	NASA Ames	79	13	30	.90	701	-.3

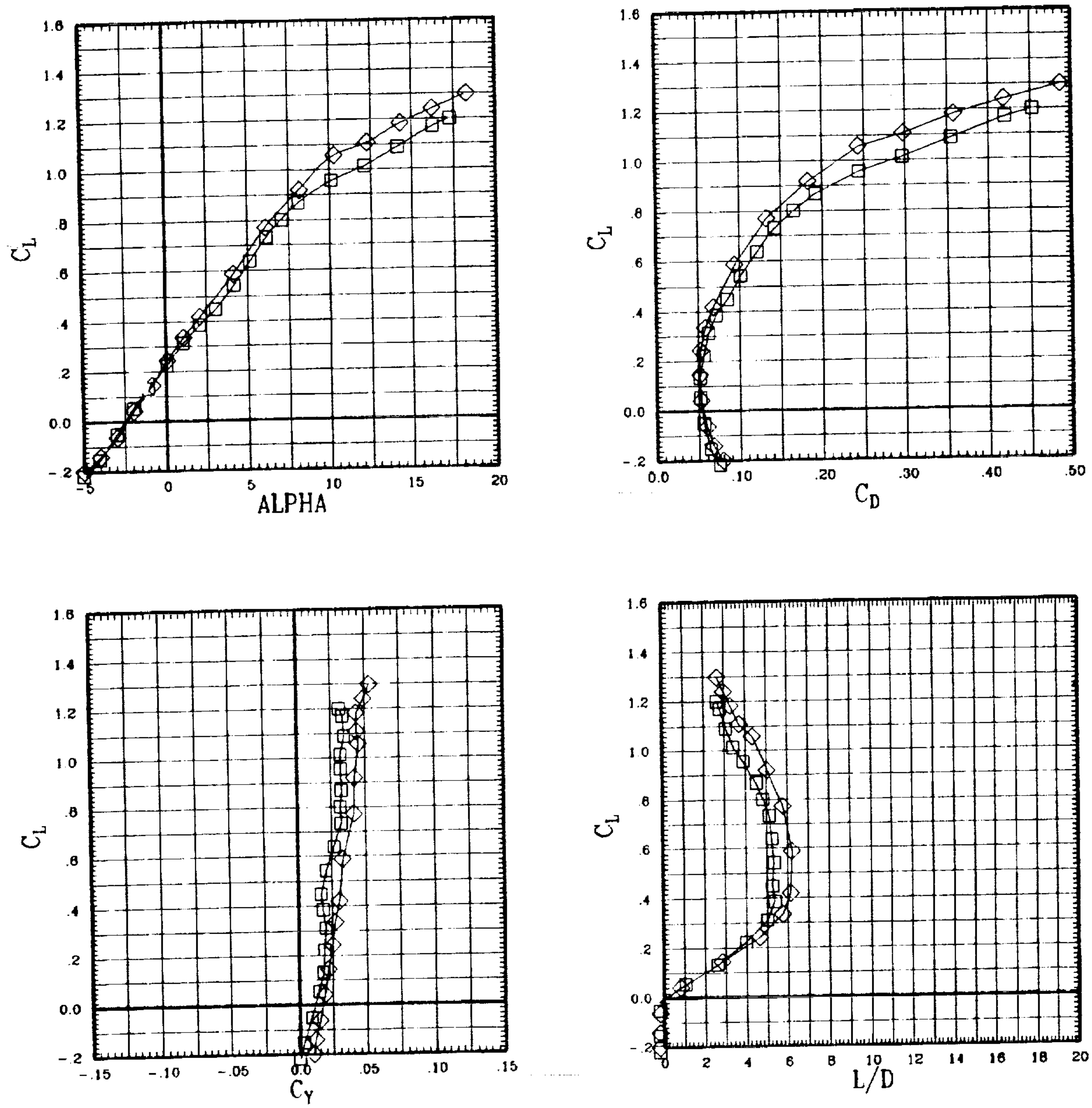

Figure A-1(b). Rockwell and NASA Ames wings for sweep = 30 deg.

SYMBOL	CONFIGURATION	TEST	RUN	SWEEP	MACH	Q	BETA
—□—	Rockwell	100	50	30	.90	698	-.1
—◇—	NASA Ames	79	13	30	.90	701	-.3

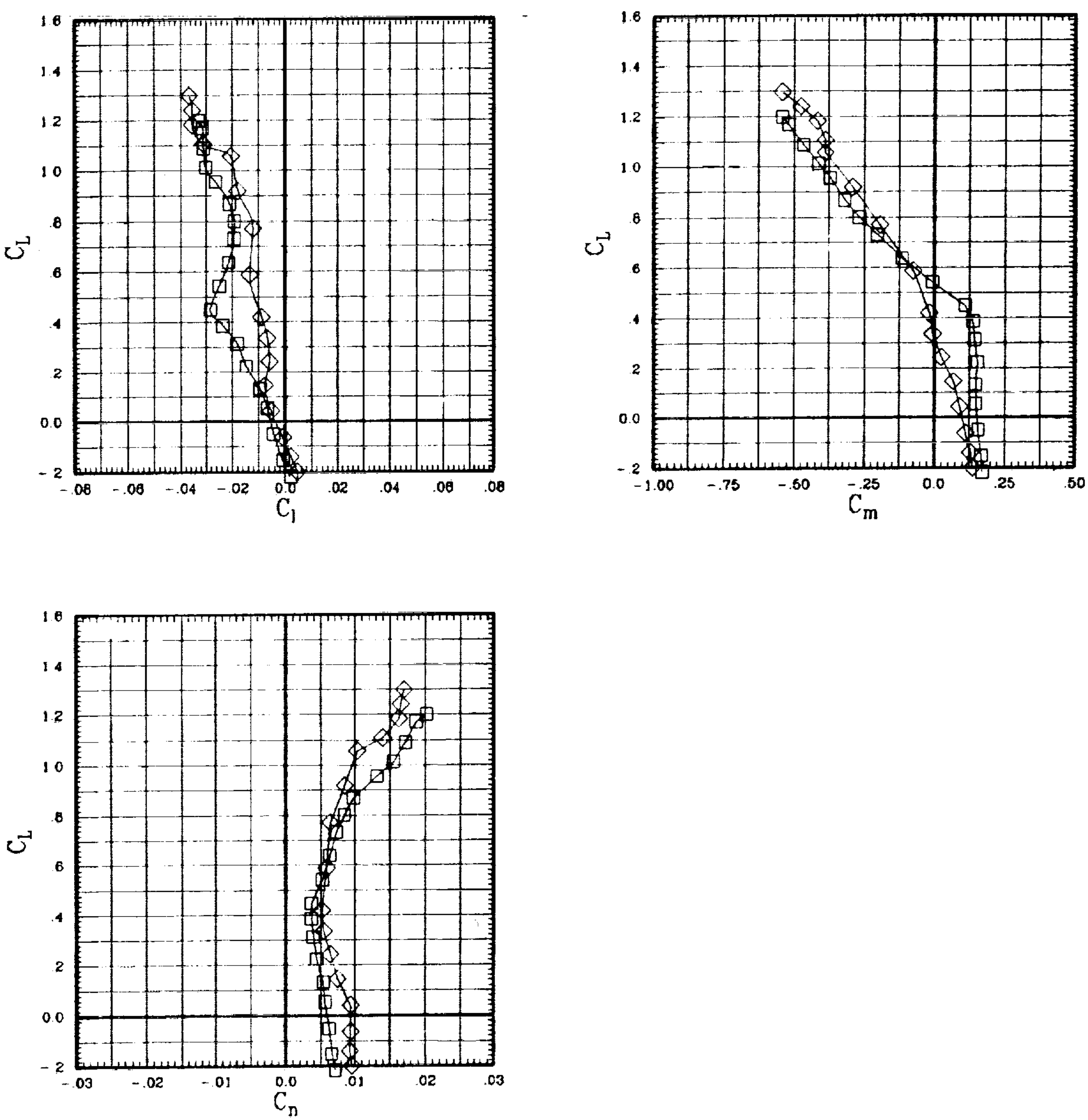

Figure A-1(b). Rockwell and NASA Ames wings for sweep = 30 deg.

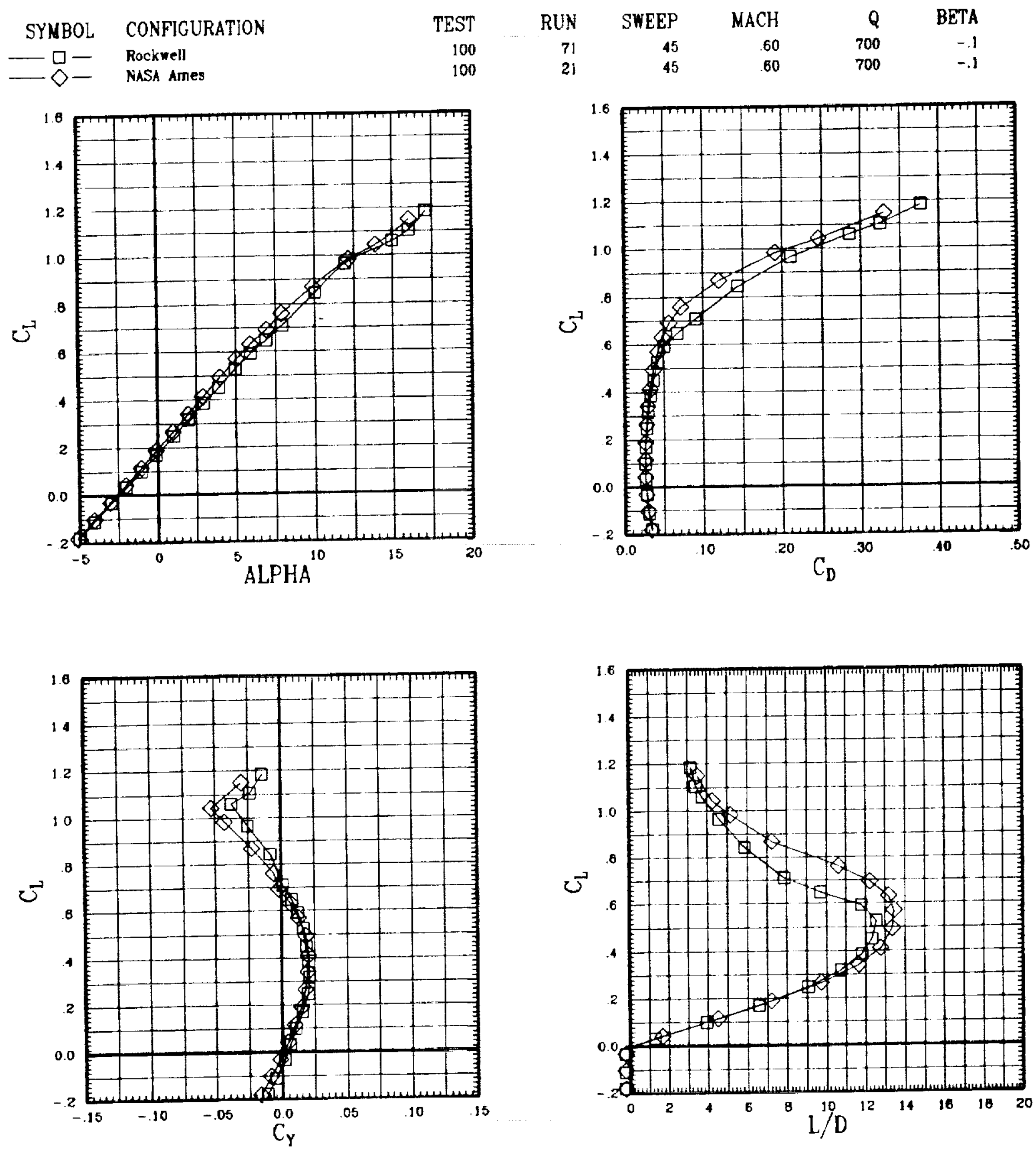

Figure A-1(c). Rockwell and NASA Ames wings for sweep = 45 deg.

SYMBOL	CONFIGURATION	TEST	RUN	SWEEP	MACH	Q	BETA
—□—	Rockwell	100	71	45	.60	700	-.1
—◇—	NASA Ames	100	21	45	.60	700	-.1

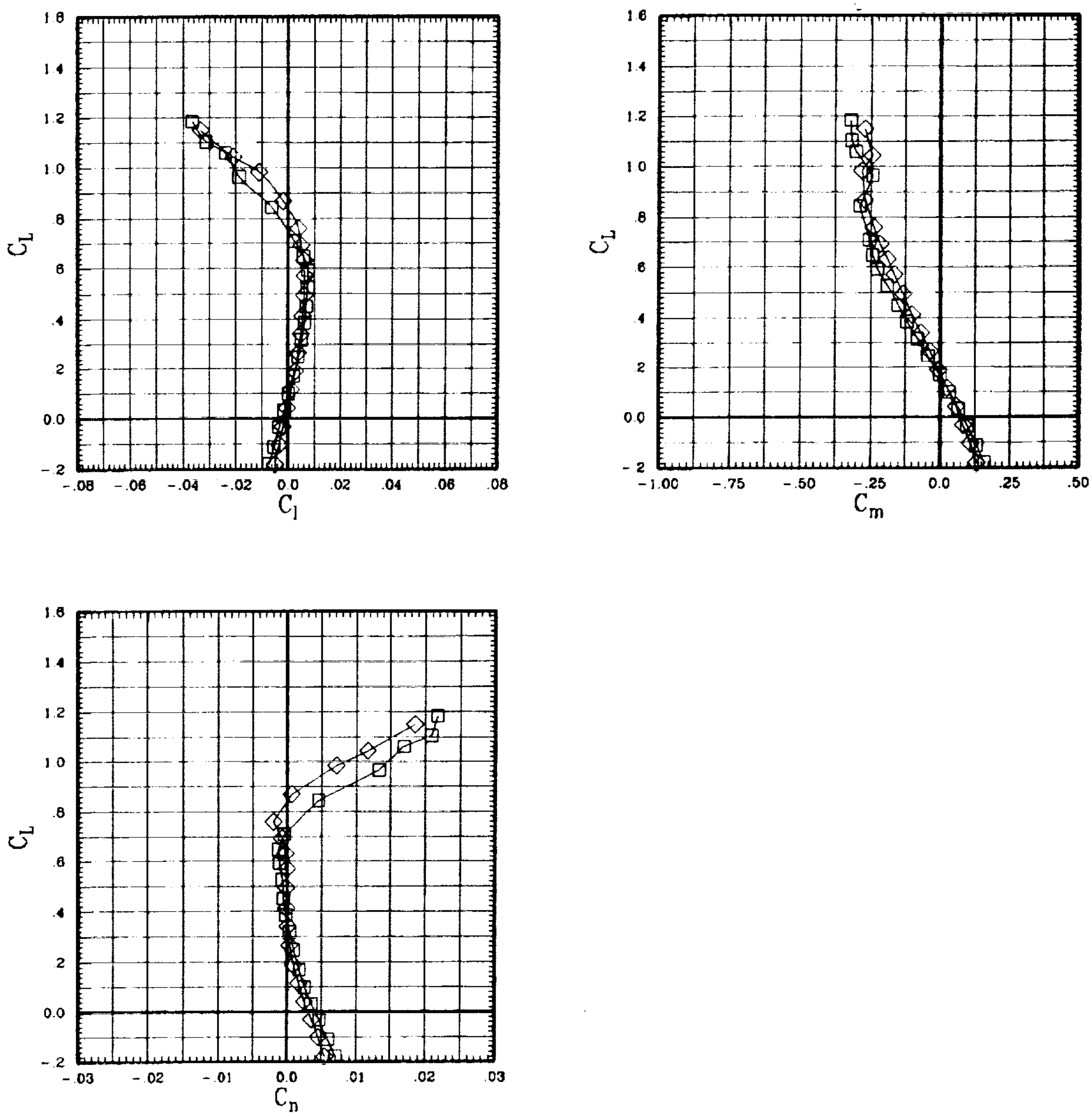

Figure A-1(c). Rockwell and NASA Ames wings for sweep = 45 deg.

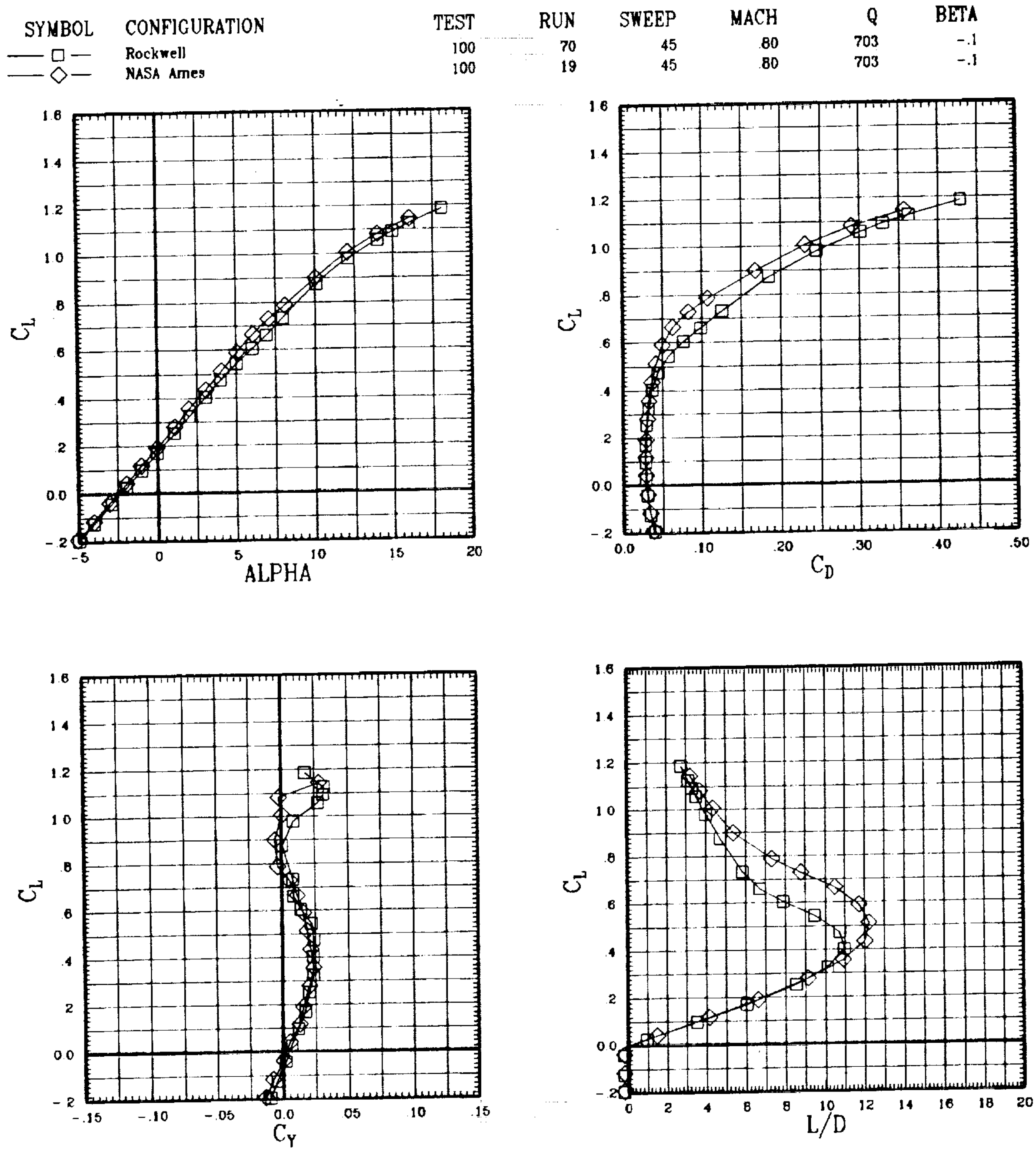

Figure A-1(c). Rockwell and NASA Ames wings for sweep = 45 deg.

SYMBOL	CONFIGURATION	TEST	RUN	SWEEP	MACH	Q	BETA
—□—	Rockwell	100	70	45	.80	703	-.1
—◇—	NASA Ames	100	19	45	.80	703	-.1

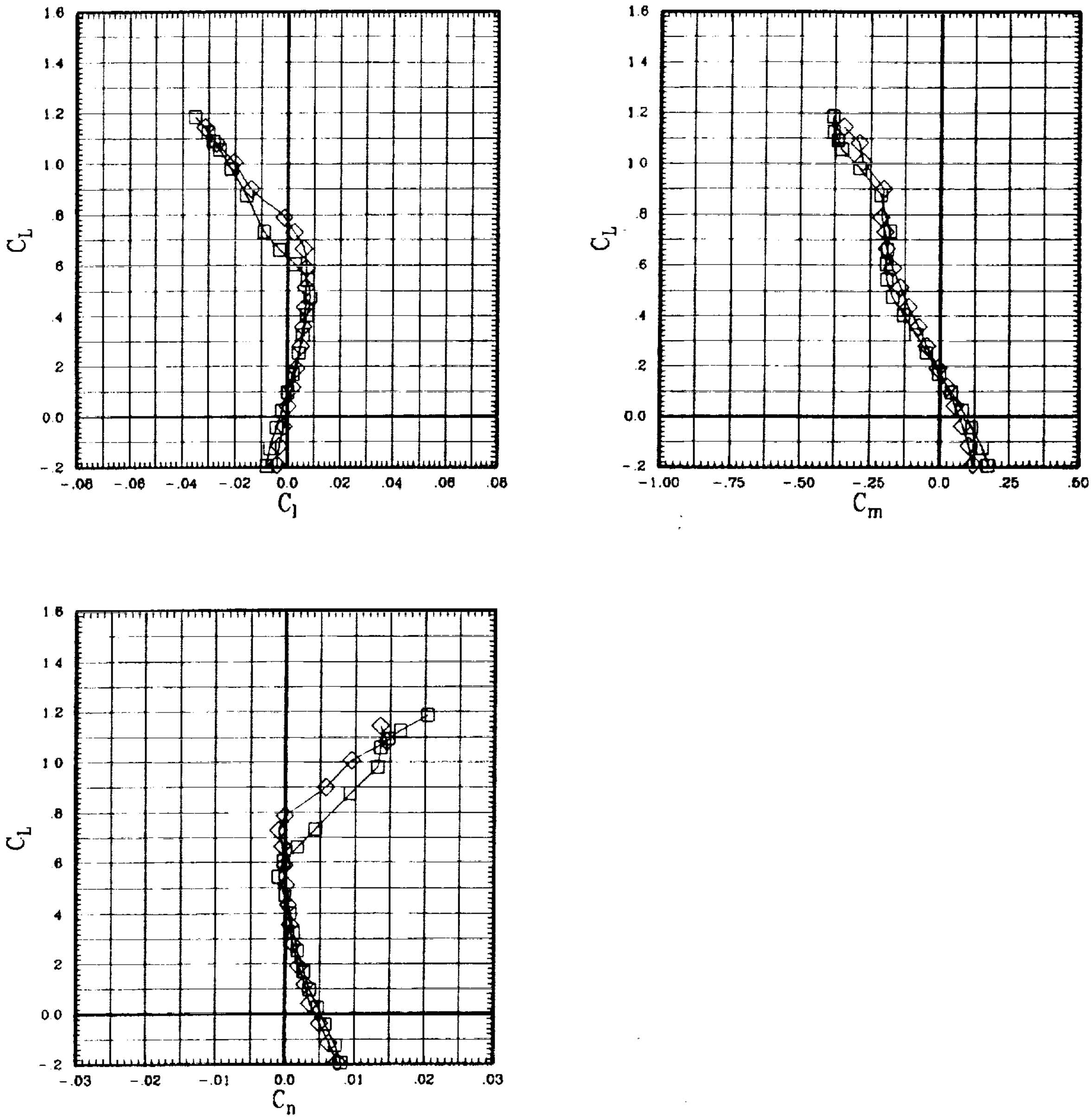

Figure A-1(c). Rockwell and NASA Ames wings for sweep = 45 deg.

SYMBOL	CONFIGURATION	TEST	RUN	SWEEP	MACH	Q	BETA
—□—	Rockwell	100	69	45	.90	704	-.1
—◇—	NASA Ames	79	19	45	.90	704	-.3

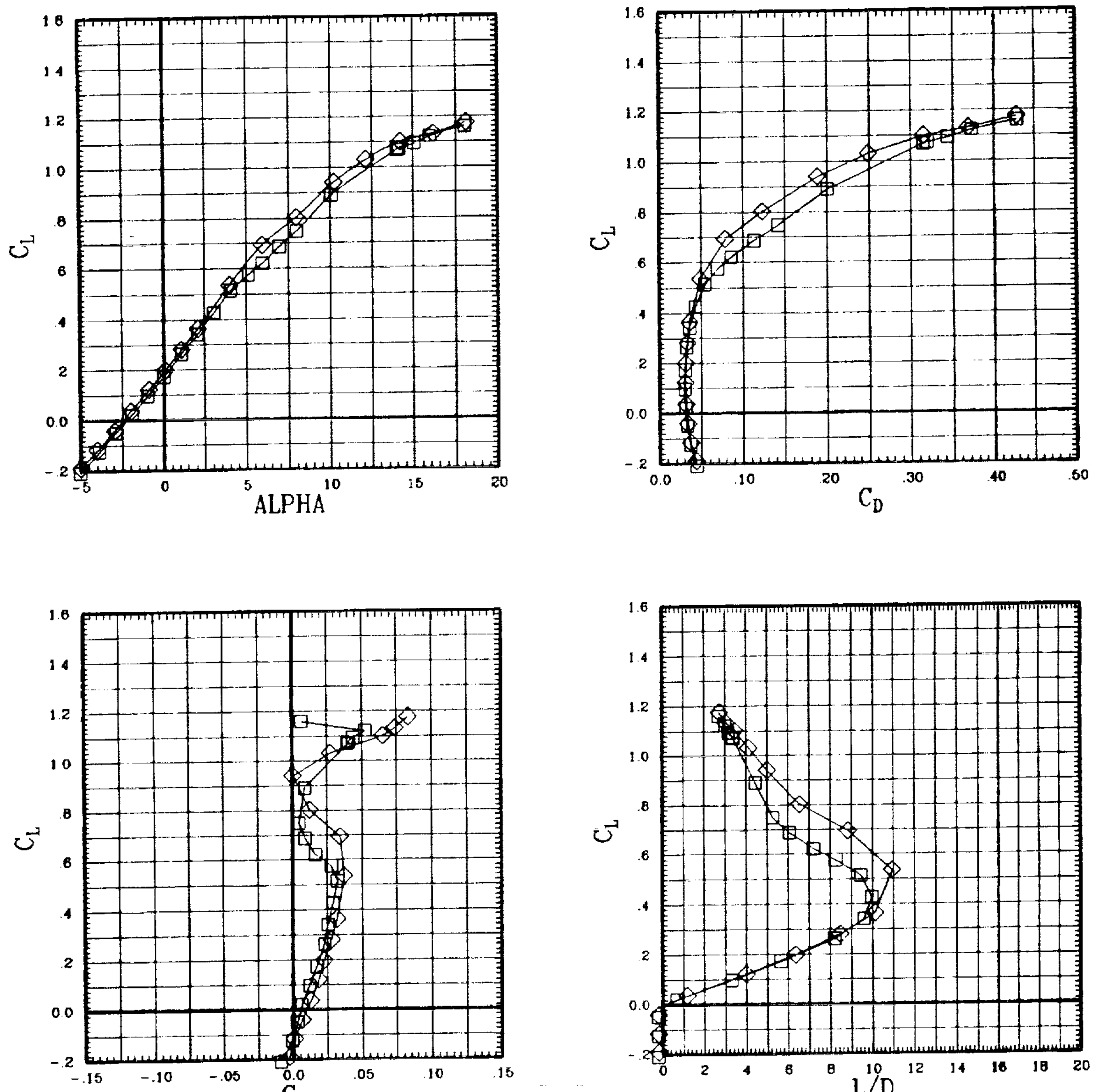

Figure A-1(c). Rockwell and NASA Ames wings for sweep = 45 deg.

SYMBOL	CONFIGURATION	TEST	RUN	SWEEP	MACH	Q	BETA
—□—	Rockwell	100	69	45	.90	704	-.1
—◇—	NASA Ames	79	19	45	.90	704	-.3

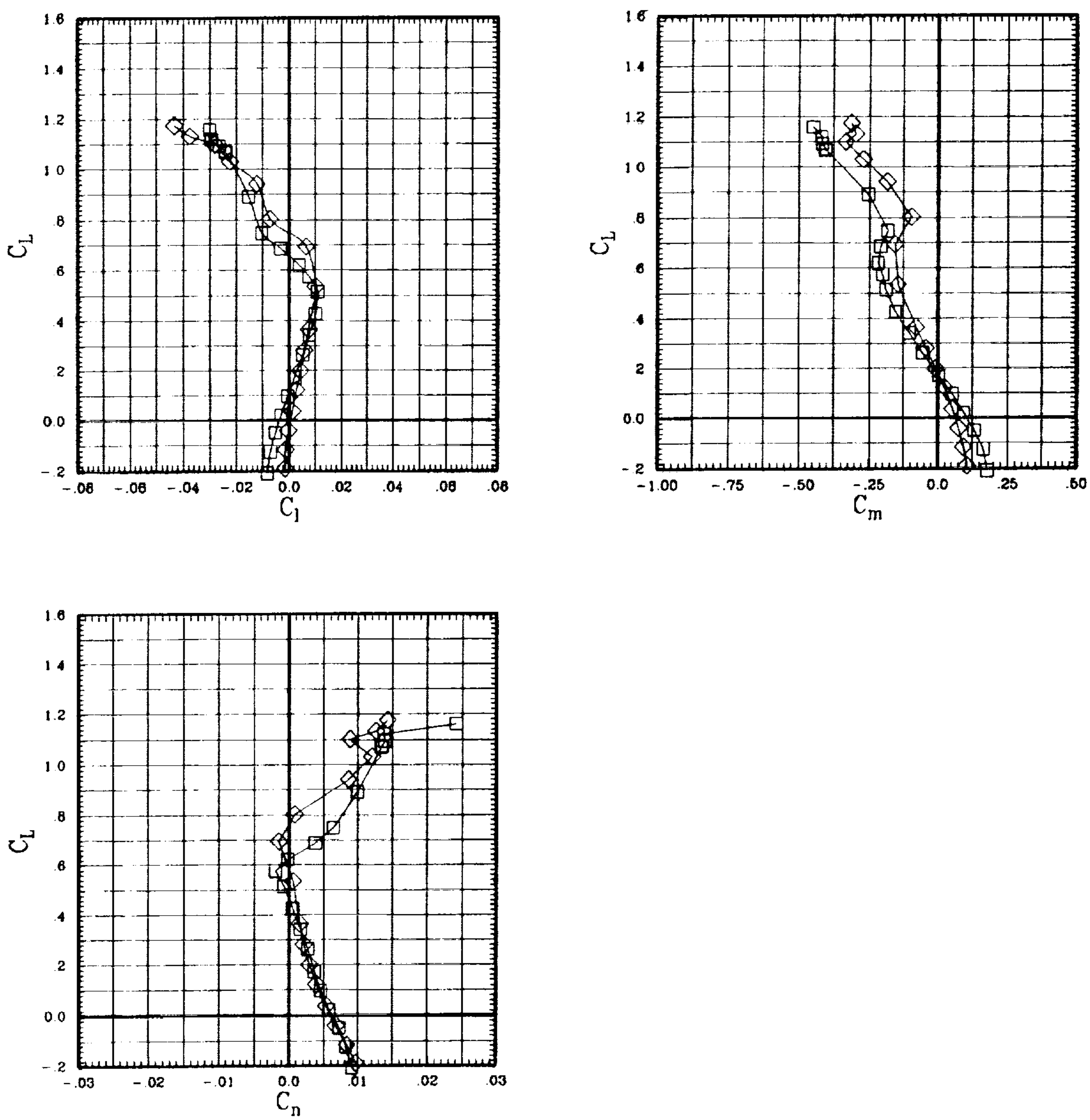

Figure A-1(c). Rockwell and NASA Ames wings for sweep = 45 deg.

SYMBOL	CONFIGURATION	TEST	RUN	SWEEP	MACH	Q	BETA
—□—	Rockwell	100	68	45	.95	700	-.1
—◇—	NASA Ames	79	18	45	.95	705	-.3

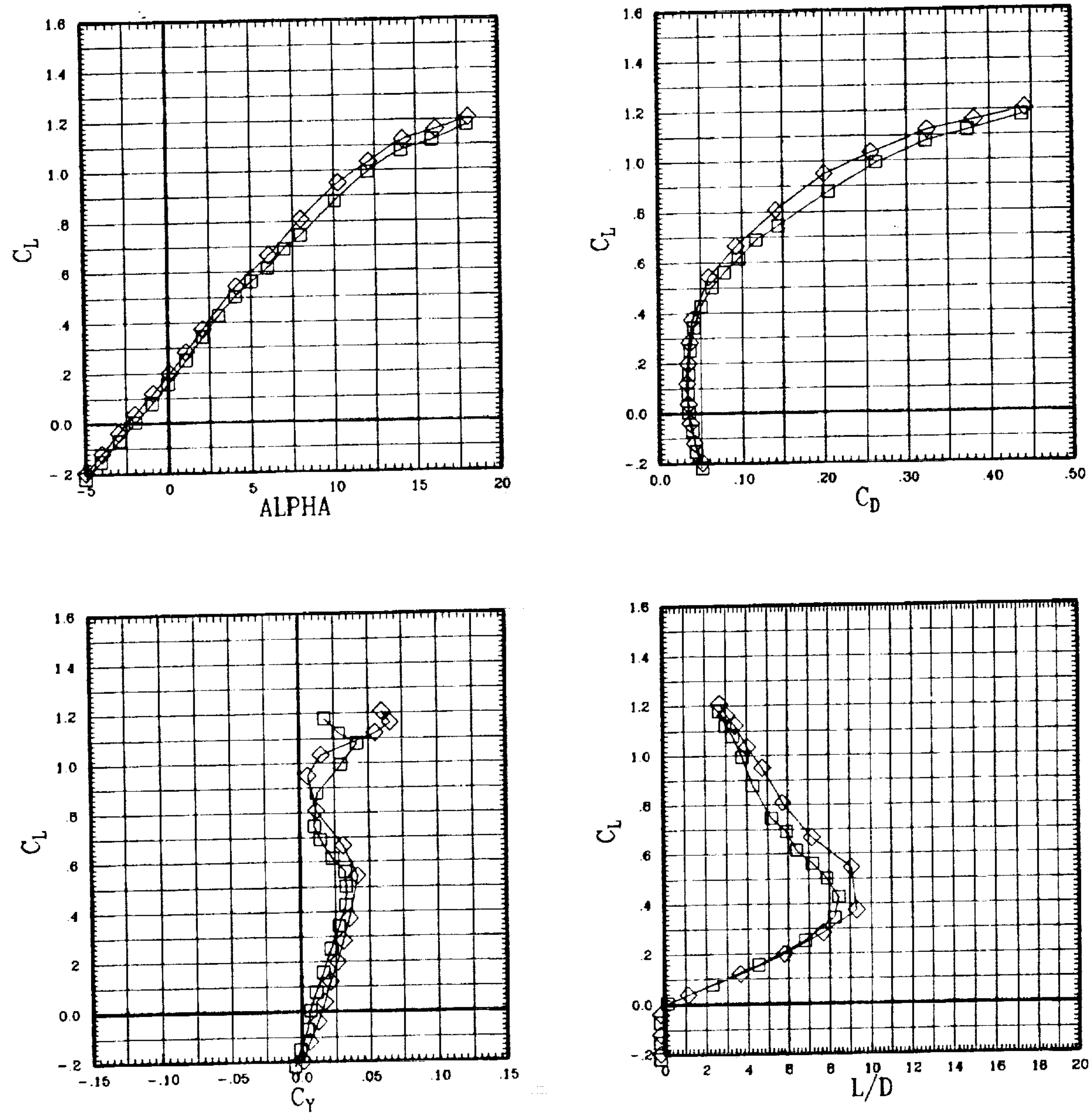

Figure A-1(c). Rockwell and NASA Ames wings for sweep = 45 deg.

SYMBOL	CONFIGURATION	TEST	RUN	SWEEP	MACH	Q	BETA
—□—	Rockwell	100	68	45	.95	700	-.1
—◇—	NASA Ames	79	18	45	.95	705	-.3

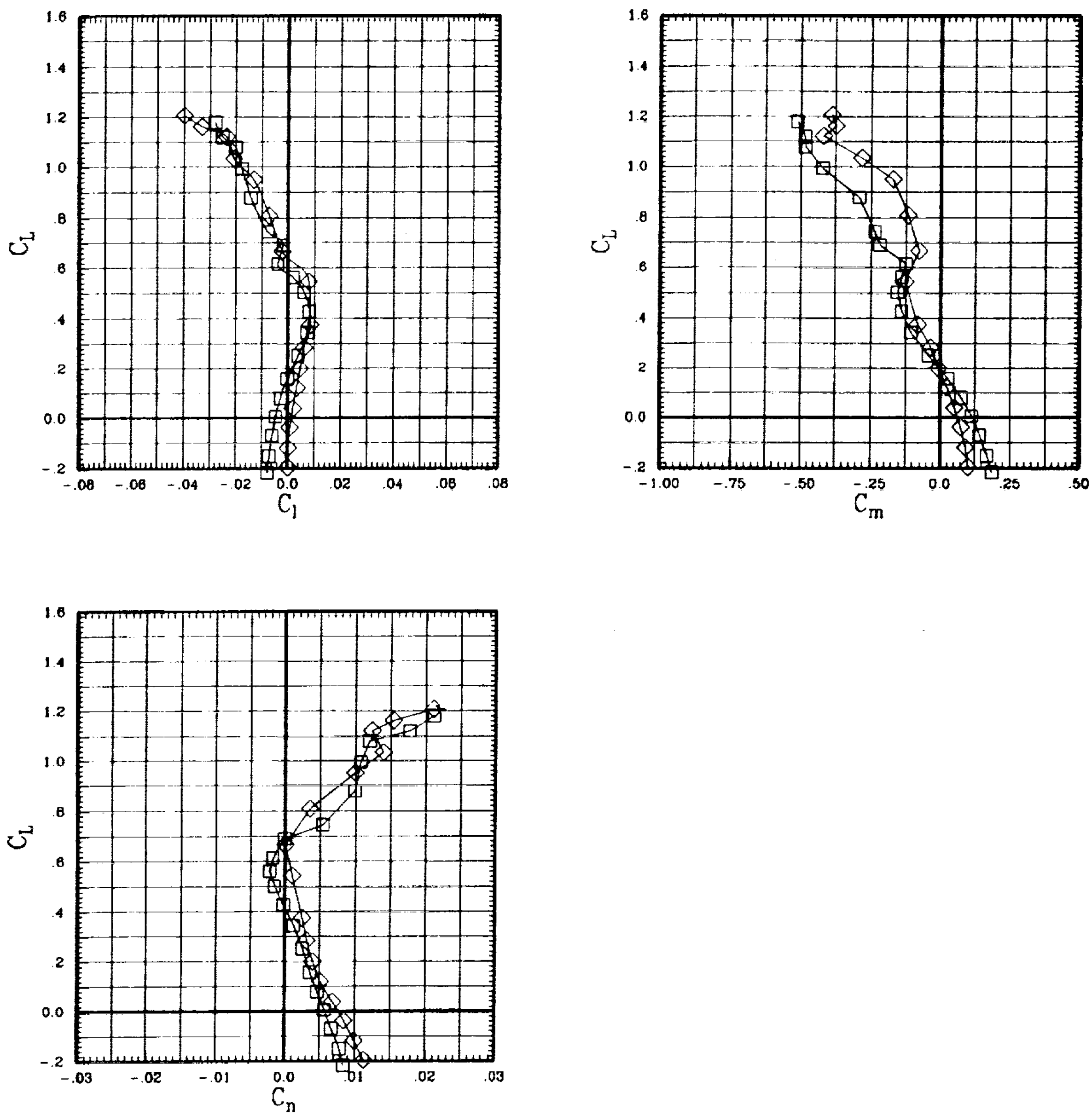

Figure A-1(c). Rockwell and NASA Ames wings for sweep = 45 deg.

SYMBOL	CONFIGURATION	TEST	RUN	SWEEP	MACH	Q	BETA
—□—	Rockwell	100	67	45	1.10	691	-.2
—◇—	NASA Ames	79	17	45	1.09	696	-.3

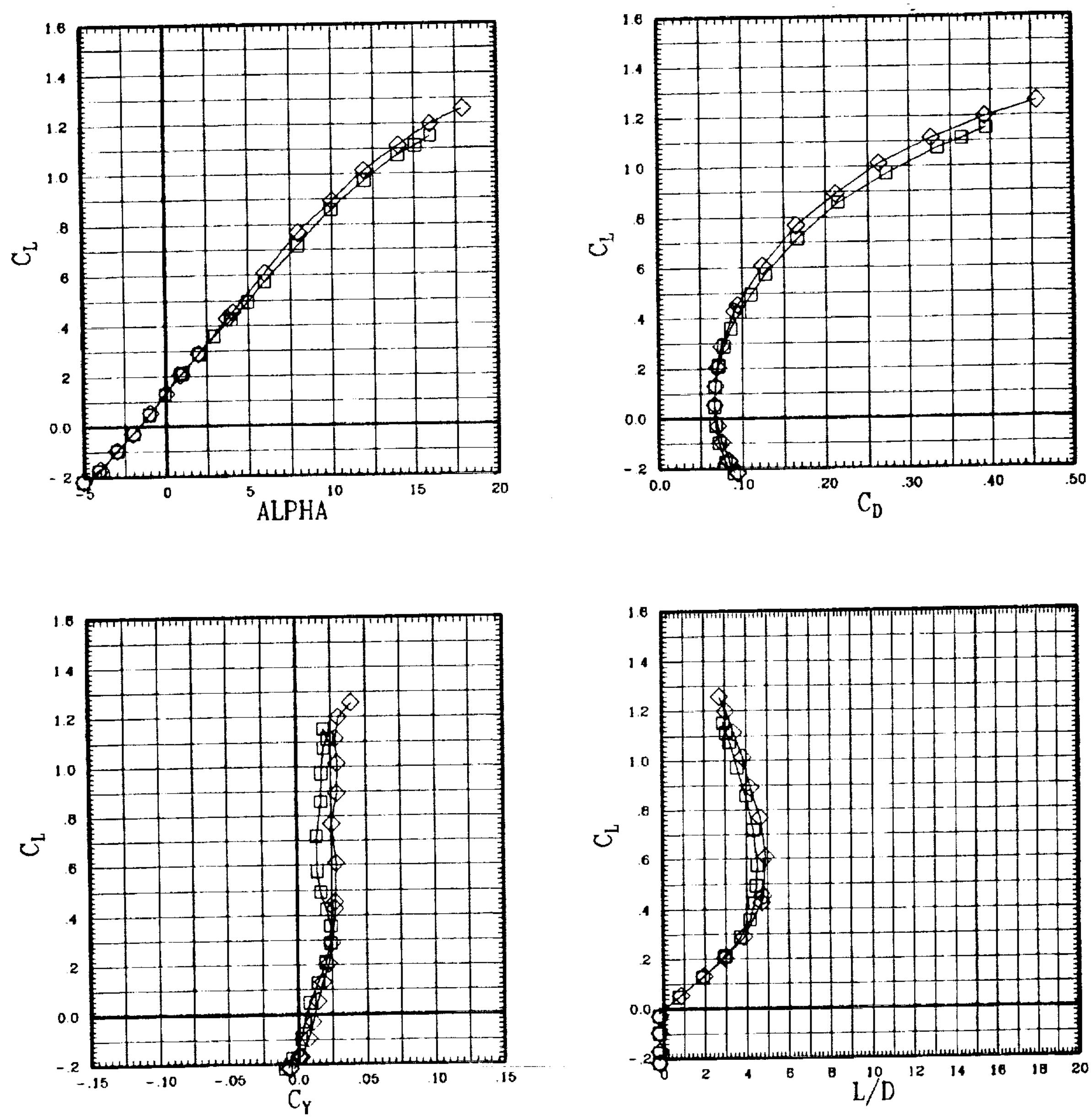

Figure A-1(c). Rockwell and NASA Ames wings for sweep = 45 deg.

SYMBOL	CONFIGURATION	TEST	RUN	SWEEP	MACH	Q	BETA
—□—	Rockwell	100	67	45	1.10	691	-.2
—◇—	NASA Ames	79	17	45	1.09	696	-.3

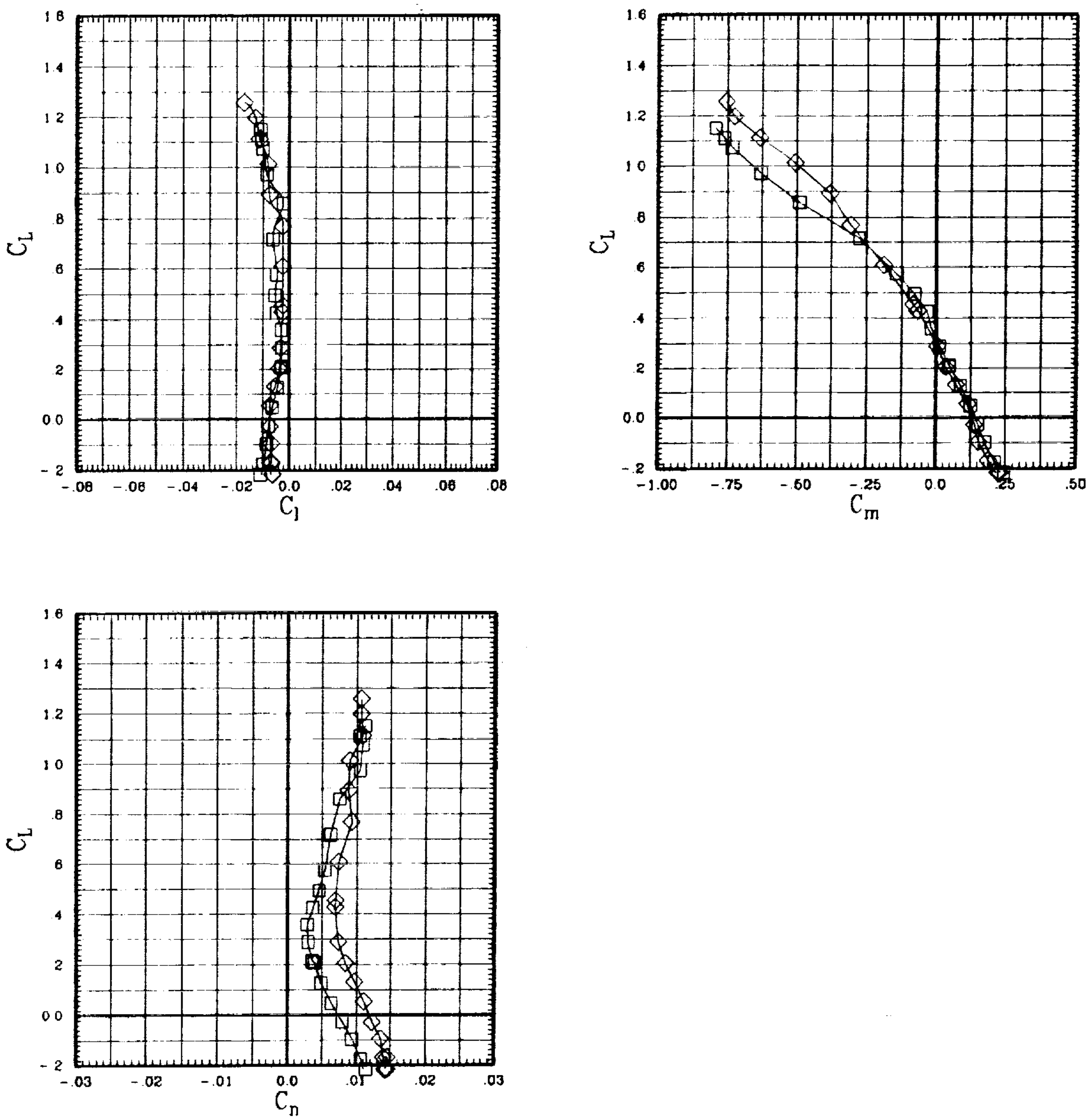

Figure A-1(c). Rockwell and NASA Ames wings for sweep = 45 deg.

SYMBOL	CONFIGURATION	TEST	RUN	SWEEP	MACH	Q	BETA
—□—	Rockwell	100	66	45	1.20	703	-2
—◇—	NASA Ames	100	18	45	1.20	705	-2

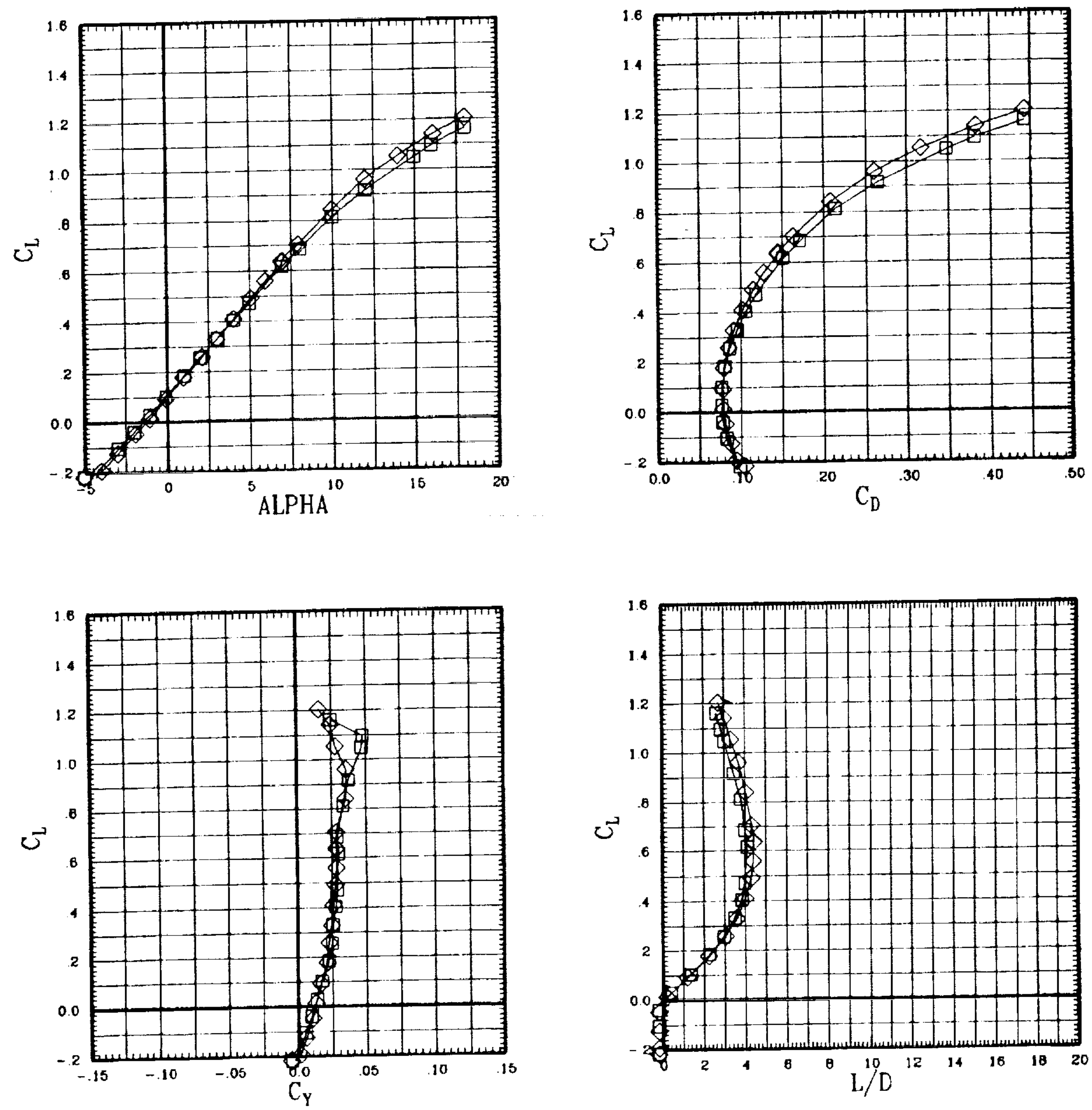

Figure A-1(c). Rockwell and NASA Ames wings for sweep = 45 deg.

SYMBOL	CONFIGURATION	TEST	RUN	SWEEP	MACH	Q	BETA
—□—	Rockwell	100	66	45	1.20	703	-.2
—◇—	NASA Ames	100	18	45	1.20	705	-.2

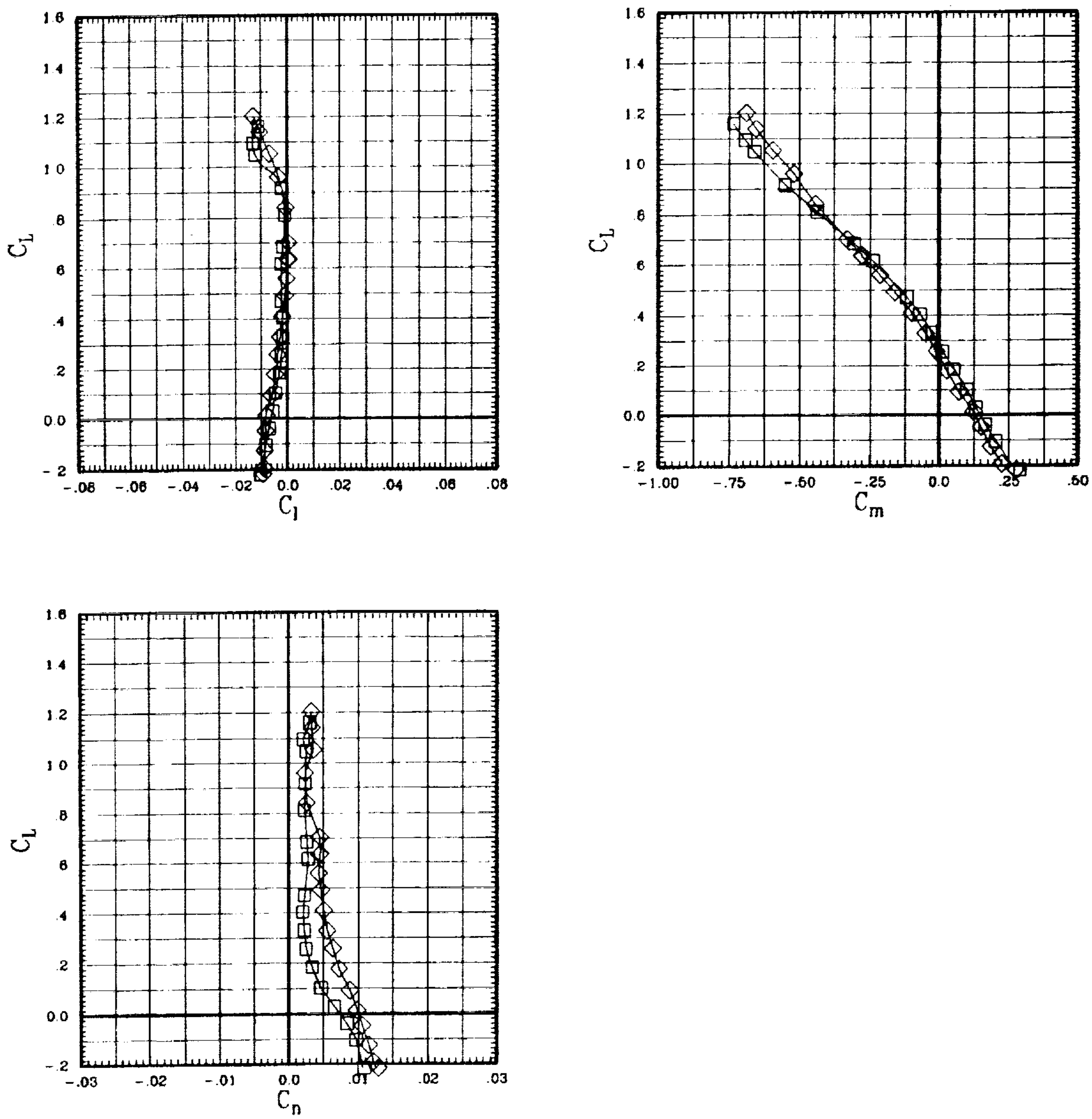

Figure A-1(c). Rockwell and NASA Ames wings for sweep = 45 deg.

SYMBOL	CONFIGURATION	TEST	RUN	SWEEP	MACH	Q	BETA
—□—	Rockwell	100	76	60	.80	699	-.1
—◇—	NASA Ames	100	135	60	.80	699	-.1

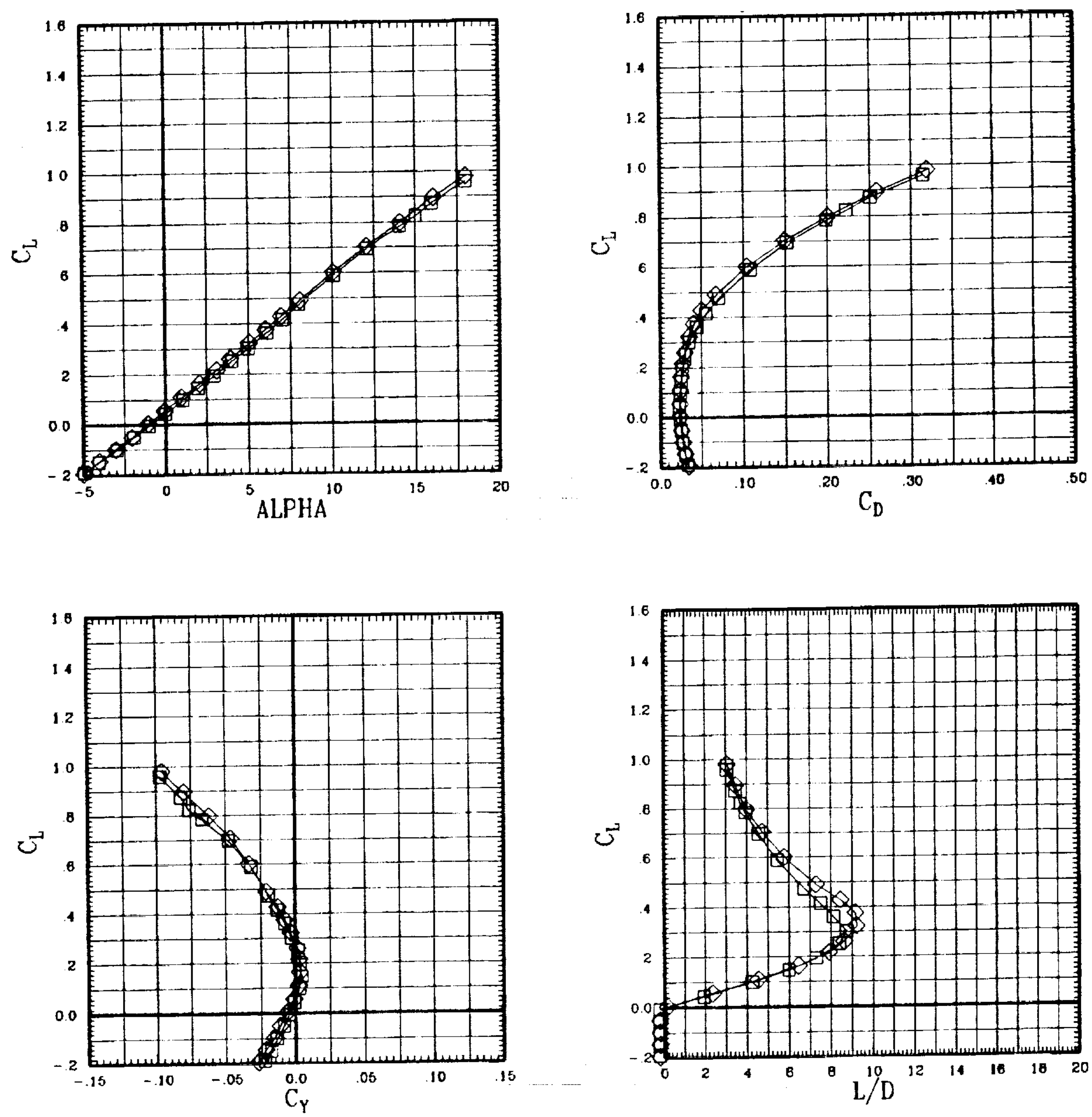

Figure A-1(d). Rockwell and NASA Ames wings for sweep = 60 deg.

SYMBOL	CONFIGURATION	TEST	RUN	SWEEP	MACH	Q	BETA
—□—	Rockwell	100	76	60	.80	699	-.1
—◇—	NASA Ames	100	135	60	.80	699	-.1

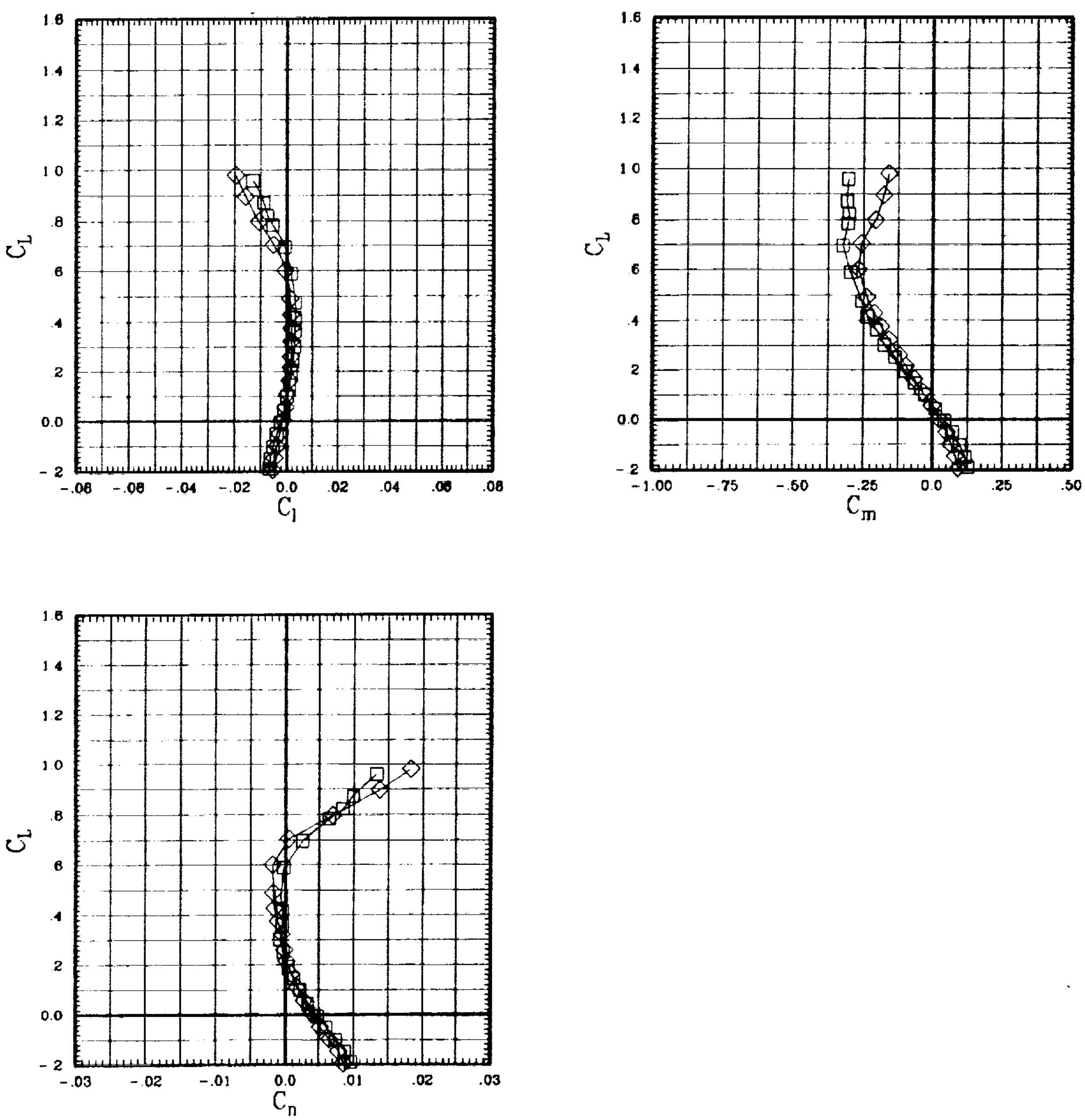

Figure A-1(d). Rockwell and NASA Ames wings for sweep = 60 deg.

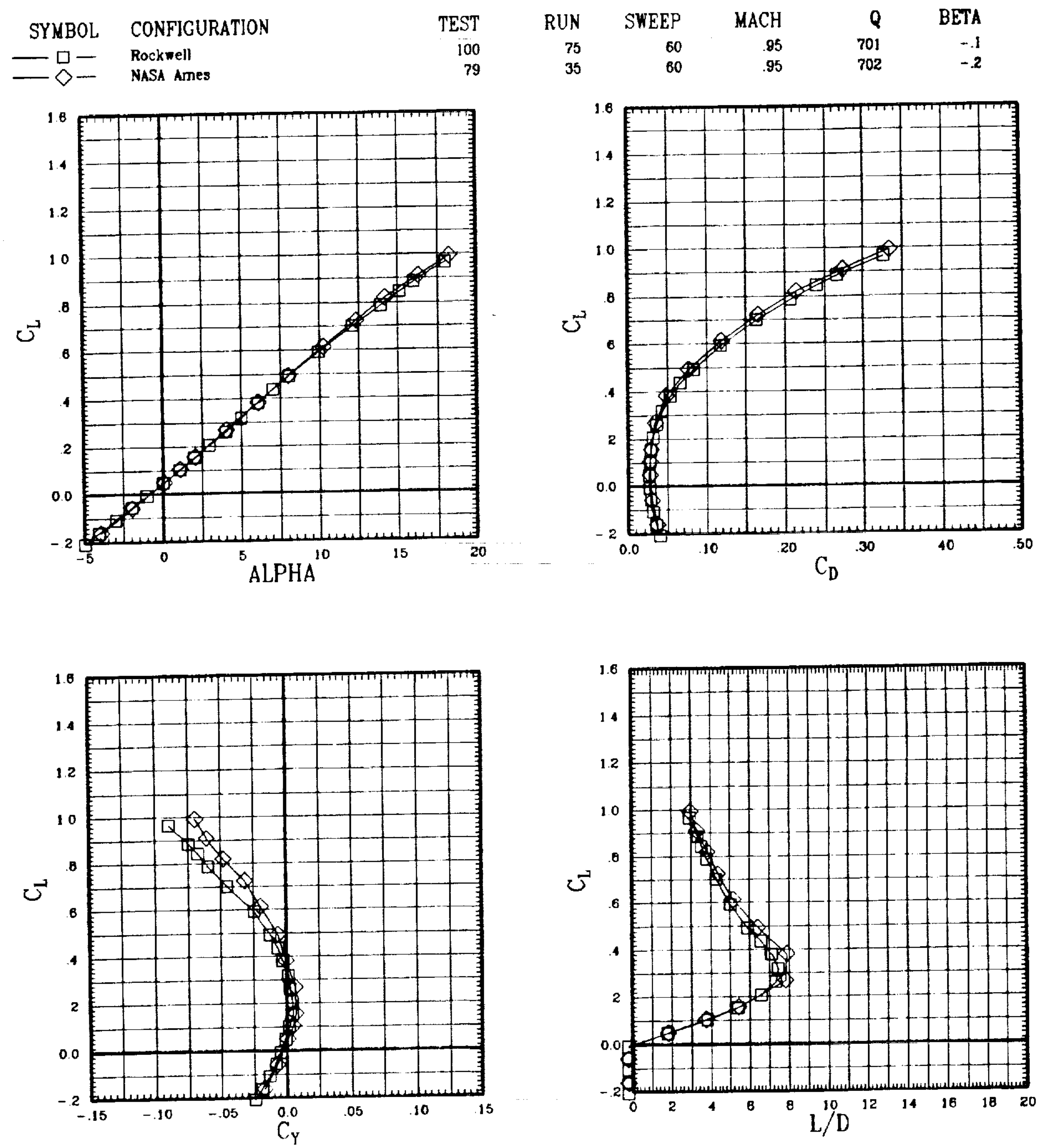

Figure A-1(d). Rockwell and NASA Ames wings for sweep = 60 deg.

SYMBOL	CONFIGURATION	TEST	RUN	SWEEP	MACH	Q	BETA
—□—	Rockwell	100	75	60	.95	701	-.1
—◇—	NASA Ames	79	35	60	.95	702	-.2

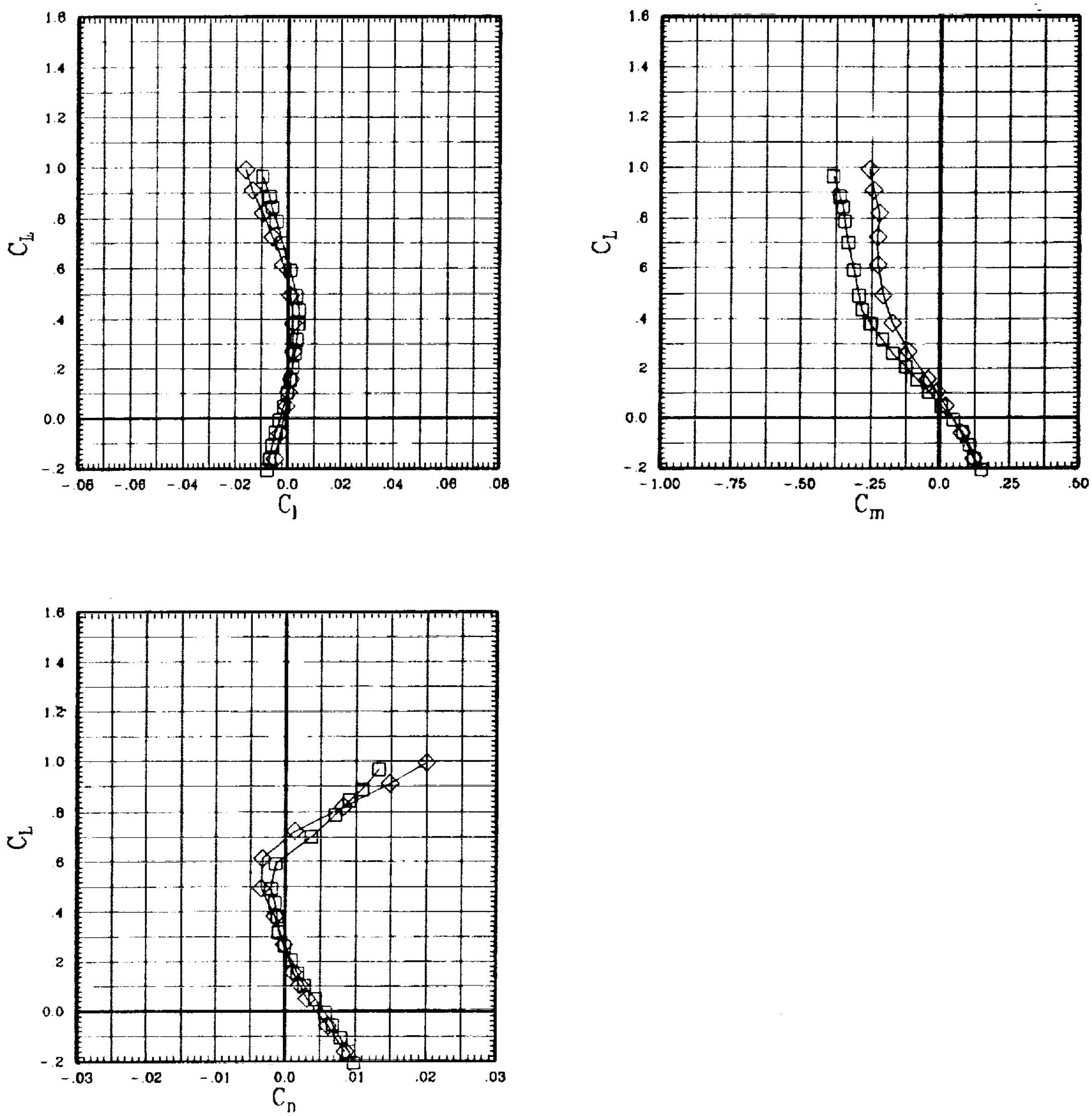

Figure A-1(d). Rockwell and NASA Ames wings for sweep = 60 deg.

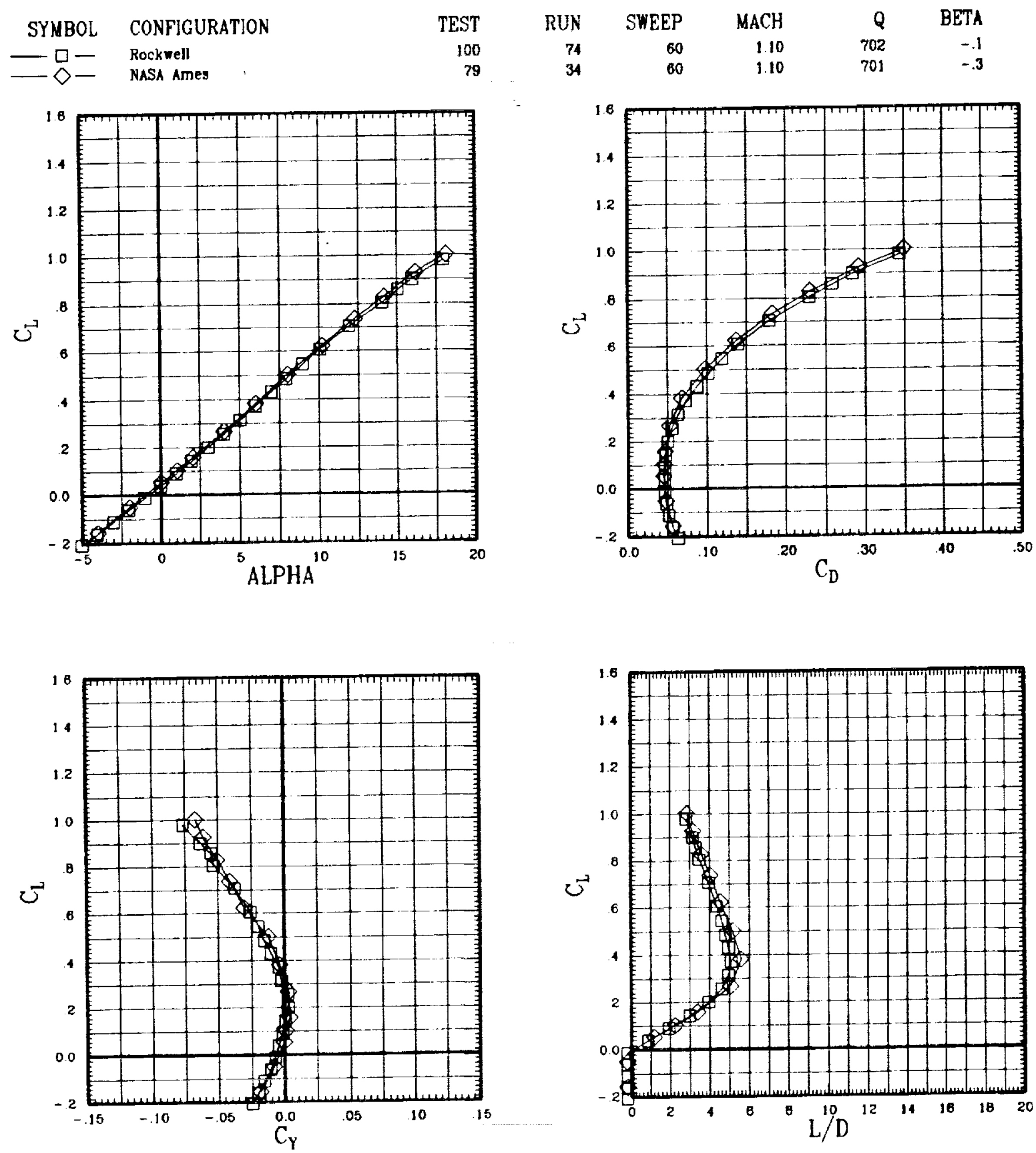

Figure A-1(d). Rockwell and NASA Ames wings for sweep = 60 deg.

SYMBOL	CONFIGURATION	TEST	RUN	SWEEP	MACH	Q	BETA
—□—	Rockwell	100	74	60	1.10	702	-.1
—◇—	NASA Ames	79	34	60	1.10	701	-.3

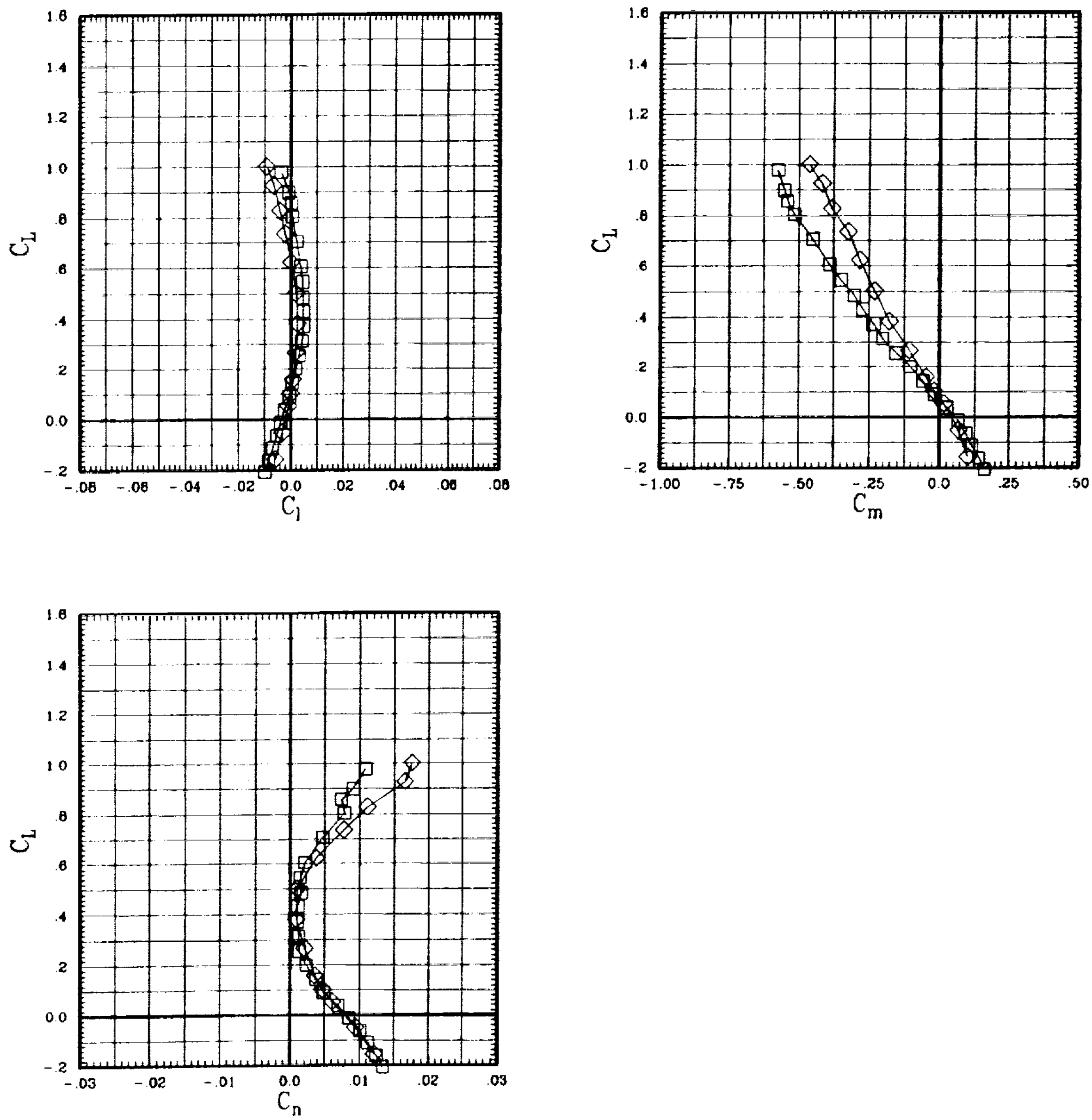

Figure A-1(d). Rockwell and NASA Ames wings for sweep = 60 deg.

SYMBOL	CONFIGURATION	TEST	RUN	SWEEP	MACH	Q	BETA
—□—	Rockwell	100	73	60	1.20	705	-.2
—◇—	NASA Ames	100	134	60	1.20	698	-.1

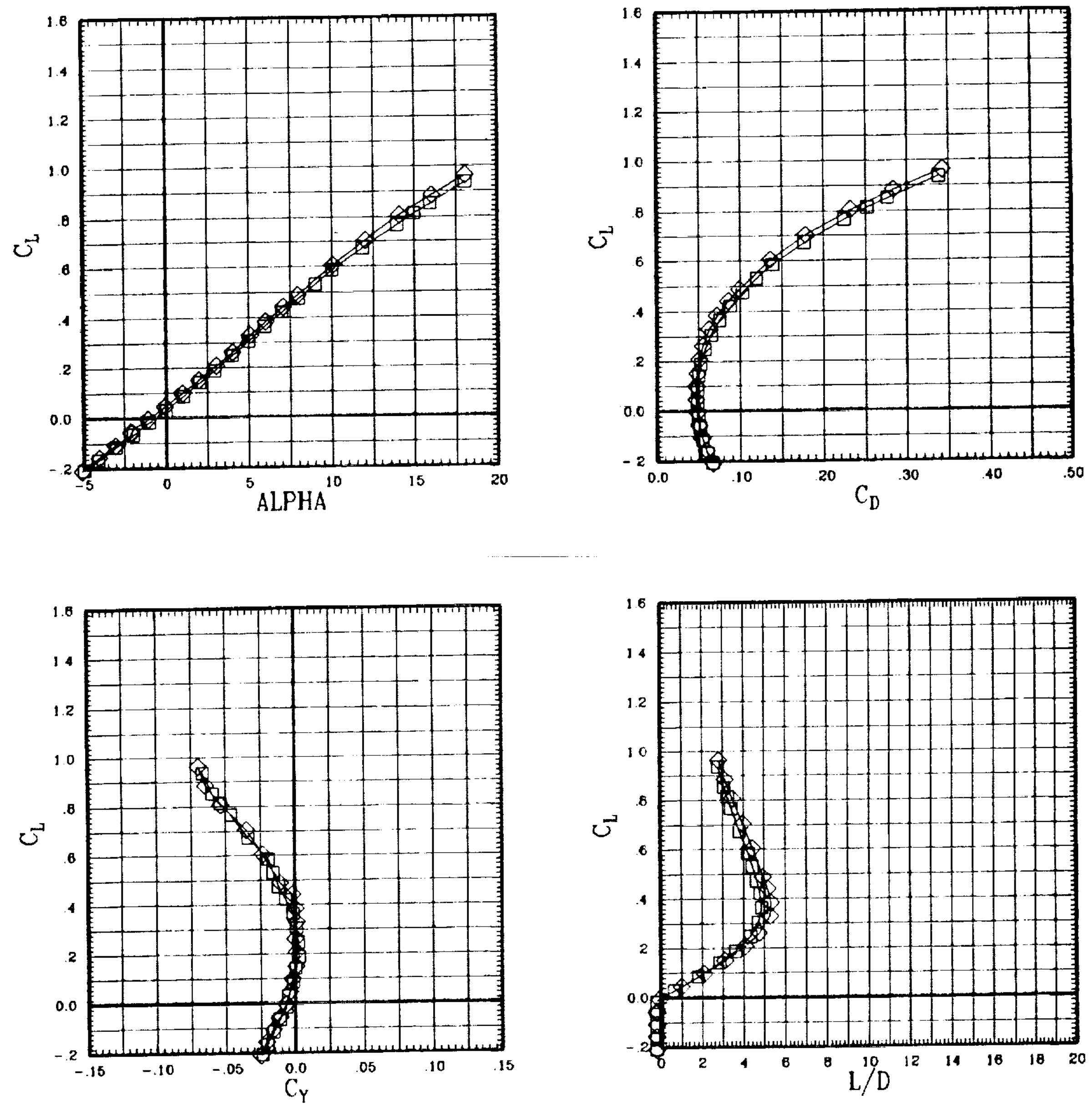

Figure A-1(d). Rockwell and NASA Ames wings for sweep = 60 deg.

SYMBOL	CONFIGURATION	TEST	RUN	SWEEP	MACH	Q	BETA
—□—	Rockwell	100	73	60	1.20	705	-.2
—◇—	NASA Ames	100	134	60	1.20	698	-.1

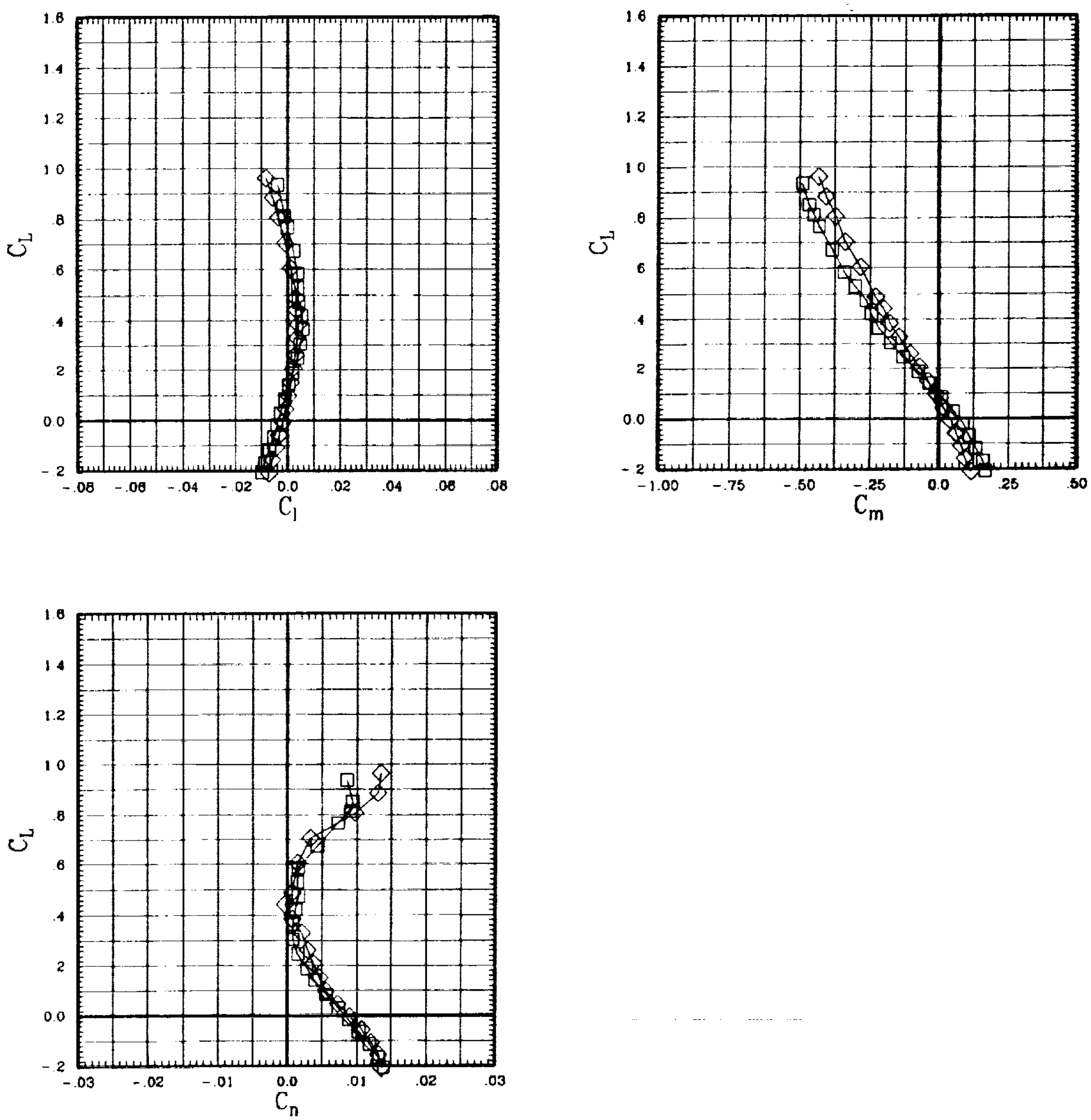

Figure A-1(d). Rockwell and NASA Ames wings for sweep = 60 deg.

SYMBOL	CONFIGURATION	TEST	RUN	SWEEP	MACH	Q	BETA
—□—	Rockwell	100	72	60	1.40	700	0.0
—◇—	NASA Ames	79	32	60	1.40	702	-.2

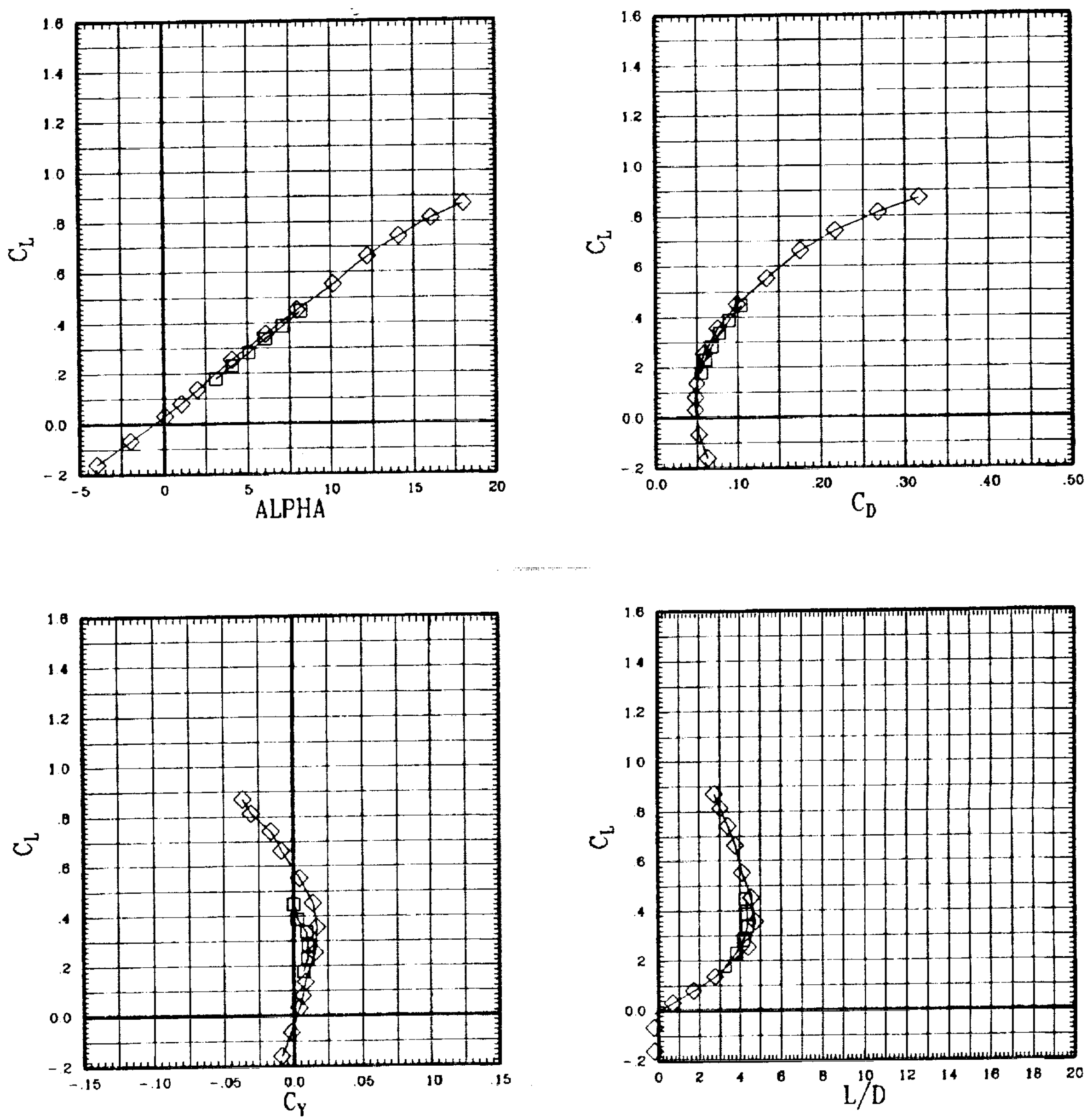

Figure A-1(d). Rockwell and NASA Ames wings for sweep = 60 deg.

SYMBOL	CONFIGURATION	TEST	RUN	SWEEP	MACH	Q	BETA
—□—	Rockwell	100	72	60	1.40	700	0.0
—◇—	NASA Ames	79	32	60	1.40	702	-.2

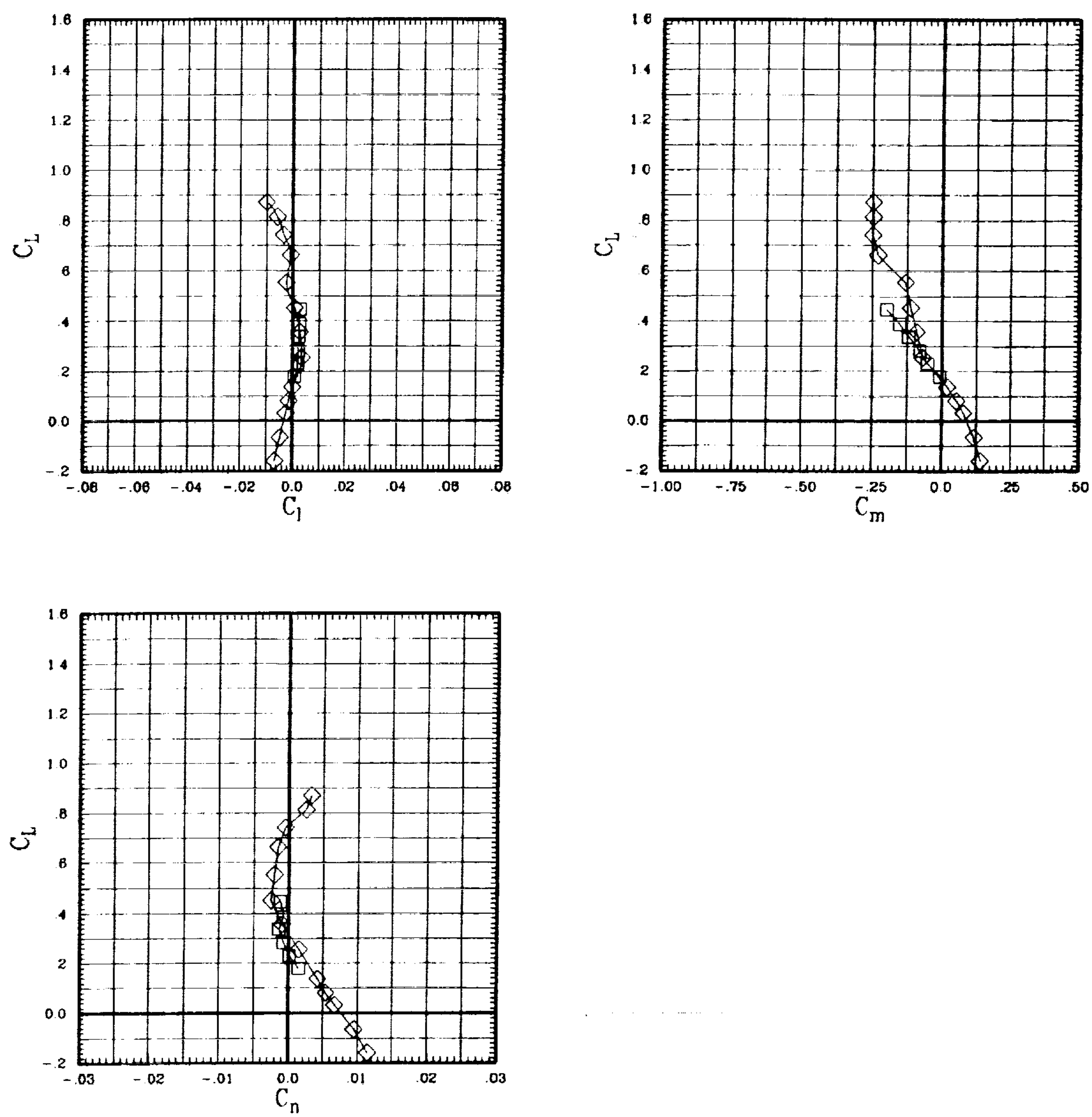

Figure A-1(d). Rockwell and NASA Ames wings for sweep = 60 deg.

SYMBOL	CONFIGURATION	TEST	RUN	SWEEP	MACH	Q	BETA
—□—	Rockwell	100	194	65	.60	698	-.1
—◇—	NASA Ames	100	29	65	.60	704	-.1

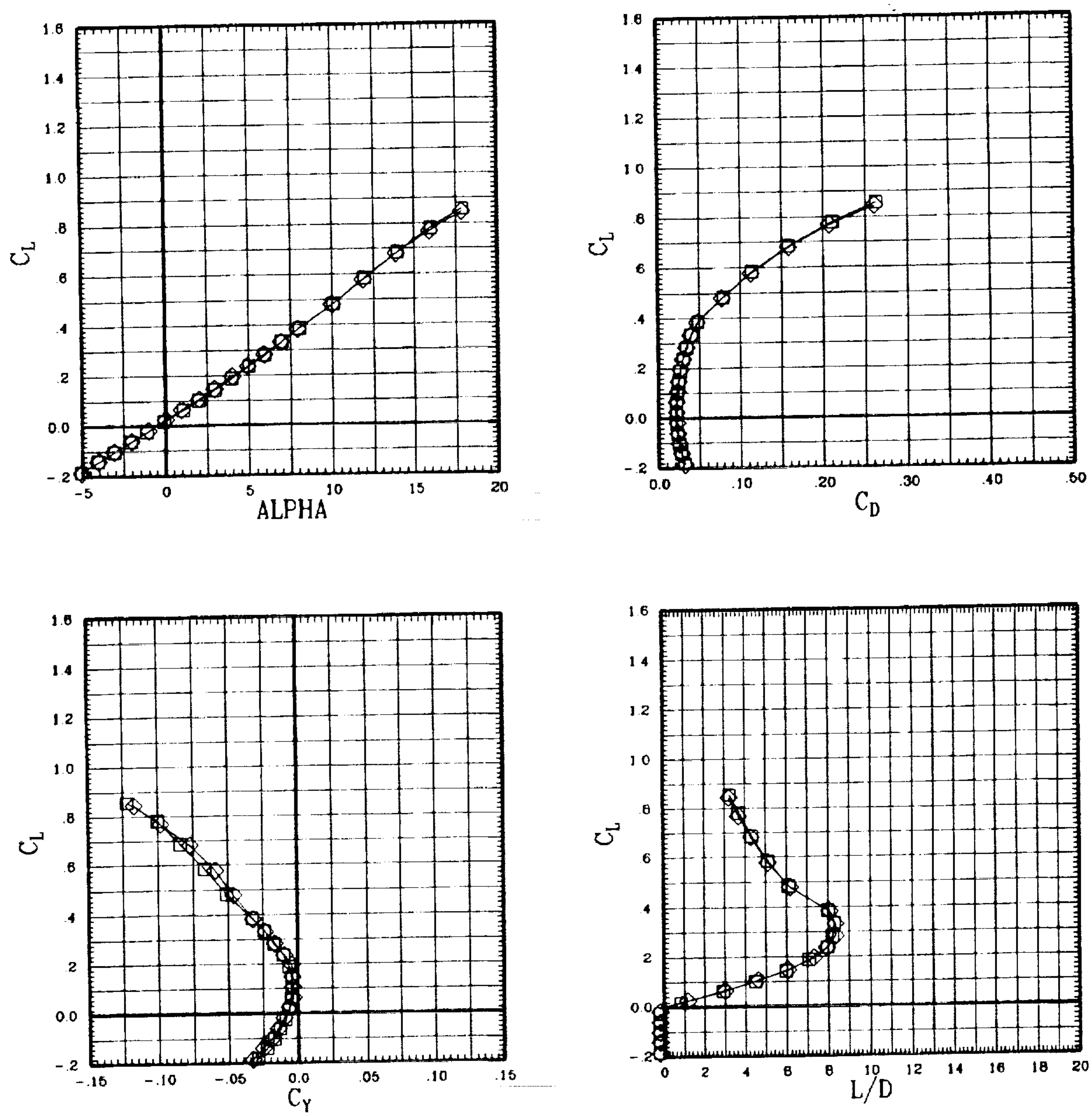

Figure A-1(e). Rockwell and NASA Ames wings for sweep = 65 deg.

SYMBOL	CONFIGURATION	TEST	RUN	SWEEP	MACH	Q	BETA
—□—	Rockwell	100	194	65	.60	698	-.1
—◇—	NASA Ames	100	29	65	.60	704	-.1

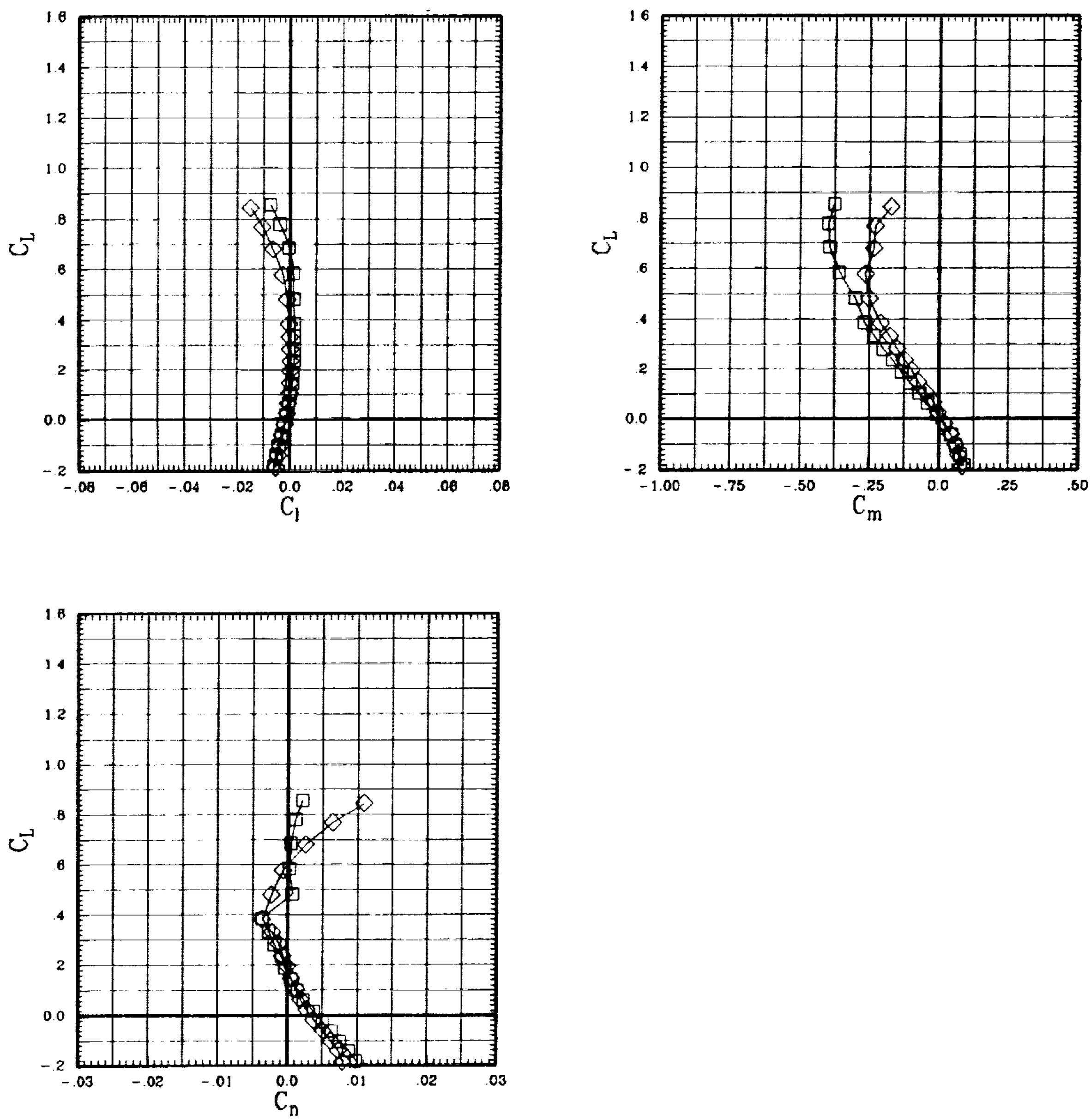

Figure A-1(e). Rockwell and NASA Ames wings for sweep = 65 deg.

SYMBOL	CONFIGURATION	TEST	RUN	SWEEP	MACH	Q	BETA
—□—	Rockwell	100	193	65	.80	698	-.1
—◇—	NASA Ames	100	27	65	.80	698	0.0

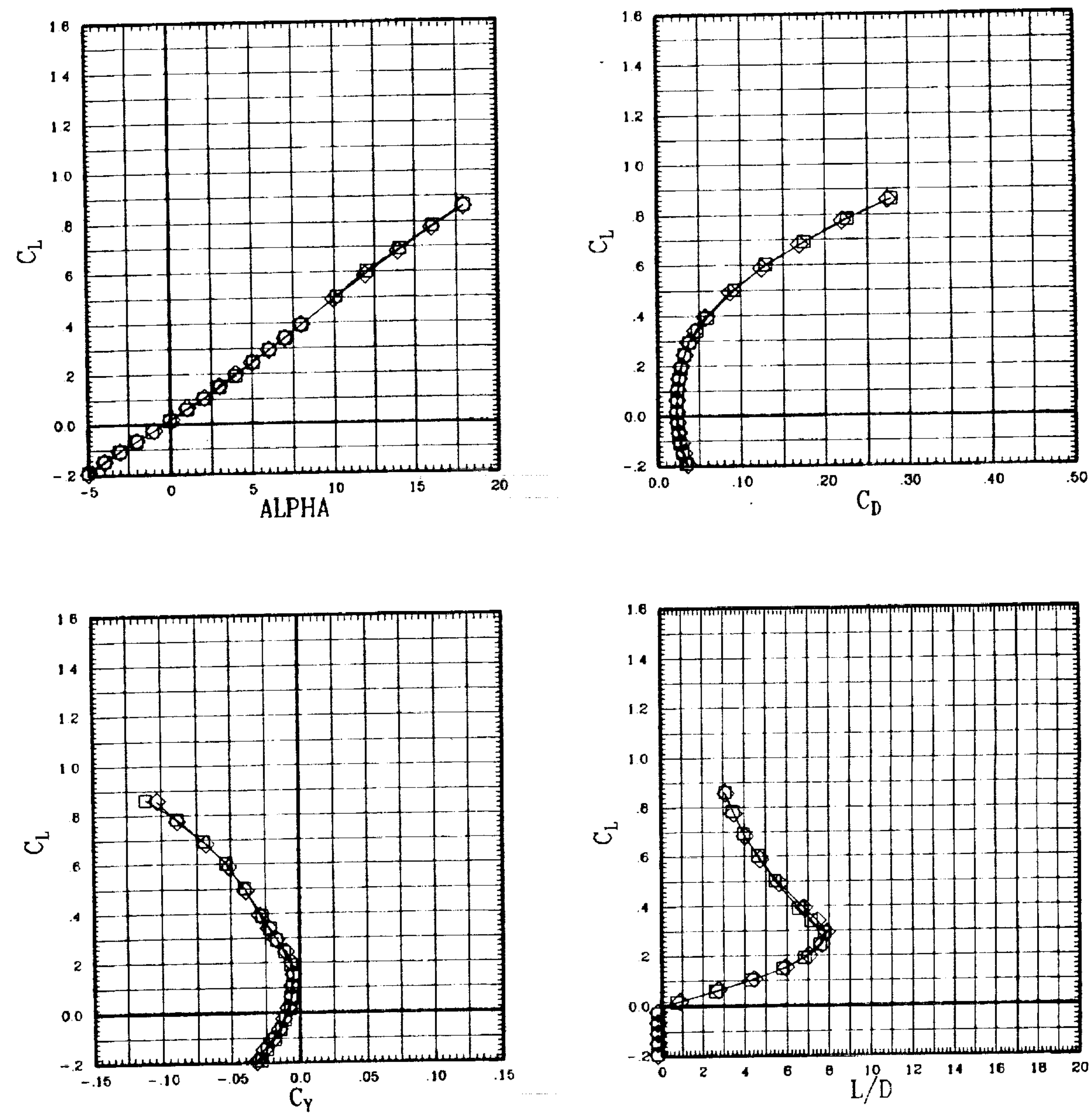

Figure A-1(e). Rockwell and NASA Ames wings for sweep = 65 deg.

SYMBOL	CONFIGURATION	TEST	RUN	SWEEP	MACH	Q	BETA
—□—	Rockwell	100	193	65	.60	698	-.1
—◇—	NASA Ames	100	27	65	.60	698	0.0

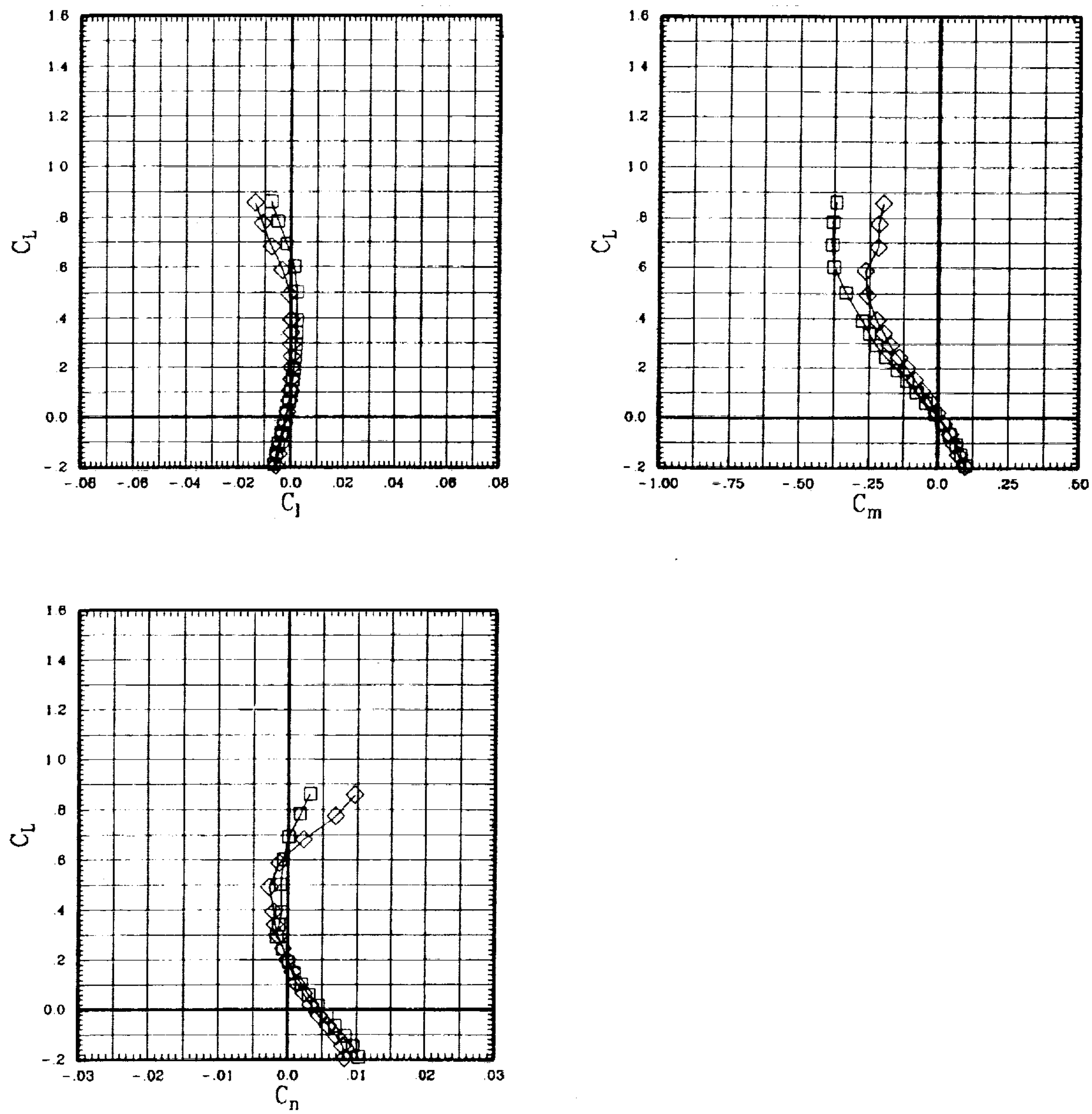

Figure A-1(e). Rockwell and NASA Ames wings for sweep = 65 deg.

SYMBOL	CONFIGURATION	TEST	RUN	SWEEP	MACH	Q	BETA
—□—	Rockwell	100	192	65	1.10	710	-.1
—◇—	NASA Ames	100	24	65	1.10	699	-.1

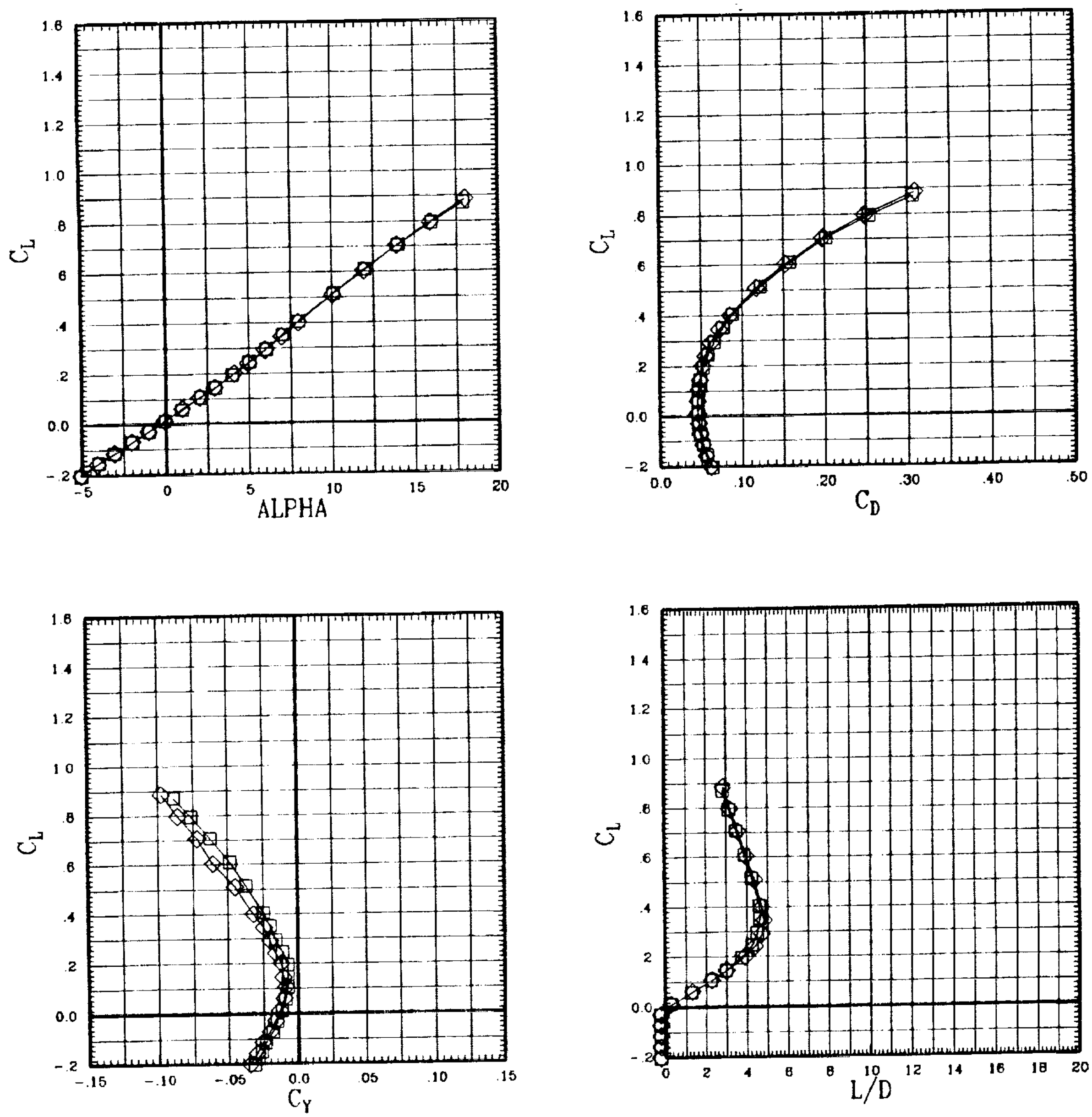

Figure A-1(e). Rockwell and NASA Ames wings for sweep = 65 deg.

SYMBOL	CONFIGURATION	TEST	RUN	SWEEP	MACH	Q	BETA
—□—	Rockwell	100	192	65	1.10	710	-.1
—◇—	NASA Ames	100	24	65	1.10	699	-.1

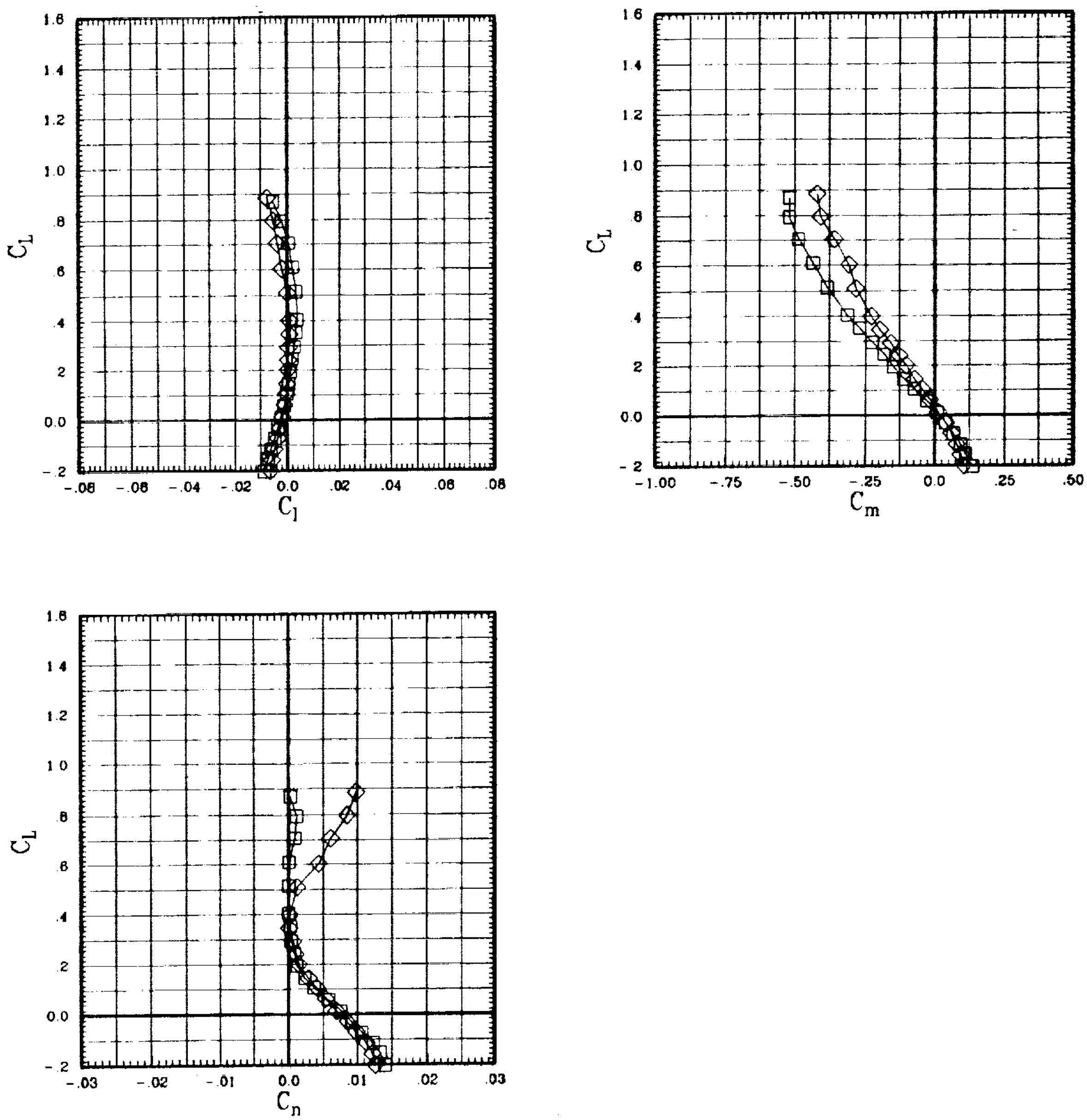

Figure A-1(e). Rockwell and NASA Ames wings for sweep = 65 deg.

SYMBOL	CONFIGURATION	TEST	RUN	SWEEP	MACH	Q	BETA
—□—	Rockwell	100	191	65	1.20	707	-.1
—◇—	NASA Ames	100	23	65	1.20	695	-.1

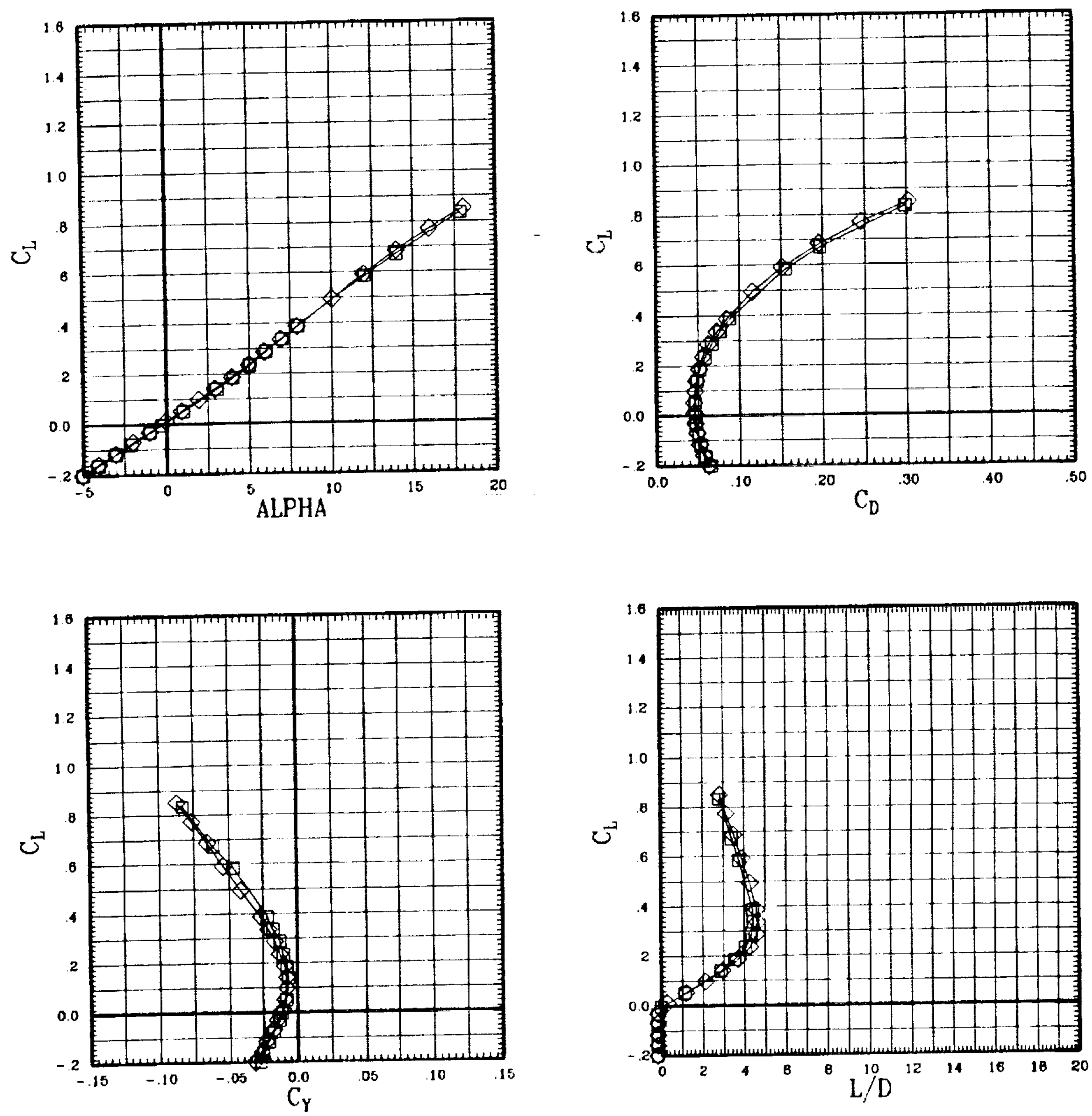

Figure A-1(e). Rockwell and NASA Ames wings for sweep = 65 deg.

SYMBOL	CONFIGURATION	TEST	RUN	SWEEP	MACH	Q	BETA
—□—	Rockwell	100	191	65	1.20	707	-.1
—◇—	NASA Ames	100	23	65	1.20	695	-.1

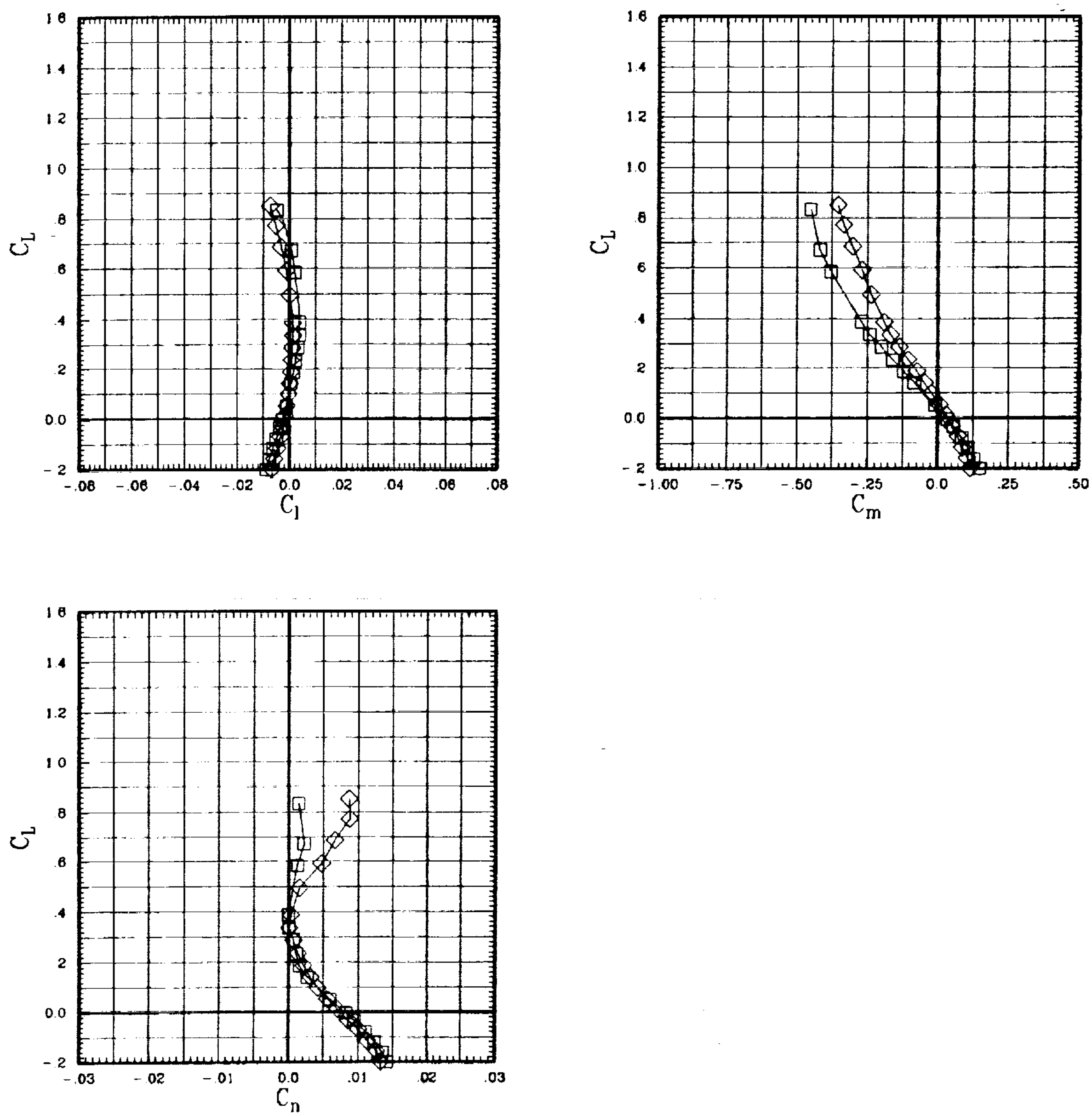

Figure A-1(e). Rockwell and NASA Ames wings for sweep = 65 deg.

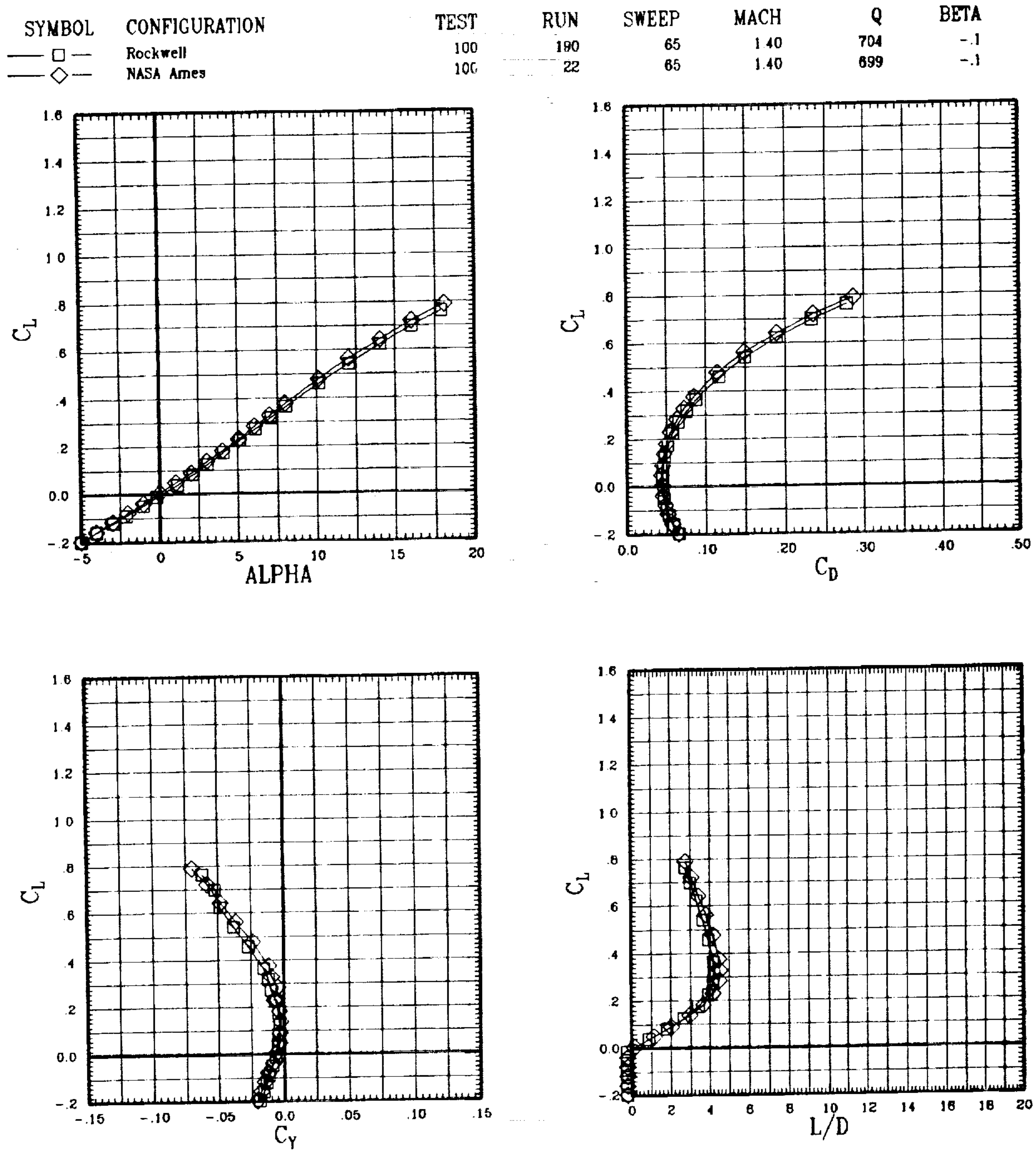

Figure A-1(e). Rockwell and NASA Ames wings for sweep = 65 deg.

SYMBOL	CONFIGURATION	TEST	RUN	SWEEP	MACH	Q	BETA
—□—	Rockwell	100	190	65	1.40	704	-.1
—◇—	NASA Ames	100	22	65	1.40	699	-.1

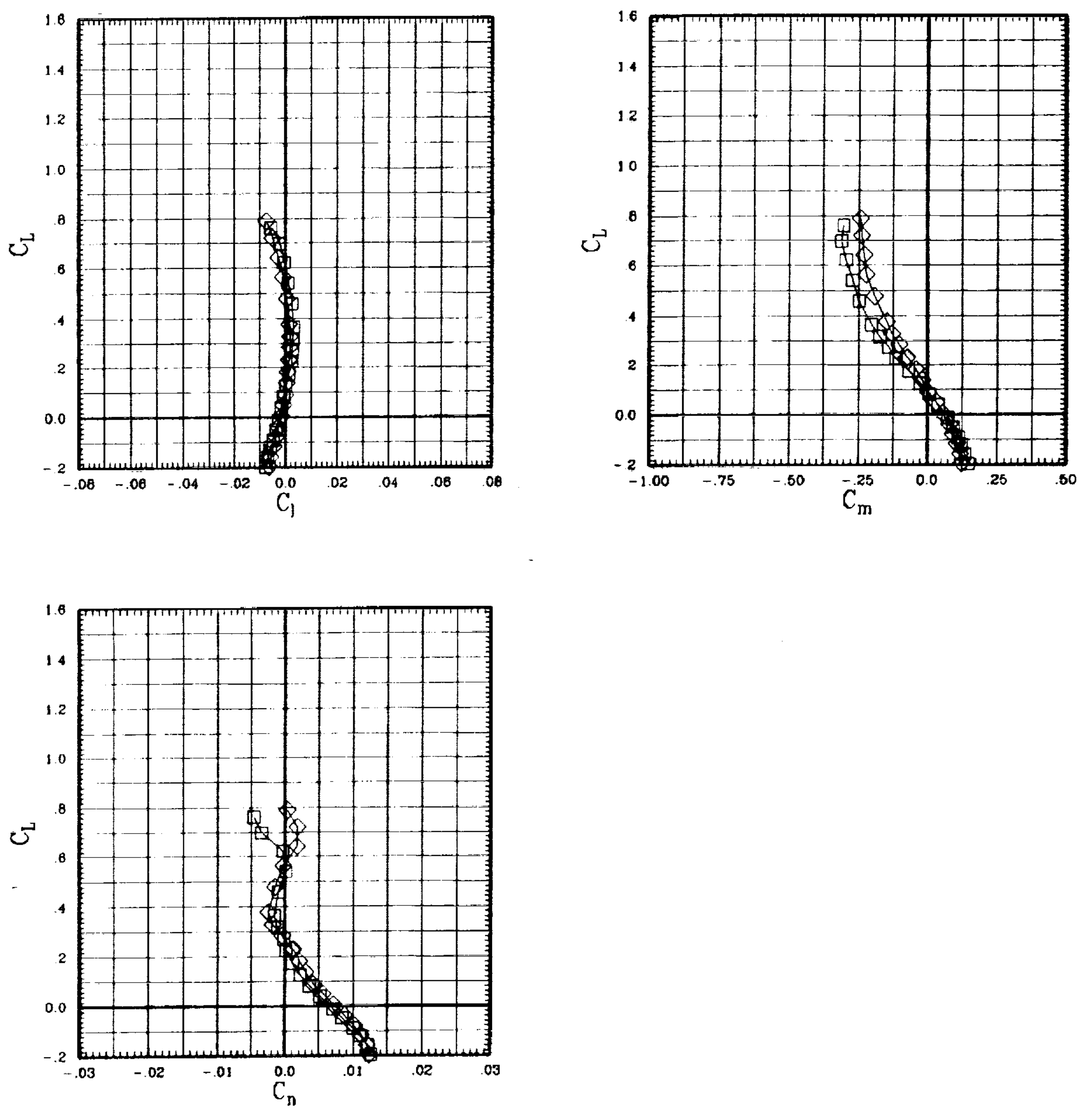

Figure A-1(e). Rockwell and NASA Ames wings for sweep = 65 deg.

NASA
National Aeronautics and Space Administration

Report Documentation Page

1. Report No.	2. Government Accession No.	3. Recipient's Catalog No.
NASA TM-102230		

4. Title and Subtitle	5. Report Date
Transonic Wind Tunnel Test of a 14% Thick Oblique Wing	August 1990
	6. Performing Organization Code
7. Author(s) Robert A. Kennelly, Jr., Ilan M. Kroo,* James M. Strong, and Ralph L. Carmichael	8. Performing Organization Report No. A-89236
	10. Work Unit No. 533-06-01
9. Performing Organization Name and Address Ames Research Center Moffett Field, CA 94035-1000	11. Contract or Grant No.
	13. Type of Report and Period Covered Technical Memorandum
12. Sponsoring Agency Name and Address National Aeronautics and Space Administration Washington, DC 20546-0001	14. Sponsoring Agency Code

15. Supplementary Notes

Point of Contact: Robert A. Kennelly, Jr., Ames Research Center, MS 227-6,
Moffett Field, CA 94035-1000, (415) 604-5860 or FTS 464-5860

*Dept. of Aeronautics and Astronautics, Stanford University, Stanford, California

16. Abstract

An experimental investigation was conducted in the NASA Ames 11- by 11-Foot Transonic Wind Tunnel as part of the Oblique Wing Research Aircraft program to study the aerodynamic performance and stability characteristics of a 0.087-scale model of an F-8 airplane fitted with an oblique wing designed by Rockwell International. The aspect ratio 10.3, straight-tapered wing of 0.14 thickness/chord ratio was tested at two different mounting heights above the fuselage. Additional tests were conducted to assess low-speed behavior with and without flaps, aileron effectiveness at representative flight conditions, and transonic drag divergence with 0° wing sweep.

Longitudinal stability data were obtained at sweep angles of 0°, 30°, 45°, 60°, and 65°, at Mach numbers ranging from 0.25 to 1.40. Test Reynolds number varied from 3.2 to 6.6×10^6/ft. Angle of attack ranged from –5° to +18°. Most data were taken at zero sideslip, but a few runs were made at sideslip angles of ±5°.

The raised wing position proved detrimental overall, although side force and yawing moment were reduced at some conditions. Maximum lift coefficient with the flaps deflected was found to fall short of the value predicted in the preliminary design document. The performance and trim characteristics of the present wing are generally inferior to those obtained for a previously tested wing designed at Ames.

17. Key Words (Suggested by Author(s))	18. Distribution Statement
Oblique wing, Transonic, Supersonic, Wind tunnel test, Skewed wing, Aerodynamics	Unclassified-Unlimited Subject Category - 02

19. Security Classif. (of this report)	20. Security Classif. (of this page)	21. No. of Pages	22. Price
Unclassified	Unclassified	432	A19

NASA FORM 1626 OCT 86